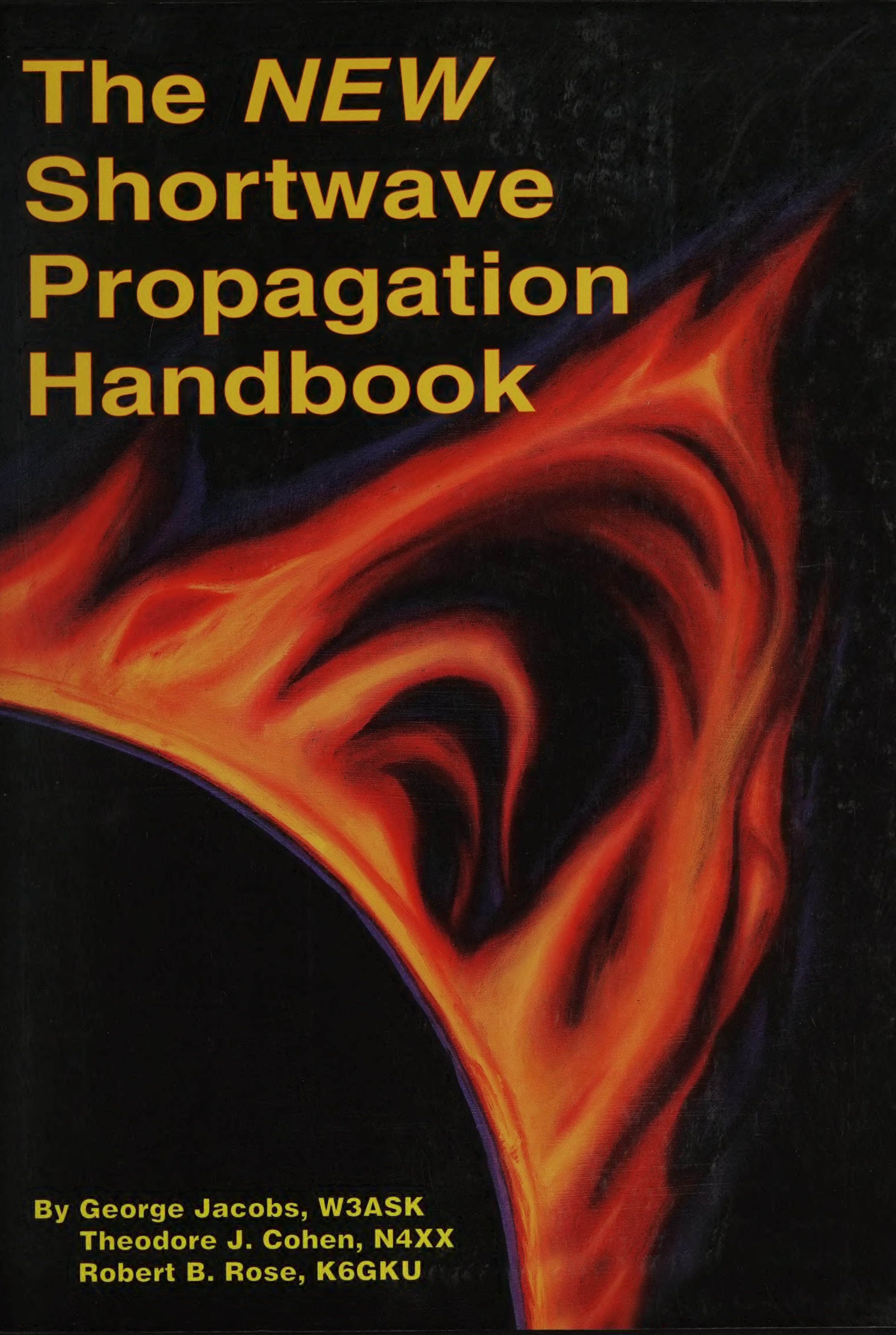

The *NEW* Shortwave Propagation Handbook

By George Jacobs, W3ASK
Theodore J. Cohen, N4XX
Robert B. Rose, K6GKU

Digitized by the Internet Archive
in 2024 with funding from
Amateur Radio Digital Communications, Grant 151

https://archive.org/details/newshortwaveprop00unse

The *NEW* Shortwave Propagation Handbook

By

George Jacobs, W3ASK
Theodore J. Cohen, N4XX
Robert B. Rose, K6GKU

CQ Communications, Inc.

Library of Congress Catalog Card Number 95-68269
ISBN 0-943016-11-8

Editor: Gail M. Schieber
Layout and Design: Elizabeth Ryan
Edmond Pesonen
Illustrations: Hal Keith, K&S Graphics
Cover art: Janine Perry

Published by CQ Communications, Inc.
76 North Broadway
Hicksville, New York 11801 USA

Printed in the United States of America.

Copyright © 1995 George Jacobs, Theodore J. Cohen, and Robert B. Rose

All rights reserved. No part of this book may be used or reproduced in any form, or stored in a database or retrieval system, without express written permission of the publisher except in the case of brief quotes included in articles by the author or in reviews of this book by others. Making copies of editorial or pictorial content in any manner except for an individual's own personal use is prohibited, and is in violation of United States copyright laws.

While every precaution has been taken in the preparation of this book, the authors and publisher assume no responsibility for errors or omissions. The information contained in this book has been checked and is believed to be entirely reliable. However, no responsibility is assumed for inaccuracies. Neither the authors nor the publisher shall be liable to the purchaser or any other person or entity with respect to liability, loss, or damage caused or alleged to have been caused directly or indirectly by this book or the contents contained herein.

Dedication

Shortwave Radio, The First 100 Years—Almost

Shortwave radio, the frequency band between 3 and 30 MHz, may be about to go full circle in its evolutionary development. First used as an experimenters' band, it rapidly became a communications mainstay for the military, civil, and international broadcasting communities. With the increasing use of fiber-optic cable and Earth-orbiting satellites, however, HF may eventually revert back to its use as an experimenters' band . . . a band that primarily will be used by radio amateurs and others seeking to further the science of HF propagation.

It has been called "wireless" (circa 1910), "radio" (1930), "shortwave radio" (1940), and "high frequency" (HF) radio (present). Around the turn of the century Marconi observed that the energy generated by an electrical spark, when passed through a resonant circuit, generated a signal on a discrete frequency. It was this type of technique that was used to produce the first trans-Atlantic transmission in 1901. A circuit that resembled the simplest of crystal sets could hear that signal. When the signal was turned on and off, using, for example, a telegraph key, the electromagnetic signal could send messages. This resulted in the birth of radio as we know it today.

The radio waves that were discovered in 1901 primarily were what we know as the low-frequency (LF) or medium-frequency (MF) bands. The AM broadcast band is in the MF band. The wavelength of these bands is relatively long, and so they were referred to as the "long-wave bands." In the early days development was accomplished experimentally because the theory of how radio worked was poorly understood. In the 1920s the first radio amateurs looked for a way to use radio for more consistent long-range communications, and in doing so they started experimenting with frequencies ranging up to 14 MHz. Compared to wavelengths in the MF bands, these new experimental wavelengths were relatively short; hence, the term "shortwave" was adopted.

In those early days of radio, experimenters tried all sorts and manner of new ideas. If something worked, it was adopted; if it did not work, the idea was discarded and something new was tried. Basically, shortwave radio evolved through a trial-and-error process. Furthermore, little or nothing was known about how signals propagated. The existence of an ionized layer was theorized in 1902 by two scientists—Arthur Kennelly in the United States and Oliver Heaviside in Great Britain. However, it was not until the 1920s that these new theories about an ionized layer and how it bent shortwave signals back to Earth were proved using the first measurement of the ionosphere's height. The "Kennelly-Heaviside" layer was described in the September 1936 issue of *QST*; the model for this layer was based on the first real measurements of the ionosphere's height and electron density.

Industrially, the science was pursued by broadcasting giants such as RCA and AT&T's Bell Laboratories. In a 1936 issue of "RCA Review," David Sarnoff classified the first three decades of radio as the Marine Decade, the War Decade, and the Broadcast Decade. For the most part, the art of radio was practiced at wavelengths of 200 meters or lower (that is, below 1500 kHz).

World War I (1914–1917) gave radio its greatest "kick-start." Because amateur experimentation was suspended during WW I, the war's conclusion saw a resurgence and acceleration in experimentation. During this period the world saw the discovery of high-vacuum tubes, regenerative circuits, improved detectors and amplifiers, and continuous-wave generators that operated at much higher frequencies than ever before.

During the 1920s the gradual perfection of radio telephony (that is, voice communications) was the development that overshadowed all others. The Broadcast Decade of the 1920s brought the introduction of radio to the masses with the Harding-Cox presidential election results being broadcast to an audience of several thousand amateurs and others with homemade radio sets. This "stunt," brought about by amateur experimenters, marked the birth of radio broadcasting.

Experimentally, radio amateurs pioneered the exploitation of the new shortwave bands, pushing their work to the unheard of frequencies of 50 MHz (6 meters). Frequencies of 28 MHz and above were referred to as "ultra-high" frequencies. At a convention in Washington, D.C., in 1927, international frequency assignments, as we know them today, were established and the "ham bands" were born.

In the late 1930s and during the 1940s the shortwave frequencies between 3 and 30 MHz (100 to 10 meters) matured into supporting communications worldwide, primarily through the use of radio telegraph and radio telephony. Radio telegraph, or "Morse," or "CW," as it is known in various circles, flourished with the transmission of global telegrams, ship-to-shore messages, ship-to-ship messages, and shortwave broadcasting. During World War II shortwave radio was the backbone of Allied and Axis communications. Amateur radio transmissions were terminated for the duration, and much of the equipment existing at that time was donated to the war effort. Communications became more sophisticated, and encryption became a new art; the ability to code your traffic so that no one else could read it became a necessity. This led to counter-encryption developments, together with new direction-finding initiatives that were needed to locate and destroy Axis submarines. In the latter phases of WW II the shortwave bands were bustling with signals 24 hours a day, as every country in the world was using this medium. Interestingly, this was a time of solar minimum, when only the lower half of the HF band was usable.

The development of new hardware was paralleled with a greater understanding of how HF worked. During WW II, for example, U.S. amateurs were not allowed to transmit, so they spent their time improving their receivers and antennas, and working on the theory of how shortwaves propagated.

Solar Cycle 18 reached a record peak in 1949, and radio amateurs first tasted the thrills of worldwide 10 meter propagation and what shortwave communication was "all about." Through this period and into the 1950s, hardware technology in vacuum tubes and other devices blossomed. Shortwave radio was about to hit full stride. It was the primary communications medium for the military, industrial, and overseas broadcasting services. The frequencies between 3 and 30 MHz were fully allocated, and during the record-breaking maximum of sunspot Cycle 19 in the late 1950s, congestion and competition for spectrum space increased. During these years, too, the science of shortwave radio and how propagation works at these frequencies started to accelerate. The International Geophysical Year (IGY) was announced. It signaled the beginning of a concentrated effort throughout the worldwide scientific community to collaborate on making experimental ionospheric measurements that could be correlated on a global basis. During this period amateur radio experimenters perfected the new, more efficient method of voice communications called "single sideband" (SSB). By the time commercial and industrial users started using SSB it had almost fully replaced amplitude modulation (AM) in the amateur community.

The development of the radio art continued into the 1960s, a time when our knowledge of the physics of the ionosphere, how shortwaves propagate, and how the Sun influences all of these processes prospered and grew. Newly born orbiting Earth satellite technologies permitted even more sophisticated work to be performed on propagation. The first real HF propagation prediction program emerged from the Central Radio Propagation Laboratory (CRPL), Boulder, Colorado, and the development of HF propagation predictions became an art unto itself. All communication services were heavily investing in ways to use shortwave frequencies in a more efficient manner. The U.S. military and U.S. Government invested heavily in solar observatories and the methods used to forecast solar effects on ionospheric conditions. Sciences involving ionospheric physics and propagation were taught in many U.S. universities. Solar-terrestrial sciences became of the utmost importance with initiation of the series of Apollo Manned Moon missions and the recognition that solar radiation could have a serious impact on astronauts and satellites alike. This scientific activity peaked in the period between 1966 and 1972. Shortwave broadcasting also was growing, and with millions of people worldwide depending on this service for their daily news, the need to understand HF propagation was paramount.

In the early 1970s HF technology started competing with new, more expensive satellite communication technologies. Almost overnight HF communications was relegated to a backup role by the U.S. military. While HF broadcasting services were still in full swing because of the Cold War, the funding for further military-related research started to wane. The most prominent loss was in the area of academic studies, where programs in ionospheric physics and solar/terrestrial relationships disappeared. By the 1980s most ionospheric-related programs had been eliminated. Important communications were moved to satellite-borne systems because of their inherent higher reliability, greater bandwidth, and the use of new, digital signal processing techniques. Simply put, HF radio became too inefficient to use.

In this time period the Navy deleted its use of manual Morse, a modulation technique it had used since the 1900s (the Marine Decade). By the late 1980s HF was primarily used by the shortwave broadcasters, the Coast Guard, elite military forces, Third World nations, and radio amateurs. The other U.S. communication services and the military had adopted a high-speed traffic mind set, and HF was just too slow. It is interesting to note, however, that during this period the use of HF prediction programs flourished, spurred on by the new desktop personal computer (PC) technology. Anyone could use just about any program available. This became a period of "users" and not "thinkers." Most people who used shortwave propagation prediction programs really did not know how to interpret the results. New digital communication technologies gave rise to "error free" printed text. All that was required of the user was the ability to read. The mystique of shortwave radio was relegated by many to the status of an obsolete art form.

In 1992 Desert Storm demonstrated that modern communications must be global, instantaneous, and capable of conveying real-time visual images—something HF cannot do. HF lost its backup role to common carrier (in particular, commercial communication satellites and cellular telephone). Virtually all research and development (R&D) was eliminated by the middle of the decade as Cold War threats diminished. While shortwave broadcasting is still important on a global basis, it may be leveling off in the next few years as a result of the end of the Cold War. Most military users have placed HF capabilities in a caretaker status. Besides international broadcasters, only the amateur experimenter and some special-purpose users still support expanding the use of shortwave capabilities. In HF communications, open voice transmissions are giving way to hard-to-detect, spread-spectrum modulation techniques. Morse code is gone, except for its use in the radio amateur community.

By the year 2000 development in the shortwave spectrum in all likelihood could revert mainly to its original developers, the radio amateurs—the original experimenters. Clearly, new opportunities for using HF were demonstrated in the Navy's Project PENEX, where it was shown that a 40 kHz wide, direct-sequence, spread-spectrum signal could be transmitted reliably at very low power levels. Furthermore, this signal could not be detected by conventional means, and several similar signals could share the same frequency reliably without interfering with one another.

In 1986 the radio amateur community was given permission to start experimenting with spread-spectrum communications. New innovations in this modulation technique will come from this community as they have for almost a hundred years. If it can be done, the amateur will do it.

This book, then, is dedicated to the radio amateur, the pioneer of shortwave radio. It also is dedicated to the new breed of experimenters who will "show the way" toward using shortwave radio ever more efficiently through the use of modern technology and a better understanding of how shortwave signals propagate.

Preface

Thirteen years have passed since publication of our last book, *The Shortwave Propagation Handbook*, second edition. During this time we have witnessed the labored demise of sunspot Cycle 21 and the rapid ascent, plateau, and initial decline of Cycle 22. During this time, too, tens of thousands of radio amateurs and other users of the high-frequency (HF) spectrum have successfully used the information and techniques presented in that handbook to communicate worldwide and to raise their DX scores to levels some thought unreachable. The WWV broadcasts of solar and geomagnetic activity have become commonplace, and virtually all radio amateur publications devoted to DXing now publish 27-day recurrence forecasts of ionospheric propagation conditions.

The above notwithstanding, it may come as a surprise to some readers that our *unified* approach to "do it yourself" propagation predictions and to the use of the Master Propagation Charts that have been published for many years in *CQ* was only developed in the late 1970s, almost 70 years after Guglielmo Marconi first bridged the Atlantic Ocean using ionospheric propagation. Clearly, the time was long overdue for the development of a more objective approach to employing the ionosphere for radio-wave propagation, an approach we first presented in *The Shortwave Propagation Handbook*. To our delight, your embrace and use of the techniques presented have been phenomenal.

Still, there is always need for improvement. So much has happened over the last thirteen years that nothing less than a new, up-to-date, comprehensive guide to mastering the art of shortwave propagation would meet the needs of today's operators. First, we have updated our earlier work on both solar phenomena and sunspot cycle behavior. References and data sources have been expanded. At the request of many readers, extensive material has been included on various microcomputer programs that are available for use in developing customized ionospheric circuit analyses. And for those who can't wait to see what the next cycle will bring, we present a summary of the sunspot cycle predictions for Cycle 23 that have been developed by recognized professionals in the field of solar physics. Our intent is to make *The NEW Shortwave Propagation Handbook* the single most comprehensive source available to the amateur, CBer, or SWL interested in optimizing his or her use and enjoyment of the HF spectrum.

The publication of this new book also marks the debut of Robert (Bob) Rose, K6GKU, as our third author. Bob has more than 25 years of professional HF communications experience, and among his other accomplishments, he was responsible for the development of the MINIMUF model in the middle 1970s and of the ionospheric prediction program known as PROPHET, widely used by the military over the last decade. We are honored to have a man of this stature working with us; his contributions were invaluable.

With Cycle 22 now on the wane, users of the HF spectrum not only have to work harder at their DX activities, they also have to work "smarter." At solar minimum the band of frequencies available for worldwide communications is almost half of that available at solar maximum. It is little wonder, then, that anyone interested in communicating worldwide, in understanding skip interference, or in receiving radio broadcasts from around the world is going to need an extra edge—one which turns an average session on the bands into a winning performance. That is what this book promises, and if used properly, that is what this book will deliver.

George Jacobs, W3ASK
Theodore J. Cohen, N4XX
Robert B. Rose, K6GKU
April 1995

Acknowledgements

The preparation of this book involved the efforts of a number of people and organizations around the world. All gave generously of their reference material, software, and technical know-how. The authors specifically thank Brian Satterlee, KD6SC, Shel Shallon, W6EL, and David Cole (Ionospheric Prediction Service [IPS], Australia) for their valuable input on HF prediction programs. We also are indebted to the staff at the National Oceanic and Atmospheric Administration (NOAA), Boulder, Colorado, including Joe Allen and Helen Coffey of the National Geophysical Data Center (NGDC) and Gary Heckman of the Space Environmental Services Center (SESC) for the extensive material they so generously provided on the last solar cycle and how users of the HF spectrum can access NOAA's geophysical databases. We acknowledge with thanks the contributions of Terry Kelly (KEL Aerospace, Australia), Joseph Ahlgren (Geoclock), and Richard Thompson (IPS) for permitting us to use material they graciously provided at our request. And without the efforts of Tom LaPuzza, Public Information Officer at the Naval Command, Control, and Ocean Surveillance Center, Research, Development, Test, and Evaluation (RDT&E) Division, San Diego, California, we would not have had access to the valuable data gleaned from many years of HF propagation research performed at that facility. Dr. Neil Sheeley of the Naval Research Center (NRL), Washington, D.C., generously provided photographs of solar phenomena that were used as a reference by artist Janine Perry to produce the original artwork shown on the cover.

Our thanks also to Susan Cohen, who lent us her considerable proofreading skills, without which our job would have been made more difficult. Lew Ozimek, N2OZ, and Nancy Barry contributed their time in inputting the authors' final changes to the text and charts. And finally, we gratefully acknowledge the many and varied contributions made by our editor, Gail M. Schieber, of CQ Communications, Inc. Without her infinite patience, undying enthusiasm, and strict attention to detail, this book never would have been published.

Thank you all!

George Jacobs, W3ASK
Theodore J. Cohen, N4XX
Robert B. Rose, K6GKU

About The Authors

George Jacobs, W3ASK

Born in 1924 on the same day that the ionosphere was discovered, George Jacobs is a legend in the field of shortwave communications.

Amateur radio has been a part of George's life for almost as long as he can remember. First licensed in 1941, but exposed to amateur radio a decade earlier, George credits amateur radio with launching him into telecommunications professionally.

In a distinguished career that has spanned more than half a century, George has successfully combined innovative engineering talents, diplomacy, and a fierce belief in the free flow of information to forge the Government-funded Voice of America, Radio Free Europe, and Radio Liberty. In private practice since 1980, he has continued to develop shortwave broadcasting stations throughout the world.

Of his many contributions to amateur radio, George is most proud of his simplified propagation forecasts and predictions which have appeared monthly in *CQ* magazine since March 1951, and of the pioneering role he played in the development and launching of the OSCAR and AMSAT radio amateur satellite projects. Included in the honors bestowed upon him are the Air Medal for radar service during World War II, rank of Life Fellow in both the IEEE and the Radio Club of America, two U.S. Government awards for outstanding and superior achievements, a Commission from President Reagan, the Marconi Gold Medal Award for Engineering Achievement, and the Jack Poppele Award for excellence in engineering.

George is a Charter Life Member of the American Radio Relay League. Academically he has an MSEE from the University of Maryland, and he is a Registered Professional Engineer. He has represented the United States at every major international telecommunication conference dealing with the shortwave bands, including WARC-59, WARC-79, and WARC-92. George is a prolific writer, having authored hundreds of articles that have appeared in technical publications throughout the world.

Dr. Theodore J. Cohen, N4XX

Dr. Theodore J. (Ted) Cohen, N4XX, has been involved in communications and electronics for over 40 years. First licensed in 1952, he now holds an amateur Extra Class license. Active in a number of technical areas, Ted is best known within the amateur radio community for his early (c. 1964) work in slow-scan television, for his pioneering efforts on technical and legislative approaches to the problem of radio frequency interference (RFI) to electronic home-entertainment equipment, and for the development of simplified techniques for the preparation of ionospheric propagation forecasts.

Ted is a Senior Member of the IEEE, a Fellow of the Radio Club of America, a former Regional Vice-President At-Large for the Armed Forces Communications and Electronics Association (AFCEA), and a Life Member of the ARRL. In 1981 Ted created the first radio feature on personal computers. Between 1981 and 1985 it was heard continuously in the Baltimore-Washington market, with selected features syndicated nationwide by the CBS Radio Station's News Service. In all, over 500 features were aired for listeners in the U.S. and Canada.

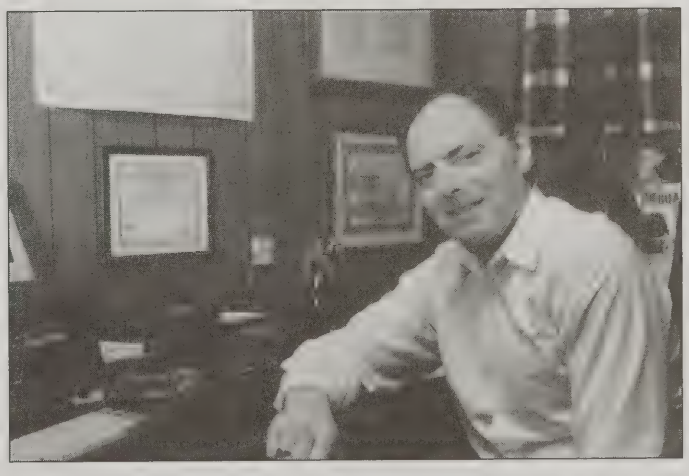

Ted has published well over 300 columns, papers, construction articles, and essays on communications, electronics, computer technology, and political aspects of amateur radio in the scientific, technical, and popular literature. The holder of advanced degrees in physics and geophysics, he currently directs the business development activities of a professional services firm that supports clients in the defense, civil, and commercial sectors. Ted enjoys chasing DX on the high-frequency bands from his home outside Washington, D.C., where he has worked more than 345 countries.

Robert B. Rose, K6GKU

Amateur radio was the "great motivator" in Bob Rose's life. First licensed in 1954 at the age of 15, he spent most of his teenage years on "40 phone" as Cycle 19 climbed to its record peak. Because of his amateur radio background, Bob went on to get a BS degree in Electrical Engineering in 1962 from California State Polytechnic College. Subsequently, he went to work for the Department of the Navy.

In the early 1970s Bob managed the La Posta Astrogeophysical Observatory near San Diego, California. This facility was involved in a number of solar and ionospheric measurement programs. After the closing of the La Posta facility in 1976, Bob went on to a career in ionospheric experimental science and the development of HF signal assessment systems to do advanced signals warfare analysis. He was the co-developer of the MINIMUF HF MUF prediction model in 1975 (with Dr. Paul Levine). This model, published in *QST* in 1982, is the backbone of many PC-based HF prediction programs.

Until his retirement from Government service in January 1994, Bob was involved with a variety of ionospheric experimental measurement programs that led to the revision of many ionospheric theories. Bob regularly lectures at amateur radio clubs and conventions on solar-terrestrial relationships and what these relationships mean to amateur radio operators. He also is a regular guest lecturer at the Naval Postgraduate School in Monterey, California, where he teaches courses on the art of HF radio.

K6GKU has been active on the HF bands for 40 years, mostly on 10 meters. In early 1995 Bob moved to his new home in Arizona, where he is heard regularly on HF using CW and RTTY. Bob is a prolific writer, although most of his papers and articles have appeared in the technical literature. This is his first book.

Table of Contents

DEDICATION iii

PREFACE vii

ACKNOWLEDGEMENTS ix

ABOUT THE AUTHORS xi

Chapter 1 PRINCIPLES OF IONOSPHERIC PROPAGATION 1-1
- 1.1 The Ionosphere 1-1
- 1.2 Regular Ionospheric Variations 1-10
- 1.3 Optimizing High-Frequency Communications 1-12
- 1.4 Ionospheric Disturbances and Shortwave Radio Effects 1-19
- 1.5 1989 and The Disturbed Sun 1-28
- 1.6 References 1-29

Chapter 2 SUNSPOTS AND THE SUNSPOT CYCLE 2-1
- 2.1 Sunspots 2-1
- 2.2 Cycle 19 (1954–1964) 2-7
- 2.3 Cycle 20 (1964–1976) 2-7
- 2.4 Cycle 21 (1976–1986) 2-10
- 2.5 Cycle 22 (1986–1996/97) 2-11
- 2.6 Solar Flux 2-12
- 2.7 References 2-13
- 2.8 Appendix 2-14

Chapter 3 SUNSPOT CYCLE PREDICTIONS 3-1
- 3.1 Prediction Methods 3-3
- 3.2 How Good Were The Predictions? 3-8
- 3.3 References 3-12

Chapter 4 DO-IT-YOURSELF PROPAGATION PREDICTIONS AND MASTER PROPAGATION CHARTS 4-1
- 4.1 How To Use The Master DX Propagation Charts 4-1
- 4.2 How To Use The Master Short-Skip Propagation Charts 4-5
- 4.3 Master Propagation Charts—Low Solar Phase (SSN 0–30) 4-7
- 4.4 Master Propagation Charts—Moderate Solar Phase (SSN 30–60) 4-12
- 4.5 Master Propagation Charts—High Solar Phase (SSN 60–90) 4-18

4.6 Master Propagation Charts—Very High Solar Phase (SSN 90–120) 4-24
4.7 Summary of DX Band Conditions Throughout A Complete Solar Cycle 4-31
4.8 References 4-31

Chapter 5 IONOSPHERIC FORECASTS 5-1
5.1 Short-Term Forecasts for Ionospheric Propagation 5-2
5.2 A Breakthrough in Simplifying Ionospheric Forecasts 5-6
5.3 WWV Broadcasts; Other Sources of Solar Flux & Geomagnetic Activity Indices ..5-11
5.4 Worldwide HF Beacon Transmissions 5-17
5.5 References 5-18
5.6 Addendum for Educators 5-18
5.7 Appendix 5-19

Chapter 6 HF PROPAGATION PREDICTION PROGRAMS 6-1
6.1 HF Propagation Programs—What Are They? 6-1
6.2 The Evolution of HF Prediction Programs 6-2
6.3 Types of HF Prediction Programs 6-3
6.4 The Two Parts of Propagation Prediction Programs 6-5
6.5 How Accurate Are The HF Prediction Programs? 6-8
6.6 Examples of HF Propagation Prediction Programs 6-9
6.7 The Future of HF Prediction Programs 6-22
6.8 References 6-25

Chapter 7 UNUSUAL HF AND VHF IONOSPHERIC PROPAGATION 7-1
7.1 VHF Propagation By Regular F_2-layer Ionization 7-1
7.2 Sporadic-*E* Ionization 7-2
7.3 Auroral Ionization 7-6
7.4 Meteor Ionization 7-11
7.5 Trans-Equatorial VHF Scatter 7-12
7.6 Ionospheric Scatter 7-14
7.7 Summary of Unusual VHF Propagation Phenomena 7-15
7.8 Spread-*F* 7-15
7.9 Gray-Line Propagation 7-17
7.10 Long-Path Propagation 7-20
7.11 Non-Reciprocal Communications 7-24
7.12 Fading 7-25
7.13 References 7-26

INDEX I-1

Chapter 1

Principles of Ionospheric Propagation

The *high-frequency,* or HF, portion of the radio spectrum lies between approximately 3 and 30 megahertz (MHz), or between 3,000 and 30,000 kilohertz (kHz). In the metric system it is called the *shortwave* range, and expressed in *wavelength,* it lies between 100 and 10 meters. In this book high frequency and shortwave will be used interchangeably.

Wavelength, expressed in meters, and frequency, expressed in kilohertz, are related by the following equation:

$$\text{Wavelength} = \frac{300{,}000}{\text{Frequency}} \qquad (1)$$

Radio communication in the high-frequency range is possible because there exists in the Earth's upper atmosphere a region called the *ionosphere,* which reflects (actually, refracts, or bends) radio waves over long distances. In this chapter we will review how the ionosphere was first detected, how it is formed and measured, how its structure varies with time and other factors, and how it makes possible long-distance radio communications. We also will discuss the role of the ionosphere in high-frequency communications from a practical point of view by examining the relationship among factors such as the maximum usable frequency (MUF), signal absorption, and optimum antenna design.

1.1 The Ionosphere

There exists in the Earth's upper atmosphere a region consisting of several electrified layers that are capable of bending high-frequency radio waves and returning them to earth at great distances.

The electrified characteristics of these layers, which are collectively referred to as the ionosphere, are subject to wide variations. This is so because the ionosphere is formed by ultraviolet radiation from the Sun, and the intensity of the radiation changes radically with time and geographical location.

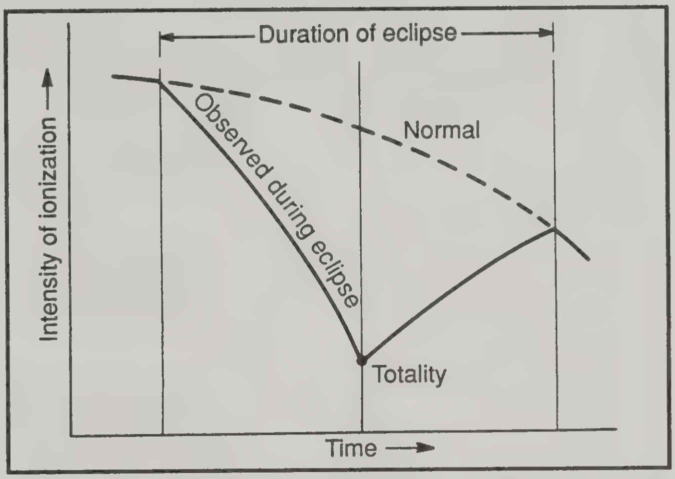

Figure 1.1. The Moon's shielding effect prevents solar radiation from reaching the Earth's atmosphere during a solar eclipse. A sharp decrease in ionization is observed, corresponding to the progress of the eclipse.

The amount of radiation illuminating the ionosphere varies hourly, seasonally, and geographically, depending on the relationship between the Sun and the Earth. In addition, year-to-year variations over an approximately 11-year cycle occur in the ionosphere's capability to reflect radio waves. These changes result from the difference in the number of sunspots that occur on the face of the Sun.

Sunspots are stormy areas on the solar surface that produce considerable ultraviolet radiation. When the Sun's surface is covered with a great number of spots, the ionosphere is electrically strong and shortwave radio communications are generally very good; when the number of sunspots diminishes, conditions become poorer.

The present sunspot cycle, the 22nd observed since accurate records have been kept, began in September 1986. Since then, the number of spots on the Sun increased until the cycle reached its maximum value in June 1989. Solar activity is now declining towards the next solar minimum, which is expected to occur in 1996 or 1997.

Because the ionosphere plays such a vital role in long-distance high-frequency communication, it is desirable at this point to go into greater detail about its characteristics as well as the factors that influence changes in its behavior. Once this has been accomplished, the reader will be better equipped to interpret the changes that take place, and to determine how they affect transmission and reception on the HF bands.

Early Discoveries

In 1901 Marconi successfully completed one of the most historic experiments ever conducted—the transmission of a radio signal without wires across two thousand miles of ocean.

Prior to Marconi's experiment, it had generally been believed that radio propagation was restricted to line of sight. However, a German physicist, Heinrich Hertz, demonstrated that while radio waves travel in straight lines, their direction of travel can be altered by interposing an electrically conducting obstacle in their path.

In 1902, a year after Marconi's initial success, two scientists, Arthur Kennelly in the United States, and Oliver Heaviside in Great Britain, suggested in independent scientific papers that the Earth's upper atmosphere consists of an electrically conducting region. It was this region, they theorized, that acted as an obstacle and deflected Marconi's signals across the Atlantic Ocean. They reasoned that such a region was probably produced by solar radiation, but two decades were to pass before the existence of this region was verified.

Early radio experimenters knew little or nothing about the physics of propagation. The experimental sciences had not evolved, and so the characteristics of a propagating signal could only be guessed at. Early radio was primarily practiced at long waves—what we know today as the LF and MF (including AM broadcast) bands (that is, the bands between 30 and 3000 kHz). Here, the normal mode of propagation is by ground wave. At night, however, especially in winter, early experimenters noted that distant stations could be heard. It also was noted that the higher frequencies in the MF bands demonstrated this phenomenon more often than did the lower frequencies, and so, early theories of "skywave" or "skip" were formulated.

One early theory was that the "ether" in the Earth's atmosphere was modulated by the transmitted signal's waveform. This modulated wavefront propagated outward from the aerial in a manner similar to the way ripples propagate away from a point when a rock is thrown into a pond. In one early paper Dr. Lee de Forest stated:

> "Radio is simply a cause and effect. The cause is the transmitter. It makes an electro-magnetic splash that sets up radio waves. These waves travel through space in all directions. The effect is the setting up of delicate currents in the aerial or loop. These delicate currents are detected and converted into audible sounds by means of the radio receiving set. Imagine a boy operating a paddle at one end of a pond of still water. Ripples are set up in the water. They travel farther and farther away from the paddle, getting weaker as they move along until they reach a piece of wood which bobs up and down as it rides the waves. Put a bell on the piece of wood, in order that it will ring with the action of the waves. This illustrates the mechanical parallel of radio communication."[1]*

The sought-after electrified region was discovered in 1924 by a British scientist, Edward Appleton. In 1925 he and his co-workers found conclusive evidence of its existence by measuring the angle of arrival of radio signals from a nearby transmitter. The angle of arrival was such that the signals could have arrived from only one direction—by reflection from an area in the Earth's atmosphere about 100 miles high. Kennelly and Heaviside's visionary theory of 22 years earlier had been verified. For this pioneering work in the field of radio-wave propagation Edward Appleton was subsequently Knighted by the British Empire.

In 1925 Briet and Tuve, two American physicists, demonstrated the existence of a reflecting region high above the Earth's surface in an even more striking manner. By transmitting short bursts of radio energy straight up, they were able to detect, using suitable receiving and measurement equipment, the presence of an echo that had been reflected and returned to earth. By determining the time that had elapsed between the transmission of the pulse and the echo, and by know-

---

**References are listed at the end of each chapter.*

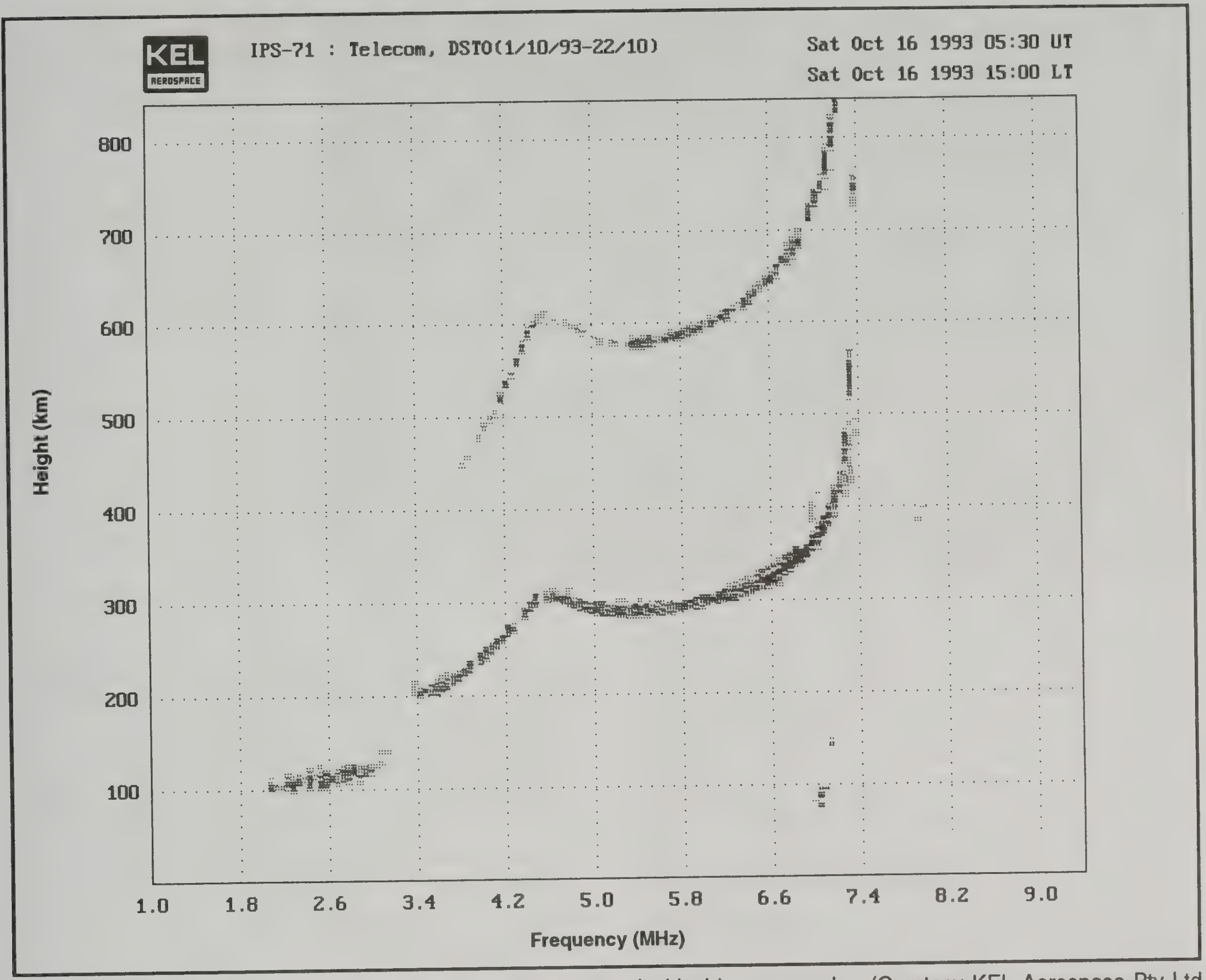

Photo 1.A. Example of an ionogram produced by a modern vertical-incidence sounder. (Courtesy KEL Aerospace Pty Ltd., Victoria, Australia.)

ing that radio waves travel with the speed of light, they were able to deduce the height of the reflecting medium with considerable accuracy. Later, by varying the frequency of the transmitted pulses over a wide range, they discovered that above a certain "critical frequency," the reflecting region would no longer return signals to earth. This was the first documented use of a vertical incidence ionospheric sounder.

Extensive studies using the Briet-Tuve technique, made at a large number of locations throughout the world, soon showed that the critical frequency varied hourly, seasonally, and geographically. This strongly implied that the reflecting layer was under solar influence.

Further evidence linking ionospheric behavior with the characteristics of solar radiation was obtained in 1927 when a sharp decrease in the critical frequency was observed during a total eclipse of the Sun. Figure 1.1 shows graphically how the intensity of ionization (and hence the critical frequency) varied as the eclipse progressed.

It was concluded from this historic experiment that the primary solar agent responsible for forming the ionized layer was ultraviolet radiation, an amazingly accurate deduction, as the chemical constituency of the ionosphere was unknown at that time. As we know today, ultraviolet (UV) and extreme ultraviolet (EUV) are the primary photo-ionizing agents for what became known as the *F* region, which supports most long-range shortwave transmissions. This observation has been verified further during each eclipse of the Sun that has occurred since 1927.

In the late 1920s amateur experimenters started probing what was later to be known as the ionosphere.

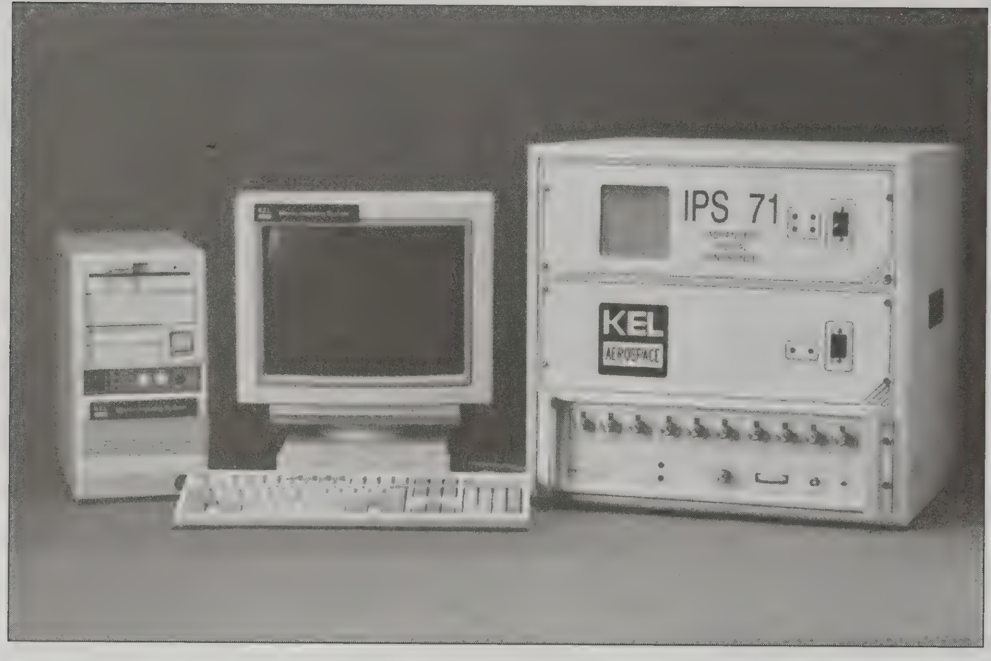

Photo 1.B. The IPS-71 Advanced Digital Ionosonde. (Courtesy KEL Aerospace Pty Ltd., Victoria, Australia.)

They noted that when a very short 200 microsecond pulse was transmitted and the receiver output was recorded on an oscilloscope, they could see the ground-wave signal and a delayed signal that was reflected (more correctly, refracted) overhead. The duration of the delay was roughly equivalent to the height of the reflecting medium. This work further substantiated the existence of the Kennelly-Heaviside Layer that was theorized 20 years earlier. The Kennelly-Heaviside Layer, or ionosphere, as it came to be known in the middle 1930s, is used to designate that electrically conducting region high up in the stratospheric regions of the Earth's atmosphere that is responsible for the propagation of radio waves to great distances by means of multiple refractions, or reflections, between the conducting surface of the earth and this "layer." The ionosphere is not a sharply defined region, but rather, it extends to several hundred miles in altitude. Conductivity begins to be important at various heights above the earth, depending on the wavelength, but the conductivity at heights as low as 50 miles may be of importance in the case of low-frequency (long-wave) propagation. Subsequently, the term *ionosphere* has been introduced to describe this whole region. However, the ionosphere does have subregions in which the conductivity varies more rapidly with altitude than in others. These are given special names according to their refracting properties for waves of different frequencies.[2]

As early as 1930 Marconi theorized that "radio waves may travel long distances, even millions of miles, beyond the Earth's atmospheric layer." He did

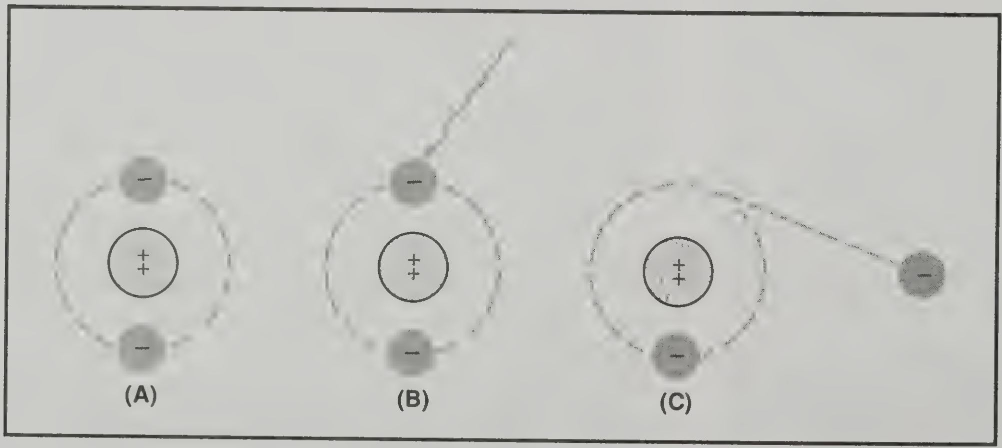

Figure 1.2. Diagram illustrating how ionization is produced by energy from ultraviolet radiation. In (A) the atom is in electrical equilibrium; in (B) the high-energy ultraviolet radiation strikes an electron; in (C) the free electron is "torn out" of the atom by energy from the ultraviolet radiation. The resulting electrically unbalanced atom is called an ion.

not see any reason why waves produced on Earth should not travel such a distance, since light and heat waves reach the Earth from the Sun by penetrating the atmospheric layer.

Ionospheric Measurements

The rapid development of long-distance radio communication stimulated intensive investigation of the ionosphere throughout the 1930s. The need to solve newly developing communication problems required the establishment of more modern engineering techniques that would meet the demands for uninterrupted use of the ionosphere for reliable worldwide communication.

Equipped with pulse-sounding equipment, ionospheric measuring stations began to spring up in all areas of the world. Ionospheric sounding is similar to radar. A pulse is emitted upward and the time it takes to reflect back to the receiver is measured. This time is easily equated to the height of the layer that reflected the signal back. The frequency is incremented upward and the procedure is repeated. This process continues until a frequency is reached where the pulse is not reflected (that is, it continues upward into space, where it may hit a second layer and reflect back). The frequency where the signal penetrated the first layer is called the critical frequency (f_o), and this frequency can be related to the maximum electron density (N_{max}) of that particular layer by the expression:

$$N_{max} = 1.24 \times 10^{10} (f_o)^2 \text{m}^{-3} \qquad (2)$$

where: f_o is in MHz.

This procedure is repeated for each layer until a picture (called an ionogram) of the ionized medium and how it is structured is formed. Photo 1.A shows a typical vertical incidence sounder (VIS) ionogram. Note that *electron density* is the controlling factor in determining the reflective (refractive) properties of the ionosphere.

From a mere handful in the 1930s, to a peak of about 250 stations in the late 1980s, approximately 100 stations today are charting the ionosphere hourly throughout the world. In 1957, the International Geophysical Year, over 250 VIS stations collaborated in mapping the global ionosphere. At one point in the 1970s and 1980s, the former Soviet Union had a large, integrated ionosonde network that could literally map the overhead ionosphere over their entire country as well as neighboring countries. Modern ionosondes consist of both FM-CW swept frequency sounders, called "chirpers," and modern pulse sounders. Each has advantages. Photo 1.B shows a typical VIS station.

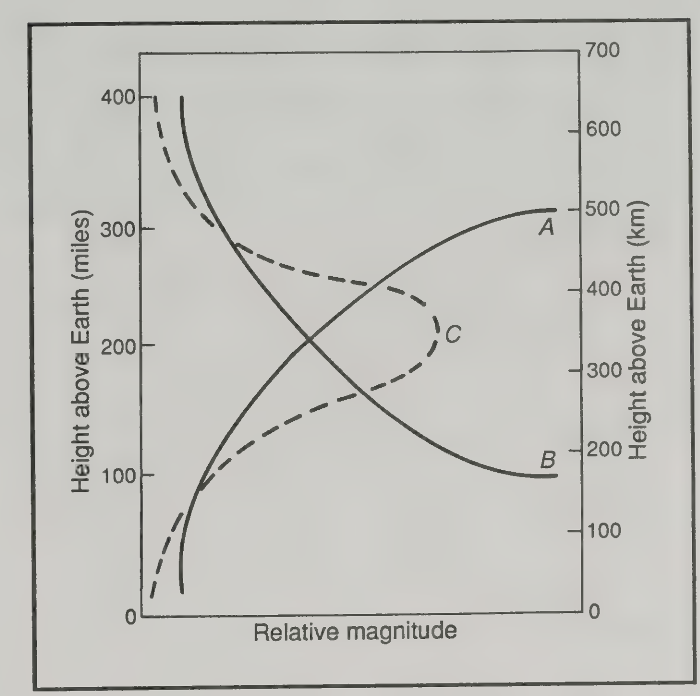

Figure 1.3. The formation of an ionized layer by single-frequency ultraviolet radiation. At (A) the intensity of ultraviolet radiation increases with height; at (B) the molecular density of gas decreases with height; at (C) the intensity of ionization varies with altitude.

Formation of the Ionosphere

In 1927 the upper atmosphere was thought to consist mostly of helium, nitrogen, and argon. Above 140 km it was theorized that the atmosphere was entirely helium.[3] We now know that the Earth's upper atmosphere is composed mainly of oxygen and nitrogen and their compounds, with small amounts of hydrogen, helium, and several other gases. This description has been experimentally derived from rocket, high-altitude balloon, and satellite measurements over the last few decades.

Gases, like all material, are composed of atoms made up of negatively charged electrons that are classically portrayed as traveling in orbit about a positively charged center (or nucleus). Atoms, unless they are under the influence of energy forces, are in electrical equilibrium, with the negatively charged electrons counter-balancing an equal number of protons in the nucleus. A neutral atom exerts no electrical force outside its own structure. An atom remains neutral until subjected to external energy forces that are great enough to detach electrons from its structure, causing it to become unbalanced, or charged.

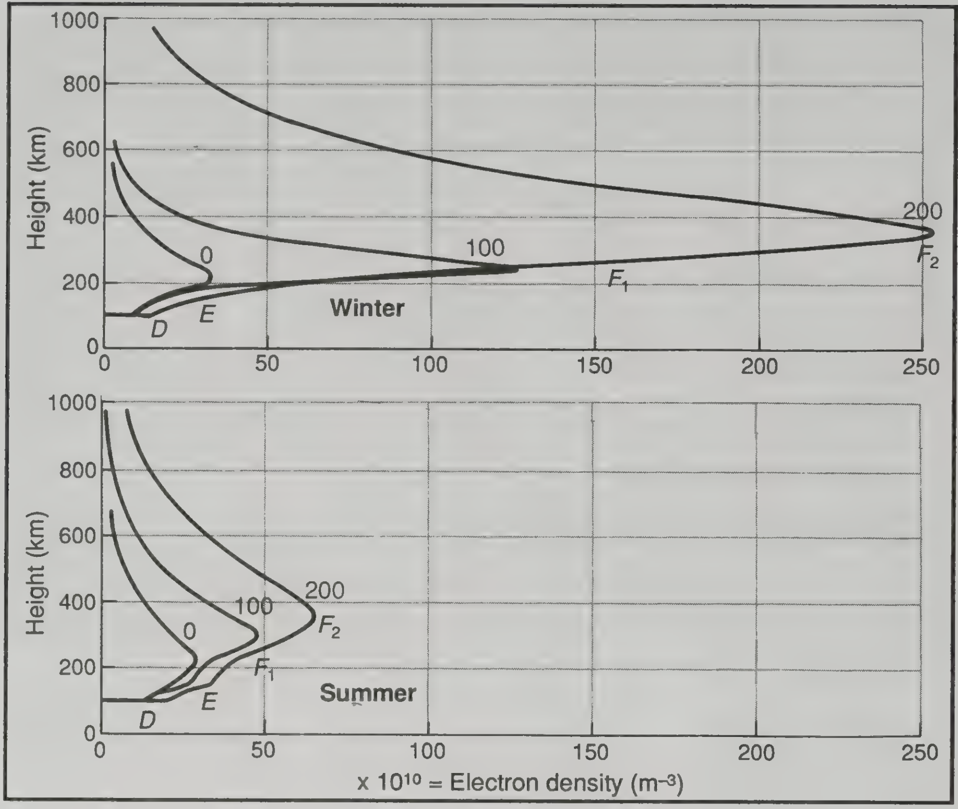

Figure 1.4. Typical daytime (N_{max}) profiles at sunspot numbers 0, 100, and 200. (Modified after Wright, 1962.)

Data gathered from rocket and satellite probes of the ionosphere have confirmed earlier theories based on solar eclipses that ultraviolet radiation from the Sun is the principal agent responsible for the formation of ionization in the upper ionosphere. The great amount of energy associated with this radiation, sweeping through the upper atmosphere, causes electrons to become detached from the gas atoms present there. This leaves the originally neutral gas atoms unbalanced, with an excess of positive charge. Such unbalanced atoms are called ions, and the process by which they are formed is called ionization (see Figure 1.2).

If the ultraviolet energy is removed, the detached electrons recombine with the ions to again form atoms in electrical equilibrium. This process is the opposite of ionization, and it is called *recombination.* Recombination takes place during the nighttime hours, when the ionosphere is shielded from the Sun's direct radiation. The ionization process starts up again when direct sunlight strikes the ionosphere, which means that the daytime ionosphere starts forming immediately at sunrise. Recombination, however, because it is a relatively slower process, causes the ionospheric electron density to decay at a slower rate after sunset as compared to the rapid rate of increase in electron density observed at sunrise.

It is of interest to note that although ultraviolet radiation from the Sun is considered the principal ionizing agent for the upper ionosphere, modern aeronomy (the science dealing with the chemistry of the ionosphere) shows that solar x-rays, certain spectral lines (such as Lyman alpha), and cosmic rays also play a major role in the formation of the lower ionosphere.

The Structure of the Ionosphere

As ultraviolet radiation sweeps into the Earth's atmosphere from above, it first produces ionization of the rarefied gases it encounters. As the radiation penetrates deeper into the atmosphere, it encounters greater densities of gases, and the amount of ionization increases. Penetrating further, it produces more and more ionization, but the radiation also is attenuated because it is giving up energy in the ionization process. Finally, the radiation penetrates to a level where its energy is completely dissipated and the ionization process stops. Thus, there is formed a region of maximum ionization, with intensity falling off above and below it. The details of the formation of an ionized region in the Earth's atmosphere are shown in Figure 1.3.

Solar radiation, which includes UV and EUV, comprises the entire electromagnetic spectrum from visible light to heavy particles. Because the gases comprising the upper atmosphere respond to different frequencies in the ultraviolet spectrum, there is a tendency for ionization to occur at several different levels. These layers are between approximately 30 and 400 miles above the surface of the Earth.

While these ionized regions are usually referred to as "layers," they are not completely separated one from the other. Each region, or layer, overlaps to some extent, forming a continuous but nonuniformly ionized area with at least four levels of peak intensity that, as we will see, are designated the *D, E, F_1*, and *F_2* regions. Figure 1.4 shows typical electron density profiles and the relationship among the regions.[4] Note the drastic difference between the summer and winter profiles, denoting the change in electron density with proximity to the Sun or its position in the sky. This "position" is called the *solar zenith angle.* Everything else being equal, the higher the Sun gets, the higher the electron density. But while the northern hemisphere winter Sun is low in the sky, peak electron densities are higher than in the summer, when the Sun is more overhead. This is because the ionosphere is colder (more dense) and the Earth is physically closer to the Sun during the northern hemisphere's winter. Also shown is the difference in the peak electron densities between solar maximum and solar minimum.

In the early days of radio, scientists operated with a lot of deduction and conjecture and without a lot of experimental evidence to back them up. Surprisingly, they were close to the truth at times. In 1920 Chapman and Milne, using certain assumptions, calculated the distribution of ionization that would result from the absorption of various types of radiation in the Earth's atmosphere.[5] Their calculations showed that the ionization should start with a small value near the Earth and increase with height, reaching a maximum value somewhere in the upper atmosphere. Ionization should then decrease again to a small value at very great heights. This distribution is shown in Figure 1.5, first presented in a 1927 *QST* article.[3]

The allocation of the letters to designate the various regions of the ionosphere was the work of Sir Edward Appleton upon his discovery of the Kennelly-Heaviside layer in 1924. He allocated the letter *"E"* to this layer, using the symbol generally employed to designate an electric vector. In 1925, when he discovered another ionized region at a greater altitude, he used the term *"F"* to designate the electric vector reflected from it. This, as he has said, left several letters at the disposal of future workers for allocation to other layers they might discover, either above or below the layers identified by him. Sir Robert Watson-Watt, an early coworker of Appleton and one of the original developers of radar, gave the name *ionosphere* to the entire region, and it was adopted internationally.

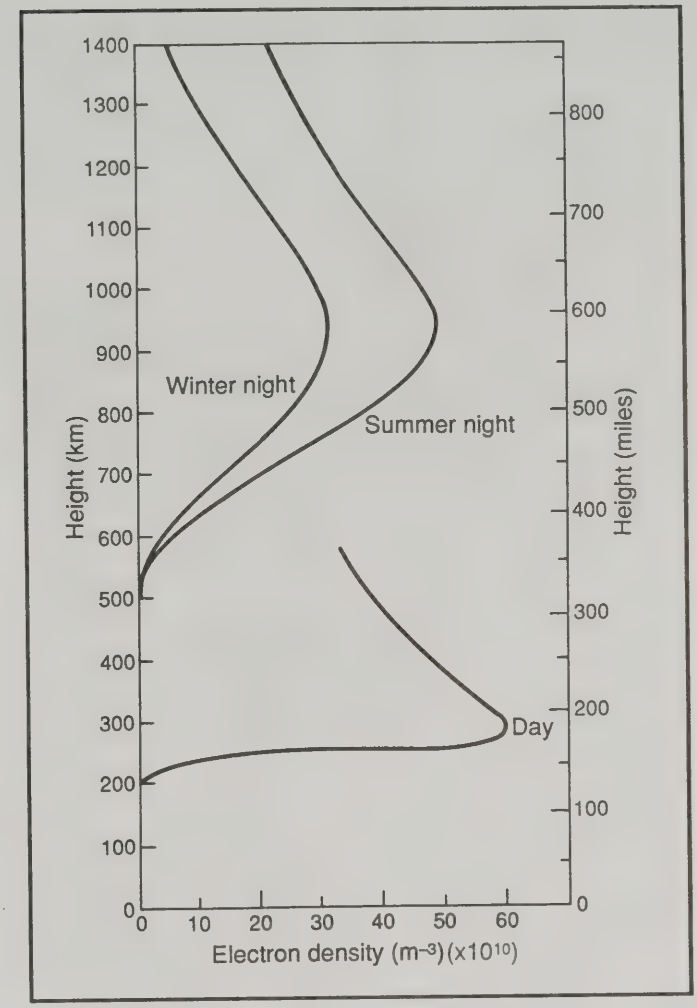

Figure 1.5. An early attempt to chart the distribution of ionization in the upper atmosphere from radio transmission experiments. (Modified after Rice, 1927.)

The height and characteristics of these layers change from day to night, and season to season. Several of these changes are illustrated in Figure 1.6. A brief description of each layer follows.

The *D* Layer

Even in the heyday of ionospheric experimentation in the late 1960s and into the 1970s, the *D* layer remained somewhat of an enigma. This layer, which extends from 40 to 60 miles (65 to 100 kilometers) above the Earth's surface, was originally thought to exist only during the day while it was illuminated by the Sun. However, its exact chemistry was difficult to

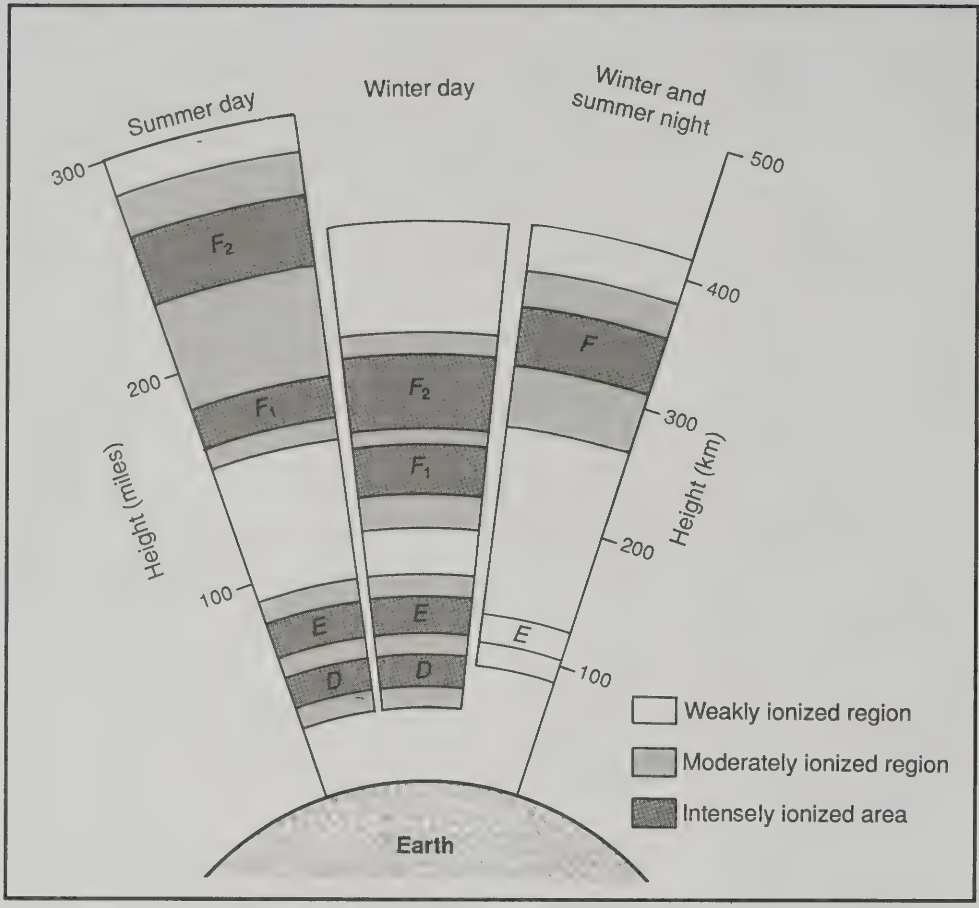

Figure 1.6. Daily and seasonal variations in the ionospheric regions (typical characteristics shown). Note that there is some residual ionization in the *E* layer during the nighttime hours.

determine, even using modern experimental probes. At these altitudes the pressure is large, producing a high electron collision frequency; as such, conventional study techniques cannot be used. Vertical sounding is not possible, because the collision frequency exceeds the critical frequency, and a signal return is never seen. Normal rocket experiments do not work well at these altitudes for several reasons. And satellites cannot function this low in altitude because of drag. Of all the ionospheric layers, the chemistry of the *D* layer is the least well defined.

The *D* layer is thought to be ionized by three sources, depending on altitude. Between 55 and 60 miles (90 and 100 kilometers) the primary source is solar 1-8 Ångström x-rays. At heights between 50 and 55 miles (80 and 90 kilometers) the Lyman-alpha line (1215.7 Ångströms) is the controlling source. Between 40 and 50 miles (65 and 80 kilometers) galactic cosmic rays have been shown to be a primary ionizing source. Enhancements in any of these sources cause an immediate increase in ionization of the *D* layer.

With respect to shortwave communications, the *D* layer is a gigantic attenuator, absorbing HF signals as they pass through it. Because attenuation varies as the inverse square of frequency, the higher the HF frequency used, the less the *D* layer absorbs the signal. After sunset the layer quickly recombines, and lower frequencies "go skywave." That is why at night at certain times of the year you will hear AM broadcast signals over very long skywave distances by means of skywave (ionospheric) propagation.

The *E* Layer

The upper boundary of the *D* layer blends into another distinct region called the *E* layer, which occurs mainly during the daylight hours at heights between 60 and 75 miles (100 to 125 kilometers). It is a thin layer, roughly 5–10 kilometers in thickness, and it remains at a predictable height throughout the day. There are many types of ionization mechanisms that appear to operate at this altitude depending on latitude, season, and level of solar activity. For now this discussion will center on the simple mid-latitude *E* layer.

Traditionally, this layer has been typified as a simple Chapman-type layer* that ionizes and recombines with the rise and fall of solar radiation. Theoretically, the *E* layer disappears at night. During the day, photoionization is produced by soft x-rays in the 10–100 Ångström region of the spectrum and EUV in the 1000–1500 Ångström range.[6]

Experiments in the early 1980s, during the peak of solar Cycle 21, demonstrated that contrary to popular belief, the *E* layer did not go away at night, but in fact was a steady, but inefficient, source of nighttime propagation. The decade of the 1980s was one in which experimental science raised more questions about ionospheric structure and mechanics than were answered. It also was during a five-year experiment, which measured ionospheric variations between the peak and minimum of Cycle 21, that the correlation time of an ionospheric phenomenon was found to be two minutes. Put another way, it was observed that the value of any given ionospheric measurement will change after two minutes have elapsed. This was an early indicator of turbulence in the ionosphere.[7]

Sporadic-*E*

In addition to the regular *D, E,* and *F* regions of the ionosphere, there exist ionized regions that occur sporadically. Unlike the regular layers, these sporadic regions come and go irregularly, and there are several theories as to their cause. The height of these regions, or patches, is variable, but they occur most commonly at an altitude of about 60 miles (100 kilometers). Since this is about the same height as that of the regular *E* layer, the phenomenon is collectively called sporadic-*E*.

Sporadic-*E* has very definite geographical characteristics. Mid-latitude sporadic-*E*, that which is most observed by the amateur radio community, occurs mainly in May, June, July, and August during daylight hours (peaking in late morning and at sunset) and in December (peaking at night). It appears as a very intensely ionized (f_oE_s>5 MHz)† thin region, several kilometers thick and of very limited geographical extent. A sporadic-*E* cloud might be 50 to 100 miles (80 to 170 kilometers) in diameter, and it may last only for a few hours before dissipating.

Many sporadic-*E* clouds appear to drift with velocities as great as a few hundred miles per hour. In the northern hemisphere the drift is usually in a westerly direction.

What produces sporadic-*E* ionization is not yet fully understood. It is known that meteors disintegrate at *E*-layer altitudes and that shearing forces on the metallic ion residue create patches of high ionization. This may be but one factor involved in sporadic-*E* formation.

In the equatorial regions sporadic-*E* is a daytime phenomenon, thought to be caused by plasma instability in the equatorial electrojet. The high electron drift velocities found here creates dense patches. Around the geomagnetic equator sporadic-*E* exists during 90% of the daylight hours.[6]

In the auroral and polar cap regions there are several forms of sporadic-*E*, each of which has a different signal support capability. During daylight summer hours the same type of sporadic-*E* that is seen at mid-latitudes is observed in the auroral region. During the nighttime hours a form of sporadic-E called auroral-*E* can be observed centered around local midnight. Auroral-*E* is associated with disturbed magnetic activity when the *K*-index rises above 3 (see Chapter 5). Also, there are two forms of auroral-*E*, one associated with the eastward auroral electrojet (occurring prior to local midnight) and one associated with the westward electrojet (occurring after local midnight). Auroral-*E* is best described as random ionized "blobs" driven by the high-latitude electric current system that forms the electrojets. Average auroral-*E* events tend to last about 10 minutes, although some have been observed to last up to two hours and to produce signals of 20 to 30 dB above the receiver detection threshold.[8]

The *F* Layers

The *F* layers are the most important regions of the ionosphere insofar as long-distance shortwave radio communications are concerned. During the daylight hours there are two well-defined regions, the F_1 layer and the F_2 layer. The winter day F_1 layer begins slightly above the upper boundary of the *E* layer at about 90 miles (150 kilometers), and it extends up to about 150 miles (250 kilometers). During the summer day the F_1 layer is found at somewhat higher altitudes (see Figure 1.6). The F_2 layer, the height of which varies seasonally, ranges up to about 200 miles (350 kilometers) during the winter and close to 300 miles (500 kilometers) during the summer. Most shortwave

---

**A so-called "Chapman layer" is characterized by its having only one type of gas, plane stratification, single wavelength ionizing radiation, and a constant-temperature atmosphere (also see reference 12 at the end of this chapter).*

†f_oE_s is the scientific notation used to denote the critical frequency of the E_s phenomenon. Similarly, f_oF_2 is used to denote the critical frequency for the F_2 layer.

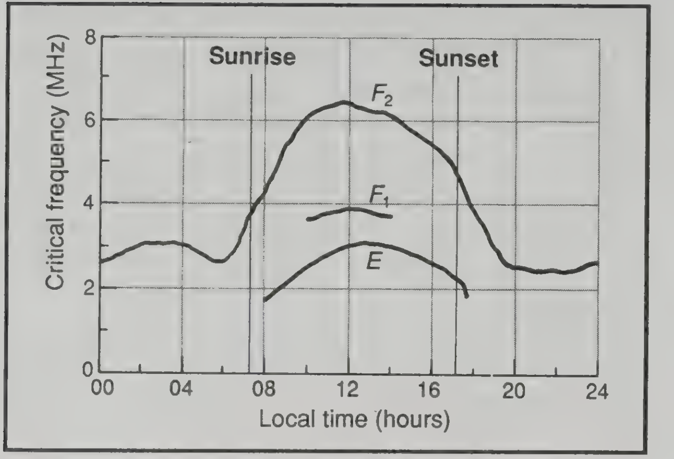

Figure 1.7. Typical hour-to-hour changes in the reflection capability of the ionospheric layers.

communications are accomplished using the F_2 layer. This layer is formed from UV solar radiation in the 170 to 911 Ångström region of the spectrum.

The F_1 layer, at least at solar minimum, also approximates a Chapman Layer. This means that it rises and falls with the rise and setting of the Sun. By this process the F_1 layer should disappear at night; experimental evidence shows that it does. During the day the F_1 layer supports shortwave circuits of short to medium length. The F_1 layer behaves much like the *E* layer. Maximum ionization occurs near noon at midpath.

Unlike all of the other layers, the F_2 layer exists throughout the day and night, and it almost always is capable of sustaining skywave propagation at some HF frequency. This is the most ionized layer of all, and it is the most important to shortwave signal propagation. It is the behavior of this region that most elementary HF prediction programs, such as MINIMUF, attempt to model. (See Chapter 6 for more information on computerized prediction programs.)

During the nighttime hours the F_2 layer height varies from approximately 150 to 250 miles (250 to 420 kilometers). Because the recombination rate of this region is relatively slow, the layer exists around the clock. Were it not for this fact, long-distance shortwave radio communication would be virtually impossible during the hours of darkness.

The intensity of ionization in the F_2 region is in an almost continuous state of flux, with hourly, seasonal, geographical, and solar cyclical changes interacting in a somewhat complicated manner. Experiments between 1980 and 1985 indicated, for example, that instead of being characterized by a nice stable plasma*, the *F* layer is in a constant state of motion.[7]

Above The *F* Region

Roughly 95% of the molecular elements that form the ionosphere are contained below 1000 kilometers altitude. Topside sounder measurements from orbiting satellites indicate that the electron density in the region between 600 and 1000 kilometers altitude is of such a low value that it has very little relevance to amateur radio or shortwave broadcasting.

1.2 Regular Ionospheric Variations

Because the existence of the ionosphere depends on solar radiation, it is evident that changes in the position of the Earth with respect to the Sun (rotation and revolution), as well as changes in the patterns of solar radiation, will influence the variations that take place in the ionosphere.

The regular variations of the Sun, that is, those which are relatively predictable and can be anticipated, fall into the following categories:

1. Diurnal (Day-Night)
2. Seasonal
3. Geographical
4. Cyclical

Day-Night Variation

The diurnal variation, or the hour-to-hour changes in the various layers of the ionosphere, is caused by the rotation of the Earth about its axis. This rotation not only is responsible for variations in the amount of sunlight reaching the Earth, resulting in day and night, but also for a corresponding variation in the intensity of ultraviolet radiation reaching the ionosphere at any point. During the daylight hours, when ultraviolet radiation strikes the Earth's upper atmosphere, the ionosphere can become highly ionized with several stratified layers; during the hours of darkness very little radiation reaches the upper atmosphere on the side of the Earth away from the Sun, the ionosphere loses its electron density, and it becomes a single, relatively weak layer.

As already indicated, diurnal variations in the *D*, *E*, and F_1 layers exhibit a regular pattern that principally is dependent on the Sun's elevation (i.e., the solar zenith angle). Ionization in these layers increases from a very low level at sunrise, reaches a maximum at noon, and then decreases towards sunset. At night,

---

**A plasma is a highly ionized gas cloud.*

for all practical purposes, these layers exhibit such a low electron density that they have no usefulness at shortwave frequencies.

Typical hour-to-hour changes in the critical frequency for the various layers are shown in Figure 1.7. From this figure it can be seen that only the F_2 layer's existence is not dependent on the Sun's position.

Ionization in the F_2 region, as shown by the increase in critical frequency, rises steeply at sunrise. Maximum ionization is reached about the time that the Sun has reached its zenith, or its highest point in the sky (local noon). Ionization then decreases, reaching low values during the nighttime hours. The lowest electron density is found just before sunrise, and the dip observed in the critical frequency is called the "pre-sunrise" depression.

The F_2 layer is the most highly ionized of the regular layers, with the ability to support the propagation of higher shortwave frequencies. In addition, because of slow recombination rates, it remains in existence several hours after sunset (something called "F_2 hang"). For these reasons, the F_2 layer is of greater importance to long-distance shortwave radio communications than are all of the other layers of the ionosphere. Almost all DX openings take place by reflection from the F_2 layer.

Seasonal Variation

Because the position of any point on the Earth relative to the Sun is constantly changing as the Earth moves in its year-long orbit around the Sun, so, too, do ionospheric properties change.

Ionization in the *E* layer behaves regularly, being dependent almost entirely on the solar zenith angle. Ionization is much stronger in the summer because the Sun is higher in the sky.

During all but the winter months, the F_1-layer critical frequency varies in much the same manner as does the *E* layer's, being dependent on the Sun's elevation. During the winter, however, the F_1 layer usually merges with the F_2 layer, and it cannot be separately identified, except in the equatorial regions.

The seasonal behavior of the F_2 layer is rather complicated. During the northern hemisphere winter months the atmosphere is cold, the Earth is closer to the Sun, and daytime ionization is very intense; thus, critical frequencies are high. During the long hours of winter darkness, on the other hand, the ionosphere has more time to lose its electrical charge, and nighttime critical frequencies fall to very low levels.

In the summer a heating effect takes place in the F_2 layer, causing it to expand during the daylight hours and resulting in a lower ionization density than is observed during the winter. As a result, summer daytime F_2-layer critical frequencies are lower than winter values. On the other hand, because of the longer hours of daylight during the summer, recombination does not occur to the extent that it does in winter. As a result, nighttime F_2-layer critical frequencies during the summer months are significantly higher than they are during the winter months. The variation between day and night critical frequencies during the summer is much smaller than during the winter.

The complex seasonal behavior of the F_2-layer's critical frequency is shown in Figure 1.8.

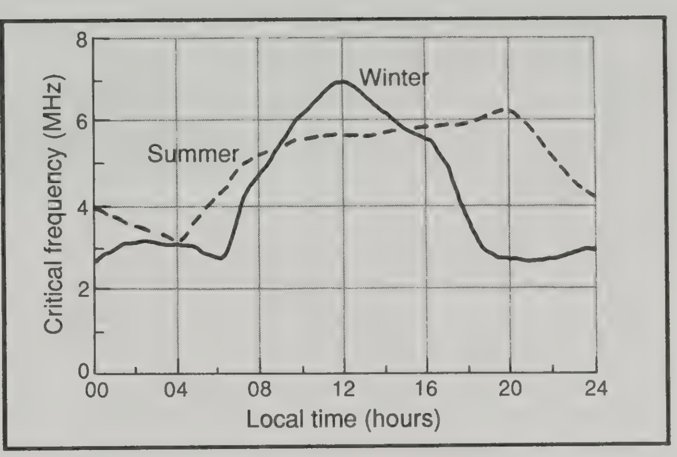

Figure 1.8. Typical seasonal variation in the F_2 layer of the ionosphere.

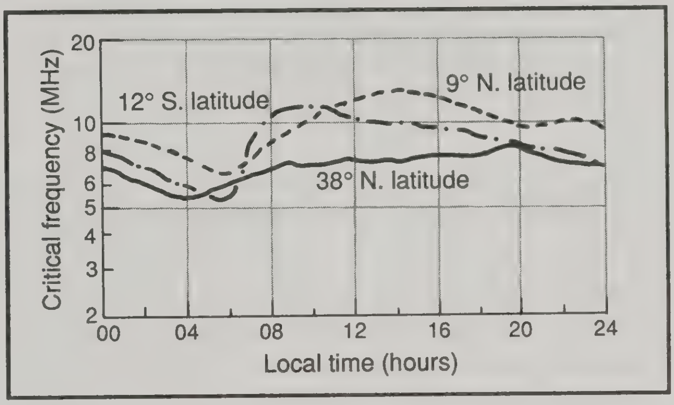

Figure 1.9. Latitude variation in F_2-layer critical frequencies. Comparison of measurements made at three locations of different latitude but along the same meridian of longitude (in this case, 77 degrees west longitude). Measurements were made at the same local standard time during June.

Geographical Variation

The intensity of ionizing radiation that strikes the ionosphere varies with latitude, being considerably

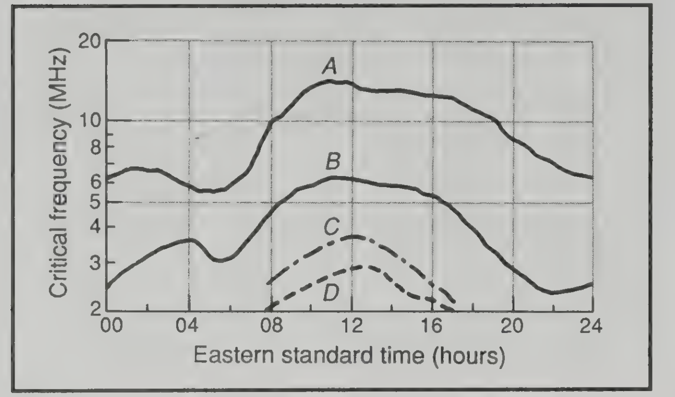

Figure 1.10. Comparison of diurnal variation in *E*-layer (dashed curves) and F_2-layer (solid curves) critical frequencies during maximum and minimum sunspot activity. The data shown in the curves marked A and C were measured near Washington, D.C., during December 1957 when a sunspot number of 200 was recorded. The data shown in curves B and D were recorded during December 1964 when the sunspot number was 11.

greater in the equatorial regions, where the Sun is more directly overhead, than in the higher latitudes.

Critical frequencies for the *E* and F_1 regions vary directly with the Sun's elevation, being highest in equatorial regions and decreasing proportionately north and south of these latitudes.

F_2-layer variations with latitude are more complex. This also is probably due to ionization from other sources. There is considerable evidence that the Earth's magnetic field exerts a significant influence on the degree of ionization in the F_2 layer.

Although complex, the F_2-layer critical frequency does follow a general pattern of being higher in equatorial regions and lower in the higher latitude and polar regions. In Figure 1.9 the latitudinal variation in the F_2 layer is shown by comparing critical frequency measurements made at three locations of different latitude.

Although not as complex as the latitude variation, F_2-layer ionization also differs along meridians of longitude (at the same local time and along the same parallel of latitude). Much of this variation is believed to be due to the influence of the Earth's magnetic field. F_2-layer critical frequencies are generally higher in the Asiatic region and Australasia than they are in Europe, Africa, or the Western Hemisphere.

Cyclical Variation

If diurnal and seasonal variations were the only influences affecting ionospheric behavior, the long-range pattern of critical frequencies would be easy and straightforward to establish, with seasonal values expected to repeat from year to year at the same geographical location. Unfortunately, this is not the case. There also is a cyclical variation, of an approximately 11-year duration, that is the most influential factor affecting the ionosphere. This variation depends on the level of sunspot activity, which is constantly changing throughout an approximately 11-year cycle. This solar cycle influence will be touched upon only lightly at this point, because sunspots, what they are, and how they influence the ionosphere and shortwave propagation, will be discussed at greater length in Chapter 2.

Figure 1.10 shows the variation in the F_2- and *E*-layer critical frequencies during the periods of maximum and minimum sunspot activity. It can be seen that the sunspot cycle exerts considerable influence on the level of ionization in the Earth's upper atmosphere.

The greatest change throughout the entire solar cycle takes place in the F_2 layer, with noontime critical frequencies approximately twice as high during the maximum of the cycle than at the minimum. The variation during the nighttime hours is about the same, with the midnight critical frequency being about two times greater during the peak of the cycle than at sunspot minimum.

The critical frequencies of both the *E* and F_1 layers also show a close, linear correlation to the sunspot numbers, although the *E*-layer variations between the extremes of the cycle are not as pronounced as they are in the F_2 layer.

Up to this point we have discussed the electrical characteristics of the ionosphere in terms of the *critical frequency.* This is the highest frequency from which an echo is received when a pulse of radio energy is sent vertically into the ionosphere. Next we will show that frequencies used for communication between any two points (oblique propagation, as compared to vertical pulse transmission) bear a direct relationship to the critical frequency.

1.3 Optimizing High-Frequency Communications

A fairly wide range of shortwave frequencies when transmitted vertically will be returned to earth by the ionosphere. The highest frequency so returned by each of the layers of the ionosphere is called the "critical frequency" for that layer.

In the previous section we discussed the importance of the critical frequency in determining the physical characteristics of the ionosphere. Although the critical frequency is invaluable for this purpose, it is not use-

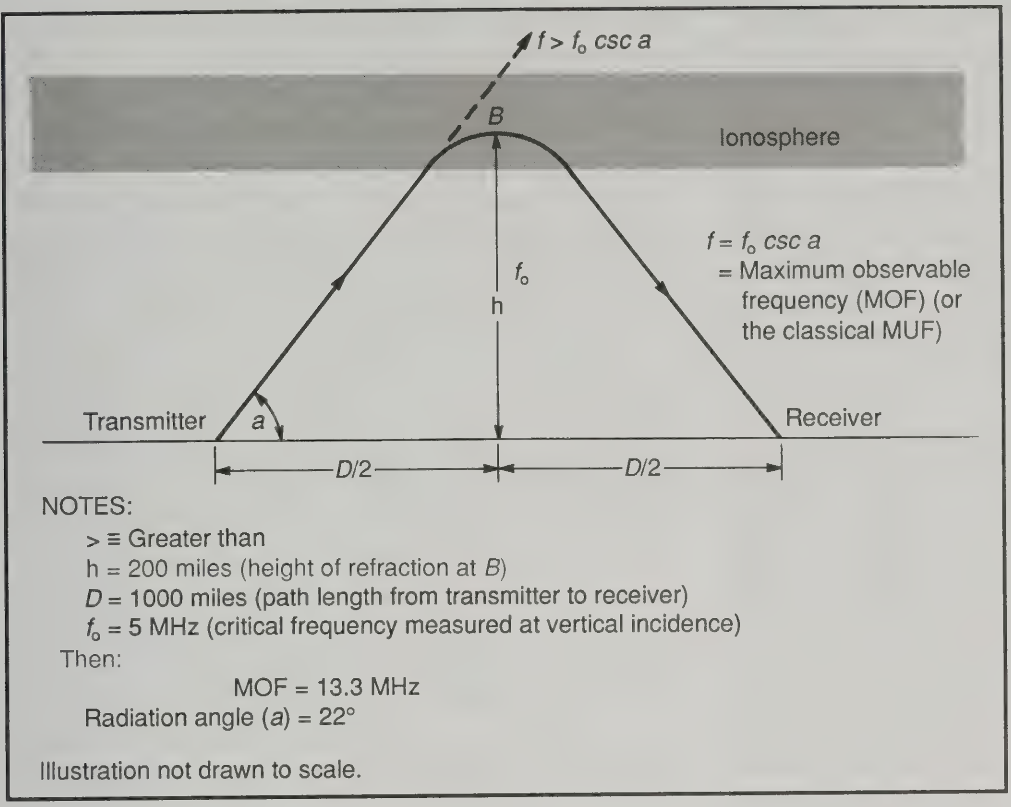

NOTES:
$>$ ≡ Greater than
h = 200 miles (height of refraction at *B*)
D = 1000 miles (path length from transmitter to receiver)
f_o = 5 MHz (critical frequency measured at vertical incidence)
Then:
MOF = 13.3 MHz
Radiation angle (*a*) = 22°

Illustration not drawn to scale.

Figure 1.11. Illustrative example of MOF calculations.

ful for long-distance communication because vertically incident energy is returned to earth near the transmitter. To enable a signal to cover the great distances required in radio communication, the radio wave must leave the transmitting antenna at an angle such that the wave will enter the ionosphere obliquely, or at a slant.

The proper slant, or radiation angle, as well as the optimum frequency to use over a particular path, depends on many factors, including the height of the reflecting layer, the extent to which it is electrified, and the distance between the transmitting and receiving locations. There also is a direct relationship between the critical frequency at the point the wave enters the ionosphere and the optimum frequency for the path.

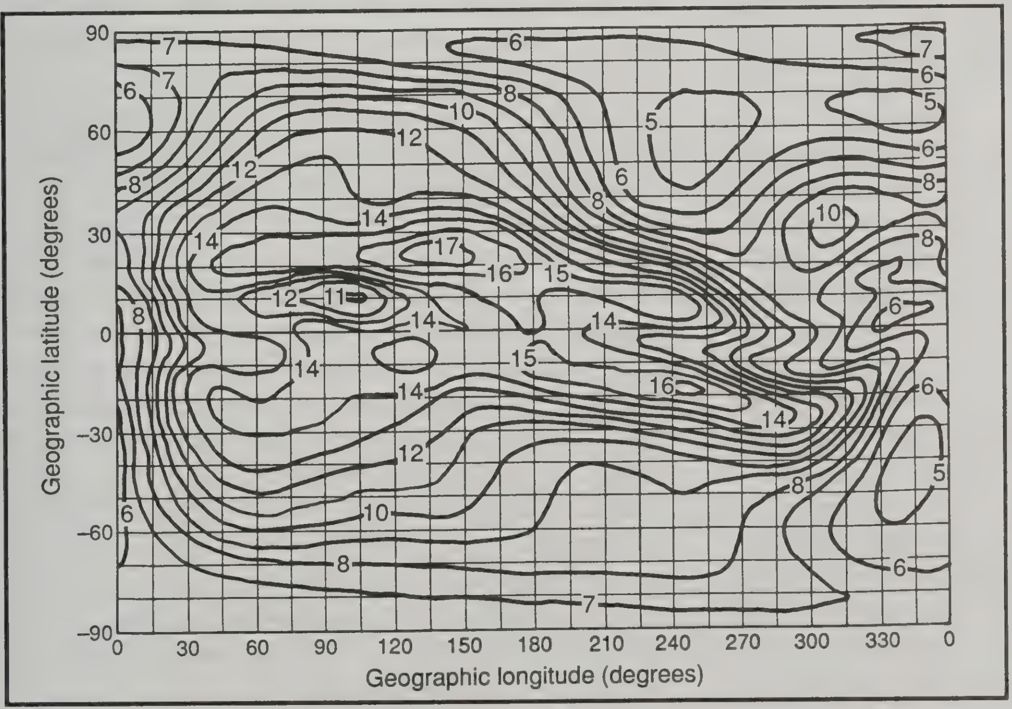

Figure 1.12. Contour map (in megahertz) of the global representation of the median value of f_oF_2 for March 1979 at 0600 UTC. (Modified after Davies, 1990.)

A knowledge of the relationships that exist among the critical frequency, layer height, radiation angle, path length, etc., are fundamental to understanding the principles of long-distance shortwave communication via the ionosphere.

This section explains, in a simplified manner, how some of these factors are related to each other, and how these relationships may be used to determine which specific frequency bands will be most useful over any given circuit, at any time of the day or night.

Trigonometric Relationships

To begin with, there is a simple trigonometric relationship that exists among the critical frequencies measured at vertical incidence, the height of the ionosphere at which reflection takes place, and the optimum radiation angle and frequency required for long-distance transmission. This relationship is expressed by the equation:

$$f = f_o/\sin a = f_o \csc a \qquad (3)$$

where: f is the equivalent signal frequency for oblique transmission;
f_o is the critical frequency; and
a is the radiation angle for oblique transmission.

The mathematics expressed in equation 3 are shown pictorially in Figure 1.11.

Using geometrical relationships shown in Figure 1.11, equation 3 can be modified as follows to permit an even more direct solution for the optimum frequency required for long-distance transmission:

$$f = f_o\sqrt{\frac{D^2}{4h^2} + 1} \qquad (4)$$

where: f is the signal frequency that will give optimum long-distance transmission over a path length of D;
f_o is the critical frequency; and
h is the height at which ionospheric reflection takes place (D and h must be given in the same units, either miles or kilometers).

The significance of equations 3 and 4 is that given the critical frequency and the height of the ionosphere, and knowing the distance between the transmitting and receiving locations, it is possible to determine the highest frequency that the ionosphere will support over this path. This frequency, f in equations 3 and 4, is called the Maximum Observable Frequency (MOF) or the Classical Maximum Usable Frequency (MUF). This is the upper frequency limit at any given time and over any given path. This is not to be confused with the MUF values produced from prediction programs, which are median values of the Classical MUF computed from data taken over long periods of time. (We will discuss these topics later in this chapter.)

For a radio wave to be reflected between two distant points via the ionosphere, its frequency must be equal to, or less than, the Classical MUF. As the operating frequency is raised toward the Classical MUF, the signal will be received with increasing strength. When the frequency exceeds the Classical MUF, ionization at the point where the signal reflects off the ionosphere will not be strong enough to bend the wave back to earth at the receiving location, and it will continue on through into outer space. To ensure satisfactory communications between two distant points, the operating frequency must be as near to the Classical MUF as is possible, but it should never exceed it.

Maximum Usable Frequency (MUF) Calculation

Because the Classical MUF is related directly to the critical frequency, its value is a function of the intensity of ionization in the Earth's upper atmosphere. For a given transmission path, the Classical MUF follows the same diurnal, seasonal, geographical, and cyclical variations as does the critical frequency. During periods of high solar activity Classical MUF values are approximately twice as high as they are during periods of low sunspot activity.

It should be noted at this point that the amount of power radiated does not enter into the determination of the Classical MUF. The ionosphere either has sufficient electron density to refract (or bend) the signal back to earth or the signal escapes into space. It depends entirely on the frequency and the electron density. This situation applies to normal shortwave signal propagation and does not apply to the case of "scatter" reflections from the ionosphere that may occur under certain abnormal conditions, or when powers on the order of hundreds of kilowatts are radiated. Under the last two conditions, radiated power will enter into the determination of the Classical MUF, but these are conditions that are not generally encountered in amateur radio communications.

The Classical MUF is a very important quantity in radio communications, but it is extremely difficult to predict. However, relatively straightforward graphical methods have been devised for predicting its *median* value for transmission paths for any distance, without the necessity for resorting to mathematics. Such a median value is what we refer to simply as the Maximum Usable Frequency (MUF).

Contour charts containing worldwide values of predicted critical frequencies for the F_2 layer (denoted as f_oF_2), predicted (median) MUF values calculated for a standard distance of 4000 kilometers (2400 miles), and appropriate graphs for determining from these values the MUF for any distance appear in the document *Ionospheric Predictions* published by the Institute of Telecommunication Sciences of the U.S. Department of Commerce.[9] Figure 1.12 shows an example of a global plot of f_oF_2 for 0600 UTC (Time of Day), Summer (Season), and at Solar Maximum (Solar Cycle).

Similar data also appear in the *Atlas of Ionospheric Characteristics* published by the International Telecommunication Union (ITU).[10]

This graphical method, called the "manual method," is quite tedious and not very flexible. Although it was used for four decades, it has given way to computerized methods that are discussed in Chapter 6. It should be noted, however, that these data on global critical frequencies as a function of time of day, season, and sunspot number were the basis for the tables of ionospheric coefficients used in the first computerized HF prediction programs.

Ionospheric Absorption

Up to now we have discussed the characteristics of the ionosphere as a reflector of radio waves. Ionization, however, not only causes a radiowave to bend, it causes energy to be absorbed as well. Ionospheric absorption is one of the main reasons the signal strength of a radio wave is reduced as it passes through parts of the ionosphere, primarily the *D* region.

As a radio wave passes through the *D* layer, it imparts energy to the electrons that exist in this electrified region. The electrons are set into motion by the transfer of energy, and thus convey the radio wave through the ionized region. While moving through the ionosphere, electrons vibrating in rhythm with the radio wave collide with much larger gas molecules and with ions that also are present in this region. As a result of such collisions, the electrons lose some of the energy imparted to them by the radio wave. In effect, this lost energy is not propagated, and the amount of energy in the radio wave when it emerges from the ionosphere is less than when it entered, resulting in decreased signal strength. Simply put, the *D* layer acts as an "RF sponge" at shortwave frequencies. Technically, there also are some minor losses in the *F* layer; however, they are negligible compared to the twin passage for each hop through the *D* layer.

Exactly how much energy is lost as the radio wave propagates through the *D* layer depends on the number of collisions per second between electrons and molecules of gas. This quantity, in turn, depends on the radio wave's frequency as well as on the number of electrons and molecules present. As the wave frequency increases, the wavelength decreases, and the number of collisions between electron and gas molecules also decreases. The higher the frequency, the less the absorption.

The amount of ionospheric absorption incurred varies inversely with the square of the signal frequency. If the signal frequency is doubled, the ionospheric absorption will decrease by a factor of four. For example, the absorption on the 27–30 MHz (10 meter amateur band; 11 meter Citizen's Band) is one fourth the intensity of the absorption found on 14 MHz (20 meter band). When both bands are open at the same time, it will require considerably more power on 20 meters to equal the strength of the 10 meter transmission over the same path. This accounts for the strong signals often observed on the 10 meter band, even when relatively low power is used.

Because the Classical MUF is the highest frequency that can be used at any given time on a given circuit, and because ionospheric absorption decreases rapidly with the increase in frequency, this type of absorption is minimum near the Classical MUF.

Ionospheric absorption on HF signals depends upon the intensity of ionization in the *D* layer. This level of absorption varies throughout the day, with the season of the year, and geographically, being proportional to the solar zenith angle. The higher the Sun is in the sky, the more absorption there is. Absorption is much more intense in equatorial regions, where the Sun is more directly overhead, than in the temperate latitudes, and it generally is greater during the summer than in the winter.

The best example of absorption can be found in the AM broadcast band. Typically, these medium-frequency signals propagate by surface waves (also known as ground waves). But during the winter, at night, these signals propagate via the ionosphere because the absorption as dropped drastically. This is the reason why AM signals are heard hundreds of miles away from their source during the winter nighttime hours.

As you might expect, the absorption of HF radio waves as they pass through the ionosphere varies throughout the solar cycle. During the years of low sunspot count, when ionization is at a minimum, ionospheric absorption also is at a minimum.

Signal-strength measurements made during previous sunspot cycles show that during the daylight hours, ionospheric absorption on a frequency of 20 MHz is approximately 25% less during periods of low solar activity than it is at the peak of a cycle. The difference at 10 MHz is close to 50%, and at 5 MHz it is 75%.

During the hours of darkness, when ionospheric absorption normally drops to very low values, there is a reduction of between 25 and 50% as the solar cycle declines from maximum to minimum activity, with the greatest reduction taking place in the lower frequency bands.

Lower absorption means stronger signals. Consequently, the signal strengths of radio waves reflected by the ionosphere during years of low solar activity are often noticeably stronger than during years of higher solar activity, particularly on the 40, 80, and 160 meter amateur bands and on the corresponding broadcast bands.

Lowest Usable Frequency

The Lowest Usable Frequency, or LUF, is the lowest frequency that can be used for satisfactory communications over a particular path at a particular time. The LUF is defined as the frequency at which the received signal strength is equal to the minimum signal strength required for satisfactory reception.

The strength of the received signal depends upon the power of the transmitter, the gain and directivity of the transmitting and receiving antennas, the path length, and absorption losses.

In effect, the LUF is a signal-to-noise boundary. Further, the minimum level of signal intensity required for satisfactory reception depends upon the noise level at the receiving location and the type of modulation used. Atmospheric noise, or static, is generally the predominant type of noise that the signal must overcome. For satisfactory reception a manual Morse (or CW) signal requires a signal-to-noise ratio of about 3:1; a speech-quality single-sideband (SSB) signal with 3 kHz bandwidth requires a signal-to-noise ratio of about 7:1; and a speech-quality double-sideband (DSB) signal with a 6 kHz bandwidth requires a signal-to-noise ratio of at least 15:1.

At frequencies below the LUF, satisfactory reception will not be possible because the received signal will be lost in the prevailing noise. As the operating frequency is raised above the LUF, the signal-to-noise ratio improves. Optimal conditions occur near the Classical MUF, where both the signal-to-noise ratio and the propagation reliability are maximum.

Unlike the MUF, which is dependent entirely upon ionospheric characteristics, the LUF can be controlled to some degree by adjustments in the effective radiated power or by changes in the type of modulation used. As a general rule of thumb, the LUF can be lowered approximately 2 MHz for each ten-fold increase in effective radiated power, and visa versa. Also, new digital signal processing (DSP) techniques have the capability to effectively "lower" the LUF. In reality, this technology allows us to see deeper (20–30 dB) into the noise through the use of coherent signal detection techniques.

Because ionospheric absorption increases as solar activity increases, the LUF for any particular circuit is expected to be somewhat higher during a period of peak solar activity than during a period of low sunspot activity.

Circuit Analysis Curves

Between the Classical MUF and the LUF there is a range of frequencies over which radio communications can be maintained on a particular circuit. The upper limit of the range (the Classical MUF) is determined by the ionization density at the point of reflection, while the lower limit (the LUF) is determined by ionospheric absorption along the path and by noise conditions at the receiving terminal. It is of great operational importance to know both of these limits as well as the intervening range of useful frequencies. Such data, plotted conveniently in graphical form, are often referred to as "circuit" (or propagation) analysis curves.

On a real-time basis the highest frequency that will support propagation between any two points, as we noted earlier, is referred to as the Classical MUF. In Figure 1.13 the circuit analysis curve shows the "predicted median MUF" for the given month. This means that on 50% percent of the days the Classical MUF will be above this value, and on 50% of the days the Classical MUF will fall below this value. Frequencies lying between the median MUF and the LUF will support propagation on a greater percentage of the days. It should be noted that if the predicted (median) MUF is multiplied by 0.85, the resulting frequency "should" support propagation on 90% of the days of the month, provided that it is above the LUF. This frequency is referred to as the Frequency of Optimum Traffic, or FOT. If the predicted (median) MUF is multiplied by 1.15, the resulting frequency should support propagation on 10% of the days of the month. This frequency is referred to as the Highest Possible Frequency, or HPF.

For example, using Figure 1.13, at 12 noon EST the predicted median MUF is seen to be 20 MHz, the FOT = 20 × 0.85, or 17 MHz; and the HPF = 20 × 1.15, or 23 MHz.

Figure 1.13, which is a typical circuit analysis curve, represents data for the circuit between the east coast of the U.S.A. and western Europe for a winter period of low solar activity (here, December 1986). From this example it is possible to see at a glance what bands are expected to be open at any time of the day. For example, the 15 meter band should open approximately 50% of the days between 9 AM and 12 noon EST, while 20 meters should be open 90% of the days between 8 AM and noon. The figure also shows that 40 meters should open a bit more than half the days of the month between 1500 and 2000 EST (3 and 8 PM). The circuit analysis shown in Figure 1.13 is based on an "effective radiated power" of 250 watts. Effective radiated power, or ERP, is defined as the power supplied to an antenna multiplied by the gain of the antenna in the given direction relative to gain of a dipole antenna at a height of one-half wavelength above the ground.

During periods of time when the LUF exceeds the MUF, a "blackout" condition occurs, and it becomes very difficult, if not impossible, to maintain communications on the circuit. In Figure 1.13 a blackout condition is seen to occur between 4 and 7 AM. Further, between 1300 and 1500 EST (1 and 3 PM) only a narrow band of frequencies around 10 MHz should support propagation on this path. Since there now is an amateur frequency allocation in this range, however, communications between the east coast of the U.S. and western Europe still should be possible in this time period.

It can been seen from Figure 1.13 that unless we are familiar with ionospheric conditions, the chances of maintaining effective radio communications are slim, especially during periods of sunspot minimum. Haphazard selection of the operating band easily can result in the signal either penetrating the ionosphere and being lost in space, or being completely lost in the noise. On the other hand, proper band selection based on propagation analysis will result in reflection of the signal between transmitter and receiver with a minimum loss of energy.

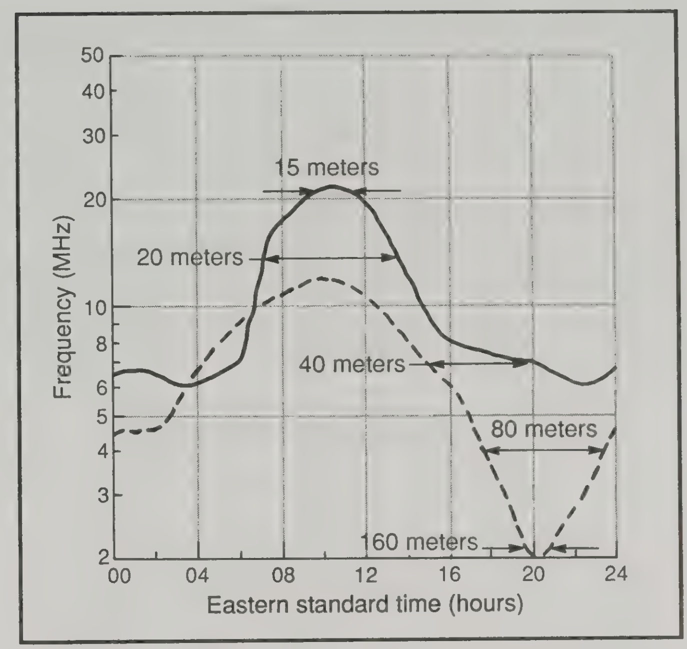

Figure 1.13. Circuit analysis curves, east coast U.S.A. to western Europe; low sunspot activity (SSN 10); winter season, December. Solid line is predicted median MUF; dashed line is LUF. LUF based on 250 watts of CW effective radiated power.

The ability to maintain efficient long-distance shortwave communications depends to a great extent on the ability to predict, far enough in advance, what ionospheric conditions will be so that adequate operational plans can be made. Such long-range propagation studies are made possible because of the close relationship that is known to exist between ionospheric conditions and smoothed sunspot numbers. Figures 1.13 and 1.14 are examples of propagation analyses calculated for the path between the eastern U.S. and western Europe during the winter months of previous periods of low and high solar activity, respectively.

Today there are two methods by which the radio amateur can develop circuit analyses such as those shown in Figures 1.13 and 1.14. These methods are the "Tabular" method and "Computer Modeling." So that the readers of this book can perform tabular circuit analyses, we have chosen paths to major points on all the world's continents from the three main geographical regions of North America (eastern, central, and western) and have constructed circuit analysis curves similar to those shown in Figures 1.13 and 1.14. The results are presented in Chapter 4 in a simplified tabular format that permits reliable do-it-your-

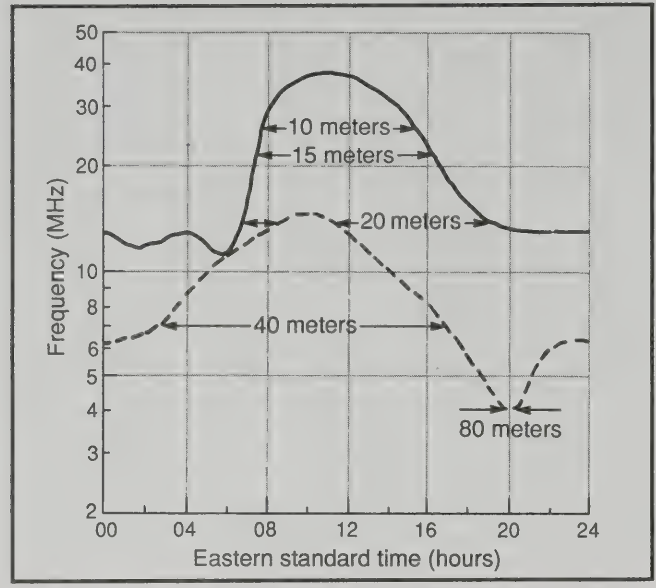

Figure 1.14. Circuit analysis curves, east coast U.S.A. to western Europe; high sunspot activity (SSN 110); winter season, December. Solid line is predicted median MUF; dashed line is LUF. LUF based on 250 watts of CW effective radiated power.

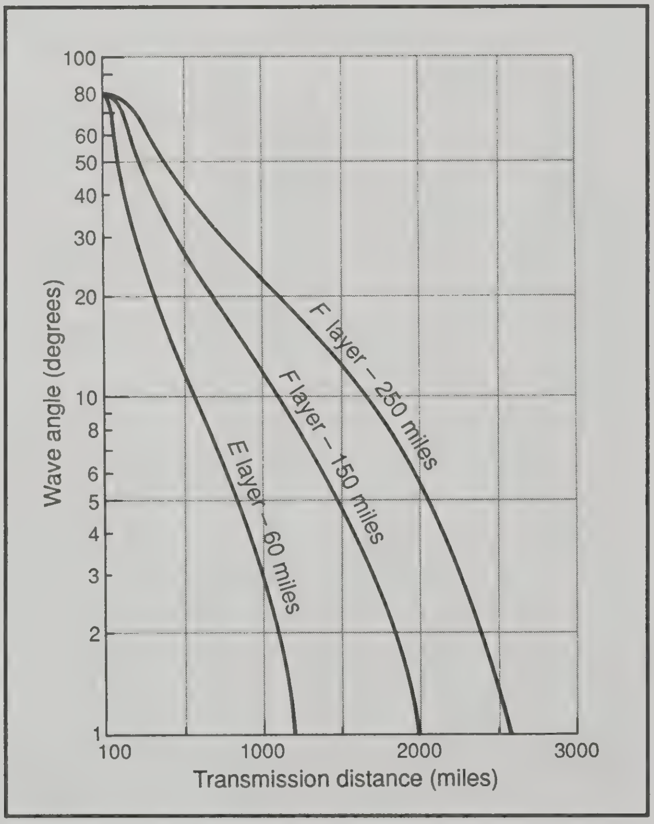

Figure 1.15. Relationship between optimum antenna wave angle, transmission distances, and height of the *E* and *F* layers.

self forecasts to be made to just about any part of the world for any time during a solar cycle.

For readers who are comfortable using modern personal computers, Chapter 6 will discuss in some detail computerized methods for circuit analysis, what software is available, and how to interpret the results. It is important for the reader to remember one fundamental fact: no matter which method you use, the MUF values derived are **median** values. That is, 50% of the time the Classical MUF values observed each day will be higher than the median, and 50% of the time they will be lower.

A more detailed explanation of the complexities involved in constructing circuit analyses can be found in *Ionospheric Radio Propagation.*[12] Detailed data for calculating LUF and field strengths appear in "Skywave Field Strength at Frequencies between 2 and 30 MHz."[13]

Optimum Radiation Angle

Figure 1.15 shows the optimal relationship between radiation angle, or the slant angle at which the radio wave must leave the earth, and distance for transmission via the ionosphere. Radiation angles (or wave angles, as they also are called) are shown for reflection from an average *E*-layer height of 60 miles, and for normal *F*-layer limits of 150 and 250 miles. From Figure 1.15, assuming one degree as the minimum attainable wave angle, it can be seen that the geometry of skywave propagation is such that one-hop reflection from the *E* layer is limited to approximately 1200 miles, and one-hop *F*-layer propagation is limited to a maximum distance of between approximately 2000 and 2600 miles. Propagation beyond these distances is usually accomplished by means of multi-hop propagation (successive reflections between the earth and the ionosphere).

For the most efficient shortwave propagation, the radiation angle of the transmitting antenna (and receiving antenna, as well) should be optimized according to the geometry of propagation. This is directly a function of the type and height of the antenna used. Figure 1.16 illustrates the radiation angles for a typical amateur three-element beam at various heights above the ground. This type of antenna is called a "directive antenna" because it can focus energy into certain directions instead of radiating uniformly in all directions. It is the vertical radiation pattern that controls the distance of transmission. For distances less than the one-hop limit, the optimum wave angles can be determined directly from Figure 1.15. For multi-hop propagation, experience has shown that the lower the radiation angle, the more efficiently the wave is propagated.

The radiation angle of the antenna is determined primarily by its electrical height above ground. Figure 1.17 shows how the wave angle varies with the antenna height. Basically, the higher the antenna, the lower the wave angle. Using the data in Figure 1.15, and for an *F*-layer height of 250 miles, the coverage of the three-element beam is approximately 750 miles when the beam is up one-half wavelength. When the antenna is raised to a full wavelength in height, one-hop coverage extends to 1400 miles.

Here is an example that ties together the geometry of propagation, optimum radiation angles, and height of the antenna above ground. Suppose that shortwave communications must be conducted between two points 1000 miles apart. From Figure 1-15 for an *F*-layer height of 150 miles, the optimum wave angle is 13 degrees; for a height of 250 miles, it is 23 degrees. In practice, the antenna's design radiation angle is generally taken as the average value of the two limiting heights, which in this example would be 18 degrees.

From Figure 1.17 a wave angle of 18 degrees can be achieved with a horizontal antenna approximately 0.8 wavelength above ground. If the optimum band for this circuit is 20 meters, the antenna should be placed 16 meters, or 53.5 feet, above ground (1 meter = 3.281 feet).

Additional data concerning the design of antennas for use by radio amateurs can be found in *The ARRL Antenna Book.*[11]

In summary, to optimize shortwave communications over a particular path use only those amateur bands that lie between the predicted median MUF and the LUF, and make sure your transmitting antenna is designed for the optimum radiation angle.

1.4 Ionospheric Disturbances and Shortwave Radio Effects

One of the challenges in using shortwave radio—as an experimenter, communicator, or listener—is dealing with the continuous variation in propagation conditions. Even when solar conditions are undisturbed, the variability of the ionosphere is enough to cause changes in day-to-day signal conditions. These changes are caused by variations in absorption, changes in ionospheric electron density, and turbulence in the upper atmosphere. However, from time to time, significant abnormalities occur in the ionosphere that make signal transmission and reception exceptionally difficult, if not impossible. These abnormalities are called "ionospheric disturbances."

Ionospheric disturbances are characterized by (1)

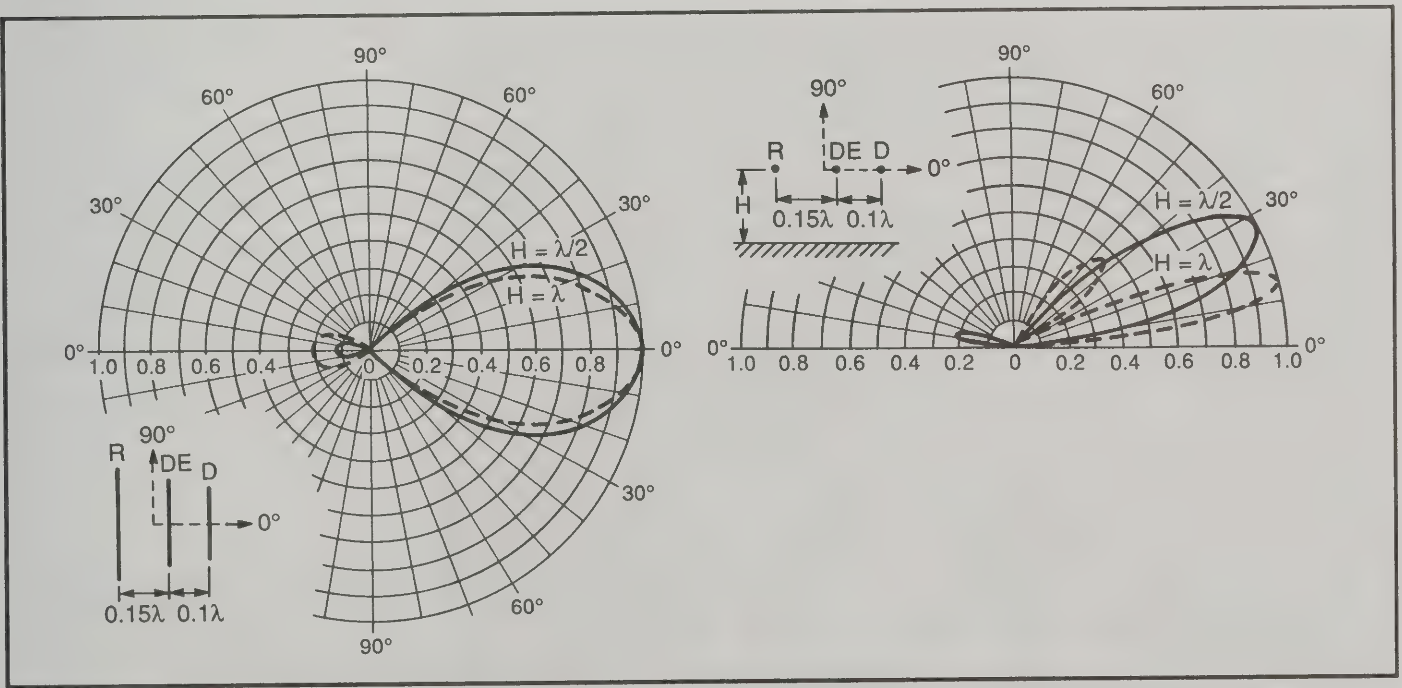

Figure 1.16. Horizontal and vertical polar diagram of a three-element Yagi antenna at a height H = λ/2 and H = λ. The spacing of the elements is given in the figure. (Modified after Dieminger, 1968.)

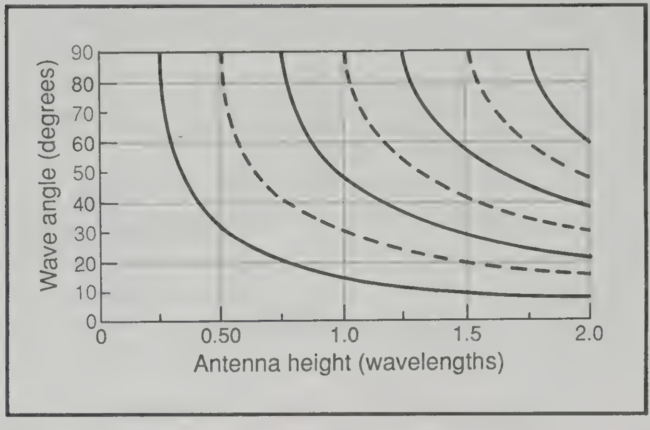

Figure 1.17. Antenna radiation angles for various antenna heights above ground. The solid lines are maxima, dashed lines are nulls, for all horizontal antennas and for vertical antennas having a length equal to an even multiple of one-half wavelength. For vertical antennas an odd number of half waves long, the dashed lines are maxima and the solid lines are nulls. For example, a horizontal antenna 0.75 wavelengths above ground will have maximum radiation at a wave angle of 20 degrees, minimum radiation at a wave angle of 40 degrees, and a second maximum at 90 degrees.

increased ionization in the *D* layer, resulting in the absorption of the shortwave signal; or (2) weakening or decomposition of F_2-layer ionization; or (3) both. The *primary* source of these ionospheric disturbances is enhanced radiation from flares in those regions around sunspots.

For years it was thought that ionospheric disturbances resulted solely from solar flares. With modern technology, however, it is now known that low-energy particle clouds that are not flare-related are ejected from the Sun. These events include (1) the High-Speed Solar Wind System (HSSWS), which emits "streamers" of particles through coronal holes; (2) Coronal Mass Ejections (CMEs), which are theorized to be flares that have no optical brightening, but that do have enough power to eject low-energy solar particles; and (3) Disappearing Filaments (large curtains) of cool, solar gases that disappear and are followed by a disturbance in the Earth's magnetic field. By far, solar flares provide events that have the most profound impact on the Earth's magnetic field and the ionosphere. However, as far as the radio amateur is concerned, the question is: How well do signals propagate? It is an accumulation of all of the events mentioned above that influence day-to-day propagation conditions.

Occasionally, an active region (that bright area around the sunspot) will erupt into a solar flare. Photo 1.C shows a solar flare from an active region on the Sun. Seen is the plasma surge from the flare, in which hot, ionized hydrogen shoots out at about 200 km per second along magnetic field lines and then retracts along the same path. In extreme instances, when surge speeds exceed the 700 km per second escape velocity for the Sun, the plasma cloud goes into interplanetary

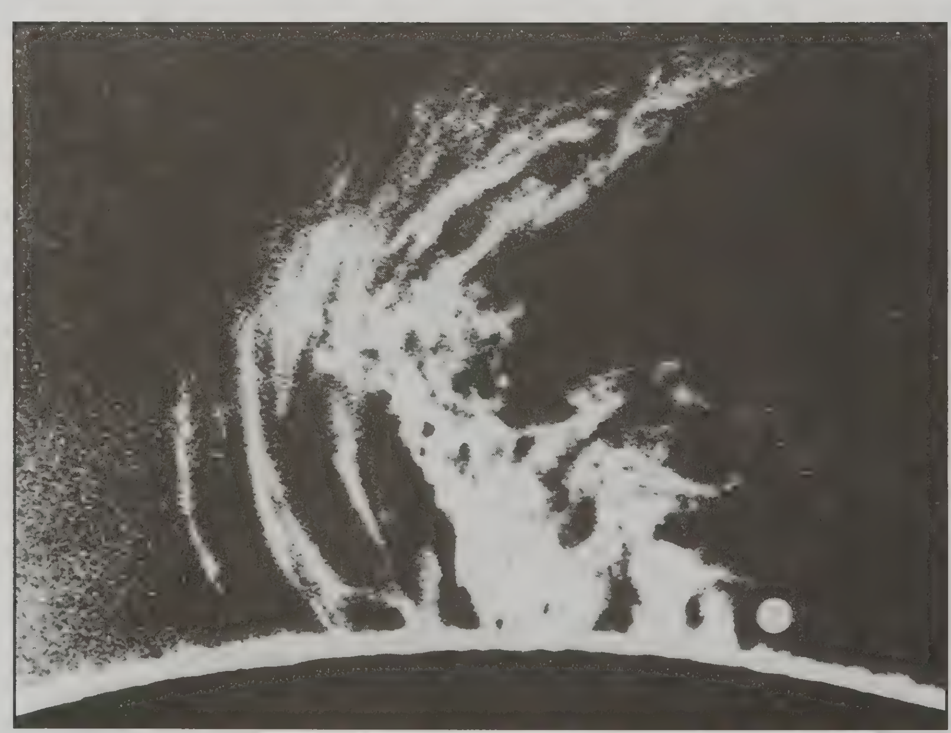

Photo 1.C. A flare on the surface of the Sun ejecting gaseous material and solar radiation millions of miles into space. (Photographed with a special telescopic camera at the Palomar Observatory, Mt. Wilson, California.)

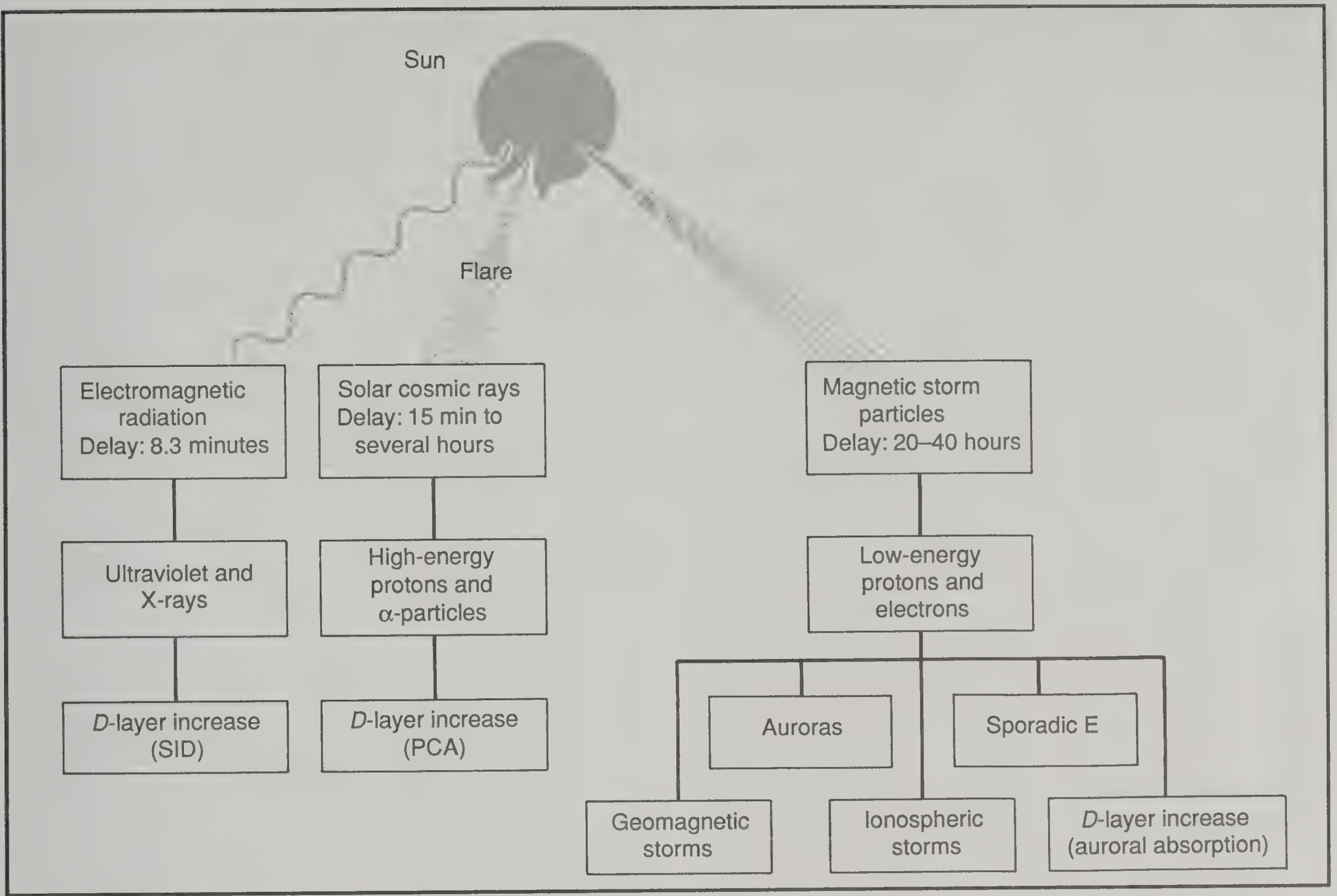
Sun
Flare
Electromagnetic radiation Delay: 8.3 minutes
Solar cosmic rays Delay: 15 min to several hours
Magnetic storm particles Delay: 20–40 hours
Ultraviolet and X-rays
High-energy protons and α-particles
Low-energy protons and electrons
D-layer increase (SID)
D-layer increase (PCA)
Auroras
Sporadic E
Geomagnetic storms
Ionospheric storms
D-layer increase (auroral absorption)

Figure 1.18. Flare emissions and ionosphere effects. (Modified after R. W. Knect [unpublished]; see also Reference 12.)

space. When this occurs, dramatic effects are observed on Earth.

Solar-Flare-Related Disturbances (Causes and Effects)

Generally, the effect of ionospheric disturbances on the HF bands is to weaken the signal levels either abruptly or gradually, sometimes to the point where signals (and even the atmospheric noise) completely disappear. The effect can be quite dramatic, and when the noise level is greatly reduced, one even may suspect that a receiver is defective. On the other hand, certain disturbances can cause rapid, erratic signal fading, echoes, or spreading (that "head-in-a-barrel" sound), and a great increase in the noise level in portions of the HF spectrum.

Three types of radiation produced by solar flares affect shortwave propagation. These are: (1) electromagnetic radiation; (2) solar high-energy particle cosmic radiation; and (3) low-energy particle radiation. Each affects the ionosphere in a different way, and all are disruptive to shortwave service.

Solar Flares and Their Radiation Products

Solar flares are thought to be produced in the following manner. Very intense magnetic fields, the frequency-of-occurrence of which follows the evolution and demise of the solar cycle, set up between a pair of sunspots. These magnetic fields lie below the surface of the Sun, but they can become so large that they erupt through the solar surface, extending in large loops up to 35,000 miles above the solar surface. As the magnetic field evolves, it becomes more complex, and the area around the sunspot is heated. This increases the level of ambient solar radiation and creates even more volatility in the magnetic field. As the complexity of the sunspot pair increases even further, the likelihood that a flare will be produced increases. However, modern technology cannot foretell exactly when a flare will occur or what its magnitude will be.

There is one theory which states that as sunspot

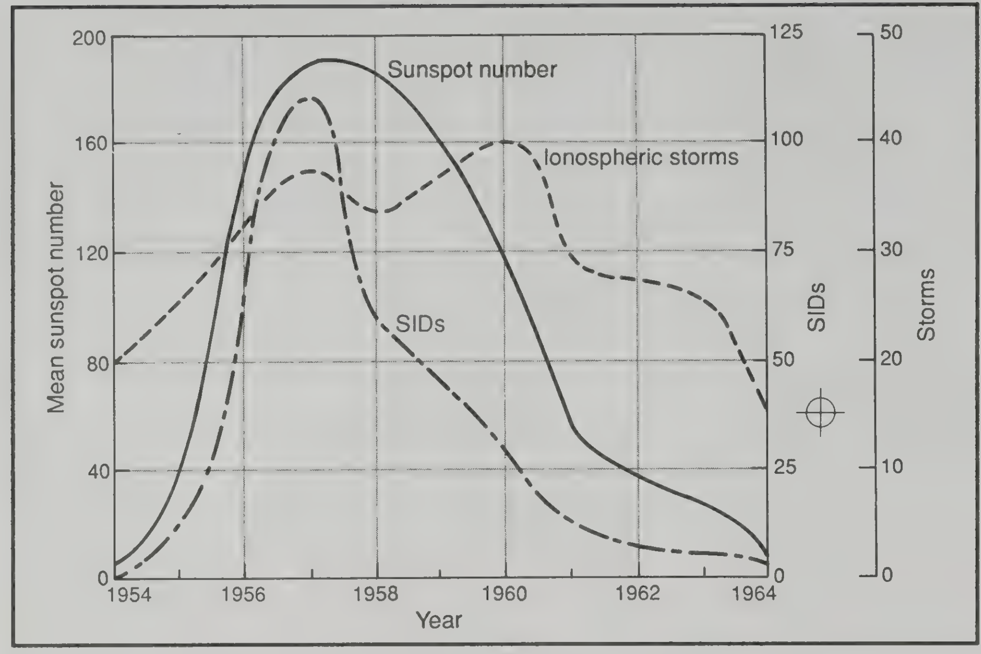

Figure 1.19. Relationship among mean sunspot numbers during Cycle 19 (1954–1964), the annual number of SIDs, and the annual number of ionospheric storms observed over the North Atlantic path during Cycle 19.

groups become more complicated and the interaction between their magnetic fields increases, two fields of cross polarity "bump," causing an electric discharge in the over-dense solar plasma and breaking the field lines. (It is very much like what happens when a balloon is blown up to the point of just about breaking, and then it is punctured with a pin.) In the first minute following the break, a cloud of very high-energy protons is ejected at about one-third the speed of light. Simultaneously, electromagnetic radiation (EUV, UV, x-rays, and cosmic rays) are emitted. Within 5 minutes a cloud of lower energy particles is ejected, traveling at a velocity of about 1,000 kilometers per second. Within an hour, however, the magnetic fields are thought to reconnect between the two sunspots, and the level of radiation from the region subsides. A really big solar flare can produce enough energy to supply a major city for 200 million years, with most of this release coming in the first 5 minutes.[15] Figure 1.18 illustrates the three types of radiation that come from a solar flare, the time it takes for each to manifest itself in the near-Earth environment, and some of the ionospheric disturbance effects that result from the flare's radiation and energetic particles.

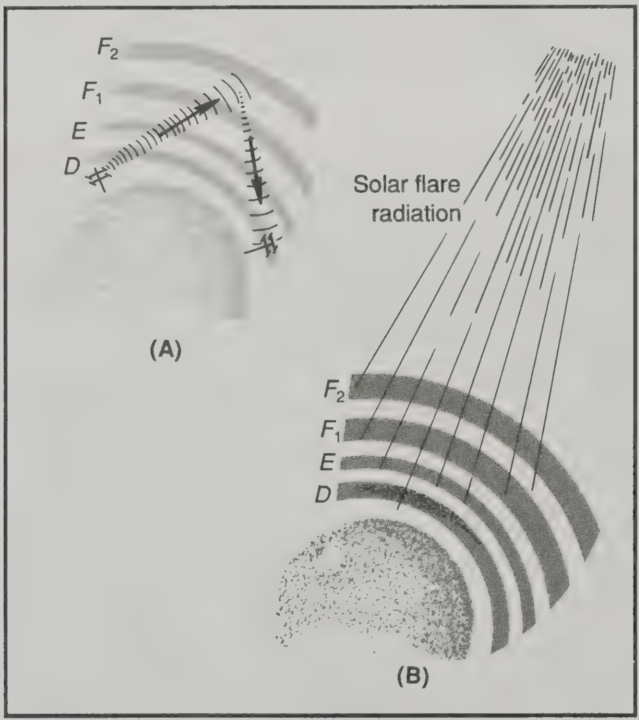

Figure 1.20. Under normal conditions the daylight ionospheric layers can be represented as shown at (A). The radiation from an intense solar flare produces unusual ionization of the lower layers, particularly in the *D* layer (B), and the result is a sudden ionospheric disturbance.

Intuition alone would tell you that solar flares should occur more frequently during solar maximum, when the sunspot number is high. That is a valid conclusion. At this time the ionosphere not only is more energized, it is more frequently disturbed as well. Figure 1.19 shows this relationship.

Sudden Ionospheric Disturbances (SIDs)

The Sudden Ionospheric Disturbance (SID) also has been referred to as a shortwave fadeout (SWF) or as the Dellenger effect (named after the late Dr. John H. Dellenger, an American pioneer in radio propagation research who was among the first to identify this type of disturbance). SIDs only affect HF circuits in the sunlit hemisphere. Depending on the intensity of the flare, and the angular relationship between the Sun and the Earth, the effect of a SID on HF propagation can range from nothing to a complete blackout.

Because the electromagnetic radiation produced by the flare travels at the speed of light, the effect of the flare on Earth takes place within about 8 minutes after it has occurred. The *D*-layer portion of the ionosphere is abruptly enhanced by the 1-8 Ångström x-rays, causing an almost immediate increase in HF absorption. This is illustrated in Figure 1.20. The solar zenith angle influences the amount of absorption that is experienced. Therefore, an HF circuit having an ionospheric control point (the part of the ionosphere where the signal is reflected) in the mid-day sun will experience a more dramatic and longer lasting blackout than will a circuit that has its control point in the early morning or late afternoon part of the day. HF circuits in the nighttime half of the Earth will experience no effect.

There are a number of characteristics about this type of disturbance that should be noted. Remembering that absorption is a function of the inverse square of the frequency, the increased *D*-layer ionization affects frequencies in the lower portion of the HF range first—for example, the 80 and 40 meter bands. Higher frequency signals are the last affected, and they also are the first to recover when the flare effect diminishes. Obviously, a higher frequency band, such as 10, 12, or 15 meters, should be tried during such a disturbance. In the equatorial regions, where the Sun is more directly overhead, SIDs are usually more intense. Transequatorial circuits with control points near the equator, therefore, will often experience abrupt, total blackouts.

What does a SID "sound" like? It can easily be simulated. Find a frequency on your shortwave radio that is very crowded, with many very loud signals. Put on a pair of earphones and turn up the volume. Then pull the antenna connector out of the receiver. The instantaneous silence is often traumatic to inexperienced users of the shortwave bands, and they immediately suspect a faulty radio or antenna. (Even trained communicators, however, can fall victim to this effect.) When an SID is so intense that no signals seem to be reflected from the ionosphere, there is nothing you can do but wait until the end of the disturbance, trying the higher frequency bands first after an hour or so.

Most SIDs subside in an hour or two. However, during solar maximum, there will be "monster" flares (such as in August 1972 and in September 1989) that will black out the sunlit hemisphere for the better portion of the day.

The Day The Ionosphere Disappeared

One of the severest SIDs on record occurred during Cycle 20. Often referred to as a "monster storm," K6GKU described how he observed it.

On August 7, 1972, Bob was making vertical incidence sounder measurements in the early afternoon at the Navy's La Posta Astrogeophysical Observatory in California. Abruptly, all traces of the ionosphere disappeared from the oscilloscope screen. After checking to make sure that there were no equipment failures, and having seen the effects of SIDs before, the scientific crew waited patiently for the remainder of the afternoon for the return of the ionosphere. What had happened was an intense x-ray burst from a major solar flare caused the *D* region of the ionosphere to literally absorb all HF radio signals in the eastern Pacific area. Frantic calls from the Navy communication stations in the area confirmed that almost all HF communications were suddenly "blacked out." It remained that way for the rest of the daylight hours.

This "monster storm" has some additional historical significance. In the early 1970s, manned space missions were on the increase in both the U.S.A. and the former U.S.S.R., and numerous satellite systems for communication, weather, navigation, spying, and other environmental and military purposes were being designed and launched in greatly increasing numbers. Recognizing that solar radiation was a potential danger to these satellites, it was the high-energy radiation recorded during this event that became the model for assessing "worst case" potential radiation hazards to both humans and equipment in space.

Geomagnetic Activity and The Ionospheric Storm

The primary disturbance that disrupts HF communications and broadcasting is the *ionospheric storm.* There is a close association between the observation of disturbances in the Earth's magnetic field and bad propagation conditions. Thus, the poor propagation often is attributed erroneously to a "geomagnetic storm," "magnetic storm," or "magstorm"; seldom is the term "ionospheric storm" used. But it is the ionospheric storm HF users dislike so much.

Geomagnetic activity. Geomagnetic disturbances are caused by the bombardment of low-energy parti-

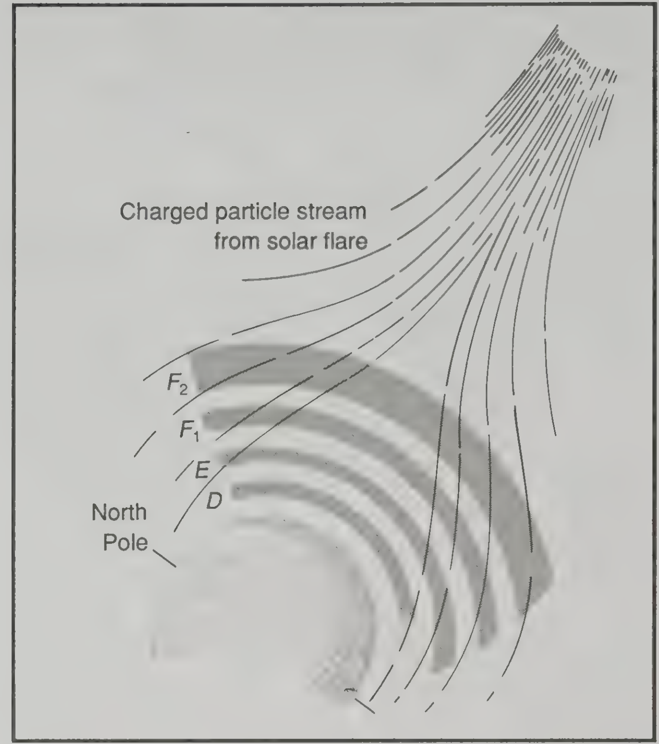

Figure 1.21. The charged particle stream from a solar flare tends to divert to the polar regions because of the Earth's magnetic field. The velocity of these particles passing through the ionospheric layers, particularly the higher layers, disturbs these layers and produces a geomagnetic storm, which often results in an ionospheric storm. These events will be explained more fully later in this chapter.

cles from the Sun. Historically, these events tended to be modulated by the 11-year solar cycle, peaking at solar maximum. However, studies of solar Cycles 11 through 21 indicate that the level of geomagnetic activity does not peak at sunspot maximum, but rather it has a double peak—one slightly prior to the maximum and a major peak in the declining phase of the cycle.[16] The latter results from a tendency of strong solar wind streams to occur in the declining phase of the solar cycle. This high-speed solar wind system (HSSWS) results from "coronal holes" that produce an unrestricted outward flow of solar particles into interplanetary space. A coronal hole is just that—a breakdown (or hole) in the magnetic fields in the solar corona. When the Earth crosses one of these solar "streamers," a disturbance in the Earth's magnetic field results. Coronal holes occur more often in the declining phase of the solar cycle, and they are a primary source of geomagnetic storms during solar minimum. HSSWS disturbance activity tends to recur in approximately 27-day periods, the time of one solar rotation.

There are two other "suspected" sources of solar particle ejection that can cause terrestrial magnetic activity and that are not related to solar flares. Coronal mass ejections (CME) are thought to be solar flares that just did not have enough energy to produce the bright optical explosion of a typical flare. However, there is enough energy in the surge for some particles to escape the Sun's magnetic fields into interplanetary space.

Disappearing filaments also have been associated with magnetic activity here on Earth. A solar filament is a large curtain of cool gas in the Sun's photosphere. Several studies have noted that shortly (several days) after the disappearance of some filaments, we experience a geomagnetic storm on Earth. While the mechanism for the eruption of the filament is not known, this event can severely disrupt HF communications.

A primary source of particle bombardment that causes geomagnetic storms is the solar flare. The low-energy particle cloud it produces arrives in the Earth's vicinity roughly 20-40 hours after the occurrence of the flare. This cloud, having had more time to expand, impacts one side of the magnetosphere, causing a "ripple" effect in the Earth's magnetic fields that is called a "magnetic storm." Because the particle cloud tends to travel along field lines, the particles concentrate in the Earth's polar regions. The higher the latitude, the greater the magnetic disturbance (see Figure 1.21).

The geomagnetic storm itself does not disrupt HF propagation. However, during these periods, the disturbed geomagnetic field causes the mid-latitude and high-latitude chemistry of the atmosphere to change. This change is a recombination effect, much like what happens in the ionosphere at night. The severity of this change increases with latitude. This effect, called an "ionospheric storm" (or "radio storm"), is the disturbance that degrades HF propagation as the daytime ionosphere decomposes. It is possible to have a geomagnetic storm without experiencing an ionospheric storm. The converse, however, is not true.

Ionospheric storms. The ionospheric storm produces many effects, all of which degrade HF communications. The *F* layer may seem to disappear, to change its ionization rapidly, or to seemingly split into many layers. The first effect, of course, means the loss of signals that are too high in frequency, while the other effects will produce rapid fading and echoes.

During ionospheric storms the highest frequency that the *F* layer will reflect may be reduced by as much as 50% below normal. Although the *F* layer is primarily affected, severe storms cause similar behav-

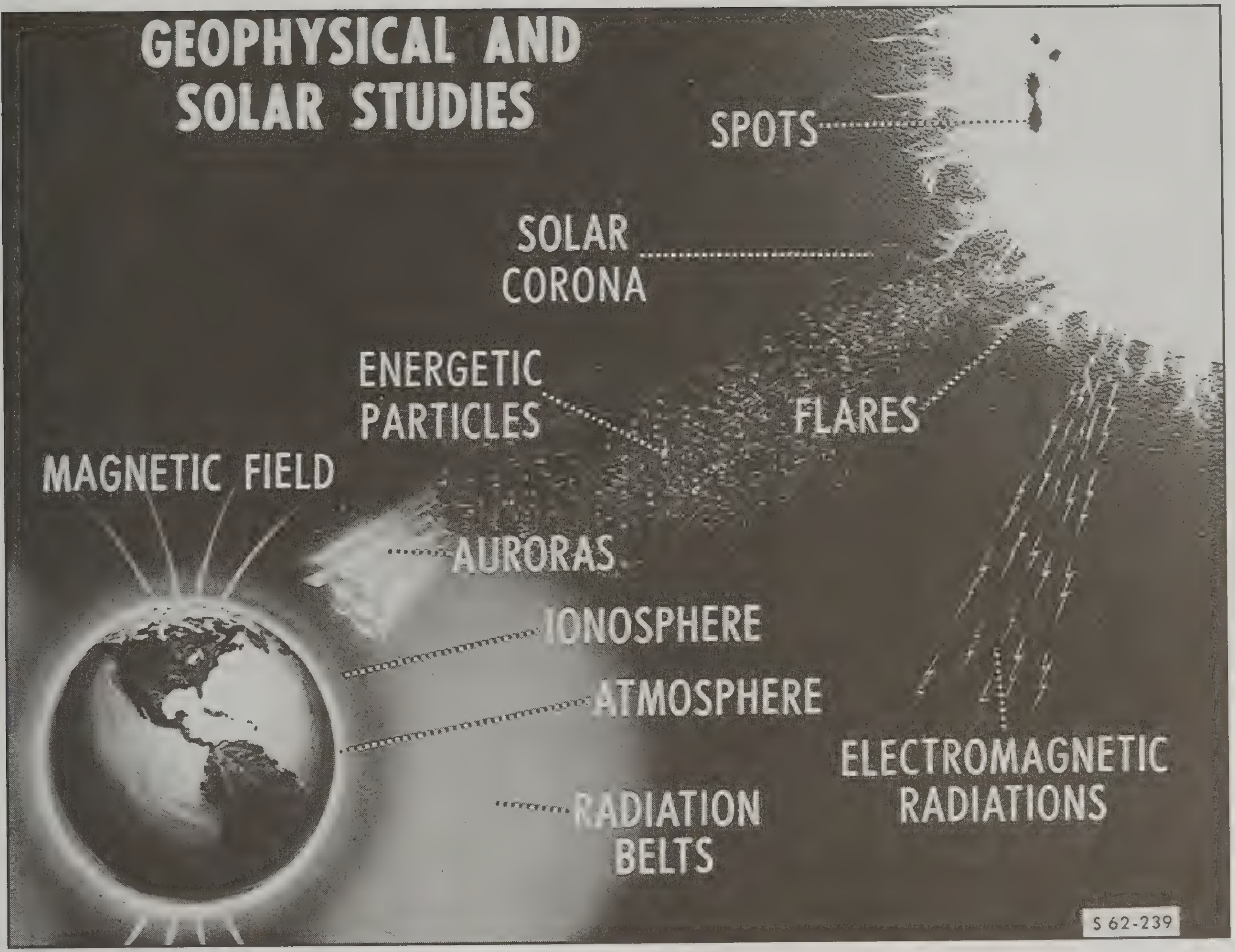

Photo 1.D. The influence of solar radiation upon the Earth's atmosphere as shown in a NASA pictorial representation.

ior in the *E* region as well. Under extreme conditions the combination of a weaker ionosphere and increased absorption results in a radio blackout, during which time long-distance communications may become impossible to many areas of the world. This is especially observed on circuits passing near the Earth's magnetic poles, where the concentration of charged particles is greatest.

The onset of an ionospheric storm usually is detected in both the daylight and dark areas of the world at the same time. The storm generally begins simultaneously in the northern and southern polar regions of the Earth, expanding into the middle and low latitudes over a several-day period as the severity of the storm increases.

Ionospheric storms may occur over as much as 100 hours per month during periods of maximum sunspot activity, while during periods of low sunspot activity, they occur about half as often. In this latter case, however, these storms are more likely caused by a high-speed solar wind system.

Obviously, one countermeasure against this type of disturbance is to try a lower frequency band to continue communications. The relaying of traffic by different paths also may help. Because the charged particles concentrate at the magnetic poles, a signal path passing through the equatorial region may be completely unaffected by such a storm while a trans-polar path may be useless. The use of a dark-side path generally will not help. The disturbance develops and disappears gradually as compared to a sudden ionospheric disturbance, and it generally will last much longer—from one to three days or more.

High-Energy Protons and Polar Cap Absorption

The high-energy particles (mostly protons) that are

	SID	Ionospheric Storm	Polar Blackout (PCA)	Polar Blackout (auroral)
Commences	Suddenly	Gradually	Suddenly	Gradually
Duration	Several Minutes to Several Hours	Several Hours to Several Days	Several Minutes to Several Hours	Several Hours to Several Days
Region Most Affected	Daylight Areas	Polar Regions and Mid-Latitudes, Day and Night	Polar Regions, Day or Night	Polar Regions and Mid-Latitudes Day and Night
Region Least Affected	Darkness Areas	Low Latitude and Equatorial Regions	Mid-Latitude and Equatorial Regions	Low Latitude and Equatorial Regions
Bands Most Affected	20–160 Meters	10–40 Meters	15–160 Meters	10–160 Meters
Bands Least Affected	10–15 Meters	80–160 Meters	—	—
Seasonal Peak	Any Season	Early Fall Through Spring	Any Season	Early Fall Through Spring
Sunspot Cycle	Peaks During High Period	Peaks During High and Medium Periods	Peaks During High Period	Peaks During High and Medium Periods
Corrective Action	Work Dark Paths. Go Higher in Frequency on Daylight Paths	Work Low Latitude and Equatorial Paths. Go Lower in Frequency on High Latitude and Trans-Polar Paths	Work Low Latitude and Equatorial Paths. Go Higher in Frequency on High Latitude and Trans-Polar Paths	Work Low Latitude and Equatorial Paths

Table 1.1. Types of ionospheric disturbances.

explosively ejected from a flaring region arrive somewhere in the Earth's vicinity one to four hours after the flare (although not every flare produces a terrestrial proton event). This cloud consists of highly radioactive particles. For reasons due to Sun-Earth geometry, only a limited portion of the solar disk where the solar eruption occurred can place the particle cloud in a trans-Earth trajectory. Once the particles arrive near the Earth, they are propagated along the magnetic field lines into the polar regions. Once in the polar regions, the protons cause a large increase in the *D*-layer ionization. This causes a Polar Cap Absorption (PCA) event, increasing absorption levels for HF signals by 40 to 80 dB. This is a far larger increase than can be compensated for using conventional communication techniques. Polar blackouts suppress signals for three to five days. Stations inside the polar cap region will hear no shortwave signals from anywhere for this period. Trans-polar circuits will be totally blacked out. Most users of the HF spectrum will not know a PCA has started, only that no signals are coming "over the poles." While high-energy particle events often have been a source of grief for HF communicators, it is only in the past 10 to 15 years, when a greater reliance has been placed on satellites at geostationary orbit (outside the Earth's magnetic field's protection), that the high-energy particle event has taken on a new ominous role—that of satellite killer.

Very strong auroral displays usually are associated with most polar blackouts, especially those occurring during severe ionospheric storms.

SIDs, ionospheric storms, and polar blackouts are often inter-related. An SID will occur minutes after the flare takes place on the Sun's surface, followed in 20 to 40 hours by an ionospheric storm. Polar Cap Absorption usually will take place within an hour or so after the SID, while vivid auroral displays will occur during the ionospheric storm, as the absorption belt moves southward.

The influence of solar radiation on the atmosphere is shown in Photo 1.D. Table 1.1 summarizes the different ionospheric disturbances and their attributes.

The sequential effects of disturbances can be a warning. When an SID is in progress, the chances are high that more prolonged, widespread storm activity will occur in 20 to 40 hours.

During SIDs use the higher frequency bands and try dark-side paths. More often than not, just wait and the event will subside.

During ionospheric storms and polar blackouts, use the lower frequency bands and avoid paths that pass through or near the polar regions.

Although ionospheric disturbances cannot yet be predicted in the same manner as, nor with the high accuracy of, normal propagation conditions, relatively simple and fairly accurate methods for predicting the possible recurrence of these disturbances have been developed. These are discussed in greater detail in Chapter 5, "Ionospheric Forecasts."

For serious students of shortwave propagation who

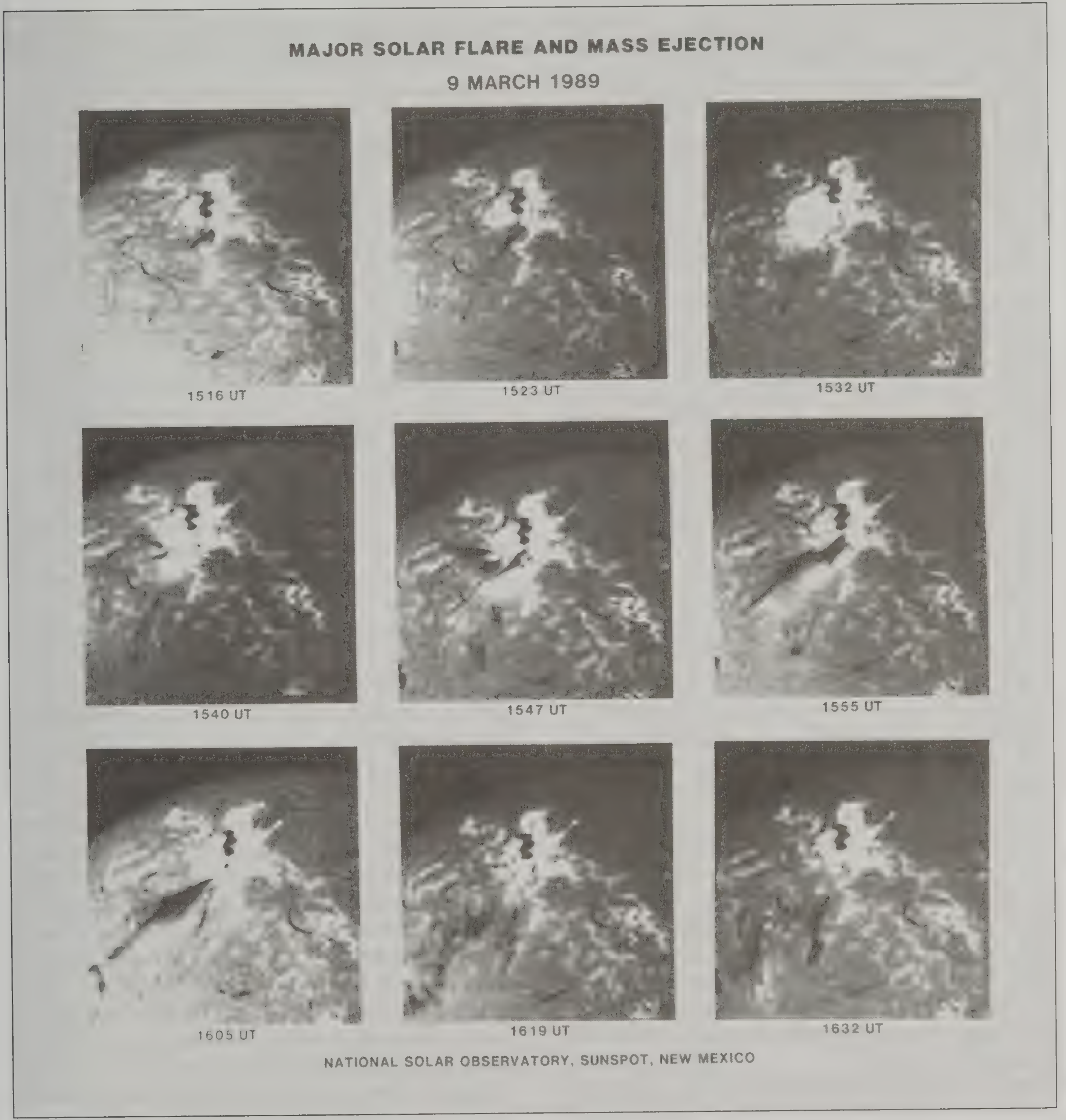
MAJOR SOLAR FLARE AND MASS EJECTION
9 MARCH 1989
1516 UT
1523 UT
1532 UT
1540 UT
1547 UT
1555 UT
1605 UT
1619 UT
1632 UT
NATIONAL SOLAR OBSERVATORY, SUNSPOT, NEW MEXICO

Photo 1.E. The flare and massive particle ejection of 9 March 1989 is thought to be the largest flare ever observed.

Solar Flare Activity—1989

Number	Type	Effect
452	Minor Flares	Little effect on HF radio
372	Moderate Flares	Minor effect to lower daylight HF spectrum
32	Major Flares	Radio blackout to most daylight frequencies
2	Extraordinary	Long-duration daylight radio flares blackouts

Average of 4 flares per day.
Average of one disruptive flare per week.

Table 1.2. The year 1989 was marked by severe solar disturbances, including the largest and most energetic solar particle events on record.

desire more information on solar-terrestrial effects and the ionosphere, refer to References 17 and 18 at the end of this chapter.

1.5 1989 and The Disturbed Sun

As discussed in a previous section, the influence of solar flares on space and the Earth's atmosphere extends far beyond the interests of radio amateurs and other users of the HF spectrum.

In 1989 Dr. James Van Allen discovered the radioactive belts above the Earth that now bear his name—the Van Allen Belts.[19] These are two huge, doughnut-shaped belts of intense radiation that encircle the Earth beginning at several miles into space. The Van Allen Belts consist of high-energy protons, electrons, other particles, and associated magnetic fields. With this discovery, theories of a benign space environment above the ionosphere had to be reconsidered and revised. Moreover, it subsequently was discovered that the radiation levels in these Belts are greatly enhanced during solar disturbances by radiation that occurs during such events.

The unusually high number of solar disturbances recorded during 1989 has earned that year the unofficial title of "the year of the turbulent Sun." This was coincident with the peak of sunspot Cycle 22. These disturbances not only were associated with major HF radio blackouts, but also, they caused damage to satellite solar panels and caused errors in satellite tracking equipment, particularly to those satellites that passed through the Van Allen Belts.[20, 21] Simply put, solar flares and other solar disturbances can affect space and satellite systems as well as terrestrial HF communications.

An example of the turbulence of 1989 is in the number of Ground Level Events (GLEs) that occurred that year. When the energy level of a solar proton event reaches or exceeds 500 MeV, energetic nuclei enter the Earth's upper atmosphere and collide with the atoms there; the result is a cascade of neutrons that arrive at the Earth's surface in the polar regions. There exists a global array of sensors to record these events in the two polar regions. It takes a very hard, intense solar flare to produce a GLE. Although no GLEs were recorded in the 11 years prior to 1989, there were seven during 1989! Each had associated space and terrestrial consequences.[19]

When it first appeared on the solar disk on 6 March 1989, sunspot region 5395 gave hints of what was to come. It initially was observed as a massive, complex spot group and was classified at the highest level of complexity. It maintained that complexity for the remaining 13½ days of its passage on the solar disk. (Actually, this volatile region was detected both before and after it came into view.) This active region is noteworthy with respect to the amount of activity it produced on its first and only passage. But what a passage it was![20]

Photo 1.E, provided by the National Solar Observatory in Sunspot, New Mexico, shows a nine-panel photograph of the 9 March 1989 flare and massive particle ejection. The pictures taken at 1555 UTC and 1605 UTC show a massive particle cloud being ejected from the flaring region. Solar astronomers speculated that this may have been the largest flare in terms of size that ever was observed.[20] Ionospheric effects from this flare were dramatic, and they produced degradation on all HF systems. This is one of ten large flares that occurred between 6 and 17 March. From 6 March onward, each large flare caused operational problems for LORAN navigation systems worldwide, and HF radio could not be used to notify ships at sea that there were environmental causes for their navigation problems. Low-altitude, high-inclination satellites began to experience periods of uncontrolled tumbling as they transited regions of high magnetic-field gradients caused by field-aligned currents. During one large flare, satellite operators even indicated that they were not aware of any satellite anomalies because their communication links to the satellites were out of operation due to the storm![21]

As a result of a major flare on 10 March, a severe magnetic storm occurred on Earth on 13–14 March. During this period overhead aurora was observed as far south as Texas. The huge geomagnetic variations above Canada caused induction problems that disabled portions of that country's power distribution system. During magnetic storms on 17 and 18 March, increased atmospheric drag, produced by continuous particle bombardment from the succession of flares, caused orbiting satellites and "space junk" to change orbits, resulting in their positions being moved outside expected "windows" of observation.

Throughout all of these events operators of satellites in geostationary orbit were kept quite busy re-initiating systems that were knocked out by energetic particles and performing station-keeping operations when the shock waves from large particle clouds knocked their satellites "off station." This solar disturbance also produced SIDs, and major HF blackouts and disturbances, that lasted several days.

While the Sun remained active during the next four months (April through July), even the large flares observed during that time seemed tame compared to those observed in March. Then, on 12 August 1989 the first of six major flares occurred, almost on a daily basis. Very high-energy protons reached the Earth's atmosphere anywhere from minutes to hours after each flare. On the 16th of August a major flare launched a high-energy proton cloud that reached Earth minutes after this event occurred. It started an SID on Earth that was followed by a severe and prolonged ionospheric disturbance. It also had serious consequences in space. During this event, half of the GOES-6 weather satellite telemetry system was lost. Users of satellite systems that employed star sensors for navigation reported spurious events as the sensors became confused by the solar particles. Many satellite systems operators reported having to reset or re-initiate their space-borne digital hardware.[21]

On 29 September a large flare produced another of the numerous GLEs seen in 1989. Very high-energy solar protons measured by monitors worldwide exhibited the largest increase measured in 33 years (since the start of the satellite age)! Again, users of the HF spectrum faced long periods of blackouts and severe disturbances. This event also had its effects on satellites in Earth orbit. For example, it was reported that photo-sensitive components on the MAGELLAN space probe, enroute to Venus, were damaged; GOES power panel outputs were permanently damaged; NOAA-10 experienced rare "phantom commands"; and numerous geostationary and orbiting satellites experienced "hits" in their digital systems.

Another series of solar flares occurred between 19 and 26 October; they had a serious effect on terrestrial HF communication systems as well as on satellites. Specifically, a large number of satellites, including GOES-5, -6, and -7, were reported to have received severe damage to their solar-panel arrays. It also was reported that astronauts aboard the Shuttle Atlantis and cosmonauts aboard the MIR Space Station experienced physical effects. For a more complete review of the effects caused by the unusually large solar events of 1989, see Reference 21.

Summary of Record 1989 Solar Flare Activity

In summary, 1989 was an unprecedented year for solar disturbances (see Table 1.2). It was marked by seven major solar events. These were among the largest events on record, as measured by the high degree of solar particle radiation ejected into space (and, consequently, into the Earth's atmosphere). By the time 1989 ended, HF propagation was completely or badly disturbed during one-third of the year, and a large number of space-borne satellite systems were damaged.

1.6 References

1. *Radiomans' Guide,* Theo. Audel & Co., New York, 1939.

2. Kendrick, G.W., "The Kennelly-Heaviside Layer—Its Relationship to Our Everyday Communication Problems," G. W. Kendrick, *QST,* September 1936.

3. Rice, C. W., "Short-Wave Radio Transmissions and Its Practical Uses," *QST*, July 1927.

4. Wright, J. W., "Dependence of the ionospheric *F* region on the solar cycle," *Nature,* 194, 1962, p. 461.

5. Chapman and Milne, *Quarterly Journal of the Royal Meteorological Society,* Vol. 46, 1920, p. 357.

6. Landmark, B., "The Ionosphere," NATO AGARD Lecture Series, Radiowave Propagation, XXIX, July 1968.

7. Rose, R. B., "High Resolution HF Time of Arrival Measurements (1981–1985)," *Radio Science,* Vol. 23, No. 3, May–June 1988, pp. 257–264.

8. Rose, R. B., and R. D. Hunsucker, "Auroral-*E*

Observations: The First Year's Data," NRaD Technical Document 2449, February 1993.

9. *Ionospheric Predictions,* Institute of Telecommunication Science, U.S. Department of Commerce. Copies available from National Technical Information Service (NTIS), P.O. Box 1553, Springfield, VA 22151.

10. *Atlas of Ionospheric Characteristics,* Radio Communications Sector,* International Telecommunications Union (ITU), Place des Nations, Geneva, Switzerland.

11. *The ARRL Antenna Book,* 1995, available from the American Radio Relay League, 225 Main Street, Newington, CT 06111.

12. Davis, K., *Ionospheric Radio,* Peter Peregrinus Ltd., London, U.K., 1990.

13. "Sky-wave Field Strength at Frequencies between 2 and 30 MHz," Report 252-2, Radio Communications Sector,* International Telecommunication Union (ITU), Place des Nations, Geneva, Switzerland.

14. Dieminger, W., "Ionospheric Propagation of High Frequency Radio Waves," AGARD Lecture Series, Radiowave Propagation, XXIX, July 1968.

15. Jaroff, L., "Fury on the Sun," *Time*, July 3, 1989, pp. 46–55.

16. Gorney, D. J., "Solar Cycle Effects on the Near-Earth Space Environment," *Review of Geophysics,* 28,3/August 1990, pp. 315–336.

17. Goodman, J. M., *HF Communications: Science and Technology,* Van Nostrand Reinhold, New York, 1990.

18. McNamara, L. F., *The Ionosphere: Communications, Surveillance, and Direction Finding,* Krieger Publishing Co., Malabar, Florida, 1991.

19. Allen, J. H., "Major Solar Activity of 1989 and Its Consequences at Earth and In Near-Earth Space," Proceedings on the First Annual Conference on Prediction and Forecasting of Radio Propagation at High-Latitudes for C3 Systems, U.S. Naval Postgraduate School, Monterey, California, 12–14 February 1991.

20. Cliffswallow, Maj. Willow, "Region 5395 of March 1989," NOAA Technical Memorandum ERL SEL-82, November 1993.

21. Allen, J.H., and D.C. Wilkinson, "Solar Terrestrial Activity Affecting Systems in Space and on Earth," NOAA, NGDC, 1991.

**In 1992, the International Radio Consultative Committee (CCIR) was renamed the Radio Communications Sector of the International Telecommunication Union.*

Chapter 2

Sunspots and The Sunspot Cycle

When the Jesuit Friar Joseph Scheiner, one of the first specialists in solar research, saw his first sunspot with an early telescope in 1611, his fellow astronomers called it a stain on the lens of the telescope! Today, of course, we know that sunspots are relatively cool regions on the Sun's surface that are characterized by tremendous eruptions of whirling, electrified gases (plasma) associated with strong magnetic fields. Because these gases are cooled to temperatures below those of the Sun's surface, they appear darker, and so, they are called sunspots. We also know that the number of sunspots on the solar surface rises and falls with a period of roughly 11 years, and that because of the ultraviolet and x-ray radiation associated with them, sunspots are responsible for forming the ionosphere, a region in the Earth's atmosphere that makes possible shortwave communications.

In this chapter we discuss sunspots and the sunspot cycle. In particular, using data on sunspot observations that have been collected since 1755, we examine the characteristics of the 22 cycles reported to date. Particular emphasis is placed on the most intense cycle to date (Cycle 19), on a cycle with an unusually high peak and record plateau (Cycle 20), on a cycle that was very active and that reached a higher level than predicted by most observers (Cycle 21), as well as on the current cycle (Cycle 22), which has produced an unprecedented number of solar flares and other solar phenomena and which is expected to end in 1996 or 1997. For those readers who would like to attempt their own studies of solar activity, we include a complete listing of the smoothed sunspot numbers recorded since 1749 by the Swiss Federal Observatory in Zurich, Switzerland, and more recently (since the second half of 1980) by the Royal Observatory of Belgium.

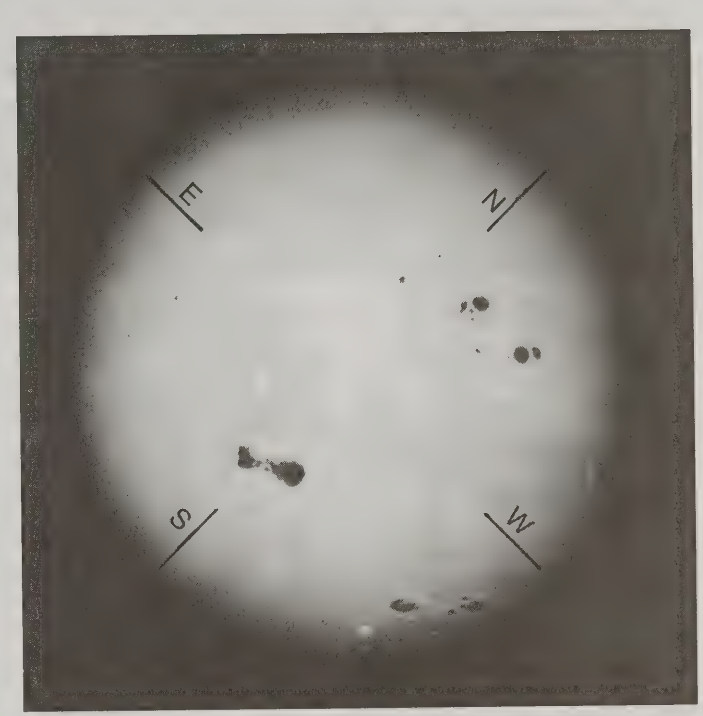

Photo 2.A. A large group of sunspots seen on the face of the Sun. The sunspots move from the east limb of the Sun towards the west as the Sun rotates. (Official U.S. Navy photo.)

2.1 Sunspots

Sunspots are thought to exist as a result of intense, localized magnetic fields that are trapped below the surface of the Sun. Following is one explanation as to how sunspots form.

At solar minimum, spots associated with the new cycle appear at the mid-latitudes. The magnetic fields are longitudinal, running north and south. However, as the Sun rotates, the magnetic fields under the solar surface rotate at different speeds, with the equatorial region of the Sun spinning at a slower rate than do

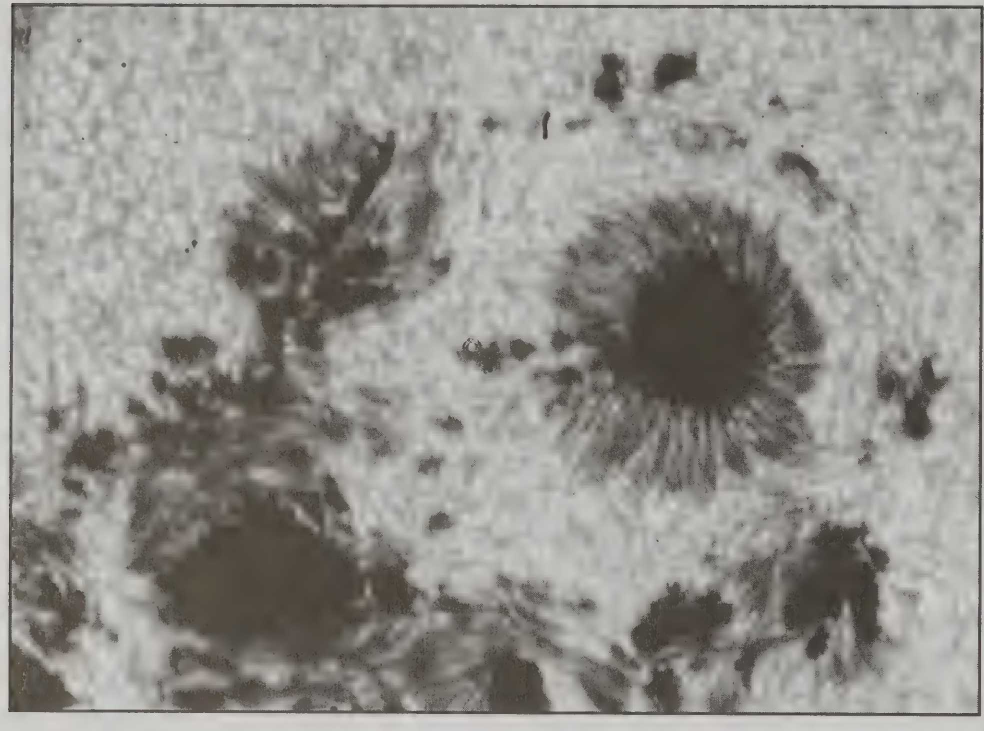

Photo 2.B. Large sunspots embedded in the solar surface. Photographed with unprecedented sharpness from an unmanned research balloon at an altitude of 80,000 feet. Note the granular composition of the Sun's surface. (Official National Science Foundation photo.)

regions at the higher latitudes. This causes the magnetic fields to distort and to realign slowly in an east-west direction. Tremendous energy builds up under the solar surface, starting at the higher (mid) latitudes and migrating toward the solar equator over the four- to five-year period to solar maximum. As these fields build in magnetic potential, they erupt through the surface, forming a huge magnetic loop. The solar surface, where this eruption appears, cools significantly, causing that region to be darker than the surrounding solar surface. At solar maximum the magnetic fields are almost completely latitudinal. From this point, sunspot activity begins its decline. At the end of roughly 11 years, the polarity at the poles associated with sunspots will reverse, the magnetic fields for spots associated with the new cycle will again be longitudinal, and the process starts over.[1]

The area around the sunspot, called the *plage* (because of the associated temperature differential and turbulent magnetic field), becomes an electromagnetic and cosmic-ray generator. Energy levels in the spectrum ranging from the visible through ultraviolet and x-ray emissions are elevated. When the magnetic field breaks down, a flare results, emitting tremendous quantities of radiation and energetic particles.

Photo 2.A of the Sun was taken at the U.S. Naval Observatory in Washington, D.C. The sunspots appear as black spots on the solar surface. Photo 2.B is an unprecedented close-up of sunspots embedded in the solar surface.

Sunspots almost always appear in groups, probably the most notorious of which was Region 5395 in March 1989, which was accompanied by a series of large solar flares and massive ejections of energized particles. (What happened over the 14-day period as Region 5395 crossed the visible solar disk will be discussed later in this chapter.) Groups may range in size from small clusters of tiny specks a few hundred miles in diameter to enormous groups stretching nearly a quarter of a million miles across the Sun's surface and containing individual spots as large as 80,000 miles in diameter . . . an area into which several planets the size of the Earth could easily disappear!

Sunspots, although embedded in the Sun's surface, appear to move in an east to west direction as the Sun rotates. If a spot is born on the side of the Sun out of view from the Earth, it will first become visible as it crosses the Sun's eastern edge. It will then drift westward across the visible face of the solar disk, and disappear out of sight behind the western edge in slightly more than 13½ days, which corresponds roughly to half the period of rotation of the Sun. The spot then enters the hidden side of the Sun for the next 13½ days.

The lifetime of a sunspot, or of a sunspot group, varies from a few days to several months. Larger sunspots often are visible during several solar rotations, reappearing roughly every 27 days. For this reason, many terrestrial phenomena that are believed to be influenced by sunspots tend to recur at intervals of about 27 days.

High-Flying Animal or Electro-Magnetic Eruption?

History vaguely records that sightings of sunspots before the invention of the telescope, if they drew any explanation at all, were usually thought to be either slow, high-flying animals or far-away clouds. It was, in fact, Galileo, inventor of the telescope in 1610, who offered the first serious explanation of sunspots. In 1613, he wrote:

> "Having made repeated observations, I am at last convinced that the spots are objects close to the surface of the solar globe, where they are continually being produced and then dissolved, some quickly and some slowly; also that they are carried around the Sun by its rotation, which is completed in a period of about one lunar month. This is an occurrence of the first importance in itself, and still greater in its implications." [2]

In this explanation, elementary as it was, Galileo was far closer to the truth than were many of his successors during the next 300 years.

During the 18th and 19th centuries various explanations for sunspots were given by noted astronomers. Some considered sunspots to be cold mountain peaks towering above the luminous surface of the Sun; others, believing that a fiery, luminous cloud surrounded the Sun, thought that sunspots were holes in this cloud, caused by hurricanes, through which could be seen the cool areas of the Sun!

One of the most significant discoveries concerning sunspots took place in 1908. Using his newly invented spectro-heliograph, Dr. George E. Hale of the Mount Wilson Observatory in California photographed certain characteristics of the Sun for the first time. From these he was able to demonstrate that large sunspots are frequently engulfed in whirling masses of gas, or vortices.

Six years later, in 1914, Dr. Hale made another remarkable discovery. He proved that magnetic fields, often more powerful than the magnetic field surrounding the Earth, occur at the center of sunspots.

Working with these two important facts, that sunspots are engulfed in whirling masses of gas and that they are surrounded by magnetic fields, scientists have developed the explanation for the evolution of sunspots discussed earlier.

The Sunspot Cycle

Sunspots are known to have been observed by the Chinese many years before the birth of Christ. But it was not until 1611, one year after Galileo's invention of the telescope, that permanent records of sunspot activity were first made. In that year Galileo and his contemporaries began to draw pictures of the Sun's surface by projecting telescopic views upon a white wall or screen. A number of Galileo's drawings of the solar disk made in 1612 still exist, and these show many large sunspots.

It was not until the middle of the 18th century, however, that many European astronomers independently began keeping sunspot records on a regular

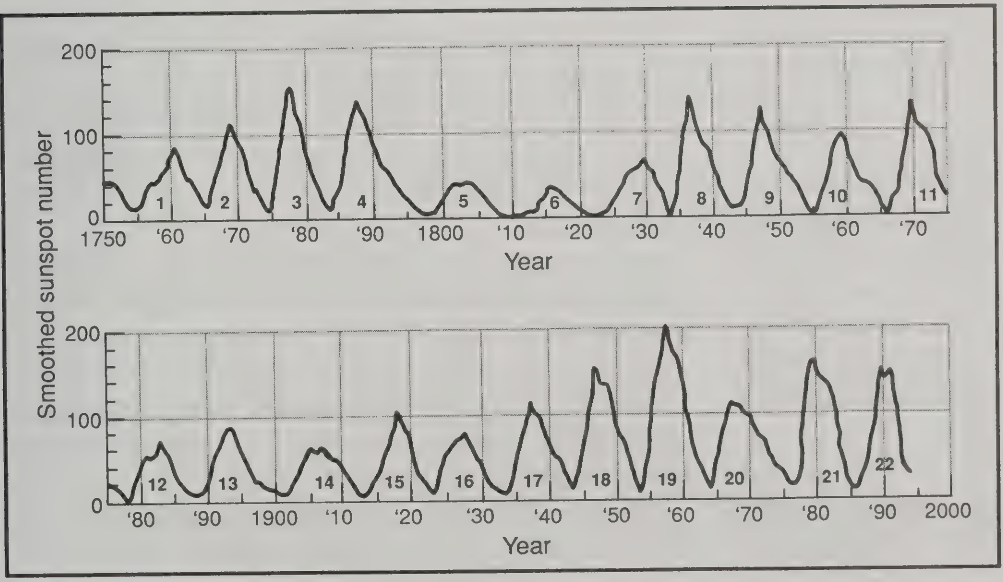

Figure 2.1. A plot of all solar cycles recorded between 1750 and 1994. Twenty–one complete cycles have been recorded; in 1994, the 22nd was decreasing steadily towards a minimum.

basis. To one of these—Hendrick S. Schwabe, a pharmacist from Dessau, Germany, who engaged in astronomy as a hobby—goes credit for the discovery of the sunspot cycle.

With the intellectual curiosity characteristic of a true scientist, Schwabe began his work on the Sun in the early part of the 19th century, painstakingly counting the spots he saw with his small telescope, day after day and year after year. After several years he observed that the number of sunspots he saw varied over wide limits in a fairly regular manner. During some years he found the face of the Sun almost completely free of sunspots, month after month. During other years he saw hundreds of spots day after day. After observing the Sun almost every day for nearly 20 years, Schwabe concluded that sunspots came and went in a periodic fashion, varying from a minimum, to a maximum, to a minimum again in about a decade's time. He published his findings in 1843.

Sunspot Numbers

Shortly after Schwabe's discovery the director of the Zurich Solar Observatory, Rudolph Wolf, devised a means for all astronomers to describe relative sunspot activity in terms of a common standard. The Zurich Solar Observatory had been recording sunspot data on a regular basis since 1749, and Wolf realized the great importance of having other observatories and astronomers, who used various types and sizes of telescopes, report their observations according to a common standard.

Wolf called his standard a *sunspot number.* The sunspot number is obtained from daily solar observations of individual sunspot groups according to the following equation:

$$R = k(10g + f) \qquad (1)$$

where: R is Wolf's relative sunspot number;
g is the observed number of sunspot groups;
f is the total number of sunspots, either individually or in groups; and
k is a factor for bringing observations of many different observers into general agreement; it takes into account the type and power of telescope used, the viewing conditions, and observer biases.

The factor 10, which multiplies g, was selected by Wolf in order to give greater weight to the large active sunspot groups, which he intuitively judged to be a more important criterion of general activity, than to small spots of short duration. Thus, the sunspot number is more an index of solar activity than of the actual number of spots on the face of the Sun.

From 1849 to 1981 the Zurich Observatory published daily sunspot numbers, recorded near mid-day, according to Equation 1. These numbers are known as the *Zurich Sunspot Numbers,* and they represent the official sunspot count upon which sunspot information is based. Because a record of daily sunspot observations, R, exhibits wide fluctuations, it is necessary to smooth the data in order that trends may be observed. The first smoothing is done by averaging the daily numbers over a one-month period; the result is the monthly mean relative sunspot number, R_m. Even the monthly mean numbers are subject to month-to-month fluctuations that tend to mask trends, and they do not correlate too well with general shortwave propagation conditions. As such, monthly means are smoothed by taking a 12-month running average. The 12-month running smoothed sunspot number, R_s (also referred to as SSN) is derived from the following equation:

$$R_s = \frac{\tfrac{1}{2} R_{m1} + R_{m2} + R_{m3} + \ldots + R_{m12} + \tfrac{1}{2} R_{m13}}{12} \qquad (2)$$

where: R_s (or SSN) is the 12-month running smoothed sunspot number centered on R_{m7};
R_{m1} through R_{m13} are monthly mean relative sunspot numbers for 13 consecutive months.

Values of 12-month running smoothed sunspot numbers reported since 1749 are given in the appendix of this chapter[3,4,5] and are plotted in Figure 2.1. It is the smoothed sunspot number, plotted over a long period of time, that exhibits the well-known solar cycle variation and that is used to define the sunspot cycle. The 12-month running smoothed sunspot number correlates closely with overall ionospheric propagation conditions.

Wolf began publishing daily sunspot numbers in 1849. This effort, carried on by his successors at the Zurich Observatory, resulted in a long, unbroken, and very valuable series of solar data over more that a century's duration. In 1852, Wolf, using the sunspot records of earlier observers, reduced to sunspot numbers those data going back to 1749.

Beginning on 1 January 1981, responsibility for the determination of the so-called Zurich sunspot num-

Characteristic	Average
Sunspot minimum	New cycle begins with 12-month running smoothed sunspot number between 0 and 12; 6 is average.
Ascending period to maximum value	Varies between 2.6 and 6.9 years, with 4.0 years as average.
Maximum values	Ranges between 49 and 201, with an average of 112.
Descending period from maximum to minimum	Varies between 4 and 10.2 years, with 6.8 years as average.
Period from minimum to maximum to minimum	Average is 10.8 years.
Interval between the maxima of two adjacent cycles	Ranges from 7.3 to 17.1 years, with an average of 10.9 years.

Table 2.1. The "average" sunspot cycle (Cycles 1–21, inclusive).

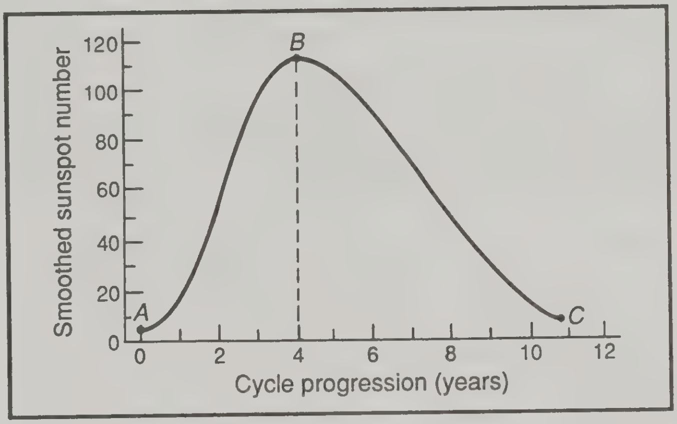

Figure 2.2. The average sunspot cycle based on the characteristics of the 21 cycles which have taken place since 1750. At (A) the minimum value is 6; at (B) the average maximum value is 112; and (C) marks the end of the cycle, 10.8 years after its beginning. The average time interval for the rising portion (A-B) is 4.0 years, while the average time interval for the descending portion (B-C) is 6.8 years.

bers was officially transferred from the Swiss Federal Observatory to the Royal Observatory of Belgium in Brussels. Numbers are still based on observations made at the solar observatory in Locarno, Switzerland, thus assuring continuity between the pre-1981 sunspot numbers and those numbers prepared by the Royal Observatory.

Monthly average sunspot numbers and the corresponding smoothed values also appear each month in *CQ*'s "Propagation" column.

While sunspots are now under daily scrutiny by the giant telescopes of dozens of solar observatories throughout the world, large sunspots often can be seen with the naked eye, **provided that a special aluminized Mylar filter, or some other suitable ray filter (e.g., a welder glass shade #14) is used to protect the eye's retina from serious damage by the Sun's rays. Under no circumstances should the Sun be viewed with the naked eye.**

Occasionally, at sundown or when light haze or fog obscures the Sun's rays, large sunspots may be seen, often accidentally, without use of a telescope or Sun filter. Such was the case in London some years ago, where the *Daily Telegraph* and *Morning Post* reported that thousands of persons were able to see two enormous spots on the face of the Sun during a foggy sunset. It no doubt was due to accidental occurrences of this sort that history recorded the sightings of sunspots by the Chinese, Greeks, and Egyptians more than 1000 years before the invention of the telescope.

Sunspots and The Ionosphere

From a radio communications viewpoint, perhaps the greatest discovery concerning sunspots was made during the early 1930s, when Edison Pettit and his associates at the Mount Wilson Observatory found a direct relationship between the smoothed sunspot number and the intensity of ultraviolet energy radiated by the Sun.

Beginning in 1924, Dr. Pettit undertook daily systematic measurements of the intensity of ultraviolet radiation emanating from the Sun. During the years from 1924 through 1928, he found a steady increase in the ultraviolet level as the smoothed sunspot numbers increased. After 1928, when the sunspot cycle began to decline, Dr. Pettit observed a corresponding decrease in ultraviolet intensity.

Because ultraviolet radiation from the Sun is mainly responsible for forming the ionosphere, which makes possible shortwave radio communications over long distances, Dr. Pettit's discovery was of paramount importance. In relating the sunspot number to the intensity of ultraviolet radiation, he also was relating it to the intensity of ionization in the upper atmosphere.

The more sunspots, or plage areas, that produce emissions that cause photo-ionization of the ionosphere, the denser will be the ionosphere and the higher will be the frequencies that it will propagate. During solar maximum, frequencies over 30 MHz will be propagated; during solar minimum, nothing much above 15–20 MHz is reliable. Simply put, the

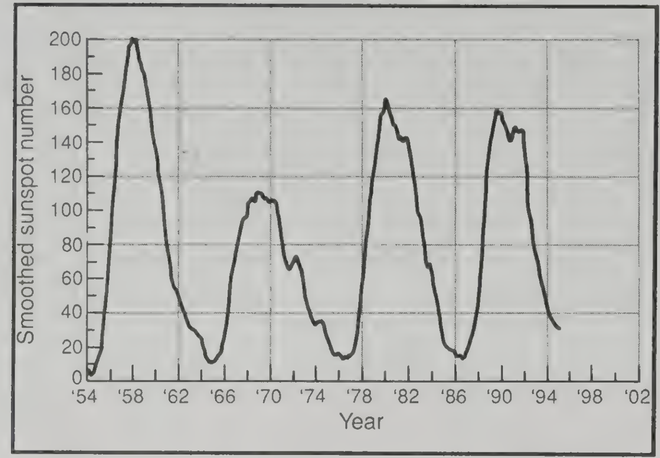

Figure 2.3. The last four sunspot cycles, Cycles 19-22 inclusive, despite their regular appearance, have exhibited a variety of unusual characteristics.

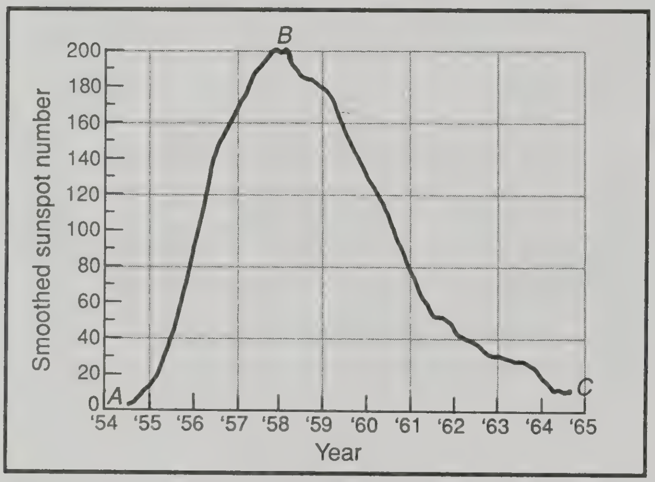

Figure 2.4. Sunspot Cycle 19, April 1954 to October 1964. At (A), the cycle began with a smoothed sunspot number of 3. The record-breaking peak occurred during March 1958 with a level of 201 (B). The cycle ended with a smoothed sunspot number of 10 at (C).

HF user loses at least the upper third of his spectrum during solar minimum, and sometimes he loses as much as half.

Sunspot Cycle Behavior

Figure 2.1, based on the smoothed sunspot numbers computed since 1749, shows the cyclic nature of this solar index. In accordance with the Zurich Observatory's cycle numbering system, the cycle that began in 1755 is shown as Cycle 1. Since that time, 21 complete cycles have occurred, with this being written during the decline of Cycle 22, now estimated to end in 1996 or 1997.

Inspection of Figure 2.1 shows that sunspot activity varies in a periodic manner, resulting in alternate minima and maxima at intervals of several years. The number of years for a complete cycle of activity—from minimum, through maximum, and back to minimum again—varies somewhat with each cycle, but has an average period close to 11 years. For this reason, the variation in sunspot activity is called the 11-year sunspot cycle. It should be noted, however, that no two cycles are exactly alike, and some cycles are as short as 9 years and others last as long as 14 years. The last complete cycle, Cycle 21, began in June 1976 and ended in September 1986.

The average cycle determined from data for the first 21 recorded cycles is summarized in Table 2.1 and Figure 2.2, and will serve to orient the reader to general sunspot cycle behavior. It must be emphasized, however, that there have been rather large deviations from these average values in the characteristics of many individual cycles.

In recent years correlation between observed solar cycle and proxy data such as radiocarbon dating of soil sediments and ancient tree rings suggests that our relatively regular 11-year solar cycle over the last 250 years may well be anomalous when viewed using proxy data that date to about 3000 BC. Other indicators of past sunspot activity include auroral observations from high-latitude monasteries in Europe. Most recently there is evidence that between 1645 and 1715, there seems to have been virtually no sunspot activity at all, and certainly there is no evidence for a solar cycle. This period was the early era of using telescopes for solar observation, and at first, this lack of sunspot observations was attributed to an inconsistent measurement program and poor equipment. It was Walter Maunder, upon reviewing the historical data in the 1890s, who pointed out that an extended minimum, in fact, had occurred. This period is now known as the "Maunder Minimum."[6] It also has been suggested that there was another extended sunspot minimum between 1460 and 1550, called the "Sporer Minimum." Radiocarbon dating indicates that there was a 200-year maximum between 1140 AD and 1340 AD (the "Medieval Maximum") and another 140-year maximum between 1 AD and 140 AD (the "Roman Maximum"). Compared to the last 5000 years, the last 21 solar cycles have been well behaved indeed!

The following sections will discuss the last four solar cycles and the highlights of each. Figure 2.3 shows the last four solar cycles—Cycles 19 through

	1954	1955	1956	1957	1958	1959	1960	1961	1962	1963	1964
Jan.		14	89	170	199	179	129	80	45	29	20
Feb.		16	99	172	201	177	125	75	42	30	18
Mar.		20	109	174	201	175	122	69	40	30	15
Apr.	3	23	119	181	197	169	120	64	39	29	13
May	4	29	127	186	191	165	117	60	39	29	11
Jun.	4	35	137	188	187	161	114	56	38	28	10
Jul.	5	40	146	191	185	156	109	53	37	28	10
Aug.	7	47	150	194	185	151	102	53	35	27	10
Sep.	8	56	152	197	184	146	98	52	33	27	10
Oct.	8	64	156	200	182	141	93	51	31	26	10
Nov.	10	73	160	201	181	137	88	51	30	24	
Dec.	12	81	164	200	181	133	84	49	30	21	

Table 2.2. Cycle 19 exhibited the highest level of sunspot activity ever observed.

the present one, Cycle 22. While Cycle 19 still is acknowledged as the "grand-daddy" of modern solar maxima, Cycle 22 to date has proved to be very exciting. Some of the events associated with the current cycle will be discussed in the section on Cycle 22.

2.2 Cycle 19 (1954–1964)

Solar Cycle 19 peaked during March 1958, and it exhibited the most intense level of solar activity ever recorded. It is this cycle to which all other cycles are at least qualitatively compared, and so, we briefly review Cycle 19 before proceeding with the review of the last three cycles.

Unprecedented Activity

Cycle 19 officially began during April 1954, with a smoothed sunspot number of 3.3 (see Figure 2.4 and Table 2.2). By November 1956, the cycle had already exhibited intense activity and had exceeded the previous record count of 159 that was recorded in May 1778 during Cycle 3. In the months that followed, solar activity continued to increase, and by March 1958, the smoothed number had reached an unprecedented peak of 201.

As a result of the unusually high level of solar activity, high-frequency radio conditions were better during the years 1957–1959 than they had ever been in the entire history of radio. Also in this time period, work in ionospheric sciences accelerated. The International Geophysical Year (IGY) in 1957 coordinated a global campaign to measure and correlate ionospheric characteristics. At about the same time, technology in electronics expanded in all directions, giving users of the shortwave spectrum the equipment they needed to exploit the exceptionally good propagation conditions. Together with the period of unprecedented activity, there came a new generation of HF users.

Once In A Lifetime Conditions

Because of the intense ionization of the ionosphere during the period 1957–1959, shortwave radio conditions—especially on the 20, 15, 11, 10, and 6 meter bands—were exceptionally good. Worldwide propagation was observed on 6 meters, while the 20 meter band was open around the clock. Ten meters was open from sunrise to sunset (and beyond, in some cases), and 25 watts of power on AM radiotelephone was sufficient to work the world. Then, too, direct reception of European and Latin American TV broadcasts in the 45–65 MHz bands, while amusing, caused considerable interference in the United States. Such conditions obviously occur very seldom . . . perhaps only once in a lifetime.

The Decline

From its peak in March 1958, Cycle 19 slowly declined towards its minimum. It reached this point in October 1964 with a smoothed sunspot number of 10. The cycle had lasted 11.5 years, and it had exhibited the most intense level of solar activity ever recorded since regular telescopic observations of the Sun were begun in 1749. Even before Cycle 19 ended, however, the first spots of the new cycle were observed on the face of the Sun (specifically, in September 1963), and they signaled the beginning of Cycle 20 activity.

2.3 Cycle 20 (1964–1976)

The 20th sunspot cycle recorded since solar records have been kept on a regular basis began in October 1964. Reaching its peak in November 1968, this cycle

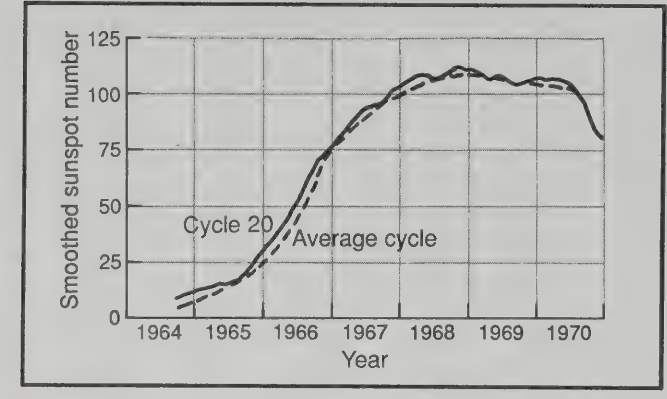

Figure 2.5. Comparison between the first six years of Cycle 20 and the average cycle derived from the previous 19 cycles.

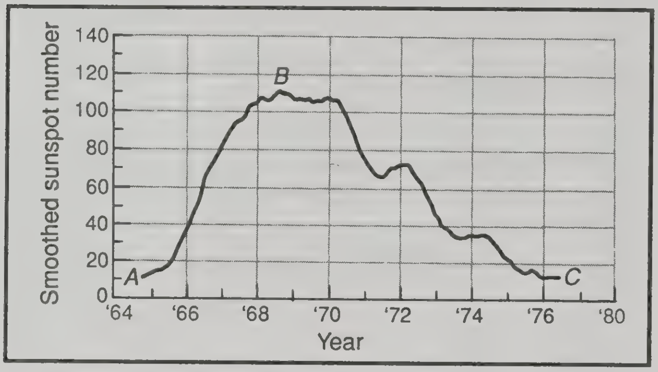

Figure 2.6. Sunspot Cycle 20, October 1964 to June 1976. At (A,) the cycle began with a smoothed number of 10. The peak occurred during November 1968 with a level of 111 (B). The cycle ended June 1976 with a smoothed sunspot number of 12 (C).

gave indications of paralleling the average sunspot cycle (Cycles 1–19) more closely than did any previous cycle. During its decline, however, Cycle 20 exhibited a prolonged decay in activity, and it continued on until June 1976, somewhat longer than the average cycle. Cycle 20's life span was 11.8 years.

Cycle 20—The Beginning

Cycle 20 officially began during October 1964 with a smoothed sunspot number of 10. Figure 2.5 shows that it began at a slightly higher-than-average level of solar intensity, and that it followed the average cycle almost exactly until reaching its peak in late 1968. In fact, the first four years of Cycle 20 paralleled that of the average cycle more closely than did any previous cycle.

Cycle 20 reached its peak during November 1968 with a smoothed sunspot number of 111. This peak is considerably lower than the peak values of the previous two cycles. Cycle 19, for example, soared to a record-breaking maximum of 201 during March 1958, while Cycle 18 peaked during June 1947, with a smoothed sunspot number of 152.

Unusual Behavior At The Maximum

Because its behavior paralleled so well the average sunspot cycle, it was expected to continue to follow the average cycle; that is, it was expected to decline in 6.7 years and to reach a minimum by July 1975. Such was not to be the case.

By July 1970, Cycle 20 had established a new type of record: it had stood practically still for 17 months! Specifically, the cycle hovered at the 106 mark, plus or minus 2, between March 1969 and July 1970. Year-long plateaus have occurred occasionally during previous cycles, but always at lower levels of activity. For example, the longest plateau on record took place during Cycle 5, when the solar index remained in the 40s for more than three years, from January 1802 through mid-1805. Then, too, between December 1827 and April 1829, the cycle remained practically constant at 62. More recently a plateau occurred between November 1926 and December 1927, when solar activity remained at the 70 mark, plus or minus 2. Only once previously, however, has a year-long plateau occurred at a relatively high level of solar activity, and that was during Cycle 11, when a smoothed sunspot count around 100 was recorded during 1872.

By mid-1970, Cycle 20 had distinguished itself by displaying the longest, highest plateau ever recorded in the history of solar observations.

The plateau near Cycle 20's maximum ended in July 1970, when the running smoothed sunspot numbers started to decline once again. However, the unexpected high solar activity observed during 1970 was most welcome, and it provided a continuation of the excellent HF propagation conditions observed during 1968 and 1969. During 1970, the 10 meter band continued in full bloom, with excellent DX openings to almost every corner of the world during the daylight hours of all but the summer months. Excellent worldwide conditions also were observed on 15 meters from shortly after sunrise through the early evening hours throughout almost the entire year. Twenty meters continued to be an around-the-clock DX band, with excellent openings possible at almost any hour. Good DX conditions during the hours of darkness

	1964	1965	1966	1967	1968	1969	1970	1971	1972	1973	1974	1975	1976
Jan.		12	28	75	103	110	106	80	71	51	33	23	15
Feb.		12	31	79	103	110	106	78	71	47	34	22	13
Mar.		13	35	82	105	108	106	74	72	44	34	21	12
Apr.		14	37	85	107	106	106	71	73	43	34	19	13
May		15	41	88	108	106	106	68	73	41	35	17	13
Jun.		15	45	91	107	106	105	67	71	39	35	16	12
Jul.		16	50	94	105	106	104	65	68	38	34	15	
Aug.		16	57	95	105	107	101	65	66	36	33	14	
Sep.		17	63	95	107	105	97	66	62	34	32	14	
Oct.	10	20	68	95	110	104	94	66	61	33	30	15	
Nov.	10	22	70	97	111	105	89	67	59	32	28	16	
Dec.	11	25	73	101	110	105	84	69	55	32	25	16	

Table 2.3. Twelve-month running smoothed sunspot numbers, Cycle 20 (October 1964 to June 1976).

	1976	1977	1978	1979	1980	1981	1982	1983	1984	1985	1986
Jan.		17	61	124	164	140	137	93	60	21	14
Feb.		18	65	131	163	142	133	90	56	20	13
Mar.		20	70	137	161	143	129	86	53	19	13
Apr.		22	77	141	159	143	124	81	50	18	14
May		24	83	147	156	143	120	71	48	18	14
Jun.	12	26	89	153	155	142	117	70	47	18	14
Jul.	13	29	97	155	153	140	115	65	44	17	14
Aug.	14	33	104	155	150	141	109	66	40	17	13
Sep.	14	39	108	156	150	143	101	68	34	17	12
Oct.	14	46	111	158	150	142	96	68	29	17	
Nov.	14	52	113	162	148	139	95	67	25	17	
Dec.	15	57	117	165	143	138	95	64	22	15	

Table 2.4. Twelve-month running mean smoothed sunspot numbers, Cycle 21 (June 1976 to September 1986).

also were observed on 40 and 80 meters throughout most of the year, and even some good 160 meter openings were recorded during the hours of darkness and the sunrise period, particularly during the winter, spring, and fall months.

The Decline

Between July 1970 and July 1971, Cycle 20's activity dropped off considerably—by a count of 40 in a span of year. With this decline came some noticeable changes in shortwave radio propagation conditions. For example, regular F_2-layer DX openings on 10 meters decreased considerably, and although excellent DX conditions held up on 15 meters, especially during the hours of daylight, the band opened less often than during the previous years of higher solar activity. A decrease in band openings also was observed on 20 meters during the hours of darkness, but the band continued to hold up well for daytime DX openings.

Then, in September 1971, Cycle 20 took another strange turn—this time upward again! Solar activity increased from 65 in August 1971 to 73 in May 1972 before the count began to decline again (see Figure 2.6).

From May 1972 through December 1973, the 12-month running smoothed sunspot numbers declined steadily from a count of 73 to 32. Then, Cycle 20 hit another plateau, this one lasting from September 1973 through September 1974, a one-year period during which time solar activity remained practically constant at 33, plus or minus 2. By October 1974, the cycle once again began to decline, but very, very slowly. At times it stalled for a month or two, and at other times, it reversed direction and increased slightly.

Finally, in June 1976, Cycle 20 reached its minimum level of activity with a smoothed sunspot number of 12. This minimum level established a new record: it was the highest level of minimum activity ever recorded in the 225 years that sunspot records had been kept at the Swiss Federal Observatory. The lifespan of Cycle 20 was 11.8 years, one year longer than the average cycle.

Cycle 20 Summary

A list of the 12-month running smooth sunspot numbers calculated for Cycle 20 is shown in Table 2.3 (the values are plotted above in Figure 2.6). Cycle 20 will

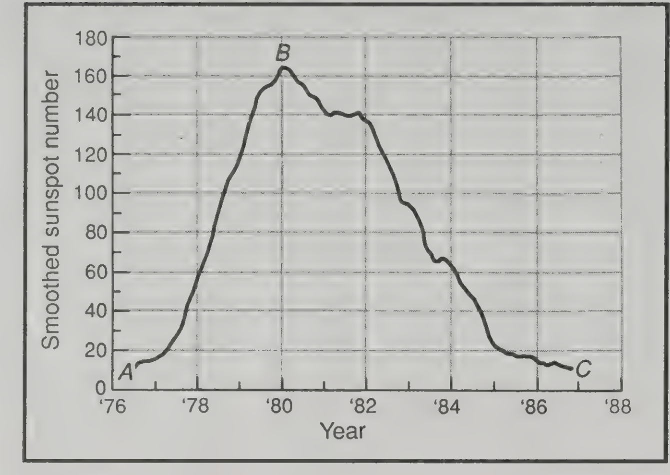

Figure 2.7. Sunspot Cycle 21, June 1976 to September 1986. At (A), the cycle began with a smoothed sunspot number of 12. The peak occurred during December 1979 with a level of 165. The cycle ended in September 1986 with a smoothed sunspot number of 12 (C).

be recorded as one of the most unusual cycles in the historical record because of its many plateaus and its unusually high level of minimum activity.

2.4 Cycle 21 (1976–1986)

Sunspot Cycle 21 started in June 1976 at a count of 12. During the minimum, scientists around the world made forecasts of the expected level of the next maximum. Early on, some scientists were forecasting a very low maximum smoothed sunspot number of approximately 50. Then, in 1976, Dr. Jay Hill at the Naval Ocean Systems Center in San Diego, California, working with Dr. Adolf Paul at ITS, Boulder, Colorado, predicted that the maximum for Cycle 21 would be substantially higher, somewhere in the range around an SSN of 150.[7] Predictions for Cycle 21 became a very controversial subject until independent studies in the U.K. and the U.S.S.R. produced essentially the same results as those developed by Hill and Paul. As history shows, these predictions were correct.

Cycle 21, shown in Table 2.4 and Figure 2.7, was 10.3 years long. The rise, from June 1976 to the maximum SSN of 165 in December 1979, took 43 months. Sunspot numbers greater than 100 generally produce good propagation conditions over the entire HF band, and the activity of Cycle 21 was no exception! Ten meters was open almost every day, and virtually from sunrise to sunset in the fall and winter months. In fact, during this period, active DXers found daylight conditions superb on everything from 20 meters to 6 meters. Even if Cycle 20's numbers were not as high as those of Cycle 19, conditions were still excellent. Cycle 21 produced a maximum over which the SSNs were above 100 for 50 months, above 120 for 41 months, and above 150 for 17 months. Trans-polar paths were especially reliable in the period 1979–1981. There were no really major sustained periods of solar disturbances, and when this is the case, HF propagation is excellent most of the time.

The only major plateau during Cycle 21 occurred between December 1980 and December 1981, when the sunspot number stalled between 138 and 143 (not a bad place to stall for 12 months!). In February 1982, the decline started from a SSN of 133, and the count steadily dropped over the next 52 months to the minimum of 12 in September 1986.

There were several large proton events during this cycle's maximum, although nothing that rivaled the August 1972 event (still considered a benchmark solar disturbance). However, manned space travel, such as

	1986	1987	1988	1989	1990	1991	1992	1993	1994
Jan.		18	58	142	151	148	123	71	37*
Feb.		20	65	145	153	148	115	69	35*
Mar.		22	71	150	152	147	108	67	34*
Apr.		24	78	154	149	146	103	64	34*
May		26	84	157	147	146	100	60	33*
Jun.		28	94	158	144	145	97	56	31*
Jul.		31	104	158	141	146	91	55	
Aug.		35	114	157	140	147	84	52	
Sep.	12	39	121	157	142	145	80	48	
Oct.	13	44	125	157	142	142	76	45	
Nov.	15	47	130	157	142	138	74	41	
Dec.	16	51	138	154	144	132	73	38	

**Provisional; may be subject to slight change.*

Table 2.5. Twelve-month running mean smoothed sunspot number, Cycle 22 (September 1986 to June 1994).

the Apollo missions, had subsided, and there were few satellites in geostationary orbit. High-frequency communications were falling from favor with the military, who opted instead for satellite communications, and interest in the space and ionospheric sciences was starting to wane. This solar maximum, however, was enjoyed by radio amateurs, by CBers, and by shortwave broadcasters and their listeners. Between 1979 and 1982, Navy scientists in San Diego monitored and recorded the DL0IGI beacon on 10 meters. Review of these old strip charts indicates that during this period there were few times when it could not be heard, indicating stable and quiet conditions.

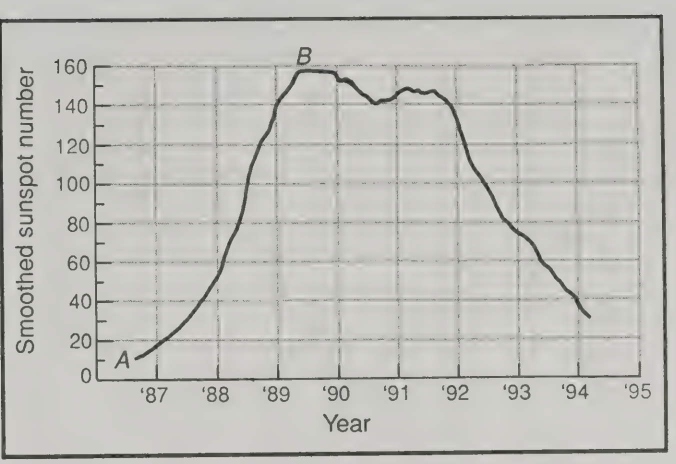

Figure 2.8. Cycle 22 had a broad maximum that exhibited two peaks. Beginning in September 1986 with a smoothed sunspot number of 12 (A), it peaked at a count of 158 in June 1989 (B). The sunspot count, as we go to press, is dropping rapidly, with the minimum expected sometime in 1996 or 1997.

2.5 Cycle 22 (1986–1996/97)

Solar Cycle 22 will go on record as something of an enigma as far as these cycles go. It originally was predicted to have a maximum that probably would not exceed 100. But it did, and not just once, but twice! It had two peaks—the highest in June, July, and August 1989 with an SSN of 158, and a second peak in early 1991 at a count of 148. Overall, Cycle 22 had a volatile, broad maximum in which the smoothed sunspot numbers remained over 130 for 38 months. The decline of Cycle 22 began in November 1991, and a minimum is expected during 1996 or 1997. Predictions for the remainder of Cycle 22 and beyond are discussed in Chapter 3. Table 2.5 lists the smoothed sunspot number through June 1994, while Figure 2.8 shows the somewhat strange shape of the cycle maximum.

Cycle 22—The Beginning

Cycle 22 began in September 1986 with a sunspot number of 12. The rise took place over the next 33 months, until the first of two peaks occurred in June 1989 at an SSN of 158. The cycle's ascent was smooth, with amateurs starting to experience good band openings on 10 and 15 meters by mid-1988.

An Exciting Maximum

The twelve-month running smoothed sunspot numbers for Cycle 22 remained over 150 until April 1990, when they dipped into the low 140s for the remainder of the year. In January 1991, a second peak occurred, with the count rising to 148. It hovered in the mid-140s until November 1991, when the cycle decline abruptly commenced. Propagation conditions during this 40-month maximum were both exciting and volatile. While Cycle 19 was the most spectacular with respect to the sunspot numbers, Cycle 22 will be remembered as the most unpredictable and turbulent. Throughout its maximum it produced a record number of major solar disturbances, with one in 1989 (discussed in Chapter 1) leading the way. Monthly sunspot numbers varied wildly. For example, in June 1990, the monthly mean sunspot number dipped to 105. It rose to 149 in the following month, and peaked in August 1990 with a monthly mean sunspot number of 200. Whereas the rise and fall of Cycle 21 was relatively smooth, with its peak accurately predicted by many scientists, Cycle 22 was marked with large variations in monthly sunspot numbers.

Cycle 22 peaked during an era when the world had placed a lot of reliance on modern satellite communications in general and on space systems parked in geostationary orbit in particular. It is this orbit where there is no protection from solar radiation hazards. Initially, the susceptibility of modern communications to solar disturbances was thought to have diminished because there was less use of the narrow-bandwidth, disturbance-prone HF spectrum. However, in eliminating one vulnerability to solar disturbances, the modern communicator now was faced with a new one: space radiation hazards.

The Decline

Cycle 22 is expected to bottom out sometime in 1996 or 1997. A prediction method has been devised by Patrick McIntosh at the Space Environmental Services Center (SESC), Boulder, Colorado. Basically, he

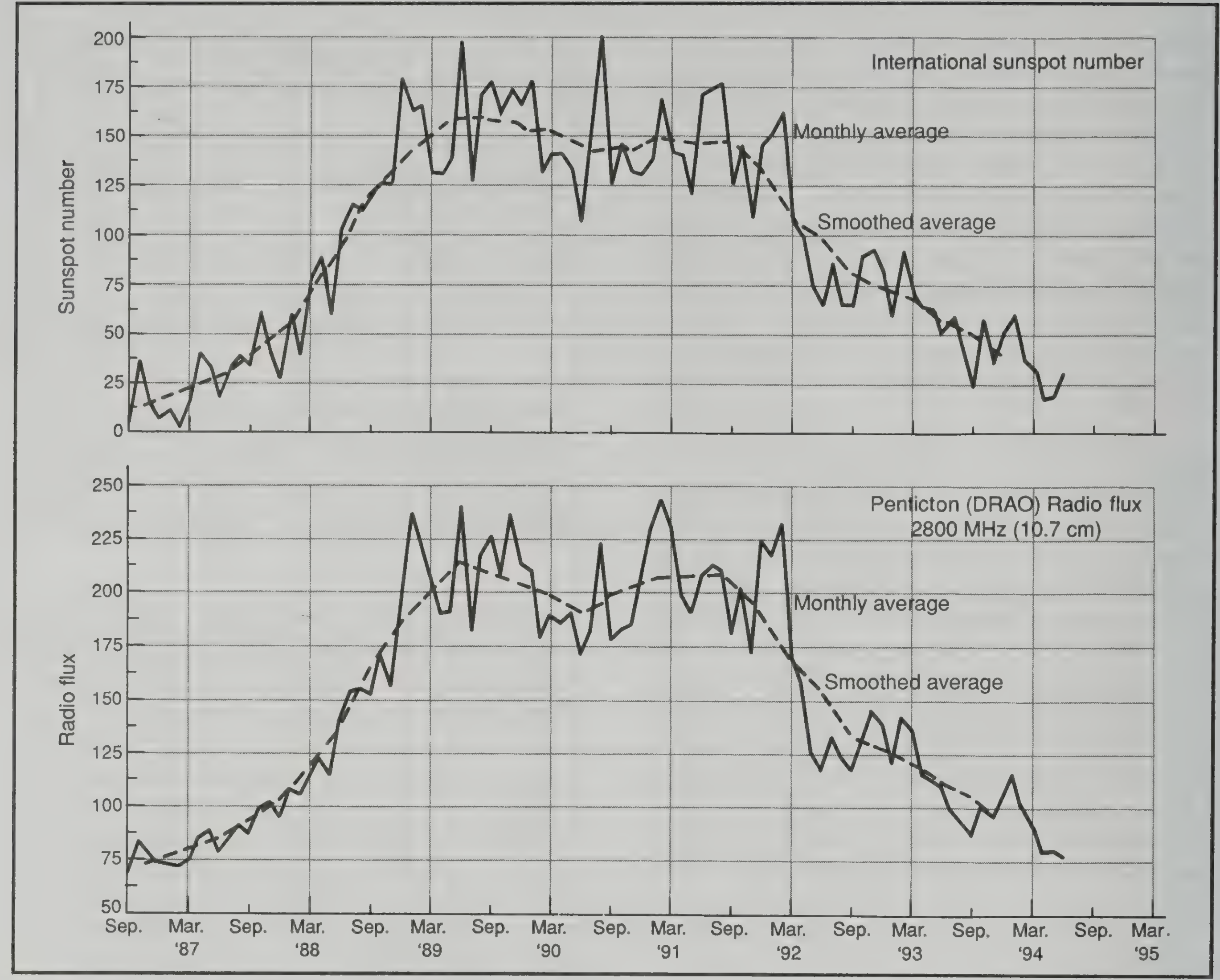

Figure 2.9. Progress of sunspot Cycle 22; note the close correlation between International Sunspot Numbers and 10.7 cm Solar Radio Flux units. (SESC/Hirman/Sutton.)

observes that a cycle ends about three to five years after the first spotless day is recorded following the peak of the cycle. This "event" took place during the fall of 1993, and so, it would indicate that the end of Cycle 22 could occur as soon as the early fall 1996. Cycle 22 appears to fit the "short-cycle" pattern, which has a 10.2-year lifetime.[8] Chapter 3 will discuss in more detail the end of Cycle 22 and what looms ahead for Cycle 23.

2.6 Solar Flux

Sunspots have been observed telescopically for more than 300 years, and daily records are available for observations made since the mid-20th century. Today sunspots are observed daily from a worldwide network of solar observatories. While the telescope at each participating observatory is carefully calibrated against a standard, results can vary between observatories because the measurements are strongly dependent on observer interpretation and experience, and on the visibility conditions in the Earth's atmosphere above the observing site. To compensate for differences, the daily international sunspot number is computed by the Royal Observatory of Belgium as a weighted average of measurements made from the network of participating observatories.

In addition to cosmic and ultraviolet radiation, the Sun is a massive generator of radio energy in the microwave range. This radio energy, or solar flux, changes gradually from day to day. These emissions are caused by a variety of phenoma in the solar atmosphere, including the random collisions of electrons.

Shortly after World War II, scientists found that changes in the level of solar flux were closely associated with the number and size of sunspot groups on the face of the Sun. Using sophisticated and sensitive receiving equipment, with huge, high-gain antennas beamed towards the Sun, many observatories throughout the world now measure solar flux levels on about a dozen selected frequencies between approximately one meter and one centimeter in wavelength. Canadian scientists have been leaders in this field, and they have measured the solar flux on 2,800 MHz (or 10.7 cm) daily at 1700 UTC since February 1947. Observations now are conducted at the Dominion Radio Astrophysical Observatory located at Penticton, British Columbia.

Solar flux measurements are more consistent, considerably less variable, and more objectively determined than are the counts derived from telescopic viewing of sunspots. There is a very close correlation between solar flux and sunspot numbers. Figure 2.9 shows the progress of sunspot Cycle 22 between 1986 and 1993 in both sunspots and solar flux units. Figure 2.10 shows the relationship between sunspots and solar flux based on a long period of measurements. Based on these data, the relationship between solar flux (*SF*) and daily sunspot count (*R*) is approximately linear:

$$SF = 73.4 + 0.62R \qquad (3)$$

A better approximation to the relationship between these two parameters, and one that still is essentially linear, was derived by Stewart and Leftin[9]:

$$SF = 63.7 + 0.73R = 0.0009R^2 \qquad (4)$$

During low periods of solar activity, the flux never falls to zero because the Sun emits some radio energy at all wavelengths, even when there are no visible sunspots. The lowest daily flux since 1947, as measured at a Canadian observatory, was 62.6 units on 3 November 1954. The highest observed value was 457.0, which occurred on 7 April 1947. Another advantage of solar flux measurements is that they are broadcast daily at 18 minutes past each hour over National Institute of Standards and Technology (NIST) radio station WWV located in Colorado, and at 45 minutes past each hour from station WWVH located in Hawaii. Solar flux is rapidly becoming the favored measure of solar activity for use in preparing shortwave propagation predictions and forecasts because it is a more sensitive and objective measure of solar activity and because it is more readily available to the general public than is the daily sunspot number. How solar flux indices and other propagation data transmitted by WWV and WWVH can be used to prepare updated shortwave propagation forecasts and predictions will be discussed in greater detail in Chapter 5.

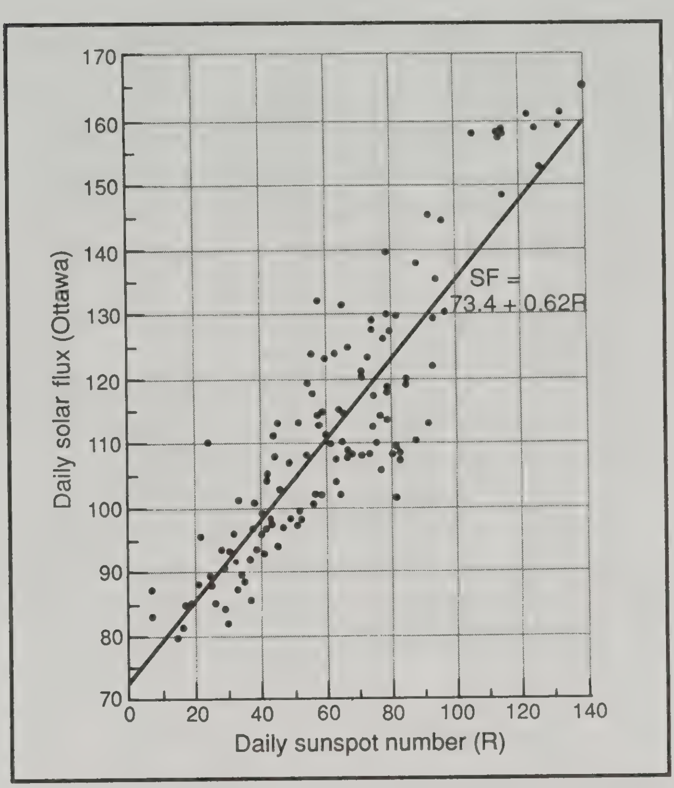

Figure 2.10. Daily solar flux versus daily sunspot number *R*, April–May 1972, 1973. Similar results have been obtained with other data sets.

Despite the increasing use of solar flux units to describe solar activity, telescopic observations of sunspots will continue. Solar flux data do not have the 300-year link with the past that sunspot numbers have. To keep that record unbroken and to provide additional solar and other solar-related cyclic data, sunspots will continue to be studied and counted by observatories throughout the world.

2.7 References

1. Goodman, J. M., *HF Communications Science and Technology,* Van Nostrand Reinhold, New York, 1992.

2. Galileo, "Three Letters on Sunspots," Academia dei Lincei, Rome, 1613.

3. Waldmeier, M. "The Sunspot Activity in the Years 1610–1960," Techniche Hochschule, Zurich, 1961.

4. Waldmeier, M., "Monthly Sunspot Bulletin from the Swiss Federal Observatory," Zurich, 1960–1980.

5. Anon., Royal Observatory of Belgium, 1980 to present.

6. Eddy, J. A. (Ed), *The New Solar Physics,* Westview Press, Boulder, Colorado, 1978.

7. Hill, J.R., "Long Term Solar Activity Forecasting Using High-Resolution Time Spectral Analysis," *Nature,* Vol. 266, No. 5598, March 10, 1977, pp. 151–153.

8. Jacobs, G. "Propagation," *CQ,* July 1994.

9. Stewart, F. G., and M. Leftin, "Relationship between Ottawa 10.7 cm Solar Radio Noise Flux and Zurich Sunspot Number," *Telecommunication Journal,* Vol. 39, No. III, 1972.

2.8 Appendix

Tabulated in this appendix is an update of the first presentation in the popular literature of the 12-month running sunspot numbers recorded since 1749. These data, assembled by the Swiss Federal Observatory, Zurich, Switzerland, were first made available to the scientific community by Prof. M. Waldmeier in 1961. The entries between 1960 and 1980 were derived from monthly mean sunspot numbers that appeared in the Monthly Bulletin of the Swiss Federal Observatory using Equation (2) given earlier in this chapter. Numbers for the second half of 1980 and later were computed using data provided by Dr. Andre Koeckelenbergh of the Royal Observatory of Belgium. The 12-month running smoothed sunspot numbers form one of the longest continuous scientific records of a natural phenomenon, and they are the basis for most studies made of long-term solar activity.

The Solar-Terrestrial Physics Division of the National Geophysical Data Center has copied its master digital Sun, sunspots, and geomagnetism databases onto floppy disks for use on PCs. The *Zurich, Brussels and International Sunspot Numbers (Wolf)* file is available. This file includes daily means (1818 to present), monthly and smoothed monthly data (1749 to present), and yearly means (1700 to present). Floppy disk files also are available for Canadian 10.7 cm solar flux values (1947 to present), geomagnetic indices (1947 to present), sunspot region histories, and coronal indices. Additional information and pricing can be obtained directly from the National Geophysical Data Center, Code E/GC2, Dept. 925, 325 Broadway, Boulder, CO 80303-3328 (phone 303-497-6761, or FAX 303-497-6513).

Year	Jan.	Feb.	Mar.	Apr.	May	Jun.	Jul.	Aug.	Sep.	Oct.	Nov.	Dec.
1749							82	83	84	86	88	89
1750	89	90	92	93	88	84	83	82	79	76	73	70
1751	67	64	60	55	52	49	46	45	46	48	48	47
1752	47	46	45	46	48	48	48	48	46	44	42	41
1753	38	36	37	36	34	32	29	26	23	20	18	17
1754	17	16	14	13	13	12	13	14	14	14	13	11
1755	9	8	8	9	9	9	10	10	9	9	10	11
1756	11	11	11	11	11	11	10	11	12	14	16	17
1757	18	21	24	26	28	31	33	36	38	41	43	45
1758	47	47	47	48	48	47	48	48	48	47	46	46
1759	47	48	50	52	53	53	55	56	58	60	61	62
1760	63	63	63	62	62	63	63	64	66	67	69	72
1761	76	78	80	83	86	87	85	83	81	79	76	72
1762	68	65	63	60	59	60	62	61	58	57	55	53
1763	52	52	50	49	47	46	45	47	48	48	49	49
1764	48	47	46	43	41	38	35	32	30	29	27	26
1765	25	25	25	24	23	22	20	19	19	19	19	18
1766	16	14	13	12	11	11	12	14	15	16	17	19
1767	21	23	26	29	33	36	39	42	43	44	46	50
1768	53	55	58	61	64	67	71	72	72	75	77	78
1769	81	86	92	98	104	106	107	112	116	115	113	112
1770	111	111	109	105	102	101	98	91	86	85	89	94
1771	94	89	86	85	84	82	84	89	90	91	87	80
1772	77	78	75	73	71	68	65	60	58	57	54	53
1773	50	46	44	40	37	36	35	36	37	38	39	39

Year	Jan.	Feb.	Mar.	Apr.	May	Jun.	Jul.	Aug.	Sep.	Oct.	Nov.	Dec.
1774	39	38	37	36	34	32	29	24	20	17	13	11
1775	9	9	9	8	8	7	8	9	9	10	10	11
1776	11	12	13	15	16	19	21	23	25	30	36	41
1777	48	55	63	70	78	88	98	107	114	120	128	139
1778	145	148	152	156	159	157	152	152	153	153	148	142
1779	139	138	134	130	127	126	124	119	116	113	109	107
1780	104	100	98	96	91	87	86	86	83	80	79	80
1781	79	78	75	72	70	69	66	63	61	59	56	51
1782	47	45	43	42	40	39	37	36	36	35	33	31
1783	31	29	28	27	25	24	22	20	18	17	16	14
1784	12	11	10	10	10	10	10	10	10	10	11	12
1785	14	16	17	19	22	24	25	28	32	36	42	46
1786	50	55	61	67	73	79	87	93	98	101	104	108
1787	111	115	119	123	126	130	132	133	137	138	136	138
1788	141	141	141	139	137	133	130	129	128	127	128	127
1789	125	123	120	117	116	118	118	117	116	114	112	109
1790	106	103	101	100	97	93	89	85	81	79	78	76
1791	75	73	71	70	68	67	66	66	65	65	64	63
1792	62	62	62	62	61	61	60	60	59	58	56	55
1793	55	54	51	49	48	47	47	46	44	43	42	41
1794	41	41	41	39	40	41	40	39	38	36	35	33
1795	31	29	28	28	26	23	21	21	20	21	21	20
1796	20	20	19	19	18	17	16	15	13	12	10	10
1797	9	8	8	7	7	7	6	5	6	6	6	5
1798	4	4	4	3	3	4	4	4	5	6	7	7
1799	8	8	8	8	7	7	7	7	7	6	6	6
1800	7	9	10	11	12	13	15	17	19	20	23	24
1801	25	27	28	30	32	34	35	37	38	39	40	41
1802	42	43	44	45	45	45	45	45	45	44	43	43
1803	42	42	41	41	43	43	43	43	43	45	46	45
1804	44	44	45	45	46	47	48	49	49	48	48	48
1805	49	49	49	47	45	43	41	40	38	37	36	35
1806	34	33	32	31	30	29	27	25	24	22	22	20
1807	19	18	16	15	13	11	10	9	8	7	7	7
1808	7	6	7	7	7	8	8	9	9	9	8	7
1809	7	6	5	5	4	3	2	2	1	1	1	0
1810	0	0	0	0	0	0	0	0	0	0	0	0
1811	0	1	1	1	1	1	2	3	3	3	3	3
1812	3	3	4	4	4	5	5	4	5	6	6	7
1813	8	9	9	10	12	12	13	14	14	15	15	15
1814	15	15	15	14	14	14	14	15	16	17	18	20
1815	22	25	28	29	31	34	36	38	41	44	47	48
1816	47	46	46	48	49	47	46	46	47	46	44	43
1817	43	45	45	43	42	41	41	40	35	33	35	36
1818	35	33	32	32	31	31	30	30	29	27	25	24
1819	24	24	23	23	23	24	23	23	23	23	24	23
1820	22	21	21	20	18	17	16	15	14	14	12	11
1821	10	8	7	7	8	7	6	5	5	6	6	6
1822	6	6	6	5	4	4	4	4	3	2	2	1
1823	0	0	0	0	0	1	3	4	5	5	6	6
1824	6	6	7	9	10	9	8	7	9	9	9	10
1825	12	14	15	14	14	16	17	18	18	20	21	23
1826	25	26	27	29	31	34	37	39	41	43	45	47
1827	47	47	49	51	51	51	51	52	53	54	56	60
1828	61	63	64	63	62	63	62	61	61	63	63	61
1829	62	63	63	64	66	67	67	69	70	71	72	71
1830	69	66	65	67	68	70	71	70	69	67	64	62
1831	60	60	60	57	54	50	47	47	45	43	42	41

Year	Jan.	Feb.	Mar.	Apr.	May	Jun.	Jul.	Aug.	Sep.	Oct.	Nov.	Dec.
1832	40	37	33	31	29	28	27	24	21	18	16	14
1833	12	12	12	11	10	9	8	8	8	8	7	7
1834	8	8	8	8	10	12	13	14	15	18	22	24
1835	28	32	38	45	50	55	60	67	74	81	87	93
1836	100	104	106	107	110	116	126	133	137	138	138	139
1837	143	146	147	146	146	142	137	131	127	127	128	126
1838	121	117	114	111	109	105	102	101	99	94	87	82
1839	80	81	86	88	88	87	85	83	82	81	82	82
1840	81	77	71	67	65	64	61	56	53	51	50	50
1841	49	47	44	42	40	37	37	36	36	35	32	29
1842	27	26	25	24	25	25	24	23	21	20	19	19
1843	18	17	16	14	12	11	11	11	12	12	12	12
1844	12	13	14	14	15	15	16	18	20	23	26	28
1845	30	31	32	34	36	38	41	41	43	44	45	47
1846	49	51	55	59	60	61	63	63	64	64	64	65
1847	66	70	75	88	92	97	102	109	113	117	120	123
1848	128	132	127	124	121	122	124	124	125	125	124	121
1849	116	111	108	105	102	99	98	88	85	82	79	78
1850	76	74	74	73	72	69	66	67	67	67	67	67
1851	67	66	65	64	64	64	64	62	61	61	61	60
1852	59	59	57	56	56	55	53	51	49	47	46	45
1853	44	45	45	44	42	40	38	36	34	33	31	30
1854	28	26	24	22	21	21	20	20	19	18	17	16
1855	14	12	11	10	9	7	6	5	5	4	4	3
1856	3	4	4	4	4	4	5	6	6	6	8	9
1857	10	12	14	17	19	22	24	26	30	33	34	36
1858	39	42	45	49	51	54	57	61	64	68	72	76
1859	79	83	86	88	91	93	94	94	94	94	94	95
1860	97	98	97	95	94	95	95	94	93	95	94	91
1861	89	86	85	83	80	78	77	77	74	69	68	68
1862	68	67	65	64	63	61	59	58	58	59	58	55
1863	51	50	47	45	44	44	44	44	44	44	43	43
1864	45	46	47	47	47	48	47	46	44	43	43	41
1865	39	37	36	35	33	31	30	29	28	27	26	24
1866	23	21	19	19	18	17	15	12	10	9	8	7
1867	6	5	5	5	5	6	8	9	11	13	15	17
1868	19	22	24	28	32	36	39	43	46	47	50	57
1869	61	65	68	69	71	73	75	78	84	94	102	106
1870	110	116	120	128	134	138	140	140	140	140	138	135
1871	132	129	125	120	116	113	111	110	108	103	99	98
1872	99	98	99	101	102	102	102	102	102	101	98	92
1873	87	85	81	76	71	68	65	62	58	54	52	52
1874	52	52	50	49	47	45	43	39	37	36	35	33
1875	30	26	23	21	19	18	17	17	16	15	14	13
1876	12	12	12	12	12	11	12	12	11	11	12	13
1877	13	13	13	13	13	13	11	10	10	9	8	7
1878	7	6	5	5	4	3	3	3	2	2	2	2
1879	3	3	3	4	5	6	7	9	11	12	14	16
1880	18	20	24	28	30	31	33	34	37	39	42	44
1881	47	50	50	50	52	54	55	56	57	60	62	62
1882	60	58	58	58	59	60	60	60	58	56	55	55
1883	57	59	59	60	61	62	65	68	71	73	75	74
1884	72	72	72	72	68	65	61	59	57	54	54	55
1885	57	57	56	55	54	53	52	49	48	47	45	41
1886	37	34	32	30	28	26	25	23	20	17	15	14
1887	13	13	13	12	12	13	13	13	13	13	12	11
1888	10	9	8	8	8	7	6	6	6	6	6	5
1889	6	7	7	7	7	6	6	6	6	6	6	6

Year	Jan.	Feb.	Mar.	Apr.	May	Jun.	Jul.	Aug.	Sep.	Oct.	Nov.	Dec.
1890	5	5	5	6	7	7	7	9	10	11	13	17
1891	20	23	26	29	32	35	38	42	46	50	54	56
1892	58	61	65	66	68	71	73	73	74	75	76	77
1893	78	80	81	82	83	84	85	86	86	85	86	87
1894	88	86	83	83	82	79	77	76	75	75	74	71
1895	68	65	65	64	63	64	63	61	60	58	55	53
1896	52	50	48	47	45	43	42	42	39	38	37	35
1897	33	32	31	30	28	27	26	26	26	26	26	26
1898	26	26	25	26	28	28	27	25	23	22	21	20
1899	20	19	17	15	13	12	12	11	11	11	11	11
1900	11	11	11	11	10	10	9	8	8	7	6	5
1901	5	4	4	3	3	3	3	3	3	4	3	3
1902	3	3	3	4	5	5	5	6	7	7	10	11
1903	12	15	16	17	19	23	25	27	28	30	31	33
1904	35	38	40	41	41	42	43	46	50	50	51	51
1905	53	53	55	57	61	63	63	60	59	59	61	62
1906	63	64	64	61	56	53	55	60	63	62	62	60
1907	57	55	56	60	63	63	60	56	51	50	50	51
1908	51	52	53	52	50	49	49	51	53	53	52	51
1909	49	46	42	41	42	43	43	41	38	35	34	33
1910	32	30	29	28	25	21	17	16	14	14	14	13
1911	12	11	10	8	6	6	6	5	5	4	3	3
1912	3	3	3	3	3	3	4	4	4	3	3	3
1913	3	3	2	2	2	2	1	1	2	2	3	4
1914	5	5	6	7	7	9	10	13	16	19	21	24
1915	29	35	39	42	45	47	48	50	52	54	57	59
1916	56	56	54	54	55	56	58	60	62	63	66	69
1917	73	81	90	94	96	101	105	105	104	103	102	98
1918	96	93	89	87	87	84	79	77	78	77	75	78
1919	78	75	73	70	67	65	64	63	62	60	57	51
1920	47	43	40	39	39	38	37	35	32	31	31	31
1921	31	32	31	29	27	27	25	24	26	26	24	23
1922	20	18	17	16	15	14	14	14	13	10	7	7
1923	6	6	6	7	7	6	6	6	6	6	7	8
1924	10	12	13	14	15	16	17	18	19	21	23	24
1925	25	27	29	33	36	41	47	52	56	58	59	61
1926	63	64	65	65	65	65	64	66	67	70	72	72
1927	72	72	72	72	72	71	69	68	68	68	68	69
1928	73	75	77	78	77	77	77	76	75	72	70	68
1929	66	64	61	59	60	63	65	64	63	62	60	57
1930	54	50	48	47	44	39	34	31	31	30	29	28
1931	28	27	26	24	23	22	21	20	18	16	15	15
1932	15	15	13	13	12	11	11	12	12	12	11	9
1933	8	8	8	8	7	6	5	4	4	4	5	5
1934	6	6	7	7	7	8	9	11	12	13	13	15
1935	18	20	22	26	30	34	38	42	47	51	55	57
1936	59	62	66	69	73	77	83	88	90	92	96	101
1937	108	114	117	119	119	116	113	111	111	111	111	110
1938	109	109	108	106	107	109	109	106	104	103	103	103
1939	100	97	98	98	95	91	88	86	86	84	80	76
1940	74	73	71	68	66	67	68	67	65	62	60	58
1941	57	55	53	53	51	49	47	47	48	49	50	48
1942	44	40	37	33	32	31	30	28	26	23	21	21
1943	20	20	20	19	17	17	16	14	13	11	9	9
1944	8	8	8	8	9	9	10	11	12	14	16	19
1945	22	24	25	28	32	33	34	39	44	48	52	56
1946	61	67	73	77	82	89	95	100	104	110	118	126
1947	132	137	143	149	152	152	151	149	146	146	146	145

Year	Jan.	Feb.	Mar.	Apr.	May	Jun.	Jul.	Aug.	Sep.	Oct.	Nov.	Dec.
1948	145	143	141	138	136	135	137	141	148	149	144	139
1949	137	135	133	133	135	136	134	130	124	121	120	118
1950	115	112	106	100	93	87	82	79	75	72	71	72
1951	72	70	70	71	70	70	69	66	63	59	53	47
1952	43	42	39	36	33	32	30	29	28	27	27	26
1953	24	21	20	18	17	15	12	11	11	10	9	7
1954	6	5	4	3	4	4	5	7	8	8	10	12
1955	14	16	20	23	29	35	40	47	56	64	73	81
1956	89	99	109	119	127	137	146	150	152	156	160	164
1957	170	172	174	181	186	188	191	194	197	200	201	200
1958	199	201	201	197	191	187	185	185	184	182	181	181
1959	179	177	175	169	165	161	156	151	146	141	137	133
1960	129	125	122	120	117	114	109	102	98	93	88	84
1961	80	75	69	64	60	56	53	53	52	51	51	49
1962	45	42	40	39	39	38	37	35	33	31	30	30
1963	29	30	30	29	29	28	28	27	27	26	24	21
1964	20	18	15	13	11	10	10	10	10	10	10	11
1965	12	12	13	14	15	15	16	16	17	20	22	25
1966	28	31	35	37	41	45	50	57	63	68	70	73
1967	75	79	82	85	88	91	94	95	95	95	97	101
1968	103	103	105	107	108	107	105	105	107	110	111	110
1969	110	110	108	106	106	106	106	107	105	104	105	105
1970	106	106	106	106	106	105	104	101	97	94	89	84
1971	80	78	74	71	68	67	65	65	66	66	67	69
1972	71	71	72	73	73	71	68	66	62	61	59	55
1973	51	47	44	43	41	39	38	36	34	33	32	32
1974	33	34	34	34	35	35	34	33	32	30	28	25
1975	23	22	21	19	17	16	15	14	14	15	16	16
1976	15	13	12	13	13	12	13	14	14	14	14	15
1977	17	18	20	22	24	26	29	33	39	46	52	57
1978	61	64	70	77	83	89	97	104	108	111	113	117
1979	124	131	137	141	147	153	155	155	156	158	162	165
1980	164	163	161	159	156	155	153	150	150	150	148	143
1981	140	142	143	143	143	142	140	141	143	142	139	138
1982	137	133	129	124	120	117	115	109	101	96	95	95
1983	93	90	86	81	71	70	65	66	68	68	67	64
1984	60	56	53	50	48	47	44	40	34	29	25	22
1985	21	20	19	18	18	18	17	17	17	17	17	15
1986	14	13	13	14	14	14	14	13	12	13	15	16
1987	18	20	22	24	26	28	31	35	39	44	47	51
1988	58	65	71	78	84	94	104	114	121	125	130	138
1989	142	145	150	154	157	158	158	158	157	157	158	154
1990	151	153	152	149	147	144	141	140	142	142	142	144
1991	148	148	147	146	146	145	146	147	145	142	138	132
1992	124	115	108	103	100	97	91	84	80	76	74	73
1993	71	69	67	64	60	56	55	52	48	45	41	38
1994	37*	35*	34*	34*	33*	31*						

** Provisional; may be subject to slight change.*

Chapter 3

Sunspot Cycle Predictions

Since the discovery of the sunspot cycle by Schwabe in the middle of the nineteenth century, considerable interest has been shown in forecasting the trends of future cycles. For years, predicting the next sunspot cycle was somewhat of a sport for mathematicians, statisticians, and those who had a flare for studying cycles. Until 1928 these predictions were largely of academic interest.

With the discovery of the relationship between sunspot numbers and ultraviolet radiation, however, the prediction of sunspot activity has assumed considerable practical importance, because long-range forecasts of shortwave propagation conditions are based on predicted smoothed sunspot numbers. These predictions have taken on even more importance during the last two decades, as the sunspot numbers are used to guide the extent to which semiconductors used in satellites should be "hardened" against galactic radiation. If a cycle is predicted to have a relatively low maximum, satellite designers will not harden the circuitry as much as they might otherwise think necessary, because this technology adds weight and considerable cost to the satellite. If the prediction proves wrong and the maximum smoothed sunspot number (SSN) is higher than predicted or a higher number of solar proton events occur than was expected, accumu-

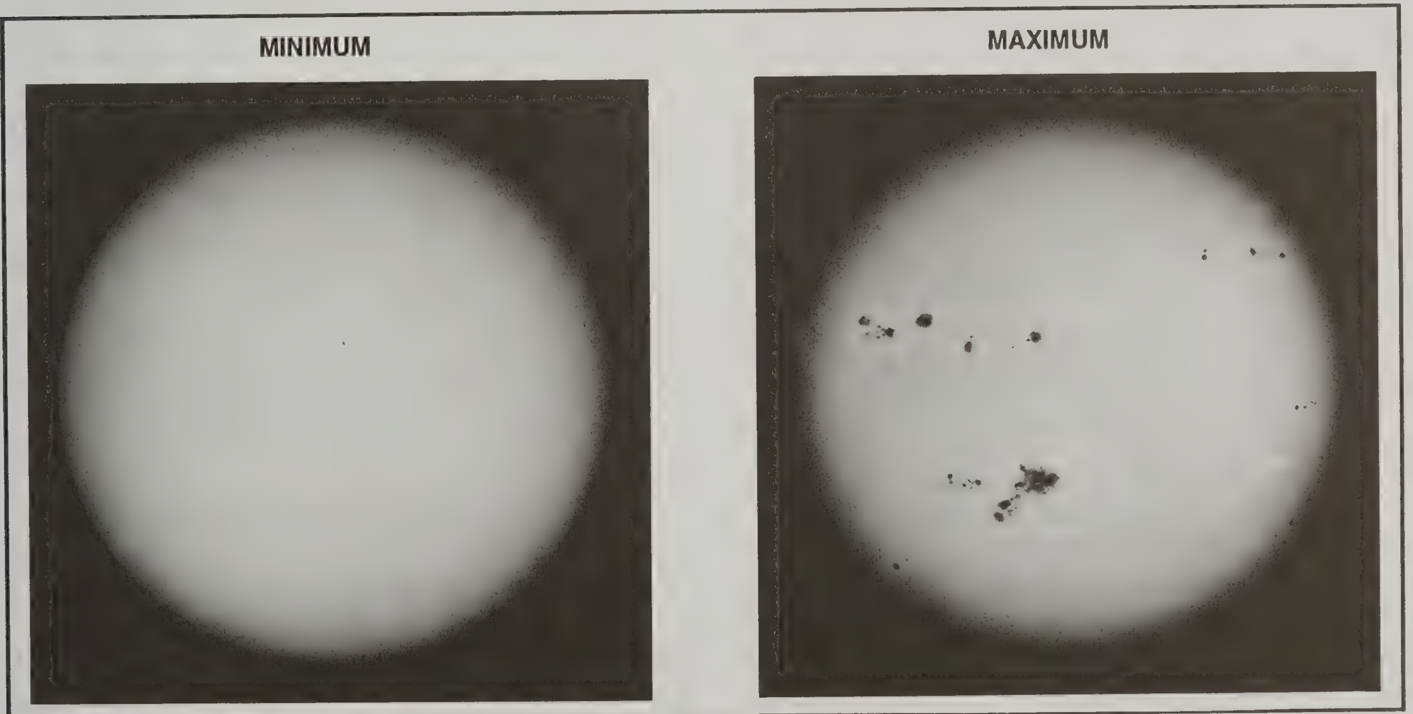

Photo 3.A. The Sun as seen in white light at solar minimum (16 June 1986) and maximum (13 June 1989). (Photograph provided by the National Solar Observatory, Sacramento Peak, New Mexico.)

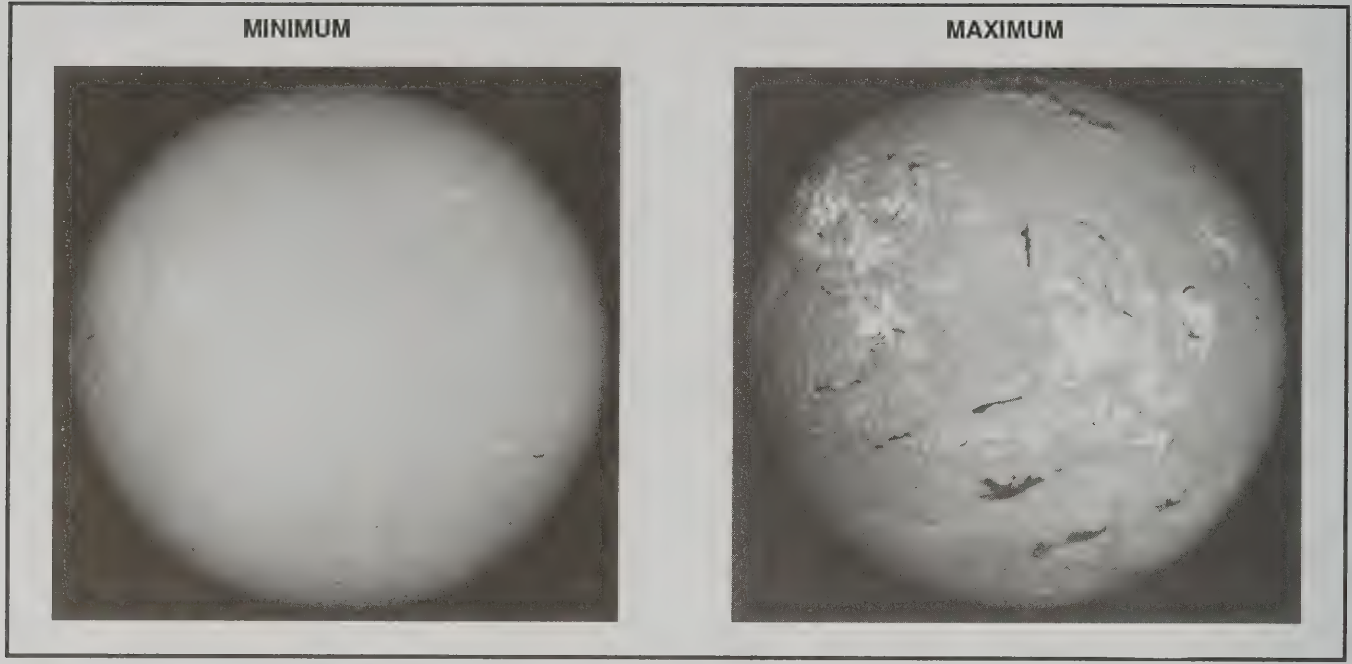

Photo 3.B. The Sun as viewed through a telescope with an Hα filter at solar minimum and maximum. (Photograph provided by the National Solar Observatory, Sacramento Peak, New Mexico.)

lated radiation damage will occur in the satellite. This is what happened during Cycle 22, the maximum of which was under-predicted by most experts.

Sunspot Cycle 22 experienced a double peak during July and November 1989, each with a smoothed sunspot count of 159. Since then, it has steadily declined. How good were the sunspot predictions for Cycle 22? What levels of solar activity can we expect for the remainder of the cycle? When can we expect the minimum of Cycle 22 to occur? The answers to these questions are very important to the radio amateur, CBer, and shortwave listener. They are particularly important to a new breed of radio amateur who came into HF radio in the 1988 to 1991 time-frame. They may not be aware that there is a solar cycle; nor may they know that 15, 12, and 10 meters will be considerably less reliable than they were during the years of high sunspot count.

To answer the very important questions stated above for users of the shortwave bands, we will examine some of the methods used to predict solar activity. We also will summarize what some of the world's leading solar scientists are predicting for Cycle 23. Much of the information in this chapter summarizes results from a workshop on the "International Decade of Solar Cycle Studies (IDSCS)" held in 1992.[1] For those who are interested in studying the finer details of solar cycle prediction, an extensive bibliography is contained at the end of this chapter.

Just what is a solar cycle prediction? It is a prediction of when to expect a minimum condition (when the Sun is virtually featureless) and a maximum condition (when the solar surface is covered with dark spots). Until modern times the Sun was viewed in "white light." This was accomplished by using a telescope to project a focused solar image of sufficient size so that the number and details of the sunspots could be counted and recorded manually. Photo 3.A illustrates how the Sun appears to most astronomers.

In the 1950s new technology allowed scientists to view the Sun at the frequency of the red spectral line emitted by hydrogen. Newly developed filters, called H-alpha filters, were used to produce what appears to be a larger solar image. This is because the layer above the photosphere (the region we see as white light) now can be observed. This layer is called the chromosphere. The chromosphere emits massive amounts of extreme ultraviolet (EUV) radiation, which is responsible for forming the ionosphere. It also is where the features of active regions around sunspots can better be studied. Photo 3.B shows examples of the Sun observed at both solar maximum and solar minimum when viewed through a telescope with a hydrogen-alpha (Hα) filter. Because of the cost and

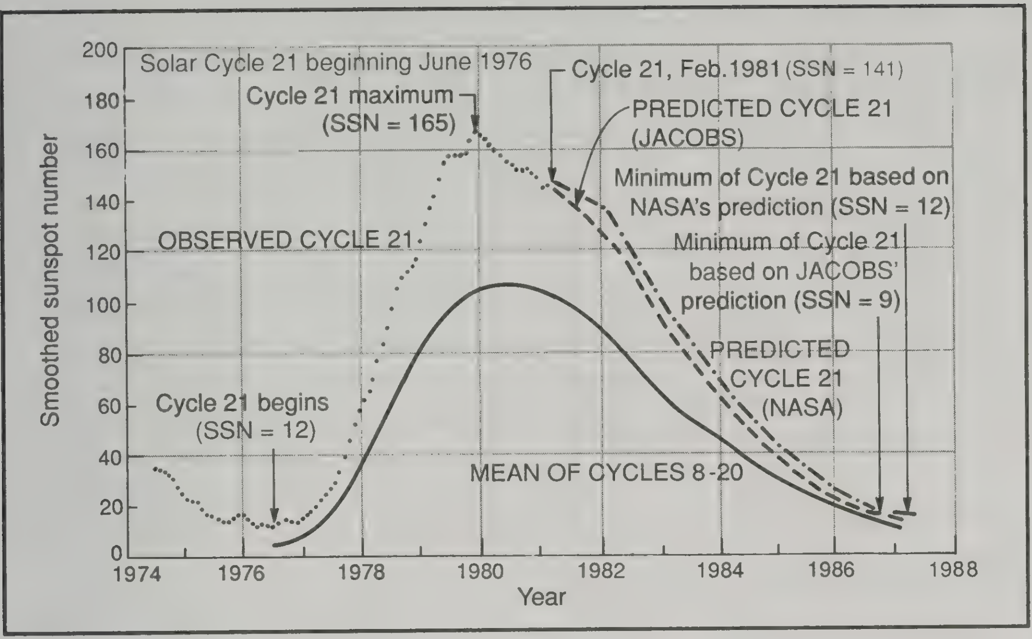

Figure 3.1. Observed and predicted smoothed sunspot numbers for Cycle 21.

complexity of these filters, few amateur astronomers have this viewing capability. However, use of these filters yields more consistent sunspot counts and more detailed information on the complexity of sunspots than do those data produced using "white light."

3.1 Prediction Methods

Methods for predicting the future course of sunspot cycle activity are as numerous as are the number of investigators who have attempted such predictions. While theories exist as to the origin of sunspots, the mechanisms that start a cycle and result in the number of spots being formed are still a mystery. For that reason the prediction of sunspot numbers years in advance of their occurrence must be considered as an imprecise science and the predictions should be treated with caution.

Currently three types of prediction methods are used to forecast solar cycle behavior. These are (1) the statistical (or empirical) method; (2) the precursor method; and (3) the planetary method. Each is discussed in this section.

Statistical Prediction Methods

There is one scientific community whose method for predicting the behavior of future sunspot activity is almost totally based on data observed from previous cycles. These statistical (or empirical) prediction methods fall into two categories: those which consider each solar cycle as an independent event, and those which assume solar activity to be a periodic phenomenon. Some attempts also have been made to predict solar behavior based on the assumption that planetary tides on the Sun trigger solar activity.

Independent Event Theory

One family of solar prediction methods is based on the premise that each 11-year (approximate) solar cycle is a relatively independent event. No assumptions are made as to the existence of long-term periodicities, but rather, each rise and subsequent fall is considered to be an independent outburst. In this method extensive studies on the behavior of previous cycles are used to derive empirical relationships between the various solar-cycle parameters. For example, the following empirical law derived by Waldmeier[2] relates the time, Θ, in years between the maximum and minimum of a given cycle to the maximum smoothed sunspot number, R_s for the cycle:

$$\Theta = 3 + 0.03R_s \text{ years} \qquad (1)$$

For cycle 20, the maximum 12-month running smoothed sunspot number, 111, was reached in November 1968. Using the value in Equation 1 yields a decay time of roughly 6.3 years. As such, this method predicts that the minimum for Cycle 20 should have occurred early in 1975; it actually occurred in June 1976. For Cycle 21, the maximum 12-month running smoothed sunspot number, 165, was reached in December 1979. Again, using Equation 1 we compute a decay time of 7 years and 11 months.

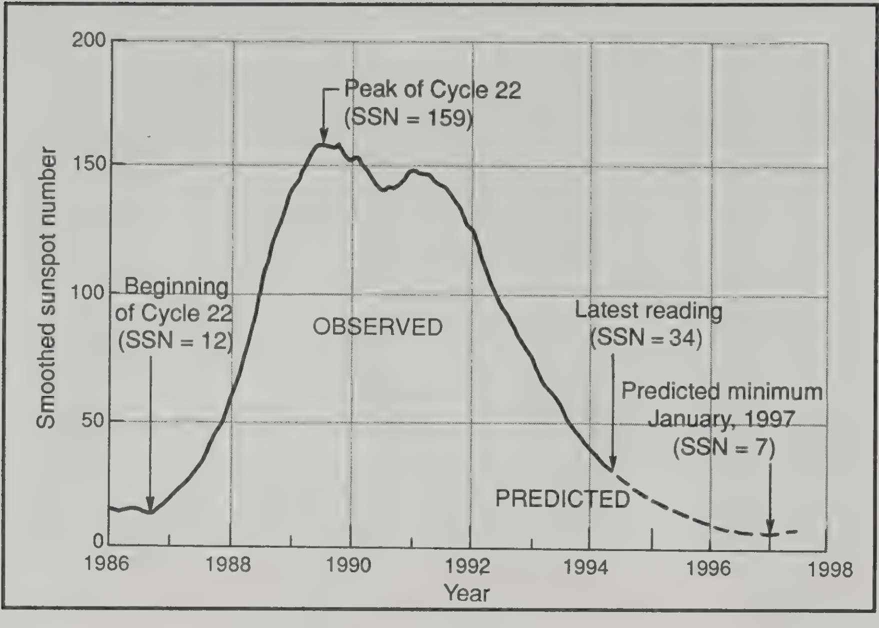

Figure 3.2. Observed and predicted smoothed sunspot numbers for Cycle 22. (Jacobs[3], 1994.)

The minimum actually occurred 6 years and 9 months after the maximum, in September 1986. Using this method for Cycle 22, the predicted decay time is 7 years and 9 months; thus, the minimum is expected to occur in March 1997.

Another empirical method developed by W3ASK is interesting to consider. In using this method one first selects about five or six cycles that more or less are similar to the cycle under study. Moving three years forward in time from the peak of each cycle, the *monthly* sunspot numbers are averaged over the cycles selected. This yields an average level of monthly sunspot activity that can be projected into the current cycle. Using these projected numbers, one then calculates the predicted 12-month running smoothed sunspot numbers for the remainder of the current cycle.

For Cycle 21, application of Jacobs' technique in 1981 suggested that the minimum should be reached in September 1986, with an expected minimum 12-month running smoothed sunspot number of 9. The actual minimum occurred in September 1986 with a number of 12 (see Figure 3.1).

In June 1992, Jacobs[3], based on matching characteristics of Cycle 22 with similar characteristics of Cycles 11, 18, 19, and 21, predicted that the most likely date for Cycle 22's minimum is January 1997, with a smoothed sunspot count of approximately 7 (see Figure 3.2).

Empirical methods such as those developed by Waldmeier and Jacobs may only be used for predicting the course of a cycle once it has begun. It is desirable, however, to predict the behavior of future cycles. To do this, consideration must be given to those methods which assume that solar activity is a periodic phenomenon.

Periodic Phenomenon

Empirical methods for predicting solar activity that are based on the periodic behavior of the solar cycle seek to describe the short- and long-period recurrence behavior of previous cycles and to extrapolate these results to portions of the current cycle and to future cycles.

One method for predicting solar activity which assumes that the sunspot cycle is periodic was developed by McNish and Lincoln.[4] This method takes, as a first approximation to the prediction of a future value for a particular period in the current cycle, the mean of the values observed during similar periods of the ten previous cycles. The values associated with this mean cycle then are modified by adding correction factors that are based on the amount of deviation observed between earlier values of the current cycle and the mean cycle. These correction factors are computed by the method of least squares.

The McNish-Lincoln prediction method is recommended only for use in predicting 12-month running smoothed sunspot numbers up to one year in advance. Using this method it is possible to predict two and three years into the future, but by the fourth year, activity in future years is best predicted using the mean of the previous ten cycles.

Boykin and Richards[5] modified the McNish-Lincoln technique so that the smoothed sunspot numbers could be predicted up to 15 years in advance. A good background in matrix algebra is required to understand Boykin and Richards' work, so no attempt will be made here to elucidate the statistical technique employed. Predictions for Cycle 21 based on Boykin and Richards' method were published by Smith[6], and values updated by Smith in 1978 are compared to predictions by other observers in Figure 3.3.

A new approach to predicting long-range solar activity was devised by Cohen and Lintz[7] in 1974 using the Maximum Entropy Spectral Analysis (MESA) technique.[8,9] A MESA analysis of 214 years of sunspot data (1750–1963) indicated that the spectrum of the 12-month running smoothed sunspot numbers exhibits significant components at 89.6, 57.1, 11.2, 9.9, and 8.1 years. As such, the period that is common to each of these components is roughly 179 years. This 179-year recurrence in solar activity can be seen by comparing Cycles 1 and 17, 2 and 18, 3 and 19, and 4 and 20 in Figure 3.4.

If the major characteristics of the sunspot cycle repeat every 179 years, then by definition the data are periodic outside an interval of this length. To predict future sunspot observations, therefore, we simply can shift the sunspot data 179 years forward in time so that the predictions for 1972 are given by the data for 1793, the predictions for 1973 are given by the data for 1794, and so forth.

An equivalent prediction method, similar to the above, would be to use the spectral components corresponding to the data for any given 179-year interval to reconstruct the smoothed sunspot numbers in this interval. Then, by repeating the waveform outside the interval, smoothed sunspot numbers could be predicted forward or backward in time. Applying this method (components at periods of less than 4.5 years are eliminated) yields the results shown in Figure 3.5.

The MESA technique did not yield good estimates for the predicted sunspot numbers for Cycle 21, so the MESA-predicted date for that cycle's minimum (late 1988) was wrong, being almost two years late (see Figure 3.3). Finally, the characteristics of Cycle 21 indicate that a 179-year period does not exist in the solar cycle.

Ohl[10] proposed a method for predicting solar activity that is based on an apparent correlation between geomagnetic activity in the years immediately preceding a solar minimum and the solar maximum for the succeeding cycle. More specifically, Ohl suggested that the geomagnetic activity that accompanies each cycle has two components: a "sporadic" component and a "recurrent" component (see Figure 3.6). It is the activity of the recurrent component that appears to be related to the following solar cycle, and, in fact, to be correlated with the maximum count of the succeeding sunspot cycle.

Sargent[11] modified Ohl's method by correcting for the contamination of the recurrent geomagnetic-activity component by the sporadic geomagnetic-activity component. He did this by multiplying the value of

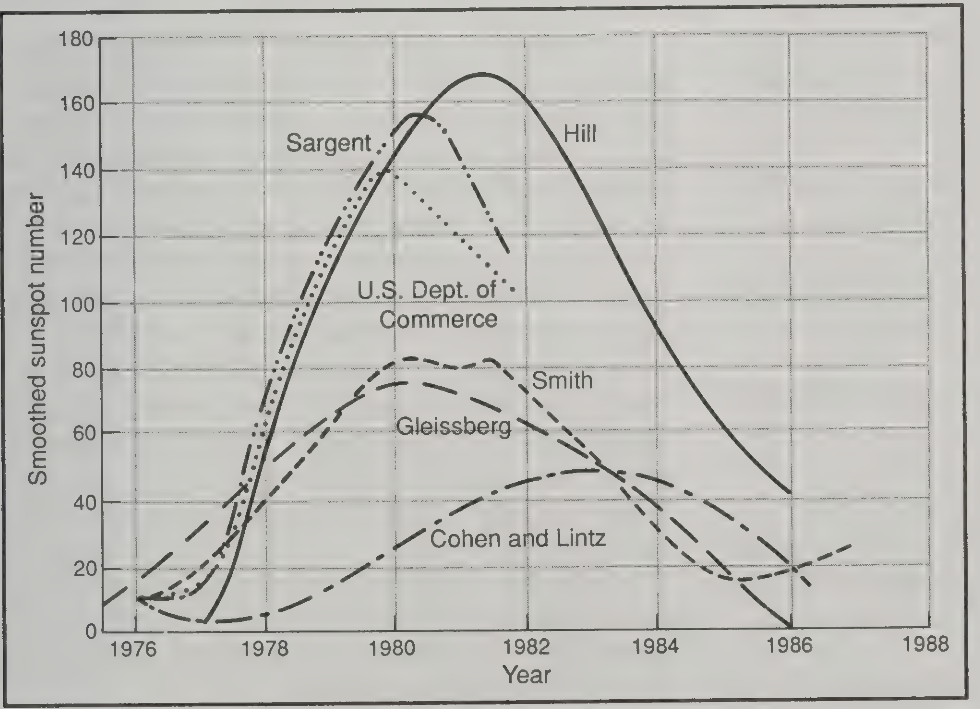

Figure 3.3. Predictions for Cycle 21 as of mid-1978. In addition to those shown, Jose[15] predicted the maximum would occur in 1984, and the minimum would occur in 1990. On the other hand, Wood[16] predicted the maximum count of 60 for Cycle 21, with the maximum occurring in 1982; he predicted the minimum to occur in late 1988. The maximum actually occurred during December 1979, with a smoothed sunspot count of 165; the minimum occurred during 1986, with a count of 12.

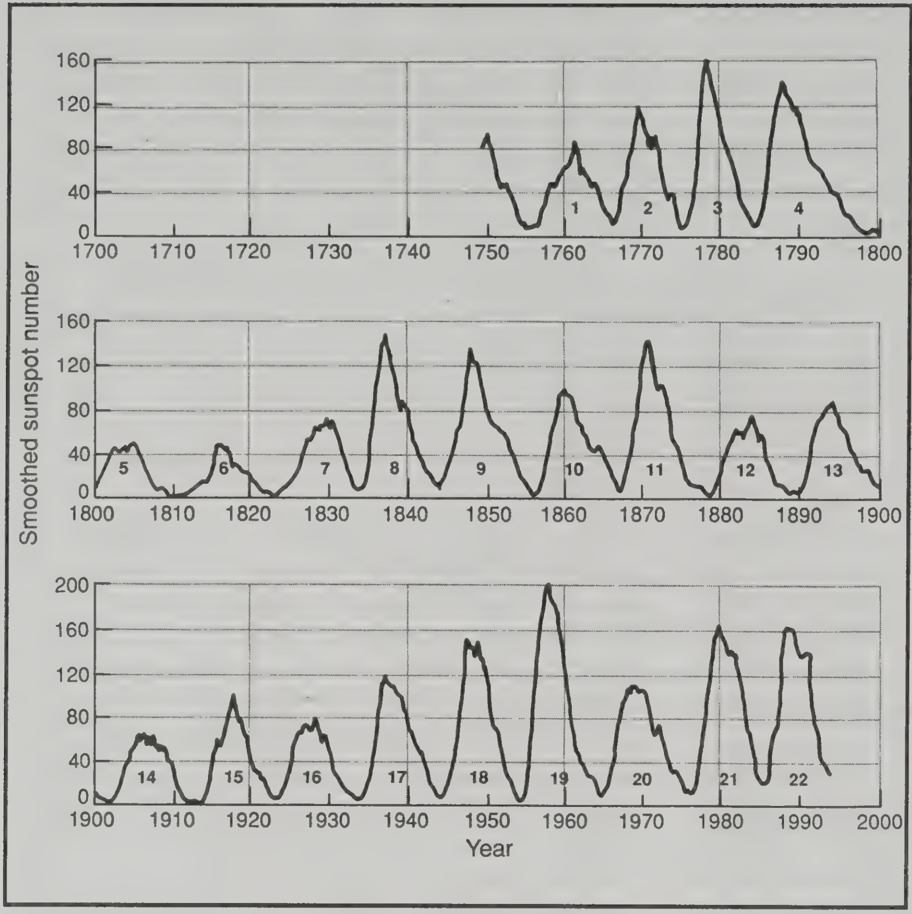

Figure 3.4. Twelve-month smoothed sunspot numbers since 1749. (Data courtesy National Geophysical Data Center, Boulder, Colorado.)

the 12-month running smoothed sunspot number at solar minimum by a constant, and then by subtracting this factor from the geomagnetic activity indices used in the study. The geomagnetic indices so obtained were then used in a multiple regression analysis to yield the best predictive equation for the maximum smoothed value of the succeeding sunspot cycle, $R_{max}(n+1)$.

In performing his multiple regression analysis, Sargent used a linear combination of the two variables:

$X1$—the average value of the monthly geomagnetic indices for the 36-month period preceding a sunspot minimum;

$X2$—the smoothed sunspot number at solar minimum, $R_{min}(n)$.

Using solar and geomagnetic activity for the previous nine cycles (Cycles 12 through 20, inclusive; see Figure 3.7), the regression equation obtained by Sargent is given as follows:

$$R_{max}(n+1) = 3.91 + 8.56 \cdot X1 - 7.84 \cdot X2 \qquad (2)$$

Equation 2 may be rewritten as follows:

$$R_{max}(n+1) = 3.91 + 2.85\ (3 \cdot X1 - 2.75 \cdot X2) \qquad (3)$$

In Equation 3, the quantity in parenthesis is the modified Ohl variable, and it is three times the average value of geomagnetic activity over the three-year period prior to solar minimum, adjusted by the sunspot value at the minimum. Hence, this quantity is a measure of recurrent geomagnetic activity.

For the three years prior to the solar minimum in March 1976, the average geomagnetic-index value was 28.7. Further, the smoothed sunspot value at the minimum was 12.2, and so, using Equation 3, the maximum sunspot value for Cycle 21 was predicted to be 154. The 95% confidence interval for this determination, by the way, extends from 104 to 204, a consequence of the limited database used. Finally, based on a rise time of 4.1 years for the average solar cycle, Sargent predicted that Cycle 21 would peak in early 1980. Predictions based on Sargent's work are shown in Figure 3.3. The peak for Cycle 21 actually took place during December.

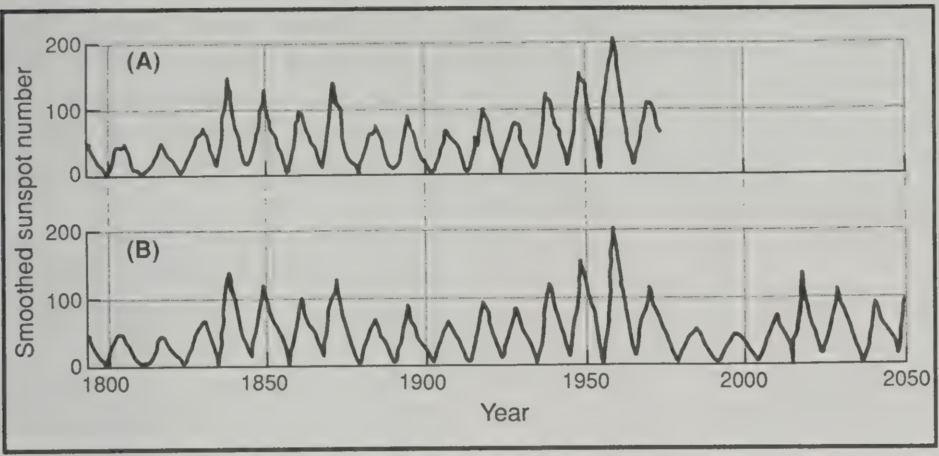

Figure 3.5. Twelve-month sunspot numbers. (A) Observed 1793-1971. (B) Predicted up to the year 2050. (After Cohen and Lintz [7], 1974.)

Also during the mid-1970s, a Navy scientist, J. Hill, was working on a method to predict solar cycle activity using high-resolution spectral analysis. This method, called Anharmonic Frequency Analysis[12], was designed mainly to search for discrete frequencies in a time series. This method yields the determination of the frequency components in a complex periodic cycle (the solar cycle) and also, the amplitude of the harmonic components. Using this technique Hill[13] predicted a solar maximum peak of between 130 and 200, centered around 165, during 1981 and 1982. This prediction was "on the mark." However, it also is interesting to note from the data published by Hill in 1977 that Cycle 22 was drastically under-predicted by this method (more specifically, the method predicted a count of slightly over 100 at the maximum, versus the observed count of 158).

Precursor Methods

The prediction methods that appear to have general approval within the modern solar scientific community are those based on the notion of the "extended solar cycle"—that is, on the notion that a new cycle actually starts before the old one reaches minimum. The extended solar cycle can be observed by a number of indicators, such as the appearance of sunspots at high solar latitudes prior to minimum, the appearance of the so-called coronal "green line," and the overlap at the end of a solar cycle of reverse- and normal-polarity sunspots. Another indicator of the birth of a new cycle is the formation of stable, large-scale magnetic structures on the Sun called *coronal holes.* Coronal holes are the source of high-velocity solar winds that may produce geomagnetic disturbances on Earth. These disturbances tend to recur at 27-day intervals. The number, strength, and stability of these recurrent disturbances during the decaying phase of a cycle appear to indicate the size or strength of the next cycle. Thompson[14] describes one precursor prediction technique that is useful in illustrating the process. As will be seen in later sections, his method was quite accurate in predicting Cycle 22 activity.

Precursor methods predicated on terrestrial geomagnetic disturbances assume two classes of phenomena generate activity; the first is normal solar disruptions such as flares, coronal mass ejections, and disappearing filaments, while the second is associated with new-cycle phenomena. The first set of phenomena peaks and wanes as the cycle varies, while the second can be found after solar maximum. In Thompson's method it is assumed that if these two classes of phenomena produce geomagnetic activity, then the total number of disturbances during a solar cycle are a function of both the peak of the current cycle as well as the peak of the next cycle. To test this theory the number of geomagnetic disturbances for every cycle since Cycle 11 were determined using geomagnetic indices. An A_p (planetary A-index; see Chapter 5) of greater than 25 was used to define a disturbance. This threshold was chosen to provide a sufficient sample size and to ensure that the disturbances were caused by solar influences. From this review, Thompson derived the following expression:

$$N_c = -47.7 + 2.04(R_c + R_n) \qquad (4)$$

where: N_c is the number of geomagnetic disturbances in the current cycle from solar minimum to solar minimum;
R_c is the peak sunspot number of the current cycle; and
R_n is the expected peak sunspot number for the next cycle.

The prediction of the peak smoothed sunspot num-

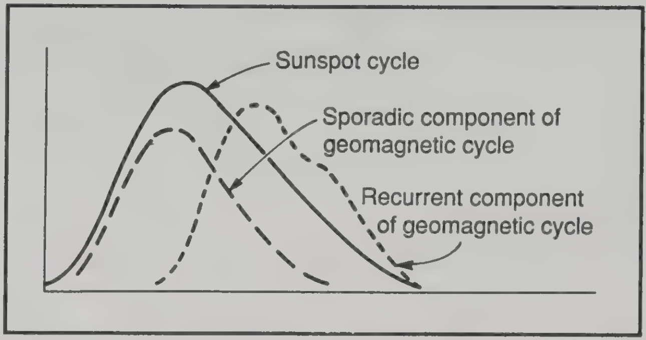
Sunspot cycle
Sporadic component of geomagnetic cycle
Recurrent component of geomagnetic cycle

Figure 3.6. A sporadic and a recurrent component of geomagnetic activity is thought to be associated with each solar cycle. (After Ohl[10], 1976).

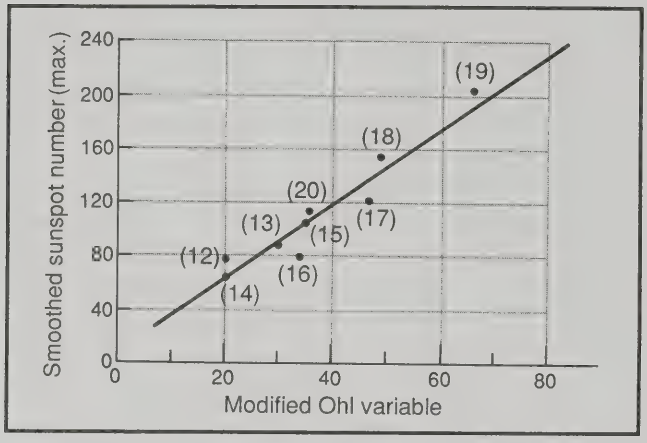

Figure 3.7. A plot showing the relationship between maximum smoothed sunspot number and values for the modified Ohl variable. Cycle numbers are shown in parentheses. The regression line determined by Sargent predicted a maximum sunspot count of 154 for Cycle 21. The actual peak occurred during 1979, with a count of 165. (Modified after Sargent[11], 1978.)

ber of the next solar cycle can be attempted by solving Equation 4, once N_c is known, as is the situation at solar minimum. As with any model that tries to fit observations with geophysical phenomena, there is some margin of uncertainty. This is due to the scatter of the data and to the choice of the threshold as to what constitutes a disturbance. However, this simple relationship illustrates the precursor prediction method. Using this method, Thompson correctly predicted a peak value of 159 for Cycle 22.

Planetary Theory of Sunspots

No discussion of sunspot predictions would be complete without some reference to the planetary theory of sunspot causation. Basically, this theory holds that sunspot activity is affected by planetary positions, and that planetary tides on the Sun vary in the same manner as do sunspot variations. Jose[15], for example, observed that the variations in the motion of the Sun about the center of mass of the solar system have a periodicity of 178.7 years, and by visual inspection of sunspot data, he asserted that the sunspot cycle exhibits the same period.

Wood[16], in his analysis of solar tides, found a similarity between the solar induced tidal height fluctuations and sunspot numbers. He postulated that the minimum for Cycle 20 would occur in early 1977. Cycle 20 actually ended during June 1976. Similarities in solar-tide effects and sunspot numbers notwithstanding, the planetary theory of sunspot causation has came under renewed criticism. Writing in *Nature*, Okal and Anderson[17] stated that the apparent agreement of the sunspot cycle with planetary tidal effects is an artifact of the calculations. By analyzing 1,800 years of solar-tide databased on planetary positions, they showed that the spectrum of these data exhibited only a single long-period peak of 11.86 years (the orbital period of Jupiter). No planetary peaks were found at 8.1, 9.9, 57.1, or 89.6 years, as were observed by Cohen and Lintz; further, no peak was found at about 179 years, again indicating that this peak is not an intrinsic periodicity of the solar cycle.

At the least, the planetary theory of sunspot causation is considered speculative. For that matter, any of the methods used for sunspot prediction must be considered speculative, for the period on which these predictions are based (245 years) represents only the smallest fraction of the Sun's 11-billion-year life.

3.2 How Good Were The Predictions?

Cycle 21 (1976 to 1986)

Figure 3.3, shown earlier, compares some of the predictions made for Cycle 21. In addition to the work previously discussed, the predictions of Gleissberg[18], the U.S. Department of Commerce[19], and Smith[20] are included here. Hill and Sargent predicted that the activity of Cycle 21 would be equivalent to, or greater than, the second highest sunspot cycle observed in the last 100 years. Hill correctly predicted the maximum count, while Sargent under-predicted it by 11 counts. With the large confidence limits most researchers place around their predictions, these two predictions were incredibly accurate.

Other investigators, such as Cohen and Lintz, and Gleissberg, however, predicted that the activity of Cycle 21 would be less than the activity observed dur-

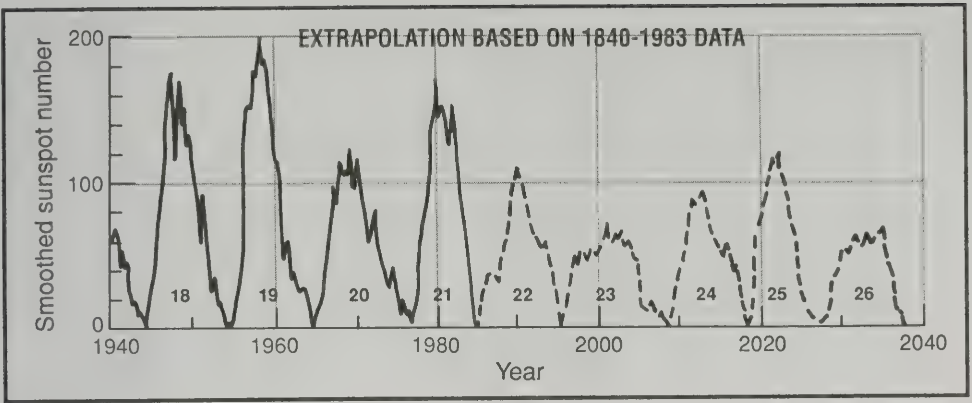

Figure 3.8. Smoothed sunspot number predictions for Cycles 22–26, inclusive. (Data courtesy the Naval Ocean Systems Center; see also Reference 22.)

ing the previous cycle, Cycle 20. In fact, until Hill published his prediction in 1977, the solar community held the general feeling that the next cycle would be close to what Cohen and Lintz had predicted. It wasn't until Sargent's paper in 1978 that Hill's work was taken seriously. Prior to the publication of Hill's work in *Nature,* his prediction was previewed by K6GKU in 1977 in a presentation to an aerospace conference.[20] The prediction was the subject of much discussion among those members of the satellite-building community who were responsible for designing satellite circuitry that would be used over the next several years.

Cycle 22 (1986 to 1997)

To say the least, large uncertainties characterize all solar cycle predictions. This may be the result of random phenomena that at times overwhelm the periodic component in the 11-year cycle *(private communication, A.K. Paul).* Because of the large variations in the predictions shown in Figure 3.3, many scientists were reluctant to be so open with their forecasts for Cycle 22. As a result, fewer predictions were published. Using the same method that Hill used in 1977 to predict Cycle 21, Navy scientists in San Diego made a prediction for Cycle 22 in the middle 1980s. The early predictions indicated a maximum smoothed sunspot number of around 100, but the confidence limits spanned plus-or-minus 50 counts. That meant Cycle 22 could peak with a count of between 50 and 150.[22] Figure 3.8 shows the prediction for Cycle 22 using the same method, Anharmonic Analysis, that accurately forecast Cycle 21.[23] Note that these data under-predicted Cycle 22 by about 50 counts. In fact, in a study[24] of 46 different predictions for the Cycle 22 peak, 65% under-predicted the maximum, with 20% of the predicted values below 100. The results of those using statistical methods tended to cluster at the lower end of the distribution, while precursor predictions tended to lie at the higher end. Two forecasts using the planetary alignment theory did not compare well to each other; one predicted a peak value of 60, while the other was quite close to the actual value of 158. Within the 46 predictions studied, three were quite close to the actual value. Thompson[25] in 1985 used the precursor method to predict a SSN of 159. In 1984 Smith[26] predicted a maximum value of 160 using statistical methods. In 1987, as Cycle 22 started, Thompson[27] and Gonzales and Schatten[28] predicted a maximum of 163 using precursor methods. The behavior of Cycle 22, when compared to the predictions made, underscored the Sun's inherent unpredictability. While every solar cycle has certain deterministic features that have some level of predictability, it is the random component that is so difficult to forecast. Generally speaking, empirical or statistical predictions for Cycle 22 predicted lower maximum values, while precursor-based predictions tended to be higher (and more accurate).

Sunspot Drift and Magnetic Field Reversal

Although current sunspot predictions are based upon empirical methods developed from the behavior of previous cycles, there is an observable pattern on the Sun itself that makes it possible to know, with a fair degree of accuracy, when we are approaching the final stages of a cycle. This is the drift pattern of spots from high solar latitudes toward the solar equator as the cycle progresses.

At the start of a new solar cycle, sunspots first appear in two zones, 25 to 40 degrees north and south of the Sun's equator (see Figure 3.9). As the cycle progresses, the zones in which sunspots occur slowly drift toward the equator by about two degrees per year. By sunspot maximum, most spots break out at about 15 degrees, and by the end of the cycle the

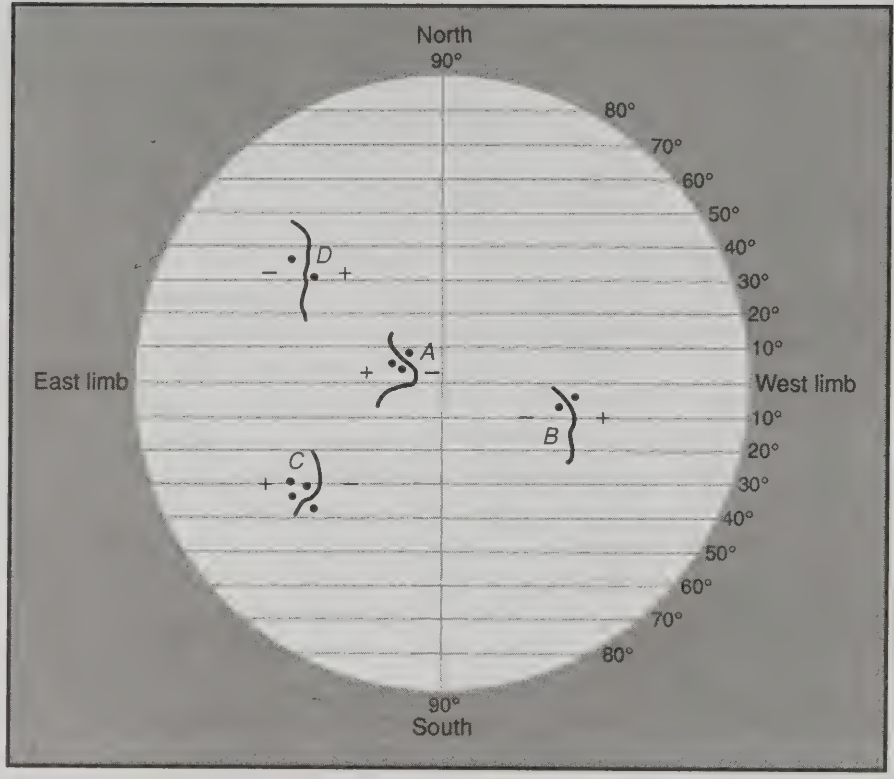

Figure 3.9. Positions of sunspots associated with an old solar cycle (A and B) and with the start of a new solar cycle (C and D). Note the opposite polarity of the magnetic fields associated with the old and new spots on a given side of the solar equator.

sunspots nearly touch the equator. For two years or more, both the new and old cycles overlap, with the spots of the new cycle seen in the high latitudes while the few remaining spots of the old cycle appear near the equator. This produces what is called the "solar butterfly diagram," or a time/solar latitude scatter diagram of sunspots. Figure 3.10 illustrates how these patterns emerged throughout ten solar cycles.[29] As we go to press in early 1995, we have yet to observe sunspots associated with Cycle 23.

Cycle 23—What Can Be Expected?

Given the comparisons of predictions to observations for Cycles 21 and 22, one might be reluctant to ever predict solar cycle activity. Of course, there always will be those who will try, just to see how well they can do. Further, because the solar events of 1989 provided an unexpected "wake-up" call to those who use space systems that are directly affected by solar-terrestrial relationships, there now is serious interest worldwide in predicting the behavior of Cycle 23.

We present in Table 3.1 some predictions from the world scientific community as to how the next cycle may behave. The list is incomplete because those who make precursor predictions cannot do so until Cycle 22's solar minimum bottoms in the 1996–1997 time frame. Some forecasts are available, however, from the statistical/empirical community.

First let's look at the results obtained using the Anharmonic Technique that so accurately predicted Cycle 21, but that performed poorly in forecasting Cycle 22. Figure 3.11 shows graphically what this analytical method predicts. This plot, developed in March 1993, indicates that the solar minimum for Cycle 22 will occur in late 1997 or in 1998. Minimum solar activity, and resultant poor HF propagation, will remain through 2000. The next solar maximum will occur in mid-2003, with a predicted smoothed sunspot number of approximately 128. Maximum conditions and good HF propagation, with smoothed sunspot numbers remaining above 100, are expected to continue through 2005 *(private communication, A.K. Paul).*

Another source of very interesting data was presented in the "International Decade of Solar Cycle Studies (IDSCS)."[1] There is feeling throughout the world solar community that Cycle 23 will produce smoothed sunspot numbers that either will be very high or very low, with some scientists even predicting a solar maximum that will rival Cycle 19. Table 3.1 shows that prior to the start of Cycle 23, there is a wide variation in the estimates available.

The consequences of an abnormally high or low cycle also are a subject of much conjecture. If Cycle 23 turns out to be abnormally low (i.e., SSNs between 50 and 100), we may experience difficulties with long-range HF radio communications and internation-

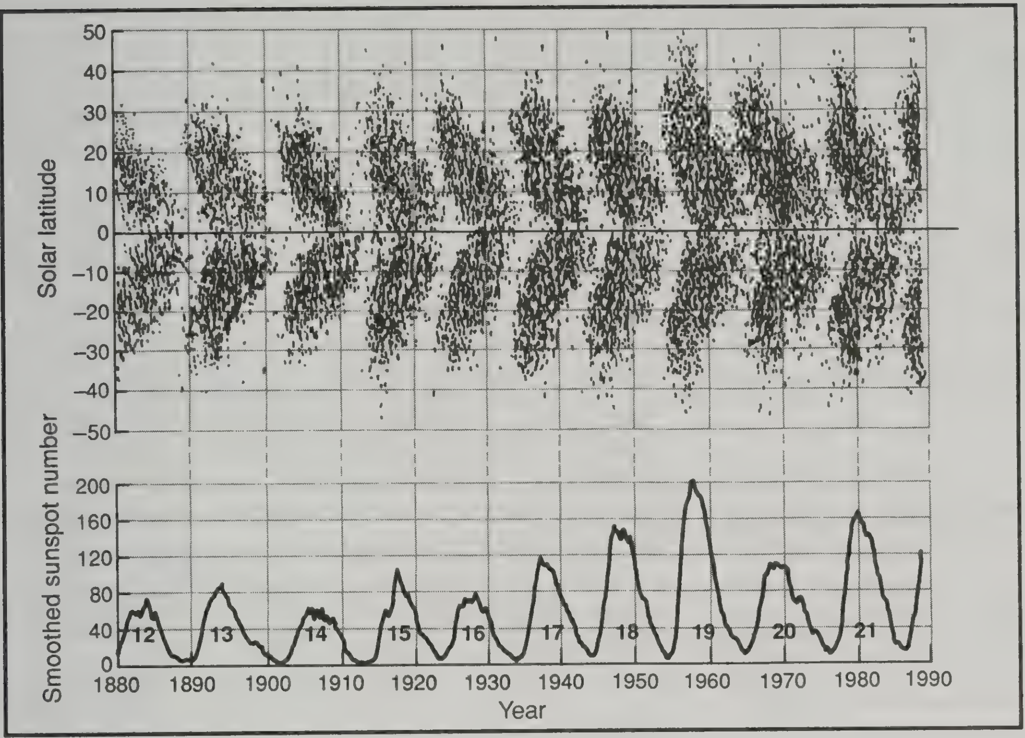

Figure 3.10. Solar butterfly diagram (modified after Allen[29], 1991).

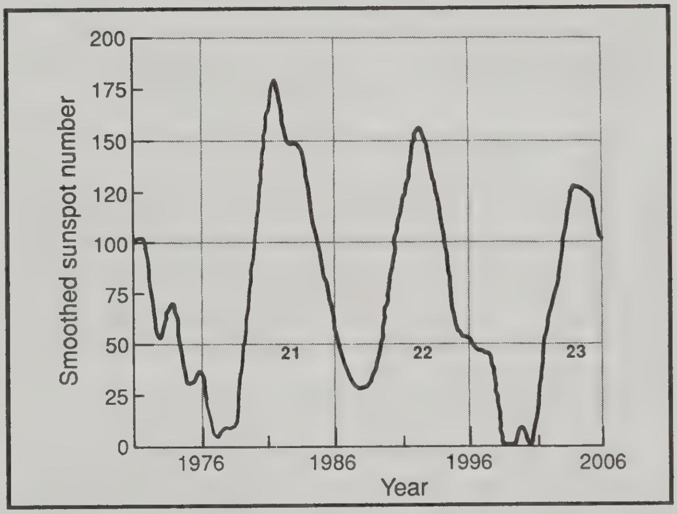

Figure 3.11. Predicted sunspot numbers for solar Cycle 23. (Personal Communication, A. K. Paul, 1993.)

al broadcasting. Based on recent studies, the ionosphere could resemble a loosely organized network of ionized patches that becomes spottier at the higher latitudes. Under such conditions, ionospheric scintillation should be unusually effective at disturbing communications via satellite. On the whole, solar-induced disturbances are likely to be weak and infrequent, but when they occur, they may produce quite noticeable effects owing to the diminished adaption properties of systems that are adjusted to operate under prevailing low solar activity conditions. Finally, shortwave broadcasters will be forced down into the lower frequency bands, causing increased congestion.

On the other hand, if Cycle 23 is abnormally active (i.e., high sunspot counts), HF propagation will be outstanding worldwide. However, it would then be expected that solar disturbances would occur at unprecedented levels, causing a “replay” of 1989. Under such conditions, space systems will incur more radiation damage. Even though shortwave broadcasters will have more spectrum to use, low-power broadcasters will achieve wider coverage, increasing congestion.

Only time will tell what Cycle 23 will bring. However, as the precursor prediction community starts to add their estimates, the picture will become a little clearer. For now, all we can do is wait and watch for the first signs that Cycle 23 has started.

Updated, long-range solar cycle predictions appear regularly in W3ASK’s monthly “Propagation” column in *CQ* magazine published by CQ Communications, 76 North Broadway, Hicksville, NY 11801.

Fortunately, an accurate prediction of solar activity is not required to produce usable forecasts of conditions on the HF bands. Simply by knowing the current phases of solar activity, it is possible to predict the average behavior of the ionosphere, and hence, the average conditions to be expected on the bands.

Using sunspot data recorded by the Swiss Federal Observatory for the 20 solar cycles since 1749, *low, moderate, high, very high,* and *intense* phases of solar

Author (Ref)	Year Min-22	Year Max-23	Year Min-23	Peak SSN-23
Wilson (30)	—	—	—	135–215
Kopecky (31)	—	—	—	208–215
Markov (32)	—	—	—	>160
Vitinsky (33)	1997	2000	2009	>160
Rivin (34)	—	—	—	217–233
Obridko (35)	—	—	—	175–225
Tritakis (36)	—	—	—	130–150
Analog of Cycle 4	1996	1999	2009	141
Paul (private communication)	1997	2003	—	128
Wilson (37)	—	—	—	126
Schove (38)	2000	2004	2009	85–120
Kontor (39)	—	—	—	110
Chistyakov (40)	2001	2006	2011	75
Mordvinov (41)	—	2002	—	81
SESC Mean	—	2000–01	—	90–130

Table 3.1. Solar cycle predictions for Cycle 23 (1997 to 2009 est.). (Adapted from Reference 1.)

Phase	Range of Smoothed Sunspot Numbers
Low	Less than 30 (centered on 15)
Moderate	Between 30 and 60 (centered on 45)
High	Between 60 and 90 (centered on 75)
Very High	Between 90 and 120 (centered on 105)
Intense	Higher than 120

Table 3.2. Phases and ranges of solar activity.

activity can be defined by the ranges of the 12-month running smoothed sunspot numbers shown in Table 3.2. Further, Table 3.3 summarizes the phases of solar activity observed or expected for Cycles 22 and 23 based on the most recent predictions prepared by NASA[42] and plotted in Figure 3.12.

The significance of knowing the phase of solar activity for use in predicting shortwave propagation conditions is discussed in greater detail in Chapter 4, "Do-it-yourself Propagation Predictions and Master Propagation Charts." Note that even if the times for each solar phase shown in Table 3.3 shift, you will still be able to make shortwave propagation predictions by knowing the smoothed solar flux or smoothed sunspot number.

3.3 References

1. Obridko, V.N., Oraevsky, V. N. (IZMIRAN, Russia), and J. H. Allen (NOAA/NESDIS/NGDC, Boulder, Colorado, U.S.), International Decade of Solar Cycle Studies (IDSCS)," 1992 Conference Paper.

2. Waldmeier, M. "A Prediction of the Next Maximum of Solar Activity," *Terrestrial Magnetism and Atmospheric Electricity,* Vol. 51, 1946.

3. Jacobs, G., "Propagation" column, *CQ,* August 1992.

4. McNish, A. G., and J. V. Lincoln, "Predictions of Sunspot Numbers," *Transactions of the American Geophysical Union,* Vol. 30, 1949.

5. Boykin, E. P., and T. J. Richards, "Application of the Lincoln-McNish Technique to the Prediction of the Remainder of the Twentieth Sunspot Cycle," Lockheed Missiles and Space Company, Technical Memorandum 54/30-89, Huntsville, Alabama, March 1966.

6. Smith, R. E., "Solar Activity Indices," George C. Marshall Space Flight Center, National Aeronautics and Space Administration, 1975.

7. Cohen, T. J., and P. R. Lintz, "Long Term Periodicities in the Sunspot Cycle," *Nature,* Vol. 250, August 2, 1974.

8. Burg, J. P., " Maximum Entropy Spectral Analysis," paper presented at the 37th meeting, Society of Exploration Geophysics, Oklahoma City, Oklahoma, 1967.

9. Ulrych, T. J.,"Maximum Entropy Power Spectrum of Truncated Sinusoids," *Journal of Geophysical Research,* Vol. 77, No. 8, 1972.

10. Ohl, A. L., "A Preliminary Forecast of Some Parameters of Cycle 21 of the Solar Activity," *Solnechnaya Dannyye,* No. 9, 1976.

11. Sargent, III, H. H., "A Prediction for the Next Sunspot Cycle," published in the Proceedings, 28th IEEE Vehicular Technology Conference, Denver, Colorado, March 22–24, 1978.

12. Paul, A. K.,"Anharmonic Frequency Analysis,"

Mathematics of Computation, Vol. 26, No. 118, April 1972.

13. Hill, J. R., "Long-Term Solar Activity Forecasting Using High-Resolution Time Spectral Analysis, *Nature,* Vol. 266, March 10, 1977.

14. Thompson, R. J., "A Technique for Predicting the Amplitude of the Solar Cycle," *Solar Physics,* Vol. 148, pp. 383–388, 1993.

15. Jose, P. D., "Sun's Motion and Sunspots," *The Astronomical Journal,* Vol. 70, No. 3, April 1965.

16. Wood, K. D., "Sunspots and Planets," *Nature,* Vol. 240, November 1972.

17. Okal, E., and D. L. Anderson, "On the Planetary Theory of Sunspots," *Nature,* Vol. 253, February 6, 1975.

18. Gleissberg, W., "The Probable Behavior of the Sunspot Cycle 21," *Solar Physics,* Vol. 21, 1971.

19. "Solar-Geophysical Data" 385, Part I, U.S. Department of Commerce, Boulder, Colorado, January 1978.

20. Smith, R. E., "Solar Activity Indices," George Marshall Space Flight Center, NASA, 1989 (monthly publication).

21. Rose, R. B., "Solar Effects on HF Propagation," Proceedings of the AIAA 15th Aerospace Science Meeting, Los Angeles, California, January 1972.

22. *The 1989 ARRL Handbook For The Radio Amateur,* American Radio Relay League, Newington, Connecticut.

23. Paul, A. K., "Anharmonic Frequency Analysis: The Complement to Fourier Analysis," *Ann. Telecommunic,* March–April 1979.

24. Kunches, J. M., "A Retrospective Look at the Predictions for Sunspot Cycle 22," Proceedings of the Solar-Terrestrial Predictions Workshop, Vol. 2, Ottawa, Canada, May 18–22, 1992.

25. Thompson, R. J. "Recurrent Geomagnetic Disturbances in 53 years of A_p Indices," IPS Radio and Space Services Technical Report IPS TR-85-06, 1985.

26. Smith, P. A.,"Some Techniques Used to Predict Solar Activity Through the 11-Year Cycle," Solar-Terrestrial Predictions: Proceedings of a Workshop in Meudon, France, edited by P. A. Simon, G. Heckman, and M. A. Shea, pp. 8–12, 1984.

27. Thompson, R. J., "The Amplitude of Solar Cycle Number 22," IPS Radio and Space Services Technical Report, IPS TR-87-03, 1987.

28. Gonzales, G. and K. H. Schatten," Using Geomagnetic Indices to Forecast the Next Sunspot Maximum," *Solar Physics,* Vol. 114, pp. 189–192, 1987.

29. Allen, J., "Major Solar Activity of 1989 and Its

Phase	Expected Years of Occurrence
Low	1995 – early 1999
Moderate	early 1999 – late 1999
High	late 1999 – late 2000
Very High	late 2000 –
Intense	no intense activity
Very High	– early 2003
High	early 2003 – early 2004
Moderate	early 2004 – early 2006
Low	early 2006 – ?

Table 3.3. Phases of solar activity for Cycle 23 based on and the work of NASA (Reference 42).

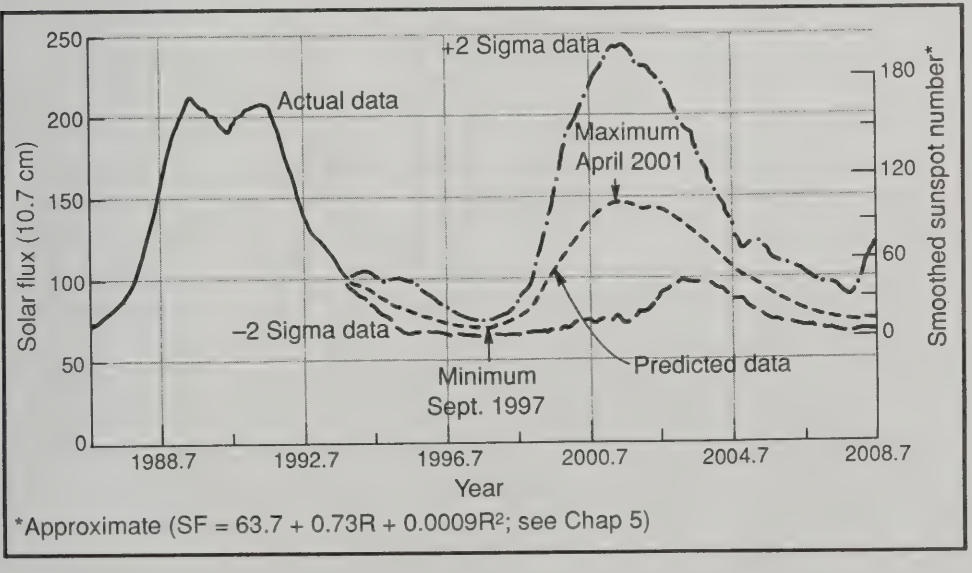

*Approximate (SF = 63.7 + 0.73R + 0.0009R²; see Chap 5)

Figure 3.12. Long-range estimates of solar activity for Cycles 22 and 23. (After NASA[43], 1994.)

Consequences at Earth and In Near-Earth Space," Proceedings on Conference on Prediction and Forecasting of Radio Propagation at High-Latitudes for C^3 Systems, Naval Postgraduate School, Monterey, California, February 12–14, 1991.

30. Wilson, R. M., "Bimodality and the Hale Cycle," *Solar Physics,* Vol. 117, No. 2, 1988, pp. 269–278.

31. Kopecky, M., "Forecast of the Maximum of the Next 11-Year Cycle of Sunspots N 23," *Bulletin of Astronomical Institutes of Czechoslovakia* 42, 157 (1991).

32. Markarov, V. I. and V. P. Mikhailutsa, "A relationship between the latitude of bands at sunspot minimum and the activity level in the two following 11 year solar cycle," Problemy solnechnoi aktivnosti (in Russian), 1991, pp. 146–157.

33. Vitinsky, V. I., private communication, 1992.

34. Rivin, Yu. R., "The Forecast of Unusually High Values of Solar Activity at the End of the Current Century and Its Discussion," *Cycles of Natural Processes, Dangerous Phenomena, and Ecological Forecasting* (in Russian), MNTK "Geos," Moscow, 1992, pp. 144–147.

35. Obridko, V. N., "Remarks on some forecasts of Cycle 23," in preparation (1992).

36. Tritakis, V. P., "A General Outlook for the Coming 22-year Cycle (No. 22–23)," Solar-Terrestrial Predictions, Proc. Workshop in Meudon (France), 1986, NOAA, Boulder, Colorado, 1986, p. 106.

37. Wilson, R. M., E. J. Reichmann and D. L. Teuber, "On Empirical Methods for Estimating Sunspot Number," Solar-Terrestrial Predictions, Proc. Workshop in Meudon (France), NOAA, Boulder, Colorado, 1986, p. 26.

38. Schove, D. J., "Sunspot, Auroral, Radiocarbon and Climatic Data since 7000 BC," *Annales Geophysicae* 1, 4–5, 1983, pp. 391–396.

39. Kontor, N. N., G. P. Lyubimov, N. V. Pereslegina, and T. G. Khotilovckaya, "A prediction of the Sunspot Maxima for Solar Cycles NN 22–44," Solnechnye Dannye (in Russian), No. 9, 1987, pp. 71–74.

40. Chistyakoav, V. F., "A Forecast of Solar Activity Till the Year 2030," Solnechnye Dannye, N1 (in Russian), 1983, pp. 97–100.

41. Mordvinov, A. V., Private communication, 1992.

42. "Solar Activity Inputs for Upper Atmospheric Models used in the Programs to Estimate Spacecraft Orbital Lifetime," NASA, George C. Marshall Space Flight Center, May 1994.

Chapter 4

Do-It-Yourself Propagation Predictions and Master Propagation Charts

While the rest of this book discusses the "why" and the "how" of ionospheric behavior, this chapter is devoted to the practical aspects of ionospheric propagation; that is, how to utilize the ionosphere effectively for HF radio communications. No previous knowledge of the ionosphere or ionospheric propagation is required to use the charts and the do-it-yourself prediction method discussed in this chapter. However, reading Chapter 1 will provide some basic background.

Normally, predicting HF radio propagation conditions can be a tedious task because it involves computation of the "maximum usable frequency" and the "lowest usable frequency," and the construction of circuit analysis curves similar to those described in Chapter 1 (see Section 1.3). Excellent computer programs that perform these functions have been developed for use by radio amateurs and shortwave listeners, and we will review some in Chapter 6. In this chapter, however, large quantities of complicated data have been reduced to relatively simple-to-use Master Propagation Charts, and these charts make the task of predicting either DX or short-skip HF propagation conditions no more difficult or time consuming than reading an airline timetable or a road map!

The Master DX Propagation Charts and the Master Short-Skip Propagation Charts contained in Sections 4.3 to 4.6 of this chapter make it possible for users of the HF radio spectrum to predict propagation conditions from most areas of the USA and Canada to just about any spot on Earth, given the frequency, time of day, season of the year, and phase of the solar cycle. The charts have been derived from a computer analysis of hundreds of DX and short-skip paths, and they have been well tested for utility and accuracy over a period of more than 40 years through the "Propagation" column that appears monthly in *CQ* magazine.[1]

In short, the Master Propagation Charts provide everything that is required to make do-it-yourself HF propagation predictions of relatively high accuracy in a matter of a few moments.

4.1 How To Use The Master DX Propagation Charts

Table 4.1 is a sample of a portion of a Master DX Propagation Chart. The DX Charts are intended for use to areas of the world outside the U.S.A. and Canada.

The chart contains *five* variables that require an explanation: **solar phase, season, frequency, time,** and **propagation index.**

Solar Phase: Sets of charts have been prepared for the major phases of a solar cycle, as shown in Table 4.2.

These phases are expected to occur in the present sunspot cycle, Cycle 22, and the forthcoming cycle, Cycle 23, during the years shown in Table 4.3. See Section 3.2 in Chapter 3 for more details.

In using the Master DX Propagation Charts, it is advisable to check for the latest smoothed sunspot number[2] rather than relying on the information given in Tables 4.2 and 4.3, because actual solar activity may differ from predicted values. Charts for a Very High phase of solar activity also can be used during an Intense period of solar activity.

Once a smoothed sunspot number is known, or assumed from Table 4.3, the Master DX Propagation

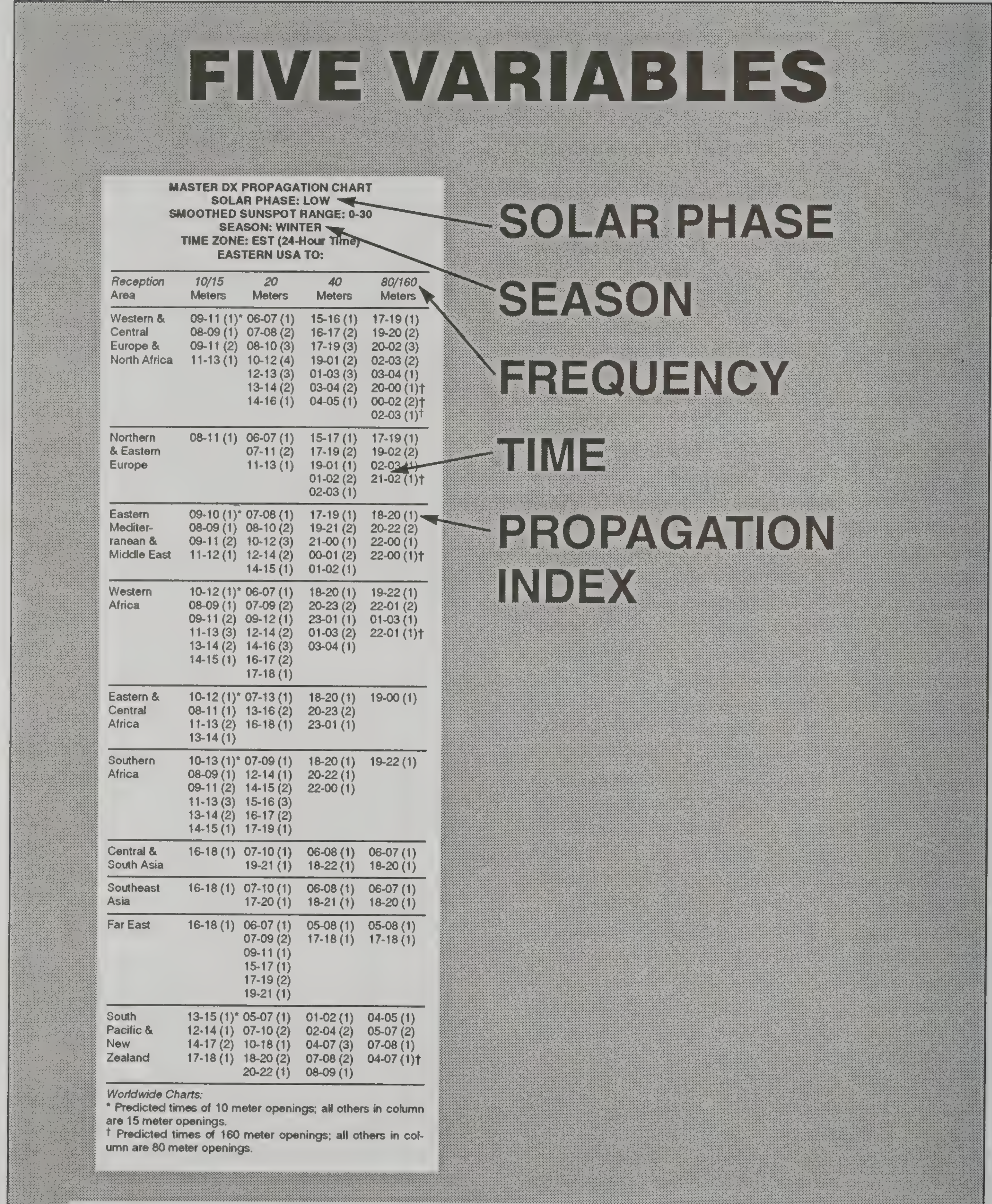
FIVE VARIABLES
SOLAR PHASE
SEASON
FREQUENCY
TIME
PROPAGATION INDEX

MASTER DX PROPAGATION CHART
SOLAR PHASE: LOW
SMOOTHED SUNSPOT RANGE: 0-30
SEASON: WINTER
TIME ZONE: EST (24-Hour Time)
EASTERN USA TO:

Reception Area	*10/15* Meters	*20* Meters	*40* Meters	*80/160* Meters
Western & Central Europe & North Africa	09-11 (1)* 08-09 (1) 09-11 (2) 11-13 (1)	06-07 (1) 07-08 (2) 08-10 (3) 10-12 (4) 12-13 (3) 13-14 (2) 14-16 (1)	15-16 (1) 16-17 (2) 17-19 (3) 19-01 (2) 01-03 (3) 03-04 (2) 04-05 (1)	17-19 (1) 19-20 (2) 20-02 (3) 02-03 (2) 03-04 (1) 20-00 (1)† 00-02 (2)† 02-03 (1)†
Northern & Eastern Europe	08-11 (1)	06-07 (1) 07-11 (2) 11-13 (1)	15-17 (1) 17-19 (2) 19-01 (1) 01-02 (2) 02-03 (1)	17-19 (1) 19-02 (2) 02-03 (1) 21-02 (1)†
Eastern Mediterranean & Middle East	09-10 (1)* 08-09 (1) 09-11 (2) 11-12 (1)	07-08 (1) 08-10 (2) 10-12 (3) 12-14 (2) 14-15 (1)	17-19 (1) 19-21 (2) 21-00 (1) 00-01 (2) 01-02 (1)	18-20 (1) 20-22 (2) 22-00 (1) 22-00 (1)†
Western Africa	10-12 (1)* 08-09 (1) 09-11 (2) 11-13 (3) 13-14 (2) 14-15 (1)	06-07 (1) 07-09 (2) 09-12 (1) 12-14 (2) 14-16 (3) 16-17 (2) 17-18 (1)	18-20 (1) 20-23 (2) 23-01 (1) 01-03 (2) 03-04 (1)	19-22 (1) 22-01 (2) 01-03 (1) 22-01 (1)†
Eastern & Central Africa	10-12 (1)* 08-11 (1) 11-13 (2) 13-14 (1)	07-13 (1) 13-16 (2) 16-18 (1)	18-20 (1) 20-23 (2) 23-01 (1)	19-00 (1)
Southern Africa	10-13 (1)* 08-09 (1) 09-11 (2) 11-13 (3) 13-14 (2) 14-15 (1)	07-09 (1) 12-14 (1) 14-15 (2) 15-16 (3) 16-17 (2) 17-19 (1)	18-20 (1) 20-22 (1) 22-00 (1)	19-22 (1)
Central & South Asia	16-18 (1)	07-10 (1) 19-21 (1)	06-08 (1) 18-22 (1)	06-07 (1) 18-20 (1)
Southeast Asia	16-18 (1)	07-10 (1) 17-20 (1)	06-08 (1) 18-21 (1)	06-07 (1) 18-20 (1)
Far East	16-18 (1)	06-07 (1) 07-09 (2) 09-11 (1) 15-17 (1) 17-19 (2) 19-21 (1)	05-08 (1) 17-18 (1)	05-08 (1) 17-18 (1)
South Pacific & New Zealand	13-15 (1)* 12-14 (1) 14-17 (2) 17-18 (1)	05-07 (1) 07-10 (2) 10-18 (1) 18-20 (2) 20-22 (1)	01-02 (1) 02-04 (2) 04-07 (3) 07-08 (2) 08-09 (1)	04-05 (1) 05-07 (2) 07-08 (1) 04-07 (1)†

Worldwide Charts:
* Predicted times of 10 meter openings; all others in column are 15 meter openings.
† Predicted times of 160 meter openings; all others in column are 80 meter openings.

Table 4.1. Sample Master DX Propagation Chart.

Solar Phase	Smoothed Sunspot Number Range	10.7 cm Solar Flux Range	Section In Which Charts Appear
LOW	0–30	< 70–90	4.3
MODERATE	30–60	90–110	4.4
HIGH	60–90	110–130	4.5
VERY HIGH	90–120	130–150	4.6
INTENSE	>120	> 150	Use 4.6

Table 4.2. Major phases of a solar cycle for which Master DX Propagation Charts appear in this chapter.

Chart for the appropriate solar phase can be selected from Sections 4.3 through 4.6.

Season: There are three sets of charts covering the four seasons, as shown in Table 4.4.

The appropriate seasonal chart can be selected from Table 4.4, depending upon the month for which the prediction is to be made.

Frequency: Predictions are contained in the charts for the amateur 10, 15, 20, 40, 80, and 160 meter HF bands. The charts also can be used with the WARC and HF broadcasting bands, as shown in Tables 4.5 and 4.6, respectively.

LOW	1995–early 1999
MODERATE	early 1999–late 1999
HIGH	late 1999–late 2000
VERY HIGH	late 2000–
INTENSE	no intense activity
VERY HIGH	–early 2003
HIGH	early 2003–early 2004
MODERATE	early 2004–early 2006
LOW	early 2006–?

Table 4.3. Solar phases expected during sunspot Cycles 22 and 23.

Time: Time in the charts is given by the 24-hour system. Charts are available for three sets of time zones: EST, CST and MST, and PST. Standard time is used throughout. Table 4.7 can be used to convert from 24-hour to regular time, to daylight time during the months when it is applicable, and to UTC.

Propagation Index: This is the number that appears in ( ) after the time of each predicted opening shown in the charts. The propagation index indicates the number of days during a month on which the predicted opening is expected to occur, as shown in Table 4.8. The higher the propagation index, the better is the chance for the opening to occur.

The propagation index statistically tells the number of days to expect the predicted opening during the month, but it does not indicate the specific days on which the opening is likely to occur. In Chapter 5, two methods are examined for merging the propagation predictions discussed in this chapter with short-term, day-to-day forecasts so that the *actual* days on which an expected opening may occur can be determined.

The Master DX Propagation Charts are based on an Effective Radiated Power (ERP) of 1000 watts. For each 10 dB gain above this reference, the propagation index will increase by one level; for each 10 dB drop, it will decrease by one level. The ERP is the power output from the transmitter, multiplied by the gain of the transmitting antenna system, taking into account feeder line losses.

The following are several examples which illustrate the ease with which the Master DX Propagation Charts can be used.

Example 1: It is December 1997, and you want to work a radio amateur friend in France at noon. You live in Washington, D.C. What is the best band to use?

1. From Table 4.3, December 1997 is expected to correspond to a Low Solar Phase. From Table 4.2, Master Propagation Charts for Low Solar Phase are found in Section 4.3 of this chapter.

2. From Table 4.4, the Winter seasonal chart should be used for December. Because Washington, D.C. is in the EST zone, the EST chart should be used. From Table 4.7, noon EST corresponds to 12 in the 24-hour time system.

3. From the appropriate Master DX Propagation Chart contained in Section 4.3 (for EST, Winter, Low Solar Phase), or in this case, from the sample con-

SUMMER Charts—For use during **May, June, July,** and **August**
WINTER Charts—For use during **November, December, January,** and **February**
SPRING & FALL Charts—For use during **March, April, September,** and **October**

Table 4.4. Months during which seasonal propagation charts can be used.

For 12 meter openings, interpolate between 10 and 15 meter openings.
For 17 meter openings, interpolate between 15 and 20 meter openings.
For 30 meter openings, interpolate between 40 and 20 meter openings.

Table 4.5. WARC bands included in Master DX Propagation Charts.

tained in Table 4.1, you find under "Western and Central Europe and North Africa" a propagation index of (1) under 15 meters at 12 hours; (3) under 20 meters; and no entries for 12 hours under 40, 80, or 160 meters. The best band to use, therefore, would be 20 meters.

Example 2: You live in California, and you want to try to hear an elusive broadcast station located in Liberia, Western Africa, that operates around-the-clock in the 25 meter broadcasting band. It is June, and you have determined that the smoothed sunspot number is 80. When would be the best time to listen for the station?

1. From Table 4.2, a smoothed sunspot number of 80 is found to correspond to a High Solar Phase, and appropriate charts will be found in Section 4.5 of this chapter.

2. From Table 4.4, the Summer seasonal chart should be used for June, and the PST zone chart would be applicable for California.

3. From Table 4.6, it is found that the 25 meter broadcasting band corresponds to the 20 meter amateur band.

4. From the appropriate Master DX Propagation Chart found in Section 4.5 (Summer, PST, High Solar Phase), you find at the intersection of "20 meters" and "West and Central Africa" that the highest propagation index is (4), and that this occurs between 19 and 21 hours. This would be the best time to listen for the desired station. From Table 4.7, this corresponds to between 8 and 10 PM PDT.

Example 3: It is 3 PM in Denver on a day in March, and you want to operate on the HF band for an hour or so. From what area of the world can you expect the strongest signals on 15 meters and on 20 meters? You already know that the smoothed sunspot number is around 40.

1. From Table 4.3, you find that a smoothed sunspot number of 40 corresponds to a Moderate Solar Phase, and that the appropriate charts for this phase can be found in Section 4.4 of this chapter.

2. From Table 4.4, for the month of March the appropriate seasonal chart to use would be Spring & Fall. For Denver, the CST & MST zones chart would be applicable. From Table 4.7, you find that 3 PM MST corresponds to 15 hours in the 24-hour time system used in the charts.

3. From the appropriate Master DX Propagation Chart contained in Section 4.4 (Moderate, Spring & Fall, CST & MST zones), you find under "15 meters" that the highest propagation index that is shown anywhere in the world for 15 hours is (4) to the "Caribbean, Central America & Northern Countries of South America" and (4) also to "Peru, Bolivia, Paraguay, Brazil, Chile, Argentina & Uruguay."

4. Under "20 meters," the highest propagation index shown at 15 hours is a (4), for "West & Central Africa."

4.2 How To Use The Master Short-Skip Propagation Charts

Table 4.9 is a sample of a Master Short-Skip Propagation Chart. The Short-Skip Charts are intended for use within the United States and Canada over distances ranging up to 2300 miles, which is considered to be the maximum possible distance for one-hop F_2-layer propagation.

The explanations given for **Solar Phase, Season,** and **Frequency** in Section 4.1 for the Master DX Propagation Charts also apply to the Master Short-Skip Propagation Charts. The Short-Skip Charts are found following the DX Charts in Sections 4.3 through 4.6. Tables 4.2 through 4.7 also are applicable to the Short-Skip Charts.

The explanation for the **Propagation Index** given in Table 4.8 also applies to the Short-Skip Charts except that often, *two* numerals are shown within a single set of parentheses. Where this is the case, the first applies to the shorter distance of the distance range shown, while the second is for the greater distance.

In the Short-Skip Charts, appropriate *standard* time is given in the 24-hour time system, but it applies at the *path mid-point* rather than at the receiving or transmitting ends. For example, on an opening

10 meter amateur band applies to 11 meter BC band
15 meter amateur band applies to 13 and 16 meter BC bands
20 meter amateur band applies to 19 and 25 meter BC bands
40 meter amateur band applies to 31, 41, and 49 meter BC bands
80 meter amateur band applies to 60, 75, and 90 meter BC bands
160 meter amateur band applies to 120 meter BC band

Table 4.6. HF broadcasting bands included in Master DX Propagation Charts.

EST ZONE

24-hour Time	EST	EDT	UTC
00	Midnight	1 AM	0500
01	1 AM	2 AM	0600
02	2 AM	3 AM	0700
03	3 AM	4 AM	0800
04	4 AM	5 AM	0900
05	5 AM	6 AM	1000
06	6 AM	7 AM	1100
07	7 AM	8 AM	1200
08	8 AM	9 AM	1300
09	9 AM	10 AM	1400
10	10 AM	11 AM	1500
11	11 AM	Noon	1600
12	Noon	1 PM	1700
13	1 PM	2 PM	1800
14	2 PM	3 PM	1900
15	3 PM	4 PM	2000
16	4 PM	5 PM	2100
17	5 PM	6 PM	2200
18	6 PM	7 PM	2300
19	7 PM	8 PM	0000
20	8 PM	9 PM	0100
21	9 PM	10 PM	0200
22	10 PM	11 PM	0300
23	11 PM	Midnight	0400
24	Midnight	1 AM	0500

CST ZONE

24-hour Time	CST	CDT	UTC
00	Midnight	1 AM	0600
01	1 AM	2 AM	0700
02	2 AM	3 AM	0800
03	3 AM	4 AM	0900
04	4 AM	5 AM	1000
05	5 AM	6 AM	1100
06	6 AM	7 AM	1200
07	7 AM	8 AM	1300
08	8 AM	9 AM	1400
09	9 AM	10 AM	1500
10	10 AM	11 AM	1600
11	11 AM	Noon	1700
12	Noon	1 PM	1800
13	1 PM	2 PM	1900
14	2 PM	3 PM	2000
15	3 PM	4 PM	2100
16	4 PM	5 PM	2200
17	5 PM	6 PM	2300
18	6 PM	7 PM	0000
19	7 PM	8 PM	0100
20	8 PM	9 PM	0200
21	9 PM	10 PM	0300
22	10 PM	11 PM	0400
23	11 PM	Midnight	0500
24	Midnight	1 AM	0600

MST ZONE

24-hour Time	MST	MDT	UTC
00	Midnight	1 AM	0700
01	1 AM	2 AM	0800
02	2 AM	3 AM	0900
03	3 AM	4 AM	1000
04	4 AM	5 AM	1100
05	5 AM	6 AM	1200
06	6 AM	7 AM	1300
07	7 AM	8 AM	1400
08	8 AM	9 AM	1500
09	9 AM	10 AM	1600
10	10 AM	11 AM	1700
11	11 AM	Noon	1800
12	Noon	1 PM	1900
13	1 PM	2 PM	2000
14	2 PM	3 PM	2100
15	3 PM	4 PM	2200
16	4 PM	5 PM	2300
17	5 PM	6 PM	0000
18	6 PM	7 PM	0100
19	7 PM	8 PM	0200
20	8 PM	9 PM	0300
21	9 PM	10 PM	0400
22	10 PM	11 PM	0500
23	11 PM	Midnight	0600
24	Midnight	1 AM	0700

PST ZONE

24-hour Time	PST	PDT	UTC
00	Midnight	1 AM	0800
01	1 AM	2 AM	0900
02	2 AM	3 AM	1000
03	3 AM	4 AM	1100
04	4 AM	5 AM	1200
05	5 AM	6 AM	1300
06	6 AM	7 AM	1400
07	7 AM	8 AM	1500
08	8 AM	9 AM	1600
09	9 AM	10 AM	1700
10	10 AM	11 AM	1800
11	11 AM	Noon	1900
12	Noon	1 PM	2000
13	1 PM	2 PM	2100
14	2 PM	3 PM	2200
15	3 PM	4 PM	2300
16	4 PM	5 PM	0000
17	5 PM	6 PM	0100
18	6 PM	7 PM	0200
19	7 PM	8 PM	0300
20	8 PM	9 PM	0400
21	9 PM	10 PM	0500
22	10 PM	11 PM	0600
23	11 PM	Midnight	0700
24	Midnight	1 AM	0800

Table 4.7. This table simplifies converting from 24-hour time shown in the Master Propagation Charts to regular time, and from regular time to daylight time and UTC, for each of the continental U.S.A. time zones.

(4)	Openings expected on more than 22 days during the month
(3)	Openings expected between 14 and 22 days during the month
(2)	Openings expected between 7 and 13 days during the month
(1)	Openings expected on less than 7 days during the month

Table 4.8. Propagation index in relation to the number of days an opening is expected to occur during a month.

between Maine and Florida, the time at the path mid-point would be EST; on an opening between New York and Colorado, the time in the chart would be CST, since the path mid-point falls in this time zone.

The following are several examples that illustrate the use of the Master Short-Skip Propagation Charts.

Example 1: You live in Los Angeles and you want to contact another radio amateur in California, about 350 miles away. You want to set up a schedule every Saturday during March 1999 at noon PST. You have no idea what the smoothed sunspot number might be. What is the best band to use?

1. From Table 4.3, March 1999 is expected to correspond to a Moderate Solar Phase. From Table 4.2, Master Propagation Charts for a Moderate Solar Phase can be found in Section 4.4 of this chapter. The Short-Skip Charts follow the DX Charts.

2. From Table 4.4, the Spring & Fall seasonal chart should be used for March. Because the path mid-point in this example falls in the PST zone, the charts will give results in PST. From Table 4.7, noon PST corresponds to 12 hours.

3. From the appropriate Master Short-Skip Propagation Chart contained in Section 4.4 (Moderate, Spring & Fall), or in this case, from the sample chart shown in Table 4.9, you find that under the range 250–750 miles between stations, the highest propagation index occurring at 12 hours is a (4-2) for "40 meters." The "4" applies to the shorter distance. This means 40 meters would be the best band to use for contacting a station 350 miles away at noon PST during March 1999.

Example 2: What would be the best time to keep a regular schedule on 15 meters between a station in New York City and one in Denver during the winter months when the smoothed sunspot number is expected to be around 70?

1. From Table 4.2, a smoothed sunspot number of around 70 corresponds to a High Solar Phase, and appropriate Short-Skip Charts can be found in Section 4.5.

2. The distance between New York City and Denver is measured on a map to be 1600 miles. The path mid-point falls in the CST zone.

3. Finding the appropriate Short-Skip Chart in Section 4.5 (High, Winter), enter the chart under the column heading marked "Distance Between Stations (miles)" for the range 1300–2300 miles. Note the propagation index shown next to each opening at the intersection of this column and the one marked "15

MASTER SHORT-SKIP PROPAGATION CHART
SOLAR PHASE: MODERATE
SMOOTHED SUNSPOT RANGE: 30-60
SEASONS: SPRING & FALL
TIME ZONES: LOCAL STANDARD AT PATH MID-POINT
(24-Hour Time)

Band	*Distance Between Stations (Miles)*			
(Meters)	*50-250*	*250-750*	*750-1300*	*1300-2300*
10	*Nil*	*Nil*	08-09 (0-1) 09-12 (0-2) 12-14 (0-3) 14-16 (0-2) 16-18 (0-1)	08-09 (1-0) 09-12 (2-1) 12-14 (3-2) 14-16 (2) 16-17 (1-2) 17-18 (1) 18-20 (0-1)
15	*Nil*	08-09 (1) 09-15 (0-2) 15-17 (0-1)	07-08 (0-1) 08-09 (1) 09-10 (2) 10-15 (2-4) 15-17 (1-3) 17-18 (0-2) 18-20 (0-1)	07-08 (1-0) 08-09 (1) 09-10 (2-3) 10-15 (4) 15-17 (3) 17-18 (2-3) 18-20 (1-2) 20-21 (0-1)
20	11-13 (0-1) 13-15 (0-2) 15-16 (0-1)	07-10 (0-1) 10-11 (0-2) 11-13 (1-3) 13-15 (2-4) 15-16 (1-3) 16-18 (0-3) 18-20 (0-2) 20-07 (0-1)	06-08 (1-2) 08-10 (1-3) 10-13 (3-4) 13-15 (4) 15-18 (3-4) 18-20 (2-3) 20-22 (1-2) 22-06 (1)	06-07 (2-1) 07-08 (2) 08-10 (3) 10-15 (4-3) 15-18 (4) 18-20 (3-4) 20-22 (2-3) 22-02 (1-2) 02-06 (1)
40	06-07 (1-2) 07-09 (2-3) 09-18 (3-4) 18-19 (2-3) 19-21 (1-2) 21-00 (0-1)	06-07 (2-3) 07-09 (3-4) 09-11 (4-3) 11-13 (4-2) 13-15 (4-3) 15-18 (1) 18-19 (3-4) 19-20 (2-4) 20-21 (2-3) 21-00 (1-2) 00-06 (0-1)	06-07 (3-2) 07-08 (4-2) 08-09 (4-1) 09-11 (3-1) 11-13 (2-1) 13-15 (3-1) 15-17 (4-2) 17-19 (4-3) 19-20 (4) 20-21 (3-4) 21-00 (2-3) 00-02 (1-3) 02-06 (1-2)	06-08 (2-1) 08-15 (1-0) 15-16 (2-0) 16-17 (2-1) 17-19 (3-2) 19-21 (4-3) 21-22 (4) 22-00 (3-4) 00-02 (3) 02-05 (2-3) 05-06 (2)
80	07-08 (2-3) 08-11 (3-4) 11-18 (4-3) 18-20 (3-4) 20-22 (2-3) 22-02 (1-2) 02-05 (1) 05-07 (1-2)	07-08 (3-2) 08-11 (4-1) 11-16 (3-0) 16-18 (3-2) 18-20 (4-3) 20-22 (3-4) 22-02 (2-4) 02-05 (1-2) 05-07 (2)	07-08 (2-1) 08-11 (1-0) 11-16 (0) 16-18 (2-1) 18-20 (3-2) 20-02 (4) 02-05 (2-3) 05-07 (2)	07-08 (1-0) 08-16 (0) 16-18 (1-0) 18-20 (2-1) 20-22 (1-2) 22-02 (4-3) 02-05 (3-2) 05-07 (2-1)
160	05-07 (4-2) 07-09 (3-1) 09-17 (2-0) 17-19 (3-1) 19-20 (4-2) 20-05 (4)	05-06 (2-1) 06-07 (2-0) 07-09 (1-0) 09-17 (0) 17-19 (1-0) 19-20 (2) 20-22 (4-3) 22-03 (4) 03-05 (4-3)	05-06 (1) 06-19 (0) 19-20 (2-1) 20-22 (3-2) 22-03 (4-2) 03-05 (3-2)	05-06 (1) 06-19 (0) 19-20 (1-0) 20-22 (2-1) 22-03 (2) 03-05 (2-4)

Table 4.9. Sample Master Short-Skip Propagation Chart.

meters." The highest propagation index, (4), occurs between 11 and 16 hours. From Table 4.7, this corresponds to 11 AM to 4 PM CST.

This means that the best time to make contact between New York City and Denver during the winter of High solar activity on 15 meters would be between 11 AM and 4 PM CST. This would be between noon and 5 PM EST at the end of the path and between 10 AM and 3 PM MST in Denver.

Example 3: You live in Boston and you want to set up a three-way schedule with a radio amateur in Washington, D.C., about 500 miles away, and with another in central North Carolina, about 750 miles away. What would be the best band to use at 7 PM EDT during the summertime when solar activity is at a Moderate level? In this case, all stations must be able to work each other.

1. From Table 4.2, Short-Skip Charts for the Summer season of a Moderate Solar Phase can be found in Section 4.4. From Table 4.7, 7 PM EDT corresponds to 18 hours EST in 24-hour time. Because all three stations are in the EST Zone, the results in the chart also will be in EST.

2. Finding the appropriate Short-Skip Chart in Section 4.4 (Moderate, Summer), enter the chart under the column heading marked "Distance Between Stations (miles)" for the distance range that corresponds to the 500 miles between Boston and Washington, D.C. The highest propagation index at 18, (4), occurs on "40 meters." Next, do the same for the range that corresponds to the distance of 750 miles between Boston and central North Carolina. On 40 meters at 18 hours for this distance, the propagation index also is (4), so there should be no problem communicating between Boston and Washington, D.C., and Boston and central North Carolina. Now, to finish the network, check 40 meters at 18 hours for the 250 miles between Washington, D.C., and central North Carolina. Here, again, the propagation index is found to be (4), so this three-way contact should work out very well.

4.3 Master Propagation Charts—Low Solar Phase Smoothed Sunspot Number Range 0–30

Band-By-Band Summary

10 meters. DX possibilities in this band are very poor, although an occasional F_2-layer opening should be possible towards South America and other tropical areas during the daylight hours of the fall, winter, and early spring months. During the summer months, when sporadic-*E* ionization is at a maximum, fairly regular short-skip openings should be possible from a few hundred miles up to a distance of approximately 1300 miles. When sporadic-*E* ionization is particularly intense and widespread, multi-hop openings considerably beyond this range also may occur.

15 meters. ***Summer:*** DX openings in this band are expected to be fairly good, and fairly regular, particularly on circuits into the southern hemisphere. Because of relatively high sporadic-*E* activity, short-skip activity should be good to excellent at distances of from 300 to 1300 miles.

Winter: Through the daylight hours, DX openings should be generally fair to good, particularly during the period from noon to around sunset. Short-skip should be fairly consistent from around sunrise to sunset, but not much can be expected at night, when critical frequencies are depressed.

Equinox: About the only consistent DX in this band in the spring and fall occurs on circuits to Africa and Latin America from the northern hemisphere. Short-skip openings may be fairly good over distances of 1000 miles or more.

20 meters. ***Summer:*** During the summer in the low part of the sunspot cycle, the 20 meter band is the best band for consistent daytime DX to all parts of the world. It should remain open from sunrise to sunset, and often, to as late as midnight. Peak conditions can be expected for an hour or two after sunrise and again during the late afternoon. In addition to DX, the seasonal increase in sporadic-*E* activity should make short-skip openings a frequent occurrence over distances ranging from a few hundred miles to approximately 2300 miles.

Winter: Although the hours of daylight are considerably fewer than during the summer, what daylight hours there are will be good for DX activity in the 20 meter band. Peak conditions, with openings possible to all areas of the world, should occur for several hours after sunrise and again during the early afternoon. The band normally will close for DX an hour or so after sundown, but it may occasionally remain open to midnight for openings towards South America and Antarctica. Short-skip openings from a few hundred miles to approximately 2300 miles should be possible throughout the daylight hours.

Equinox: Again, this should be the best band for DX openings to all areas of the world between sunrise and sunset. The band should remain open from time to time well past sunset, particularly for long openings into the southern hemisphere. Excellent short-skip openings between distances of a few hundred and approximately 2300 miles should be possible during the daylight hours.

40 meters. ***Summer:*** In the summertime, because of greater thunderstorm activity, there is an increase in the static level on most shortwave bands; as the frequency is lowered, the noise becomes more pronounced. In spite of increased static in the 40 meter band, nighttime DX openings should be numerous and consistent from just before sunset to just after sunrise, to all parts of the world. Daytime short-skip should range between distances of 100 and approximately 1000 miles. Nighttime short-skip should be possible between distances of 500 and 2300 miles.

Winter: Forty meters should open for DX in an easterly direction towards Europe and Africa during the late afternoon, and towards the south just after sundown, after which time the MUF will fall below 7 MHz to many areas of the world. Openings towards the South Pacific and in a westerly direction should be possible after midnight and should peak just before sunrise. Short-skip openings during the daytime should range between distances of approximately 100 and 1000 miles, and between 1000 and 2300 miles at night.

Equinox: The band should remain open for DX from just before sunset, through the hours of darkness, and until just after sunrise. Signals from the east should peak between sunset and midnight; signals from all other directions should peak between midnight and sunrise. Daytime short-skip should range between distances of 100 and 1000 miles; nighttime short-skip should range between 1000 and 2300 miles.

80 Meters. ***Summer:*** Generally fair DX is possible on this band during the hours of darkness to many areas of the world, although static levels will be high. During daylight hours, short-skip openings to distances of up to 250 miles should be likely, ranging between

MASTER DX PROPAGATION CHART
SOLAR PHASE: LOW
SMOOTHED SUNSPOT RANGE: 0-30
SEASON: SUMMER
TIME ZONE: EST (24-Hour Time)
EASTERN USA TO:

Reception Area	*10/15 Meters*	*20 Meters*	*40 Meters*	*80/160 Meters*
Western & Central Europe & North Africa	15-18 (1)	05-06 (1) 06-09 (3) 09-13 (2) 13-15 (3) 15-17 (4) 17-19 (3) 19-20 (2) 20-21 (1)	19-22 (1) 22-00 (2) 00-02 (1)	21-23 (1) 23-00 (2) 00-01 (1) 23-01 (1)†
Northern & Eastern Europe	*Nil*	05-07 (1) 07-09 (2) 09-14 (1) 14-16 (2) 16-19 (1)	22-00 (1)	22-00 (1)
Eastern Mediter-ranean & East Africa	11-13 (1)	05-06 (1) 06-07 (2) 07-09 (1) 09-11 (2) 11-15 (1) 15-17 (2) 17-19 (1)	20-00 (1)	21-23 (1)
Western Africa	14-17 (1)	04-06 (1) 06-08 (2) 08-15 (1) 15-16 (2) 16-18 (3) 18-19 (2) 19-21 (1)	21-00 (1) 00-02 (2) 02-04 (1)	00-02 (1)
Central & South Africa	*Nil*	05-06 (1) 06-07 (2) 07-14 (1) 14-16 (2) 16-18 (1) 01-03 (1)	22-23 (1) 23-01 (2) 01-03 (1)	23-01 (1)
Central & South Asia	*Nil*	05-08 (1) 18-21 (1)	*Nil*	*Nil*
Southeast Asia	*Nil*	05-06 (1) 06-08 (2) 08-10 (1) 18-21 (1)	*Nil*	*Nil*
Far East	*Nil*	06-07 (1) 07-09 (2) 09-11 (1) 20-23 (1)	*Nil*	*Nil*
South Pacific & New Zealand	18-20 (1)	16-22 (1) 22-00 (2) 00-06 (1) 06-09 (2) 09-11 (1)	01-02 (1) 02-05 (2) 05-06 (1)	02-05 (1) 02-04 (1)†
Australasia	19-22 (1)	15-22 (1) 22-00 (2) 00-06 (1) 06-09 (2) 09-11 (1)	01-02 (1) 02-05 (2) 05-06 (1)	03-05 (1) 03-04 (1)†
Carribbean, Central America & Northern Countries of South America	13-15 (1)* 15-17 (2)* 17-18 (1)* 08-09 (1) 09-11 (3) 11-13 (2) 13-14 (3) 14-17 (4) 17-19 (3) 19-21 (1)	06-07 (3) 07-09 (4) 09-11 (3) 11-16 (2) 16-18 (3) 18-21 (4) 21-22 (3) 22-00 (2) 00-06 (1)	19-21 (1) 21-00 (2) 00-03 (3) 03-05 (2) 05-06 (1)	22-01 (1) 01-04 (2) 04-05 (1) 01-03 (1)†
Peru, Bolivia, Paraguay, Brazil, Chile, Argentina & Uruguay	14-17 (1)* 08-11 (1) 11-14 (2) 14-15 (3) 15-16 (4) 16-17 (3) 17-18 (2) 18-20 (1)	05-06 (1) 06-10 (2) 10-14 (1) 14-17 (2) 17-18 (3) 18-20 (4) 20-22 (3) 22-23 (2) 23-01 (1)	21-00 (1) 00-02 (2) 02-06 (1)	00-04 (1) 02-04 (1)†
McMurdo Sound, Antarctica	14-17 (1)	14-16 (1) 16-18 (2) 18-22 (1)	03-07 (1)	*Nil*

MASTER DX PROPAGATION CHART
SOLAR PHASE: LOW
SMOOTHED SUNSPOT RANGE: 0-30
SEASON: SUMMER
TIME ZONES: CST & MST (24-Hour Time)
CENTRAL USA TO:

Reception Area	*10/15 Meters*	*20 Meters*	*40 Meters*	*80/160 Meters*
Western & Central Europe & North Africa	15-17 (1)	05-06 (1) 06-08 (2) 08-12 (1) 12-14 (2) 14-17 (3) 17-19 (2) 19-20 (1)	20-22 (1) 22-00 (2) 00-01 (1)	21-23 (1)
Northern & Eastern Europe	*Nil*	05-07 (1) 07-09 (2) 09-13 (1) 13-15 (2) 15-18 (1)	21-23 (1)	*Nil*
Eastern Mediterranean & East Africa	*Nil*	05-06 (1) 06-07 (2) 07-14 (1) 14-16 (2) 16-18 (1)	20-23 (1)	*Nil*
Western Africa	*Nil*	05-06 (1) 06-09 (2) 09-14 (1) 14-16 (2) 16-17 (3) 17-18 (2) 18-20 (1)	21-00 (1) 00-01 (2) 01-03 (1)	00-01 (1)
Central & South Africa	*Nil*	05-06 (1) 06-07 (2) 07-14 (1) 14-16 (2) 16-18 (1) 00-02 (1)	22-23 (1) 23-00 (2) 00-02 (1)	22-00 (1)
Central & South Asia	*Nil*	05-09 (1) 18-21 (1)	*Nil*	*Nil*
Southeast Asia	*Nil*	05-06 (1) 06-09 (2) 09-11 (1) 18-20 (1) 20-22 (2) 22-23 (1)	*Nil*	*Nil*
Far East	21-23 (1)	06-07 (1) 07-10 (2) 10-20 (1) 20-22 (2) 22-00 (1)	04-06 (1)	*Nil*
South Pacific & New Zealand	14-18 (1) 18-20 (2) 20-22 (1)	02-06 (1) 06-09 (2) 09-17 (1) 17-19 (2) 19-22 (3) 20-02 (2)	00-02 (1) 02-06 (2) 06-07 (1)	01-06 (1) 03-05 (1)†
Australasia	15-17 (1) 17-19 (2) 19-22 (1)	06-07 (1) 07-09 (2) 09-13 (1) 13-15 (2) 15-18 (1) 18-20 (2) 20-23 (3) 23-01 (2) 01-03 (1)	00-02 (1) 02-05 (2) 05-07 (1)	02-03 (1) 03-05 (2) 05-06 (1) 03-05 (1)†

200 and approximately 2300 miles during the night.

Winter: This should be the best band for DX during most of the hours of darkness. DX to most areas of the world should be possible from sundown to sunrise, with peaks at about midnight and again just before sunrise. Short-skip openings to distances of up to about 500 miles should be possible during the day, and between distances of 750 and 2300 miles at night.

Equinox: Fairly good DX conditions to most areas of the world should be possible between sundown and sunrise. Excellent short-skip openings should be possible during the day over distances of up to about 350 miles. During the hours of darkness, short-skip openings should range between 500 and 2300 miles.

160 meters. ***Summer:*** During the daylight hours, high levels of static and solar absorption will prevent any short-skip openings. During the hours of darkness, short-skip openings should be possible at ranges out to approximately 1000 miles and, at times, to greater distances. Conditions do not favor DX openings on this band during the summer, although an occasional opening may be possible during the hours of darkness.

Winter: In spite of low sunspot conditions, solar absorption rules out any skip during the daylight hours. Around sunset, the band will begin to open for skip. Regular short-skip openings to distances of up to 1500 miles should be possible, with frequent openings up to 2300 miles. DX openings should be possible, with conditions peaking towards Europe and the east near midnight, and towards the west, south, and other directions just before sunrise.

Equinox: No daylight skip is possible, but look for short-skip and DX openings during the hours of darkness. Expect short-skip openings regularly to distances of up to 1200 miles and occasionally up to 2300 miles. DX openings are expected to some areas of the world, with conditions expected to peak around midnight and again just before sunrise.

Caribbean, Central America & Northern Countries of South America	14-15 (1)* 15-16 (2)* 16-17 (1)* 08-10 (1) 10-12 (2) 12-14 (3) 14-16 (4) 16-18 (3) 18-19 (2) 19-20 (1)	06-07 (3) 07-09 (4) 09-11 (3) 11-16 (2) 16-18 (3) 18-20 (4) 20-22 (3) 22-00 (2) 00-06 (1)	19-21 (1) 21-23 (2) 23-02 (3) 02-04 (2) 04-05 (1)	21-23 (1) 23-02 (2) 02-04 (1) 00-02 (1)†
Peru, Bolivia, Paraguay, Brazil, Chile, Argentina & Uruguay	13-16 (1)* 08-11 (1) 11-13 (2) 13-14 (3) 14-16 (4) 16-17 (3) 17-18 (2) 18-19 (1)	05-06 (1) 06-09 (2) 09-14 (1) 14-16 (2) 16-17 (3) 17-19 (4) 19-21 (3) 21-22 (2) 22-00 (1)	20-23 (1) 23-01 (2) 01-05 (1)	23-04 (1) 01-03 (1)†
McMurdo Sound, Antarctica	13-15 (1)	12-16 (1) 16-18 (2) 18-21 (1)	03-07 (1)	*Nil*

MASTER DX PROPAGATION CHART
SOLAR PHASE: LOW
SMOOTHED SUNSPOT RANGE: 0-30
SEASON: SUMMER
TIME ZONE: PST (24-Hour Time)
WESTERN USA TO:

Reception Area	*10/15* Meters	*20* Meters	*30* Meters	*80/160* Meters
Western & Central Europe & North Africa	*Nil*	20-22 (1) 05-06 (1) 06-08 (2) 08-13 (1) 13-16 (2) 16-17 (1)	19-23 (1)	*Nil*
Northern & Eastern Europe	*Nil*	05-07 (1) 07-09 (2) 09-16 (1) 20-22 (1)	20-22 (1)	*Nil*
Eastern Mediterranean & East Africa	*Nil*	06-11 (1) 11-14 (2) 14-16 (1) 20-22 (1)	*Nil*	*Nil*
Western & Central Africa	09-11 (1)	21-23 (1) 05-06 (1) 06-08 (2) 08-13 (1) 13-16 (3) 16-17 (2) 17-18 (1)	20-23 (1)	*Nil*
Southern Africa	*Nil*	05-07 (1) 07-08 (2) 08-13 (1) 21-23 (1)	19-21 (1) 20-21 (2) 21-22 (1)	19-21 (1)
Central & South Asia	*Nil*	07-11 (1) 17-18 (1) 18-20 (2) 20-21 (1)	*Nil*	*Nil*
Southeast Asia	20-22 (1)	06-08 (1) 08-09 (2) 09-13 (1) 19-21 (1) 21-23 (2) 23-00 (1)	02-06 (1)	*Nil*
Far East	12-14 (1) 20-22 (1)	06-07 (1) 07-09 (2) 09-18 (1) 18-20 (2) 20-22 (1) 22-00 (2) 00-02 (1)	01-02 (1) 02-05 (2) 05-07 (1)	01-04 (1)
South Pacific & New Zealand	14-17 (1) 17-20 (2) 20-21 (1)	02-07 (1) 07-09 (2) 09-11 (1) 11-17 (2) 17-18 (3) 18-22 (4) 22-00 (3) 00-02 (2)	23-01 (1) 01-04 (3) 04-06 (2) 06-07 (1)	23-01 (1) 01-04 (2) 04-06 (1) 02-04 (1)†
Australasia	14-17 (1) 17-20 (2) 20-22 (1)	01-07 (1) 07-09 (2) 09-12 (1) 12-14 (2) 14-18 (1) 18-20 (2) 20-23 (3) 23-01 (2)	23-01 (1) 01-04 (2) 04-07 (1)	00-02 (1) 02-04 (2) 04-06 (1) 02-04 (1)†
Caribbean, Central America & Northern Countries of South America	14-17 (1)* 08-10 (1) 10-12 (2) 12-14 (3) 14-16 (4) 16-18 (2) 18-19 (1)	06-08 (3) 08-10 (2) 10-13 (1) 13-15 (2) 15-17 (3) 17-20 (4) 20-22 (3) 22-23 (2) 23-04 (1) 04-06 (2)	19-21 (1) 21-23 (2) 23-01 (3) 01-03 (2) 03-04 (1)	20-22 (1) 22-00 (2) 00-03 (1) 00-02 (1)†
Peru, Bolivia, Paraguay, Brazil, Chile, Argentina & Uruguay	12-14 (1)* 08-11 (1) 11-12 (2) 12-13 (3) 13-15 (4) 15-16 (2) 16-18 (1)	05-06 (1) 06-08 (2) 08-14 (1) 14-16 (2) 16-18 (4) 18-20 (2) 20-22 (1)	20-22 (1) 22-01 (2) 01-04 (1)	22-04 (1) 00-02 (1)†
McMurdo Sound, Antarctica	12-16 (1)	11-16 (1) 16-18 (2) 18-20 (1)	19-21 (1) 02-07 (1)	

MASTER DX PROPAGATION CHART
SOLAR PHASE: LOW
SMOOTHED SUNSPOT RANGE: 0-30
SEASON: WINTER
TIME ZONE: EST (24-Hour Time)
EASTERN USA TO:

Reception Area	*10/15* Meters	*20* Meters	*40* Meters	*80/160* Meters
Western & Central Europe & North Africa	09-11 (1)* 08-09 (1) 09-11 (2) 11-13 (1)	06-07 (1) 07-08 (2) 08-10 (3) 10-12 (4) 12-13 (3) 13-14 (2) 14-16 (1)	15-16 (1) 16-17 (2) 17-19 (3) 19-01 (2) 01-03 (3) 03-04 (2) 04-05 (1)	17-19 (1) 19-20 (2) 20-02 (3) 02-03 (2) 03-04 (1) 20-00 (1)† 00-02 (2)† 02-03 (1)†
Northern & Eastern Europe	08-11 (1)	06-07 (1) 07-11 (2) 11-13 (1)	15-17 (1) 17-19 (2) 19-01 (1) 01-02 (2) 02-03 (1)	17-19 (1) 19-02 (2) 02-03 (1) 21-02 (1)†
Eastern Mediterranean & Middle East	09-10 (1)* 08-09 (1) 09-11 (2) 11-12 (1)	07-08 (1) 08-10 (2) 10-12 (3) 12-14 (2) 14-15 (1)	17-19 (1) 19-21 (2) 21-00 (1) 00-01 (2) 01-02 (1)	18-20 (1) 20-22 (2) 22-00 (1) 22-00 (1)†
Western Africa	10-12 (1)* 08-09 (1) 09-11 (2) 11-13 (3) 13-14 (2) 14-15 (1)	06-07 (1) 07-09 (2) 09-12 (1) 12-14 (2) 14-16 (3) 16-17 (2) 17-18 (1)	18-20 (1) 20-23 (2) 23-01 (1) 01-03 (2) 03-04 (1)	19-22 (1) 22-01 (2) 01-03 (1) 22-01 (1)†
Eastern & Central Africa	10-12 (1)* 08-11 (1) 11-13 (2) 13-14 (1)	07-13 (1) 13-16 (2) 16-18 (1)	18-20 (1) 20-23 (2) 23-01 (1)	19-00 (1)
Southern Africa	10-13 (1)* 08-09 (1) 09-11 (2) 11-13 (3) 13-14 (2) 14-15 (1)	07-09 (1) 12-14 (1) 14-15 (2) 15-16 (3) 16-17 (2) 17-19 (1)	18-20 (1) 20-22 (1) 22-00 (1)	19-22 (1)

Central & South Asia	16-18 (1)	07-10 (1) 19-21 (1)	06-08 (1) 18-22 (1)	06-07 (1) 18-20 (1)
Southeast Asia	16-18 (1)	07-10 (1) 17-20 (1)	06-08 (1) 18-21 (1)	06-07 (1) 18-20 (1)
Far East	16-18 (1)	06-07 (1) 07-09 (2) 09-11 (1) 15-17 (1) 17-19 (2) 19-21 (1)	05-08 (1) 17-18 (1)	05-08 (1) 17-18 (1)
South Pacific & New Zealand	13-15 (1)* 12-14 (1) 14-17 (2) 17-18 (1)	05-07 (1) 07-10 (2) 10-18 (1) 18-20 (2) 20-22 (1)	01-02 (1) 02-04 (2) 04-07 (3) 07-08 (2) 08-09 (1)	04-05 (1) 05-07 (2) 07-08 (1) 04-07 (1)†
Australasia	14-16 (1)* 12-15 (1) 15-17 (2) 17-18 (1)	06-07 (1) 07-10 (2) 10-12 (1) 15-16 (1) 16-19 (2) 19-21 (1)	03-05 (1) 05-08 (2) 08-09 (1) 17-19 (1)	05-06 (1) 06-07 (2) 07-08 (1) 17-18 (1) 05-07 (1)†
Caribbean, Central America & Northern Countries of South America	10-15 (1)* 08-09 (1) 09-12 (2) 12-16 (3) 16-17 (2) 17-18 (1)	05-07 (1) 07-08 (3) 08-09 (4) 09-11 (3) 11-15 (2) 15-17 (3) 17-18 (4) 18-19 (3) 19-20 (2) 20-02 (1)	17-18 (1) 18-19 (2) 19-21 (3) 21-03 (2) 03-06 (3) 06-07 (2) 07-08 (1)	18-20 (1) 20-21 (2) 21-04 (3) 04-06 (2) 06-07 (1) 21-03 (1)† 03-05 (2)† 05-06 (1)†
Peru, Bolivia, Paraguay, Brazil, Chile, Argentina & Uruguay	11-15 (1)* 08-09 (1) 09-11 (2) 11-13 (1) 13-14 (2) 14-16 (3) 16-17 (2) 17-18 (1)	06-07 (1) 07-09 (2) 09-10 (1) 12-14 (1) 14-15 (2) 15-16 (3) 16-18 (4) 18-19 (3) 19-20 (2) 20-22 (1) 22-00 (2) 00-02 (1)	19-21 (1) 21-02 (2) 02-05 (1) 05-06 (2) 06-07 (1)	21-03 (1) 03-05 (2) 05-06 (1) 03-05 (1)†
McMurdo Sound, Antarctica	15-17 (1)	07-09 (1) 17-18 (1) 18-20 (2) 20-22 (1) 22-00 (2) 00-02 (1)	22-00 (1) 00-02 (2) 02-06 (1)	*Nil*

MASTER DX PROPAGATION CHART
SOLAR PHASE: LOW
SMOOTHED SUNSPOT RANGE: 0-30
SEASON: WINTER
TIME ZONES: CST & MST (24-Hour Time)
CENTRAL USA TO:

Reception Area	*10/15 Meters*	*20 Meters*	*40 Meters*	*80/160 Meters*
Western Europe & North Africa	08-09 (1) 09-11 (2) 11-12 (1)	06-08 (1) 08-10 (2) 10-12 (3) 12-13 (2) 13-15 (1)	15-17 (1) 17-19 (2) 19-12 (3) 23-01 (2) 01-02 (1)	17-19 (1) 19-00 (2) 00-01 (1) 20-01 (1)†
Northern, Central, & Eastern Europe	08-11 (1)	07-08 (1) 08-11 (2) 11-12 (1)	16-18 (1) 18-19 (2) 19-22 (1) 22-00 (2) 00-01 (1)	18-00 (1) 20-00 (1)†
Eastern Mediterranean & Middle East	08-11 (1)	07-09 (1) 09-12 (2) 12-14 (1) 22-00 (1)	17-19 (1) 19-22 (2) 22-23 (1)	19-22 (1)
Western Africa	09-12 (1)* 08-09 (1) 09-11 (2) 11-13 (3) 13-14 (2) 14-15 (1)	06-07 (1) 07-09 (2) 09-11 (1) 11-13 (2) 13-15 (3) 15-16 (2) 16-18 (1) 22-00 (1)	17-20 (1) 20-23 (2) 23-01 (1)	19-22 (1) 22-23 (2) 23-00 (1) 21-23 (1)†
Eastern & Central Africa	10-12 (1)* 08-11 (1) 11-13 (2) 13-14 (1)	06-12 (1) 12-14 (2) 14-16 (3) 16-17 (1)	18-19 (1) 19-21 (2) 21-23 (1)	19-22 (1)
Southern Africa	10-12 (1)* 08-10 (1) 10-13 (2) 13-14 (1)	07-13 (1) 13-15 (2) 15-16 (3) 16-17 (2) 17-18 (1) 22-00 (1)	18-19 (1) 19-21 (2) 21-23 (1)	19-22 (1)
Central & South Asia	17-19 (1)	07-10 (1) 19-22 (1)	06-08 (1) 18-21 (1)	06-07 (1) 18-20 (1)
Southeast Asia	17-19 (1)	06-07 (1) 07-09 (2) 09-12 (1) 17-20 (1)	06-08 (1) 17-19 (1)	06-07 (1) 17-19 (1)
Far East	17-19 (1)	06-07 (1) 07-09 (2) 09-11 (1) 15-17 (1) 17-19 (2) 19-20 (1)	01-03 (1) 03-07 (2) 07-08 (1)	02-04 (1) 04-06 (2) 06-07 (1) 04-06 (1)†
South Pacific & New Zealand	12-16 (1)* 11-13 (1) 13-15 (2) 15-17 (3) 17-18 (2) 18-19 (1)	06-07 (1) 07-11 (2) 11-16 (1) 16-17 (2) 17-19 (3) 19-20 (2) 20-22 (1)	23-01 (1) 01-02 (2) 02-06 (3) 06-07 (2) 07-09 (1)	00-01 (1) 01-06 (2) 06-08 (1) 13-07 (1)†
Australasia	14-17 (1)* 11-15 (1) 15-18 (2) 18-19 (1)	06-07 (1) 07-11 (2) 11-18 (1) 18-21 (2) 21-22 (1)	01-03 (1) 03-07 (3) 07-08 (2) 08-09 (1)	03-05 (1) 05-07 (2) 07-08 (1) 04-07 (1)†
Caribbean, Central America & Northern Countries of South America	10-15 (1)* 07-08 (1) 08-10 (2) 10-13 (3) 13-15 (4) 15-16 (3) 16-18 (1)	04-06 (1) 06-07 (2) 07-10 (3) 10-14 (2) 14-16 (3) 16-18 (4) 18-19 (3) 19-20 (2) 20-22 (1) 22-00 (2) 00-02 (1)	18-20 (1) 20-22 (2) 22-00 (3) 00-04 (2) 04-06 (3) 06-07 (1)	19-21 (1) 21-05 (2) 05-06 (1) 23-05 (1)†
Peru, Bolivia, Paraguay, Brazil, Chile, Argentina & Uruguay	11-15 (1)* 07-09 (1) 09-11 (2) 11-13 (1) 13-14 (2) 14-16 (3) 16-17 (2) 17-18 (1)	06-07 (1) 07-09 (2) 09-13 (1) 13-14 (2) 14-15 (3) 15-17 (4) 17-18 (3) 18-19 (2) 19-21 (1) 21-23 (2) 23-00 (1)	19-21 (1) 21-02 (2) 02-04 (1) 04-06 (2) 06-07 (1)	21-05 (1) 00-04 (1)†
McMurdo Sound, Antarctica	15-17 (1)	06-07 (1) 07-09 (2) 09-11 (1) 17-18 (1) 18-20 (2) 20-22 (1) 22-00 (2) 00-02 (1)	22-00 (1) 00-02 (2) 02-06 (1)	*Nil*

MASTER DX PROPAGATION CHART
SOLAR PHASE: LOW
SMOOTHED SUNSPOT RANGE: 0-30
SEASON: WINTER
TIME ZONE: PST (24-Hour Time)
WESTERN USA TO:

Reception Area	*10/15 Meters*	*20 Meters*	*40 Meters*	*80/160 Meters*
Western Europe & North Africa	08-10 (1)	06-07 (1) 07-11 (2) 11-13 (1) 23-01 (1)	17-21 (1) 21-23 (2) 23-01 (1)	18-20 (1) 20-22 (2) 22-23 (1) 19-22 (1)†
Northern, Central & Eastern Europe	08-10 (1)	06-07 (1) 07-10 (2) 10-12 (1) 23-01 (1)	17-00 (1)	19-22 (1) 19-21 (1)†
Eastern Mediterranean & Middle East	08-10 (1)	07-10 (1) 10-12 (2) 12-13 (1) 21-23 (1)	06-08 (1) 18-22 (1)	06-08 (1) 18-21 (1)
Western Africa	09-11 (1)* 08-09 (1) 09-12 (2) 12-13 (1)	07-10 (1) 10-13 (2) 13-16 (3) 16-17 (2) 17-18 (1)	18-23 (1)	19-22 (1)
Eastern & Central Africa	09-11 (1)	08-10 (1) 13-16 (1) 21-23 (1)	06-08 (1) 18-22 (1)	06-08 (1) 18-21 (1)
Southern Africa	08-10 (1) 10-12 (2) 12-14 (1)	09-13 (1) 13-16 (2) 16-18 (1) 23-01 (1)	18-21 (1)	18-20 (1)
Central & South Asia	17-19 (1)	08-10 (1) 17-18 (1) 18-19 (2) 19-20 (1)	15-08 (1) 17-19 (1)	05-07 (1)
Southeast Asia	14-16 (1)* 14-15 (1) 15-17 (2) 17-18 (1)	08-09 (1) 09-11 (2) 11-16 (1) 16-19 (2) 19-20 (1)	01-04 (1) 04-07 (2) 07-09 (1)	04-07 (1)
Far East	14-15 (1) 15-17 (2) 17-19 (1)	08-10 (1) 13-14 (1) 14-15 (2) 15-17 (3) 17-18 (2) 18-19 (1)	22-00 (1) 00-02 (2) 02-06 (3) 06-08 (2) 08-10 (1)	23-01 (1) 01-06 (2) 06-08 (1) 01-06 (1)†
South Pacific & New Zealand	14-16 (1)* 11-13 (1) 13-14 (2) 14-16 (3) 16-18 (2) 18-19 (1)	07-08 (1) 08-13 (2) 13-15 (1) 15-16 (2) 16-18 (4) 18-19 (2) 19-21 (1)	20-22 (1) 22-00 (2) 00-07 (3) 07-08 (2) 08-09 (1)	00-03 (1) 03-06 (2) 06-08 (1) 03-06 (1)†
Australasia	14-16 (1)* 10-13 (1) 13-15 (2) 15-17 (3) 17-18 (1)	07-08 (1) 08-11 (2) 11-17 (1) 17-18 (2) 18-19 (3) 19-20 (2) 20-22 (1)	01-03 (1) 03-05 (2) 05-07 (3) 07-08 (2) 08-09 (1)	03-05 (1) 05-06 (2) 06-08 (1) 04-07 (1)†
Caribbean, Central America & Northern Countries of South America	10-14 (1)* 07-08 (1) 08-10 (2) 10-12 (3) 12-14 (4) 14-15 (3) 15-16 (2) 16-17 (1)	04-06 (1) 06-07 (2) 07-09 (3) 09-13 (2) 13-15 (3) 15-17 (4) 17-18 (3) 18-19 (2) 19-21 (1) 21-23 (2) 23-01 (1)	18-20 (1) 20-21 (2) 21-23 (3) 23-01 (2) 01-03 (3) 03-04 (2) 04-05 (1)	19-21 (1) 21-03 (2) 03-04 (1) 21-03 (1)†
Peru, Bolivia, Paraguay, Brazil, Chile, Argentina & Uruguay	11-14 (1)* 08-10 (1) 10-12 (2) 12-14 (3) 14-16 (2) 16-17 (1)	05-07 (1) 07-09 (2) 09-13 (1) 13-15 (2) 15-16 (3) 16-17 (4) 17-18 (3) 18-19 (2) 19-20 (1) 22-00 (1)	19-21 (1) 21-00 (2) 00-02 (1) 02-04 (2) 04-06 (1)	22-05 (1) 00-04 (1)†
McMurdo Sound, Antarctica	14-16 (1)	06-07 (1) 07-09 (2) 09-11 (1) 15-17 (1) 17-19 (2) 19-21 (1) 21-23 (2) 23-01 (1)	21-00 (1) 00-02 (2) 02-05 (1)	*Nil*

MASTER DX PROPAGATION CHART
SOLAR PHASE: LOW
SMOOTHED SUNSPOT RANGE: 0-30
SEASONS: SPRING & FALL
TIME ZONE: EST (24-Hour Time)
EASTERN USA TO:

Reception Area	*10/15 Meters*	*20 Meters*	*40 Meters*	*80/160 Meters*
Western & Central Europe & North Africa	08-10 (1) 10-12 (2) 12-14 (1)	06-07 (1) 07-08 (2) 08-12 (3) 12-13 (4) 13-14 (3) 14-15 (2) 15-18 (1)	16-18 (1) 18-19 (2) 19-23 (3) 23-02 (2) 02-05 (1)	18-20 (1) 20-23 (3) 23-01 (2) 01-03 (1) 20-23 (1)† 23-01 (2)† 01-02 (1)†

Northern & Eastern Europe	09-12 (1)	06-07 (1) 07-10 (2) 10-14 (1)	18-02 (1)	20-00 (1) 21-23 (1)†
Eastern Mediter-ranean & East Africa	09-11 (1)	06-11 (1) 11-13 (2) 13-15 (1)	18-20 (1) 20-21 (2) 21-23 (1)	19-23 (1) 20-22 (1)†
Western Africa	08-10 (1) 10-12 (3) 12-13 (2) 13-16 (1)	06-07 (1) 07-09 (2) 09-12 (1) 12-14 (2) 14-16 (3) 16-17 (2) 17-19 (1)	18-19 (1) 19-22 (2) 22-01 (1)	19-21 (1) 21-22 (2) 22-00 (1) 20-22 (1)†
Central & South Africa	10-13 (1)* 07-10 (1) 10-12 (2) 12-14 (3) 14-15 (2) 15-18 (1)	07-14 (1) 14-15 (2) 15-17 (3) 17-18 (2) 18-21 (1)	18-20 (1) 20-22 (2) 22-00 (1)	19-22 (1) 19-21 (1)†
Central & South Asia	*Nil*	06-07 (1) 07-09 (2) 09-11 (1) 19-22 (1)	05-07 (1) 18-21 (1)	*Nil*
Southeast Asia	17-19 (1)	06-07 (1) 07-09 (2) 09-11 (1) 17-20 (1)	06-08 (1) 17-20 (1)	*Nil*
Far East	16-19 (1)	06-07 (1) 07-09 (2) 09-11 (1) 17-20 (1)	05-08 (1)	06-07 (1)
South Pacific & New Zealand	15-17 (1)* 12-16 (1) 16-18 (2) 18-20 (1)	07-09 (2) 09-20 (1) 20-22 (2) 22-07 (1)	00-02 (1) 02-06 (3) 06-07 (2) 07-08 (1)	02-03 (1) 03-05 (2) 05-07 (1) 02-06 (1)†
Australasia	12-16 (1) 16-18 (2) 18-20 (1)	06-07 (1) 07-09 (2) 09-15 (1) 20-23 (1)	03-05 (1) 05-07 (2) 07-09 (1)	04-05 (1) 05-07 (2) 07-08 (1) 05-07 (1)†
Caribbean, Central America & Northern Countries of South America	12-16 (1)* 07-08 (1) 08-09 (2) 09-11 (4) 11-13 (2) 13-15 (4) 15-16 (3) 16-18 (2) 18-20 (1)	00-06 (1) 06-07 (2) 07-10 (3) 10-15 (2) 15-17 (3) 17-19 (4) 19-21 (3) 21-00 (2)	18-19 (1) 19-20 (2) 20-03 (3) 03-05 (2) 05-07 (1)	19-21 (1) 00-02 (2) 02-06 (1) 00-04 (1)†
Peru, Bolivia, Paraguay, Brazil, Chile, Argentina & Uruguay	12-15 (1)* 07-09 (1) 09-11 (2) 11-13 (1) 13-15 (2) 15-17 (3) 17-19 (1)	06-07 (1) 07-10 (2) 10-14 (1) 14-16 (2) 16-18 (3) 18-20 (4) 20-22 (2) 22-03 (1)	19-21 (1) 21-03 (2) 03-07 (1)	21-06 (1) 01-04 (1)†
McMurdo Sound, Antarctica	15-17 (1)	16-18 (1) 18-20 (2) 20-23 (1) 06-07 (1) 07-09 (2) 09-11 (1)	23-05 (1)	*Nil*

Western Africa	08-10 (1) 10-12 (2) 12-15 (1)	06-07 (1) 07-09 (2) 09-11 (1) 11-13 (2) 13-15 (3) 15-17 (2) 17-18 (1)	18-19 (1) 19-21 (2) 21-00 (1)	19-20 (1) 20-22 (2) 22-23 (1) 20-22 (1)†
Central & South Africa	11-13 (1)* 08-10 (1) 10-12 (2) 12-14 (3) 14-15 (2) 15-18 (1)	07-14 (1) 14-15 (2) 15-16 (3) 16-17 (2) 17-20 (1)	18-20 (1) 20-22 (2) 22-00 (1)	19-22 (1) 19-21 (1)†
Central & South Asia	*Nil*	06-07 (1) 07-09 (2) 09-11 (1) 19-21 (1)	06-08 (1) 19-21 (1)	*Nil*
Southeast Asia	10-14 (1) 17-20 (1)	06-07 (1) 07-09 (2) 09-12 (1) 19-21 (1)	06-08 (1) 17-19 (1)	*Nil*
Far East	16-19 (1)	06-07 (1) 07-09 (2) 09-11 (1) 16-18 (1) 18-20 (2) 20-22 (1)	02-09 (1)	05-07 (1)
South Pacific & New Zealand	14-17 (1)* 12-16 (1) 16-18 (2) 18-21 (1)	18-19 (2) 19-21 (3) 21-00 (2) 00-06 (1) 06-09 (2) 09-18 (1)	22-01 (1) 01-06 (3) 06-07 (2) 07-09 (1)	00-03 (1) 03-06 (2) 06-07 (1) 03-07 (1)†
Australasia	12-16 (1) 16-18 (2) 18-20 (1)	06-07 (1) 07-09 (2) 09-14 (1) 17-19 (1) 19-21 (2) 21-23 (1)	02-04 (1) 04-07 (2) 07-09 (1)	04-05 (1) 05-07 (2) 07-08 (1) 05-07 (1)†
Caribbean, Central America & Northern Countries of South America	11-15 (1)* 07-08 (1) 08-09 (2) 09-11 (3) 11-13 (2) 13-15 (4) 15-17 (2) 17-19 (1)	00-06 (1) 06-07 (2) 07-09 (3) 09-14 (2) 14-16 (3) 16-18 (4) 18-20 (3) 20-00 (2)	18-19 (1) 19-20 (2) 20-02 (3) 02-04 (2) 04-06 (1)	20-21 (1) 21-02 (2) 02-06 (1) 00-03 (1)†
Peru, Bolivia, Paraguay, Brazil, Chile, Argentina & Uruguay	12-14 (1)* 07-08 (1) 08-10 (2) 10-12 (1) 12-13 (2) 13-16 (3) 16-17 (2) 17-19 (1)	06-07 (1) 07-09 (2) 09-13 (1) 13-15 (2) 15-17 (3) 17-19 (4) 19-21 (2) 21-02 (1)	19-21 (1) 21-03 (2) 03-06 (1)	21-05 (1) 01-04 (1)†
McMurdo Sound, Antarctica	15-17 (1)	16-18 (1) 18-20 (2) 20-00 (1) 06-07 (1) 07-09 (2) 09-11 (1)	00-07 (1)	*Nil*

West & Central Africa	07-08 (1) 08-10 (2) 10-13 (1)	06-10 (1) 10-13 (2) 13-15 (3) 15-16 (2) 16-18 (1)	18-22 (1)	19-21 (1) 19-21 (1)†
Southern Africa	09-11 (1)* 07-10 (1) 10-13 (2) 13-15 (1)	05-14 (1) 14-17 (2) 17-18 (1) 23-01 (1)	19-22 (1)	20-21 (1)
Central & South Asia	17-19 (1)	07-09 (1) 16-18 (1) 18-20 (2) 20-21 (1)	05-08 (1)	*Nil*
Southeast Asia	11-15 (1) 15-17 (2) 17-19 (1)	07-09 (1) 09-11 (2) 11-13 (1) 19-22 (1)	02-05 (1) 05-07 (2) 07-09 (1)	*Nil*
Far East	12-14 (1) 14-18 (2) 18-20 (1)	07-12 (1) 12-14 (2) 14-16 (1) 16-17 (2) 17-19 (3) 19-20 (2) 20-22 (1)	22-00 (1) 00-02 (2) 02-06 (3) 06-08 (2) 08-09 (1)	00-02 (1) 02-05 (2) 05-07 (1) 03-06 (1)†
South Pacific & New Zealand	15-17 (1)* 10-13 (1) 13-15 (2) 15-17 (4) 17-18 (2) 18-20 (1)	07-08 (1) 08-10 (2) 10-16 (1) 16-17 (2) 17-19 (4) 19-21 (2)	21-22 (1) 22-05 (3) 05-07 (2) 07-09 (1)	22-00 (1) 00-05 (2) 05-07 (1) 02-06 (1)†
Australasia	15-17 (1)* 13-17 (1) 17-19 (3) 19-20 (1)	07-08 (1) 08-10 (2) 10-17 (1) 17-18 (2) 18-20 (3) 20-21 (2) 21-22 (1)	00-03 (1) 03-05 (3) 05-07 (2) 07-08 (1)	02-03 (1) 03-05 (2) 05-07 (1) 04-06 (1)†
Caribbean, Central America & Northern Countries of South America	10-14 (1)* 06-08 (1) 08-13 (2) 13-15 (3) 15-16 (2) 16-18 (1)	00-05 (1) 05-06 (2) 06-08 (3) 08-14 (2) 14-16 (3) 16-18 (4) 18-20 (3) 20-00 (2)	18-20 (1) 20-00 (3) 00-03 (2) 03-05 (1)	20-21 (1) 21-01 (2) 01-04 (1) 23-02 (1)†
Peru, Bolivia, Paraguay, Brazil, Chile, Argentina & Uruguay	10-14 (1)* 06-08 (1) 08-10 (2) 10-12 (1) 12-13 (2) 13-15 (3) 15-16 (2) 16-18 (1)	05-07 (1) 07-09 (2) 09-13 (1) 13-15 (2) 15-17 (3) 17-19 (2) 19-00 (1)	19-21 (1) 21-02 (2) 02-05 (1)	21-04 (1) 00-03 (1)†
McMurdo Sound, Antarctica	08-10 (1) 14-16 (1)	15-17 (1) 17-19 (3) 19-00 (1) 05-06 (1) 06-08 (2) 08-11 (1)	00-06 (1)	*Nil*

MASTER DX PROPAGATION CHART
SOLAR PHASE: LOW
SMOOTHED SUNSPOT RANGE: 0-30
SEASONS: SPRING & FALL
TIME ZONES: CST & MST (24-Hour Time)
CENTRAL USA TO:

Reception Area	*10/15 Meters*	*20 Meters*	*40 Meters*	*80/160 Meters*
Western & Central Europe & North Africa	06-08 (1) 08-09 (1) 09-12 (2) 12-14 (1)	06-08 (1) 08-12 (2) 12-14 (3) 14-15 (2) 15-17 (1)	16-19 (1) 19-22 (2) 22-02 (1)	18-20 (1) 20-22 (2) 22-00 (1) 20-00 (1)†
Northern & Eastern Europe	08-12 (1)	07-08 (1) 08-10 (2) 10-13 (1)	19-01 (1)	20-23 (1)
Eastern Mediter-ranean & East Africa	09-12 (1)	07-11 (1) 11-13 (2) 13-15 (1)	19-23 (1)	20-22 (1)

MASTER DX PROPAGATION CHART
SOLAR PHASE: LOW
SMOOTHED SUNSPOT RANGE 0-30
SEASONS: SPRING & FALL
TIME ZONE: PST (24-Hour Time)
WESTERN USA TO:

Reception Area	*10/15 Meters*	*20 Meters*	*40 Meters*	*80/160 Meters*
Western & Central Europe & North Africa	09-11 (1)	23-01 (1) 06-08 (1) 08-11 (2) 11-15 (1)	18-00 (1)	19-22 (1) 19-21 (1)†
Northern & Eastern Europe	07-10 (1)	23-01 (1) 06-07 (1) 07-09 (2) 09-12 (1)	18-23 (1)	20-23 (1)
Eastern Mediter-ranean & East Africa	*Nil*	07-12 (1) 19-21 (1)	18-21 (1)	*Nil*

MASTER SHORT-SKIP PROPAGATION CHART
SOLAR PHASE: LOW
SMOOTHED SUNSPOT RANGE: 0-30
SEASON: SUMMER
TIME ZONES: LOCAL STANDARD AT PATH MID-POINT (24-Hour Time)

Band	*Distance Between Stations (Miles)*			
(Meters)	*50-250*	*250-750*	*750-1300*	*1300-2300*
10	*Nil*	07-09 (0-1)* 09-13 (0-3)* 13-17 (0-1)* 17-21 (0-2)* 21-23 (0-1)*	07-09 (1)* 09-13 (3)* 13-17 (1-2)* 17-21 (2-3)* 21-07 (1)*	07-09 (1-0)* 09-13 (3-0)* 13-17 (2-0)* 17-21 (3-0)* 21-07 (1-0)*
15	*Nil*	07-09 (0-2)* 09-13 (0-3)* 13-17 (0-2)* 17-19 (0-3)* 19-21 (0-2)* 21-07 (0-1)*	07-09 (2)* 09-13 (3)* 13-17 (2)* 17-19 (3)* 19-21 (2)* 21-23 (1-2)* 23-07 (1)*	07-09 (2-0) 09-13 (3-2) 13-17 (2-0) 17-19 (3-1) 19-20 (2-1) 20-23 (2-0) 23-07 (1-0)

20	09-00 (0-1)*	06-09 (0-2)* 09-15 (0-4)* 15-20 (0-3)* 20-00 (0-2)* 00-06 (0-1)*	06-09 (2-3)* 09-16 (4)* 16-21 (3-4)* 21-00 (2-3)* 00-06 (1-2)*	06-09 (2-0) 09-15 (3-2) 15-16 (4-2) 16-21 (4) 21-23 (3) 23-00 (3-2) 00-06 (2-1)
40	07-09 (1-2)* 09-15 (1-4)* 15-19 (2-4) 19-22 (1-2) 22-07 (0-1)*	07-09 (2)* 09-11 (4-2) 11-15 (4-1) 15-17 (4-3) 17-19 (4) 19-22 (2-4) 22-07 (1-3)*	07-09 (2-1) 09-11 (2-0) 11-15 (1-0) 15-17 (3-1) 17-20 (4-3) 20-22 (4) 22-05 (3-4) 05-07 (3)	07-09 (1-0) 09-15 (0) 15-17 (1-0) 17-20 (3-2) 20-05 (4) 05-07 (3-1)
80	06-09 (3-4) 09-17 (4-3) 17-21 (4) 21-04 (3-4) 04-06 (3)	07-09 (4-1) 09-17 (3-0) 17-19 (4-0) 19-21 (4-2) 21-23 (4-3) 23-04 (4) 04-06 (3) 06-07 (4-2)	07-09 (1-0) 09-19 (0) 19-21 (2-1) 21-23 (3) 23-04 (4) 04-06 (3) 06-07 (2-1)	07-19 (0) 19-21 (1) 21-23 (3) 23-03 (4-3) 03-04 (4-2) 04-05 (3-2) 05-06 (3-1) 06-07 (1)
160	17-18 (1-0) 18-19 (1) 19-21 (3-1) 21-23 (4-2) 23-05 (4-3) 05-07 (3-2) 07-09 (1-0)	18-20 (1-0) 20-21 (1) 21-22 (2-1) 22-23 (2) 23-05 (3-0) 05-06 (2-1) 06-07 (2-0)	20-22 (1) 22-00 (2-1) 00-02 (2) 02-06 (2-1)	20-22 (1-0) 22-00 (1) 00-02 (2-1) 02-05 (1)

MASTER SHORT-SKIP PROPAGATION CHART
SOLAR PHASE: LOW
SMOOTHED SUNSPOT RANGE: 0-30
SEASON: WINTER
TIME ZONES: LOCAL STANDARD AT PATH MID-POINT
(24-Hour Time)

Band (Meters)	*Distance Between Stations (Miles)* 50-250	250-750	750-1300	1300-2300
10	*Nil*	*Nil*	11-16 (0-1)	11-16 (1-0)
15	*Nil*	10-16 (0-1)	09-10 (0-1) 10-12 (1) 12-16 (1-2) 16-17 (0-1)	09-10 (1) 10-12 (1-3) 12-14 (2-4) 14-15 (2-3) 15-16 (2) 16-17 (1) 17-18 (0-1)
20	*Nil*	09-11 (0-1) 11-16 (0-2) 16-19 (0-1)	08-09 (0-1) 09-11 (1-4) 11-16 (2-4) 16-17 (1-3) 17-18 (1-2) 18-19 (1) 19-21 (0-1)	07-08 (0-1) 08-09 (1-3) 09-11 (4) 11-15 (4-3) 15-16 (4) 16-17 (3) 17-18 (2-3) 18-19 (1-2) 19-20 (1)
40	07-09 (0-1) 09-10 (1-3) 10-15 (3-4) 15-16 (2-3) 16-18 (1-2) 18-20 (0-1)	07-09 (1-3) 09-10 (3) 10-15 (4-3) 15-16 (3-4) 16-18 (2-4) 18-20 (1-2) 20-00 (0-2) 00-07 (0-1)	07-09 (3) 09-14 (3-1) 14-15 (3-2) 15-16 (3) 16-18 (4) 18-20 (2-4) 20-22 (2-3) 22-00 (2) 00-04 (1-2) 04-07 (1-3)	07-08 (3-2) 08-09 (3-1) 09-14 (1-0) 14-15 (2-0) 15-16 (3-1) 16-17 (4-2) 17-18 (4-3) 18-20 (4) 20-22 (3-4) 22-00 (2-3) 02-04 (2-3) 04-06 (3)
80	08-16 (4) 16-18 (2-4) 18-20 (1-3) 20-06 (1-2) 06-08 (2-3)	08-09 (4-2) 09-16 (4-1) 16-18 (4-2) 18-20 (3-4) 20-06 (2-4) 06-07 (3-4) 07-08 (3)	08-09 (2-1) 09-16 (1-0) 16-18 (2-1) 18-20 (4-3) 20-06 (4) 06-07 (4-2) 07-08 (3-1)	08-09 (1-0) 09-16 (0) 16-18 (1-0) 18-20 (3-2) 20-04 (4-3) 04-06 (4-2) 06-07 (2-1) 07-08 (1)
160	07-09 (3-2) 09-11 (2-0) 11-17 (1-0) 17-19 (3-2) 19-07 (4)	07-09 (2-1) 09-17 (0) 17-19 (2-1) 19-04 (4) 04-05 (4-3) 05-07 (4-2)	06-07 (2-1) 07-09 (1-0) 17-19 (1-0) 19-20 (4-2) 20-21 (4-3) 21-04 (4) 04-06 (3-2)	06-07 (1-0) 07-19 (0) 19-20 (2-1) 20-21 (3-2) 21-04 (4-2) 04-06 (2-1)

MASTER SHORT-SKIP PROPAGATION CHART
SOLAR PHASE: LOW
SMOOTHED SUNSPOT RANGE: 0-30
SEASONS: SPRING & FALL
TIME ZONES: LOCAL STANDARD AT PATH MID-POINT
(24-Hour Time)

Band (Meters)	*Distance Between Stations (Miles)* 50-250	250-750	750-1300	1300-2300
10	*Nil*	09-13 (0-1)	07-09 (1) 09-13 (1-2) 13-21 (0-1)	07-09 (1-0) 09-11 (2-0) 11-13 (2-1) 13-17 (1) 17-21 (1-0)
15	*Nil*	07-09 (0-1) 09-13 (0-2) 13-21 (0-1)	07-09 (1) 09-13 (2) 13-17 (1-2) 17-21 (1) 21-07 (0-1)	07-09 (1) 09-15 (2) 15-17 (2-1) 17-19 (1) 19-07 (1-0)
20	*Nil*	07-09 (0-1) 09-11 (0-2) 11-14 (0-4) 14-16 (0-3) 16-18 (0-2) 18-07 (0-1)	07-09 (1-2) 09-11 (2-4) 11-14 (4) 14-16 (3-4) 16-18 (2-4) 18-20 (1-3) 20-22 (1-2) 22-07 (1)	07-09 (2) 09-13 (4-2) 13-15 (4-3) 15-18 (4) 18-20 (3) 20-22 (2) 22-00 (1) 00-05 (1-0) 05-07 (1)
40	07-09 (0-2) 09-11 (2-4) 11-15 (3-4) 15-17 (2-3) 17-19 (1-2) 19-21 (0-1)	07-09 (2-3) 09-11 (4-3) 11-15 (4-2) 15-17 (3) 17-19 (2-4) 19-21 (1-4) 21-23 (0-3) 23-02 (0-2) 02-05 (0-1) 05-07 (0-2)	07-09 (3-2) 09-11 (3-1) 11-15 (2-1) 15-17 (3-2) 17-19 (4-3) 19-21 (4) 21-23 (3-4) 23-02 (2-3) 02-05 (1-2) 05-07 (2-4)	07-09 (2-1) 09-15 (1-0) 15-17 (2-1) 17-19 (3-2) 19-23 (4) 23-02 (3-4) 02-05 (2-3) 05-07 (4-2)
80	06-08 (3-4) 08-21 (4) 21-03 (3-4) 03-06 (2-3)	06-08 (4-2) 08-16 (4-1) 16-18 (4-2) 18-21 (4-3) 21-03 (4) 03-05 (3-4) 05-06 (3)	06-08 (2-1) 08-16 (1-0) 16-18 (2-1) 18-21 (3-2) 21-03 (4) 03-05 (4-2) 05-06 (3-2)	06-08 (1) 08-16 (0) 16-18 (1) 18-21 (2) 21-03 (4-3) 03-06 (2)
160	16-18 (1-0) 18-20 (2-1) 20-05 (4) 05-07 (3-2) 07-09 (2-1) 09-11 (1-0)	17-19 (1-0) 19-20 (1) 20-02 (4-3) 02-05 (3-2) 05-07 (2-1) 07-09 (1-0)	19-20 (1-0) 20-22 (3-1) 22-02 (3) 02-05 (2-1) 05-07 (1)	20-22 (1-0) 22-02 (3-2) 02-05 (1) 05-07 (1-0)

FOOTNOTES

Worldwide Charts:
* Predicted times of 10 meter openings; all others in column are 15 meter openings.
† Predicted times of 160 meter openings; all others in column are 80 meter openings.

Short Skip Charts:
* Predominately sporadic-E openings.

4.4 Master Propagation Charts—Moderate Solar Phase Smoothed Sunspot Number Range: 30–60

Band-By-Band Summary

10 Meters. ***Summer:*** Some north-south DX openings should be possible during the afternoon hours, but in general, DX opportunities on this band will only be poor to fair. Short-skip openings due to sporadic-*E* ionization, however, should provide communications on paths of up to 1300 miles in length during most days throughout this season. When sporadic-*E* ionization is intense and widespread, multi-hop openings over considerably greater distances should also be possible.

Winter: DX activity in the 10 meter band should be fair during this season. While F_2-layer openings will occur only during the daytime hours, possibilities exist for occasional morning openings to Europe, fairly frequent mid-day openings to South America and Africa, and late afternoon openings to the South Pacific and Australia. Then, too, short-skip openings to distances between 1000 and 2300 miles also should be possible.

Equinox: Some fairly good north-south daytime openings should be possible on the 10 meter band during the spring and fall months, particularly during the afternoon. Further, some F_2-layer DX openings should be possible on east-west paths, especially to Africa, and to the South Pacific and New Zealand. An occasional opening to Europe also may be possible earlier in the day. Some fairly good short-skip propagation should be possible to distances between approximately 1300 and 2300 miles, particularly during the afternoon hours.

15 meters. ***Summer:*** Watch for fairly good DX openings on a regular basis towards the southern hemisphere during the daylight hours. Peak conditions should occur, along with an occasional east-west opening towards Europe and Africa, during the afternoon hours. Then, too, sporadic-*E* peaks during this season, and it should provide excellent short-skip propagation to distances between 750 and 1300 miles, and often beyond.

Winter: Worldwide DX conditions should be very good during the daytime hours. The band should peak towards Europe and the east a few hours after sunrise, towards the southern hemisphere during the early afternoon, and towards the South Pacific, the Far East and in a generally westerly direction during the late afternoon. Consistent short-skip openings also should be possible during the daylight hours to distances of between approximately 1000 and 2300 miles.

Equinox: Expect fairly good DX openings to all areas of the world, with excellent propagation from the northern hemisphere to Africa, South America, and the South Pacific during the hours of daylight; signals should peak during the afternoon. Good short-skip openings should be possible over distances greater than approximately 1000 miles.

20 meters. *Summer:* Twenty meters should be the best band for worldwide propagation during the summer months. The band, which will open shortly after sunrise and remain open until well after sunset, should provide good openings to all areas of the world on most of the days during this season. Look for peak conditions for an hour or two after sunrise and again during the late afternoon and early evening. Excellent short-skip openings should be possible for distances beyond approximately 500 miles.

Winter: While the band will not be open as long as it is during other times of the year, 20 meters should provide excellent DX openings to all areas of the world between sunrise and sunset. Excellent short-skip openings should also be possible during the daylight hours over distances beyond approximately 500 miles.

Equinox: Expect very good DX openings to all areas of the world from sunrise through the early hours of darkness. Openings should peak for an hour or two after sunrise and again during the afternoon. Further, short-skip openings should provide excellent propagation conditions over distances beyond approximately 750 miles during the daylight hours.

40 meters. *Summer:* Good DX openings should be possible on this band during the evening, nighttime, and sunrise hours; however, atmospheric noise (static) generated by thunderstorms will frequently limit activity. Peak conditions should occur at about midnight for openings towards Europe and the east, and just before sunrise for openings in other directions. Short-skip openings over ranges of up to approximately 1000 miles should be possible during the daytime, and between 500 and 2300 miles at night.

Winter: The band should first open towards Europe and the east during the late afternoon, and remain open to different areas of the world during the hours of darkness and until just after sunrise. This should be the best band for DX during the nighttime hours. Excellent short-skip openings should be possible during the daytime for distances of up to approximately 1000 miles, and during the hours of darkness to distances beyond 1000 miles.

Equinox: Expect fairly good worldwide DX openings from early evening through sunrise. Short-skip openings should occur during the daylight hours in the range from 100 to 1000 miles, and during the hours of darkness to distances beyond 1000 miles.

80 meters. *Summer:* Due to high daytime ionospheric absorption and generally high static levels, expect no daytime DX openings on this band. Some fairly good openings should be possible, however, during the hours of darkness and just before sunrise to some areas of the world. Short-skip openings should be possible to ranges of up to 250 miles during the day, and up to approximately 2300 miles at night.

Winter: Fairly good DX openings should be possible to almost all areas of the world between sunset and sunrise, with peaks expected around midnight for signals from Europe and an easterly direction, and just before sunrise for signals from all other directions. Excellent daytime short-skip openings should be possible over distances of up to approximately 500 miles, with nighttime openings ranging between 500 and 2300 miles.

Equinox: Expect fairly good DX openings to many parts of the world, particularly to the southern hemisphere, during the hours of darkness and the sunrise period. Excellent daytime short-skip openings should be possible over distances of up to about 350 miles, while nighttime openings should range between 500 and 2300 miles.

160 meters. *Summer:* Due to intense solar absorption, no ionospheric propagation will be possible on this band during the daylight hours. An occasional DX opening may be possible during the hours of darkness and the sunrise period, but high static levels often will make it difficult, if not impossible, to communicate on this band. During the nighttime hours, short-skip openings over distances of up to approximately 1000 miles may often be possible, despite heavy static.

Winter: No ionospheric propagation is expected during the daytime, but by late afternoon, conditions should begin to improve and some fairly good DX openings should be possible to many parts of the world during the hours of darkness and the pre-dawn period. Short-skip openings should be possible over distances of up to approximately 1500 miles during the nighttime hours, and at times, up to 2300 miles.

Equinox: Expect no daytime openings, but fairly good openings to some areas of the world should be possible during the nighttime hours and the pre-dawn period. Nighttime short-skip openings should provide communications on paths up to 1200 miles long on a regular basis, and often out to distances as great as 2300 miles. Conditions should peak around midnight, and again just before dawn.

MASTER DX PROPAGATION CHART
SOLAR PHASE: MODERATE
SMOOTHED SUNSPOT RANGE: 30-60
SEASON: SUMMER
TIME ZONE: EST (24-Hour Time)
EASTERN USA TO:

Reception Area	*10 Meters*	*15 Meters*	*20 Meters*	*40/80 Meters*
Western & Central Europe & North America	*Nil*	14-18 (1)	06-08 (2) 08-11 (1) 11-13 (2) 13-15 (3) 15-19 (4) 19-20 (3) 20-21 (2) 21-06 (1)	19-21 (1) 21-22 (2) 22-00 (3) 00-01 (2) 01-02 (1) 21-23 (1)* 23-00 (2)* 00-01 (1)*
Northern & Eastern Europe	*Nil*	14-17 (1)	08-14 (1) 14-18 (2) 18-22 (3) 22-00 (2) 00-05 (1) 05-08 (2)	20-21 (1) 21-23 (2) 23-01 (1) 20-23 (1)*
Eastern Mediterranean & Middle East	*Nil*	15-17 (1)	11-13 (1) 13-17 (2) 17-23 (3) 23-00 (2) 00-05 (1) 05-07 (2) 07-09 (1)	19-21 (1) 21-23 (2) 23-00 (1) 21-23 (1)*
Western Africa	*Nil*	10-13 (1) 13-16 (2) 16-18 (1)	00-06 (1) 06-08 (2) 08-14 (1) 14-16 (2) 16-18 (3) 18-21 (4) 21-23 (3) 23-00 (2)	19-21 (1) 21-23 (2) 23-01 (1)
East & Central Africa	*Nil*	12-14 (1) 14-16 (2) 16-18 (1)	13-15 (1) 15-17 (2) 17-20 (3) 20-21 (2) 21-23 (1) 23-01 (2) 01-05 (1)	20-23 (1)
Southern Africa	*Nil*	09-12 (1)	23-00 (1) 00-03 (2) 03-06 (1) 14-15 (1) 15-17 (2) 17-18 (1)	20-21 (1) 21-23 (2) 23-01 (1) 22-00 (1)*
Central & South Asia	*Nil*	*Nil*	16-19 (1) 19-21 (2) 21-23 (1) 06-08 (1)	18-20 (1)
Southeast Asia	*Nil*	*Nil*	05-06 (1) 06-08 (2) 08-10 (1) 18-20 (1)	*Nil*
Far East	*Nil*	*Nil*	05-06 (1) 06-09 (2) 09-11 (1) 19-23 (1)	*Nil*
South Pacific & New Zealand	17-20 (1)	15-17 (1) 17-20 (2) 20-21 (1)	17-20 (1) 20-22 (2) 22-02 (3) 02-05 (2) 05-08 (1)	00-02 (1) 02-05 (2) 05-07 (1) 03-05 (1)*
Australasia	*Nil*	18-21 (1)	22-00 (1) 00-01 (2) 01-03 (3) 03-04 (2) 04-07 (1) 07-09 (2) 09-11 (1) 15-17 (1)	02-03 (1) 03-05 (2) 05-06 (1) 03-05 (1)*
Caribbean, Central America & Northern Countries of South America	10-14 (1) 14-16 (2) 16-17 (1)	07-08 (1) 08-14 (2) 14-15 (3) 15-17 (4) 17-19 (3) 19-20 (2) 20-21 (1)	05-06 (2) 06-07 (3) 07-09 (4) 09-11 (3) 11-15 (2) 15-17 (3) 17-21 (4) 21-23 (3) 23-00 (2) 00-05 (1)	20-22 (1) 22-03 (2) 03-05 (1) 22-03 (1)*
Peru, Bolivia, Paraguay, Brazil, Chile, Argentina & Uruguay	13-14 (1) 14-16 (2) 16-17 (1)	07-08 (1) 08-10 (2) 10-14 (1) 14-15 (2) 15-16 (3) 16-17 (4) 17-18 (3) 18-20 (2) 20-21 (1)	15-16 (1) 16-18 (2) 18-19 (3) 19-21 (4) 21-23 (3) 23-01 (2) 01-06 (1) 06-08 (2) 08-10 (1)	22-00 (1) 00-03 (2) 03-05 (1) 00-04 (1)*
McMurdo Sound, Antarctica	*Nil*	14-17 (1)	16-18 (1) 18-22 (2) 22-00 (1)	02-04 (1)

MASTER DX PROPAGATION CHART
SOLAR PHASE: MODERATE
SMOOTHED SUNSPOT RANGE: 30-60
SEASON: SUMMER
TIME ZONES: CST & MST (24-Hour Time)
CENTRAL USA TO:

Reception Area	10 Meters	15 Meters	20 Meters	40/80 Meters
Western & Central Europe & North Africa	*Nil*	14-17 (1)	05-06 (1) 06-08 (2) 08-12 (1) 12-14 (2) 14-19 (3) 19-21 (2) 21-23 (1)	19-22 (1) 22-00 (2) 00-01 (1) 21-23 (1)*
Northern & Eastern Europe	*Nil*	14-16 (1)	04-06 (1) 06-08 (2) 08-15 (1) 15-21 (2) 21-23 (1)	19-23 (1)
Eastern Mediterranean & Middle East	*Nil*	13-15 (1)	12-16 (1) 16-18 (2) 18-20 (3) 20-22 (2) 22-00 (1) 06-08 (1)	20-23 (1)
West & Central Africa	*Nil*	09-12 (1) 12-15 (2) 15-17 (1)	13-15 (1) 15-17 (2) 17-20 (3) 20-22 (2) 22-00 (1) 04-07 (1)	19-23 (1) 22-23 (1)*
East Africa	*Nil*	11-15 (1)	14-17 (1) 17-20 (2) 20-23 (1) 05-07 (1)	19-22 (1)
Southern Africa	*Nil*	09-11 (1)	21-23 (1) 23-02 (2) 02-06 (1) 12-14 (1)	20-22 (1) 22-23 (2) 23-00 (1) 22-00 (1)*
Central & South Asia	*Nil*	*Nil*	16-18 (1) 18-21 (2) 21-23 (1) 04-06 (1) 06-08 (2) 08-09 (1)	*Nil*
Southeast Asia	*Nil*	19-21 (1)	04-06 (1) 06-09 (2) 09-10 (1) 20-23 (1)	*Nil*
Far East	*Nil*	19-22 (1)	06-07 (1) 07-09 (3) 09-10 (2) 20-21 (1) 21-23 (2) 23-00 (1)	03-04 (1) 04-05 (2) 05-08 (1)
South Pacific & New Zealand	17-19 (1)	12-15 (1) 15-17 (2) 17-20 (3) 20-21 (2) 21-22 (1)	16-18 (1) 18-21 (2) 21-22 (3) 22-00 (4) 00-02 (3) 02-06 (2) 06-08 (3) 08-10 (2) 10-12 (1)	22-00 (1) 00-02 (2) 02-04 (3) 04-06 (2) 06-07 (1) 00-06 (1)*
Australasia	*Nil*	13-14 (1) 14-16 (2) 16-18 (1) 18-20 (2) 20-22 (1)	21-23 (1) 23-00 (2) 00-02 (3) 02-06 (2) 06-08 (3) 08-10 (2)	00-02 (1) 02-06 (2) 06-07 (1) 03-06 (1)*
Caribbean, Central America & Northern Countries of South America	10-14 (1) 14-16 (2) 16-17 (1)	07-08 (1) 08-10 (2) 10-15 (3) 15-17 (4) 17-18 (3) 18-19 (2) 19-20 (1)	01-04 (1) 04-05 (2) 05-06 (3) 06-08 (4) 08-10 (3) 10-15 (2) 15-17 (3) 17-21 (4) 21-23 (3) 23-01 (2)	20-22 (1) 22-03 (2) 03-05 (1) 23-02 (1)*
Peru, Bolivia, Paraguay, Brazil, Chile, 23-03 (1)* Argentina & Uruguay	13-17 (1)	06-07 (1) 07-09 (2) 09-13 (1) 14-15 (3) 15-17 (4) 17-18 (3) 18-20 (2) 20-21 (1)	13-15 (1) 15-16 (2) 16-17 (3) 13-14 (2) 21-23 (3) 23-02 (2) 02-04 (1) 04-06 (2) 06-09 (1)	21-22 (1) 22-01 (2) 01-04 (1) 17-21 (4)
McMurdo Sound, Antarctica	*Nil*	14-17 (1)	16-18 (1) 18-22 (2) 22-00 (1)	02-05 (1)

MASTER DX PROPAGATION CHART
SOLAR PHASE: MODERATE
SMOOTHED SUNSPOT RANGE: 30–60
SEASON: SUMMER
TIME ZONE: PST (24-Hour Time)
WESTERN USA TO:

Reception Area	*10 Meters*	*15 Meters*	*20 Meters*	*40/80 Meters*
Western Europe & North Africa	*Nil*	14-16 (1)	04-05 (1) 05-07 (2) 07-14 (1) 14-16 (2) 16-18 (3) 18-21 (2) 21-23 (1)	19-22 (1)

Central, Northern & Eastern Europe	*Nil*	*Nil*	04-05 (1) 05-07 (2) 07-09 (1) 09-12 (1) 12-16 (1) 16-21 (2) 21-22 (1)	19-21 (1)
Eastern Mediter-ranean & Middle East	*Nil*	*Nil*	16-19 (1) 19-21 (2) 21-22 (1) 05-07 (1)	*Nil*
West & Central Africa	*Nil*	09-11 (1) 11-14 (2) 14-15 (1)	14-17 (1) 17-19 (2) 19-21 (3) 21-23 (2) 23-02 (1) 06-08 (1)	20-23 (1)
East Africa	*Nil*	12-15 (1)	16-19 (1) 19-21 (2) 21-22 (1)	*Nil*
Southern Africa	*Nil*	09-11 (1)	14-16 (1) 21-22 (1) 22-00 (2) 00-01 (1)	19-22 (1)
Central & South Asia	*Nil*	*Nil*	04-06 (1) 06-08 (2) 08-10 (1) 16-20 (1) 20-22 (2) 22-00 (1)	*Nil*
Southeast Asia	*Nil*	19-21 (1)	20-22 (1) 22-00 (2) 00-06 (1) 06-08 (2) 08-10 (1)	02-06 (1)
Far East	*Nil*	19-21 (1)	17-19 (1) 19-21 (2) 21-23 (3) 23-01 (4) 01-03 (2) 03-06 (1) 06-09 (2) 09-11 (1)	01-02 (1) 02-05 (2) 05-06 (1) 02-04 (1)*
South Pacific & New Zealand	15-10 (1)	10-12 (1) 12-16 (2) 16-20 (3) 20-22 (2) 22-23 (1)	16-18 (1) 18-20 (2) 20-00 (4) 00-02 (3) 02-07 (2) 07-09 (3) 09-10 (2) 10-12 (1)	21-22 (1) 22-00 (2) 00-05 (3) 05-06 (2) 06-07 (1) 23-01 (1)* 01-04 (2)* 04-06 (1)*
Australasia	*Nil*	12-14 (1) 14-17 (2) 17-20 (3) 20-21 (2) 21-22 (1)	19-21 (1) 21-23 (2) 23-00 (3) 00-06 (2) 06-08 (3) 08-09 (2) 09-12 (1) 12-14 (2) 14-15 (1)	23-01 (1) 01-03 (2) 03-05 (3) 05-06 (2) 06-07 (1) 01-06 (1)*
Caribbean, Central America & Northern Countries of South America	10-14 (1) 14-16 (2) 16-18 (1)	07-10 (1) 10-12 (2) 12-14 (3) 14-16 (4) 16-17 (3) 17-18 (2) 18-20 (1)	08-10 (2) 10-13 (1) 13-15 (2) 15-17 (3) 17-21 (4) 21-23 (3) 23-01 (2) 01-03 (1) 03-06 (2) 06-08 (3)	20-22 (1) 22-03 (2) 03-05 (1) 22-03 (1)*
Peru, Bolivia, Paraguay, Brazil, Chile, Argentina & Uruguay	11-16 (1)	07-10 (1) 10-13 (2) 13-14 (3) 14-16 (4) 16-17 (3) 17-19 (2) 19-20 (1)	13-15 (1) 15-17 (2) 17-18 (3) 18-20 (4) 20-22 (3) 22-00 (2) 00-04 (1) 04-06 (2) 06-09 (1)	21-23 (1) 23-01 (2) 01-03 (1) 23-02 (1)*
McMurdo Sound, Antarctica	*Nil*	13-17 (1)	16-18 (1) 18-20 (2) 20-22 (1)	02-06 (1)

MASTER DX PROPAGATION CHART
SOLAR PHASE: MODERATE
SMOOTHED SUNSPOT RANGE: 30–60
SEASON: WINTER
TIME ZONE: EST (24-Hour Time)
EASTERN USA TO:

Reception Area	*10 Meters*	*15 Meters*	*20 Meters*	*40/80 Meters*
Western & Central Europe & North Africa	09-11 (1)	07-08 (1) 08-09 (3) 09-11 (4) 11-12 (3) 12-13 (2) 13-14 (1)	06-07 (1) 07-09 (4) 09-11 (3) 11-13 (4) 13-14 (3) 14-15 (2) 15-17 (1)	15-16 (1) 16-17 (2) 17-19 (3) 19-00 (4) 00-04 (2) 04-05 (1) 17-19 (1)* 19-20 (2)* 20-02 (3)* 02-03 (2)* 03-04 (1)*
Northern & Eastern Europe	08-10 (1)	07-08 (1) 08-10 (2) 10-12 (1)	06-07 (1) 07-09 (3) 09-12 (2) 12-14 (1)	16-19 (1) 19-23 (2) 23-03 (1) 19-02 (1)*
Eastern Mediter-ranean & Middle East	08-10 (1)	07-08 (1) 08-09 (2) 09-10 (3) 10-11 (2) 11-12 (1)	06-09 (1) 09-10 (2) 10-12 (3) 12-14 (2) 14-17 (1) 19-21 (1)	18-20 (1) 20-22 (2) 22-00 (1) 20-23 (1)*
Western & Central Africa	09-11 (1) 11-13 (2) 13-15 (1)	07-08 (1) 08-09 (2) 09-12 (3) 12-14 (4) 14-15 (3) 15-16 (2) 16-17 (1)	06-07 (1) 07-09 (2) 09-13 (1) 13-15 (2) 15-17 (4) 17-18 (3) 18-19 (2) 19-20 (1)	18-22 (1) 22-02 (2) 02-03 (1) 00-02 (1)*
East Africa	10-13 (1)	08-10 (1) 10-12 (2) 12-14 (3) 14-15 (2) 15-16 (1)	07-13 (1) 13-15 (2) 15-18 (3) 18-19 (2) 19-20 (1) 00-02 (1)	18-00 (1)
Southern Africa	09-10 (1) 10-12 (2) 12-13 (1)	07-09 (1) 09-12 (2) 12-14 (3) 14-16 (2) 16-17 (1)	06-09 (1) 12-14 (1) 14-15 (2) 15-17 (3) 17-18 (2) 18-20 (1)	18-19 (1) 19-21 (2) 21-00 (1) 19-22 (1)*
Central & South Asia	*Nil*	08-10 (1) 17-19 (1)	06-07 (1) 07-09 (2) 09-11 (1) 18-21 (1)	06-08 (1) 20-22 (1)
Southeast Asia	*Nil*	08-11 (1) 17-19 (1)	06-07 (1) 07-09 (2) 09-12 (1) 19-21 (1)	06-08 (1) 20-22 (1)
Far East	*Nil*	16-17 (1) 17-19 (2) 19-20 (1)	06-07 (1) 07-09 (2) 09-11 (1) 16-18 (1) 18-20 (2) 20-21 (1)	05-08 (1) 05-07 (1)*
South Pacific & New Zealand	13-17 (1)	11-14 (1) 14-15 (2) 15-17 (3) 17-18 (2) 18-20 (1)	03-07 (1) 07-09 (2) 09-11 (1) 16-18 (1) 18-20 (2) 20-22 (1)	01-02 (1) 02-04 (2) 04-07 (3) 07-08 (2) 08-09 (1) 04-05 (1)* 05-07 (2)* 07-08 (1)*
Australasia	16-18 (1)	09-12 (1) 15-16 (1) 16-18 (2) 18-20 (1)	06-07 (1) 07-10 (2) 10-14 (1) 14-16 (2) 16-18 (1) 18-20 (2) 20-22 (1)	03-05 (1) 05-07 (2) 07-09 (1) 05-08 (1)*
Caribbean, Central America & Northern Countries of South America	09-10 (1) 10-12 (2) 12-14 (1) 14-16 (2) 16-17 (1)	07-08 (1) 08-11 (3) 11-13 (2) 13-15 (4) 15-16 (3) 16-17 (2) 17-18 (1)	06-07 (2) 07-09 (4) 09-11 (3) 11-15 (2) 15-17 (3) 17-18 (4) 18-19 (3) 19-20 (2) 20-22 (1) 22-00 (2) 00-06 (1)	17-18 (1) 18-19 (2) 19-21 (3) 21-04 (4) 04-05 (3) 05-06 (2) 06-07 (1) 19-20 (1)* 20-22 (2)* 22-02 (3)* 02-04 (2)* 04-06 (1)*
Peru, Bolivia, Paraguay, Brazil, Chile, Argentina & Uruguay	09-12 (1) 12-15 (2) 15-16 (1)	07-08 (1) 08-10 (2) 10-12 (1) 12-14 (2) 14-16 (4) 16-17 (3) 17-18 (1)	13-14 (1) 14-15 (2) 15-17 (3) 17-18 (4) 18-19 (3) 19-20 (2) 20-22 (1) 22-00 (2) 00-03 (1) 05-06 (1) 06-08 (2) 08-09 (1)	19-21 (1) 21-02 (2) 02-05 (1) 21-03 (1)*
McMurdo Sound, Antarctica	*Nil*	07-10 (1) 16-18 (1)	07-09 (1) 17-18 (1) 18-22 (2) 22-00 (1) 00-02 (2) 02-03 (1)	00-05 (1)

MASTER DX PROPAGATION CHART
SOLAR PHASE: MODERATE
SMOOTHED SUNSPOT RANGE: 30-60
SEASON: WINTER
TIME ZONES: CST & MST (24-Hour Time)
CENTRAL USA TO:

Reception Area	*10 Meters*	*15 Meters*	*20 Meters*	*40/80 Meters*
Western & Southern Europe & North Africa	09-11 (1)	07-08 (1) 08-09 (2) 09-11 (3) 11-12 (2) 12-13 (1)	06-08 (1) 08-09 (2) 09-12 (3) 12-13 (2) 13-15 (1) 22-00 (1)	16-18 (1) 18-20 (2) 20-00 (1) 00-02 (2) 02-03 (1) 17-22 (1)* 22-01 (2)* 01-02 (1)*
Northern, Central & Eastern Europe	*Nil*	07-08 (1) 08-10 (2) 10-12 (1)	07-08 (1) 08-11 (2) 11-13 (1) 23-01 (1)	17-19 (1) 19-22 (2) 22-01 (1) 19-00 (1)*
Eastern Mediter-ranean & Middle East	*Nil*	08-11 (1)	06-09 (1) 09-12 (2) 12-14 (1) 22-00 (1)	18-20 (1) 20-22 (2) 22-23 (1) 20-22 (1)*
West & Central Africa	08-10 (1) 10-12 (2) 12-13 (1)	07-09 (1) 09-11 (2) 11-13 (3) 13-14 (2) 14-15 (1)	06-11 (1) 11-13 (2) 13-16 (3) 16-17 (2) 17-19 (1) 22-02 (1)	18-22 (1) 22-23 (2) 23-01 (1) 19-22 (1)*
East Africa	10-12 (1)	07-11 (1) 11-13 (2) 13-14 (1)	06-12 (1) 12-14 (2) 14-16 (3) 16-17 (2) 17-19 (1)	19-23 (1)
Southern Africa	08-09 (1) 09-12 (2) 12-13 (1)	07-09 (1) 09-11 (2) 11-13 (3) 13-15 (2) 15-16 (1)	07-13 (1) 13-15 (2) 15-17 (3) 17-18 (2) 18-20 (1) 23-01 (1)	18-19 (1) 19-21 (2) 21-23 (1)
Central & South Asia	*Nil*	08-10 (1) 19-21 (1)	06-07 (1) 07-09 (2) 09-11 (1) 19-22 (1)	06-08 (1) 19-21 (1)
Southeast Asia	*Nil*	08-11 (1) 17-20 (1)	07-08 (1) 08-10 (2) 10-12 (1) 16-17 (1) 17-19 (2) 19-20 (1)	04-07 (1)

Far East	*Nil*	07-09 (1) 16-17 (1) 17-19 (2) 19-20 (1)	06-07 (1) 07-09 (2) 09-11 (1) 15-17 (1) 17-19 (2) 19-21 (1)	02-04 (1) 04-06 (2) 06-07 (1) 04-07 (1)*
South Pacific & New Zealand	12-14 (1) 14-16 (2) 16-18 (1)	10-12 (1) 12-14 (2) 14-17 (3) 17-19 (2) 19-20 (1)	06-07 (1) 07-09 (3) 09-12 (2) 12-15 (1) 15-17 (2) 17-20 (3) 20-21 (2) 21-22 (1) 02-04 (1)	23-01 (1) 01-02 (2) 02-06 (3) 06-07 (2) 07-08 (1) 03-07 (1)*
Australasia	14-15 (1) 15-17 (2) 17-18 (1)	09-11 (1) 13-15 (1) 15-17 (3) 17-19 (2) 19-20 (1)	06-07 (1) 07-08 (2) 08-10 (3) 10-12 (2) 12-18 (1) 18-21 (2) 21-22 (1)	02-04 (1) 04-07 (2) 07-09 (1) 03-06 (1)*
Caribbean, Central America & Northern Countries of South America	08-10 (1) 10-14 (2) 14-16 (1)	07-08 (1) 08-09 (2) 09-13 (3) 13-16 (4) 16-17 (2) 17-19 (1)	06-07 (2) 07-11 (3) 11-14 (2) 14-16 (3) 16-18 (4) 18-19 (3) 19-20 (2) 20-22 (1) 22-00 (2) 00-06 (1)	18-20 (1) 20-22 (2) 22-03 (3) 03-05 (2) 05-07 (1) 19-21 (1)* 21-01 (2) 01-04 (1)*
Peru, Bolivia, Paraguay, Brazil, Chile, Argentina & Uruguay	08-11 (1) 11-15 (2) 15-17 (1)	07-08 (1) 08-13 (2) 13-15 (4) 15-16 (3) 16-17 (2) 17-19 (1)	05-06 (1) 06-08 (2) 08-10 (1) 12-14 (1) 14-15 (2) 15-17 (3) 17-19 (4) 19-20 (2) 20-22 (1) 22-00 (2) 00-03 (1)	19-21 (1) 21-02 (2) 02-05 (1) 21-04 (1)*
McMurdo Sound, Antarctica	*Nil*	07-09 (1) 16-18 (1)	06-07 (1) 07-09 (2) 09-11 (1) 17-18 (1) 18-22 (2) 22-00 (1) 00-02 (2) 02-03 (1)	22-05 (1)

MASTER DX PROPAGATION CHART

SOLAR PHASE: MODERATE
SMOOTHED SUNSPOT RANGE: 30-60
SEASON: WINTER
TIME ZONE: PST (24-Hour Time)
WESTERN USA TO:

Reception Area	*10 Meters*	*15 Meters*	*20 Meters*	*40/80 Meters*
Western Europe & North Africa	07-09 (1)	07-08 (1) 08-10 (2) 10-11 (1)	05-07 (1) 07-10 (2) 10-12 (1) 23-01 (1)	18-20 (1) 20-23 (2) 23-01 (1) 19-23 (1)*
Northern, Central & Eastern Europe	*Nil*	07-09 (1)	06-07 (1) 07-10 (2) 10-13 (1) 23-01 (1)	17-00 (1) 19-23 (1)*
Eastern Mediterranean & Middle East	*Nil*	07-09 (1)	06-07 (1) 07-09 (2) 09-11 (1) 21-23 (1)	18-21 (1)
West & Central Africa	09-12 (1)	07-09 (1) 09-10 (2) 10-12 (3) 12-13 (2) 13-14 (1)	06-10 (1) 10-13 (2) 13-16 (3) 16-18 (2) 18-19 (1)	18-22 (1)
East Africa	*Nil*	08-11 (1)	08-10 (1) 13-16 (1) 21-23 (1)	18-20 (1)
Southern Africa	08-11 (1)	06-08 (1) 08-10 (2) 10-12 (3) 12-13 (2) 13-14 (1)	07-11 (1) 11-13 (2) 13-16 (3) 16-18 (2) 18-19 (1) 00-02 (1)	18-20 (1)
Central & South Asia	*Nil*	09-11 (1) 17-19 (1)	08-10 (1) 17-19 (1) 19-20 (2) 20-21 (1)	05-07 (1) 18-20 (1)
Southeast Asia	15-18 (1)	09-11 (1) 15-16 (1) 16-18 (2) 18-19 (1)	07-09 (1) 09-11 (2) 11-16 (1) 16-19 (2) 19-20 (1)	03-08 (1)
Far East	15-17 (1)	14-15 (1) 15-16 (2) 16-17 (3) 17-18 (2) 18-19 (1)	08-10 (1) 13-14 (1) 14-15 (2) 15-18 (3) 18-19 (2) 19-21 (1)	00-01 (1) 01-03 (2) 03-06 (3) 06-08 (2) 08-10 (1) 02-08 (1)*
South Pacific & New Zealand	12-14 (1) 14-16 (2) 16-17 (1)	09-12 (1) 12-14 (2) 14-16 (4) 16-17 (3) 17-18 (2) 18-20 (1)	07-08 (1) 08-10 (2) 10-15 (1) 15-16 (2) 16-18 (4) 18-19 (3) 19-20 (2) 20-22 (1) 03-05 (1)	22-00 (1) 00-03 (2) 03-06 (3) 06-07 (2) 07-08 (1) 00-03 (1)* 03-06 (2)* 06-07 (1)*
Australasia	13-15 (1) 15-17 (2) 17-18 (1)	08-12 (1) 12-15 (2) 15-17 (3) 17-18 (2) 18-19 (1)	07-08 (1) 08-10 (3) 10-12 (2) 12-17 (1) 17-18 (2) 18-20 (3) 20-21 (2) 21-22 (1)	01-03 (1) 03-06 (2) 06-08 (1) 01-03 (1)* 03-06 (2)* 06-07 (1)*
Caribbean, Central America & Northern Countries of South America	09-11 (1) 11-14 (2) 14-16 (1)	06-07 (1) 07-08 (2) 08-12 (3) 12-14 (4) 14-15 (3) 15-16 (2) 16-17 (1)	06-07 (2) 07-09 (3) 09-13 (2) 13-15 (3) 15-17 (4) 17-18 (3) 18-20 (2) 20-22 (1) 22-00 (2) 00-06 (1)	18-20 (1) 20-22 (2) 22-02 (3) 02-04 (2) 04-05 (1) 19-21 (1)* 21-01 (2)* 01-04 (1)*
Peru, Bolivia, Paraguay, Brazil, Chile, Argentina & Uruguay	10-12 (1) 12-14 (2) 14-15 (1)	07-10 (1) 10-12 (2) 12-13 (3) 13-15 (4) 15-16 (2) 16-18 (1)	08-14 (1) 14-15 (2) 15-16 (3) 16-18 (4) 18-19 (3) 19-20 (2) 20-23 (1) 23-01 (2) 01-06 (1) 06-08 (2)	20-22 (1) 22-01 (2) 01-04 (1) 22-02 (1)*
McMurdo Sound, Antarctica	*Nil*	07-09 (1) 12-15 (1) 15-17 (2) 17-18 (1)	16-18 (1) 18-19 (2) 19-22 (3) 22-01 (2) 01-03 (1) 07-09 (1)	23-05 (1)

MASTER DX PROPAGATION CHART

SOLAR PHASE: MODERATE
SMOOTHED SUNSPOT RANGE: 30-60
SEASONS: SPRING & FALL
TIME ZONE: EST (24-Hour Time)
EASTERN USA TO:

Reception Area	*10 Meters*	*15 Meters*	*20 Meters*	*40/80 Meters*
Western & Central Europe & North Africa	09-12 (1)	08-09 (1) 09-10 (2) 10-13 (3) 13-14 (2) 14-15 (1)	06-07 (1) 07-09 (3) 09-11 (2) 11-12 (3) 12-14 (4) 14-15 (3) 15-17 (2) 17-19 (1)	17-18 (1) 18-19 (2) 19-22 (3) 22-01 (4) 01-02 (3) 02-03 (2) 03-04 (1) 19-21 (1)* 21-00 (2)* 00-02 (1)*
Northern & Eastern Europe	08-11 (1)	08-09 (1) 09-12 (2) 12-13 (1)	06-07 (1) 07-09 (3) 09-11 (2) 11-13 (1) 13-15 (2) 15-17 (1) 00-03 (1)	17-19 (1) 19-02 (2) 02-03 (1) 20-01 (1)*
Eastern Mediterranean & Middle East	08-11 (1)	08-09 (1) 09-11 (2) 11-13 (1)	06-07 (1) 07-09 (2) 09-12 (1) 12-15 (2) 15-16 (3) 16-18 (2) 18-20 (1) 00-02 (1)	18-20 (1) 20-23 (2) 23-00 (1) 20-23 (1)*
West & Central Africa	09-11 (1) 11-13 (2) 13-14 (1)	07-09 (1) 09-10 (2) 10-12 (3) 12-14 (4) 14-15 (3) 15-16 (2) 16-17 (1)	05-06 (1) 06-08 (2) 08-13 (1) 13-14 (2) 14-15 (3) 15-17 (4) 17-18 (3) 18-20 (2) 20-22 (1)	18-21 (1) 21-01 (2) 01-03 (1) 22-02 (1)*
Southern Africa	09-10 (1) 10-12 (2) 12-14 (1)	07-10 (1) 10-13 (2) 13-15 (3) 15-17 (2) 17-18 (1)	07-14 (1) 14-16 (2) 16-18 (3) 18-20 (2) 20-22 (1) 22-00 (2) 00-01 (1)	18-20 (1) 20-23 (2) 23-00 (1) 21-23 (1)*
East Africa	10-13 (1)	07-09 (1) 09-11 (2) 11-13 (3) 13-14 (2) 14-16 (1)	12-14 (1) 14-16 (2) 16-18 (3) 18-19 (2) 19-20 (1)	19-23 (1) 23-01 (2) 01-02 (1)
Central & South Asia	08-11 (1) 19-21 (1)	08-10 (1) 19-21 (1)	06-07 (1) 07-09 (2) 09-11 (1) 19-21 (1)	19-22 (1) 04-06 (1)
Southeast Asia	10-13 (1) 18-20 (1)	08-10 (1) 17-19 (1)	06-07 (1) 07-09 (2) 09-11 (1) 19-21 (1)	05-07 (1) 19-22 (1)
Far East	17-19 (1)	16-17 (1) 17-19 (2) 19-20 (1)	06-07 (1) 07-09 (2) 09-11 (1) 17-18 (1) 18-20 (2) 20-22 (1)	05-08 (1) 05-07 (1)*
South Pacific & New Zealand	12-14 (1) 14-16 (2) 16-18 (1)	10-14 (1) 14-16 (2) 16-18 (3) 18-19 (2) 19-20 (1)	09-11 (2) 11-19 (1) 19-23 (2) 23-06 (1) 06-07 (2) 07-09 (3)	00-01 (1) 01-02 (2) 02-05 (3) 05-07 (2) 07-08 (1) 03-07 (1)*
Australasia	09-11 (1) 16-18 (1)	08-12 (1) 14-16 (1) 16-19 (2) 19-21 (1)	06-07 (1) 07-09 (3) 09-10 (2) 10-14 (1) 14-16 (2) 16-19 (1) 19-22 (2) 22-00 (1)	02-04 (1) 04-06 (2) 06-08 (1) 04-06 (1)*
Caribbean, Central America & Northern Countries of South America	09-11 (1) 11-12 (2) 12-14 (3) 14-16 (2) 16-18 (1)	07-08 (1) 08-09 (2) 09-11 (4) 11-13 (2) 13-16 (4) 16-17 (3) 17-18 (2) 18-20 (1)	22-00 (2) 00-06 (1) 06-07 (2) 07-09 (4) 09-10 (3) 10-14 (2) 14-16 (3) 16-19 (4) 19-22 (3)	18-19 (1) 19-20 (2) 20-03 (4) 03-05 (3) 05-06 (2) 06-07 (1) 20-22 (1)* 22-03 (2)* 03-05 (1)*
Peru, Bolivia, Paraguay, Brazil, Chile, Argentina & Uruguay	09-11 (1) 11-14 (2) 14-16 (3) 16-17 (2) 17-18 (1)	07-08 (1) 08-10 (2) 10-13 (1) 13-15 (2) 15-16 (3) 16-17 (4) 17-18 (2) 18-19 (1)	13-15 (1) 15-16 (2) 16-18 (3) 18-20 (4) 20-21 (3) 21-23 (2) 23-06 (1) 06-08 (2) 08-10 (1)	19-21 (1) 21-03 (2) 03-06 (1) 21-05 (1)*
McMurdo Sound, Antarctica	*Nil*	14-17 (1) 17-19 (2) 19-20 (1)	17-19 (1) 19-23 (2) 23-01 (1) 06-08 (1)	22-00 (1) 00-04 (2) 04-06 (1)

MASTER DX PROPAGATION CHART
SOLAR PHASE: MODERATE
SMOOTHED SUNSPOT RANGE: 30-60
SEASONS: SPRING & FALL
TIME ZONES: CST & MST (24-Hour Time)
CENTRAL USA TO:

Reception Area	*10 Meters*	*15 Meters*	*20 Meters*	*40/80 Meters*
Western & Central Europe & North Africa	09-11 (1)	08-09 (1) 09-13 (2) 13-14 (1)	00-07 (1) 07-09 (2) 09-11 (1) 11-13 (2) 13-15 (3) 15-16 (2) 16-18 (1) 22-00 (1)	17-19 (1) 19-22 (2) 22-00 (3) 00-01 (2) 01-02 (1) 20-22 (1)* 22-00 (2)* 00-01 (1)*
Northern & Eastern Europe	09-11 (1)	07-09 (1) 09-11 (2) 11-12 (1)	06-07 (1) 07-10 (2) 10-12 (1) 12-13 (2) 13-15 (3) 23-01 (1)	19-22 (1) 22-00 (2) 00-02 (1) 22-01 (1)*
Eastern Mediter-ranean & Middle East	09-11 (1)	07-09 (1) 09-11 (2) 11-13 (1)	07-12 (1) 12-15 (2) 15-17 (1) 22-00 (1)	19-22 (1) 20-22 (1)*
West & Central Africa	09-10 (1) 10-12 (2) 12-14 (1)	07-09 (1) 09-10 (2) 10-12 (3) 12-13 (4) 13-15 (3) 15-16 (2) 16-17 (1)	06-12 (1) 12-14 (2) 14-15 (3) 15-16 (4) 16-17 (3) 17-19 (2) 19-21 (1)	18-20 (1) 20-23 (2) 23-01 (1) 21-00 (1)*
East Africa	09-12 (1)	08-11 (1) 11-15 (2) 15-17 (1)	06-12 (1) 12-14 (2) 14-16 (3) 16-18 (2) 18-19 (1)	19-22 (1)
Southern Africa	08-09 (1) 09-12 (2) 12-13 (1)	07-09 (1) 09-11 (2) 11-14 (3) 14-15 (2) 15-16 (1)	05-07 (2) 07-13 (1) 13-15 (2) 15-17 (3) 17-18 (2) 18-20 (1) 23-01 (1)	19-22 (1) 20-21 (1)*
Central & South Asia	07-09 (1) 17-19 (1)	08-10 (1) 19-21 (1)	06-07 (1) 07-09 (2) 09-11 (1) 19-21 (2)	05-07 (1) 18-20 (1)
Southeast Asia	08-10 (1) 18-20 (1)	09-12 (1) 16-17 (1) 17-19 (2) 19-20 (1)	06-07 (1) 07-10 (2) 10-12 (1) 16-18 (1) 18-20 (2) 20-21 (1)	04-07 (1)
Far East	16-19 (1)	14-16 (1) 16-18 (2) 18-20 (1)	06-07 (1) 07-09 (2) 09-11 (1) 16-18 (1) 18-21 (2) 21-23 (1)	02-04 (1) 04-06 (2) 06-08 (1) 05-07 (1)*
South Pacific & New Zealand	11-13 (1) 13-14 (2) 14-15 (3) 15-16 (2) 16-17 (1)	10-12 (1) 12-15 (2) 15-17 (3) 17-19 (2) 19-20 (1)	06-07 (1) 07-09 (3) 09-11 (2) 11-18 (1) 18-20 (2) 20-22 (3) 22-00 (2) 00-02 (1)	22-00 (1) 00-01 (2) 01-06 (3) 06-07 (2) 07-08 (1) 00-02 (1)* 02-05 (2)* 05-07 (1)*
Australasia	14-15 (1) 15-16 (2) 16-18 (1)	08-14 (1) 14-16 (2) 16-18 (3) 18-19 (2) 19-21 (1)	06-07 (1) 07-09 (3) 09-12 (2) 12-15 (1) 15-17 (2) 17-19 (1) 19-21 (2) 21-01 (1)	02-04 (1) 04-06 (3) 06-07 (2) 07-08 (1) 04-05 (1)* 05-06 (2)* 06-07 (1)*
Caribbean, Central America & Northern Countries of South America	08-09 (1) 09-10 (2) 10-14 (3) 14-15 (2) 15-16 (1)	07-08 (1) 08-09 (2) 09-13 (3) 13-16 (4) 16-17 (3) 17-18 (2) 18-19 (1)	07-09 (4) 09-11 (3) 11-15 (2) 15-16 (3) 16-18 (4) 18-21 (3) 21-00 (2) 00-06 (1) 06-07 (2)	18-19 (1) 19-20 (2) 20-00 (3) 00-02 (4) 02-03 (3) 03-04 (2) 04-06 (1) 19-21 (1)* 21-03 (2)* 03-05 (1)*
Peru, Bolivia, Paraguay, Brazil, Chile, Argentina & Uruguay	08-11 (1) 11-14 (2) 14-16 (3) 16-17 (2) 17-18 (1)	07-08 (1) 08-13 (2) 13-14 (3) 14-16 (4) 16-17 (3) 17-18 (2) 18-20 (1)	14-15 (2) 15-16 (3) 16-19 (4) 19-20 (3) 20-00 (2) 00-02 (1) 04-06 (1) 06-08 (2) 08-14 (1)	19-20 (1) 20-02 (2) 02-05 (1) 21-03 (1)*
McMurdo Sound, Antarctica	*Nil*	13-16 (1) 16-18 (2) 18-20 (1)	16-19 (1) 19-23 (2) 23-02 (1) 07-09 (1)	22-02 (1) 02-04 (2) 04-06 (1)

MASTER DX PROPAGATION CHART
SOLAR PHASE: MODERATE
SMOOTHED SUNSPOT RANGE: 30-60
SEASONS: SPRING & FALL
TIME ZONE: PST (24-Hour Time)
WESTERN USA TO:

Reception Area	*10 Meters*	*15 Meters*	*20 Meters*	*40/80 Meters*
Western Europe & North Africa	09-11 (1)	08-09 (1) 09-12 (2) 12-14 (1)	05-07 (1) 07-09 (2) 09-11 (1) 11-13 (2) 13-14 (3) 14-16 (2) 16-18 (1) 22-00 (1)	19-20 (1) 20-22 (2) 22-00 (1) 20-22 (1)*
Northern, Central & Eastern Europe	*Nil*	07-08 (1) 08-10 (2) 10-12 (1)	06-07 (1) 07-09 (2) 09-12 (1) 12-13 (2) 13-15 (1) 22-00 (1)	19-21 (1) 21-23 (2) 23-00 (1) 21-23 (1)*
Eastern Mediter-ranean & Middle East	*Nil*	07-08 (1) 08-10 (2) 10-12 (1)	07-12 (1) 12-14 (2) 14-17 (1) 22-02 (1)	18-21 (1)
West & Central Africa	08-10 (1) 10-12 (2) 12-14 (1)	07-09 (1) 09-12 (2) 12-15 (3) 15-16 (2) 16-17 (1)	04-06 (1) 06-08 (2) 08-12 (1) 12-14 (2) 14-17 (3) 17-19 (2) 19-21 (1)	18-22 (1)
East Africa	09-12 (1)	08-10 (1) 10-13 (2) 13-14 (1)	06-08 (1) 12-14 (1) 14-16 (2) 16-18 (1)	18-20 (1)
Southern Africa	09-12 (1)	07-10 (1) 10-14 (2) 14-15 (1)	06-08 (2) 08-13 (2) 13-15 (2) 15-17 (3) 17-18 (2) 18-19 (1) 23-01 (1)	18-21 (1)
Central & South Asia	17-19 (1)	07-09 (1) 16-17 (1) 17-19 (2) 19-20 (1)	16-18 (1) 18-20 (2) 20-22 (1) 06-07 (1) 07-09 (2) 09-12 (1)	05-07 (1) 19-21 (1)
Southeast Asia	09-11 (1) 17-19 (1)	08-10 (1) 15-17 (1) 17-19 (2) 19-22 (1)	07-08 (1) 08-11 (2) 11-13 (1) 20-22 (1) 22-00 (2) 00-02 (1)	00-02 (1) 02-05 (2) 05-07 (1)
Far East	15-17 (1)	12-14 (1) 14-17 (2) 17-18 (3) 18-19 (2) 19-20 (1)	06-07 (1) 07-09 (2) 09-11 (1) 11-13 (2) 13-15 (1) 15-17 (2) 17-20 (3) 20-22 (2) 22-02 (1)	00-02 (1) 02-07 (2) 07-08 (1) 02-06 (1)*
South Pacific & New Zealand	12-15 (1) 15-17 (2) 17-18 (1)	10-14 (1) 14-16 (2) 16-19 (3) 19-21 (2) 21-22 (1)	06-07 (1) 07-09 (3) 09-11 (2) 11-17 (1) 17-19 (2) 19-20 (3) 20-22 (4) 22-00 (3) 00-02 (2) 02-04 (1)	19-21 (1) 21-22 (2) 22-23 (3) 23-05 (4) 05-06 (3) 06-07 (2) 07-08 (1) 22-01 (1)* 01-05 (2)* 05-06 (1)*
Australasia	12-15 (1) 15-17 (1) 17-18 (1)	09-12 (1) 12-16 (2) 16-19 (3) 19-20 (2) 20-21 (1)	07-08 (1) 08-10 (3) 10-12 (2) 12-17 (1) 17-19 (2) 19-22 (3) 22-01 (2) 01-04 (1)	00-01 (1) 01-02 (2) 02-05 (3) 05-06 (2) 06-08 (1) 02-04 (1)* 04-06 (2)* 06-07 (1)*
Caribbean, Central America & Northern Countries of South America	09-11 (1) 11-12 (2) 12-14 (3) 14-15 (2) 15-16 (1)	06-07 (1) 07-09 (2) 09-12 (3) 12-15 (4) 15-16 (3) 16-17 (2) 17-18 (1)	06-07 (2) 07-09 (3) 09-14 (2) 14-16 (3) 16-19 (4) 19-21 (3) 21-23 (2) 23-06 (1)	18-20 (1) 20-01 (3) 01-03 (2) 03-06 (1) 19-21 (1)* 21-02 (2)* 02-04 (1)*
Peru, Bolivia, Paraguay, Brazil, Chile, Argentina & Uruguay	09-11 (1) 11-13 (2) 13-15 (3) 15-16 (2) 16-17 (1)	07-08 (1) 08-09 (2) 09-11 (1) 11-13 (2) 13-15 (3) 15-16 (4) 16-17 (3) 17-18 (2) 18-19 (1)	12-14 (1) 14-15 (2) 15-16 (3) 16-18 (4) 18-20 (3) 20-23 (2) 23-05 (1) 05-07 (2) 07-09 (1)	18-20 (1) 20-01 (2) 01-03 (1) 22-02 (1)*
McMurdo Sound, Antarctica	13-16 (1)	12-15 (1) 15-18 (2) 18-20 (1)	16-19 (1) 19-20 (2) 20-22 (3) 22-00 (2) 00-02 (1) 05-06 (1) 06-08 (2) 08-10 (1)	22-02 (1) 02-04 (2) 04-06 (1)

MASTER SHORT-SKIP PROPAGATION CHART
SOLAR PHASE: MODERATE
SMOOTHED SUNSPOT RANGE: 30-60
SEASON: SUMMER
TIME ZONES: LOCAL STANDARD AT PATH MID-POINT
(24-Hour Time)

Band (Meters)	*Distance Between Stations (Miles)*			
	50-250	*250-750*	*750-1300*	*1300-2300*
10	*Nil*	07-09 (0-1)* 09-13 (0-3)* 13-17 (0-1)* 17-21 (0-2)* 21-23 (0-1)*	07-09 (1)* 09-13 (3)* 13-17 (1-2)* 17-21 (2-3)* 21-07 (1)*	07-09 (1-0) 09-13 (3-1) 13-17 (2-1) 17-21 (3-1) 21-07 (1-0)
15	*Nil*	07-09 (0-2)* 09-13 (0-3)* 13-17 (0-2)* 17-19 (0-3)* 19-21 (0-2)* 21-07 (0-1)*	07-09 (2)* 09-13 (3)* 13-17 (2)* 17-19 (3)* 19-21 (2)* 21-23 (1-2)* 23-07 (1)*	07-09 (2-1) 09-13 (3-2) 13-17 (2-3) 17-19 (3) 19-21 (2) 21-23 (2-1) 23-07 (1-0)
20	09-00 (0-1)*	06-09 (0-2)* 09-15 (1-4)* 15-20 (1-3)* 20-00 (1-2)* 00-06 (0-1)*	06-09 (2-3)* 09-16 (4)* 16-21 (3-4)* 21-00 (2-3)* 00-06 (1-2)*	06-09 (3-2) 09-15 (4-2) 15-16 (4-3) 16-21 (4) 21-00 (3-2) 00-06 (2-1)
40	07-11 (1-2)* 11-16 (2-4) 16-20 (3-4) 20-22 (1-2) 22-07 (0-1)*	07-09 (2-3)* 09-11 (2) 11-16 (4-2) 16-17 (4-3) 17-20 (4) 20-22 (2-4) 22-07 (1-3)*	07-09 (3-1) 09-16 (2-1) 16-17 (3-1) 17-20 (4-3) 20-22 (4) 22-05 (3-4) 05-07 (3)	07-17 (1-0) 17-20 (3-2) 20-05 (4) 05-07 (3-1)
80	06-11 (3-4) 11-15 (4-3) 15-21 (4) 21-04 (3-4) 04-06 (3)	07-09 (4-1) 09-11 (4-0) 11-15 (3-0) 15-17 (4-1) 17-19 (4-2) 19-21 (4-3) 21-04 (1) 04-06 (3) 06-07 (4-2)	07-09 (1-0) 09-15 (0) 15-17 (1-0) 17-19 (2-1) 19-21 (3-1) 21-04 (4) 04-06 (3) 06-07 (2-1)	07-17 (0) 17-19 (1-0) 19-21 (1) 21-03 (4-3) 03-04 (4-2) 04-05 (3-2) 05-06 (3-1) 06-07 (1)

160	17-18 (1-0) 18-19 (1) 19-21 (3-2) 21-23 (4-3) 23-05 (4) 05-07 (3-2) 07-08 (1) 08-09 (1-0)	18-19 (1-0) 19-20 (2-0) 20-21 (2-1) 21-23 (3-2) 23-03 (4-2) 03-05 (4-3) 05-07 (2-1) 07-08 (1-0)	20-21 (1) 21-00 (2-1) 00-03 (2) 03-05 (3-2) 05-06 (1) 06-07 (1-0)	20-22 (1-0) 22-00 (1) 00-05 (2-1) 05-06 (1-0)

MASTER SHORT-SKIP PROPAGATION CHART
SOLAR PHASE: MODERATE
SMOOTHED SUNSPOT RANGE: 30-60
SEASON: WINTER
TIME ZONES: LOCAL STANDARD AT PATH MID-POINT
(24-Hour Time)

Band	*Distance Between Stations (Miles)*			
(Meters)	*50-250*	*250-750*	*750-1300*	*1300-2300*
10	*Nil*	*Nil*	11-16 (0-1)	09-11 (0-1) 11-15 (1-2) 15-16 (1) 16-17 (0-1)
15	*Nil*	10-12 (0-1) 12-14 (0-2) 14-16 (0-1)	08-10 (0-1) 10-11 (1-2) 11-12 (1-3) 12-14 (2-4) 14-15 (1-3) 15-16 (1-2) 16-18 (0-1)	07-09 (1) 09-11 (2-3) 11-12 (3-4) 12-14 (4) 14-15 (3) 15-16 (2-3) 16-17 (1-2) 17-18 (1) 18-19 (0-1)
20	*Nil*	07-09 (0-1) 09-11 (0-2) 11-14 (0-4) 14-15 (0-3) 15-17 (0-2) 17-20 (0-1)	07-08 (1) 08-09 (1-3) 09-11 (2-4) 11-14 (4) 14-15 (3-4) 15-17 (2-4) 17-18 (1-3) 18-20 (1-2) 20-22 (0-1)	06-07 (1) 07-08 (1-2) 08-09 (3) 09-15 (4-3) 15-17 (4) 17-18 (3) 18-20 (2-3) 20-22 (1)
40	07-08 (0-1) 08-09 (1-2) 09-16 (3-4) 16-17 (2-3) 17-18 (1-2) 18-20 (0-1)	07-08 (1-3) 08-09 (2-3) 09-16 (4-3) 16-17 (3-4) 17-18 (2-4) 18-20 (1-3) 20-02 (0-2) 02-07 (0-1)	07-09 (3) 09-14 (3-1) 14-16 (3-2) 16-18 (4) 18-20 (3-4) 20-22 (2-3) 22-02 (2) 02-04 (1-2) 04-07 (1-3)	07-08 (3-2) 08-09 (3-1) 09-14 (1-0) 14-16 (2-0) 16-17 (4-2) 17-18 (4-3) 18-20 (4) 20-22 (3-4) 22-00 (2-3) 00-02 (2) 02-04 (2-3) 04-07 (3)
80	08-18 (4) 18-19 (3-4) 19-00 (1-2) 00-07 (1-3) 07-08 (2-3)	08-09 (4-2) 09-16 (4-1) 16-18 (4-2) 18-19 (4-3) 19-00 (2-4) 00-07 (3-4) 07-08 (3)	08-09 (2-0) 09-16 (1-0) 16-18 (2-1) 18-19 (3) 19-20 (4-3) 20-04 (4) 04-06 (4-3) 06-07 (4-2) 07-08 (3-1)	08-16 (0) 16-18 (1-0) 18-20 (3-2) 20-04 (4-3) 04-06 (3-2) 06-07 (2-1) 07-08 (1)
160	07-09 (3-2) 09-11 (2-0) 11-17 (1-0) 17-19 (3-2) 19-07 (4)	07-09 (2-0) 09-17 (0) 17-19 (2-1) 19-04 (4) 04-06 (4-2) 06-07 (4-1)	07-09 (1-0) 09-17 (0) 17-19 (1-0) 19-20 (4-2) 20-21 (4-3) 21-04 (4) 04-06 (2-1) 06-07 (1-0)	06-19 (0) 19-20 (2-1) 20-21 (3-2) 21-04 (4-2) 04-06 (1)

MASTER SHORT-SKIP PROPAGATION CHART
SOLAR PHASE: MODERATE
SMOOTHED SUNSPOT RANGE: 30-60
SEASONS: SPRING & FALL
TIME ZONES: LOCAL STANDARD AT PATH MID-POINT
(24-Hour Time)

Band	*Distance Between Stations (Miles)*			
(Meters)	*50-250*	*250-750*	*750-1300*	*1300-2300*
10	*Nil*	*Nil*	08-09 (0-1) 09-12 (0-2) 12-14 (0-3) 14-16 (0-2) 16-18 (0-1)	08-09 (1-0) 09-12 (2-1) 12-14 (3-2) 14-16 (2) 16-17 (1-2) 17-18 (1) 18-20 (0-1)
15	*Nil*	08-09 (1) 09-15 (0-2) 15-17 (0-1)	07-08 (0-1) 08-09 (1) 09-10 (2) 10-15 (2-4) 15-17 (1-3) 17-18 (0-2) 18-20 (0-1)	07-08 (1-0) 08-09 (1) 09-10 (2-3) 10-15 (4) 15-17 (3) 17-18 (2-3) 18-20 (1-2) 20-21 (0-1)
20	11-13 (0-1) 13-15 (0-2) 15-16 (0-1)	07-10 (0-1) 10-11 (0-2) 11-13 (1-3) 13-15 (2-4) 15-16 (1-3) 16-18 (0-3) 18-20 (0-2) 20-07 (0-1)	06-08 (1-2) 08-10 (1-3) 10-13 (3-4) 13-15 (4) 15-18 (3-4) 18-20 (2-3) 20-22 (1-2) 22-06 (1)	06-07 (2-1) 07-08 (2) 08-10 (3) 10-15 (4-3) 15-18 (4) 18-20 (3-4) 20-22 (2-3) 22-02 (1-2) 02-06 (1)
40	06-07 (1-2) 07-09 (2-3) 09-18 (3-4) 18-19 (2-3) 19-21 (1-2) 21-00 (0-1)	06-07 (2-3) 07-09 (3-4) 09-11 (4-3) 11-13 (4-2) 13-15 (4-3) 15-18 (1) 18-19 (3-4) 19-20 (2-4) 20-21 (2-3) 21-00 (1-2) 00-06 (0-1)	06-07 (3-2) 07-08 (4-2) 08-09 (4-1) 09-11 (3-1) 11-13 (2-1) 13-15 (3-1) 15-17 (4-2) 17-19 (4-3) 19-20 (4) 20-21 (3-4) 21-00 (2-3) 00-02 (1-3) 02-06 (1-2)	06-08 (2-1) 08-15 (1-0) 15-16 (2-0) 16-17 (2-1) 17-19 (3-2) 19-21 (4-3) 21-22 (4) 22-00 (3-4) 00-02 (3) 02-05 (2-3) 05-06 (2)
80	07-08 (2-3) 08-11 (3-4) 11-18 (4-3) 18-20 (3-4) 20-22 (2-3) 22-02 (1-2) 02-05 (1) 05-07 (1-2)	07-08 (3-2) 08-11 (4-1) 11-16 (3-0) 16-18 (3-2) 18-20 (4-3) 20-22 (3-4) 22-02 (2-4) 02-05 (1-2) 05-07 (2)	07-08 (2-1) 08-11 (1-0) 11-16 (0) 16-18 (2-1) 18-20 (3-2) 20-02 (4) 02-05 (2-3) 05-07 (2)	07-08 (1-0) 08-16 (0) 16-18 (1-0) 18-20 (2-1) 20-22 (1-2) 22-02 (4-3) 02-05 (3-2) 05-07 (2-1)
160	05-07 (4-2) 07-09 (3-1) 09-17 (2-0) 17-19 (3-1) 19-20 (4-2) 20-05 (4)	05-06 (2-1) 06-07 (2-0) 07-09 (1-0) 09-17 (0) 17-19 (1-0) 19-20 (2) 20-22 (4-3) 22-03 (4) 03-05 (4-3)	05-06 (1) 06-19 (0) 19-20 (2-1) 20-22 (3-2) 22-03 (4-2) 03-05 (3-2)	05-06 (1) 06-19 (0) 19-20 (1-0) 20-22 (2-1) 22-03 (2) 03-05 (2-4)

FOOTNOTES

Worldwide Charts:
* Predicted times of 80 meter openings. Openings on 160 meters are also likely to occur during those times when 80 meter openings are shown with a forecast rating of (2) or higher.

Short Skip Charts:
* Predominately sporadic-E openings.

4.5 Master Propagation Charts—High Solar Phase Smoothed Sunspot Number Range: 60–90

Band-By-Band Summary

10 meters. ***Summer:*** Fairly good daytime DX should be possible on north-south paths, particularly into the southern hemisphere. Conditions should peak during the afternoon. Plenty of short-skip openings due to sporadic-*E* ionization should be possible between distances of approximately 500 and 1300 miles, and considerably beyond this range when intense and widespread sporadic-*E* ionization permits multi-hop propagation.

Winter: Excellent worldwide DX conditions are expected during the daytime hours. Conditions should peak before noon for openings towards Europe, Africa, and the east; during the early afternoon for openings towards the south; and during the late afternoon for openings towards the northwest and west. There also should be frequent short-skip openings from just after sunrise until shortly before sunset over distances ranging between approximately 1000 and 2300 miles.

Equinox: Some fairly good openings should be possible towards Europe and the east before noon, and towards Africa shortly after noon. Good openings also should be possible towards South America, into the South Pacific, and to other areas in the southern hemisphere during the afternoon. Expect fairly good short-skip openings during most of the day over distances of between 1000 and 2300 miles.

15 meters. ***Summer:*** Fairly good worldwide DX propagation should be possible on most days from a few hours after sunrise until sunset. Conditions should peak to most areas of the world during the afternoon. Short-skip openings should be possible during the hours of daylight over distances of 500 to 2300 miles.

Winter: Excellent DX conditions are expected to most areas of the world from shortly after sunrise until past sunset. Openings should peak towards Europe and the east before noon; towards Africa and South America during the early afternoon; and towards the Far East, the South Pacific, and areas in a westerly direction during the late afternoon and early evening. Regular short-skip openings should be possible at ranges of beyond approximately 750 miles.

Equinox: Excellent daytime DX is expected to almost all areas of the world, particularly to the southern hemisphere. Signals should peak towards Europe before noon, but to most other areas of the world during the afternoon. Excellent short-skip openings should be possible beyond a range of about 1000 miles.

20 meters. *Summer:* This band should remain open for DX around the clock. It should peak for signals from practically all directions for an hour or two after sunrise and again during early evening. Daytime short-skip openings should range between 500 and 2300 miles; nighttime, between 1000 and 2300 miles.

Winter: DX conditions should be excellent from sunrise, through the hours of daylight, and until a few hours after sunset. Openings can be expected to all areas of the world, particularly during peak periods, for an hour or two after sunrise and again during the late afternoon. Some DX openings into the southern hemisphere should also be possible during the hours of darkness. Daytime short-skip openings should be excellent over a range of between 500 and 2300 miles.

Equinox: Excellent DX conditions can be expected from sunrise, through the daylight hours, and well into the evening. It should be possible to work into all areas of the world on 20 meters, particularly during peak periods, which should occur for an hour or two after sunrise and again during the late afternoon and early evening. The band should remain open fairly regularly during the hours of darkness as well, particularly towards the southern hemisphere. The short-skip range during the daylight hours should extend out to between 500 and 2300 miles.

40 meters. *Summer:* Good DX conditions should be possible to most areas of the world from sunset, through the hours of darkness, until just after sunrise, despite seasonally high static levels. Excellent short-skip should be possible during the hours of daylight between distances of approximately 100 and 1000 miles, and during the hours of darkness to distances between 500 and 2300 miles.

Winter: This band should be an optimum band for worldwide DX during the hours of darkness and the sunrise period. The band should be open in the late afternoon towards Europe and the east, with signals peaking towards the east and south after sundown. Signals from the northwest and west should begin to build up by midnight, and reach a peak just before sunrise. Expect excellent short-skip openings between distances of 100 and 1000 miles during the day, and between 750 and 2300 miles at night.

Equinox: Expect good DX to most parts of the world, particularly into the southern hemisphere from sundown, through the hours of darkness, until just after sunrise. During the daylight hours expect excellent short-skip openings between distances of 100 and 1000 miles, and during the night, beyond 750 miles.

80 meters. *Summer:* Some DX should be possible to several areas of the world during the hours of darkness and the sunrise period, despite seasonally high static levels. Daytime skip will be limited to a range up to approximately 250 miles; nighttime skip should be possible between approximately 200 and 2300 miles.

Winter: Fairly good DX should be possible to most areas of the world during the hours of darkness and the sunrise period. Daytime short-skip openings should be possible up to about 500 miles, increasing to between approximately 500 and 2300 miles at night.

Equinox: Some fairly good worldwide DX should be possible from sunset, through the hours of darkness, until sunrise. Excellent short-skip openings should be possible during the day up to about 350 miles, increasing to between 500 and 2300 miles at night.

160 meters. *Summer:* No daytime openings are expected on this band due to high solar absorption. An occasional DX opening might be possible at night, but seasonally high static levels will severely limit openings on this band most of the time. Short-skip openings to distances of up to about 1000 miles should be possible during the hours of darkness, with openings considerably beyond this range occasionally possible.

Winter: No daylight openings are expected, but some fairly good DX should be possible to many areas of the world during the hours of darkness and the sunrise period. Signals from Europe and from the east and south should peak about midnight, while signals from the northwest and west should peak just before sunrise. Expect fairly good short-skip openings during the hours of darkness over ranges up to 1500 miles and occasionally up to 2300 miles.

Equinox: No daytime skip possible, but fairly good DX should be possible during the hours of darkness and the sunrise period to some areas of the world. Nighttime short-skip should be possible to distances of up to approximately 1200 miles, and at times up to 2300 miles.

MASTER DX PROPAGATION CHART

SOLAR PHASE: HIGH
SMOOTHED SUNSPOT RANGE: 60-90
SEASON: SUMMER
TIME ZONE: EST (24-Hour Time)
EASTERN USA TO:

Reception Area	*10 Meters*	*15 Meters*	*20 Meters*	*40/80 Meters*
Western & Central Europe & North Africa	*Nil*	07-08 (1) 08-11 (2) 11-14 (1) 14-17 (2) 17-19 (1)	08-13 (1) 13-14 (2) 14-16 (3) 16-21 (4) 21-00 (3) 00-04 (2) 04-06 (3) 06-08 (2)	19-21 (1) 21-22 (2) 22-00 (3) 00-01 (2) 01-02 (1) 21-23 (1)* 23-00 (2)* 00-01 (1)*
Northern & Eastern Europe	*Nil*	10-13 (1) 13-15 (2) 15-18 (1)	08-14 (1) 14-16 (2) 16-17 (3) 17-20 (4) 20-23 (3) 23-01 (2) 01-06 (1) 06-08 (2)	20-21 (1) 21-23 (2) 23-01 (1) 20-23 (1)*
Eastern Mediterranean & Middle East	*Nil*	10-12 (1) 12-16 (2) 16-17 (3) 17-18 (2) 18-19 (1)	11-13 (1) 13-15 (2) 15-18 (3) 18-22 (4) 22-00 (3) 00-02 (2) 02-05 (1) 05-07 (2) 07-09 (1)	19-21 (1) 21-23 (2) 23-00 (1) 21-23 (1)*
Western Africa	10-12 (1) 15-18 (1)	09-11 (1) 11-13 (2) 13-14 (3) 14-16 (4) 16-18 (3) 18-19 (2) 19-21 (1)	13-14 (1) 14-15 (2) 15-17 (3) 17-22 (4) 22-01 (3) 01-03 (2) 03-06 (1)	19-21 (1) 21-23 (2) 23-01 (1)
East & Central Africa	09-11 (1) 15-17 (1)	08-11 (1) 11-13 (2) 13-15 (3) 15-16 (4) 16-17 (3) 17-19 (2) 19-20 (1)	13-15 (1) 15-16 (2) 16-17 (3) 17-20 (4) 20-23 (3) 23-02 (2) 02-05 (1)	20-23 (1)
Southern Africa	09-12 (1)	07-09 (1) 09-10 (2) 10-12 (3) 12-13 (2) 13-14 (1)	23-00 (1) 00-02 (3) 02-04 (2) 04-07 (1) 12-13 (1) 13-15 (2) 15-17 (1)	20-21 (1) 21-23 (2) 23-01 (1) 22-00 (1)*
Central & South Asia	*Nil*	08-10 (1) 13-18 (1) 18-21 (2) 21-22 (1)	16-19 (1) 19-22 (2) 22-02 (1) 02-05 (2) 05-07 (1)	18-20 (1)
Southeast Asia	*Nil*	09-12 (1) 15-18 (1) 18-20 (2) 20-21 (1)	05-06 (1) 06-08 (2) 08-10 (1) 15-18 (1) 18-20 (2) 20-23 (1) 23-01 (2) 01-02 (1)	*Nil*
Far East	*Nil*	09-11 (1) 15-17 (1) 17-19 (2) 19-21 (1)	05-06 (1) 06-08 (3) 08-09 (2) 09-11 (1) 17-19 (1) 23-01 (1)	*Nil*
South Pacific & New Zealand	14-17 (1) 17-19 (2) 19-21 (1)	08-10 (1) 13-15 (1) 15-18 (2) 18-22 (3) 22-23 (2) 23-00 (1)	17-20 (1) 20-22 (2) 22-00 (3) 00-03 (4) 03-04 (3) 04-06 (2) 06-08 (3) 08-09 (2) 09-11 (1)	00-02 (1) 02-05 (2) 05-07 (1) 03-05 (1)*
Australasia	18-20 (1)	08-10 (1) 16-17 (1) 17-19 (2) 19-21 (3) 21-22 (2) 22-23 (1)	22-00 (1) 00-02 (2) 02-04 (3) 04-07 (2) 07-09 (3) 09-11 (2) 11-13 (1)	02-03 (1) 03-05 (2) 05-06 (1) 03-05 (1) 03-05 (1)*
Caribbean, Central America & Northern Countries of South America	10-13 (1) 13-15 (2) 15-17 (3) 17-18 (2) 18-19 (1)	07-08 (1) 08-10 (2) 10-15 (3) 15-19 (4) 19-21 (3) 21-23 (2) 23-00 (1)	05-06 (3) 06-08 (4) 08-10 (3) 10-15 (2) 15-17 (3) 17-00 (4) 00-03 (3) 03-05 (2)	20-22 (1) 22-03 (2) 03-05 (1) 22-03 (1)*
Peru, Bolivia, Paraguay, Brazil, Chile, Argentina & Uruguay	10-13 (1) 13-15 (2) 15-17 (3) 17-18 (2) 18-19 (1)	06-07 (1) 07-10 (2) 10-14 (1) 14-15 (2) 15-16 (3) 16-19 (4) 19-22 (3) 22-00 (2) 00-01 (1)	15-16 (1) 16-18 (2) 18-19 (3) 19-00 (4) 00-02 (3) 02-04 (2) 04-06 (1) 06-08 (2) 08-10 (1)	23-05 (1) 00-04 (1)*
McMurdo Sound, Antarctica	*Nil*	13-15 (1) 15-19 (2) 19-20 (1)	16-18 (1) 18-22 (2) 22-02 (3) 02-06 (2) 06-08 (1)	01-04 (1)

MASTER DX PROPAGATION CHART

SOLAR PHASE: HIGH
SMOOTHED SUNSPOT RANGE: 60-90
SEASON: SUMMER
TIME ZONES: CST & MST (24-Hour Time)
CENTRAL USA TO:

Reception Area	*10 Meters*	*15 Meters*	*20 Meters*	*40/80 Meters*
Western & Central Europe & North Africa	*Nil*	10-15 (1) 15-17 (2) 17-19 (1) 22-00 (1)	00-04 (1) 04-06 (2) 06-15 (1) 15-16 (2) 16-17 (3) 17-19 (4) 19-22 (3) 22-00 (2)	19-22 (1) 22-00 (2) 00-01 (1) 21-23 (1)*
Northern & Eastern Europe	*Nil*	08-11 (1) 11-15 (2) 15-17 (1)	01-06 (1) 06-08 (2) 08-14 (1) 14-17 (2) 17-21 (3) 21-01 (2)	19-23 (1)
Eastern Mediterranean & Middle East	*Nil*	12-14 (1) 14-17 (2) 17-19 (1)	12-15 (1) 15-17 (2) 17-21 (3) 21-23 (2) 23-00 (1) 06-08 (1)	20-23 (1)
Western Africa	09-11 (1) 15-17 (1)	09-11 (1) 11-14 (2) 14-16 (3) 16-18 (2) 18-20 (1)	13-14 (1) 14-15 (2) 15-17 (3) 17-21 (4) 21-23 (3) 23-02 (2) 02-04 (1)	19-23 (1) 22-23 (1)*
East & Central Africa	15-18 (1)	12-14 (1) 14-15 (2) 15-17 (3) 17-18 (2) 18-19 (1)	14-16 (1) 16-17 (2) 17-19 (3) 19-21 (4) 21-22 (3) 22-00 (2) 00-01 (1)	19-22 (1)
Southern Africa	09-11 (1)	23-01 (1) 07-09 (1) 09-11 (2) 11-12 (1)	22-23 (1) 23-01 (2) 01-04 (1) 10-12 (1) 12-14 (2) 14-16 (1)	20-22 (1) 22-23 (2) 23-00 (1) 22-00 (1)*
Central & South Asia	*Nil*	14-17 (1) 17-20 (2) 20-22 (1) 08-10 (1)	16-18 (1) 18-21 (2) 21-05 (1) 05-07 (2) 07-09 (1)	*Nil*
Southeast Asia	*Nil*	09-12 (1) 16-18 (1) 18-20 (2) 20-22 (1)	02-06 (1) 06-09 (2) 09-10 (1) 21-22 (1) 22-00 (2) 00-01 (1)	*Nil*
Far East	*Nil*	08-10 (1) 12-14 (1) 17-19 (1) 19-22 (2) 22-00 (1)	00-03 (1) 03-05 (2) 05-09 (3) 09-10 (2) 10-12 (1)	03-04 (1) 04-05 (2) 05-08 (1)
South Pacific & New Zealand	12-17 (1) 17-19 (2) 19-20 (1)	12-15 (1) 15-17 (2) 17-19 (3) 19-21 (4) 21-22 (3) 22-23 (2) 23-00 (1)	16-18 (1) 18-22 (2) 22-00 (4) 00-04 (3) 04-06 (2) 06-08 (4) 08-10 (2) 10-12 (1)	22-00 (1) 00-02 (2) 02-04 (3) 04-06 (2) 06-07 (1) 00-06 (1)*
Australasia	16-20 (1)	13-14 (1) 14-16 (2) 16-18 (1) 18-19 (2) 19-21 (3) 21-22 (2) 22-23 (1)	21-23 (1) 23-00 (2) 00-02 (4) 02-04 (3) 04-06 (2) 06-08 (4) 08-10 (2) 10-11 (1)	00-02 (1) 02-06 (2) 06-07 (1) 03-06 (1)*
Caribbean, Central America & Northern Countries of South America	10-12 (1) 12-14 (2) 14-16 (3) 16-17 (2) 17-18 (1)	07-08 (1) 08-10 (2) 10-15 (3) 15-18 (4) 18-19 (3) 19-20 (2) 20-22 (1)	02-04 (2) 04-06 (3) 06-08 (4) 08-10 (3) 10-15 (2) 15-17 (3) 17-22 (4) 22-02 (3)	20-22 (1) 22-03 (2) 03-05 (1) 22-04 (1) 23-02 (1)*
Peru, Bolivia, Paraguay, Brazil, Chile, Argentina & Uruguay	08-12 (1) 12-15 (2) 15-18 (3) 18-19 (2) 19-20 (1)	06-07 (1) 07-09 (2) 09-13 (1) 13-15 (2) 15-16 (3) 16-19 (4) 19-20 (3) 20-22 (2) 22-00 (1)	13-15 (1) 15-17 (2) 17-18 (3) 18-22 (4) 22-00 (3) 00-02 (2) 02-04 (1) 04-06 (2) 06-09 (1)	21-22 (1) 22-01 (2) 01-04 (1) 23-03 (1)*
McMurdo Sound, Antarctica	*Nil*	13-15 (1) 15-18 (2) 18-20 (1)	13-16 (1) 16-18 (2) 18-23 (3) 23-02 (2) 02-06 (1) 06-08 (2) 08-09 (1)	22-03 (1)

MASTER DX PROPAGATION CHART

SOLAR PHASE: HIGH
SMOOTHED SUNSPOT RANGE: 60-90
SEASON: SUMMER
TIME ZONE: PST (24-Hour Time)
WESTERN USA TO:

Reception Area	*10 Meters*	*15 Meters*	*20 Meters*	*40/80 Meters*
Western Europe & North Africa	*Nil*	07-08 (1) 08-10 (2) 10-14 (1) 14-16 (2) 16-17 (1) 20-22 (1)	23-05 (1) 05-07 (2) 07-14 (1) 14-16 (2) 16-21 (3) 21-23 (2)	19-22 (1)
Northern, Central & Eastern Europe	*Nil*	06-08 (1) 13-16 (1) 20-22 (1)	13-15 (1) 15-20 (2) 20-22 (3) 22-00 (2) 00-07 (1)	19-21 (1)

Eastern Mediterranean & Middle East	*Nil*	07-09 (1) 09-11 (2) 11-14 (1) 19-21 (1)	12-15 (1) 15-19 (2) 19-21 (3) 21-23 (2) 23-00 (1) 05-07 (1)	*Nil*
West & Central Africa	07-10 (1)	06-10 (1) 10-12 (2) 12-16 (1) 16-18 (2) 18-19 (1)	12-14 (1) 14-17 (2) 17-19 (3) 19-21 (4) 21-23 (3) 23-03 (2) 03-07 (1)	20-23 (1)
East Africa	*Nil*	08-12 (1) 12-15 (2) 15-16 (1) 19-21 (1)	14-16 (1) 16-18 (2) 18-21 (3) 21-23 (2) 23-00 (1)	*Nil*
Southern Africa	*Nil*	07-09 (1) 09-11 (2) 11-12 (1) 22-00 (1)	14-16 (1) 21-22 (1) 22-00 (2) 00-06 (1) 06-08 (2) 08-10 (1)	19-22 (1)
Central & South Asia	*Nil*	07-09 (1) 09-11 (2) 11-13 (1) 17-19 (1) 19-21 (2) 21-22 (1)	22-04 (1) 04-08 (2) 08-11 (1)	*Nil*
Southeast Asia	*Nil*	07-08 (1) 08-10 (2) 10-12 (1) 16-19 (1) 19-21 (2) 21-22 (1)	22-00 (1) 00-02 (2) 02-04 (3) 04-06 (2) 06-08 (3) 08-10 (2) 10-13 (1)	02-06 (1)
Far East	13-15 (1)	08-09 (1) 09-11 (2) 11-13 (1) 13-14 (2) 14-16 (3) 16-18 (2) 18-21 (1)	18-20 (1) 20-22 (2) 22-00 (3) 00-02 (4) 02-03 (3) 03-06 (2) 06-09 (3) 09-11 (2) 11-14 (1)	01-02 (1) 02-05 (2) 05-06 (1) 02-04 (1)*
South Pacific & New Zealand	11-13 (1) 13-18 (2) 18-19 (1)	08-10 (1) 10-11 (2) 11-13 (3) 13-15 (2) 15-17 (3) 17-19 (4) 19-20 (3) 20-21 (2) 21-22 (1)	16-18 (1) 18-20 (2) 20-01 (4) 01-05 (2) 05-07 (4) 07-10 (2) 10-12 (1)	21-22 (1) 22-00 (2) 00-05 (3) 05-06 (2) 06-07 (1) 23-01 (1)* 01-04 (2)* 04-06 (1)*
Australasia	13-16 (1) 16-19 (2) 19-21 (1)	06-08 (1) 12-14 (1) 14-17 (2) 17-19 (3) 19-21 (4) 21-22 (3) 22-00 (2) 00-02 (1)	19-21 (1) 21-23 (2) 23-04 (4) 04-06 (3) 06-08 (4) 08-09 (2) 09-12 (1)	23-01 (1) 01-03 (2) 03-05 (3) 05-06 (2) 06-07 (1) 01-06 (1)*
Caribbean, Central America & Northern Countries of South America	08-10 (1) 10-12 (2) 12-14 (1) 14-16 (2) 16-17 (1)	07-08 (1) 08-12 (2) 12-14 (3) 14-17 (4) 17-18 (3) 18-19 (2) 19-20 (1)	08-10 (2) 10-13 (1) 13-15 (2) 15-17 (3) 17-22 (4) 22-00 (3) 00-05 (2) 05-08 (3)	20-22 (1) 22-03 (2) 03-05 (1) 22-03 (1)*
Peru, Bolivia, Paraguay, Brazil, Chile, Argentina & Uruguay	08-12 (1) 12-14 (2) 14-16 (3) 16-18 (2) 18-20 (1)	05-06 (1) 06-08 (2) 08-12 (1) 12-14 (2) 14-16 (3) 16-19 (4) 19-20 (3) 20-21 (2) 21-22 (1)	13-15 (1) 15-17 (2) 17-18 (3) 18-22 (4) 22-00 (3) 00-02 (2) 02-04 (1) 04-06 (2) 06-09 (1)	21-23 (1) 23-01 (2) 01-03 (1) 23-02 (1)*
McMurdo Sound, Antarctica	*Nil*	14-16 (1) 16-20 (2) 20-21 (1)	15-17 (1) 17-18 (2) 18-00 (3) 00-03 (2) 03-06 (1)	21-04 (1)

MASTER DX PROPAGATION CHART
SOLAR PHASE: HIGH
SMOOTHED SUNSPOT RANGE: 60-90
SEASON: WINTER
TIME ZONE: EST (24-Hour Time)
EASTERN USA TO:

Reception Area	*10 Meters*	*15 Meters*	*20 Meters*	*40/80 Meters*
Western & Central Europe & North Africa	08-09 (1) 09-10 (2) 10-12 (1)	07-08 (1) 08-09 (3) 09-11 (4) 11-12 (3) 12-13 (2) 13-15 (1)	05-07 (1) 07-09 (4) 09-13 (3) 13-14 (4) 14-15 (3) 15-17 (2) 17-19 (1)	15-17 (1) 17-19 (2) 19-00 (4) 00-03 (2) 03-04 (1) 19-23 (1)* 23-01 (2)* 01-02 (1)*
Northern & Eastern Europe	08-11 (1)	07-08 (1) 08-11 (2) 11-13 (1)	05-07 (1) 07-09 (3) 09-12 (2) 12-16 (1)	16-19 (1) 19-23 (2) 23-03 (1) 19-02 (1)*
Eastern Mediterranean & Middle East	08-09 (1) 09-10 (2) 10-11 (1)	07-08 (1) 08-10 (3) 10-13 (1)	01-03 (1) 05-07 (1) 07-09 (2) 09-11 (1) 11-14 (2) 14-17 (1)	19-00 (1) 20-23 (1)*
East Africa	08-09 (1) 09-11 (2) 11-15 (1)	07-08 (1) 08-12 (2) 12-15 (3) 15-16 (2) 16-17 (1)	06-07 (1) 07-09 (2) 09-12 (1) 12-15 (2) 15-18 (3) 18-20 (2) 20-22 (1)	19-00 (1) 22-00 (1)*
West & Central Africa	08-09 (1) 09-13 (2) 13-16 (1)	07-08 (1) 08-09 (2) 09-12 (3) 12-14 (4) 14-15 (3) 15-16 (2) 16-17 (1)	01-03 (1) 06-07 (1) 07-09 (2) 09-12 (1) 12-14 (2) 14-15 (3) 15-17 (4) 17-18 (3) 18-19 (2) 19-21 (1)	18-22 (1) 22-01 (2) 01-02 (1) 00-02 (1)*
Southern Africa	08-09 (1) 09-13 (2) 13-15 (1)	07-09 (1) 09-12 (2) 12-14 (3) 14-16 (2) 16-17 (1)	05-14 (1) 14-15 (2) 15-17 (3) 17-19 (2) 19-23 (1) 23-01 (2) 01-03 (1)	18-19 (1) 19-21 (2) 21-00 (1) 19-22 (1)*
Central & South Asia	*Nil*	08-10 (1) 17-20 (1)	06-07 (1) 07-09 (2) 09-11 (1) 18-22 (1)	06-08 (1) 20-22 (1)
Southeast Asia	08-10 (1) 18-20 (1)	08-11 (1) 17-20 (1)	06-07 (1) 07-09 (2) 09-12 (1) 18-21 (1)	06-08 (1)
Far East	17-19 (1)	07-09 (1) 16-17 (1) 17-19 (2) 19-20 (1)	06-07 (1) 07-09 (2) 09-11 (1) 17-19 (1) 19-21 (2) 21-23 (1)	05-08 (1) 05-07 (1)*
South Pacific & New Zealand	12-13 (1) 13-15 (2) 15-17 (1)	11-13 (1) 13-15 (2) 15-17 (3) 17-19 (2) 19-20 (1)	05-07 (1) 07-09 (3) 09-11 (2) 11-19 (1) 19-22 (2) 22-00 (1)	01-02 (1) 02-04 (2) 04-07 (3) 07-08 (2) 08-09 (1) 04-05 (1)* 05-07 (2)* 07-08 (1)*
Australasia	09-11 (1) 16-18 (1)	08-12 (1) 15-17 (1) 17-19 (2) 19-21 (1)	06-07 (1) 07-09 (3) 09-10 (2) 10-13 (1) 13-15 (2) 15-19 (1) 19-22 (2) 22-23 (1)	04-06 (1) 06-08 (2) 08-09 (1) 05-08 (1)*
Caribbean, Central America & Northern Countries of South America	07-09 (1) 09-11 (2) 11-14 (3) 14-15 (2) 15-16 (1)	07-08 (1) 08-11 (3) 11-14 (2) 14-16 (4) 16-17 (3) 17-18 (2) 18-20 (1)	05-06 (1) 06-07 (2) 07-09 (4) 09-11 (3) 11-15 (2) 15-17 (3) 17-19 (4) 19-20 (3) 20-02 (2) 02-05 (1)	18-20 (1) 20-22 (2) 22-00 (3) 00-04 (2) 04-07 (1) 19-21 (1)* 21-02 (2)* 02-05 (1)*
Peru, Bolivia, Paraguay, Brazil, Chile, Argentina & Uruguay	08-12 (1) 12-15 (2) 15-17 (1)	07-08 (1) 08-14 (2) 14-16 (4) 16-17 (3) 17-18 (2) 18-19 (1)	01-06 (1) 06-07 (2) 07-08 (3) 08-09 (2) 09-15 (1) 15-16 (2) 16-17 (3) 17-19 (4) 19-20 (3) 20-01 (2)	19-21 (1) 21-02 (2) 02-05 (1) 21-03 (1)*
McMurdo Sound, Antarctica	08-11 (1)	08-15 (1) 15-17 (2) 17-19 (1)	06-07 (1) 07-09 (2) 09-12 (1) 15-18 (1) 18-20 (2) 20-23 (3) 23-01 (2) 01-03 (1)	22-00 (1) 00-02 (2) 02-05 (1)

MASTER DX PROPAGATION CHART
SOLAR PHASE: HIGH
SMOOTHED SUNSPOT RANGE: 60-90
SEASON: WINTER
TIME ZONES: CST & MST (24-Hour Time)
CENTRAL USA TO:

Reception Area	*10 Meters*	*15 Meters*	*20 Meters*	*40/80 Meters*
Western & Central Europe & North Africa	08-11 (1)	07-08 (1) 08-09 (2) 09-11 (3) 11-13 (2) 13-14 (1)	05-07 (1) 07-09 (3) 09-11 (2) 11-13 (3) 13-15 (2) 15-17 (1)	15-17 (1) 17-23 (2) 23-03 (1) 19-23 (1)* 23-00 (2)* 00-01 (1)*
Northern & Eastern Europe	08-10 (1)	07-09 (1) 09-10 (2) 10-12 (1)	06-07 (1) 07-09 (2) 09-11 (1) 11-12 (2) 12-14 (1)	18-01 (1) 19-00 (1)*
Eastern Mediterranean & Middle East	08-11 (1)	07-08 (1) 08-10 (2) 10-12 (1)	23-02 (1) 07-10 (1) 10-12 (2) 12-15 (1)	18-23 (1) 20-02 (1)*
East Africa	09-11 (1)	07-11 (1) 11-15 (2) 15-17 (1)	06-11 (1) 11-14 (2) 14-17 (3) 17-18 (2) 18-22 (1)	19-23 (1)
West & Central Africa	08-09 (1) 09-12 (2) 12-15 (1)	07-08 (1) 08-10 (2) 10-12 (3) 12-14 (4) 14-15 (3) 15-16 (2) 16-17 (1)	05-11 (1) 11-13 (2) 13-15 (3) 15-17 (4) 17-19 (2) 19-21 (1)	18-21 (1) 21-23 (2) 23-00 (1) 22-00 (1)*
Southern Africa	08-09 (1) 09-12 (2) 12-13 (1)	07-09 (1) 09-11 (2) 11-14 (3) 14-15 (2) 15-16 (1)	06-13 (1) 13-15 (2) 15-17 (3) 17-19 (2) 19-21 (1) 00-02 (1)	18-20 (1) 20-22 (2) 22-00 (1) 19-22 (1)*
Central & South Asia	*Nil*	08-10 (1) 19-21 (1)	06-07 (1) 07-09 (2) 09-11 (1) 19-22 (1)	06-08 (1) 19-21 (1)
Southeast Asia	08-10 (1) 18-20 (1)	08-11 (1) 16-17 (1) 17-19 (2) 19-20 (1)	06-07 (1) 07-09 (2) 09-12 (1) 17-18 (1) 18-20 (2) 20-21 (1)	06-08 (1)

Far East	16-18 (1)	07-09 (1) 14-16 (1) 16-19 (2) 19-20 (1)	06-07 (1) 07-09 (2) 09-11 (1) 15-17 (1) 17-20 (2) 20-22 (1)	03-09 (1) 04-07 (1)*
South Pacific & New Zealand	12-13 (1) 13-15 (2) 15-17 (1)	10-12 (1) 12-14 (2) 14-17 (3) 17-19 (2) 19-20 (1)	06-07 (1) 07-09 (3) 09-11 (2) 11-15 (1) 15-17 (2) 17-20 (3) 20-21 (2) 21-22 (1)	22-00 (1) 00-02 (2) 02-06 (3) 06-07 (2) 07-09 (1) 02-04 (1)* 04-06 (2)* 06-08 (1)*
Australasia	04-15 (1) 15-16 (2) 16-17 (1)	08-14 (1) 14-18 (2) 18-21 (1)	06-07 (1) 07-11 (2) 11-16 (1) 16-17 (2) 17-21 (3) 21-22 (2) 22-23 (1)	02-05 (1) 05-07 (3) 07-09 (1) 04-07 (1)*
Caribbean, Central America & Northern Countries of South America	08-10 (1) 10-13 (2) 13-14 (3) 14-15 (2) 15-16 (1)	06-07 (1) 07-08 (2) 08-12 (3) 12-16 (4) 16-17 (3) 17-18 (2) 18-19 (1)	06-07 (2) 07-11 (3) 11-14 (2) 14-16 (3) 16-18 (4) 18-20 (3) 20-22 (2) 22-00 (1) 00-02 (2) 02-06 (1)	19-21 (1) 21-23 (2) 23-01 (3) 01-03 (2) 03-06 (1) 19-21 (1)* 21-01 (2)* 01-04 (1)*
Peru, Bolivia, Paraguay, Brazil, Chile, Argentina & Uruguay	08-11 (1) 11-15 (2) 15-17 (1)	07-08 (1) 08-13 (2) 13-16 (4) 16-17 (3) 17-18 (2) 18-19 (1)	06-07 (2) 07-08 (3) 08-09 (2) 09-14 (1) 14-16 (2) 16-18 (4) 18-21 (3) 21-23 (2) 23-06 (1)	19-21 (1) 21-02 (2) 02-05 (1) 21-05 (1)*
McMurdo Sound, Antarctica	08-11 (1)	07-14 (1) 14-16 (2) 16-19 (1)	06-07 (1) 07-09 (2) 09-12 (1) 15-18 (1) 18-20 (2) 20-22 (3) 22-00 (2) 00-03 (1)	22-00 (1) 00-02 (2) 02-05 (1)

MASTER DX PROPAGATION CHART
SOLAR PHASE: HIGH
SMOOTHED SUNSPOT RANGE: 60-90
SEASON: WINTER
TIME ZONE: PST (24-Hour Time)
WESTERN USA TO:

Reception Area	*10 Meters*	*15 Meters*	*20 Meters*	*40/80 Meters*
Western & Central Europe & North Africa	07-09 (1)	06-07 (1) 07-08 (2) 08-09 (3) 09-10 (2) 10-11 (1)	05-07 (1) 07-10 (2) 10-12 (3) 12-13 (2) 13-15 (1) 00-03 (1)	17-19 (1) 19-22 (2) 22-00 (1) 19-23 (1)*
Northern & Eastern Europe	*Nil*	07-09 (1)	06-08 (1) 08-10 (2) 10-13 (1) 00-04 (1)	17-00 (1) 19-23 (1)*
Eastern Mediterranean & Middle East	*Nil*	07-09 (1)	06-07 (1) 07-09 (2) 09-13 (1)	18-21 (1)
Western Africa	08-10 (1) 10-12 (2) 12-13 (1)	06-08 (1) 08-10 (2) 10-12 (3) 12-14 (4) 14-16 (2) 16-17 (1)	05-10 (1) 10-13 (2) 13-15 (3) 15-17 (4) 17-19 (2) 19-21 (1)	18-22 (1) 19-21 (1)*
East & Central Africa	08-09 (1) 09-11 (2) 11-12 (1)	06-11 (1) 11-12 (2) 12-14 (3) 14-15 (2) 15-16 (1)	05-11 (1) 11-13 (2) 13-17 (3) 17-19 (2) 19-20 (1)	18-21 (1)
Southern Africa	08-09 (1) 09-10 (2) 10-12 (1)	06-08 (1) 08-11 (2) 11-13 (3) 13-15 (2) 15-16 (1)	07-11 (1) 11-14 (2) 14-17 (3) 17-19 (2) 19-20 (1) 00-02 (1)	18-21 (1)
Central & South Asia	*Nil*	08-10 (1) 16-17 (1) 17-19 (2) 19-20 (1)	06-07 (1) 07-09 (2) 09-11 (1) 17-19 (1) 19-20 (2) 20-21 (1)	05-07 (1) 18-20 (1)
Southeast Asia	14-15 (1) 15-17 (2) 17-18 (1)	09-11 (1) 15-16 (1) 16-17 (2) 17-18 (3) 18-19 (2) 19-20 (1)	07-09 (1) 09-11 (2) 11-13 (1) 13-15 (2) 15-18 (1) 18-20 (2) 20-21 (1)	00-02 (1) 02-07 (2) 07-08 (1) 04-06 (1)*
Far East	14-15 (1) 15-16 (2) 16-18 (1)	13-15 (1) 15-16 (2) 16-17 (3) 17-18 (2) 18-20 (1)	08-10 (1) 13-14 (1) 14-17 (3) 17-19 (2) 19-21 (1)	00-03 (1) 03-08 (2) 08-10 (1) 02-08 (1)*
South Pacific & New Zealand	12-14 (1) 14-16 (2) 16-17 (1)	09-10 (1) 10-13 (2) 13-14 (3) 14-16 (4) 16-17 (3) 17-18 (2) 18-20 (1)	07-08 (1) 08-10 (2) 10-15 (1) 15-16 (2) 16-18 (4) 18-20 (3) 20-21 (2) 21-22 (1)	20-22 (1) 22-00 (2) 00-05 (3) 05-07 (2) 07-09 (1) 00-03 (1)* 03-06 (2)* 06-08 (1)*
Australasia	14-15 (1) 15-16 (2) 16-18 (1)	08-12 (1) 12-15 (2) 15-17 (3) 17-18 (2) 18-19 (1)	07-08 (1) 08-10 (3) 10-12 (2) 12-16 (1) 16-17 (2) 17-19 (4) 19-20 (3) 20-22 (2) 22-23 (1)	01-03 (1) 03-05 (2) 05-07 (3) 07-09 (1) 03-05 (1)* 05-06 (2)* 06-08 (1)*
Caribbean, Central America & Northern Countries of South America	08-10 (1) 10-15 (2) 15-16 (1)	06-07 (1) 07-08 (2) 08-12 (3) 12-15 (4) 15-16 (3) 16-17 (2) 17-18 (1)	06-07 (2) 07-09 (3) 09-10 (2) 10-13 (1) 13-15 (2) 15-18 (4) 18-20 (3) 20-22 (2) 22-06 (1)	20-22 (1) 22-01 (2) 01-04 (1) 22-06 (1)*
Peru, Bolivia, Paraguay, Brazil, Chile, Argentina & Uruguay	08-10 (1) 10-14 (2) 14-16 (1)	07-10 (1) 10-12 (2) 12-13 (3) 13-15 (4) 15-16 (3) 16-17 (2) 17-18 (1)	05-06 (1) 06-08 (2) 08-14 (1) 14-15 (2) 15-17 (4) 17-19 (2) 19-20 (1)	20-22 (1) 22-01 (2) 01-04 (1) 22-06 (1)*
McMurdo Sound, Antarctica	08-11 (1)	07-14 (1) 14-16 (2) 16-19 (1)	06-07 (1) 07-09 (2) 09-12 (1) 16-18 (1) 18-19 (2) 19-21 (2) 21-23 (2) 23-03 (1)	21-00 (1) 00-02 (2) 02-05 (1)

MASTER DX PROPAGATION CHART
SOLAR PHASE: HIGH
SMOOTHED SUNSPOT RANGE: 60-90
SEASONS: SPRING & FALL
TIME ZONE: EST (24-Hour Time)
EASTERN USA TO:

Reception Area	*10 Meters*	*15 Meters*	*20 Meters*	*40/80 Meters*
Western & Central Europe & North Africa	09-11 (1) 11-13 (2) 13-14 (1)	07-08 (1) 08-09 (3) 09-12 (4) 12-13 (3) 13-15 (2) 15-16 (1)	04-07 (1) 07-09 (4) 09-12 (3) 12-15 (4) 15-17 (3) 17-19 (2) 19-21 (1)	17-19 (1) 19-20 (2) 20-01 (3) 01-02 (2) 02-03 (1) 19-21 (1)* 21-22 (2)* 22-23 (3)* 23-00 (2)* 00-01 (1)*
Northern & Eastern Europe	08-12 (1)	07-08 (1) 08-11 (2) 11-14 (1)	05-07 (1) 07-09 (3) 09-11 (2) 11-13 (3) 13-14 (2) 14-18 (1)	18-20 (1) 20-22 (2) 22-02 (1) 20-00 (1)*
Eastern Mediterranean & Middle East	09-13 (1)	08-09 (1) 09-11 (3) 11-13 (2) 13-15 (1)	07-09 (2) 09-12 (1) 12-14 (2) 14-16 (1) 16-18 (3) 18-22 (2) 22-23 (1) 04-07 (1)	19-20 (1) 20-22 (2) 22-23 (1) 20-22 (1)*
East Africa	10-13 (1) 13-15 (2) 15-16 (1)	07-08 (1) 08-13 (2) 13-16 (3) 16-17 (2) 17-18 (1)	06-07 (1) 07-09 (2) 09-13 (1) 13-18 (2) 18-21 (3) 21-23 (2) 23-01 (1)	19-00 (1) 21-23 (1)*
West & Central Africa	11-14 (1) 14-16 (2) 16-17 (1)	07-08 (1) 08-09 (2) 09-11 (3) 11-14 (4) 14-16 (3) 16-17 (2) 17-19 (1)	07-09 (2) 09-12 (1) 12-13 (2) 13-15 (3) 15-18 (4) 18-19 (3) 19-22 (2) 22-07 (1)	18-20 (1) 20-22 (2) 22-01 (1) 21-23 (1)*
Southern Africa	10-11 (1) 11-12 (2) 12-14 (1)	07-09 (1) 09-13 (2) 13-15 (3) 15-17 (2) 17-18 (1)	05-14 (1) 14-16 (2) 16-18 (3) 18-20 (2) 20-23 (1) 23-01 (2) 01-03 (1)	21-23 (1) 23-00 (2) 00-01 (1) 23-01 (1)*
Central & South Asia	*Nil*	07-09 (1) 18-20 (1)	07-10 (1) 19-22 (1)	05-07 (1) 19-21 (1)
Southeast Asia	*Nil*	07-09 (1) 18-20 (1)	06-07 (1) 07-09 (2) 09-10 (1) 19-21 (1)	06-08 (1) 17-20 (1)
Far East	17-19 (1)	07-09 (1) 16-17 (1) 17-19 (2) 19-21 (1)	06-07 (1) 07-09 (2) 09-11 (1) 17-20 (1) 20-22 (2) 22-00 (1)	05-08 (1) 06-07 (1)*
South Pacific & New Zealand	13-15 (1) 15-17 (2) 17-18 (1)	12-15 (1) 15-17 (2) 17-19 (3) 19-20 (2) 20-21 (1)	01-07 (1) 07-10 (2) 10-19 (1) 19-01 (2)	00-02 (1) 02-06 (3) 06-07 (2) 07-08 (1) 02-03 (1)* 03-05 (2)* 05-06 (1)*
Australasia	16-18 (1)	08-12 (1) 15-17 (1) 17-20 (2) 20-22 (1)	00-03 (2) 03-07 (1) 07-09 (3) 09-10 (2) 10-13 (1) 13-15 (2) 15-19 (1) 19-22 (2) 22-03 (3)	03-05 (1) 05-07 (2) 07-09 (1) 04-05 (1)* 05-06 (2)* 06-07 (1)*
Caribbean, Central America & Northern Countries of South America	08-10 (1) 10-12 (2) 12-15 (3) 15-16 (2) 16-18 (1)	07-08 (1) 08-11 (3) 11-14 (2) 14-15 (3) 15-17 (4) 17-19 (3) 19-20 (2) 20-21 (1)	00-03 (2) 03-06 (1) 06-07 (2) 07-09 (4) 09-11 (3) 11-15 (2) 15-17 (3) 17-22 (4) 22-00 (3)	18-19 (1) 19-20 (2) 20-03 (3) 03-05 (2) 05-07 (1) 19-21 (1)* 21-02 (2)* 02-06 (1)*
Peru, Bolivia, Paraguay, Brazil, Chile, Argentina & Uruguay	09-11 (1) 11-13 (2) 13-15 (3) 15-16 (2) 16-18 (1)	07-08 (1) 08-10 (3) 10-15 (2) 15-17 (4) 17-18 (3) 18-19 (2) 19-20 (1)	04-06 (1) 06-08 (2) 08-15 (1) 15-16 (2) 16-17 (3) 17-19 (4) 19-01 (3) 01-04 (2)	19-21 (1) 21-03 (2) 03-07 (1) 21-06 (1)*
McMurdo Sound, Antarctica	11-13 (1) 13-16 (2) 16-18 (1)	08-10 (1) 15-17 (1) 17-19 (2) 19-21 (1)	04-07 (1) 07-09 (2) 09-12 (1) 15-18 (1) 18-21 (2) 21-00 (3) 00-04 (2)	23-05 (1)

MASTER DX PROPAGATION CHART

SOLAR PHASE: HIGH
SMOOTHED SUNSPOT RANGE: 60-90
SEASONS: SPRING & FALL
TIME ZONES: CST & MST (24-Hour Time)
CENTRAL USA TO:

Reception Area	*10 Meters*	*15 Meters*	*20 Meters*	*40/80 Meters*
Western & Central Europe & North Africa	09-12 (1)	07-08 (1) 08-09 (2) 09-12 (3) 12-14 (2) 14-15 (1)	05-07 (1) 07-09 (3) 09-11 (2) 11-14 (3) 14-17 (2) 17-20 (1)	17-19 (1) 19-22 (2) 22-02 (1) 20-21 (1)* 21-22 (2)* 22-00 (1)*
Northern & Eastern Europe	08-11 (1)	07-09 (1) 09-11 (2) 11-13 (1)	06-07 (1) 07-09 (2) 09-11 (1) 11-13 (2) 13-17 (1)	19-01 (1) 20-23 (1)*
Eastern Mediter-ranean & Middle East	09-12 (1)	07-09 (1) 09-12 (2) 12-14 (1)	23-02 (1) 07-12 (1) 12-17 (2) 17-22 (1)	19-23 (1) 20-22 (1)*
East Africa	10-15 (1)	07-10 (1) 10-15 (2) 15-17 (1)	06-12 (1) 12-17 (2) 17-20 (3) 20-21 (2) 21-23 (1)	19-21 (1) 20-22 (1)*
West & Central Africa	11-13 (1) 13-15 (2) 15-16 (1)	07-08 (1) 08-10 (2) 10-12 (3) 12-14 (4) 14-15 (3) 15-16 (2) 16-18 (1)	07-12 (1) 12-13 (2) 13-15 (3) 15-17 (4) 17-20 (2) 20-00 (1)	18-19 (1) 19-21 (2) 21-00 (1) 20-22 (1)*
Southern Africa	10-13 (1)	07-09 (1) 09-13 (2) 13-14 (3) 14-16 (2) 16-17 (1)	05-14 (1) 14-16 (2) 16-18 (3) 18-19 (2) 19-21 (1) 00-02 (1)	23-00 (1) 23-00 (1)*
Central & South Asia	17-19 (1)	07-10 (1) 18-20 (1)	06-07 (1) 07-09 (2) 09-11 (1) 19-22 (1)	06-08 (1) 19-21 (1)
Southeast Asia	09-11 (1) 16-19 (1)	08-11 (1) 16-17 (1) 17-19 (2) 19-20 (1)	06-07 (1) 07-09 (2) 09-12 (1) 17-18 (1) 18-20 (2) 20-22 (1)	06-08 (1) 17-19 (1)
Far East	15-18 (1)	07-09 (1) 14-16 (1) 16-19 (2) 19-21 (1)	07-09 (2) 09-11 (1) 17-20 (1) 20-00 (2) 00-07 (1)	02-05 (1) 05-07 (2) 07-09 (1) 05-07 (1)*
South Pacific & New Zealand	12-15 (1) 15-17 (2) 17-19 (1)	10-13 (1) 13-16 (2) 16-19 (3) 19-20 (2) 20-21 (1)	06-07 (2) 07-09 (3) 09-11 (2) 11-18 (1) 18-20 (2) 20-22 (3) 22-00 (2) 00-06 (1)	22-01 (1) 01-06 (3) 06-07 (2) 07-09 (1) 00-03 (1)* 03-06 (2)* 06-07 (1)*
Australasia	15-17 (1)	09-12 (1) 12-17 (2) 17-19 (3) 19-20 (2) 20-22 (1)	07-09 (2) 09-17 (1) 17-20 (2) 20-00 (3) 00-03 (2) 03-07 (1)	02-04 (1) 04-07 (2) 07-09 (1) 04-05 (1)* 05-07 (2)* 07-08 (1)*
Caribbean, Central America & Northern Countries of South America	09-11 (1) 11-13 (2) 13-14 (3) 14-15 (2) 15-17 (1)	06-07 (1) 07-08 (2) 08-14 (3) 14-16 (4) 16-18 (3) 18-19 (2) 19-20 (1)	06-07 (2) 07-11 (3) 11-14 (2) 14-16 (3) 16-20 (4) 20-22 (3) 22-02 (2) 02-06 (1)	18-19 (1) 19-20 (2) 20-02 (3) 02-04 (2) 04-06 (1) 20-21 (1)* 21-02 (2)* 02-06 (1)*
Peru, Bolivia, Paraguay, Brazil, Chile, Argentina, & Uruguay	08-11 (1) 11-13 (2) 13-15 (3) 15-16 (2) 16-18 (1)	07-08 (1) 08-13 (2) 13-15 (3) 15-17 (4) 17-18 (3) 18-19 (2) 19-20 (1)	06-08 (2) 08-15 (1) 15-16 (2) 16-18 (4) 18-22 (3) 22-04 (2) 04-06 (1)	19-22 (1) 21-03 (2) 03-06 (1) 21-05 (1)*
McMurdo Sound, Antarctica	11-13 (1) 13-15 (2) 15-18 (1)	13-16 (1) 16-18 (2) 18-20 (1)	07-09 (2) 09-12 (1) 15-18 (1) 18-20 (2) 20-23 (3) 23-03 (2) 03-07 (1)	00-06 (1)

MASTER DX PROPAGATION CHART

SOLAR PHASE: HIGH
SMOOTHED SUNSPOT RANGE: 60-90
SEASONS: SPRING & FALL
TIME ZONE: PST (24-Hour Time)
WESTERN USA TO:

Reception Area	*10 Meters*	*15 Meters*	*20 Meters*	*40/80 Meters*
Western & Central Europe & North Africa	09-11 (1)	08-10 (1) 10-12 (2) 12-15 (1)	23-01 (1) 06-08 (1) 08-12 (2) 12-14 (3) 14-16 (2) 16-20 (1)	18-00 (1) 20-22 (1)*
Northern & Eastern Europe	*Nil*	08-12 (1)	23-01 (1) 06-07 (1) 07-09 (2) 09-13 (1)	19-23 (1) 20-22 (1)*
Eastern Mediter-ranean & East Africa	*Nil*	07-11 (1)	06-09 (1) 09-11 (2) 11-15 (1) 18-21 (1)	18-21 (1)
West & Central Africa	11-16 (1)	06-08 (1) 08-15 (2) 15-17 (3) 17-18 (2) 18-19 (1)	05-10 (1) 10-15 (2) 15-18 (3) 18-20 (2) 20-22 (1)	18-22 (1) 19-21 (1)*
Southern Africa	10-13 (1)	08-10 (1) 10-14 (2) 14-16 (1)	05-14 (1) 14-16 (2) 16-18 (3) 18-20 (1) 00-02 (1)	19-22 (1) 20-21 (1)*
Central & South Asia	17-19 (1)	07-09 (1) 16-17 (1) 17-19 (2) 19-21 (2)	06-07 (1) 07-09 (2) 09-11 (1) 17-19 (1) 19-20 (2) 20-22 (1)	05-08 (1)
Southeast Asia	16-19 (1) 09-11 (1)	08-09 (1) 09-10 (2) 10-14 (1) 14-17 (2) 17-18 (3) 18-19 (2) 19-21 (1)	07-08 (1) 08-10 (3) 10-11 (2) 11-21 (1) 21-00 (2) 00-02 (1)	00-02 (1) 02-06 (2) 06-08 (1) 02-06 (1)*
Far East	14-15 (1) 15-16 (2) 16-18 (1)	12-14 (1) 14-18 (2) 18-20 (3) 20-22 (1)	08-10 (2) 10-20 (1) 20-22 (2) 22-00 (3) 00-04 (2) 04-08 (1)	00-02 (1) 02-06 (2) 06-08 (1) 02-08 (1)*
South Pacific & New Zealand	12-15 (1) 15-17 (2) 17-19 (1)	08-12 (1) 12-16 (2) 16-17 (3) 17-18 (4) 18-20 (3) 20-21 (1)	09-10 (2) 10-12 (4) 12-16 (3) 16-19 (4) 19-20 (3) 20-00 (2) 00-09 (1)	19-20 (1) 20-22 (2) 22-06 (4) 06-08 (2) 08-09 (1) 21-23 (1)* 23-06 (2)* 06-07 (1)*
Australasia	11-15 (1) 15-17 (2) 17-18 (1)	10-12 (1) 12-17 (2) 17-19 (3) 19-20 (2) 20-21 (1)	07-08 (1) 08-10 (3) 10-12 (2) 12-17 (1) 17-18 (2) 18-20 (3) 20-22 (4) 22-00 (3) 00-02 (2) 02-04 (1)	00-03 (1) 03-05 (3) 05-07 (2) 07-08 (1) 02-03 (1) 03-05 (2) 05-07 (1)
Caribbean, Central America & Northern Countries of South America	10-12 (1) 12-14 (2) 14-16 (1)	06-07 (1) 07-08 (2) 08-14 (3) 14-16 (4) 16-17 (3) 17-18 (2) 18-19 (1)	06-07 (2) 07-09 (3) 09-10 (2) 10-14 (1) 14-16 (2) 16-18 (4) 18-22 (3) 22-00 (2) 00-06 (1)	18-20 (1) 20-00 (3) 00-03 (2) 03-05 (1) 20-21 (1)* 21-01 (2)* 01-04 (1)*
Peru, Bolivia, Paraguay, Brazil, Chile, Argentina & Uruguay	08-12 (1) 12-13 (2) 13-15 (3) 15-16 (2) 16-18 (1)	00-02 (1) 07-11 (1) 11-13 (2) 13-15 (3) 15-16 (4) 16-17 (3) 17-18 (2) 18-19 (1)	20-05 (2) 05-15 (1) 15-16 (2) 16-18 (4) 18-20 (3)	18-19 (1) 19-23 (2) 23-03 (1) 20-02 (1)*
McMurdo Sound, Antarctica	11-13 (1) 13-15 (2) 15-17 (1)	12-15 (1) 15-18 (2) 18-20 (1)	05-06 (1) 06-08 (2) 08-11 (1) 16-19 (1) 19-20 (2) 20-23 (3) 23-02 (2) 02-05 (1)	00-06 (1)

MASTER SHORT-SKIP PROPAGATION CHART

SOLAR PHASE: HIGH
SMOOTHED SUNSPOT RANGE: 60-90
SEASON: SUMMER
TIME ZONES: LOCAL STANDARD AT PATH MID-POINT (24-Hour Time)

Band	*Distance Between Stations (Miles)*			
(Meters)	*50-250*	*250-750*	*750-1300*	*1300-2300*
10	*Nil*	07-09 (0-1)* 09-13 (0-3)* 13-17 (0-1)* 17-21 (0-2)* 21-23 (0-1)*	07-09 (1)* 09-13 (3)* 13-17 (1-2)* 17-21 (2-3)* 21-07 (1)*	07-09 (1-0)* 09-13 (3-1)* 13-17 (2-1)* 17-21 (3-1)* 21-07 (1-0)*
15	*Nil*	07-09 (0-2)* 09-13 (0-3)* 13-17 (0-2)* 17-19 (0-3)* 19-21 (0-2)* 21-07 (0-1)*	07-09 (2)* 09-13 (3)* 13-17 (2)* 17-19 (3)* 19-21 (2)* 21-23 (1-2)* 23-07 (1)*	07-09 (2-1) 09-13 (3-2) 13-17 (2-3) 17-19 (3-4) 19-20 (2-3) 20-23 (2-1) 23-07 (1-0)
20	09-00 (0-1)	06-09 (0-2)* 09-15 (1-4)* 15-20 (1-3)* 20-00 (1-2)* 00-06 (0-1)*	06-09 (2-3)* 09-16 (4)* 16-21 (3-4)* 21-00 (2-3)* 00-06 (1-2)*	06-09 (3-2) 09-15 (4-2) 15-16 (4-3) 16-21 (4) 21-23 (3) 23-00 (3-2) 00-06 (2-1)
40	07-11 (1-2)* 11-16 (2-4)* 16-20 (3-4) 20-22 (1-2) 22-07 (0-2)*	07-09 (2-4)* 09-11 (2) 11-16 (4-2) 16-17 (4-3) 17-20 (4) 20-22 (2-4) 22-04 (2-4) 04-07 (2-3)	07-09 (4-1) 09-11 (2-1) 16-17 (3-1) 17-20 (4-3) 20-04 (4) 04-05 (3-4) 05-07 (3)	07-17 (1-0) 17-20 (3-2) 20-05 (4) 05-07 (3-1)
80	06-11 (3-4) 11-15 (4-3) 15-21 (4) 21-04 (3-4) 04-06 (4)	07-09 (4-1) 09-11 (4-0) 11-15 (3-0) 15-17 (4-1) 17-19 (4-2) 19-21 (4-3) 21-06 (4) 06-07 (4-2)	07-09 (1-0) 09-15 (1-0) 15-17 (1-0) 17-19 (2-1) 19-21 (3-0) 21-04 (4) 04-06 (4-3) 06-07 (2-1)	07-17 (1) 19-21 (1-0) 19-21 (1) 21-03 (4-3) 03-04 (4-2) 04-05 (3-2) 05-07 (3-1) 06-07 (1)
160	17-18 (1-0) 18-19 (1) 19-21 (3-2) 21-23 (4-3) 23-05 (4) 05-07 (3-2) 07-08 (1) 08-09 (1-0)	18-19 (1-0) 19-20 (2-0) 20-21 (2-1) 21-23 (3-2) 23-03 (4-2) 03-05 (4-3) 05-07 (2-1) 07-08 (0-1)	20-21 (1) 21-00 (2-1) 00-03 (2) 03-05 (2) 05-06 (1) 06-07 (1-0)	20-22 (1-0) 22-00 (1) 00-05 (2-1) 05-06 (1-0)

MASTER SHORT-SKIP PROPAGATION CHART

SOLAR PHASE: HIGH
SMOOTHED SUNSPOT RANGE: 60-90
SEASON: WINTER
TIME ZONES: LOCAL STANDARD AT PATH MID-POINT (24-Hour Time)

Band	*Distance Between Stations (Miles)*			
(Meters)	*50-250*	*250-750*	*750-1300*	*1300-2300*
10	*Nil*	*Nil*	09-11 (0-1) 11-15 (0-2) 15-17 (0-1)	08-09 (0-1) 09-11 (1-2) 11-15 (2) 15-17 (1-2) 17-19 (0-1)

15	*Nil*	09-18 (0-1)	07-09 (0-1) 09-11 (1-2) 11-16 (1-4) 16-18 (1-2) 18-20 (0-1)	07-09 (1) 09-11 (2-3) 11-16 (4) 16-18 (2-3) 18-20 (1-2) 20-22 (0-1)
20	11-15 (0-1)	15-09 (0-1) 09-11 (0-1) 11-13 (1-3) 13-15 (1-4) 15-17 (0-3) 17-19 (0-2) 19-21 (0-1)	05-07 (1) 07-09 (1-3) 09-11 (2-4) 11-13 (3-4) 13-15 (4) 15-17 (3-4) 17-19 (2-3) 19-21 (1-2) 21-23 (0-1)	07-09 (3-2) 09-15 (4-2) 15-17 (4) 17-19 (3-4) 19-21 (2-3) 21-23 (1-2) 23-04 (0-1)
40	07-09 (1-2) 09-17 (3-4) 17-19 (2-3) 19-21 (1)	07-09 (2-3) 09-15 (4-2) 15-17 (4-3) 17-19 (3-4) 19-21 (1-3) 21-03 (0-2) 03-07 (0-1)	07-09 (3-2) 09-15 (2-1) 15-17 (3-2) 17-19 (4) 19-21 (3-4) 21-03 (2-4) 03-07 (1-3)	07-09 (2-1) 09-15 (1-0) 15-17 (2-0) 17-19 (4-3) 19-03 (4) 03-07 (3)
80	08-21 (4) 21-01 (3-4) 01-04 (2-3) 04-7 (1-2) 07-08 (2-3)	08-09 (4-2) 09-16 (4-1) 16-18 (4-2) 18-01 (4) 01-04 (3-4) 04-07 (2-4) 07-08 (3)	08-09 (2-1) 09-16 (1-0) 16-18 (2) 18-06 (4) 06-07 (4-2) 07-08 (3-1)	08-09 (1-0) 09-16 (0) 16-18 (2-0) 18-20 (4-3) 20-04 (4) 04-06 (4-2) 06-07 (2-1) 07-08 (1)
160	09-17 (1-0) 17-19 (3-2) 19-07 (4) 07-09 (3-2)	17-19 (2-1) 19-07 (4) 07-09 (2-1)	17-19 (1-0) 19-21 (4-2) 21-04 (4) 04-06 (4-2) 06-07 (4-1) 07-09 (1-0)	19-21 (2-1) 21-04 (4-3) 04-06 (2-1) 06-07 (1-0)

MASTER SHORT-SKIP PROPAGATION CHART
SOLAR PHASE: HIGH
SMOOTHED SUNSPOT RANGE: 60-90
SEASONS: SPRING & FALL
TIME ZONES: LOCAL STANDARD AT PATH MID-POINT
(24-Hour Time)

Band	*Distance Between Stations (Miles)*			
(Meters)	*50-250*	*250-750*	*750-1300*	*1300-2300*
10	*Nil*	*Nil*	08-10 (0-1) 10-15 (1-2) 15-20 (0-1)	08-09 (1-0) 09-10 (1) 10-13 (2-1) 13-15 (2) 15-17 (1-2) 17-20 (1)
15	*Nil*	09-16 (0-1)	08-09 (0-1) 09-10 (1) 10-16 (1-3) 16-18 (0-3) 18-20 (0-1)	07-08 (0-1) 08-10 (1-2) 10-18 (3-4) 18-20 (1-3) 20-22 (0-1)
20	*Nil*	07-12 (0-2) 12-18 (0-3) 18-20 (0-2) 20-07 (0-1)	06-07 (0-2) 07-08 (2) 08-10 (2-3) 10-12 (2-4) 12-18 (3-4) 18-20 (2-3) 20-22 (1-2) 22-06 (1-2)	06-08 (2-1) 08-10 (3) 10-15 (4-3) 15-18 (4) 18-20 (3-4) 20-22 (2-3) 22-02 (1-2) 02-06 (1)
40	06-08 (1-2) 08-10 (2-4) 10-19 (3-4) 19-21 (2-3) 21-23 (1-2) 23-06 (0-1)	06-08 (2-3) 08-15 (4-3) 15-19 (4) 19-21 (3-4) 21-23 (2-3) 23-02 (1-2) 02-06 (1)	06-08 (3-2) 08-15 (3-1) 15-17 (4-2) 17-19 (4-3) 19-21 (4) 21-23 (3-4) 23-02 (2-3) 02-06 (1-2)	06-08 (2-1) 08-15 (1-0) 15-17 (2-0) 17-19 (3-2) 19-23 (4) 23-02 (3-4) 02-06 (2-3)
80	07-08 (3-4) 08-11 (4) 11-18 (4-3) 18-21 (4) 21-23 (3-4) 23-01 (2-3) 01-05 (1-2) 05-07 (2-3)	07-08 (4-2) 08-11 (4-1) 11-16 (3-0) 16-18 (4-2) 18-20 (4-3) 20-23 (4) 23-01 (3-4) 01-05 (2-3) 05-07 (3-2)	07-08 (2-1) 08-11 (1-0) 11-16 (1) 16-18 (2-1) 18-20 (3-2) 20-01 (4) 01-05 (3) 05-07 (2)	07-08 (1-0) 08-16 (0) 16-18 (1-0) 18-20 (2-1) 20-22 (4-2) 22-01 (4-3) 01-05 (3) 05-07 (2-1)
160	05-07 (4-2) 07-09 (3-1) 09-17 (2-0) 17-19 (3-1) 19-20 (4-2) 20-05 (4)	05-07 (2-1) 06-07 (2-0) 07-09 (1-0) 09-17 (1) 17-19 (1-0) 19-20 (2) 20-22 (4-3) 22-03 (4) 03-05 (4-3)	05-06 (1) 06-19 (0) 19-20 (2-1) 20-22 (3-2) 22-03 (4-3) 03-05 (3-2)	05-06 (1-0) 06-19 (0) 19-20 (1-0) 20-22 (2) 22-03 (3-2) 03-05 (2-1)

FOOTNOTES

Worldwide Charts:
* Predicted times of 80 meter openings. Openings on 160 meters are also likely to occur during those times when 80 meter openings are shown with a forecast rating of (2) or higher.

Short Skip Charts:
* Predominantly sporadic-*E* openings.

4.6 Master Propagation Charts—Very High Solar Phase Smoothed Sunspot Number Range: 90–120

Band-By-Band Summary

6 meters: During this phase, solar activity should be high enough to permit occasional F_2-layer DX openings on the amateur 6 meter band. The best time for such openings is during the afternoon hours of the spring and fall months towards South America and to other areas in the southern hemisphere. An occasional opening may also be possible during the winter months towards Europe and the east before noon, towards the south during the early afternoon, and towards the northwest and west during the late afternoon. If the 6 meter band is going to open at all, it will do so at the same time that 10 meters is peaking in the same direction.

10 meters. *Summer:* Good daytime DX should be possible on north-south paths into South America, and to many parts of Africa and the South Pacific. Conditions should peak during the afternoon. Expect plenty of short-skip openings due to sporadic-*E* ionization over a range of between 500 and 1300 miles, and considerably beyond this when sporadic-*E* ionization is intensive and widespread.

Winter: Excellent world-wide DX should be possible from shortly after sunrise to well past sunset. Conditions should peak before noon for openings towards Europe, Africa, and the east; during the early afternoon for openings towards the south; and during the late afternoon for openings towards the northwest, west, and South Pacific areas. Often signals will be exceptionally strong, even when using very low power. Exceptionally good short-skip openings should be possible from just after sunrise to an hour or so after sunset over distances ranging from between approximately 1000 and 2300 miles.

Equinox: Expect good DX openings to most areas of the world from just after sunrise until an hour or so after sunset. This should be the best season of the year for long openings into areas of the southern hemisphere. Expect the band to peak for DX during the afternoon hours. Short-skip should be possible most of the day over a range of between 1000 and 2300 miles.

15 meters. *Summer:* Good worldwide DX should be possible on this band during most of the daylight hours and into the early evening. Conditions should peak during the late afternoon. Short-skip openings should be possible during the hours of daylight and into the early evening over a range of 500 to 2300 miles.

Winter: Excellent DX is expected to all areas of the world. The band should open towards Europe and the east an hour or so after sunrise; peak towards the southwest and south during the noon and afternoon periods; and peak towards the South Pacific, Far East, and other areas in a westerly and northwesterly direction during the late afternoon and early evening. Regular short-skip should be possible beyond a range of approximately 750 miles during the daytime hours and into the early evening.

Equinox: Excellent DX conditions are expected to all areas of the world, particularly for long openings into the southern hemisphere. The band should be open for DX from an hour or so after sunrise to well after sunset. Excellent short-skip openings should be possible during most of the daylight hours beyond a range of approximately 750 miles.

20 meters. ***Summer:*** Expect good DX conditions around the clock. The band should peak in all directions just after sunrise, and again towards the east and the south during the late afternoon and evening hours. Expect a peak towards the northwest, west, and towards the South Pacific area during the hours of darkness. Excellent short-skip openings should be possible during the daylight hours over distances as short as 350 miles and as long as 2300 miles. During the hours of darkness, short-skip openings should range to distances of between 1000 and 2300 miles.

Winter: Excellent worldwide DX should be possible from just after sunrise to well into the evening hours, with the band remaining open to some areas of the world around the clock. Peak conditions should occur for several hours after sunrise and again during the late afternoon and early evening. Expect short-skip openings during the hours of darkness at ranges of from 1000 to 2300 miles.

Equinox: Excellent worldwide DX conditions can be expected, particularly for openings into the southern hemisphere. The band should open for DX shortly after sunrise and remain open well into the evening hours, and around the clock to some areas. Peak conditions should occur for several hours after sunrise and again during the late afternoon and early evening. The short-skip range during the daylight hours should extend out to distances of between 500 and 2300 miles, and to between 1300 and 2300 miles during the hours of darkness.

40 meters. ***Summer:*** Fairly good DX should be possible to most areas of the world from sunset, through the hours of darkness, to just after sunrise, despite seasonally high static levels. Excellent short-skip openings are expected during the hours of daylight up to a distance of approximately 750 miles, and again during the hours of darkness over distances of between 300 and 2300 miles.

Winter: Good worldwide DX should be possible to most areas of the world during the hours of darkness and the sunrise period. The band should open during the late afternoon towards Europe and the east, with signals peaking towards the east and the south between sunset and midnight. Signals from the northwest, west, and South Pacific should begin to build up about midnight, and reach a peak just before sunrise. Excellent short-skip openings should be possible during the daylight hours up to distances of approximately 1000 miles, and between 750 and 2300 miles during the hours of darkness.

Equinox: Fairly good DX conditions are expected from just before sunset, through the hours of darkness, to an hour or so after sunrise to most parts of the world. Check particularly for openings into the southern hemisphere, which should peak between midnight and sunrise. During the daylight hours expect excellent short-skip openings up to a range of about 1000 miles, and between 500 and 2300 miles at night.

80 meters. ***Summer:*** DX openings to some areas of the world should be possible during the hours of darkness and the sunrise period, but be prepared for seasonally high static levels and generally weak signals. Daytime skip will be limited to a range of approximately 250 miles; nighttime skip should be possible to distances of between approximately 200 and 2300 miles.

Winter: Fairly good DX should be possible to many areas of the world during the hours of darkness and the sunrise period. The band should peak towards Europe and the east, and towards the south, from an hour or so after sundown to midnight, and towards the northwest, west, and southwest between midnight and dawn. Daytime short-skip openings should be possible up to a range of about 500 miles, increasing to between approximately 500 and 2300 miles at night.

Equinox: Some DX openings should be possible from sunset, through the hours of darkness, until sunrise. Check particularly for openings into the southern hemisphere between midnight and dawn. Excellent short-skip openings should be possible during the day to ranges of up to approximately 350 miles, increasing to 2300 miles at night.

160 meters. ***Summer:*** No possibility for daytime skip due to high solar absorption and static levels. Nighttime openings to distances of up to about 1000 miles should be possible on a regular basis, with occasional openings beyond this range possible from time to time.

Winter: No daytime openings possible, but expect fair chances for DX openings during the hours of darkness and the sunrise period. Short-skip openings should be possible during the hours of darkness to ranges of up to approximately 1500 miles on a regular basis, and less frequently for distances of up to 2300 miles.

Equinox: Do not expect any daytime skip, but look for DX openings to some parts of the world during the hours of darkness and the sunrise period. Nighttime short-skip should be possible to ranges of up to approximately 1300 miles, and at times up to 2300 miles.

MASTER DX PROPAGATION CHART
SOLAR PHASE: VERY HIGH
SMOOTHED SUNSPOT RANGE: 90-120
SEASON: SUMMER
TIME ZONE: EST (24-Hour Time)
EASTERN USA TO:

Reception Area	*10 Meters*	*15 Meters*	*20 Meters*	*40/80 Meters*
Western & Central Europe & North Africa	*Nil*	07-08 (1) 08-11 (2) 11-14 (1) 14-17 (2) 17-19 (1)	08-13 (1) 13-14 (2) 14-16 (3) 16-22 (4) 22-00 (3) 00-04 (2) 04-06 (3) 06-08 (2)	19-21 (1) 21-22 (2) 22-00 (3) 00-01 (2) 01-02 (1) 21-23 (1)* 23-00 (2)* 00-01 (1)*
Northern & Eastern Europe	*Nil*	10-14 (1) 14-16 (2) 16-18 (1)	08-14 (1) 14-16 (2) 16-17 (3) 17-20 (4) 20-23 (3) 23-01 (2) 01-06 (1) 06-08 (2)	20-21 (1) 21-23 (2) 23-01 (1) 20-23 (1)*
Eastern Mediterranean & Middle East	*Nil*	10-12 (1) 12-16 (2) 16-17 (3) 17-18 (2) 18-19 (1)	11-13 (1) 13-15 (2) 15-18 (3) 18-22 (4) 22-01 (3) 01-02 (2) 02-05 (1) 05-07 (2) 07-09 (1)	19-21 (1) 21-23 (2) 23-00 (1) 21-23 (1)*
Western Africa	10-12 (1) 15-18 (1)	09-11 (1) 11-13 (2) 13-14 (3) 14-16 (4) 16-18 (3) 18-19 (2) 19-21 (1)	13-14 (1) 14-15 (2) 15-17 (3) 17-23 (4) 23-02 (3) 02-03 (2) 03-06 (1)	19-21 (1) 21-23 (2) 23-01 (1)
East & Central Africa	08-10 (1) 16-18 (1)	08-11 (1) 11-13 (2) 13-15 (3) 15-16 (4) 16-18 (3) 18-19 (2) 19-20 (1)	13-15 (1) 15-16 (2) 16-17 (3) 17-21 (4) 21-23 (3) 23-02 (2) 02-05 (1)	19-20 (1) 20-23 (2) 23-00 (1)
Southern Africa	09-12 (1)	00-02 (1) 07-09 (1) 09-10 (2) 10-12 (3) 12-13 (2) 13-14 (1)	23-00 (1) 00-02 (3) 02-04 (2) 04-07 (1) 13-14 (1) 14-16 (2) 16-18 (1)	19-20 (1) 20-22 (2) 22-01 (1) 22-00 (1)*
Central & South Asia	*Nil*	08-10 (1) 13-18 (1) 18-21 (2) 21-22 (1)	16-19 (1) 19-22 (2) 22-02 (1) 02-05 (2) 05-07 (1)	18-20 (1)
Southeast Asia	*Nil*	09-13 (1) 13-15 (2) 15-18 (1) 18-20 (2) 20-21 (1)	05-06 (1) 06-08 (2) 08-10 (1) 15-18 (1) 18-20 (2) 20-23 (1) 23-01 (2) 01-02 (1)	*Nil*
Far East	*Nil*	08-09 (1) 09-11 (2) 11-17 (1) 17-19 (2) 19-21 (1)	05-06 (1) 06-08 (3) 08-09 (2) 09-11 (1) 17-19 (1) 23-01 (1)	*Nil*
South Pacific & New Zealand	17-21 (1)	08-10 (1) 13-15 (1) 15-18 (2) 18-22 (3) 22-23 (2) 23-00 (1)	17-20 (1) 20-22 (2) 22-00 (3) 00-03 (4) 03-04 (3) 04-06 (2) 06-08 (3) 08-09 (2) 09-11 (1)	00-02 (1) 02-05 (2) 05-07 (1) 03-05 (1)*
Australasia	18-20 (1)	08-10 (1) 16-17 (1) 17-19 (2) 19-21 (3) 21-22 (2) 22-23 (1)	22-00 (1) 00-02 (2) 02-04 (3) 04-07 (2) 07-09 (3) 09-11 (2) 11-13 (1)	02-03 (1) 03-05 (2) 05-06 (1) 03-05 (1)*
Caribbean, Central America & Northern Countries of South America	10-13 (1) 13-16 (2) 16-18 (3) 18-19 (2) 19-20 (1)	07-08 (1) 08-10 (2) 10-15 (3) 15-19 (4) 19-21 (3) 21-23 (2) 23-00 (1)	05-06 (3) 06-08 (4) 08-10 (3) 10-15 (2) 15-17 (3) 17-00 (4) 00-03 (3) 03-05 (2)	18-19 (1) 19-22 (2) 22-03 (3) 03-04 (2) 04-05 (1) 19-21 (1) 21-03 (2) 03-04 (1)
Peru, Bolivia, Paraguay, Brazil, Chile, Argentina & Uruguay	10-13 (1) 13-15 (2) 15-17 (3) 17-18 (2) 18-19 (1)	06-07 (1) 07-10 (2) 10-14 (1) 14-15 (2) 15-17 (3) 17-20 (4) 20-23 (3) 23-01 (2) 01-02 (1)	15-16 (1) 16-18 (2) 18-19 (3) 19-01 (4) 01-03 (3) 03-04 (2) 04-06 (1) 06-08 (2) 08-10 (1)	20-23 (1) 23-04 (2) 04-06 (1) 00-06 (1)
McMurdo Sound, Antarctica	*Nil*	13-15 (1) 15-19 (2) 19-20 (1)	16-17 (1) 17-20 (2) 20-02 (3) 02-06 (2) 06-08 (1)	20-01 (1) 01-03 (2) 03-05 (1)

MASTER DX PROPAGATION CHART
SOLAR PHASE: VERY HIGH
SMOOTHED SUNSPOT RANGE: 90-120
SEASON: SUMMER
TIME ZONES: CST & MST (24-Hour Time)
CENTRAL USA TO:

Reception Area	*10 Meters*	*15 Meters*	*20 Meters*	*40/80 Meters*
Western & Central Europe & North Africa	*Nil*	10-15 (1) 15-17 (2) 17-19 (1) 22-00 (1)	00-04 (1) 04-06 (2) 06-15 (1) 15-16 (2) 16-18 (3) 18-20 (4) 20-22 (3) 22-00 (2)	19-22 (1) 22-00 (2) 00-01 (1) 21-23 (1)*
Northern & Eastern Europe	*Nil*	08-11 (1) 11-15 (2) 15-17 (1)	01-06 (1) 06-08 (2) 08-14 (1) 14-17 (2) 17-22 (3) 22-01 (2)	19-23 (1)
Eastern Mediterranean & Middle East	*Nil*	12-14 (1) 14-17 (2) 17-19 (1)	12-15 (1) 15-17 (2) 17-21 (3) 21-23 (2) 23-00 (1) 06-08 (1)	20-23 (1)
Western Africa	09-11 (1) 15-18 (1)	09-11 (1) 11-14 (2) 14-16 (3) 16-18 (2) 18-20 (1)	13-14 (1) 14-15 (2) 15-17 (3) 17-21 (4) 21-23 (3) 23-02 (2) 02-04 (1)	19-23 (1)
East & Central Africa	15-18 (1)	12-14 (1) 14-15 (2) 15-17 (3) 17-18 (2) 18-19 (1)	14-16 (1) 16-17 (2) 17-19 (3) 19-21 (4) 21-22 (3) 22-00 (2) 00-01 (1)	19-22 (1)
Southern Africa	08-11 (1)	23-01 (1) 07-09 (1) 09-11 (2) 11-12 (1)	22-23 (1) 23-01 (2) 01-04 (1) 10-12 (1) 12-14 (2) 14-16 (1)	20-22 (1) 22-23 (2) 23-00 (1)
Central & South Asia	*Nil*	14-17 (1) 17-20 (2) 20-22 (1) 08-10 (1)	16-18 (1) 18-21 (2) 21-05 (1) 05-07 (2) 07-09 (1)	*Nil*
Southeast Asia	*Nil*	09-10 (1) 10-13 (2) 13-18 (1) 18-21 (2) 21-23 (1)	02-06 (1) 06-09 (2) 09-10 (1) 21-22 (1) 22-00 (2) 00-01 (1)	*Nil*
Far East	*Nil*	08-10 (1) 12-14 (1) 17-19 (1) 19-22 (2) 22-00 (1)	00-03 (1) 03-05 (2) 05-09 (3) 09-10 (2) 10-12 (1)	03-04 (1) 04-05 (2) 06-08 (1)
South Pacific & New Zealand	15-21 (1)	12-15 (1) 15-17 (2) 17-19 (3) 19-21 (4) 21-22 (3) 22-23 (2) 23-00 (1)	16-18 (1) 18-22 (2) 22-01 (4) 01-04 (3) 04-06 (2) 06-08 (4) 08-10 (2) 10-12 (1)	22-00 (1) 00-02 (2) 02-04 (3) 04-06 (2) 06-07 (1) 00-06 (1)*
Australasia	16-20 (1)	13-14 (1) 14-16 (2) 16-18 (1) 18-19 (2) 19-21 (3) 21-22 (2) 22-23 (1)	21-23 (1) 23-00 (2) 00-02 (4) 02-04 (3) 04-06 (2) 06-08 (4) 08-10 (2) 10-11 (1)	00-02 (1) 02-06 (2) 06-07 (1) 03-06 (1)*
Caribbean, Central America, & Northern Countries of South America	10-12 (1) 12-14 (2) 14-16 (3) 16-17 (2) 17-18 (1)	07-08 (1) 08-10 (2) 10-15 (3) 15-18 (4) 18-19 (3) 19-20 (2) 20-22 (1)	02-04 (2) 04-06 (3) 06-08 (4) 08-10 (3) 10-15 (2) 15-17 (3) 17-22 (4) 22-02 (3)	19-20 (1) 20-22 (2) 22-03 (3) 03-04 (2) 04-05 (1) 21-00 (1)* 00-03 (2)* 03-04 (1)*
Peru, Bolivia, Paraguay, Brazil, Chile, Argentina & Uruguay	08-12 (1) 12-15 (2) 15-18 (3) 18-19 (2) 19-20 (1)	06-07 (1) 07-09 (2) 09-13 (1) 13-15 (2) 15-16 (3) 16-20 (4) 20-22 (3) 22-00 (2) 00-02 (1)	13-15 (1) 15-17 (2) 17-18 (3) 18-23 (4) 23-01 (3) 01-02 (2) 02-04 (1) 04-06 (2) 06-09 (1)	20-22 (1) 22-01 (2) 01-04 (1) 22-03 (1)*
McMurdo Sound, Antarctica	*Nil*	13-15 (1) 15-18 (2) 18-20 (1)	13-16 (1) 16-18 (2) 18-00 (3) 00-03 (2) 03-06 (1)	20-21 (1) 21-23 (2) 23-05 (1)

MASTER DX PROPAGATION CHART
SOLAR PHASE: VERY HIGH
SMOOTHED SUNSPOT RANGE: 90-120
SEASON: SUMMER
TIME ZONE: PST (24-Hour Time)
WESTERN USA TO:

Reception Area	*10 Meters*	*15 Meters*	*20 Meters*	*40/80 Meters*
Western Europe & North Africa	*Nil*	07-08 (1) 08-10 (2) 10-14 (1) 14-16 (2) 16-17 (1) 20-22 (1)	23-05 (1) 05-07 (2) 07-14 (1) 14-16 (2) 16-21 (3) 21-23 (2)	19-22 (1)
Northern, Central & Eastern Europe	*Nil*	06-08 (1) 13-16 (1) 20-22 (1)	13-15 (1) 15-20 (2) 20-23 (3) 23-00 (2) 00-07 (1)	19-21 (1)
Eastern Mediter-ranean & Middle East	*Nil*	06-08 (1) 12-19 (1) 19-21 (2) 21-22 (1)	12-15 (1) 15-19 (2) 19-21 (3) 21-23 (2) 23-00 (1) 05-07 (1)	*Nil*
West & Central Africa	07-10 (1)	06-10 (1) 10-12 (2) 12-16 (1) 16-18 (2) 18-19 (1)	12-14 (1) 14-17 (2) 17-19 (3) 19-21 (4) 21-23 (3) 23-03 (2) 03-07 (1)	20-23 (1)
East Africa	*Nil*	08-12 (1) 12-15 (2) 15-16 (1) 19-21 (1)	14-16 (1) 16-18 (2) 18-21 (3) 21-23 (2) 23-00 (1)	*Nil*
Southern Africa	*Nil*	07-09 (1) 09-11 (2) 11-12 (1) 22-00 (1)	14-16 (1) 21-22 (1) 22-00 (2) 00-06 (1) 06-08 (2) 08-10 (1)	19-22 (1)
Central & South Asia	*Nil*	07-09 (1) 09-11 (2) 11-13 (1) 17-19 (1) 19-21 (2) 21-22 (1)	22-04 (1) 04-08 (2) 08-11 (1)	*Nil*
Southeast Asia	*Nil*	07-08 (1) 08-10 (3) 10-12 (2) 12-15 (1) 18-20 (1) 20-22 (2) 22-00 (1)	22-00 (1) 00-02 (2) 02-04 (3) 04-06 (2) 06-08 (3) 08-10 (2) 10-13 (1)	02-06 (1)
Far East	13-15 (1)	08-09 (1) 09-11 (2) 11-13 (1) 13-14 (2) 14-16 (3) 16-18 (2) 18-21 (1)	18-20 (1) 20-22 (2) 22-00 (3) 00-02 (4) 02-04 (3) 04-06 (2) 06-09 (3) 09-11 (2) 11-14 (1)	01-02 (1) 02-05 (2) 05-06 (1) 02-04 (1)
South Pacific & New Zealand	11-13 (1) 13-18 (2) 18-19 (1)	08-10 (1) 10-11 (2) 11-13 (3) 13-15 (2) 15-17 (3) 17-20 (4) 20-21 (3) 21-22 (2) 22-00 (1)	16-18 (1) 18-20 (2) 20-01 (4) 01-05 (2) 05-07 (4) 07-10 (2) 10-12 (1)	21-22 (1) 22-00 (2) 00-05 (3) 05-06 (2) 06-07 (1) 23-01 (1)* 01-04 (2)* 04-06 (1)*
Australasia	13-16 (1) 16-19 (2) 19-20 (1)	06-08 (1) 12-14 (1) 14-17 (2) 17-19 (3) 19-21 (4) 21-22 (3) 22-00 (2) 00-02 (1)	19-21 (1) 21-23 (2) 23-04 (4) 04-06 (3) 06-08 (4) 08-09 (2) 09-12 (1)	23-01 (1) 01-03 (2) 03-05 (3) 05-06 (2) 06-07 (1) 01-06 (1)*
Caribbean, Central America & Northern Countries of South America	08-10 (1) 10-12 (2) 12-14 (1) 14-16 (2) 16-17 (1)	07-08 (1) 08-12 (2) 12-14 (3) 14-17 (4) 17-18 (3) 18-20 (2) 20-22 (1)	08-10 (2) 10-13 (1) 13-15 (2) 15-17 (3) 17-23 (4) 23-02 (3) 02-05 (2) 05-08 (3)	19-20 (1) 20-23 (2) 23-02 (3) 02-04 (2) 04-05 (1) 20-00 (1)* 00-02 (2)* 02-03 (1)*
Peru, Bolivia, Paraguay, Brazil, Chile, Argentina & Uruguay	08-12 (1) 12-14 (2) 14-16 (3) 16-18 (2) 18-20 (1)	05-06 (1) 06-08 (2) 08-12 (1) 12-14 (2) 14-16 (3) 16-20 (4) 20-22 (3) 22-23 (2) 23-00 (1)	13-15 (1) 15-17 (2) 17-18 (3) 18-23 (4) 23-00 (3) 00-02 (2) 02-04 (1) 04-06 (2) 06-09 (1)	20-22 (1) 22-01 (2) 01-04 (1) 21-02 (1)*
McMurdo Sound, Antarctica	16-18 (1)	14-16 (1) 16-20 (2) 20-21 (1)	15-17 (1) 17-18 (2) 18-00 (3) 00-03 (2) 03-06 (1)	20-21 (1) 21-23 (2) 23-03 (1) 03-05 (2) 05-06 (1)

MASTER DX PROPAGATION CHART
SOLAR PHASE: VERY HIGH
SMOOTHED SUNSPOT RANGE: 90-120
SEASON: WINTER
TIME ZONE: EST (24-Hour Time)
EASTERN USA TO:

Reception Area	*10 Meters*	*15 Meters*	*20 Meters*	*40/80 Meters*
Western & Central Europe & North Africa	07-08 (1) 08-09 (2) 09-11 (4) 11-12 (3) 12-13 (2) 13-14 (1)	06-07 (1) 07-08 (2) 08-09 (3) 09-12 (4) 12-13 (3) 13-14 (2) 14-15 (1)	23-01 (2) 01-05 (1) 05-07 (2) 07-09 (3) 09-11 (2) 11-12 (3) 12-15 (4) 15-16 (3) 16-19 (2) 19-23 (1)	14-16 (1) 16-17 (2) 17-19 (3) 19-02 (4) 02-03 (3) 03-04 (2) 04-05 (1) 17-19 (1)* 19-20 (2)* 20-02 (3)* 02-03 (2)* 03-01 (1)*
Northern & Eastern Europe	07-08 (1) 08-10 (2) 10-12 (1)	06-07 (1) 07-08 (2) 08-10 (3) 10-12 (2) 12-13 (1)	23-02 (1) 02-04 (2) 04-06 (1) 06-07 (2) 07-11 (3) 11-13 (2) 13-14 (1)	16-19 (1) 19-23 (2) 23-03 (1) 19-02 (1)*
Eastern Mediter-ranean & Middle East	07-08 (1) 08-10 (2) 10-12 (1)	07-08 (1) 08-09 (2) 09-11 (4) 11-12 (3) 12-13 (2) 13-14 (1)	06-08 (2) 08-10 (1) 10-13 (2) 13-16 (3) 16-21 (2) 21-23 (1) 23-02 (2) 02-06 (1)	18-20 (1) 20-22 (2) 22-00 (1) 20-23 (1)*
West & Central Africa	07-08 (1) 08-10 (2) 10-11 (3) 11-14 (4) 14-15 (3) 15-16 (2) 16-17 (1)	06-07 (1) 07-11 (2) 11-13 (3) 13-16 (4) 16-17 (3) 17-18 (2) 18-19 (1)	01-06 (1) 06-08 (2) 08-13 (1) 13-15 (2) 15-16 (3) 16-18 (4) 18-21 (3) 21-01 (2)	18-22 (1) 22-02 (2) 02-03 (1) 00-03 (1)*
East Africa	08-10 (1) 10-12 (2) 12-15 (3) 15-16 (2) 16-17 (1)	06-10 (1) 10-12 (2) 12-14 (3) 14-16 (4) 16-17 (3) 17-18 (2) 18-19 (1)	07-13 (1) 13-15 (2) 15-16 (3) 16-18 (4) 18-20 (3) 20-23 (2) 23-01 (1)	18-00 (1)
Southern Africa	07-08 (1) 08-10 (2) 10-12 (4) 12-13 (3) 13-14 (2) 14-15 (1)	07-09 (1) 09-11 (2) 11-12 (3) 12-15 (4) 15-17 (2) 17-18 (1)	12-14 (1) 14-15 (2) 15-18 (4) 18-20 (3) 20-01 (2) 01-03 (1)	18-19 (1) 19-21 (2) 21-00 (1) 19-22 (1)*
Central & South Asia	08-10 (1) 17-19 (1)	07-08 (1) 08-10 (2) 10-11 (1) 17-19 (1)	06-07 (1) 07-09 (2) 09-12 (1) 18-20 (1) 20-23 (2) 23-01 (1)	06-08 (1) 20-22 (1)
Southeast Asia	09-10 (1) 10-11 (2) 11-13 (1) 18-20 (1)	09-10 (1) 10-12 (2) 12-14 (1) 17-18 (1) 18-20 (2) 20-21 (1)	06-07 (1) 07-09 (2) 09-11 (1) 17-19 (1) 19-22 (2) 22-03 (1)	05-07 (1)
Far East	17-18 (1) 18-19 (2) 19-20 (1)	16-17 (1) 17-18 (2) 18-20 (3) 20-21 (2) 21-22 (1)	16-18 (1) 18-20 (2) 20-22 (3) 22-00 (2) 00-02 (1) 02-04 (2) 04-07 (1) 07-09 (2) 09-11 (1)	05-08 (1) 05-07 (1)*
South Pacific & New Zealand	12-14 (1) 14-17 (2) 17-19 (3) 19-20 (2) 20-21 (1)	08-10 (1) 10-13 (2) 13-16 (1) 16-18 (2) 18-20 (3) 20-21 (2) 21-22 (1)	12-19 (1) 19-22 (2) 22-00 (3) 00-02 (2) 02-04 (3) 04-06 (1) 06-07 (2) 07-09 (1) 09-12 (2)	01-02 (1) 02-04 (2) 04-07 (3) 07-08 (2) 08-09 (1) 04-05 (1)* 05-07 (2)* 07-08 (1)*
Australasia	09-10 (1) 10-11 (2) 11-12 (1) 15-17 (1) 17-19 (2) 19-20 (1)	08-10 (1) 10-12 (2) 12-16 (1) 16-18 (2) 18-20 (3) 20-21 (2) 21-22 (1)	07-10 (3) 10-12 (2) 12-15 (1) 15-17 (2) 17-20 (1) 20-22 (2) 22-02 (1) 02-04 (2) 04-07 (1)	03-05 (1) 05-07 (2) 07-09 (1) 05-08 (1)*
Caribbean, Central America & Northern Countries of South America	07-08 (1) 08-09 (3) 09-12 (4) 12-14 (3) 14-16 (4) 16-17 (3) 17-18 (2) 18-19 (1)	06-07 (1) 07-08 (3) 08-10 (4) 10-13 (3) 13-17 (4) 17-19 (3) 19-20 (2) 20-21 (1)	07-09 (4) 09-11 (3) 11-16 (2) 16-17 (3) 17-21 (4) 21-00 (3) 00-03 (2) 03-05 (1) 05-07 (2)	17-18 (1) 18-19 (2) 19-21 (3) 21-04 (1) 04-05 (3) 05-06 (2) 06-07 (1) 19-20 (1)* 20-22 (2)* 22-02 (3)* 02-04 (2)* 04-06 (1)*
Peru, Bolivia, Paraguay, Brazil, Chile, Argentina & Uruguay	07-08 (1) 08-11 (2) 11-14 (3) 14-16 (4) 16-17 (2) 17-19 (1)	06-07 (1) 07-09 (2) 09-12 (1) 12-14 (2) 14-16 (3) 16-18 (4) 18-19 (3) 19-20 (2) 20-21 (1)	13-14 (1) 14-15 (2) 15-17 (3) 17-21 (4) 21-02 (3) 02-04 (2) 04-06 (1) 06-08 (2) 08-09 (1)	19-21 (1) 21-02 (2) 02-05 (1) 21-03 (1)*
McMurdo Sound, Antartctica	*Nil*	06-09 (1) 16-18 (1) 18-20 (2) 20-21 (1)	18-19 (1) 19-20 (2) 20-00 (3) 00-02 (2) 02-04 (3) 04-06 (1) 06-08 (2) 08-09 (1)	00-05 (1)

MASTER DX PROPAGATION CHART
SOLAR PHASE: VERY HIGH
SMOOTHED SUNSPOT RANGE: 90-120
SEASON: WINTER
TIME ZONES: CST & MST (24-Hour Time)
CENTRAL USA TO:

Reception Area	*10 Meters*	*15 Meters*	*20 Meters*	*40/80 Meters*
Western Europe & North Africa	07-08 (1) 08-09 (2) 09-10 (3) 10-11 (2) 11-12 (1)	06-07 (1) 07-08 (2) 08-10 (3) 10-12 (4) 12-13 (3) 13-14 (2) 14-15 (1)	02-06 (1) 06-07 (2) 07-09 (3) 09-11 (2) 11-13 (3) 13-16 (2) 16-19 (1) 19-22 (2) 22-00 (1) 00-02 (2)	15-17 (1) 17-18 (2) 18-01 (3) 01-02 (2) 02-03 (1) 17-20 (1)* 20-01 (2)* 01-02 (1)*
Northern, Central & Eastern Europe	08-09 (1) 09-10 (2) 10-11 (1)	06-07 (1) 07-10 (2) 10-12 (1)	22-00 (1) 00-02 (2) 02-06 (1) 06-08 (2) 08-11 (3) 11-12 (2) 12-14 (1)	17-19 (1) 19-22 (2) 22-01 (1) 19-00 (1)*

Eastern Mediterranean & Middle East	08-09 (1) 09-10 (2) 10-11 (1)	07-08 (1) 08-11 (2) 11-12 (1)	04-06 (2) 06-10 (1) 10-12 (2) 12-14 (3) 14-18 (2) 18-22 (1) 22-02 (2) 02-04 (1)	18-20 (1) 20-22 (2) 22-23 (1) 20-22 (1)*
West & Central Africa	07-08 (1) 08-10 (2) 10-12 (3) 12-14 (4) 14-15 (3) 15-16 (2) 16-17 (1)	06-09 (1) 09-11 (2) 11-14 (3) 14-16 (4) 16-17 (3) 17-18 (2) 18-19 (1)	06-13 (1) 13-15 (2) 15-16 (3) 16-18 (4) 18-20 (3) 20-22 (2) 22-01 (1)	18-21 (1) 21-23 (2) 23-01 (1)
East Africa	08-09 (1) 09-12 (2) 12-14 (3) 14-15 (2) 15-16 (1)	08-10 (1) 10-13 (2) 13-15 (3) 15-17 (2) 17-18 (1)	11-14 (1) 14-16 (2) 16-19 (3) 19-22 (2) 22-00 (1)	19-00 (1)
Southern Africa	08-09 (1) 09-10 (2) 10-12 (3) 12-13 (2) 13-14 (1)	07-10 (1) 10-11 (2) 11-12 (3) 12-14 (4) 14-15 (3) 15-17 (2) 17-18 (1)	07-13 (1) 13-15 (2) 15-16 (3) 16-18 (4) 18-20 (3) 20-21 (2) 21-00 (1)	18-19 (1) 19-21 (1) 21-22 (1)
Central & South Asia	08-10 (1) 18-20 (1)	07-09 (1) 18-19 (1) 19-20 (2) 20-21 (1)	06-07 (1) 07-09 (2) 09-11 (1) 17-19 (1) 19-22 (2) 22-00 (1)	06-08 (1) 19-21 (1)
Southeast Asia	09-10 (1) 10-12 (2) 12-13 (1) 16-17 (1) 17-19 (2) 19-20 (1)	09-10 (1) 10-12 (2) 12-14 (1) 16-18 (1) 18-20 (2) 20-21 (1)	07-08 (1) 08-09 (2) 09-11 (3) 11-13 (2) 13-18 (1) 18-20 (2) 20-21 (1)	04-07 (1)
Far East	16-17 (1) 17-19 (2) 19-20 (1)	15-16 (1) 16-17 (2) 17-19 (3) 19-20 (2) 20-21 (1)	15-17 (1) 17-18 (2) 18-20 (3) 20-23 (2) 23-01 (1) 01-03 (2) 03-07 (1) 07-09 (2) 09-11 (1)	02-08 (1) 04-07 (1)*
South Pacific & New Zealand	10-14 (1) 14-16 (2) 16-18 (3) 18-19 (2) 19-20 (1)	08-09 (1) 09-11 (2) 11-13 (3) 13-14 (2) 14-16 (1) 16-17 (2) 17-19 (3) 19-20 (2) 20-21 (1)	06-07 (2) 07-09 (3) 09-12 (2) 12-18 (1) 18-20 (2) 20-00 (3) 00-03 (4) 03-04 (3) 04-05 (2) 05-06 (1)	23-01 (1) 01-02 (2) 02-06 (3) 06-07 (2) 07-08 (1) 03-07 (1)*
Australasia	08-09 (1) 09-11 (2) 11-12 (1) 15-17 (1) 17-19 (2) 19-20 (1)	08-09 (1) 09-10 (2) 10-12 (3) 12-14 (2) 14-15 (3) 15-17 (4) 17-19 (3) 19-20 (2) 20-21 (1)	05-07 (1) 07-08 (2) 08-10 (3) 10-12 (2) 12-15 (1) 15-17 (2) 17-20 (1) 20-22 (2) 22-03 (1) 03-05 (2)	02-04 (1) 04-07 (2) 07-09 (1) 03-06 (1)*
Caribbean, Central America & Northern Countries of South America	07-08 (1) 08-09 (3) 09-11 (4) 11-13 (3) 13-15 (4) 15-16 (2) 16-17 (1)	06-07 (1) 07-08 (2) 08-12 (3) 12-17 (4) 17-18 (3) 18-19 (2) 19-20 (1)	06-07 (2) 07-11 (3) 11-15 (2) 15-17 (3) 17-20 (4) 20-22 (3) 22-00 (2) 00-02 (3) 02-04 (2) 04-06 (1)	17-18 (1) 18-19 (2) 19-00 (3) 00-04 (4) 04-05 (3) 05-06 (2) 06-07 (1) 19-20 (1)* 20-22 (2)* 22-01 (3)* 01-02 (2)* 02-04 (1)*
Peru, Bolivia, Paraguay, Brazil, Chile, Argentina & Uruguay	07-08 (1) 08-11 (2) 11-14 (3) 14-16 (4) 16-17 (2) 17-18 (1)	06-07 (1) 07-09 (2) 09-12 (1) 12-14 (2) 14-15 (3) 15-17 (4) 17-18 (3) 18-19 (2) 19-20 (1)	04-06 (1) 06-08 (2) 08-14 (1) 14-15 (2) 15-17 (3) 17-20 (4) 20-02 (3) 02-04 (2)	19-21 (1) 21-02 (2) 02-05 (1) 21-04 (1)*
McMurdo Sound, Antarctica	*Nil*	07-09 (1) 16-18 (1) 18-20 (2) 20-21 (1)	17-19 (1) 19-22 (2) 22-00 (3) 00-02 (2) 02-04 (3) 04-05 (2) 05-06 (1)	22-05 (1)

MASTER DX PROPAGATION CHART
SOLAR PHASE: VERY HIGH
SMOOTHED SUNSPOT RANGE: 90-120
SEASON: WINTER
TIME ZONE: PST (24-Hour Time)
WESTERN USA TO:

Reception Area	*10 Meters*	*15 Meters*	*20 Meters*	*40/80 Meters*
Western Europe & North Africa	07-08 (1) 08-10 (2) 10-11 (1)	07-08 (1) 08-09 (2) 09-10 (3) 10-11 (2) 11-12 (1)	22-00 (1) 00-03 (2) 03-06 (1) 06-09 (2) 09-11 (3) 11-14 (2) 14-16 (1)	18-21 (1) 21-00 (2) 00-01 (1) 19-23 (1)*
Northern, Central & Eastern Europe	07-09 (1)	06-07 (1) 07-09 (2) 09-10 (1)	16-18 (1) 22-00 (1) 00-02 (2) 02-06 (1) 06-07 (2) 07-09 (3) 09-11 (2) 11-13 (1)	17-22 (1) 22-00 (2) 00-01 (1) 19-23 (1)*
Eastern Mediterranean & Middle East	07-09 (1)	07-08 (1) 08-10 (2) 10-11 (1)	22-00 (1) 00-03 (2) 03-07 (1) 07-10 (2) 10-14 (1) 14-16 (2) 16-18 (1)	18-21 (1)
West & Central Africa	08-09 (1) 09-11 (2) 11-14 (4) 14-15 (3) 15-16 (2) 16-17 (1)	06-08 (1) 08-11 (2) 11-12 (3) 12-15 (4) 15-16 (3) 16-17 (2) 17-18 (1)	05-10 (1) 10-13 (2) 13-15 (3) 15-17 (4) 17-18 (3) 18-19 (2) 19-21 (1) 00-03 (2)	18-22 (1)
East Africa	09-10 (1) 10-12 (2) 12-14 (1)	08-10 (1) 10-12 (2) 12-15 (3) 15-16 (2) 16-17 (1)	08-13 (1) 13-15 (2) 15-17 (3) 17-19 (2) 19-20 (1)	18-20 (1)
Southern Africa	08-10 (1) 10-12 (2) 12-14 (1)	07-09 (1) 09-12 (2) 12-15 (3) 15-16 (2) 16-17 (1)	07-12 (1) 12-14 (2) 14-15 (3) 15-17 (4) 17-19 (3) 19-20 (2) 20-21 (1) 00-02 (1)	18-20 (1)
Central & South Asia	17-19 (1)	07-10 (1) 16-17 (1) 17-19 (2) 19-20 (1)	06-07 (1) 07-09 (2) 09-11 (1) 16-18 (1) 18-20 (2) 20-22 (1)	05-07 (1) 17-20 (1)
Southeast Asia	09-11 (1) 14-15 (1) 15-17 (3) 17-18 (2) 18-19 (1)	08-09 (1) 09-11 (2) 11-13 (1) 13-15 (2) 15-18 (3) 18-19 (2) 19-21 (1)	07-08 (1) 08-09 (2) 09-11 (3) 11-13 (2) 13-14 (1) 18-19 (1) 19-21 (2) 21-22 (1)	03-08 (1) 04-06 (1)*
Far East	14-15 (1) 15-16 (2) 16-17 (4) 17-18 (3) 18-19 (2) 19-20 (1)	13-14 (1) 14-16 (3) 16-18 (4) 18-19 (3) 19-20 (2) 20-21 (1)	02-04 (1) 07-08 (1) 08-11 (2) 11-13 (1) 13-15 (2) 15-16 (3) 16-18 (4) 18-20 (3) 20-21 (2) 21-22 (1)	00-01 (1) 01-03 (2) 03-06 (3) 06-08 (2) 08-10 (1) 02-08 (1)*
South Pacific & New Zealand	10-12 (1) 12-14 (2) 14-16 (3) 16-17 (2) 17-19 (1)	07-08 (1) 08-09 (2) 09-11 (3) 11-15 (2) 15-17 (3) 17-19 (4) 19-20 (3) 20-21 (2) 21-22 (1)	02-06 (1) 06-07 (2) 07-09 (3) 09-11 (2) 11-17 (1) 17-18 (2) 18-20 (3) 20-23 (4) 23-00 (3) 00-02 (2)	22-00 (1) 00-03 (2) 03-06 (3) 06-07 (2) 07-08 (1) 00-06 (1)*
Australasia	10-13 (1) 13-15 (2) 15-17 (3) 17-19 (2) 19-20 (1)	08-09 (1) 09-12 (3) 12-15 (2) 15-17 (1) 17-18 (2) 18-20 (3) 20-21 (2) 21-22 (1)	18-20 (1) 20-22 (2) 22-02 (1) 02-05 (2) 05-06 (1) 06-08 (2) 08-10 (4) 10-12 (2) 12-14 (1)	01-03 (1) 03-06 (2) 06-08 (1) 01-03 (1)*
Caribbean, Central America & Northern Countries of South America	07-08 (1) 08-09 (2) 09-10 (3) 10-14 (4) 14-15 (3) 15-16 (2) 16-17 (1)	06-07 (1) 07-08 (2) 08-13 (3) 13-16 (4) 16-17 (3) 17-18 (2) 18-19 (1)	06-07 (2) 07-09 (4) 09-13 (2) 13-15 (3) 15-19 (4) 19-20 (3) 20-00 (2) 00-06 (1)	17-18 (1) 18-19 (2) 19-23 (3) 23-03 (4) 03-04 (2) 04-05 (1) 19-20 (1)* 20-22 (2)* 22-00 (3)* 00-02 (2)* 02-04 (1)*
Peru, Bolivia, Paraguay, Brazil, Chile,	07-08 (1) 08-11 (2) 11-13 (3) 13-15 (4) 15-16 (3) 16-17 (2) 17-18 (1)	06-07 (1) 07-09 (2) 09-13 (3) 13-14 (2) 14-15 (3) 15-17 (4) 17-18 (3) 18-19 (2) 19-20 (1)	12-14 (1) 14-16 (2) 16-17 (3) 17-19 (4) 19-22 (3) 22-00 (2) 00-02 (3) 02-03 (2) 03-04 (1) 06-08 (1)	20-22 (1) 22-01 (2) 01-04 (1) 22-02 (1)*
McMurdo Sound, Antarctica	*Nil*	06-09 (1) 14-16 (1) 16-19 (2) 19-21 (1)	16-18 (1) 18-20 (2) 20-00 (3) 00-04 (2) 04-06 (1) 06-08 (2) 08-10 (1)	23-05 (1)

MASTER DX PROPAGATION CHART
SOLAR PHASE: VERY HIGH
SMOOTHED SUNSPOT RANGE: 90-120
SEASONS: SPRING & FALL
TIME ZONE: EST (24-Hour Time)
EASTERN USA TO:

Reception Area	*10 Meters*	*15 Meters*	*20 Meters*	*40/80 Meters*
Western & Central Europe & North Africa	08-09 (1) 09-10 (2) 10-12 (3) 12-13 (2) 13-15 (1)	06-07 (1) 07-08 (2) 08-11 (3) 11-14 (4) 14-15 (3) 15-16 (2) 16-17 (1)	03-06 (2) 06-09 (3) 09-12 (2) 12-13 (3) 13-16 (4) 16-19 (3) 19-22 (2) 22-03 (1)	17-18 (1) 18-19 (2) 19-01 (3) 00-03 (2) 03-04 (1) 19-21 (1)* 21-00 (2)* 00-02 (1)*
Northern & Eastern Europe	08-09 (1) 09-11 (2) 11-13 (1)	06-08 (1) 08-09 (2) 09-12 (3) 12-13 (2) 13-14 (1)	08-13 (1) 13-15 (2) 15-18 (3) 18-23 (2) 23-04 (3) 04-08 (2)	18-20 (1) 20-22 (2) 22-02 (1) 20-00 (1)*
Eastern Mediterranean & Middle East	08-09 (1) 09-12 (2) 12-13 (1)	07-09 (1) 09-10 (2) 10-11 (3) 11-13 (4) 13-15 (2) 15-16 (1)	05-07 (2) 07-14 (1) 14-18 (2) 18-20 (3) 20-22 (2) 22-00 (4) 00-02 (2) 02-05 (1)	19-20 (1) 20-22 (2) 22-23 (1) 20-22 (1)*
Western Africa	07-08 (1) 08-11 (3) 11-15 (4) 15-17 (3) 17-18 (2) 18-19 (1)	05-06 (1) 06-07 (2) 07-13 (3) 13-17 (4) 17-18 (3) 18-20 (2) 20-22 (1)	06-13 (1) 13-15 (2) 15-17 (3) 17-23 (4) 23-02 (3) 02-06 (2)	18-20 (1) 20-23 (2) 23-01 (3) 01-02 (2) 02-03 (1) 22-02 (1)*

East & Central Africa	07-09 (1) 09-11 (2) 11-15 (3) 15-17 (2) 17-19 (1)	07-09 (1) 09-11 (2) 11-13 (3) 13-15 (4) 15-17 (3) 17-18 (2) 18-19 (1)	12-14 (1) 14-16 (2) 16-18 (3) 18-22 (4) 22-01 (3) 01-03 (2) 03-05 (1)	19-23 (1) 23-01 (2) 01-02 (1)
Southern Africa	07-09 (1) 09-11 (2) 11-12 (3) 12-14 (4) 14-15 (2) 15-16 (1)	06-10 (1) 10-13 (2) 13-15 (3) 15-17 (4) 17-18 (2) 18-19 (1)	12-15 (1) 15-17 (2) 17-18 (3) 18-20 (4) 20-23 (2) 23-02 (3) 02-03 (2) 03-06 (1)	18-19 (1) 19-21 (2) 21-22 (1) 19-21 (1)*
Central & South Asia	08-10 (1) 17-19 (1)	07-08 (1) 08-10 (2) 10-12 (1) 19-21 (1)	06-09 (1) 17-19 (1) 19-21 (2) 21-23 (1)	05-07 (1) 19-21 (1)
Southeast Asia	08-09 (1) 09-11 (2) 11-14 (1) 18-21 (1)	07-08 (1) 08-10 (2) 10-12 (1) 15-17 (1) 17-19 (2) 19-21 (1)	04-06 (1) 06-07 (2) 07-10 (1) 14-16 (1) 21-23 (1) 23-01 (2) 01-02 (1)	05-07 (1)
Far East	16-17 (1) 17-19 (2) 19-20 (1)	07-10 (1) 15-16 (1) 16-17 (2) 17-19 (3) 19-20 (2) 20-21 (1)	02-06 (1) 06-09 (2) 09-11 (1) 19-21 (1) 21-22 (2) 22-00 (3) 00-02 (2)	05-08 (1)
South Pacific & New Zealand	11-12 (1) 12-14 (2) 14-16 (1) 16-17 (2) 17-19 (3) 19-20 (2) 20-21 (1)	08-09 (1) 09-12 (2) 12-16 (1) 16-18 (2) 18-21 (3) 21-22 (2) 22-23 (1)	18-20 (1) 20-22 (2) 22-00 (3) 00-02 (4) 02-05 (3) 05-07 (2) 07-09 (4) 09-10 (2) 10-12 (1)	01-02 (1) 02-03 (2) 03-05 (3) 05-07 (2) 07-08 (1) 02-03 (1)* 03-05 (2)* 05-06 (1)*
Australasia	09-11 (1) 15-16 (1) 16-17 (2) 17-19 (3) 19-20 (2) 20-21 (1)	08-09 (1) 09-11 (2) 11-16 (1) 16-18 (2) 18-20 (3) 20-22 (2) 22-23 (1)	02-07 (2) 07-09 (3) 09-10 (2) 10-13 (1) 13-15 (2) 15-19 (1) 19-22 (2) 22-02 (3)	03-05 (1) 05-07 (2) 07-09 (1) 04-05 (1)* 05-06 (2)* 06-07 (1)*
Caribbean, Central America & Northern Countries of South America	07-08 (1) 08-09 (3) 09-11 (4) 11-13 (3) 13-16 (4) 16-17 (3) 17-18 (2) 18-19 (1)	06-07 (1) 07-08 (2) 08-10 (4) 10-15 (3) 15-18 (4) 18-20 (3) 20-22 (2) 22-01 (1)	06-08 (4) 08-10 (3) 10-15 (2) 15-18 (3) 18-00 (4) 00-03 (3) 03-05 (2) 05-06 (3)	18-19 (1) 19-20 (2) 20-03 (3) 03-05 (2) 05-07 (1) 19-21 (1)* 21-02 (2)* 02-06 (1)*
Peru, Bolivia, Paraguay, Brazil, Chile, Argentina & Uruguay	07-08 (1) 08-10 (3) 10-14 (2) 14-15 (3) 15-17 (4) 17-18 (2) 18-19 (1)	06-07 (1) 07-10 (2) 10-14 (1) 14-15 (2) 15-19 (4) 19-21 (3) 21-23 (2) 23-01 (1)	15-16 (1) 16-17 (2) 17-18 (3) 00-02 (3) 18-00 (4) 02-04 (2) 04-05 (1) 05-07 (2) 07-09 (1)	19-21 (1) 21-03 (2) 03-06 (1) 21-05 (1)*
McMurdo Sound, Antarctica	14-16 (1) 16-19 (2) 19-20 (1)	14-16 (1) 16-18 (2) 18-21 (3) 21-22 (2) 22-23 (1)	17-19 (1) 19-21 (2) 21-04 (3) 04-06 (2) 06-08 (1)	22-00 (1) 00-03 (2) 03-05 (1)

MASTER DX PROPAGATION CHART
SOLAR PHASE: VERY HIGH
SMOOTHED SUNSPOT RANGE: 90-120
SEASONS: SPRING & FALL
TIME ZONES: CST & MST (24-Hour Time)
CENTRAL USA TO:

Reception Area	*10 Meters*	*15 Meters*	*20 Meters*	*40/80 Meters*
Western & Central Europe & North Africa	08-10 (1) 10-13 (2) 13-14 (1)	07-08 (1) 08-09 (2) 09-13 (3) 13-14 (2) 14-15 (1)	23-06 (1) 06-09 (2) 09-11 (1) 11-13 (2) 13-17 (3) 17-19 (2) 19-22 (1) 22-23 (2)	17-19 (1) 19-23 (2) 23-02 (1) 20-21 (1)* 21-22 (2)* 22-00 (1)*
Northern & Eastern Europe	08-12 (1)	06-08 (1) 08-12 (2) 12-13 (1)	20-22 (1) 22-00 (2) 00-06 (1) 06-08 (2) 08-12 (1) 12-14 (2) 14-16 (3) 16-20 (2)	19-01 (1) 20-23 (1)*
Eastern Mediterranean & Middle East	08-12 (1)	07-08 (1) 08-09 (2) 09-11 (3) 11-12 (2) 12-13 (1)	06-13 (1) 13-16 (2) 16-18 (3) 18-19 (2) 19-21 (1) 21-23 (2) 23-01 (1)	19-22 (1) 20-21 (1)*
West & Central Africa	08-09 (1) 09-11 (2) 11-13 (3) 13-16 (4) 16-17 (3) 17-18 (2) 18-19 (1)	07-10 (1) 10-12 (2) 12-14 (3) 14-17 (4) 17-18 (3) 18-20 (2) 20-21 (1)	10-12 (1) 12-15 (2) 15-17 (3) 17-20 (4) 20-22 (3) 22-00 (2) 00-02 (1)	18-19 (1) 19-21 (2) 21-00 (1) 20-22 (1)*
East Africa	08-10 (1) 10-14 (2) 14-16 (1)	07-10 (1) 10-12 (2) 12-15 (3) 15-17 (2) 17-18 (1)	10-14 (1) 14-16 (2) 16-20 (3) 20-22 (2) 22-00 (1)	19-21 (1) 20-22 (1)*
Southern Africa	07-09 (1) 09-10 (2) 10-13 (3) 13-14 (2) 14-15 (1)	06-10 (1) 10-12 (2) 12-13 (3) 13-15 (4) 15-16 (3) 16-17 (2) 17-18 (1)	10-13 (1) 13-15 (2) 15-16 (3) 16-18 (4) 18-20 (3) 20-22 (2) 22-00 (3) 00-02 (2) 02-04 (1)	19-22 (1) 20-21 (1)*
Central & South Asia	07-09 (1) 18-20 (1)	07-08 (1) 08-10 (2) 10-11 (1) 18-19 (1) 19-20 (2) 20-21 (1)	06-07 (1) 07-09 (2) 09-11 (1) 17-19 (1) 19-21 (2) 21-22 (1)	05-07 (1) 19-21 (1)
Southeast Asia	09-10 (1) 10-12 (2) 12-14 (1) 16-17 (1) 17-19 (2) 19-20 (1)	07-08 (1) 08-10 (2) 10-12 (3) 12-13 (2) 13-17 (1) 17-20 (2) 20-22 (1)	20-22 (1) 22-00 (2) 00-06 (1) 06-09 (2) 09-11 (1) 13-15 (1)	03-07 (1)
Far East	15-16 (1) 16-17 (2) 17-18 (3) 18-19 (2) 19-20 (1)	08-11 (1) 15-16 (1) 16-17 (2) 17-20 (3) 20-21 (2) 21-22 (1)	03-06 (1) 06-09 (2) 09-12 (1) 19-21 (1) 21-22 (2) 22-01 (3) 01-03 (2)	03-08 (1) 05-07 (1)*
South Pacific & New Zealand	10-11 (1) 11-13 (2) 13-15 (3) 15-17 (2) 17-19 (3) 19-20 (2) 20-21 (1)	08-09 (1) 09-12 (2) 12-17 (1) 17-18 (2) 18-22 (3) 22-00 (2) 00-01 (1)	18-20 (1) 20-22 (2) 22-00 (3) 00-03 (4) 03-05 (3) 05-07 (2) 07-09 (3) 09-10 (2) 10-11 (1)	22-00 (1) 00-01 (2) 01-06 (3) 06-07 (2) 07-08 (1) 00-02 (1)* 02-05 (2)* 05-07 (1)*
Australasia	08-11 (1) 13-14 (1) 14-15 (2) 15-18 (4) 18-19 (3) 19-20 (2) 20-21 (1)	07-08 (1) 08-11 (2) 11-13 (1) 13-14 (2) 14-16 (3) 16-18 (2) 18-20 (3) 20-22 (4) 22-00 (2) 00-01 (1)	05-07 (2) 07-09 (3) 09-12 (2) 12-14 (1) 14-16 (2) 16-20 (1) 20-22 (2) 22-02 (3) 02-04 (4) 04-05 (3)	02-04 (1) 04-06 (3) 06-07 (2) 07-08 (1) 04-05 (1)* 05-06 (2)* 06-07 (1)*
Caribbean, Central America & Northern Countries of South America	06-07 (1) 07-08 (3) 08-11 (4) 11-13 (3) 13-16 (4) 16-17 (3) 17-18 (2) 18-20 (1)	05-06 (1) 06-07 (2) 07-10 (4) 10-14 (3) 14-18 (4) 18-20 (3) 20-22 (2) 22-01 (1)	02-07 (2) 07-10 (3) 10-15 (2) 15-17 (3) 17-00 (4) 00-02 (3)	18-19 (1) 19-20 (2) 20-02 (3) 02-04 (2) 04-06 (1) 20-21 (1)* 21-02 (2)* 02-05 (1)*
Peru, Bolivia, Paraguay, Brazil, Chile, Argentina & Uruguay	06-08 (1) 08-09 (3) 09-13 (2) 13-14 (3) 14-16 (4) 16-17 (3) 17-18 (2) 18-19 (1)	06-07 (1) 07-10 (2) 10-13 (1) 13-14 (2) 14-15 (3) 15-19 (4) 19-21 (3) 21-23 (2) 23-01 (1)	13-15 (1) 15-16 (2) 16-18 (3) 18-00 (4) 00-02 (3) 02-06 (2) 06-08 (1)	19-20 (1) 20-02 (2) 02-05 (1) 21-03 (1)*
McMurdo Sound, Antarctica	11-14 (1) 14-18 (2) 18-20 (1)	13-16 (1) 16-18 (2) 18-21 (3) 21-22 (2) 22-23 (1)	16-19 (1) 19-20 (2) 20-03 (3) 03-07 (2) 07-10 (1)	22-01 (1) 01-04 (2) 04-06 (1)

MASTER DX PROPAGATION CHART
SOLAR PHASE: VERY HIGH
SMOOTHED SUNSPOT RANGE: 90-120
SEASONS: SPRING & FALL
TIME ZONE: PST (24-Hour Time)
WESTERN USA TO:

Reception Area	*10 Meters*	*15 Meters*	*20 Meters*	*40/80 Meters*
Western Europe & North Africa	08-11 (1)	07-08 (1) 08-09 (3) 09-11 (2) 11-12 (3) 12-13 (2) 13-14 (1)	00-06 (1) 06-08 (2) 08-11 (1) 11-13 (2) 13-15 (3) 15-19 (2) 19-22 (1) 22-00 (2)	18-00 (1) 20-22 (1)*
Northern, Central & Eastern Europe	08-10 (1)	07-08 (1) 08-11 (2) 11-13 (1)	20-22 (1) 22-01 (2) 01-06 (1) 06-08 (2) 08-10 (1) 10-12 (2) 12-14 (3) 14-16 (2) 16-18 (1)	19-23 (1) 20-22 (1)
Eastern Mediterranean & Middle East	08-10 (1)	07-08 (1) 08-10 (2) 10-12 (1) 19-21 (1)	07-12 (1) 12-15 (2) 15-18 (1) 18-22 (2) 22-02 (1)	18-21 (1)
West & Central Africa	08-09 (1) 09-12 (2) 12-14 (3) 14-16 (4) 16-17 (3) 17-18 (2) 18-19 (1)	07-10 (1) 10-12 (2) 12-14 (3) 14-17 (4) 17-18 (3) 18-19 (2) 19-20 (1)	10-12 (1) 12-14 (2) 14-16 (3) 16-20 (4) 20-22 (3) 22-23 (2) 23-00 (1)	18-22 (1)
Southern Africa	08-09 (1) 09-11 (3) 11-12 (1)	06-10 (1) 10-12 (2) 12-14 (4) 14-15 (2) 15-16 (1)	06-13 (1) 13-15 (2) 15-18 (3) 18-19 (2) 19-21 (1) 21-23 (3) 23-00 (2) 00-02 (1)	19-22 (1) 20-21 (1)*
Central & South Asia	17-19 (1)	07-08 (1) 08-10 (2) 10-11 (1) 16-17 (1) 17-19 (2) 19-21 (1)	05-07 (1) 07-09 (2) 09-11 (1) 17-19 (1) 19-21 (2) 21-22 (1)	05-07 (1)
Southeast Asia	08-10 (1) 14-15 (1) 15-16 (2) 16-18 (3) 18-19 (2) 19-20 (1)	07-08 (1) 08-10 (3) 10-12 (2) 12-17 (1) 17-20 (2) 20-00 (1)	22-00 (1) 00-07 (2) 07-09 (3) 09-11 (2) 11-15 (1)	02-07 (1) 04-06 (1)*
Far East	13-14 (1) 14-16 (2) 16-17 (4) 17-18 (3) 18-19 (2) 19-20 (1)	07-12 (1) 12-15 (2) 15-17 (3) 17-19 (4) 19-20 (3) 20-21 (2) 21-22 (1)	11-21 (1) 21-22 (2) 22-03 (3) 03-06 (2) 06-08 (3) 08-11 (2)	00-02 (1) 02-04 (2) 04-08 (1) 02-06 (1)

South Pacific & New Zealand	08-09 (1) 09-11 (3) 11-15 (2) 15-16 (3) 16-18 (4) 18-20 (2) 20-21 (1)	07-08 (1) 08-11 (3) 11-16 (2) 16-18 (3) 18-20 (4) 20-21 (3) 21-22 (2) 22-00 (1)	17-19 (1) 19-21 (2) 21-22 (3) 22-00 (4) 00-02 (3) 02-04 (2) 04-06 (1) 06-09 (2) 09-11 (1)	19-21 (1) 21-23 (2) 23-05 (4) 05-06 (3) 06-07 (2) 07-08 (1) 21-23 (1)* 23-05 (2)* 05-07 (1)*
Australasia	11-13 (1) 13-16 (3) 16-18 (4) 18-20 (3) 20-21 (2) 21-22 (1)	06-07 (1) 07-09 (2) 09-11 (1) 11-13 (2) 13-16 (1) 16-18 (2) 18-20 (4) 20-22 (3) 22-00 (2) 00-02 (1)	12-20 (1) 20-22 (2) 22-00 (3) 00-03 (4) 03-07 (2) 07-09 (3) 09-12 (2)	01-03 (1) 03-05 (3) 05-06 (2) 06-08 (1) 03-04 (1)* 04-06 (21)* 06-07 (1)*
Caribbean, Central America & Northern Countries of South America	06-07 (1) 07-08 (3) 08-10 (4) 10-13 (3) 13-16 (4) 16-17 (3) 17-18 (2) 18-20 (1)	05-06 (1) 06-07 (2) 07-09 (4) 09-14 (3) 14-18 (4) 18-20 (3) 20-22 (2) 22-00 (1)	06-08 (3) 08-15 (2) 15-17 (3) 17-00 (4) 00-02 (3) 02-06 (2)	18-20 (1) 20-00 (3) 00-03 (2) 03-05 (1) 20-21 (1)* 21-01 (2)* 01-04 (1)*
Peru, Bolivia, Paraguay, Brazil, Chile, Argentina & Uruguay	07-08 (1) 08-09 (3) 09-12 (2) 12-14 (3) 14-16 (4) 16-17 (3) 17-18 (2) 18-19 (1)	06-07 (1) 07-09 (2) 09-12 (1) 12-14 (2) 14-15 (3) 15-19 (4) 19-20 (3) 20-22 (2) 22-02 (1)	12-14 (1) 14-16 (2) 16-18 (3) 18-23 (4) 23-02 (3) 02-06 (2) 06-08 (1)	18-19 (1) 19-01 (2) 01-03 (1) 20-02 (1)*
McMurdo Sound, Antarctica	11-15 (1) 15-18 (2) 18-19 (1)	14-16 (1) 16-18 (2) 18-21 (3) 21-23 (2) 23-00 (1)	16-19 (1) 19-20 (2) 20-02 (3) 02-04 (2) 04-06 (1) 06-08 (2) 08-10 (1)	22-02 (1) 02-04 (2) 04-06 (1)

MASTER SHORT-SKIP PROPAGATION CHART
SOLAR PHASE: VERY HIGH
SMOOTHED SUNSPOT RANGE: 90-120
SEASON: SUMMER
TIME ZONES: LOCAL STANDARD AT PATH MID-POINT
(24-Hour Time)

Band (Meters)	*Distance Between Stations (Miles)*			
	50-250	*250-750*	*750-1300*	*1300-2300*
10	*Nil*	07-09 (0-1)* 09-13 (0-2)* 13-17 (0-1)* 17-21 (0-2)* 21-23 (0-1)*	07-09 (1)* 09-13 (2-3)* 13-17 (1-2)* 17-21 (2-3)* 21-07 (1)*	07-09 (1-0)* 09-13 (3-1)* 13-17 (2-1)* 17-21 (3-1)* 21-07 (1-0)*
15	*Nil*	07-09 (0-2)* 09-13 (0-3)* 13-17 (0-2)* 17-19 (0-3)* 19-21 (0-2)* 21-07 (0-1)*	07-09 (2)* 09-13 (3)* 13-17 (2)* 17-19 (3)* 19-21 (2)* 21-23 (1-2)* 23-07 (1)*	07-09 (2) 09-13 (3) 13-17 (2-3) 17-19 (3-4) 19-21 (2-3) 21-23 (2) 23-07 (1)*
20	09-00 (0-1)*	06-09 (0-2)* 09-15 (1-4)* 15-20 (1-3)* 20-00 (1-2)* 00-06 (0-1)*	06-09 (2-4) 09-15 (4) 15-20 (3-4) 20-00 (2-4)* 00-02 (1-3)* 02-06 (1-2)*	06-09 (4) 09-16 (4-3) 16-00 (4) 00-02 (3) 02-06 (2)
40	07-11 (2-4) 11-20 (3-4) 20-22 (2-3) 22-00 (1-2) 00-06 (0-2)* 06-07 (1-2)	07-09 (2-4)* 09-11 (4-3) 11-16 (4-2) 16-18 (4-3) 18-20 (4) 20-22 (3-4) 22-04 (2-4) 04-07 (2-3)	07-09 (4-2) 09-11 (3-1) 11-16 (2-1) 16-17 (3-1) 17-18 (3-2) 18-20 (4-3) 20-04 (4) 04-05 (3-4) 05-07 (3)	07-17 (1-0) 17-18 (2-1) 18-20 (3-2) 20-05 (4) 05-06 (3-2) 06-07 (3-1)
80	06-10 (4) 10-18 (4-3) 18-00 (4) 00-06 (3-4)	07-09 (4-1) 09-10 (4-1) 10-16 (3-0) 16-18 (3-1) 18-19 (4-2) 19-21 (4-3) 21-06 (4) 06-07 (4-2)	06-07 (2-1) 07-09 (1-0) 09-16 (0) 16-18 (1-0) 18-19 (2-1) 19-20 (3-1) 20-21 (3-2) 21-04 (4) 04-06 (4-3)	07-18 (1) 18-19 (1-0) 19-20 (1) 20-21 (2) 21-03 (4-3) 03-04 (4-2) 04-05 (3-2) 05-06 (3-1) 06-07 (1)
160	17-18 (1-0) 18-19 (1) 19-21 (3-2) 21-23 (4-3) 23-05 (4) 05-07 (3-2) 07-08 (1) 08-09 (1-0)	18-19 (1-0) 19-20 (2-0) 20-21 (2-1) 21-23 (3-2) 23-03 (4-2) 03-05 (4-3) 05-07 (2-1) 07-08 (0-1)	21-21 (1) 21-00 (2-1) 00-03 (2) 03-05 (3-2) 05-06 (1) 06-07 (1-0)	20-22 (1-0) 22-00 (1) 00-05 (2-1) 05-06 (1-0)

MASTER SHORT-SKIP PROPAGATION CHART
SOLAR PHASE: VERY HIGH
SMOOTHED SUNSPOT RANGE: 90-120
SEASON: WINTER
TIME ZONES: LOCAL STANDARD AT PATH MID-POINT
(24-Hour Time)

Band (Meters)	*Distance Between Stations (Miles)*			
	50-250	*250-750*	*750-1300*	*1300-2300*
10	*Nil*	*Nil*	07-09 (0-1) 09-10 (0-3) 10-15 (0-4) 15-17 (0-3) 17-19 (0-1)	07-09 (1) 09-10 (3) 10-15 (4) 15-17 (3-4) 17-18 (1-3) 18-19 (1-2) 19-20 (0-1)
15	*Nil*	08-17 (0-2)	06-08 (0-1) 08-09 (2) 09-11 (2-3) 11-17 (2-4) 17-18 (0-3) 18-20 (0-2) 20-22 (0-1)	06-07 (1) 07-08 (1-2) 08-09 (2-3) 09-11 (3-4) 11-17 (4) 17-18 (3-4) 18-20 (2-4) 20-21 (1-2) 21-22 (1)
20	09-11 (1-2) 11-14 (1-3) 14-15 (1-2) 15-17 (0-1)	08-09 (0-2) 09-11 (2-4) 11-14 (3-4) 14-15 (2-4) 15-17 (1-4) 17-19 (0-3) 19-20 (0-2) 20-08 (0-1)	07-08 (1-2) 08-09 (2-3) 09-17 (4) 17-19 (3-4) 19-20 (2-3) 20-22 (1-3) 22-00 (0-2) 00-07 (1)	07-08 (2-3) 08-09 (3-4) 09-10 (4) 10-14 (4-3) 14-19 (4) 19-21 (3-4) 21-22 (3) 22-00 (2-3) 00-03 (1-2) 03-06 (1) 06-07 (1-2)
40	07-08 (0-2) 08-09 (1-3) 09-10 (2-4) 10-17 (4) 17-18 (3-4) 18-20 (2-3) 20-22 (1-2) 22-07 (0-1)	07-08 (2) 08-09 (3) 09-11 (4-3) 11-15 (4-2) 15-18 (4) 18-20 (3-4) 20-22 (2-4) 22-02 (1-3) 02-07 (1-2)	07-08 (2) 08-11 (3-1) 11-15 (2-1) 15-17 (4-2) 17-18 (4-3) 18-22 (4) 22-02 (3-4) 02-05 (2-4) 05-07 (2-3)	07-08 (2-1) 08-15 (1-0) 15-17 (2-1) 17-18 (3) 18-04 (4) 04-05 (4-3) 05-07 (3-2)
80	07-08 (2-3) 08-10 (3-4) 10-15 (4-3) 15-21 (4) 21-00 (3-4) 00-04 (2-3) 04-07 (1-2)	07-08 (3) 08-09 (4-2) 09-10 (4-1) 10-15 (3-1) 15-16 (4-1) 16-18 (4-2) 18-00 (4) 00-04 (3-4) 04-07 (2-3)	07-08 (3-1) 08-09 (2-0) 09-16 (1-0) 16-18 (2-1) 18-20 (4-3) 20-04 (4) 04-06 (3) 06-07 (3-2)	07-08 (1-0) 08-16 (0) 16-18 (1-0) 18-20 (3-2) 20-03 (4) 03-04 (4-3) 04-05 (3) 05-06 (3-2) 06-07 (2-1)
160	09-17 (1-0) 17-19 (3-2) 19-05 (4) 05-07 (3) 07-09 (2-1)	17-18 (2-1) 18-19 (2) 19-21 (4-3) 21-05 (4) 05-06 (3) 06-07 (3-1) 07-09 (1-0)	17-18 (1-0) 18-19 (2-1) 19-21 (3-1) 21-03 (4-3) 03-05 (4) 05-06 (3-2) 06-07 (1)	18-19 (1-0) 19-21 (2-1) 21-03 (3) 03-05 (4-2) 05-06 (2-1) 06-07 (1-0)

MASTER SHORT-SKIP PROPAGATION CHART
SOLAR PHASE: VERY HIGH
SMOOTHED SUNSPOT RANGE: 90-120
SEASONS: SPRING & FALL
TIME ZONES: LOCAL STANDARD AT PATH MID-POINT
(24-Hour Time)

Band (Meters)	*Distance Between Stations (Miles)*			
	50-250	*250-750*	*750-1300*	*1300-2300*
10	*Nil*	09-13 (0-1)	07-09 (1) 09-12 (1-2) 12-13 (1-3) 13-16 (0-3) 16-18 (0-2) 18-20 (0-1)	07-08 (1) 08-09 (1-2) 09-12 (2-4) 12-16 (3-4) 16-18 (2-3) 18-20 (1-2) 20-21 (0-1)
15	*Nil*	07-09 (0-1) 09-15 (0-2) 15-19 (0-1)	07-08 (1) 08-09 (1-2) 09-15 (2-4) 15-18 (1-3) 18-19 (1-2) 19-23 (0-1)	07-08 (1) 08-09 (1-3) 09-15 (4) 15-18 (3-4) 18-19 (2-3) 19-21 (1-3) 21-23 (1-2) 23-01 (0-1)
20	11-13 (0-1) 13-16 (0-2) 16-19 (0-1)	08-09 (0-3) 09-11 (0-4) 11-13 (1-4) 13-16 (2-4) 16-18 (1-4) 18-19 (1-3) 19-22 (0-2) 22-08 (0-1)	06-07 (1-2) 07-08 (3) 08-09 (3-4) 09-18 (4) 18-19 (3-4) 19-22 (2-4) 22-00 (1-3) 00-02 (1-2) 02-06 (1)	06-07 (2) 07-08 (3) 08-10 (4) 10-15 (4-3) 15-22 (4) 22-23 (3-4) 23-00 (3) 00-02 (2) 02-04 (1-2) 04-06 (1)
40	06-07 (1-2) 07-09 (2-3) 09-18 (4) 18-20 (3-4) 20-22 (2-3) 22-00 (1-2) 00-06 (1)	06-07 (2-3) 07-09 (3-4) 09-11 (4-3) 11-13 (4-2) 13-15 (4-3) 15-20 (4) 20-22 (3-4) 22-00 (2-4) 00-03 (1-3) 03-06 (1-2)	06-07 (3-2) 07-08 (4-2) 08-09 (4-1) 09-13 (2-1) 13-15 (3-1) 15-17 (4-2) 17-19 (4-3) 19-00 (4) 00-03 (3-4) 03-06 (2-3)	06-08 (2-1) 08-15 (1-0) 15-16 (2-0) 16-17 (2-1) 17-19 (3-2) 19-03 (4) 03-04 (3-4) 04-06 (3)
80	07-11 (4) 11-18 (4-3) 18-22 (4) 22-00 (3-4) 00-07 (2-3)	07-08 (4-2) 08-11 (4-1) 11-16 (3-0) 16-18 (3-2) 18-20 (4-3) 20-00 (4) 00-05 (3-4) 05-07 (3)	07-08 (2-1) 08-11 (1-0) 11-16 (0) 16-18 (2-1) 18-20 (3-2) 20-03 (4) 03-05 (4-3) 05-07 (3-2)	07-08 (1-0) 08-16 (0) 16-18 (1-0) 18-20 (2-1) 20-22 (4-2) 22-03 (4-3) 03-05 (3-2) 05-07 (2-1)
160	05-07 (4-2) 07-09 (3-1) 09-17 (2-0) 17-19 (3-1) 19-20 (4-2) 20-05 (4)	05-06 (2-1) 06-07 (2-0) 07-09 (1-0) 09-17 (0) 17-19 (1-0) 19-20 (2) 20-22 (4-3) 22-03 (4) 03-05 (4-3)	05-06 (1) 06-19 (4) 19-20 (2-1) 20-22 (3-2) 22-03 (4-3) 03-05 (3-2)	05-06 (1-0) 06-19 (0) 19-20 (1-0) 20-22 (2) 22-03 (3-2) 03-05 (2-1)

FOOTNOTES

Worldwide Charts:
* Predicted times of 80 meter openings. Openings on 160 meters are also likely to occur during those times when 80 meter openings are shown with a forecast rating of (2) or higher.

Short Skip Charts:
* Predominantly sporadic-*E* openings.

4.7 Summary of DX Band Conditions Throughout A Complete Solar Cycle

Table 4.10 summarizes the quality of DX propagation conditions that can be expected on each amateur HF band during day and night for each season of the year for each major phase of a sunspot cycle.

In summary, there is a direct relationship between the level of solar activity and DX capabilities on each of the HF bands. As the sunspot count increases, daytime DX conditions improve considerably on the 10, 15, and 20 meter bands, while nighttime conditions improve on 20 meters but decline somewhat on 40, 80, and 160 meter bands. As a solar cycle declines, nighttime DX conditions on 40, 80, and 160 meters improve, while conditions on 20 meters deteriorate. Daytime DX conditions will deteriorate somewhat on 20 meters, and considerably on 10 and 15 meters.

4.8 References

1. Jacobs, G., "Propagation," published monthly in *CQ* magazine, 76 N. Broadway, Hicksville, NY 11801.

2. Updated smoothed sunspot numbers appear monthly in "Propagation," *CQ*, 76 N. Broadway, Hicksville, NY 11801. They also can be obtained from the National Oceanic and Atmospheric Administration (NOAA), Environmental Research Laboratories, Boulder, CO 80303.

Solar Phase	Season	Time	10 meters	15 meters	20 meters	40 meters	80 meters	160 meters
Very High	Summer	Day	G	G	G	—	—	—
	Summer	Night	—	F	E	F	P	P
	Winter	Day	E	E	E	—	—	—
	Winter	Night	—	—	F	G	F	F
	Equinox	Day	E	E	E	—	—	—
	Equinox	Night	—	—	G	G	F	P
High	Summer	Day	F	G	G	—	—	—
	Summer	Night	—	—	G	G	F	P
	Winter	Day	E	E	E	—	—	—
	Winter	Night	—	—	F	E	G	F
	Equinox	Day	G	E	E	—	—	—
	Equinox	Night	—	—	F	E	G	F
Moderate	Summer	Day	P	F	G	—	—	—
	Summer	Night	—	—	G	G	F	P
	Winter	Day	F	E	E	—	—	—
	Winter	Night	—	—	P	E	G	F
	Equinox	Day	F	G	E	—	—	—
	Equinox	Night	—	—	F	G	G	F
Low	Summer	Day	P	F	G	—	—	—
	Summer	Night	—	—	F	G	F	P
	Winter	Day	P	F	E	—	—	—
	Winter	Night	—	—	P	G	G	F
	Equinox	Day	P	F	G	—	—	—
	Equinox	Night	—	—	F	G	G	F

Equinox = Spring & Fall

E = Excellent
G = Good

F = Fair
P = Poor

— = Not likely

Table 4.10. Relative quality of DX propagation in each amateur HF band during day and night, for each season of the year, for each major phase of a solar cycle. See Tables 4.5 and 4.6 for applying this summary to the WARC and HF broadcasting bands, respectively. During periods of intense solar activity (smoothed sunspot numbers greater than 120), use data shown for Very High solar phase.

Chapter 5

Ionospheric Forecasts

Chapter 4 contains Master Propagation Charts that make it relatively easy for shortwave users to predict propagation conditions from most areas of the U.S. and Canada to just about any spot on Earth, given the solar phase, the season of the year, the frequency, and the time of day.

Besides the more or less normal variations in the ionosphere that can be predicted long in advance, short-term variations also occur. These variations account for the day-to-day differences observed in the propagation of shortwave signals, and they explain why reception on a particular path may be good one day, fair another, and sometimes not possible at all.

Now that the Master Propagation Charts in Chapter 4 have provided for long-term propagation predictions, the next question to be answered is "How can shortwave users tell if conditions are going to be good or bad on a particular day and on a specific path?" In this chapter we examine two methods that permit you to determine day-to-day conditions for up to 27 days in advance.

The first method requires that a log, or record, be kept of observed signal strengths and general reception conditions for selected paths, on a day-to-day basis, as a function of solar and geomagnetic activity. Then, using your observations and current values of solar and geomagnetic activity broadcast hourly on WWV, you should be able to make short-term forecasts with a fairly high degree of accuracy.

The second method uses the Master Propagation Charts that appear in Chapter 4 (and monthly in *CQ* magazine), thus eliminating the need to make your own observations of reception conditions. Using the propagation indices shown next to the band openings in these charts, and using the solar and geomagnetic data available from WWV broadcasts and other sources, it is relatively easy to make your own short-term, day-to-day forecasts for as much as 27 days in advance and with a reliability as high as 90%.

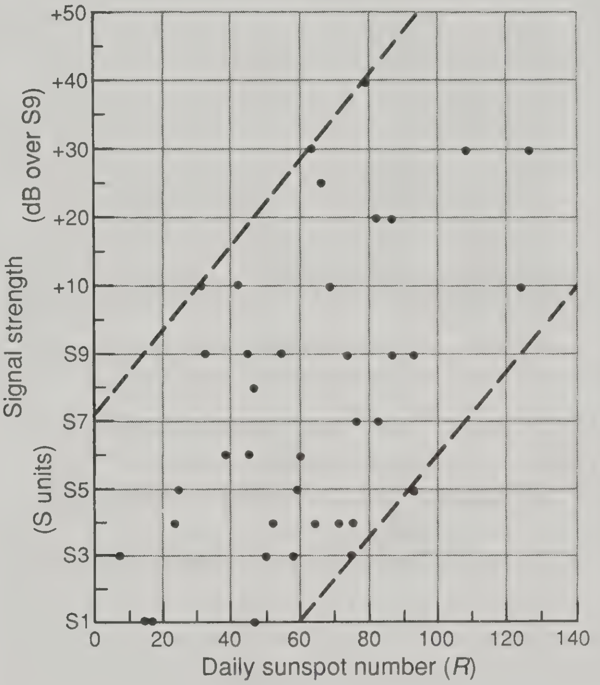

Figure 5.1. Signal strength as a function of daily sunspot number *R*, Australia to East Coast U.S., 14 MHz short path, April/May 1972/1973, 1100–1300 UTC.

Although the words are often used interchangeably in the technical literature, we will apply the term "prediction" to *long-term* determinations of band openings that can be made for any phase of the solar cycle, months and even years in advance, and that are discussed in Chapter 4. The term "forecast" will apply to the *short-term* determinations of day-to-day variations

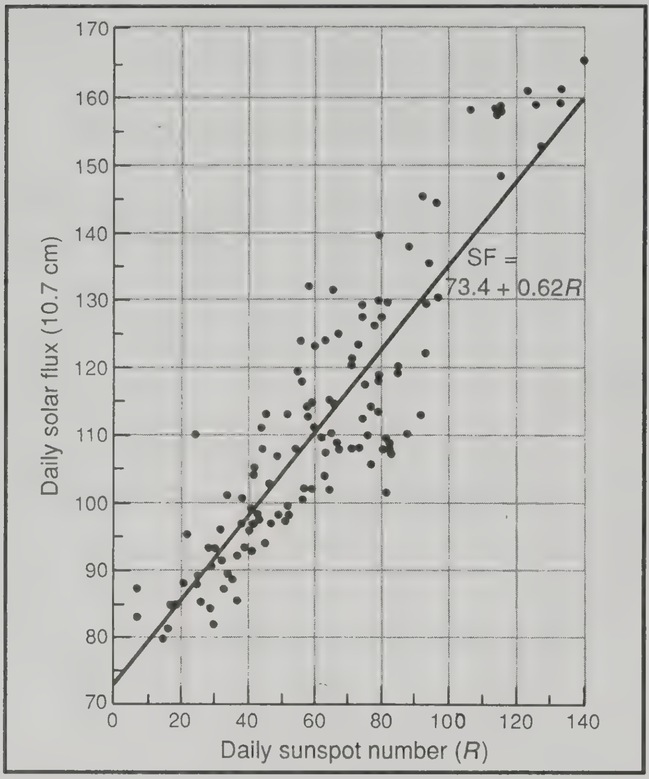

Figure 5.2. Daily solar flux versus daily sunspot number, *R*, April/May 1972/73.

in the quality of these band openings up to 27 days in advance, as is discussed in this chapter.

In this chapter, we also review the type of radio propagation forecast information provided by the time standard HF broadcast stations WWV (Ft. Collins, Colorado) and WWVH (Kauai, Hawaii). These stations are operated by the Department of Commerce, National Oceanic and Atmospheric Administration, Environmental Research Laboratory, in Boulder, Colorado.

5.1 Short-Term Forecasts For Ionospheric Propagation

In an earlier chapter we saw that solar activity is defined in terms of the 12-month running smoothed sunspot numbers. Then, too, expected ionospheric conditions over a given path as a function of time are usually described by a chart of the median (50%) maximum usable frequencies (MUFs). In each case it is the average behavior of the Sun and the ionosphere, respectively, that is being described. However, a knowledge of the average, expected behavior of the Sun and the ionosphere does not permit an assessment of the specific level of solar activity, or of the actual maximum usable frequency (i.e., the Classical MUF), at any given time.

Given this situation, the question is "How will radio operators and shortwave listeners know what to expect on the high-frequency bands from day to day?" Obviously, it is not desirable to have to monitor the bands constantly in an attempt to catch an occasional opening to an area of interest. What is needed is some method for making short-term ionospheric forecasts.

In this section we present a relatively simple method by which an operator, on the day of operation, can determine whether or not a particular path will open to a given area. To be useful, however, the method requires the use of timely measurements of solar activity (solar flux) and geomagnetic activity (solar particle radiation), which are broadcast on WWV at 18 minutes past each hour on 2.5, 5.0, 10.0, 15.0, and 20.0 MHz (see Section 5.3). Using this method, it will be possible to determine, for example, if the 14 MHz band will open to Japan and the Far East in the morning on a day in April from information obtained early in the day *on that day in April.*

While we will specifically examine 14 MHz short-path openings to select areas of the world from the East Coast of the United States, it should be emphasized that the forecast methods to be introduced can be applied to any band, and to any path, once the relationship among signal strength, solar flux, and geomagnetic activity is known.

Band Conditions and The Daily Sunspot Number (*R*)

For some time, amateurs and other users of the high-frequency bands have observed the correlation between daily sunspot activity and propagation conditions. In general, improved conditions are observed when greater numbers of sunspots are visible. This

K	0	1	2	3	4	5	6	7	8	9
a	0	3	7	15	27	48	80	180	240	400

Table 5.1. Relationship between the *K*-index and the *a*-index.

	Prefixes	Years Analyzed	Months Analyzed	Times Analyzed (UTC)
Far East Asia	HM, JA, JD, KA6, KR6, VS6	1972, 73	Apr., May	1100–1400
Australia	VK1–8	1972, 73	Apr., May	1100–1300
Asiatic Russia	UA9	1971, 72, 73	Mar., Apr., May	0100–0330
Asiatic Russia	UA9	1971, 72, 73	Aug. Sept., Oct.	0100–0330

Table 5.2. Information on the database used to derive the circuit charts.

Signal Strength	Symbol	Signal Quality
$r>S9+30$ dB	A	Excellent opening, exceptionally strong, steady signals
$S9<r\leq S9+30$ dB	B	Good opening, moderately strong signals with little fading or noise
$S3<r\leq S9$	C	Fair opening, signals between moderately strong and weak, with some fading and noise
$S1<r\leq S3$	D	Poor opening, signals weak with considerable fading and noise
	E	No opening expected

Table 5.3. Signal-strength categories.

observation is supported by the data of Figure 5.1, which are signal-strength readings for Australian stations as observed on the East Coast of the United States during the months of April and May, 1972 and 1973, between 1100 and 1300 UTC (short-path). While a considerable spread in the data is observed, due primarily to the great variety of equipment used by the Australian stations logged, the general trend is toward increased signal strength at higher daily sunspot numbers. Apparently, the increased *D*-layer absorption that accompanies higher solar activity is more than compensated for by more efficient F_2-layer propagation. That is, with the F_2 layer generally at a higher level during periods of increased sunspot activity, the distance covered per "hop" increases. Thus, fewer hops are required to traverse the distance to Australia (in this case), and the signal losses due to ground reflections (on the order of 6 dB for a poorly conducting ground surface), and due to multiple passages through the *D* layer (again, roughly 6 dB per hop), are reduced.

It would appear, therefore, that sunspot counts, if made available on a daily basis, might be useful for preparing short-term propagation forecasts. These data are available to the public through the Space Environment Services Center (SESC) Public Bulletin Board System (PBBS), which is discussed later in the chapter. If we are to make valid short-term forecasts, it will be necessary to have a timely measure of solar activity. Solar flux has been discussed in Chapter 2, and the topic will be summarized here.

Solar Flux

The Sun is a source of radio-frequency radiation. These emissions are caused by a variety of phenomena in the solar atmosphere, including the random collisions of electrons; the noise from the quiet Sun is of the latter type. The flux (or energy level) of solar radio noise here on Earth is monitored at a number of observatories, and daily values are published by the World Data Center A for Solar-Terrestrial Physics in the *Journal of Geophysical Research.*[1] Provisional solar flux values also are broadcast on WWV at 18 minutes after each hour. These values are determined officially by the Dominion Radio Astrophysical Observatory, Penticton, BC, Canada, and are issued at 2000 UTC daily.

That the solar flux measured at 10.7 cm is a good indicator of solar activity is demonstrated in Figure 5.2. It is obvious that increased solar activity results in increased solar flux with the relationship between solar flux (*SF*) and the daily sunspot count (*R*) approximately linear:

$$SF = 73.4 + 0.62R \qquad (1)$$

A better approximation to the true relationship between these two parameters, and one which is still essentially linear, was derived by Stewart and Leftin[2]:

$$SF = 63.7 + 0.73R + 0.0009R^2 \qquad (2)$$

Let us therefore adopt the solar flux as the measure of solar activity to be used in our short-term forecasts, because it not only is a more objective measure of solar activity, but also because it is more readily available than is the daily sunspot number, which requires a computer and telephone modem to access.

The Equivalent Range Index *a* and the *K*-index

If we are to make reliable short-term forecasts, a measure of the current effects produced by solar particle

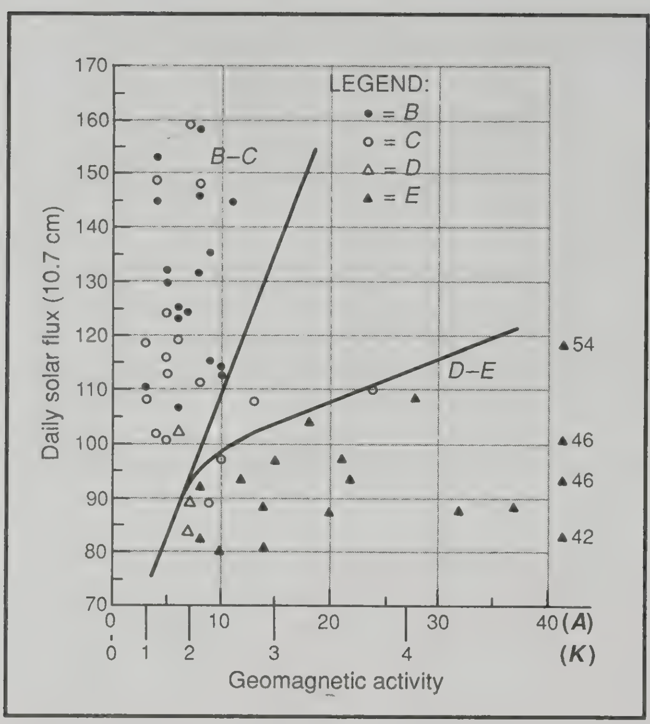

Figure 5.3. Circuit analysis, Far East Asia (HM, JA, JD, KA, KR6, VS6) to East Coast U.S. (Virginia), 14 MHz short path April/May 1972/1973, 1100–1400 UTC.

radiation (electrons and protons) is needed. The arrival of these particles in the atmosphere results in magnetic and ionospheric storms that produce signal fluctuations, fading, and noise (static). The equivalent range index, *a*, measured at a given observatory, is designed to measure solar particle radiation by its magnetic effects. Higher index values, which indicate a greater influx of solar particles, can be correlated with weaker signals and greater signal fading. Although there are exceptions, an *a*-index of less than 10 indicates periods when the ionosphere is quiet (that is, little storm activity present), while an *a*-index greater than 30 indicates times when the ionosphere is disturbed. Because magnetic disturbances are most intense in the auroral zones, effects due to the arrival of magnetic storm particles are especially pronounced on signals that pass through the higher latitudes and polar regions.

Measurements of the *a*-index are made at a number of observatories around the world and are determined at three-hour intervals.

The *K*-index also is a measure of variations in the Earth's magnetic field as determined every three hours at a given observatory. Methods to get updates on the *a*-index and the *K*-index will be discussed in a later section.

The *K*-index allows a wide range of geomagnetic activity to be expressed by a single digit, and it is related to the three-hour single-station *a*-index as is shown in Table 5.1.

Short-Term Forecasts—Methods

One way to make short-term ionospheric forecasts is to display observed signal strength on selected circuits as a function of solar flux and geomagnetic activity. Then, using current values for solar flux and the *K*-index, we will use these charts to make short-term forecasts for circuits of interest. Because the solar flux changes slowly, we even can use the previous day's value if a current reading for this parameter is not available.

In making your charts, use the *K*-index broadcast by WWV or any of the other indices of geomagnetic activity that are discussed in the following paragraphs.

Whole-Day Geomagnetic Indices, A and A_p

If you are using your logs and archival literature to prepare circuit charts, know that the preferred method for publishing information on geomagnetic activity is by means of a daily figure called the *A*-index. It may be computed as follows. Briefly, a given geomagnetic observatory will obtain eight *K*-indices, one every three hours, during a 24-hour period. Each of these is converted to an *a*-index using Table 5.1, and the eight *a*-indices so obtained are averaged to yield that station's *A*-index.

If the *a*-indices for a worldwide network of stations are averaged every three hours, we obtain the planetary three-hour index, a_p. By averaging the eight a_p indices obtained in a 24-hour period, the planetary index A_p is obtained.

To a first approximation, it makes little difference whether the *A*- or A_p-index is used to produce circuit charts. Further, regardless of the whole-day index used, the difference between this index and any one of its constituent three-hour indices (*a* or a_p) will, in 70% of the cases, be less than 5 units of measure. Thus, while three-hour indices, including the *K*-index, might better represent the geomagnetic conditions that existed at the time you made your signal-strength observations, use of the three-hour indices is not a critical factor in preparing circuit charts.

In the circuit analyses to follow, we used values for the A_p-index.[1]

Data Analysis

To produce the circuit charts that follow, signal reports were first extracted from log books for stations heard from the areas shown in Table 5.2. (This makes a good case for keeping a log with accurate signal-strength observations.) The maximum signal strength observed on a given day then was categorized according to the scheme shown in Table 5.3. Employing this technique had the effect of smoothing the data, thereby minimizing effects produced by variations in the power, antennas, and locations used by the stations logged. The categorized signal strengths then were plotted as a function of solar flux and geomagnetic activity. The results are shown in Figures 5.3, 5.5, 5.6, and 5.7. All of the circuit charts shown are for the 14 MHz (20 meter) band. We again emphasize, however, that the method can be applied to any band and to any path, and that the examples shown here are meant primarily to illustrate the type of charts that can be produced.

Far East Asia (Figure 5.3). The plot of signal strength as a function of solar flux and geomagnetic activity for the path between Far East Asia and the East Coast of the United States yields some interesting results. More than one interpretation of the data are possible. However, Figure 5.3 clearly shows that regardless of the solar flux value, A_P-indices less than 8–10 are required for good communications. Put another way, even minor geomagnetic activity (K-indices on the order of 2 or 3) can quench signals on this circuit. This effect appears to be a consequence of the fact that a significant portion of the path between the Far East and the East Coast extends along the zone of maximum frequency of occurrence of overhead aurora (Figure 5.4). As such, the Far East circuit (as well as other circuits with paths along the auroral zone) is expected to be far more sensitive to ionospheric storms (which are more intense at high latitudes) than is, for example, the Australian circuit. As we move west across the United States, absorption effects on communications with Far East stations should diminish as the path shifts to the west of the auroral zone. Similarly, even under moderately disturbed conditions, stations to the north of the East Coast of the United States (e.g., stations in the Canadian Maritime provinces) should be able to communicate somewhat more reliably with the Far East because their paths extend through the center of the auroral zone (versus along the edge).

Australia (Figure 5.5). The data for Australia indicate that geomagnetic activity is less important in determining path conditions to the East Coast than it is in determining conditions on Far East paths. This is not unexpected, since this path extends through the equatorial region, away from the debilitating effects of the zone of maximum frequency of occurrence of overhead aurora. Still, low solar activity (solar flux on the order of 80) and modest solar particle (geomagnetic) activity (A_P-indices in the range of 10–20) would appear to inhibit communications. Slightly higher values of solar flux, however, apparently override even severely disturbed ionospheric conditions. For example, solar flux values of even 92–95 were able to overcome the effects associated with ionospheric storms characterized by A_P-indices in the low 40s. Thus, even in times of major ionospheric storms, and except for the most depressed periods of sunspot activity, communications between Australia and the East Coast of the United States should be possible.

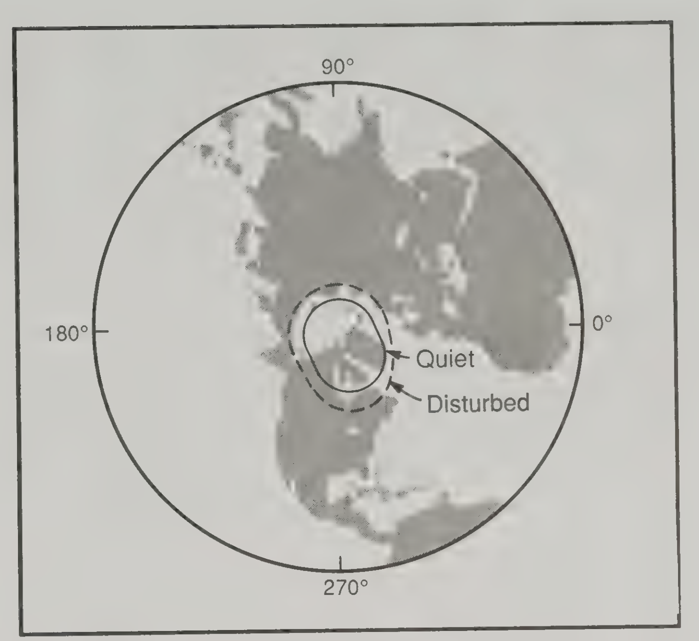

Figure 5.4. Location of the northern zone of maximum frequency of occurrence of overhead aurora on magnetically quiet days and magnetically disturbed days. (After Y.I. Fieldstein[3])

Asiatic Russia (UA9) (Figures 5.6 and 5.7). The results for the 14 MHz short path between Asiatic Russia and the East Coast in the Spring and Fall are similar, and they will be discussed together. Although it might have been expected that the circuit to Asiatic Russia would show a strong dependence on the auroral zone (Figure 5.4), as did the circuit to the Far East, such is not the case. The data suggest that even for a solar flux of 80 and an A_P-index in the low 20s, signals with fair strength still may be heard on the East Coast. The reason for this is that while the path to northern Asia does intersect the zone of maximum occurrence for overhead aurora at two places, it does not lie along this zone as is the case for a significant portion of the path from the East Coast to the Far

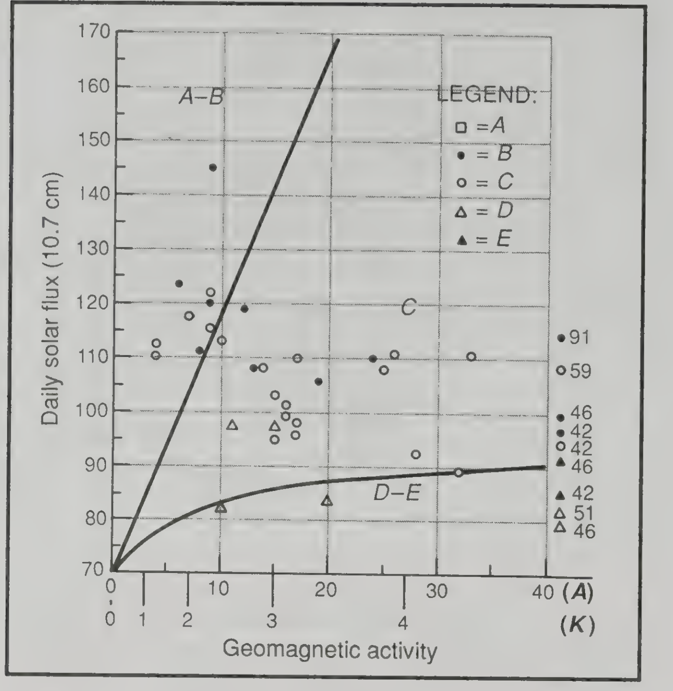

Figure 5.5. Circuit analysis, Australia to East Coast U.S. (Virginia), 14 MHz short path, April/May 1972/1973, 1100–1300 UTC.

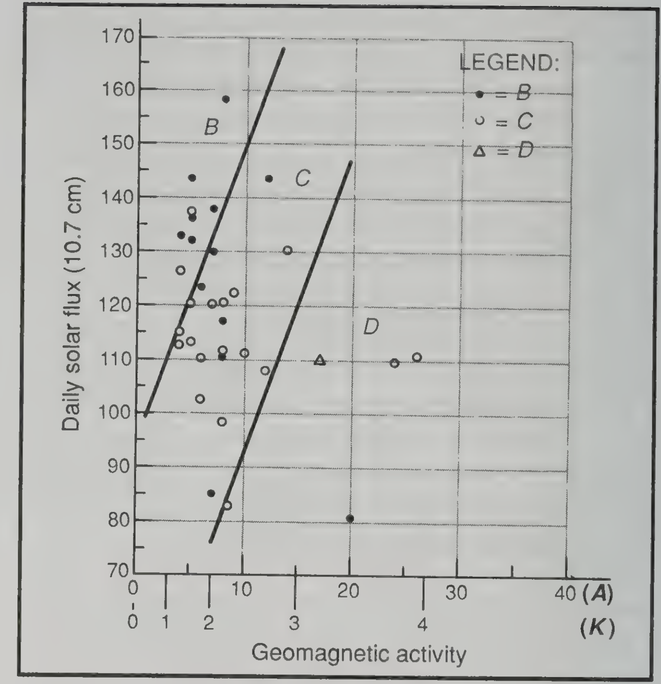

Figure 5.6. Circuit analysis, Asiatic Russia (UA9) to East Coast U.S. (Virginia), 14 MHz short path, March/April/May 1972/1973, 0100–0330 UTC.

East. Thus, while signals from northern Asia will show the effects of passing through the auroral zone (for example, auroral flutter), this path could open even under conditions when mild ionospheric storms are in progress.

Using The Circuit Analysis Charts

Once you have derived circuit analysis charts for your favorite paths (from logged signal-strength data, and from published or broadcast values of solar and geomagnetic data), simply choose the path to be used based on the time of day and the time of year. Then, listening to WWV, determine the latest values for solar flux and the Boulder *A*- or *K*-indices. By entering the graph with these values, you will obtain a fairly reliable indication of the signal-strength level to be expected.

For example, let us assume you live on the East Coast, that it is around 1200 UTC on a day in April, and that you wish to communicate with Japan. As such, reference is made to the circuit analysis chart in Figure 5.3. At 1118 UTC, WWV indicates the solar flux is 80, while the estimated *A*-index is 30. For this combination of solar and geomagnetic indices, Figure 5.3 and Table 5.3 indicate that no openings are expected.

On the other hand, if WWV had indicated a solar flux of 130 and an estimated *A*-index of 5, the 20 meter band will probably experience a good opening (B), with strong signals being heard from the Far East.

5.2 A Breakthrough in Simplifying Ionospheric Forecasts

In Section 5.1, a method of short-term forecasting was discussed that is based upon a relationship between observed variations in signal levels on a particular circuit, and solar and geomagnetic activity. However, it often is not convenient nor possible to devote time to making the day-to-day observations that are required over a period of a month or two to develop the data shown, for example, in Figure 5.3. Thus, in this section we discuss a short-term forecasting method developed by the authors that uses the long-term Master Propagation Charts contained in Chapter 4 in place of signal-level observations.

Short-Term Forecasting

Solar flux values indicate the degree of ionization in the Earth's atmosphere, and the geomagnetic indices (e.g., *A*, *K*, etc.) are a measure of the influx of solar particles and their impact in terms of activity in the Earth's magnetic field. Taken together, they give a relatively accurate picture of overall ionospheric propagation conditions.

With few exceptions, the higher the value of solar flux and the lower the level of geomagnetic activity, the better will be ionospheric conditions. Conversely, the lower the solar flux and the higher the geomagnetic activity, the poorer will be the conditions.

Figures 5.8 through 5.12 graphically show first-order relationships among solar flux, geomagnetic activity indices, and categories of high-frequency propagation expressed subjectively as **Above Normal, High Normal, Low Normal, Below Normal,** and **Disturbed**. A separate graph is provided for each of the phases of solar activity experienced during a sunspot cycle: Low, Moderate, High, Very High, and Intense. Geomagnetic activity is shown both in *A* and *K* units.

As an example of how to use figures such as Figure 5.8, assume that the solar activity is in a Low phase and that the latest WWV broadcast at 18 minutes after the hour reports a solar flux of 80 and an estimated *A*-index of 7. The intersection of the solar and geomagnetic indices broadcast by WWV falls within the area categorized as High Normal. While this result, by itself, is not related directly to any particular path or band, it does suggest that it would be worthwhile to get on the air. On the other hand, if a solar flux value of 75 is reported, along with an estimated *A*-index of 25, you can generally expect poor conditions.

Marriage Between Short-Term Forecasts and Long-Term Predictions

While a general overview of high-frequency propagation conditions obtained from Figures 5.8 through 5.12 can be very useful on a day-to-day basis, short-term forecasts are of considerably greater value when they can be related directly to particular paths on specific bands.

In Section 5.1 we related short-term forecasts to signal variations on several circuits for which careful signal-strength records had been kept for as long as three years. It is now possible to make short-term forecasts without the need for going through such a time-consuming operation by using the Master Propagation Charts given in Chapter 4.

High-frequency propagation predictions for DX from the three main geographical areas of the continental United States (eastern, central, and western) to more than a dozen different geographical areas throughout the world appear in Chapter 4. Also given in Chapter 4 are short-skip predictions for distances up to 2300 miles, and for openings from the continental United States to Hawaii and Alaska. While the explanation that follows uses the DX predictions as an example, the same method will apply to the short-skip predictions as well.

With respect to the propagation predictions in Chapter 4, a number between 1 and 4, appearing in parentheses (), follows the times given in the Master DX Propagation Charts for each band opening on a particular circuit. This number is called the **propagation index**, and it is keyed to the number of days during the month on which openings are likely to occur as follows:

(4) Openings are likely to occur on more than 22 days during the month;

(3) Openings are likely to occur between 14 and 22 days during the month;

(2) Openings are likely to occur between 7 and 13 days during the month;

(1) Openings are likely to occur on less than 7 days during the month:

While the propagation index indicates the likely number of days the opening should take place, it does

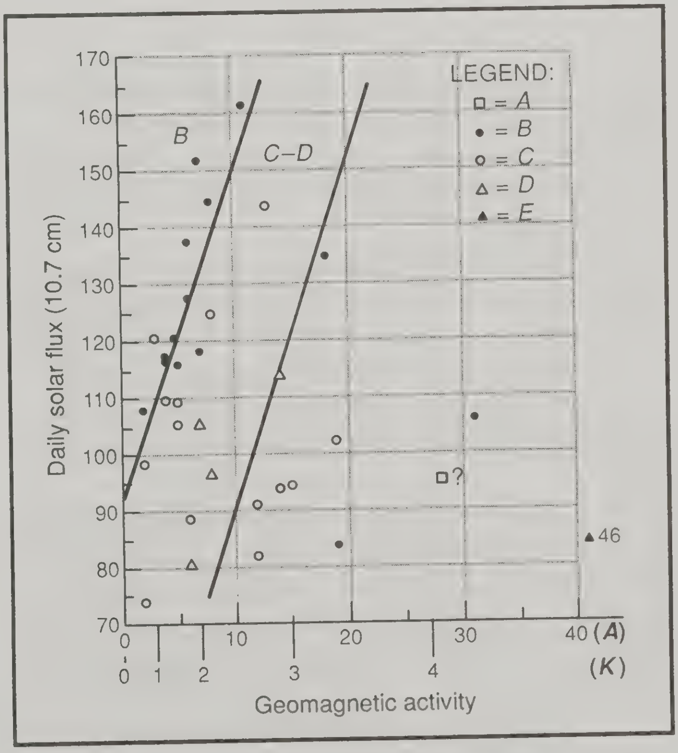

Figure 5.7. Circuit analysis, Asiatic Russia (UA9) to East Coast U.S. (Virginia), 14 MHz short path, August/September/October 1972/1973, 0100–0330 UTC.

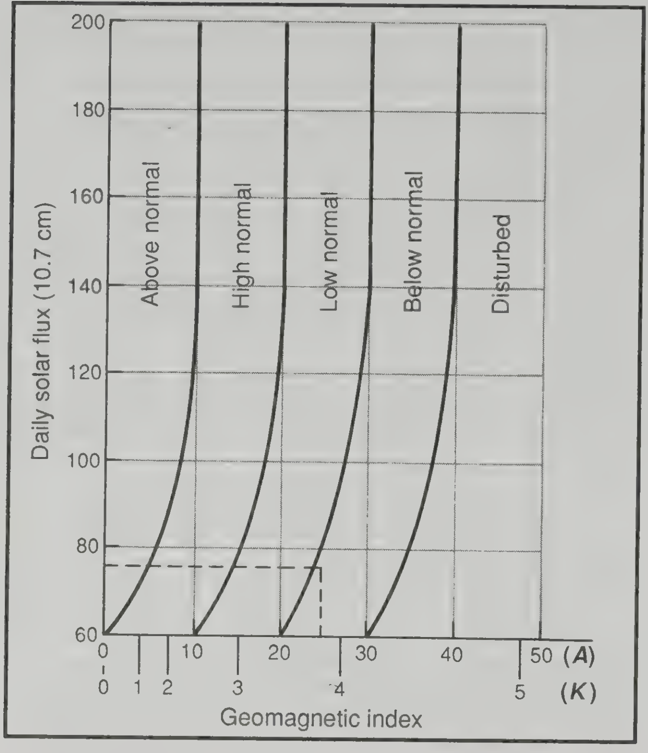

Figure 5.8. Intersection of given values of solar flux and geomagnetic activity determine expected HF ionospheric propagation conditions. (Example: Solar flux is 75 and *A*-index is 25; expect Below Normal conditions.) Use this chart during a Low phase of solar activity (smoothed sunspot range: 0 to 30).

not give the actual dates. A marriage between these predictions and short-term forecasts discussed previously *will permit the actual dates to be determined.* First, however, we will need the information given in Tables 5.4 and 5.5.

Table 5.4 ties together signal-quality ratings (*A* through *E*) and the propagation indices (1 to 4) with the categories of general conditions used in Figures 5.8 through 5.12 for short-term forecasts. Table 5.5, on the other hand, relates ranges of expected signal strength to the signal-quality ratings (*A* through *E*) of Table 5.4.

With the long-term propagation predictions given in Chapter 4, Figures 5.8 through 5.12, and Tables 5.4 and 5.5, it is now possible to determine expected conditions on a day-to-day basis for any phase of the solar cycle, for any path, on any high-frequency band, and at any time.

As an example, suppose you live in the eastern third of the U.S., and you have a schedule to keep on 20 meters between 2000 and 2100 UTC with a station in western Europe. Solar activity is Moderate. Assume that the appropriate Master DX Propagation Chart shows a propagation index of (2) for this path at the schedule time. The last WWV propagation broadcast before the schedule, at 1918 UTC, reported a solar flux of 87 and an estimated *A*-index of 15. Entering Figure 5.9, these values are found to intersect in the Low Normal range.

Next, using Table 5.4, determine the expected signal quality at the intersection of the propagation index (2) and Low Normal conditions. You find it to be *D*. A check of Table 5.5 for the definition of *D* indicates that you can expect a poor opening with weak signals and with considerable fading and noise. Specifically, you can expect the signal strength of the western European station to be on the order of S-1 to S-3.

In the same example, had the solar flux been 100 and the *A*-index 7, the resulting signal quality would have been a *C*, with chances for a fair opening and stronger signals.

Here's another example, this one showing how expected signal quality can vary on two different paths under the same category of ionospheric conditions. Assume that the Master DX Propagation Charts show that between 0400 and 0600 UTC, the 20 meter band is expected to open from the western states to the South Pacific with a propagation index of (4) and to South Asia with an index of (1). The solar phase is High. Let's assume that at 0318 UTC, WWV reports a solar flux of 120 and an estimated *A*-index of 7. From Figure 5.10, these two values are seen to fall in the area defined as High Normal. Table 5.4 shows that for High Normal conditions and a propagation index of (4), the signal quality expected on the path to the South Pacific is *A*, while for the path to South Asia, for which the propagation index is (1), the resulting signal quality is expected to be *C-D*. Table 5.5 translates these into an expected S-9 + 30 dB or higher signal from the South Pacific and an S-1 to S-9 signal from South Asia.

In summary, to relate solar flux and geomagnetic activity levels broadcast by WWV to path openings as they appear in the Master Propagation Charts contained in Chapter 4 (or in the "Propagation" column in *CQ* magazine[4], do the following:

1. Obtain the "propagation index" for the desired path opening from the appropriate Master DX or Short-Skip Propagation Chart appearing in Chapter 4;
2. Obtain the latest "solar flux" and "geomagnetic" activity values from WWV; these are broadcast at 18 minutes after each hour;
3. For the appropriate phase of solar activity (which

can be determined from the "Propagation" column in *CQ* magazine), enter Figures 5.8 through 5.12 with the "solar flux" and "geomagnetic" activity values in order to determine the "expected conditions" for HF ionospheric propagation;

4. Use Table 5.4 to determine the "expected signal quality" from the "expected conditions" and the "propagation index";
5. Use Table 5.5 to convert the "expected signal quality" into a subjective description of conditions and to obtain an "expected signal-strength range."

In sum, Figures 5.8 through 5.12, together with Tables 5.4 and 5.5, permit the solar flux and geomagnetic activity levels broadcast by WWV to be related directly to path openings as they appear in the Master Propagation Charts of Chapter 4. Further, using a similar method, it is possible to make day-to-day forecasts of ionospheric conditions up to 27 days in advance, and this is the subject to which we now turn.

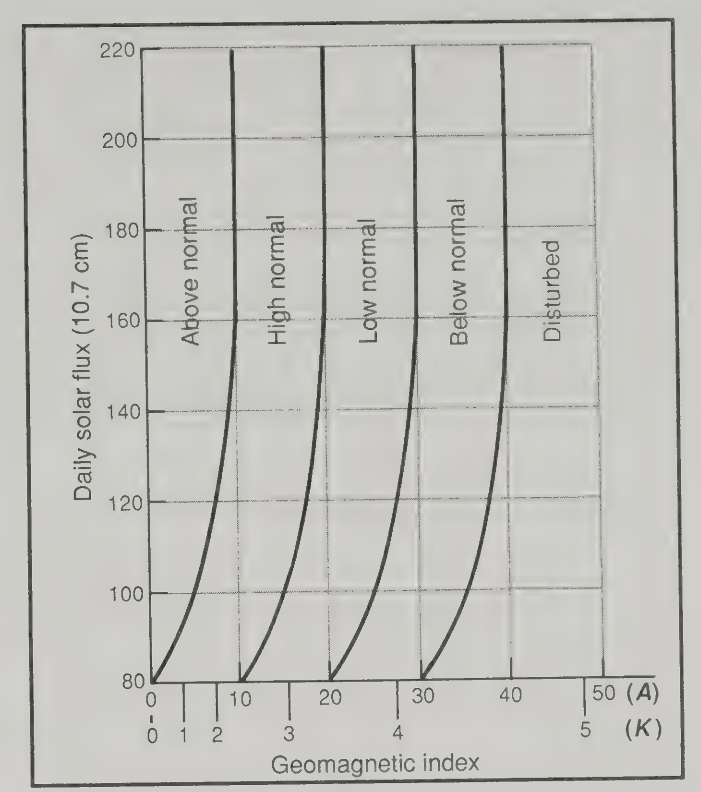

Figure 5.9. Ionospheric propagation conditions as a function of solar flux and geomagnetic activity during a Moderate phase of solar activity (smoothed sunspot range: 30 to 60).

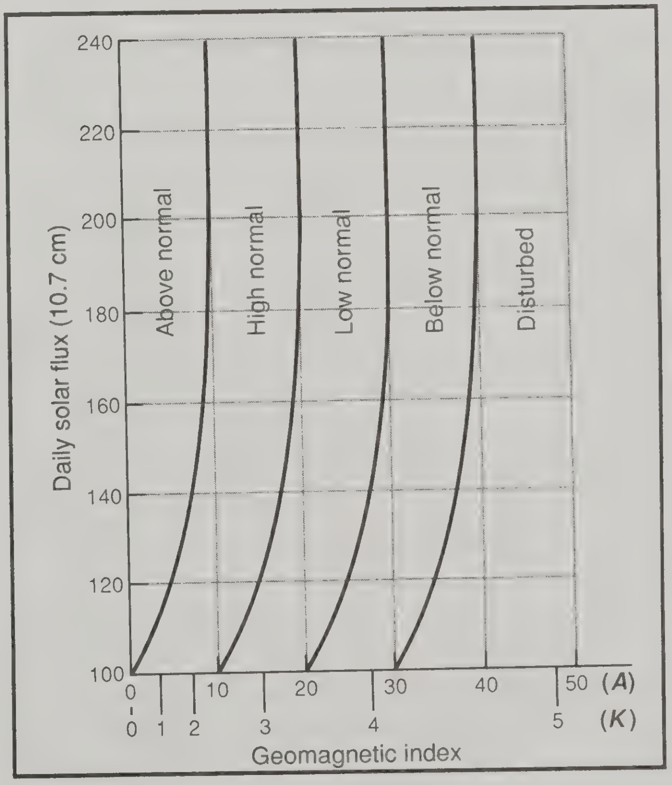

Figure 5.10. Ionospheric propagation conditions as a function of solar flux and geomagnetic activity during a High phase of solar activity (smoothed sunspot range: 60 to 90).

The 27-Day Solar Rotation Period

The Sun makes one complete rotation on its axis in about 27½ days. There is a very good chance, therefore, that if a group of sunspots is in a position to affect the Earth's ionosphere today, it will be back in the same position about 27 days from now. Thus, one might expect ionospheric propagation conditions to recur every 27 days or so. Although the recurrence of similar ionospheric conditions every 27 days is not always observed (old sunspots can disappear and new ones form during one solar rotation, as was the case of Region 5395 in March 1989), it does happen a high percentage of the time. This is particularly true during periods of low solar activity, near the end of an 11-year cycle, when a given sunspot region may remain intact over six or more consecutive rotations of the Sun.

An example of the recurrence tendency for the solar flux is shown in Figure 5.13. Shown are daily values for the solar flux that were observed during the last five months of 1974. Note that the solar flux changes slowly day to day. An example of the recurrence tendency for geomagnetic conditions is shown in Figure 5.14. Here, the *A*-index is plotted daily for the same period. While the behavior of the Earth's magnetic field is fairly erratic, the recurrence of high and low periods of activity over a 27-day period stands out.

27-Day Forecasts

Because both solar flux and geomagnetic activity show an approximate 27-day recurrence tendency,

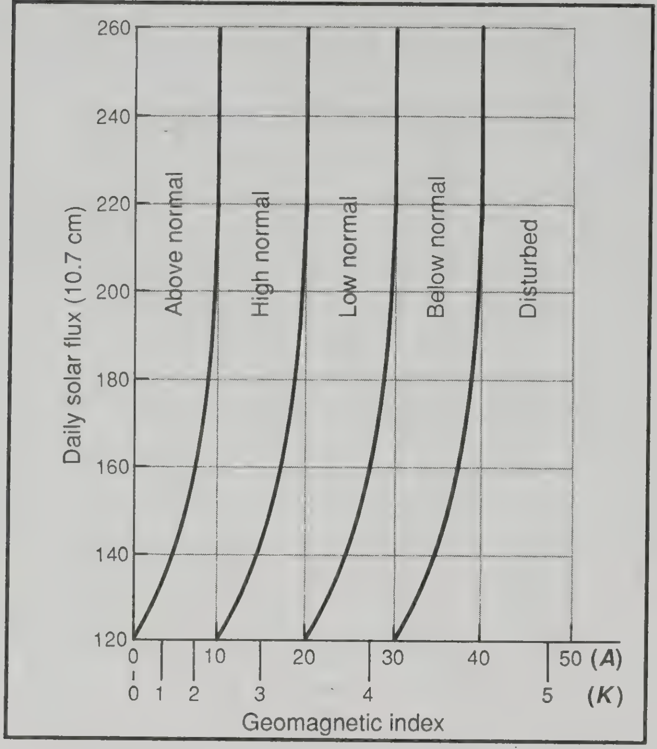

Figure 5.11. Ionospheric propagation conditions as a function of solar flux and geomagnetic activity during a Very High phase of solar activity (smoothed sunspot range: 90 to 120).

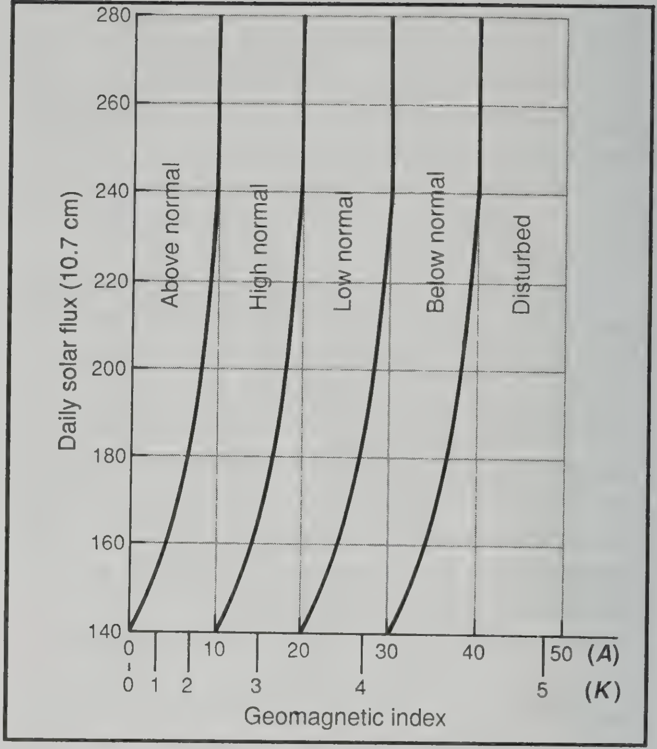

Figure 5.12. Ionospheric propagation conditions as a function of solar flux and geomagnetic activity during an Intense phase of solar activity (smoothed sunspot range: greater than 120).

observation of these parameters can be used to make a forecast for up to 27 days in advance. That is, to a first approximation, conditions that exist today are very likely to repeat in about 27 days.

To see how a radio operator or an SWL can make 27-day forecasts, consider the following example. Suppose that the solar phase is Low and that on 1 March, WWV announcements at 18 minutes past each hour indicate that the solar flux is in the mid-70s and the estimated *A*-index is 25. Reference to Figure 5.8 shows that under these circumstances, conditions on the high-frequency bands should be, in general, Below Normal. Using arithmetic or by counting days on the calendar, add 27 days to 1 March. This comes out to be 28 March, and so, you also can expect conditions to be Below Normal on this date.

If you keep a daily record of the solar flux and the *A*-index values broadcast by WWV, you should be able to predict conditions on the HF bands up to 27 days in advance. It will not always work out, of course, but you may score as high as 80–90%, especially late in the solar cycle.

Day-to-day forecasts of conditions on specific paths can be derived 27 days in advance by using the Master DX Propagation Charts in Chapter 4 together with Figures 5.8 through 5.12 and Tables 5.4 and 5.5, in the manner discussed earlier for making 24-hour forecasts. As an example, suppose this is 1 March, and you want to arrange a schedule from your station in the central part of the United States with a friend in Tokyo. Let's place the time of the schedule about a month from now on 20 meters, and at 1300 UTC. Solar activity is High. Assume that the appropriate Master DX Propagation Chart shows a propagation index of (2) for these circumstances. From Table 5.4, the signal quality expected on this path will be *B* when conditions are Above Normal and *C* when conditions are High Normal. Under poorer conditions, it would be *D* or *E*, which is unsuitable.

You begin listening today to WWV at 18 minutes past each hour for the values of the solar flux and the *A*-index. You are waiting for a combination of solar flux and *A*-index values that will produce Above Normal or High Normal conditions as defined in Figure 5.10. Assume that this occurs on 6 March, when an announcement indicates that the solar flux was 120 and the estimated *A*-index was 2. Adding 27 days to 6 March yields a recurrence date of 2 April.

You now can notify your friend in Tokyo that the best time for a schedule is at 1300 UTC on 2 April, and you can do so with confidence that there is a very good chance it will work out well.

5.3 WWV Broadcasts and Other Sources of Solar Flux and Geomagnetic Activity Indices

	Propagation Index			
Expected Conditions	**(4)**	**(3)**	**(2)**	**(1)**
Above Normal	A	A	B	C
High Normal	A	B	C	C-D
Low Normal	B	C	D	D-E
Below Normal	C	C-D	D-E	E
Disturbed	C	D	E	E

Table 5.4. Expected signal quality (A to E) as a function of propagation index (1 to 4) and expected conditions. Example: A path opening with a predicted propagation index of (3) is expected to have a signal quality of C during Low Normal conditions.

The "Information Highway" is in full operation for those readers who want more and more geophysical information. Earlier chapters of this book provided the proper foundation for interpreting the wealth of information that is available. Now, in addition to the traditional broadcasts on WWV and WWVH on the time standard frequencies of 2.5, 5.0, 10.0, 15.0, and 20 MHz (WWVH does not transmit on 20 MHz), users of the HF spectrum can obtain the information they need over the telephone. They also can access a vast amount of current geophysical data over various bulletin board systems. An organization responsible for providing these services is the Space Environment Services Center (SESC), an arm of NOAA in the Department of Commerce. The SESC monitors the Sun and the near-Earth environment from a network of ground- and satellite-based sensors that provide data in real time. Solar activity is monitored from satellites, primarily the GOES weather satellites, and by solar observatories around the world. SESC forecasters issue alerts of significant solar and geomagnetic events. Alerts and other data are disseminated worldwide via a variety of delivery systems, generally available to customers without cost. The wide variety of services are described in the document "Space Environment Services Center Products and Services User Guide." It can be obtained directly from SESC, Space Environmental Laboratory,[5] or through the National Technical Information Service.[6] Table 5.6 has been included to illustrate the variety of SESC information available and the methods used to deliver it. Note that the SESC uses two potent, global data distribution networks to update their summaries and alerts. These are the Continental Meteorological Data System (COMEDS) and the Space Environment Laboratory Data Acquisition and Display System (SELDADS). Also, the system accesses the National Geophysical Data Center (NGDC), which is the national data archive center for solar-terrestrial physics. For our purposes, we will discuss four of the services that are most appropriate for the average radio amateur or shortwave listener: the WWV broadcasts, the SESC Public Bulletin Board System, sources accessible via INTERNET, and a private bulletin board system. Specifically, we will discuss what they provide and how we can use them.

WWV/WWVH Broadcasts

In the middle 1970s, radio amateurs became aware of the relationship among 10.7 cm solar flux, geomagnetic activity, and the probability of the higher bands (15, 10, and 6 meters) opening. A rough estimation said that as the solar flux rose above 100, there was a better probability that 10 meters would open. As the peak of Cycle 21 approached, more and more amateurs listened to WWV for the current solar flux value. As the solar flux was watched more closely, it was learned that when the flux rose to a high level, it was several days before a change in propagation conditions was experienced on 10 and 15 meters. It took time to "pump up the ionosphere." Regardless, radio amateurs now had an objective way of determining

Symbol	**Signal Quality**	**Signal Strength**
A	Excellent opening, exceptionally strong, steady signals	r>S9 + 30 dB
B	Good opening, moderately strong signals with little fading or noise	S9<r≤S9 + 30 dB
C	Fair opening, signals between moderately strong and weak, with some fading and noise	S3<r≤S9
D	Poor opening, signals weak with considerable fading and noise	S1<r≤S3
E	No opening expected	

Table 5.5. Signal quality (A to E) defined in terms of expected signal levels. Based on typical amateur radio installations.

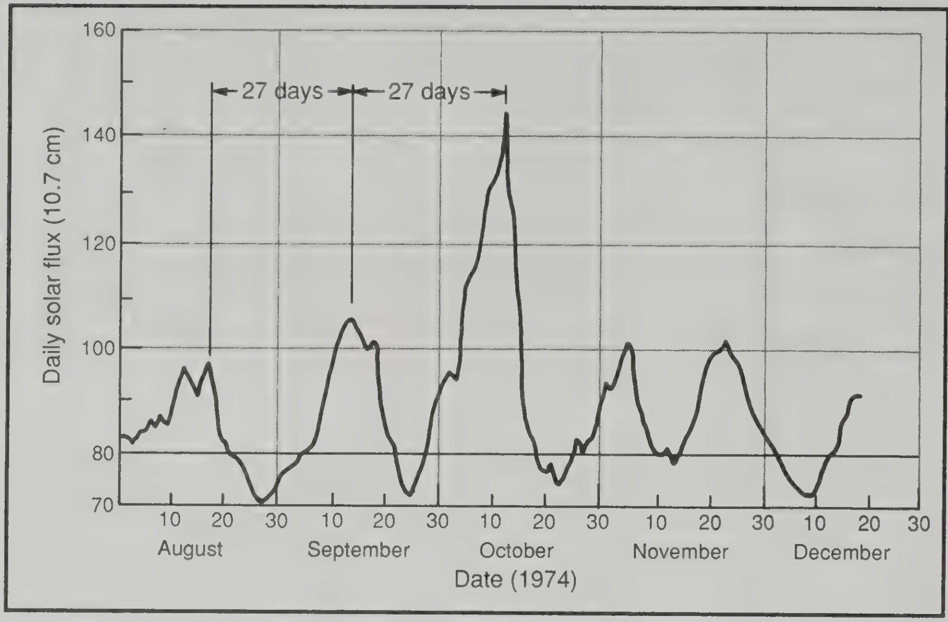

Figure 5.13. Solar flux as a function of time (August 1 through December 17, 1974). Note tendency toward 27-day recurrence.

general ionospheric conditions, and even today, the WWV broadcasts are a mainstay of high-frequency propagation forecasters.

The WWV/WWVH broadcasts at 18 minutes (WWV) and 45 minutes (WWVH) after the hour contain the Geophysical Alert Message. At these times, the SESC broadcasts a 40-second message containing the latest solar and geomagnetic indices, a summary of recent significant activity, and a forecast of activity for the next 24 hours. This message is updated every three hours. Solar flares, proton events, geomagnetic activity, and stratospheric warming alerts also are

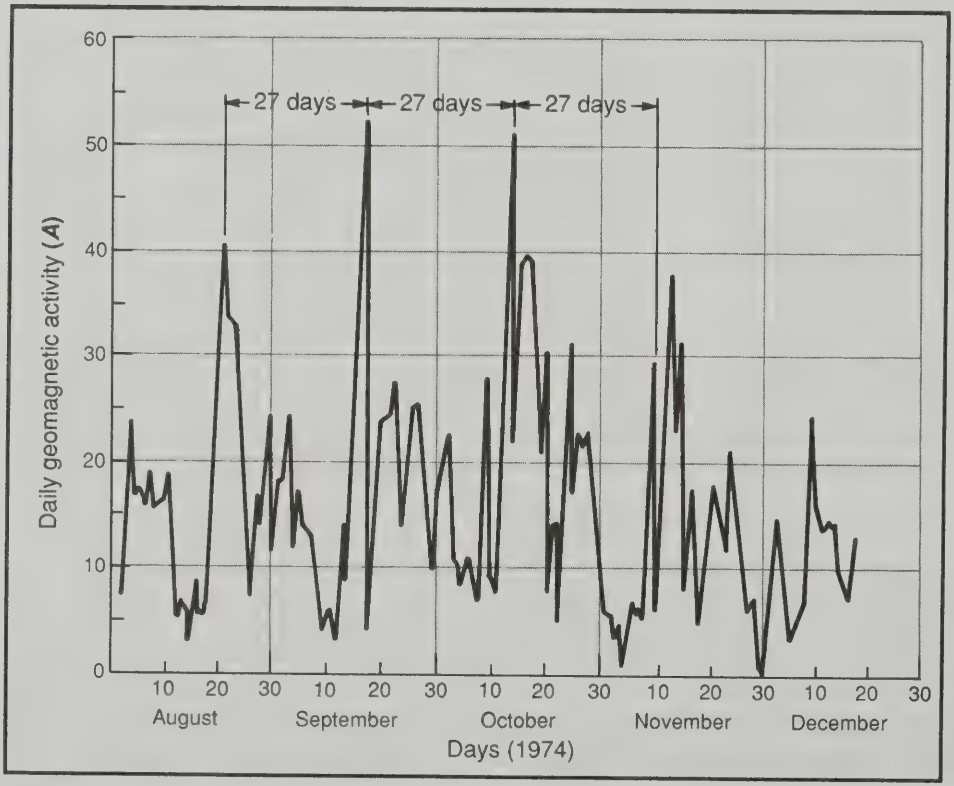

Figure 5.14. Geomagnetic activity (*A*) as a function of time (August 1 through December 17, 1974). Note tendency toward 27-recurrence.

Products & Services	Delivery Systems									
	Phone	Fax	Telephone Recording & & Radio Bcst	Satellite Broad-cast	COMEDS	SELDADS	Electronic File Transfer	Bulletin Board	Mail	NGDC
Alerts & Warnings	★	★	★	★	★					
Geophysical Alert Message			★							
Report of Solar and Geophysical Activity					★	★	★	★		
Solar Region Summary					★	★	★	★		
Solar and Geophysical Activity Summary					★	★	★	★		
Solar Corona Disturbance Report					★	★	★	★		
High-Frequency Radio Propagation Report					★	★	★	★		
World Warning Agency GEOALERT					★	★	★	★		
Space Weather Data				★	★	★	★	★		★
Solar Images							★			
Solar-Synoptic Analysis Drawing		★							★	
"The Weekly"							★	★	★	★
Publications									★	
Short-term and special support arranged with the customer.										

Table 5.6. SESC products and services (from Reference 5).

broadcast. Users who want to get this information quickly without waiting for the broadcasts can telephone the SESC directly in Boulder, Colorado, at (303) 497-3235 for a recorded announcement, or (303) 497-3171 to speak with the duty forecaster. These calls are not toll free.

The Geophysical Alert Message contains three sections:

Latest Indices

The current UTC day and month.

The latest daily 10.7 cm radio flux from the Dominion Radio Astrophysical Observatory, Penticton, BC, Canada (issued at 2000 UTC daily).

The latest observed or estimated Boulder *A*-index.

The latest 3-hour *K*-index in Boulder.

Summary

The level of solar activity and geomagnetic conditions during the last 24 hours. If appropriate, the time and size of recent solar events (solar flares, proton events), geomagnetic storms, and polar cap absorption events are noted.

Forecast

A forecast of solar activity, geomagnetic conditions, and proton events expected in the next 24 hours.

NOAA/ERL Space Environment Laboratory BBS

P)ropagation Report
S)olar Report
R)egion Report
A)ctivity Summary
O)utlook for 27 Days
Q)uick Look Data
N)ews of Services
H)elp Menu

C)oronal Data Report
G)eoalert Message
L)og of Magnetic Data
D)ata Listing Menu
W)eekly Summary
M)UF Predictions
F)eedback to Sysop
B)ye - Leave the system

(P,S,R,A,C,G,L,D,O,W,Q,M,N,F,H,B) Choice ? __

Figure 5.15. SESC Public Bulletin Board System (PBBS) Menu.

A typical verbal broadcast, either over WWV/WWVH or the telephone, sounds like this:

Solar-terrestrial indices for 25 August follow:

Solar-flux two-two-six, and estimated Boulder *A*-index one-seven.
Repeat. Solar flux two-two-six, and estimated Boulder *A*-index one-seven.
The Boulder *K*-index at zero nine hundred UTC on 25 August was four. Repeat four.

Solar-terrestrial conditions for the last 24 hours follow:
Solar activity was high.
The geomagnetic field was active.
A major flare occurred at zero eight five zero UTC on 25 August.

The forecast for the next 24 hours follows:
Solar activity will be moderate to high.

*** Data Listing Menu ***

1) Daily Sunspot Number (SESC value and estimated RI value)
2) Daily Penticton 10.7 cm radio flux value
3) Daily Boulder 24-hour geomagnetic A-index
4) 8 Boulder 3-hourly geomagnetic K-indices
5) Daily estimated Planetary 24-hour geomagnetic A_p-index
6) 8 estimated Planetary 3-hourly geomagnetic K_p-indices
7) See this sub-menu again

Figure 5.16. Selection "D" on the PBBS produces the Data Listing Menu shown here.

Minute	Call sign	Location
:00	4U1UN/B	United Nations Headquarters, NY
:01	W6WX/B	Stanford University, Palo Alto, CA
:02	KH6O/B	Honolulu City College, HI
:03	JA2IGY/B	Japan
:04	4X6TU/B	Tel Aviv, Israel
:05	OH2B	Helsinki, Finland
:06	CT3B	Madeira Island
:07	ZS6DN/B	Irene, South Africa
:08	LU4AA	Buenos Aires, Argentina

58 Second Message Format

100 watts	QST DE W6WX/B Beacon
100 watts	-(9 seconds)
10 watts	-(9 seconds)
1 watt	-(9 seconds)
0.1 watt	-(9 seconds)
100 watts	W6WX/BSK

(Provided by John G. Troster, W6ISQ, NCDXF Beacon Coordinator, IARU International Beacon Coordinator.)

Table 5.7. Northern California DX Foundation (NCDXF/International Amateur Radio Union (IARU) 14.100 MHz Worldwide Beacon Network. (See Reference 7.)

The geomagnetic field will be unsettled to active.
A proton event is expected to begin near twelve-hundred UTC on 25 August.

(Taken from Reference 5)

The complete listing of geophysical, time, and audio services provided by WWV and WWVH, as well as the radiated powers, antennas, and coverage of each station, appears annually in the *CQ Amateur Radio Almanac*, and can also be found in the Appendix to this chapter.[7]

Public Bulletin Board System (PBBS)

More and more users of the high-frequency spectrum rely on computers for various aspects of their operations, and a large part of the population now is "computer literate." For those who have a telephone modem on their computer, the SESC Public Bulletin Board System (PBBS) provides a wide variety of solar-geophysical information—more than enough to satisfy any radio amateur's or SWL's geophysical data needs. The PBBS is available 24 hours a day, seven days a week, but it only is updated during normal working hours.

PBBS Access. The PBBS is extremely easy to use. The data are obtained via modem from a dial-up personal computer (PC) at SESC. The commercial telephone number is (303) 497-5000 for initial use and sign-in. Expert users who have been issued a user number can access the PBBS faster by calling (303) 497-5042. The system supports 300, 1200, or 2400 baud. The protocol is 8-bit data with 1 stop bit and no parity. The system will ask you some questions when you first sign on in order to gain some background information about its users. It then will assign you a user number, which will speed up subsequent "log-ons." Next, the menu shown in Figure 5.15 will be displayed; 16 options are presented, of which 13 provide some manner of solar or near-Earth environmental data.

PBBS Material (from Reference 5). The SESC PBBS provides the following options:

Activity Summary—The daily report of significant x-ray flares, proton events, or geomagnetic storms. Available at 0330 UTC.

Bye—The command to exit the PBBS.

Coronal Data Report—The daily report of coronal holes, interplanetary disturbances, and mass-ejection reports. Available at 0230 UTC.

Data Listing—30-day listing of sunspot numbers, solar flux values, and geomagnetic A- and K-indices, including the Planetary 24-hour geomagnetic A_p-index (see Figure 5.16).

Feedback to Sysop—A routine that PBBS users can use to send their comments to the system operator at SESC.

Geoalert Message—A coded message of sunspot locations, flare activity, and energetic solar-geophysical activity for the previous day, and a brief forecast of solar-geophysical activity. Available at 0430 UTC.

Help—A help menu.

Log of Magnetic Data—A tabular display of the latest 24-hour UT-day A- and K-indices for a selection of geomagnetic stations.

MUF Predictions—A routine that users can run to obtain Maximum Usable Frequency predictions for propagation paths of their choice.

News of Services—A description of new products.

Outlook for 27 Days—27-day forecast of 10.7 cm solar radio flux, A_p, and largest expected daily K_p index (from the Weekly Summary). Available each Wednesday after 0100 UTC.

Propagation Report—A simple summary and forecast of HF radio propagation conditions for the Northern Hemisphere. This product is updated every 6 hours and is posted on the PBBS.

Quick-Look Data—A tabular display of the latest 24-hour UT-day values for a selection of key solar-geophysical parameters.

Region Report—A daily report of sunspot regions for the most recent 24 hour UT-day. Available at 0100 UT.

Solar Report—The daily report of solar and geophysical activity (such as solar flares, proton events, PCSs, geomagnetic storms) and forecast for the subsequent three days. Available at 2230 UT.

```
PRIMARY HF RADIO PROPAGATION REPORT ISSUED AT 14/0530Z JUN 94.
PART I. SUMMARY  14/0000Z TO 14/0600Z JUN 94/
        FORECAST 14/0600Z TO 14/1200Z JUN 94.
                                   QUADRANT
                         I          II          III          IV
                    0 TO 90W   90W TO 180   180 TO 90E   90E TO 0
REGION      POLAR     N4          N4          N4          N4
          AURORAL     N4          N4          N4          N4
           MIDDLE     N6          N6          N7          N7
              LOW     N6          N7          N7          N7
       EQUATORIAL     N6          N7          N7          N7
PART II.
GENERAL DESCRIPTION OF HF RADIO PROPAGATION CONDITIONS
OBSERVED DURING THE 24 HOUR PERIOD ENDING 13/2400Z, AND FORECAST
CONDITIONS FOR THE NEXT 24 HOURS.  NO SIGNIFICANT DEGRADATIONS
WERE OBSERVED.
FORECAST:  NO SIGNIFICANT CHANGES ARE EXPECTED UNTIL 15 JUN,
WHEN A GEOMAGNETIC STORM IS EXPECTED TO PRODUCE DEGRADED
CONDITIONS.
PART III. SUMMARY OF SOLAR FLARE INDUCED IONOSPHERIC DISTURBANCES
WHICH MAY HAVE CAUSED SHORT WAVE FADES IN THE SUNLIT HEMISPHERE
DURING THE 24 HOUR PERIOD ENDING 13/2400Z JUN 94 . . .
     START       END          CONFIRMED          FREQS AFFECTED
                           ......NONE.....
PROBABILITY FOR THE NEXT 24 HOURS . . . . NIL.
PART IV. OBSERVED/FORECAST 10.7 CM FLUX AND K/AP.
THE OBSERVED 10.7 CM FLUX FOR 13 JUN 94 WAS 085.
THE FORECAST 10.7 CM FLUX FOR 14, 15, AND 16 JUN 94
ARE 085, 085, AND 084.
THE OBSERVED K/AP VALUE FOR 13 JUN 94 WAS 03/11.
THE FORECAST K/AP VALUES FOR 14, 15, AND 16 JUN 94
ARE 03/15, 04/30, AND 05/40.
SATELLITE X-RAY BACKGROUND: A9.9 (9.8 E MINUS 05 ERGS/CM SQ/SEC).
THE EFFECTIVE SUNSPOT NUMBER FOR 13 JUN 94 WAS 040.1.
99999
```

Figure 5.17. SESC PBBS HF Radio Propagation Report.

Weekly Summary—Text containing highlights of solar and geophysical activity during the past week and a forecast for the next 27 days. Available each Wednesday after 0100 UTC.

The times indicate when each message is updated. While this amount of information may seem overwhelming to the first-time user, the product formats are very straight forward. One of the more useful is the **Propagation Report**, which takes about a minute to dial into, log-on, print, and exit. The only cost is the price of the telephone call.

PBBS Propagation Report. The High Frequency Radio Propagation Report is prepared by the U.S. Air Force Space Forecast (AFSFC), and it is issued jointly with SESC. The Primary daily forecast is issued at 0600 UTC with secondary forecasts released at 0000, 1200, and 1800 UTC. Figure 5.17 shows an example of this report. Each propagation report has four parts. Part I presents an estimate of expected propagation conditions for the Northern Hemisphere. An alpha-numeric designator representing expected propagation conditions is assigned to 20 low-, middle-, auroral-, and polar-latitude segments. Part II contains a plain-language discussion of geomagnetic and ionospheric conditions and their effects on propagation. Part III contains a summary of solar disturbances that have occurred and the probability of future occurrence. Part IV is a three-day forecast of *K*- and *A*-indices and 10.7 cm solar flux. If there is something that the reader does not understand, there is an excellent descriptive text of the Propagation Report in the "help" section. Overall, this report provides everything required to do propagation forecasting in the way described earlier in this chapter. For the price of a telephone call, SESC has provided an easy and comprehensive source of solar-geophysical data that is more than adequate for use in preparing your own specific HF circuit forecasts.

INTERNET Data

For readers who have access to the INTERNET E-Mail computer network, a comprehensive worldwide

WORLDWIDE 10 METER BEACONS

Freq.	Call	Operation	Location	Notes
28.175	VE3TEN	C	OTTAWA, ONT.	10W, GP
28.1825	SV3AQR/B	C	AMALIAS, GREECE	4W, GP
28.191	VE6YF		EDMONTON, ALTA.	10W
28.195	IY4M	ROBOT	BOLOGNA, ITALY	20W, 5/8 GP
28.200	GB3SX	C	CROWBOROUGH, ENGLAND	8W, DIPOLE
28.201	LU8ED		ARGENTINA	5W
28.202	KE5GY	I	ARLINGTON, TX	5W, VERTICAL
28.2025	ZS5VHF		NATAL, RSA	5W, GP
28.204	DLIGI	C	GERMANY	100W, VERT DIPOLE
28.205	KA3OEM		MEADVILLE, PA	27W, YAGI/WEST
28.206	KJ4X		PICKENS, SC	2W, VERTICAL
28.2075	N8ZKP	C	BROOKPARK, OH	10W, VERT
28.208	WA1IOB	C	MARLBORO, MA	75W, VERT
28.209	NX2O	C	STATEN ISLAND, NY	10W, GP
28.210	3B8MS	C	MAURITIUS	GP
28.210	K4KMZ	I	ELIZABETHTOWN, KY	20W, VERT
28.210	KC4DPC	C	WILMINGTON, NC	4W, DIPOLE
28.212	EA6RCM		PALMA DE MALLORCA	4W, 5 EL YAGI NNE
28.2125	ZD9GI	C	GOUGH ISLAND	GP
28.213	PT7BCN	C	CEARA, BRAZIL	
28.216	GB3RAL	C	SLOUGH, ENGLAND	20W, GP
28.2175	WB9VMY	C	CALUMET, OK	2W, DIPOLE
28.218	W8UR	C	MACKINAC ISLAND, MI	0.5W, VERT
28.2185	PT8AA		RIO BRANCO, BRAZIL	5W, GP
28.2195	LU4XS		CAPE HORN, ARGENTINA	
28.220	5B4CY	C	CYPRUS	26W, GP
28.221	PY2GOB		SAN PAULO, BRAZIL	15W, VERT
28.222	W9UXO	C	NR CHICAGO, IL	10W, GP
28.2225	HG2BHA	C	TAPOLCA, HUNGARY	10W, GP
28.225	N6TWX	I	GRASS VALLEY, CA	30W, 3 EL YAGI
28.225	KW7Y		EVERETT, WA	4W, OMNI
28.225	PY2AMI	C	SASO PAULO, BRAZIL	5W, DIOPOLE
28.2275	EA6AU	C	MALLORCA, BALEARIC IS	10W, 5/8 GP
28.230	ZL2MHF	C	MT.CLMIE, NEW ZEALAND	50W, VERT DIPOLE
28.232	W7JPI	C	SONOITA, AZ	5W, 3 EL YAGI NE
28.233	KD4EC	C	JUPITER, FL	7W, GP
28.235	VP9BA	C	HAMILTON, BERMUDA	10W, GP
28.237	NV6A	C	SAN DIEGO, CA	0.5W, VERT
28.2375	LA5TEN	C	OSLO, NORWAY	10W, 5/8 GP
28.2405	5Z4ERR	C	KIAMBU, KENYA	
28.244	WA6APQ	C	LONG BEACH, CA	30W, Vert
28.245	A92C		BAHRAIN	DIPOLE NW/SE
28.2455	ZS1CTB	C	CAPETOWN, RSA	20W, 1/4 VERT
28.246	N8KHE	C	MACKINAW, MI	0.050W, VERT
28.2475	EA2HB	I	SPAIN	6W, GP
28.248	K1BZ	C	BELFAST, ME	5W, VERT DIPOLE
28.2495	EA3JA		BARCELCONA, SPAIN	
28.250	W3SV	C	ELVERSON, PA	10W, VERT
28.250	KHTF	C	DES MOINES, IA	2W, GP
28.250	Z21ANB	C	BULAWAYO, ZIMBABWE	8W, GP
28.250	WA4SLT	I	HASTINGS, FL	20W, Vert
28.2505	4N3ZHK	C	MT.KUM, YUGOSLAVIA	1W, VERT
28.252	WJ7X	C	SEATTLE, WA	5W, RINGO
28.2525	OH2TEN		FINLAND	
28.255	LUIUG		GRAL PICO, ARGENTINA	5W, GP
28.2575	DK0TEN	C	ARBEITSGEN, GERMANY	40W, GP
28.258	WB4JHS	I	KISSIMMEE, FL	5W, VERT
28.259	WB9FVR	C	PEMBROKE PINES, FL	1W, DIPOLE
28.260	VK5WI	C	ADELAIDE, AUSTRALIA	10W, GP
28.262	VK2RSY	C	SYDNEY, NSW, AUSTRALIA	25W, GP
28.263	N6PEQ	C	TUSTIN, CA	2W, HORZ DIPOLE
28.264	VK6RWA	C	PERTH, WA, AUSTRALIA	

28.265	VK4RIK		CAIRNS, AUSTRALIA	
28.266	VK6RTW	C	ALBANY, WA, AUSTRALIA	
28.266	KB4UPI	C	BIRMINGTON, AL	20W, 1/4 VERT
28.268	VK8VF		DARWIN, AUSTRALIA	
28.2685	W9KFO	I	EATON, IL	0.750W, VERT
28.270	ZS6PW	C	PRETORIA, RSA	10W, 3 EL YAGI
28.270	VK4RTL	C	TOWNSVILLE, QLD, AUSTRALIA	
28.2705	KF4MS	C	ST PETERSBURG, FL	5W
28.2725	9L1FTN	I	FREETOWN, SIERRA LEONE	10W, VERT DIPOLE
28.2745	ZS1LA		STILLBAY, RSA	20W, 3 EL YAGI NW
28.275	AL7GQ	C	DENVER, CO	1W, LOOP
28.2755	N6RDX	I	STOCKTON, CA	20W, 3 EL YAGI
28.277	DF0AAB	C	KIEL, GERMANY	10W, GP
28.280	LU8EB		ARGENTINA	5W
28.282	VE1MUF	C	FREDRICKTON, NB, CANADA	0.5W, DIPOLE
28.282	VE2HOT	C	BEACONSFIELD, QUE, CANADA	5W, VERT DIPOLE
28.2825	OK0EG	C	HRADEC KRALOVE , CZECH	10W, DIPOLE
28.284	VP8ADE	C	ADELAIDE IS, NR ANTARCTICA	8W, V BEAM TO ENGLAND
28.285	N2JNT	C	TROY, NY	1W, GP
28.286	KE2DI		NR ROCHESTER, NY	2W, VERT DIPOLE
28.286	KK4M	C	LAS VEGAS, NV	5W, VERT
28.2865	N5AQM	C	ARIZONA	2W, VERTICAL
28.287	W8OMV		NR ASHEVILLE, NC	5W, GP
28.287	H44SI	C	SOLOMON IS	15W
28.288	W2NZH	I	MOORESTOWN, NJ	3W GP
28.290	SK5TEN		SWEDEN	5W
28.290	VS6TEN	C	HONG KONG	10W, VERT
28.292	ZD8HF		ASCENSION ISLAND	
28.2925	LU2FFV		SAN JORGE, ARGENTINA	5W, GP
28.284	KE0UL		GREELEY, CO	5W Omni vert
28.295	WC8E	I	CINCINNATI, OHIO	10W, RINGO
28.295	W3VD	C	LAUREL, MD	1, 5W, VERT DIPOLE
28.297	WA4DJS	I	FT LAUDERDALE, FL	30W, GP
28.3025	PT7AAC		FORTALEZA, BRAZIL	5W, GP
28.993	DF0ANN	C	NUREMBURG, GERMANY	0.30W, DELTA LOOP

C=Continuous; I=Intermittent

(Courtesy of The DX Bulletin, *Box 50 Fulton CA 95439 USA; see Reference 7.)*

Table 5.8. Worldwide 10 meter beacons.

ionospheric propagation analysis and forecast is given every day. The data consist of detailed ionospheric, geomagnetic, and solar data collected from worldwide observatories. It is presented in both graphic and narrative form. Information for accessing these data can be obtained from the following E-Mail addresses:

oler@rho.uleth.ca *or*
coler@solar.stanford.edu

Private Bulletin Board System

For readers who do not have access to INTERNET, the same data can be obtained daily from the *Solar Terrestrial Bulletin Board.* This BBS works at speeds as high as 9600 baud. There is a small annual fee for registration and full use of the resources of the BBS. Basic daily solar, geomagnetic, and ionospheric data, however, are available without charge, but a password must be requested. Additional information, registration data, and passwords can be obtained directly from Solar Terrestrial Dispatch, P.O. Box 357, Stirling, Alberta, Canada TOK 2EO.

5.4 Worldwide HF Beacon Transmissions

Radio Amateur 20 Meter Beacons

Another source of information on "real-time" propagation conditions is the dozens of HF beacon transmitters that operate around-the-clock on a worldwide basis. For example, the network of the Northern California DX Foundation (NCDXF)/International Amateur Radio Union (IARU), which consists of nine 100 watt transmitters operating on 14.100 MHz in the radio amateur 20 meter band, is shown in Table 5.7.

The beacons operate on a coordinated 10 minute sequence, with each one transmitting signals for one minute, in the order given in Table 5.7. The sequence begins with 4U1UN/B on the hour (say, 0000 UTC), with the call sign followed by four 9 second dashes at decreasing power levels of 100, 10, 1, and 0.1 watts. The sequence ends with the call sign given again. The next station, W6WX/B, starts its cycle at 0001 UTC, and so forth. These beacons provide a real-time assessment of 20 meter propagation conditions on a worldwide basis. Not only do they indicate when the band is open to various parts of the world, but they also are excellent, reliable signal sources for use in developing the type of circuit analyses and do-it-yourself forecasting aids discussed earlier in this chapter.

The IARU is in the process of developing an expanded worldwide beacon network to operate in the 14, 17, 21, 24, and 28 MHz amateur bands.

Other HF Beacons

The International Telecommunications Union (ITU) has activated a new HF beacon transmitter in Sveio, Norway, as part of a worldwide HF field strength measurement campaign. The new beacon was provided by the Norwegian Telecommunications Regulatory Authority and Norwegian Telecom, and joins a similar beacon station on the air from Australia since 1990.

LN2A operates 24 hours a day at 1 kW on CW to a 5-band trap vertical antenna. VK4IPS in Brisbane, Australia, also operates 24 hours a day, running 1 kW to an omni-directional spiral antenna.

The schedule of frequencies (in kHz) for both is as follows:

Time (min. past hr.)	VK4IPS	LN2A
0, 20, 40	5470	14405
04, 24, 44	7870	20945
08, 28, 48	10407	5470
12, 32, 52	14405	7870
16, 36, 56	20945	10407

A new beacon began operation May 13, 1993, from Cape Prince of Wales, Alaska (67N, 168W). Transmissions are narrow-band CW and FSK. Its call sign is NAF, and it runs 100 watts to a three-band fan dipole on the following schedule (all frequencies in kHz):

Time (min. past hr.)	Frequency
00, 01	5604
20, 21	11004
40, 41	16804

The beacon will be monitored by government facilities in Fairbanks, Alaska; Seattle, Washington; State College, Pennsylvania; and San Diego, California. The project's sponsor is the Naval Security Group Command in Washington, D.C.

A government spokesman said the project is "purely scientific." The purpose of the project as described is to provide a "rigorous verification" of the field strength models employed by HF propagation prediction programs such as IONCAP, which are used, for example, to generate the predictions appearing in Chapter 4.

10 Meter Beacons

A list of 10 meter beacons operating throughout the world is shown in Table 5.8.

5.5 References

1. "Geomagnetic and Solar Data," published monthly in the *Journal of Geophysical Research,* Space Physics Series, The American Geophysical Union, Washington, D.C.

2. Stewart, F. G. and M. Leftin, "Relationship between Ottawa 10.7 cm Solar Radio Noise Flux and Zurich Sunspot Number," *Telecommunication Journal,* Vol. 39, No. III, 1972.

3. Fieldstein, U. I., "Investigation of the Aurora," Moscow, 1960.

4. Jacobs, G. "Propagation," published monthly in *CQ* magazine, Hicksville, New York.

5. Space Environment Services Center, "Products and Services User Guide," Space Environment Laboratory, Boulder, Colorado, January 1993.

6. National Technical Information Service, 5285 Port Royal Road, Springfield, Virginia 22061.

7. *CQ Amateur Radio Almanac,* published annually by CQ Communications, Inc., Hicksville, New York.

5.6 Addendum For Educators

The Space Environment Laboratory at NOAA in Boulder, Colorado, has produced an excellent teaching guide entitled "Solar Physics and Terrestrial Effects; A Curriculum Guide For Teachers, Grades 7–12." This 94-page manual was written by high-school physics teachers. It is not a step-by-step guide for teachers that will take time away from their already over-crowded curriculum. Rather, it is a resource from which to pick and choose material so that existing courses can be enhanced to provide some state-of-the-art applications of physics. The guide consists of three main parts: a short textbook, a hands-on activity guide, and resource listings. The text consists of four chapters: (1) How the Sun came to be: Stellar Evolution; (2) The Structure of the Sun; (3) Studying the Sun; and (4) Solar-Terrestrial Interactions. It also contains eight hands-on projects such as "Building a Spectroscope" and "Measuring the Solar Constant."

This teaching guide, coupled with the information that can be obtained in real-time from the SESC Public Bulletin Board, provides an opportunity for science educators not only to teach solar-terrestrial interactions, but also, to monitor them. This teaching guide is available at no cost. For more information, contact NOAA, Space Environment Laboratory, 325 Broadway, Boulder, CO 80303-3328.

5.7 Appendix

The following WWV/WWVH/WWVB Information is excerpted from NIST Time and Frequency Services [Special Publication 432 (Revised 1990)]. A complete copy is available from NIST.

Abstract

NIST Time and Frequency Services [Special Publication 432 (Revised 1990)] is a revision of SP 432, last published in 1979. It describes services available, as of December 1990, from NIST radio stations WWV, WWVH, and WWVB; from GOES satellites; from Loran-C; by telephone (voice and modem); and from the NIST Frequency Measurement Service.

Key words: broadcast of standard frequencies; computer time setting; frequency calibrations; GOES satellite; high frequency; low frequency; satellite time code; shortwave; standard frequencies; time calibrations; time signals.

Introduction

Precise time and frequency information is needed by electric power companies, radio and television stations, telephone companies, air traffic control systems, participants in space exploration, computer networks, scientists monitoring data of all kinds, and navigators of ships and planes. These users need to compare their own timing equipment to a reliable, internationally recognized standard. The National Institute of Standards and Technology (NIST), formerly the National Bureau of Standards, provides this standard for most users in the United States.

NIST began broadcasting time and frequency information from radio station WWV in 1923. Since then, NIST has expanded its time and frequency services to meet the needs of a growing number of users. NIST time and frequency services are convenient, accurate, and easy to use. They contribute greatly to the nation's space and defense programs, to manufacturers, and to transportation and communications. In addition, NIST services are widely used by the general public.

Broadcast services include radio signals from NIST radio stations WWV, WWVH, and WWBV; the GOES satellites, and Loran-C. Services are also available using telephone voice and data lines. This is a guide to these services.

Shortwave Services—WWV and WWVH

NIST operates two high-frequency (shortwave) radio stations, WWV and WWVH. WWV is in Ft. Collins, CO, and WWVH is in Kauai, HI. Both stations broadcast continuous time and frequency signals on 2.5, 5, 10, and 15 MHz. WWV also broadcasts on 20 MHz. All frequencies provide the same information. Although radio reception conditions in the high-frequency band vary greatly with factors such as location, time of year, time of day, the particular frequency being used, atmospheric and ionospheric propagation conditions, and the type of receiving equipment used, at least one frequency should be usable at all times. As a general rule, frequencies above 10 MHz work best in the daytime, and the lower frequencies work best at night.

Services provided by WWV and WWVH include:

Time announcements
Standard time intervals
Standard frequencies
UT1 time corrections
BCD time code
Geophysical alerts
Marine storm warnings
OMEGA Navigation System status reports
Global Positioning System (GPS) status reports

Figures 5.18 and 5.19 show the hourly broadcast schedules of these services along with station location, radiated power, and details of the modulation.

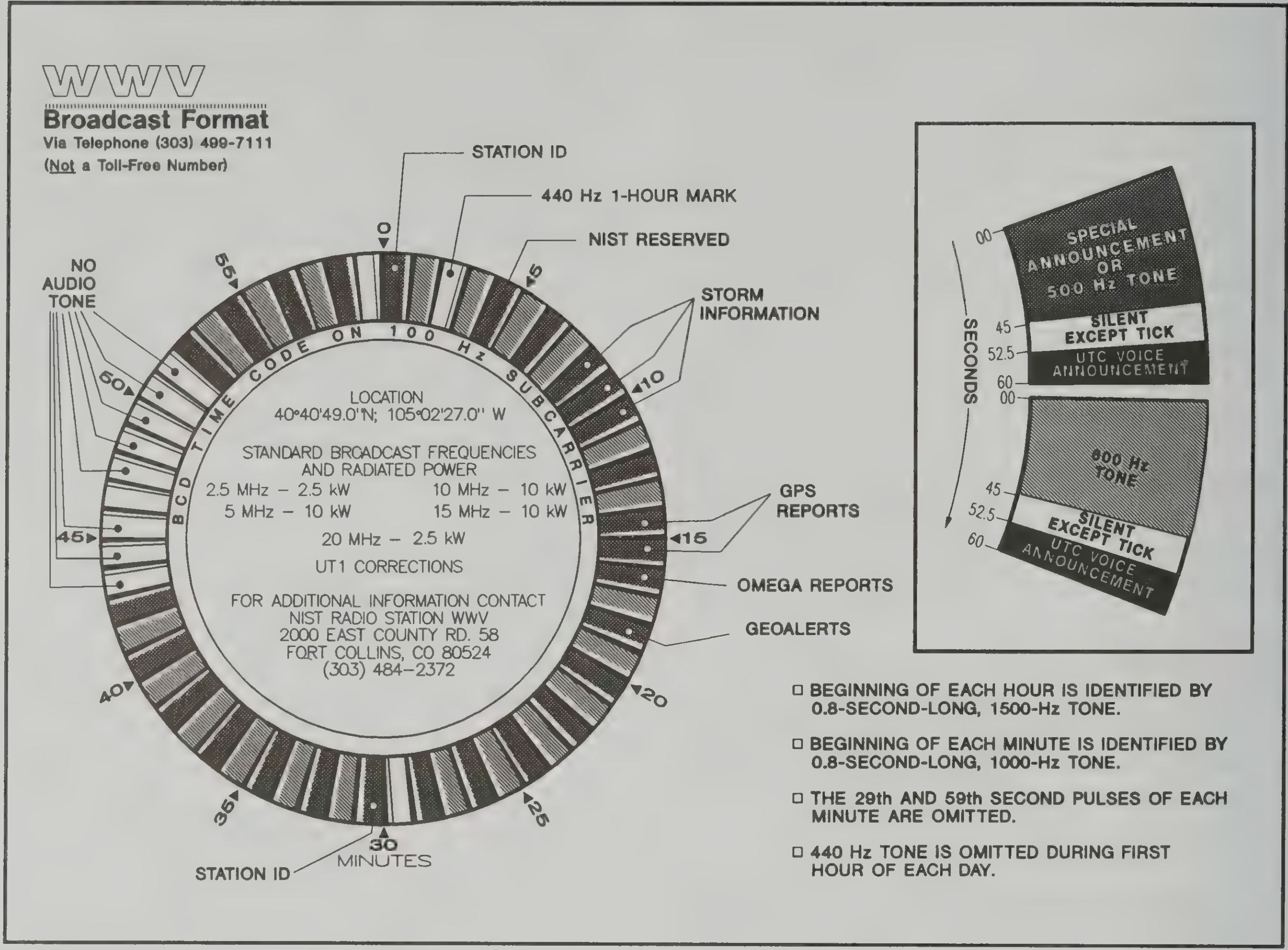

Figure 5.18. The hourly broadcast schedules of WWV.

Accuracy and Stability

WWV and WWVH are referred to the primary NIST Frequency Standard and related NIST atomic time scales in Boulder, CO. The frequencies as transmitted are accurate to about 1 part in 100 billion (1×10^{-11}) for frequency and about 0.01 ms for timing. The day-to-day deviations are normally less than 1 part in 1,000 billion (1×10^{-12}). However, the received accuracy is far less due to various propagation effects. The usable received accuracy is about 1 part in 10 million for frequency (1×10^{-7}) and about 1 ms for timing.

Radiated Power, Antennas, and Modulation

WWV and WWVH radiate 10,000 W on 5, 10, and 15 MHz. The radiated power is lower on the other frequencies: WWV radiates 2500 W on 2.5 and 20 MHz while WWVH radiates 5000 W on 2.5 MHz and does not broadcast on 20 MHz.

The WWV antennas are half-wave dipoles that radiate omnidirectional patterns. The 2.5 MHz antenna at WWVH is also of this type. The other antennas at WWVH are phased vertical half-wave dipole arrays They radiate a cardioid pattern with the maximum gain pointed toward the west.

Both stations use double sideband amplitude modulation. The modulation level is 50 percent for the steady tones, 25 percent for the BCD time code, 100 percent for the seconds pulses and the minute and hour markers, and 75 percent for the voice announcements.

Time Announcements

Voice announcements are made from WWV and WWVH once every minute. Since both stations can be heard in some locations, a man's voice is used on WWV, and a woman's voice is used on WWVH to reduce confusion. The WWVH announcement occurs first, at about 15 s before the minute. The WWV announcement follows at about 7.5 s before the minute.

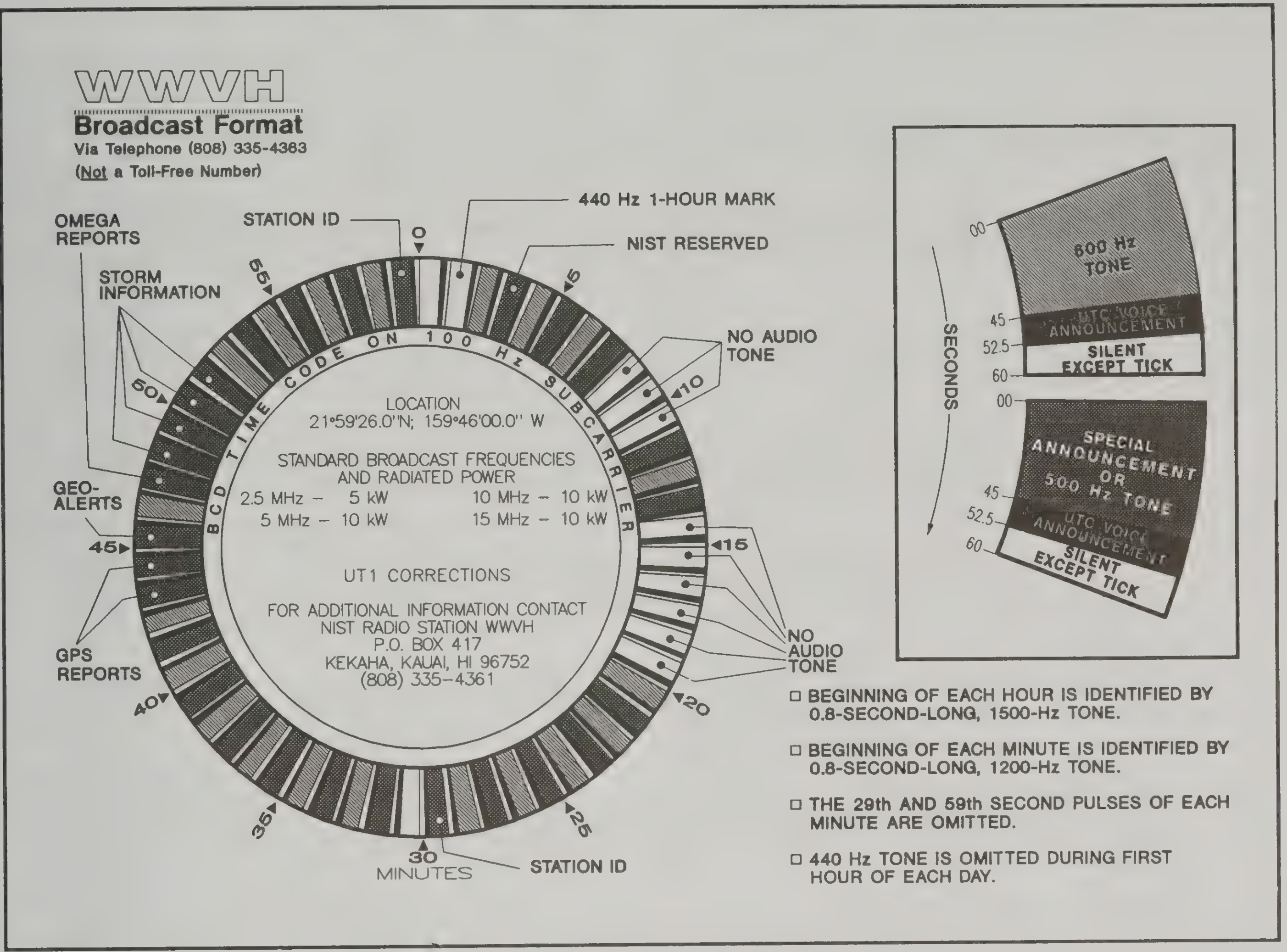

- ☐ BEGINNING OF EACH HOUR IS IDENTIFIED BY 0.8-SECOND-LONG, 1500-Hz TONE.
- ☐ BEGINNING OF EACH MINUTE IS IDENTIFIED BY 0.8-SECOND-LONG, 1200-Hz TONE.
- ☐ THE 29th AND 59th SECOND PULSES OF EACH MINUTE ARE OMITTED.
- ☐ 440 Hz TONE IS OMITTED DURING FIRST HOUR OF EACH DAY.

Figure 5.19. The hourly broadcast schedules of WWVH.

Though the announcements occur at different times, the tone markers are transmitted at the exact same time from both stations. However, they may not be received at exactly the same instant due to differences in the propagation delays from the two station sites.

The announced time is "Coordinated Universal Time" (UTC). UTC was established by international agreement in 1972, and is governed by the International Bureau of Weights and Measures (BIPM) in Paris, France. Coordination with the international UTC time scale keeps NIST time signals in close agreement with signals from other time and frequency stations throughout the world.

UTC differs from your local time by a specific number of hours. The number of hours depends on the number of time zones between your location and the location of the zero meridian (which passes through Greenwich, England). When local time changes from Daylight Saving to Standard Time, or vice versa, UTC does not change. However, the difference between UTC and local time does change—by 1 hour. Use the chart of world time zones (Figure 5.20) to find out how many hours to add to or subtract from UTC to obtain your local standard time. If DST is in effect at your location, subtract 1 hour less in the U.S. than shown on the chart. Thus, Eastern Daylight Time (EDT) is only 4 hours behind UTC, not 5 as shown on the chart for EST.

UTC is a 24-hour clock system. The hours are numbered beginning with 00 hours at midnight through 12 hours at noon to 23 hours and 59 minutes just before the next midnight.

The international agreement that established UTC in 1972 also specified that occasional adjustments of exactly 1 s will be made to UTC so that UTC should never differ from a particular astronomical time scale, UT1, by more than 0.9 s. This was done as a convenience for some time-broadcast users, such as boaters using celestial navigation, who need to know time that is based on the rotation of the Earth. These occasional 1-s adjustments are known as "leap seconds." When deemed necessary by the International Earth Rotation Service in Paris, France, the leap seconds are inserted into UTC, usually at the end of June or at the end of December, making that month 1 s longer than usual. Typically, a leap second has been inserted at intervals of 1 to 2 years.

Standard Time Intervals

The most frequent sounds heard on WWV and WWVH are the seconds pulses. These pulses are heard every second except on the 29th and 59th seconds of each minute. The first pulse of each hour is an 800-ms pulse of 1500 Hz. The first pulse of each minute is an 800-ms pulse of 1000 Hz at WWV and 1200 Hz at WWVH. The remaining seconds pulses are short audio bursts (5-ms pulses of 1000 Hz at WWV and 1200 Hz at WWVH) that sound like the ticking of a clock.

Each seconds pulse is preceded by 10 ms of silence and followed by 25 ms of silence. The silence makes it easier to pick out the pulse. The total 40-ms protected zone around each seconds pulse is shown in Figure 5.21.

Standard Audio Frequencies

In alternate minutes during most of each hour, 500-Hz or 600-Hz audio tones are broadcast. A 440-Hz tone (the musical note A above middle C) is broadcast once each hour. In addition to being a musical standard, the 440-Hz tone provides an hourly marker for chart recorders and other automated devices. The 440-Hz tone is omitted, however, during the first hour of each UTC day. See figures 5.18 and 5.19 for details.

Silent Periods

The silent periods are without tone modulation. However, the carrier frequency, seconds pulses, time announcements, and the 100-Hz BCD time code continue during the silent periods. In general, one station will not broadcast an audio tone while the other station is broadcasting a voice message.

On WWV, the silent period extends from 43 to 46 and from 47 to 52 minutes after the hour. WWVH has two silent periods; from 8 to 11 minutes after the hour, and from 14 to 20 minutes after the hour. Minutes 29 and 59 on WWV and minutes 00 and 30 on WWVH are also silent.

BCD Time Code

WWV and WWVH continuously broadcast a binary coded decimal (BCD) time code on a 100-Hz subcarrier. The time code presents UTC information in serial fashion at a rate of 1 pulse per second. The information carried by the time code includes the current minute, hour, and day of the year. The time code also contains the 100-Hz frequency from the subcarrier. The 100-Hz frequency may be used as a standard with the same accuracy as the audio frequencies.

At the time of publication of this revision of Special Publication 432 (late 1990), further changes to the content of the WWV and WWVH time codes are in the planning stage. The proposed changes will not affect currently encoded information, but will add information in the form of the last two digits of the current year, improved indicators for when Daylight Saving Time is in effect, and a warning for the insertion of a leap second at the end of the current month.

UT1 Time Corrections

The UTC time scale broadcast by WWV and WWVH meets the needs of most users. UTC runs at an almost perfectly constant rate, since its rate is based on cesium atomic frequency standards. Somewhat surprisingly, some users need time less stable than UTC but related to the rotation of the Earth. Applications such as celestial navigation, satellite observations of the Earth, and some types of surveying require time referenced to the rotational position of the Earth. These users rely on the UT1 time scale. UT1 is derived by astronomers who monitor the speed of the Earth's rotation.

You can obtain UT1 time by applying a correction to the UTC time signals broadcast from WWV and WWVH. UT1 time corrections are included in the WWV and WWVH broadcasts at two levels of accuracy. First, for those users only needing UT1 to within 1 s, occasional corrections of exactly 1 s are inserted into the UTC time scale. These corrections, called leap seconds, keep UTC within ±0.9 s of UT1. Leap seconds are coordinated under international agreement by the International Earth Rotation Service in Paris, France. Leap seconds can be either positive or negative, but so far, only positive leap seconds have been needed. A positive leap second is normally added every 1 or 2 years, usually on June 30 or December 31.

The second level of correction is for the small number of users needing UT1 accurate to within 0.1 s.

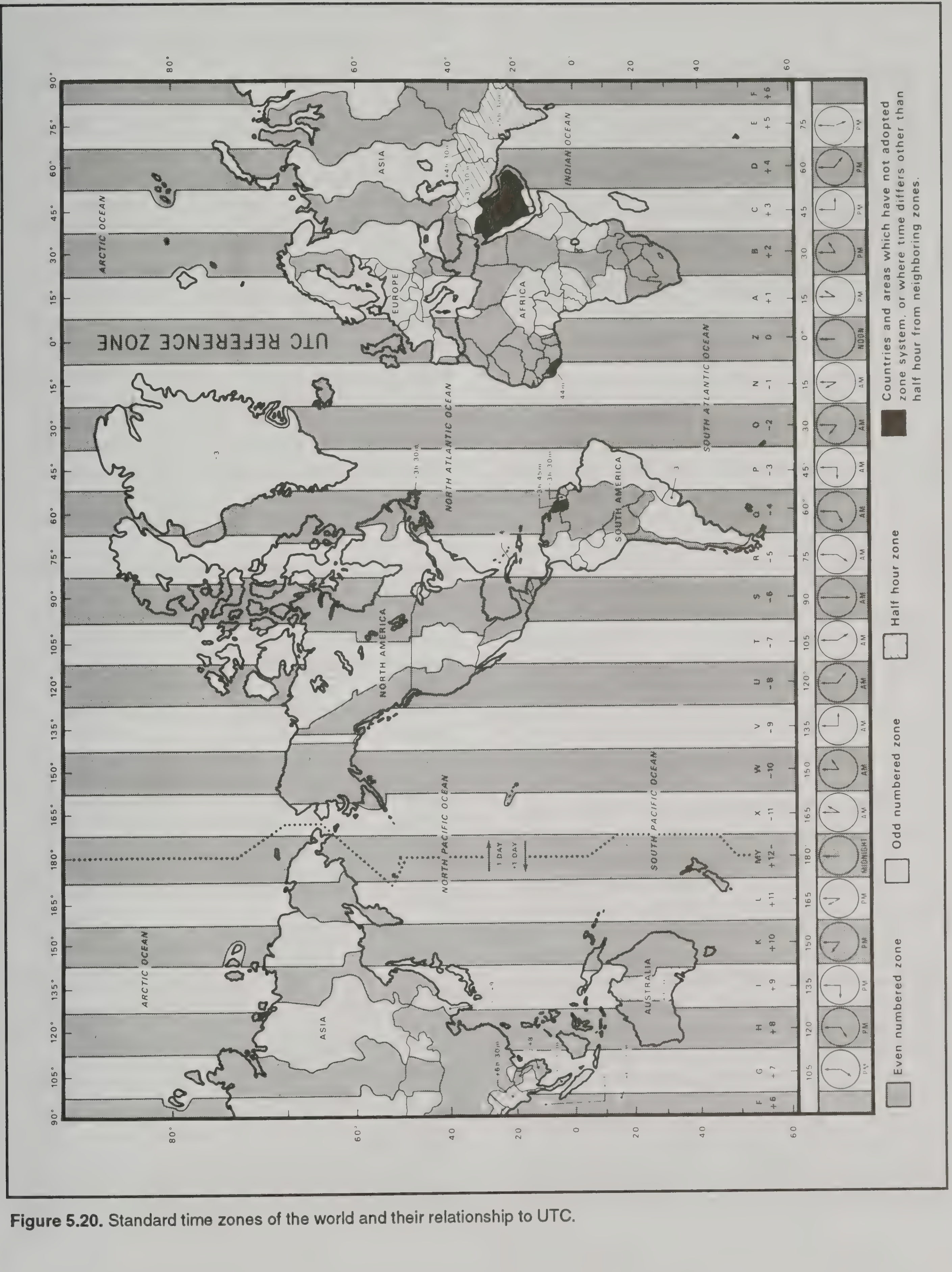

Figure 5.20. Standard time zones of the world and their relationship to UTC.

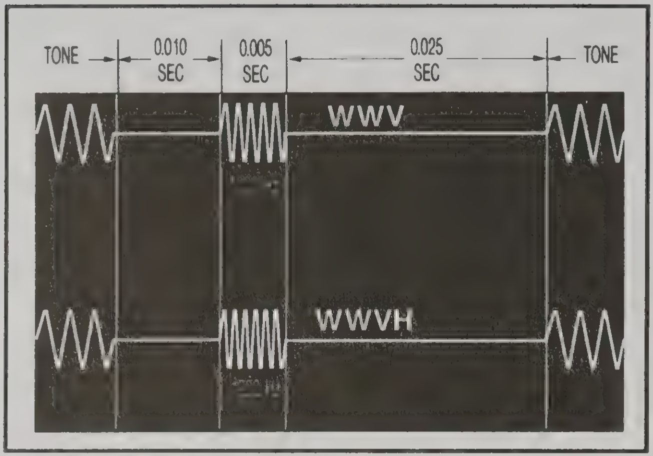

Figure 5.21 Format of WWV and WWVH second pulses.

These corrections are encoded into the broadcasts by using doubled ticks during the first 16 s of each minute. The amount of correction (in tenths of 1 s) is determined by counting the number of successive doubled ticks heard each minute. The sign of the correction depends on whether the doubled ticks are in the first 8 s of the minute or in the second 8 s. If the doubled ticks are in the first 8 s (1–8) the sign is positive, and if they are in the second 8 s (9–16) the sign is negative. For example, if ticks 1, 2, and 3 are doubled, the correction is "plus" 0.3 s. This means that UT1 equals UTC + 0.3 s. If UTC is 8:45:17, then UT1 is 8:45:17.3. If ticks 9, 10, 11, and 12 are doubled, the correction is "minus" 0.4 s. If UTC is 8:45:17, then UT1 is 8:45:16.6. An absence of doubled ticks indicates that the current correction is 0.

Official Announcements

Announcement segments 45 s long are available by subscription to other Federal agencies (see figures 5.18 and 5.19). These segments are used for public service messages. The accuracy and content of these messages is the responsibility of the originating agency.

For information about the availability of these segments, contact the NIST Time and Frequency Division.

The segments currently in use (late 1990) are described below. Since these are subject to change from time to time, contact NIST for more current status information.

OMEGA Navigation System Status Reports—The OMEGA Navigation System status reports are voice announcements broadcast on WWV at 16 minutes after the hour, and on WWVH at 47 minutes after the hour. The OMEGA Navigation System consists of eight radio stations transmitting in the 10- to 14-kHz frequency band. These stations serve as international aids to navigation. The status reports are updated as necessary by the U.S. Coast Guard.

For more information about the OMEGA Navigation System or these announcements, contact: Commanding Officer, U.S. Coast Guard OMEGA Navigation System Center, 7323 Telegraph Road, Alexandria, VA 22310-3998; telephone (703) 866-3800.

Geophysical Alerts—Current geophysical alerts (Geo-alerts) are broadcast in voice from WWV at 18 minutes after the hour and from WWVH at 45 minutes after the hour. The messages are less than 45 s in length and are updated every 3 hours (typically at 0000, 0300, 0600, 0900, 1200, 1500, 1800, and 2100 UTC). Hourly updates are made when necessary.

Part A of the message gives the solar-terrestrial indices for the day: specifically the 1700 UTC solar flux from Ottowa, Canada, at 2800 MHz, the estimated *A*-index for Boulder, CO, and the current Boulder *K*-index.

Part B gives the solar-terrestrial conditions for the previous 24 hours.

Part C gives optional information on current conditions that may exist (that is, major flares, proton or polar cap absorption [PCA] events, or stratwarm conditions).

Part D gives the expected conditions for the next 24 hours. For example:

A) "Solar-terrestrial indices for 26 October follow: Solar flux 173 and estimated Boulder *A*-index 20; repeat: Solar flux one-seven-three and estimated Boulder *A*-index two-zero.The Boulder *K*-index at 1800 UTC on 26 October was four; Repeat: four."

B) "Solar-terrestrial conditions for the last 24 hours follow:

Solar activity was high.

Geomagnetic field was unsettled to active."

C) "A major flare occurred at 1648 UTC on 26 October. A satellite proton event and PCA are in progress."

D) "The forecast for the next 24 hours follows:

Solar activity will be moderate to high. The geomagnetic field will be active."

Definitions

1. Solar Activity is defined as transient perturbations of the solar atmosphere as measured by enhanced x-

ray emission, typically associated with flares. Five standard terms are used to describe solar activity:

Very Low:	X-ray events less than C-class.
Low:	C-class x-ray events.
Moderate:	isolated (1 to 4) M-class x-ray events.
High	several (5 or more) M-class x-ray events, or isolated (1 to 4) M5 or greater x-ray events.
Very High	several M5 or greater x-ray events.

2. The geomagnetic field experiences natural variations classified quantitatively into six standard categories depending upon the amplitude of the disturbance. The Boulder *K*- and estimated *A*-indices determine the category according to the following table:

Condition	**Range of *A*-index**	**Typical *K*-indices**
Quiet	$0 \le A < 8$	usually no *K*-indices > 2
Unsettled	$8 \le A < 16$	usually no *K*-indices > 3
Active	$16 \le A < 30$	a few *K*-indices of 4
Minor storm	$30 \le A \le 50$	*K*-indices mostly 4 and 5
Major storm	$50 \le A < 100$	some *K*-indices 6 or greater
Severe storm	$100 \le A$	some *K*-indices 7 or greater.

3. Solar Flares are classified by their x-ray emission as:

Peak Flux Range (1–8 Ångströms)

Class	SI system (W m^{-2})	cgs system (erg $cm^{-2}s^{-1}$)
A	Ø < 10-7	Ø<10-4
B	10-7 ≤ Ø < 10-6	10-4 ≤ Ø < 10-3
C	10-6 ≤ Ø < 10-5	10-3 ≤ Ø < 10-1
M	10-5 ≤ Ø < 10-4	10-2 ≤ Ø < 10-1
X	10-4 ≤ Ø	10-1 ≤ Ø

The letter designates the order of magnitude of the peak value. Following the letter the measured peak value is given. For descriptive purposes, a number from 1.0 to 9.9 is appended to the letter designation. The number acts as a multiplier. For example, a C3.2 event indicates an x-ray burst with peak flux of 3.2×10^{-6} Wm^{-2}.

Forecasts are usually issued only in terms of the broad C, M, and X categories. Since x-ray bursts are observed as a full-Sun value, bursts below the x-ray background level are not discernible. The background drops to class A level during solar minimum; only bursts that exceed B1.0 are classified as x-ray events. During solar maximum the background is often at the class M level, and therefore class A, B, and C x-ray bursts cannot be seen. Data are from the NOAA GOES satellites, monitored in real time at the NOAA Space Environment Services Center. Bursts greater than 1.2×10^{-3} Wm^{-2} may saturate the GOES detectors. If saturation occurs estimated peak flux values are reported.

4. The remainder of the report is as follows:

Major Solar Flare = flare which produces some geophysical effect, usually flares that have x-rays ≥ M5 class.
Proton Flare = protons by satellite detectors (or polar cap observed in time association with H-alpha flare.
Satellite Level Proton Event = proton enhancement detected by Earth-orbiting satellites with measured particle flux of at least 10 protons $cm^{-2}s^{-1}sr^{-1}$ at ≥ 10 MeV.
Polar Cap Absorption = proton-induced absorption ≥ 2 dB daytime, 0.5 dB night, as measured by a 20-MHz riometer* located within the polar cap.
Stratwarm = reports of stratospheric warmings in the high latitude regions of the winter hemisphere of the Earth associated with gross distortions of the normal circulation associated with the winter season.

To hear these Geophysical Alert messages by telephone (at any minute of the hour, but without time information), dial (303) 497-3235.

Inquiries regarding these messages should be addressed to:

Space Environment Services Center, NOAA R/E/SE2,
325 Broadway, Boulder, CO 80303-3328. Or call (303) 497-5127.

Marine Storm Warnings—Marine storm warnings are broadcast for the marine areas that the United States has warning responsibility for under international agreement. The storm warning information is provided by the National Weather Service. Storm warnings for the Atlantic and eastern North Pacific are broadcast by voice on WWV at 8, 9, and 10 minutes after the hour. Storm warnings for the western, eastern, southern, and north Pacific are broadcast by WWVH at 48, 49, 50, and 51 minutes after the hour. An additional segment (at 11 minutes after the hour on WWV and at 52 minutes after the hour on WWVH) is used occasionally if there are unusually widespread storm conditions. The brief voice messages warn mariners of storm threats present in their areas.

**A riometer (rio = relative ionospheric opacity) is a receiver that measures the intensity of the random noise that impinges on the Earth from deep space.*

The storm warnings are based on the most recent forecasts. Updated forecasts are issued by the National Weather Service at 0500, 1100, 1700, and 2300 UTC for WWV; and at 0000, 0600, 1200, and 1800 UTC for WWVH.

A typical storm warning announcement text is as follows:

> North Atlantic weather West of 35 West at 1700 UTC; Hurricane Donna, intensifying, 24 North, 60 West, moving northwest, 20 knots, winds 75 knots; storm, 65 North, 35 West, moving east, 10 knots; winds 50 knots, seas 15 feet.

For more information about marine storm warnings, write to: The Director, National Weather Service, Silver Spring, MD 20910.

Global Positioning System (GPS) Status Announcements—Since March 1990 the U.S. Coast guard has sponsored two voice announcements per hour on WWV and WWVH, giving current status information about the GPS satellites and related operations. The 45-s announcements begin at 14 and 15 minutes after each hour on WWV and at 43 and 44 minutes after each hour on WWVH. For further information, contact the Commanding Officer, U.S. Coast Guard Center, 7323 Telegraph Road, Alexandria, VA 22310-3998.

WWV and WWVH Audio Signals By Telephone

The audio portions of the WWV and WWVH broadcasts can be heard by telephone. The accuracy of the telephone time signals is normally 20 ms or better in the continental United States. In rare instances when the telephone connection is made by satellite, there is an additional delay of 0.25 to 0.5 s.

To hear these broadcasts, dial (303) 499-7111 for WWV, and (808) 335-4363 for WWVH. Callers are disconnected after three minutes. These are not toll-free numbers; callers outside the local calling area are charged for the call at regular long-distance rates.

Chapter 6

HF Propagation Prediction Programs

A wise old ham once said that if you want to know what propagation conditions will be like tomorrow, check them today. That is called "now-casting," as contrasted with "forecasting." And while statistics have shown that now-casting will be correct a fair amount of the time, we probably are better off using HF propagation prediction programs. This chapter will discuss what HF propagation prediction programs are, the evolution of these programs, and the various types of programs available.

6.1 HF Propagation Prediction Programs—What Are They?

HF propagation prediction programs make an assessment of what is **likely** to occur sometime in the future based on a collection of historical solar and ionospheric data.

With the computer revolution of the 1980s and 1990s, many ham shacks and SWL listening-posts now sport a personal computer. Given this capability, it was inevitable that radio amateurs and other users of the HF spectrum would want to do their own propagation predictions, especially on those HF circuits that they most use or are most interested in (for example, the path to that "rare one"). They also might want to determine the "gray-line" times and coverage areas for their QTH as well as the reliability that they can expect on their "pet" paths, given current solar and geomagnetic conditions. Finally, amateurs and SWLs alike simply may want to know when propagation probably will not be possible, making it best just to leave the shack and do something else. Modern shortwave propagation prediction programs for the PC now can provide such information in the comfort of your home.

Given a specific set of geographical end-points for a desired path, an HF propagation prediction program will: (1) determine the band of frequencies that should propagate over that path; and (2) provide information on the probable modes of propagation, expected signal strengths, signal-to-noise ratios, and/or path reliability. The program should be able to do this for any time of day, for any month (season), for any portion of the solar cycle, and between any two geographical end-points in the world. Many programs do this, taking into account your transmitter power and antenna gain. Simply put, HF prediction programs indicate whether or not you can even expect to get your signal to that distant receiver, and if you can, whether or not it will be useful. Most modern PC-based programs can do all of this quickly—in a minute or less, in most cases. That is quite a capability. Modern PC technology allows the radio amateur or the SWL to use prediction programs that originally required large mainframe computers to use. However, regardless of the level of complexity of the software, all of these programs carry one important caveat—one which often is overlooked but must be remembered if the predictions from any given program are to be interpreted properly: **The numbers produced by shortwave prediction programs are "median" values that were developed on a statistical basis.** This means that 50% of the time the actual observed value of whatever you are predicting will be higher than the predicted value, and 50% of the time the observed value will be lower.

Take, for example, the *MINIMUF 3* model, originally developed by the U.S. Navy to predict MUFs on computers that only had 32K of RAM.[1] When this model was tested against median determinations of the MUF obtained using the Navy's HF oblique sounder database (also described in Reference 1), *MINIMUF's* (median) MUF predictions typically had an error of ±3.8 MHz. This meant that when *MINIMUF* predicted an MUF of 30 MHz, what most likely would be observed that day are conditions characterized by an MUF somewhere between 26.2 and 33.8 MHz. The proper interpretation of these data are that: (1) 10 meters may be open, and (2) 12 and 15 meters likely will be open. HF predictions are not absolutes, but rather, are approximate determinations that are intended to indicate the general level of certain propagation parameters. Interpreted in this manner, program users will experience good success with their predictions. With one exception, the many programs evaluated here contain no provision to make a prediction based on current solar/ionospheric conditions. They only are capable of forecasting what is **likely** to occur a high percentage of the time. If the user chooses to interpret the numbers as precise, he or she often will be disappointed, because sometimes shortwave predictions are just plain wrong!

Finally, it must be recognized that all prediction models are based on data for quiet, ambient ionospheric conditions. None of the predictive programs yields valid results for periods characterized by solar/ionospheric disturbances.

6.2 The Evolution of HF Prediction Programs

The genesis of computerized HF prediction programs can be traced back to 1966, with the development of the *ESSA-ITSA-1*. This was followed by *ITS-78* (1969), *RADARC* (1971), *HFMUFES4* (1976), *AMBCOM* (1980), *IONCAP* (1983), and *HFBC84* (1984). *AMBCOM* and *IONCAP* were substantially revised through the 1980s. Goodman[2] devotes an entire chapter to the evolution of HF predictions for the serious student of this science.

Today, several dozen HF prediction programs are available; some are fairly accessible to the radio amateur while others were developed strictly for a special customer. Historically, prediction programs were developed by scientists and engineers, and they were intended to be used by scientists and engineers. Operational communicators would take the computer listings that these programs generated, and they would try to apply these data to a real-time, ever-changing HF scenario. More often than not, the results were disappointing.

In the middle 1970s, HF prediction technology development separated into two different paths. One path continued on to employ traditional theoretical, empirical, or statistical approaches (i.e., *IONCAP*; these approaches are explained in section 6.3). The other path was directed at helping HF communicators and frequency managers do frequency selection and communications management in the field, "on the fly." Instead of doing HF predictions on a large mainframe computer in a central processing location, the idea here was to make the predictive process simple and quick, and to take into account the user's specific scenario. In addition, emphasis was given to developing products ("outputs") that reflected exactly what the users wanted.

Because PC technology was in its infancy during the 1970s, RAM storage was limited to either 32K or 64K. This limitation required some relatively innovative development work to be done by program developers because parameters (e.g., the MUF) required upwards of 150K of RAM to calculate. The concept of emulation* was borne with the development of the *MINIMUF* model mentioned earlier. It allowed the MUF to be calculated with 80 BASIC statements. This single, specific innovation spawned the development of a new, smaller, quicker breed of prediction software that could operate in a PC environment and that was operationally oriented. The best example of this new approach can be found in the Navy's *Advanced PROPHET* HF signal assessment system.

Specifically, since its inception in 1976, *PROPHET*'s developers have emphasized the operational environment. That is, its products were designed, to a large extent, to meet the needs of the operational user. Its capabilities include the ability to:

(1) predict the band of frequencies that can be used to communicate from one point to another, which is not trivial because propagation varies considerably with time of day, season, and state of the sunspot cycle;

(2) estimate the expected field strength and signal-to-noise levels at the receiving end of the circuit;

(3) present a graphical display of the skywave signal's bounce pattern between the earth and the ionosphere (signal ray-tracing); and

(4) determine communication frequencies that, due to propagation, are immune to interception by an adversary or intentional interference.

Since its inception in 1976, *PROPHET* had grown from an initial five outputs to its present 25-product capabilities, each of which has several output sub-

---

**One example of emulation is to model the rise and fall of the MUF as the charging and discharging of two different RC circuits.*

options. The last version to be developed (in the late 1980s), Version 3.2, has been used by hundreds of operators throughout the military and industrial communities. The program uses simple emulations of complex propagation phenomena to take advantage of the portability and speed of personal computers. *PROPHET* also contains large amounts of empirical and intuitive knowledge and user experience, lending it the attributes of an expert system. Throughout its development and use, the models in *PROPHET* have undergone numerous, extensive verification tests against "ground truth" oblique-sounder data.[3] While *PROPHET* was never released to the public, many of its propagation models were published in the open literature in the early 1980s.[4] These models were used by many innovative radio amateurs to develop the first of many PC shortwave prediction programs for the amateur and SWL communities. *DX* and the initial version of *MINIPROP*, discussed later in this chapter, are examples of such programs.

6.3 Types of HF Prediction Programs

Today, a wide variety of HF prediction programs are available; they span the entire range from the very simple to the very complex. Whereas earlier development of such programs was constricted by computer memory size, modern PCs can accommodate virtually any available program. This has led to the development of hybrid programs that combine the strengths of several prediction models. Generally, however, the HF predictions programs can be categorized into one or more of the following types of models:

(1) THEORETICAL—This approach presumes that the ionosphere is so well modeled that a signal ray at a discreet elevation angle can be obliquely sent into it, with the refraction (or bending) along the path accurately calculated. The result is a location where the signal returns to earth. This process, called ray-tracing, initially required the extensive "number crunching" capabilities of large mainframe computers. In the middle 1980s, however, when mini- and microcomputer technology began to mature, ray-tracing models started to increase in popularity. Users of PCs now were able to use realistic antenna vertical radiation patterns to generate signal ray patterns in the ionosphere and to see what the "footprint" at the receiving end looked like. Even ducted propagation could be observed, and the full refractive effect of all the ionospheric layers could be seen. The most important issue to be addressed in using this type of program is how well the ionospheric model that is used simulates the real ionosphere. In fact, the subject of which ionospheric model is "best" generates as much controversy as does the question of which prediction model is "best." Ambient Ionospheric Communications Predictions at HF (*AMBCOM*) is an example of a theoretical-type program.[5]

(2) STATISTICAL—Early propagation predictions were based on large statistical databases of worldwide f_oF_2 values for a variety of conditions, including the time of day, season, and state of the sunspot cycle. These methods, called "virtual methods," use a predetermined path to establish where the ionospheric control points are located. As these programs evolved into computerized systems, large sets of numerical coefficients were developed to describe f_oF_2, f_oE, f_oE_s, and noise on a global basis. While most such numerical maps have been developed by the U.S. Government in Boulder, Colorado, they have been adopted as ITU (CCIR)* standards. The numerical maps for f_oF_2 used in *ITS-78*[6], *HFMUFES4*[7], and *IONCAP*[8] were derived from vertical sounder data gathered in 1954 (solar minimum) and 1957 (solar maximum). Approximately 175 vertical incidence sounder (VIS) stations contributed to that database. Over the years, vertical sounder data have continued to be collected. Thus, it was possible in the middle 1980s for the Australian Ionospheric Prediction Service (IPS) to develop a set of numerical coefficients for its *ASAPS* propagation program[9] that used sounder data acquired over the last 40 years. While not all participating stations contributed over that period, a few have, including the one in Washington, D.C.[10]

One novel departure from what we will call the "classical STATISTICAL approach" was used in the Russian HF prediction program *SPARC*.[11] Over the past several decades, the former Soviet Union maintained a network of vertical sounders that literally mapped the ionosphere over their entire land mass. (With the major part of your homeland above 50 degrees north latitude, some innovation was indeed required to use HF effectively!) When a version of *SPARC* was secured for evaluation in 1992 by the U.S. Government, it was learned that *SPARC* had the provision to store hourly f_oF_2 values for many stations

---

**The ITU is the International Telecommunication Union in Geneva, Switzerland. The technical arm of the ITU is the Consultative Committee International du Radio (CCIR). In 1992, the CCIR was renamed the Radio Communications Sector of the ITU (ITU-R).*

and for periods of up to 30 days. When a new day's data were added, the data from 31 days earlier were dropped. These data then were used to update in near-real-time the standard CCIR f_oF_2 maps and to track 27-day trends. (This is a very effective method by which to characterize the ionosphere if an extensive vertical sounder network exists to support the effort). If no new data were forthcoming, the system fell back on data from previous days, or it even could go back to basic numerical maps. The software also contained a provision to accept K_p on a near-real-time basis. Because the software's architecture was not compatible with existing U.S. PCs, a full evaluation, using the U.S. Ionosonde system, could not be conducted easily.

There also is a subset of the STATISTICAL approach that does not use the large, complex CCIR numerical maps. Recognizing the need for simplified approaches to estimate ionospheric parameters on microcomputers, Fricker[12] proposed a method in which the f_oF_2 for a given month and sunspot number can be represented satisfactorily by using a model that is a function of local time and latitude (based on the magnetic dip equator) and that moves around the Earth with universal time (with its center line kept along the magnetic dip equator). This approach was the basis for the revised *MINIPROP*[13] and *IONSOUND*[14] series of capable programs developed for the radio amateur and SWL communities.

(3) EMPIRICAL—The EMPIRICAL method of HF prediction uses large databases of actual observed data to statistically derive an expression that describes the parameter that is desired. In many cases, the expression will have absolutely no basis in physics, but it will provide a value based on some other fixed parameter (such as time). Most often, empirical models are used in conjunction with other models, such as large statistical numerical maps, to provide a more comprehensive capability. Many of the statistical programs mentioned above contain smaller empirical models. Probably the best known empirical model is the *FTZ4*[15], which contains an empirical field-strength model that originally (1982) was written in seven BASIC statements. This simple field-strength model originally was derived from thousands of long-range signal-strength measurements of shortwave broadcast transmissions.

Another example of an EMPIRICAL model is the *QLOF* model[16] developed in the 1970s to predict the LUF. This model was developed from thousands of LUF observations in the Navy Oblique Sounder Base, and the model was used in early versions of the *PROPHET* HF prediction program.

The *MINIMUF* model mentioned earlier[16] is an example of a semi-empirical model (it is better described as an "emulation") that can be used to calculate the MUF over any HF circuit. The MUF is principally controlled by the critical frequency of the F_2 layer of the ionosphere (f_oF_2), and it is the success in predicting this quantity that primarily determines the accuracy of the MUF forecast produced by any given empirical prediction program. Unlike the *E* and F_1 layers, which can be modeled quite well as a function of a single parameter ($\cos \varkappa$, the cosine of the instantaneous solar zenith angle, which is proportional to the solar intensity), the physics of the F_2 layer are generally believed to involve an interaction of photochemical and transport processes sufficiently complex that diurnal, seasonal, and geographical f_oF_2 variations cannot be accommodated simply through the corresponding variations of $\cos \varkappa$. Indeed, one even speaks of F_2 layer "anomalies" when comparing observed f_oF_2 with expectations based on the instantaneous value of $\cos \varkappa$. For example, f_oF_2 can be higher at mid-day in winter than in summer ("seasonal" anomaly), and on a given day, it can peak in late afternoon rather than at mid-day ("diurnal" anomaly).

Therefore, while f_oF_2 cannot be modeled as a function of the instantaneous value of $\cos \varkappa$, the possibility remains that it can be modeled as a response of a dynamic system "driven" by a function of $\cos \varkappa$. Examination of the shape of observed f_oF_2 diurnal profiles, for example, suggests that a simple relaxation model, according to which f_oF_2 represents a lagged response to the instantaneous solar intensity, may be useful as a first approximation. Allowing the lag time to be long (approximately 10 hours) in summer and short (approximately one hour) in the winter at middle and equatorial latitudes could at least partially reproduce both the seasonal and diurnal anomalies.

Therefore, a semi-empirical model for f_oF_2 was developed based on the analogy to a single-lag linear system (e.g., an RC circuit) driven by a forcing function proportional to the instantaneous value of $\cos \varkappa$. Further simplifying assumptions of the model include:

(1) The lag-time constant during the day is a simple monotonic function of the mid-day solar zenith angle; and

(2) The time constant at night is a constant (two hours), independent of season or geographical location.

As with other semi-empirical models of complex geophysical processes, no attempt was made to justify the model in terms of underlying physical mechanisms. In fact, the term "f_oF_2" is a misnomer in *MIN-*

Case Tested	Number of Path Months	RMS Residual Error (MHz)			
		MINIMUF-3	ESSA-ITSA-1	ITS-78 "Red"	ITS-78 "Blue"
All cases	137	4.03	5.2	4.6	4.5
Path length<4000 km	31	4.41	5.7	6.3	6.5
Path length>4000 km	106	3.88	4.1	4.1	3.6
4000≤path length≤5000 km	53	3.88	5.4	4.2	3.7
Path length>5000 km	47	3.88	4.0	3.9	3.5
25°S<geographic latitude<25°N	59	4.59	3.8	3.4	3.8
20°N<geographic latitude<60°N	76	3.65	5.4	5.2	4.9
Geographic latitude>60°N	2	3.18	6.7	4.8	4.9
SSN<50	24	3.39	4.8	4.1	4.1
50<SSN<100	58	4.01	5.6	5.3	5.0
SSN>100	55	4.30	4.7	4.2	3.9
Winter months	27	3.64	4.7	5.6	5.1
Spring months	34	4.08	5.4	4.4	4.4
Summer months	42	3.92	5.4	3.4	3.5
Fall months	34	4.40	4.8	5.3	5.7

Table 6.1. Comparison of large-scale HF prediction codes and MINIMUF-3 (taken from Rose, et al[1]).

IMUF. It is a number that resembles how the f_oF_2 varies as a function of the "driving" forces. In this approach, the model serves to provide a mathematical framework for force-fitting F_2-layer behavior to empirical data. The sunrise and sunset time constants, together with the "bias" (maximum daytime value as a function of path length), were derived from five years of sounder data collected between Hawaii and Guam, and three years of data collected over the path between France and Iceland. By making analytical approximations to the dynamic solutions of the model (i.e., the diurnal response function), a simple, closed-form expression for f_oF_2 was derived as a function of mid-day solar zenith angle, sunspot number, and time (relative to local sunrise and sunset). By appending simple approximations for the "M" factor (i.e., MUF/f_oF_2) and for solar zenith angle as a function of location and time, a model for the MUF was developed that was sufficiently compact for coding in early mini- and microcomputers.

Over the years, *MINIMUF-3* and its successors, *MINIMUF 3.5* and ultimately *MUF85*, were repeatedly retested against oblique sounder data. Table 6.1 shows how the original *MINIMUF* program's performance compared the traditional statistical programs *ESSA-ITSA-1* and two versions of *ITS-78*. It should be noted that during this test, the sounder data used to develop the constants in *MINIMUF-3* were excluded; thus, the results represent data from the remaining 80% of the sounder database. The comparison shows that the semi-empirical (or emulative) approach can produce useful results.

6.4 The Two Parts of Propagation Prediction Programs

Propagation prediction programs are comprised of two parts: a propagation kernel and a man-machine interface.

(1) **The Propagation Kernel.** These are the programs that work together to describe the HF channel between two points with respect to the frequencies that will propagate and how strong the signals will be. A simple propagation kernel would consist of models that predict:

(a) *Maximum Usable Frequency (MUF).* This is the *median* Maximum Usable Frequency for a given path. The MUF is a function of the time of day, season, state of the solar cycle, and, to some extent, geographical location. This is a physical parameter that cannot be influenced by mechanical means (e.g., power).

(b) *Lowest Usable Frequency (LUF).* This is the lower boundary of the band of frequencies that will propagate between two points. The LUF is a signal-to-noise boundary created primarily by *D*-region absorption. It is not a clear, concise, limiting point due, in part, to the fact that noise, power, and receiver sensitivities affect where this limit occurs. The LUF is a difficult parameter to model, and many times,

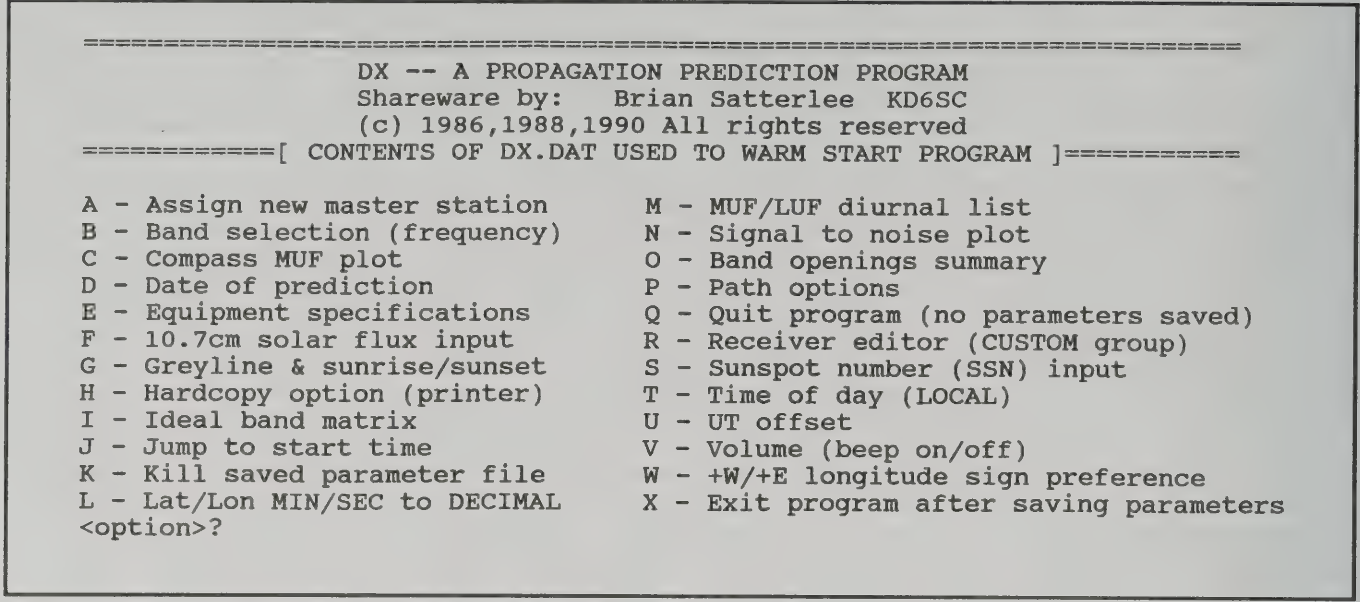

```
========================================================================
                 DX -- A PROPAGATION PREDICTION PROGRAM
                 Shareware by:   Brian Satterlee  KD6SC
                 (c) 1986,1988,1990 All rights reserved
============[ CONTENTS OF DX.DAT USED TO WARM START PROGRAM ]===========

A - Assign new master station        M - MUF/LUF diurnal list
B - Band selection (frequency)       N - Signal to noise plot
C - Compass MUF plot                 O - Band openings summary
D - Date of prediction               P - Path options
E - Equipment specifications         Q - Quit program (no parameters saved)
F - 10.7cm solar flux input          R - Receiver editor (CUSTOM group)
G - Greyline & sunrise/sunset        S - Sunspot number (SSN) input
H - Hardcopy option (printer)        T - Time of day (LOCAL)
I - Ideal band matrix                U - UT offset
J - Jump to start time               V - Volume (beep on/off)
K - Kill saved parameter file        W - +W/+E longitude sign preference
L - Lat/Lon MIN/SEC to DECIMAL       X - Exit program after saving parameters
<option>?
```

Figure 6.1. *DX* main menu.

empirical models do a better job than do any other techniques for day-to-day operations.

(c) *Field Strength.* The field strength is a measure of the signal energy that appears at the receiver's antenna. This is contrasted to the signal energy that appears at the receiver's antenna terminal. Here, the voltage measured is a function of a number of factors, including the field strength at the antenna, gain of the antenna (at the angle of arrival) compared to an isotropic antenna, the impedance match between the receive antenna and the feed-line, feed-line losses, etc. Simply put, there is no easy way to develop a general-purpose computer program that can incorporate a station's specific factors in the calculation of signal energy at the receiver's antenna terminals. Some programs, such as *ASAPS, CAPMAN, IONCAP,* and *VOACAP,* let you enter files containing receive antenna characteristics. But these data are taken into account in computing signal-to-noise and reliability values, not signal-strength values.

(d) *Noise Model.* Most HF prediction programs have some form of manmade and galactic noise models. Values usually are developed from look-up tables or numerical maps, which are compiled and available from the International Telecommunication Union, Geneva, Switzerland. These data are used to deter-

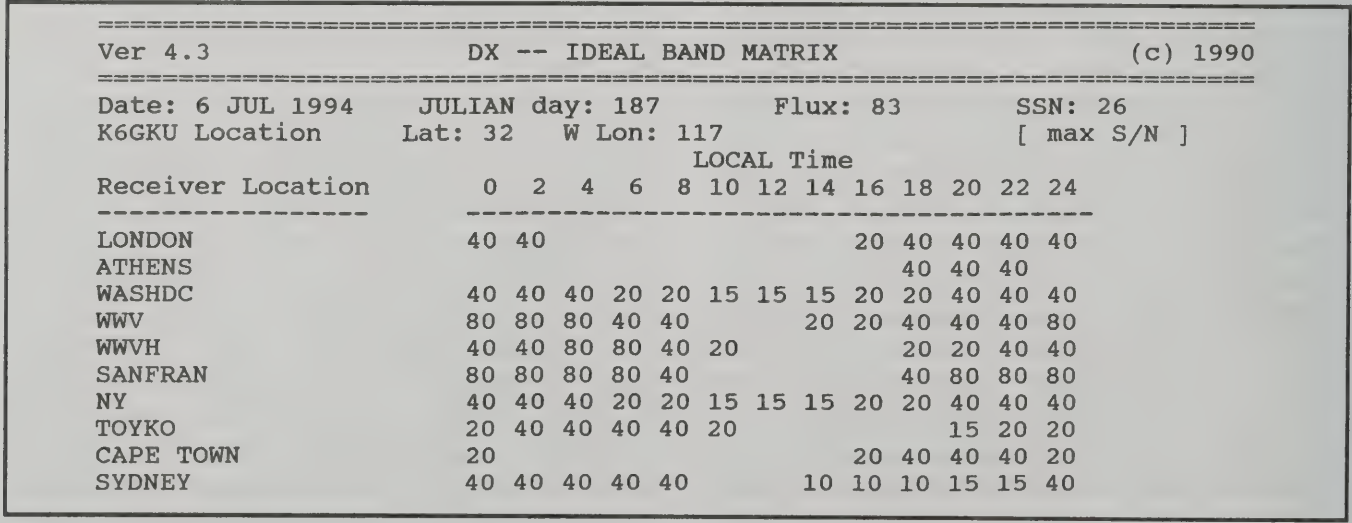

```
======================================================================
Ver 4.3                DX -- IDEAL BAND MATRIX                 (c) 1990
======================================================================
Date: 6 JUL 1994    JULIAN day: 187        Flux: 83       SSN: 26
K6GKU Location     Lat: 32   W Lon: 117                   [ max S/N ]
                                      LOCAL Time
Receiver Location       0  2  4  6  8 10 12 14 16 18 20 22 24
-----------------      --------------------------------------
LONDON                 40 40                      20 40 40 40 40
ATHENS                                               40 40 40
WASHDC                 40 40 40 20 20 15 15 15 20 20 40 40 40
WWV                    80 80 80 40 40          20 20 40 40 40 80
WWVH                   40 40 80 80 40 20             20 20 40 40
SANFRAN                80 80 80 80 40                40 80 80 80
NY                     40 40 40 20 20 15 15 15 20 20 40 40 40
TOYKO                  20 40 40 40 40 20                15 20 20
CAPE TOWN              20                         20 40 40 40 20
SYDNEY                 40 40 40 40 40          10 10 10 15 15 40
```

Figure 6.2. *DX* ideal band matrix printout.

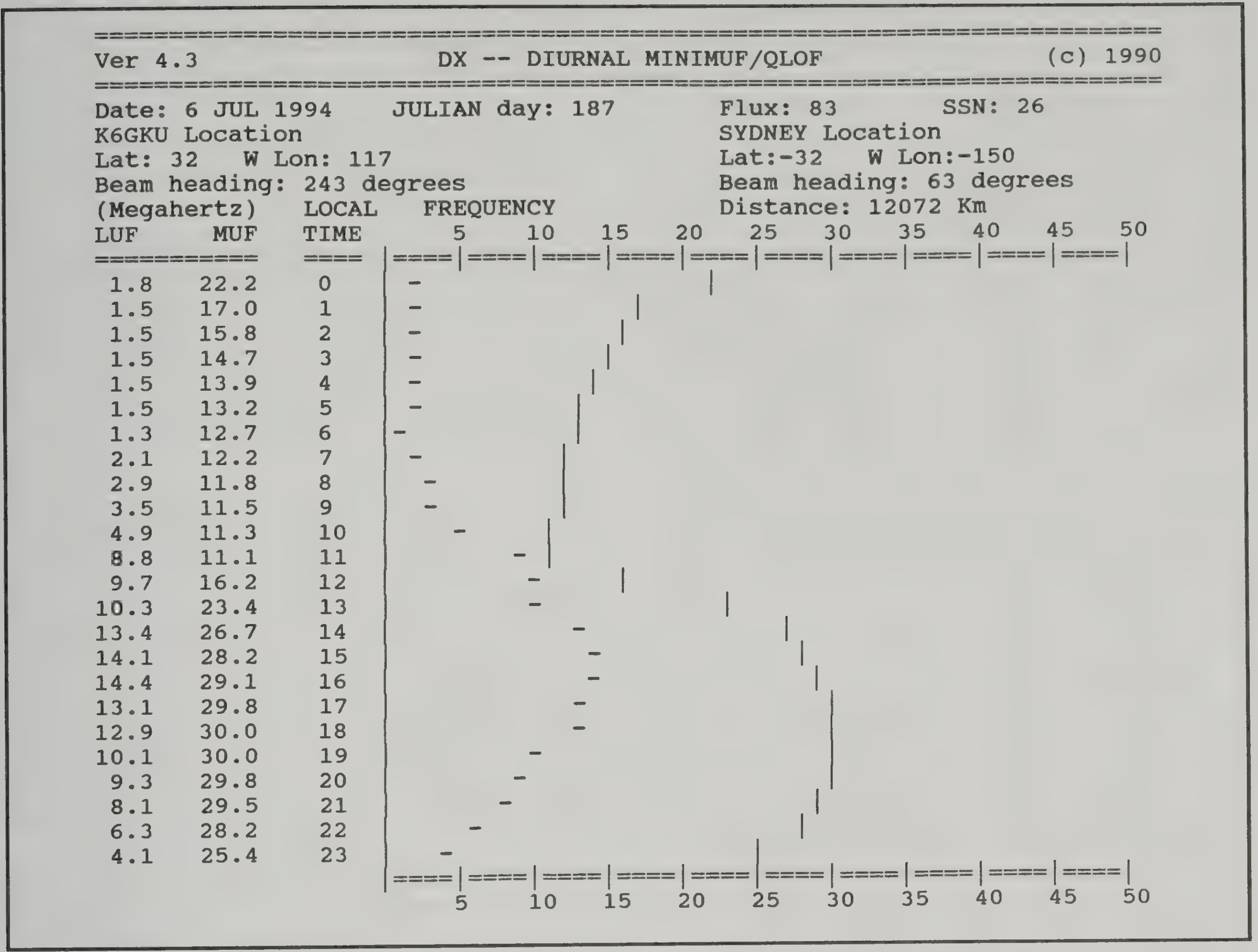

```
========================================================================
Ver 4.3                DX -- DIURNAL MINIMUF/QLOF               (c) 1990
========================================================================
Date: 6 JUL 1994    JULIAN day: 187       Flux: 83       SSN: 26
K6GKU Location                            SYDNEY Location
Lat: 32   W Lon: 117                      Lat:-32   W Lon:-150
Beam heading: 243 degrees                 Beam heading: 63 degrees
(Megahertz)   LOCAL   FREQUENCY           Distance: 12072 Km
LUF     MUF   TIME      5    10   15   20   25   30   35   40   45   50
===========   ==== |====|====|====|====|====|====|====|====|====|====|
 1.8   22.2    0   | -                   |
 1.5   17.0    1   | -              |
 1.5   15.8    2   | -             |
 1.5   14.7    3   | -            |
 1.5   13.9    4   | -           |
 1.5   13.2    5   | -          |
 1.3   12.7    6   |-           |
 2.1   12.2    7   | -         |
 2.9   11.8    8   |  -        |
 3.5   11.5    9   |  -        |
 4.9   11.3    10  |    -     |
 8.8   11.1    11  |        - |
 9.7   16.2    12  |         -     |
10.3   23.4    13  |         -            |
13.4   26.7    14  |            -             |
14.1   28.2    15  |             -             |
14.4   29.1    16  |             -              |
13.1   29.8    17  |            -                |
12.9   30.0    18  |            -                |
10.1   30.0    19  |         -                   |
 9.3   29.8    20  |        -                    |
 8.1   29.5    21  |       -                    |
 6.3   28.2    22  |     -                     |
 4.1   25.4    23  |   -                    |
                   |====|====|====|====|====|====|====|====|====|====|
                        5    10   15   20   25   30   35   40   45   50
```

Figure 6.3. *DX* diurnal printout.

mine signal-to-noise ratios, or whether or not there is sufficient received signal strength to overcome the ambient (background) noise.

(e) *Solar Zenith Angle as a function of Time of Day and Month.* This model determines the Sun's location in the sky. Almost all methods of modeling require this information because most ionospheric parameters are defined in terms of the time of day and season.

(f) *Path Length.* This is the great-circle distance between the transmitter and the receiver.

With these parameters, the average radio amateur can do a good job of determining the band of frequencies in which signals will propagate between two points and the relative signal levels to be expected. The parameters discussed above would comprise a sufficient kernel for a simple propagation model. More complicated models (e.g., *IONCAP* and *AMBCOM*) have much larger sets of models, and they provide much more detailed outputs (such a service probability, reliability, and free-space loss, to name a few). Our review of many models indicates that there are now over 30 signal parameters calculated by various HF prediction programs. For the most part, they are irrelevant to the radio amateur and SWL.

(2) **The Man-Machine Interface (MMI).** This is the part of the program that lets the user interact with the propagation kernel. In the early days, when propagation programs were only used by scientists and engineers, the MMI was very simple. The user knew the internal complexities of the program and developed ways of "coaxing" the answers out of the computer. Early programs such as *ITS-78* and *HFMUFES4*, and today *IONCAP*, require such "stroking." Their MMIs are not designed for the casual user. The demand for easy-to-use HF propagation programs, however, has led to a focus on the MMI.

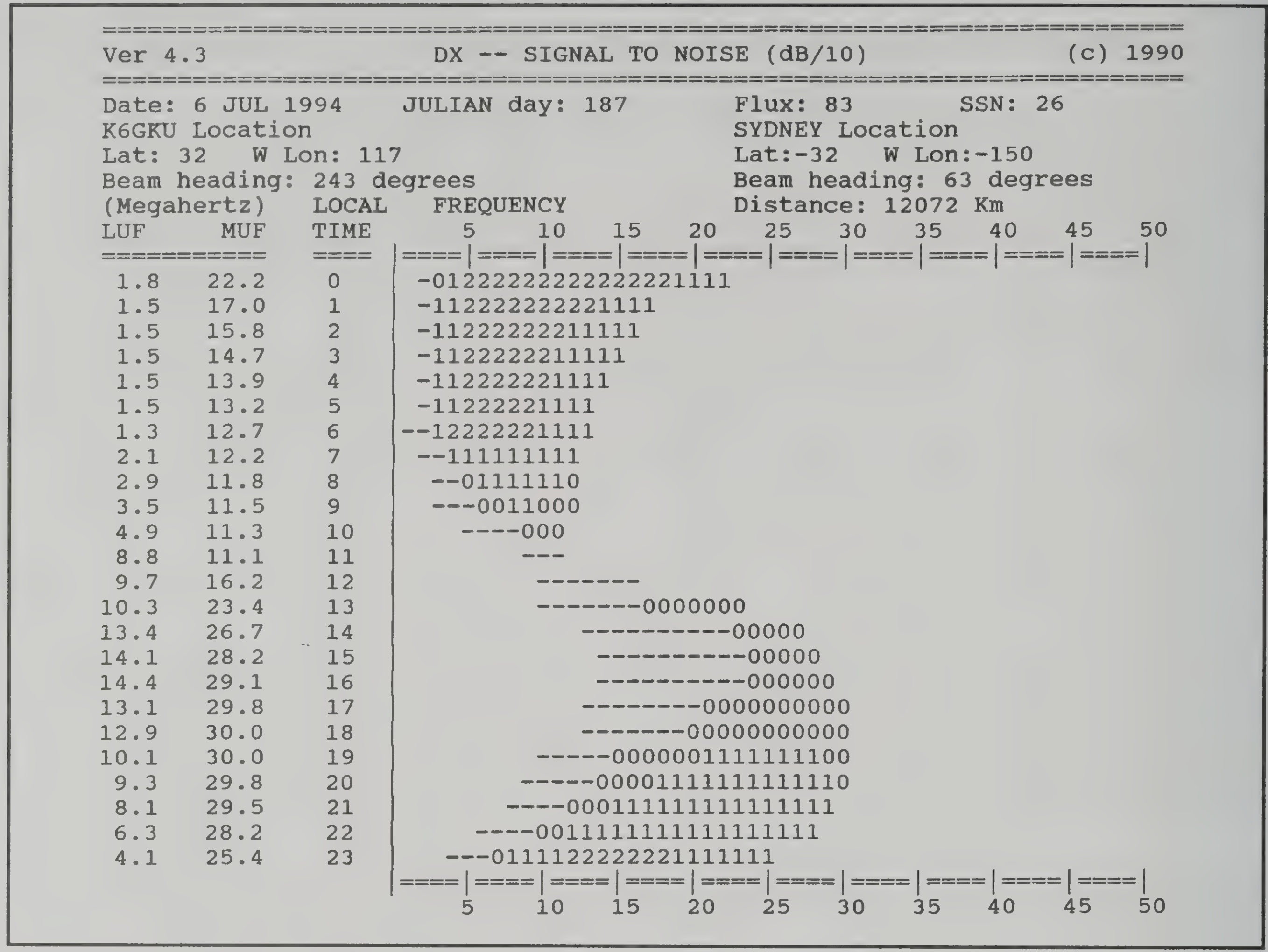

```
========================================================================
Ver 4.3               DX -- SIGNAL TO NOISE (dB/10)              (c) 1990
========================================================================
Date: 6 JUL 1994    JULIAN day: 187       Flux: 83       SSN: 26
K6GKU Location                            SYDNEY Location
Lat: 32   W Lon: 117                      Lat:-32   W Lon:-150
Beam heading: 243 degrees                 Beam heading: 63 degrees
(Megahertz)   LOCAL   FREQUENCY           Distance: 12072 Km
LUF     MUF   TIME      5    10   15   20   25   30   35   40   45   50
===========   ==== |====|====|====|====|====|====|====|====|====|====|
 1.8   22.2    0   | -01222222222222221111
 1.5   17.0    1   | -112222222221111
 1.5   15.8    2   | -11222222211111
 1.5   14.7    3   | -1122222211111
 1.5   13.9    4   | -112222221111
 1.5   13.2    5   | -11222221111
 1.3   12.7    6   |--12222221111
 2.1   12.2    7   | --111111111
 2.9   11.8    8   |  --01111110
 3.5   11.5    9   |  ---0011000
 4.9   11.3    10  |    ----000
 8.8   11.1    11  |        ---
 9.7   16.2    12  |         -------
10.3   23.4    13  |         -------0000000
13.4   26.7    14  |            ----------00000
14.1   28.2    15  |             ----------00000
14.4   29.1    16  |             ----------000000
13.1   29.8    17  |            --------0000000000
12.9   30.0    18  |            -------00000000000
10.1   30.0    19  |         -----0000001111111100
 9.3   29.8    20  |        -----00001111111111110
 8.1   29.5    21  |       ----000111111111111111
 6.3   28.2    22  |     ----0011111111111111111
 4.1   25.4    23  |   ---0111122222221111111
                   |====|====|====|====|====|====|====|====|====|====|
                        5    10   15   20   25   30   35   40   45   50
```

Figure 6.4. *DX* signal-to-noise, diurnal printout.

The easier a program is to use, and the better its "bells and whistles," the more likely that it will be used by the radio amateur and SWL.

The existence of several different propagation kernels has led to the creation of different permutations of a program wherein the kernel is the same but the MMI is different. For example, *IONCAP* has spawned *IONCAST*, *VOACAP*, *ICEPAC*, and *CAPMAN*. *IONCAST* is a PC-version of *IONCAP* developed by NRL. *VOACAP* is an updated, debugged version of an older version of *IONCAP*, and *ICEPAC* is a specialized version of *IONCAP* with a polar ionospheric model called *ICED* and a Chapman ionospheric profile. *CAPMAN* preserves the *IONCAP* kernel, improves the MMI, increases the speed of computation, provides documentation, and is customized for use by radio amateurs. Fricker's work in 1985 spawned *MINIPROP* and *IONSOUND Ver.3*. *MINIMUF* and subsequent *PROPHET* developments led to program permutations that were intended to accommodate real-time chirp sounder inputs (*CHIMPS*), while another program, created for the Australian Defence Force, replaced the simple *MINIMUF-3.5* ionospheric model with the numerical maps developed by the Australian Ionospheric Prediction Service (IPS; *PSYCHIC Ver. 1.2*).

HF prediction program development over the past two decades has shown that a new or innovative prediction process will spawn new permutations, with the major changes occurring in the MMI. Most often, the propagation kernel is left intact.

6.5 How Accurate Are The HF Prediction Programs?

Solar, geomagnetic, and ionospheric conditions are controlled by nature. Computer propagation programs attempt to emulate or predict nature, but they cannot control it. For this reason a propagation program model, no matter how complex, will always be imprecise. It is well to remember that propagation forecasting may be a highly developed art, but it is not a precise science!

Comparison of predicted and observed propagation parameters on a purely scientific basis would require a very large database of observed measurements acquired over long periods of time, at least throughout a complete sunspot cycle. Such studies require international cooperation, and they can be very expensive and time consuming. For this reason, only a limited number of such studies have been conducted. Refer to Reference 1 for details of one such study of the *MINIMUF* prediction model, which was verified against sounder data.

The general approach to verification of a particular propagation prediction program is based on user satisfaction. For example, the *IONCAP* program is used professionally for HF broadcasting and communication purposes in more than 100 countries throughout the world. W3ASK's "Propagation" column, which appears monthly in *CQ* magazine, is based on the *IONCAP* program, as are the *Master Propagation Charts* appearing in Chapter 4 of this book.

IONCAP users have had the opportunity to check the results on a "real time" or "on-air" basis, circuit by circuit, day by day, for more than a decade. If the desired results were not being achieved, users obviously would discontinue its use. Despite some shortcomings, *IONCAP* continues to be the most popular program used by HF communication professionals, and it is the one to which all others are usually compared.

In short, the propagation models in the major HF prediction programs available today are judged for accuracy mainly by the user. A radio amateur will lose confidence in a program that often predicts band openings that do not occur. Conversely, a program that is observed to consistently predict openings with a high degree of accuracy will gain a high level of confidence among users. With this in mind, for the radio amateur or the SWL, the selection of an HF prediction program usually boils down to how "user-friendly" it is, how easy it is to set up, and how easy it is to interpret the output.

Radio amateurs and other users of the HF spectrum must gain a level of comfort with how to use a particular program, and then must gain confidence in its results. The programs to be discussed in the next section, while representing varying degrees of complexity and a broad range in price, have achieved high levels of confidence with their users over a significant period of time.

6.6 Examples of HF Propagation Prediction Programs

For purposes of illustration, this section will discuss four HF prediction programs that represent four levels of scientific complexity and cost. They were chosen because: (1) we are comfortable in using them; (2) the genesis of their model set is known, and the developers are quite candid in answering questions about the models used and how they interact; and (3) they are readily accessible to the radio amateur community. We conclude with a discussion on a wider cross-sec-

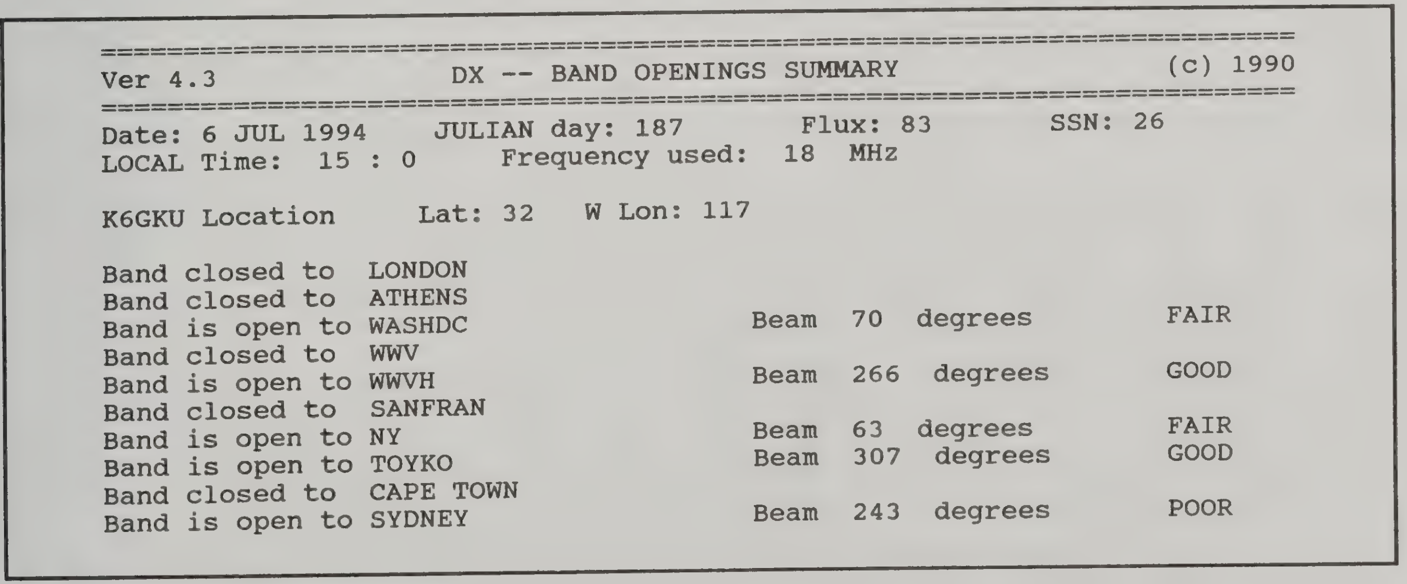

```
=========================================================================
Ver 4.3              DX -- BAND OPENINGS SUMMARY                (c) 1990
=========================================================================
Date: 6 JUL 1994    JULIAN day: 187       Flux: 83        SSN: 26
LOCAL Time:  15 : 0     Frequency used:  18  MHz

K6GKU Location     Lat: 32   W Lon: 117

Band closed to  LONDON
Band closed to  ATHENS
Band is open to WASHDC                  Beam  70  degrees          FAIR
Band closed to  WWV
Band is open to WWVH                    Beam  266  degrees         GOOD
Band closed to  SANFRAN
Band is open to NY                      Beam  63  degrees          FAIR
Band is open to TOYKO                   Beam  307  degrees         GOOD
Band closed to  CAPE TOWN
Band is open to SYDNEY                  Beam  243  degrees         POOR
```

Figure 6.5. *DX* band openings summary.

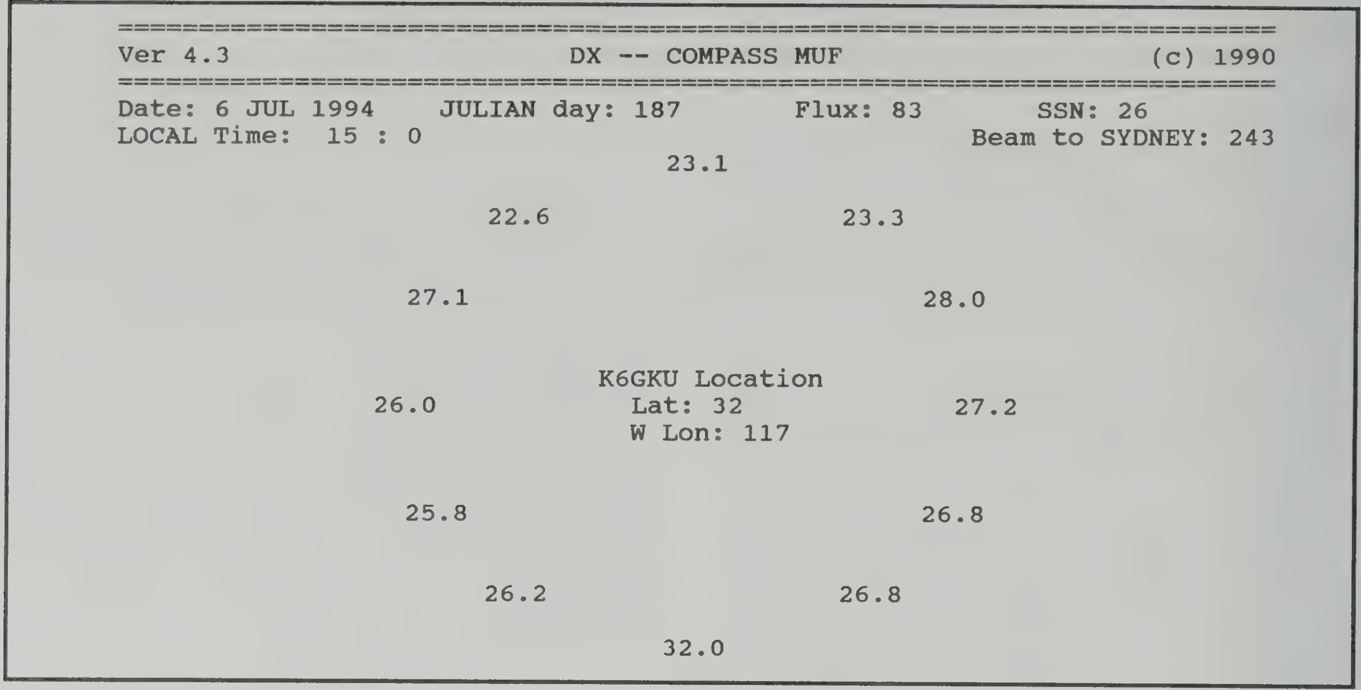

```
========================================================================
Ver 4.3                       DX -- COMPASS MUF                  (c) 1990
========================================================================
Date: 6 JUL 1994   JULIAN day: 187      Flux: 83        SSN: 26
LOCAL Time:  15 : 0                                 Beam to SYDNEY: 243
                                 23.1

                      22.6                  23.3


                 27.1                            28.0


                             K6GKU Location
               26.0            Lat: 32             27.2
                               W Lon: 117


                 25.8                            26.8


                      26.2                  26.8

                                 32.0
```

Figure 6.6. *DX* compass MUF printout.

tion of programs that is appropriate for radio amateur or SWL use.

DX (Version 4.3)

In the middle 1980s, KD6SC developed a very simple HF prediction module based on models that had been published in the open literature and, hence, that were in the public domain.[17] The propagation kernel included the *MINIMUF-3.5* model[4] to predict the MUF, the *QLOF* model[16], the original *FTZ* field strength model[18], and CCIR ambient noise models. The software is written in BASIC, and it is heavily "commented," thereby giving the user the option to modify the code. While the developer refers to this program as *DX.BAS* (signifying use of the BASIC language), the subsequent discussions and figures will refer to it solely as *DX*.

DX is quick and efficient. Version 4.3 is designed to operate on MS-DOS computer systems with all known BASIC interpreters and compilers. The version evaluated was compiled using *QUICKBASIC 4*, making it exceptionally fast for a BASIC program. The run speed will vary, depending on the version of BASIC used. The software comes with a concise eight-page manual in the "DX.DOC" file. This manual provides the user with more than enough information on how to use the software. It even devotes one page to instructing the user on how to customize his or her own version of the program. It also contains a

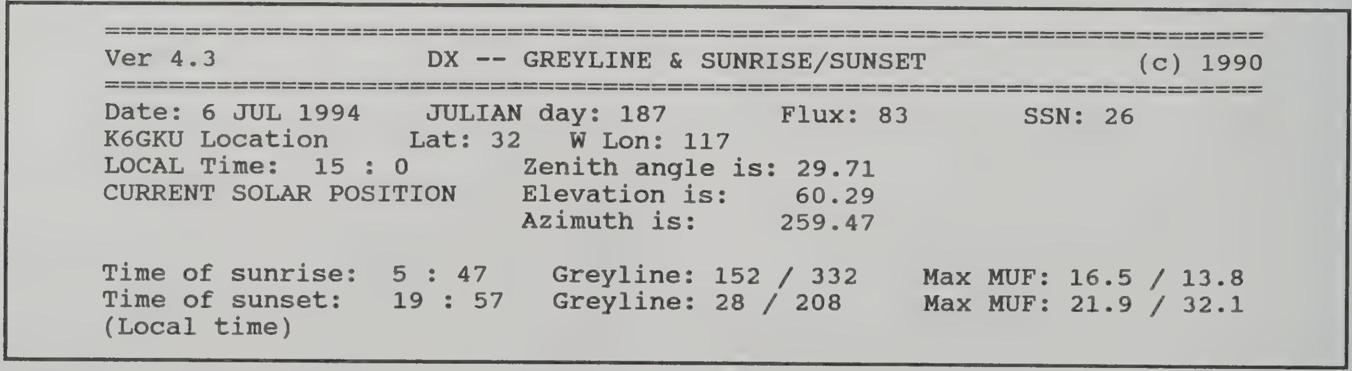

```
========================================================================
Ver 4.3                DX -- GREYLINE & SUNRISE/SUNSET           (c) 1990
========================================================================
Date: 6 JUL 1994   JULIAN day: 187      Flux: 83        SSN: 26
K6GKU Location     Lat: 32    W Lon: 117
LOCAL Time:  15 : 0      Zenith angle is: 29.71
CURRENT SOLAR POSITION   Elevation is:    60.29
                         Azimuth is:     259.47

Time of sunrise:  5 : 47   Greyline: 152 / 332   Max MUF: 16.5 / 13.8
Time of sunset:  19 : 57   Greyline: 28 / 208    Max MUF: 21.9 / 32.1
(Local time)
```

Figure 6.7. *DX* gray-line printout.

method for reporting "bugs" as well as instructions to the user for redistribution.

Even if the user chooses not to read the manual first, the simplicity of *DX* allows a person to "feel his or her way" through the first run to generate outputs. In operation, users are greeted with the menu shown in Figure 6.1. The first thing new users must do is establish where the master station is to be; normally, it is their own QTH (use the "A" command). Next, the user must select a set of receiver sites (command "R"), which normally are distant reference cities so that global conditions can be assessed. *DX* allows the user to build these reference sites in groups of 15. The next logical step is to program the user-station's power and antenna gain (command "E"). Once the user has completed these operations, he or she should exit the program (command "X"). All data will be saved, and they will be there when the program is restarted.

To run a calculation, the user updates the program for the current date (command "D"), time of day (command "T"), and solar flux (command "F"); the program now is ready to go. By the way, the solar flux can be obtained from WWV at 18 minutes after the hour on 5, 10, and 15 MHz. As we slide into the solar minimum (1996–1997), these values will hover between 65 and 85; something in between (say, 75) can be used as a default value if the user is unable to hear WWV.

The "I" command produces the Ideal Band Matrix, an example of which is shown in Figure 6.2. This product shows the best ham band as a function of time of day for each of the receiver sites in the station group selected. The selection criteria may be based either on the maximum signal-to-noise ratio (SNR) or on the band nearest the MUF. Blanks are displayed if the maximum SNR on any band is below zero, or when band selection is based on the one nearest to the MUF, if none of the bands fall between the LUF and MUF.

The "M" command (Figure 6.3) produces a standard MUF/LUF curve with an hourly MUF/LUF listing produced on the side. It also contains beam headings and distance to the receiver site.

The "N" command produces an alpha-numeric diurnal plot of signal-to-noise (S/N); see Figure 6.4. A zero means the S/N is between 0 and 10 dB. A value of "1" means the S/N is between 10 and 20 dB. A "–" means the S/N is below zero dB. The printout also contains a MUF/LUF listing for each hour.

Figure 6.5 shows the "Band Openings Summary" for a specified band. The "O" command provides this product.

The Compass Maximum MUF display "C" command yields a prediction of the highest MUF in relation to a particular compass heading. It must be understood that this display assumes ionospheric support for a single, average hop over a maximum distance of 4000 kilometers. Hops of less than this dis-

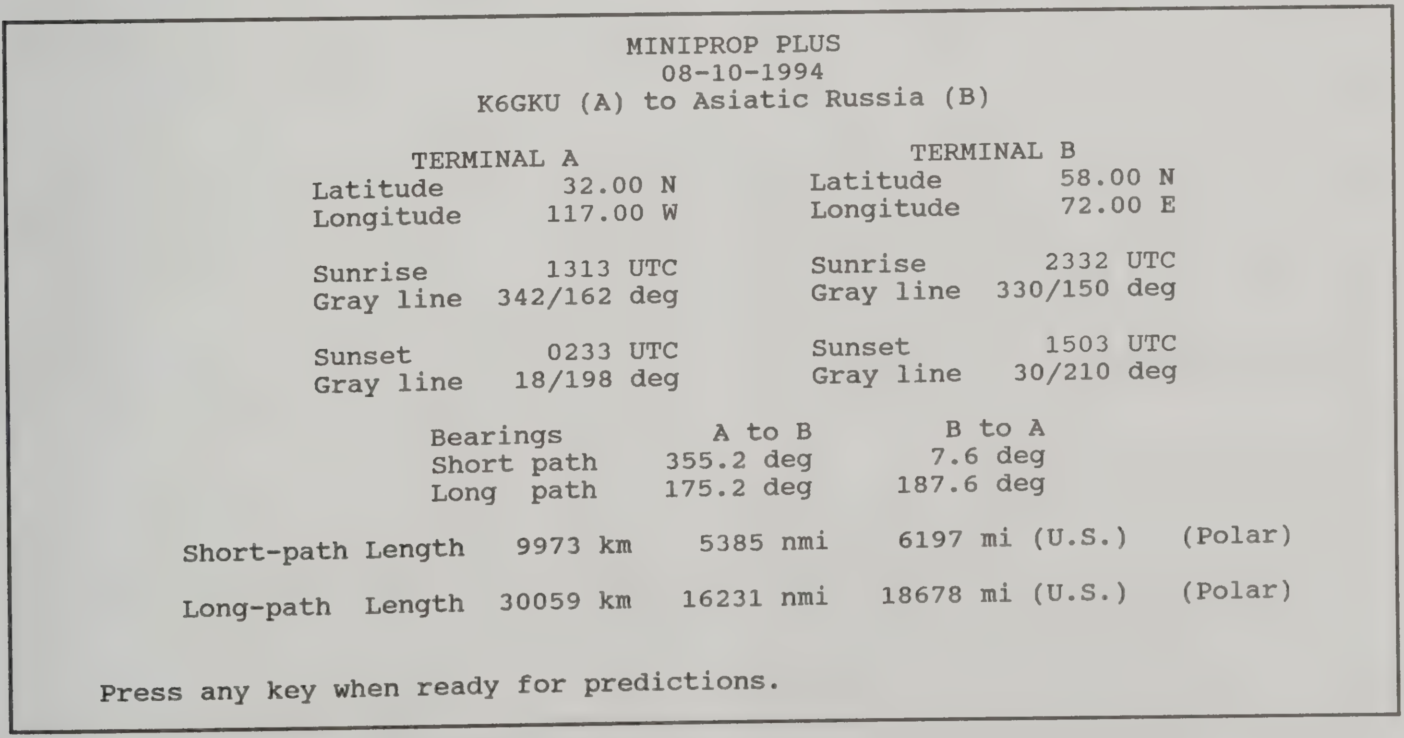

```
                          MINIPROP PLUS
                           08-10-1994
                  K6GKU (A) to Asiatic Russia (B)

            TERMINAL A                         TERMINAL B
          Latitude        32.00 N          Latitude        58.00 N
          Longitude      117.00 W          Longitude       72.00 E

          Sunrise          1313 UTC        Sunrise          2332 UTC
          Gray line   342/162 deg          Gray line   330/150 deg

          Sunset           0233 UTC        Sunset           1503 UTC
          Gray line    18/198 deg          Gray line    30/210 deg

               Bearings         A to B          B to A
               Short path     355.2 deg        7.6 deg
               Long  path     175.2 deg      187.6 deg

     Short-path Length    9973 km    5385 nmi    6197 mi (U.S.)    (Polar)

     Long-path  Length   30059 km   16231 nmi   18678 mi (U.S.)    (Polar)


  Press any key when ready for predictions.
```

Figure 6.8. *MINIPROP PLUS* opening display.

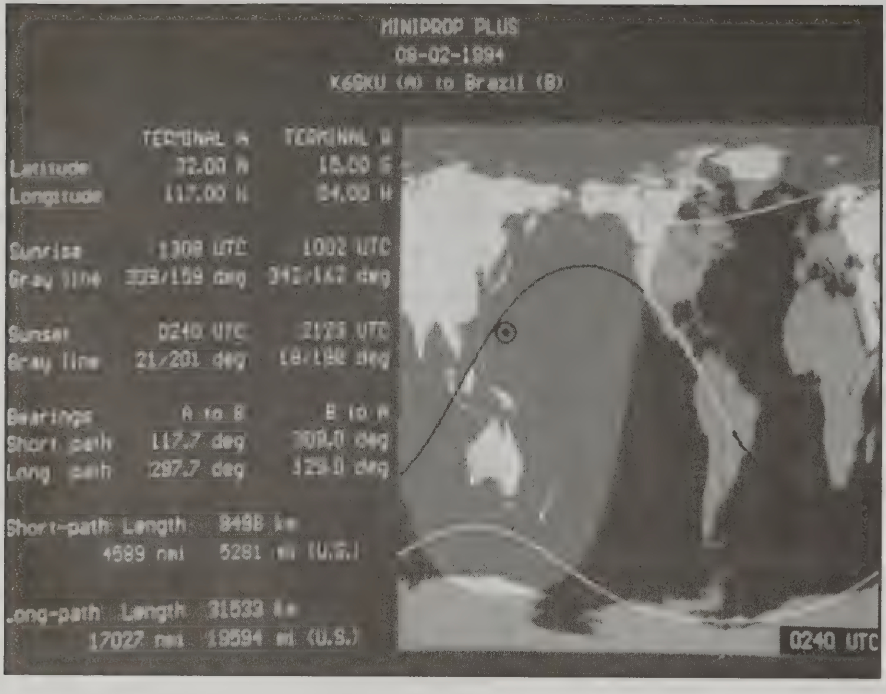

```
                         MINIPROP PLUS
                          08-02-1994
                    K6GKU (A) to Brazil (B)

             TERMINAL A    TERMINAL B
Latitude       32.00 N       16.00 S
Longitude     117.00 W       54.00 W

Sunrise       1308 UTC      1002 UTC
Gray line  339/159 deg   342/162 deg

Sunset        0240 UTC      2123 UTC
Gray line   21/201 deg    18/198 deg

Bearings        A to B        B to A
Short path   117.7 deg     309.0 deg
Long path    297.7 deg     129.0 deg

Short-path Length   8498 km
      4589 nmi   5281 mi (U.S.)

Long-path Length  31533 km
     17027 nmi  19594 mi (U.S.)
                                                         0240 UTC
```

Photo 6.A. *MINIPROP PLUS* world terminator graphic. Also shown are parts of the world covered by the proposed HF circuit.

tance will likely have lower MUFs, as will hops associated with higher antenna launch angles. Because it is unlikely that a station will be encountered such that the path length is an exact multiple of 4000 kilometers, the actual MUF to any given station may be much less than that displayed, for example, in Figure 6.6, for which the distance *is* a multiple of 4000 km.

Finally, command "G" produces gray-line times and beam headings. An example of this product is shown in Figure 6.7. Times of sunrise and sunset are displayed with the UTC offset value included so as to display the local time.

The main advantage in using the *DX* program is its speed and simplicity. It is so small that it can be "stashed" in the corner of any PC's memory. Further, it is easy to retrieve, set up, and run (less than a minute). This makes it ideal for the amateur and SWL who wants a general indication of expected "undisturbed" signal conditions, but who doesn't want to deal with the intricacies of shortwave propagation.

MINIPROP PLUS (Version 2.0)

MINIPROP PLUS is the latest in the series of *MINIPROP* programs that are in the mid-range with respect to cost and complexity.[13] Its developer, W6EL, wrote his first propagation prediction program in 1966 to help himself in working DX. His early program only computed signal strength, with the MUFs calculated manually. The publication of *MINIMUF 3.5*[4] prompted the development of *MINIPROP* version 1.0. Released in August 1985 and intended for use on early PCs, it combined the prediction of signal levels, *F*-layer MUF (using W6EL's own adjustments to *MINIMUF 3.5* for the midnight sun and polar night conditions), and *E*-layer cutoff frequency. The MS-DOS version was released the following October. *MINIPROP* version 1 and its successors are programmed in Pascal.

Using an improved *F*-layer model based on work by Fricker[12], and an improved method for predicting *E*-layer cutoff frequencies from CCIR Report 340, W6EL developed *MINIPROP* version 2.0.

In 1989, *MINIPROP* version 3.0 was introduced. This version yields improved prediction accuracy by using a mode-search algorithm that searches for the ionospheric mode yielding the strongest signal for each frequency, at every half hour. The algorithm takes into account the effects of the *D, E,* and *F* layers. Version 3.0 also provided optional support for math coprocessors in order to speed the prediction calculations. *MINIPROP PLUS* versions 1.0 and 2.0 followed in 1992 and 1994, respectively.

In *MINIPROP PLUS* version 2.0, Fricker's *F*-layer model (with a few embellishments) is used for the f_oF_2 calculations. The *K*-index adjustment is as described in Reference 6. The "k" factor correction of the secant law for converting f_oF_2 to oblique MUF is from Davies, NBS Monograph 80. The method used for *E*-layer calculations was taken from CCIR Report 340. *D*-layer absorption also is from Reference 6. In

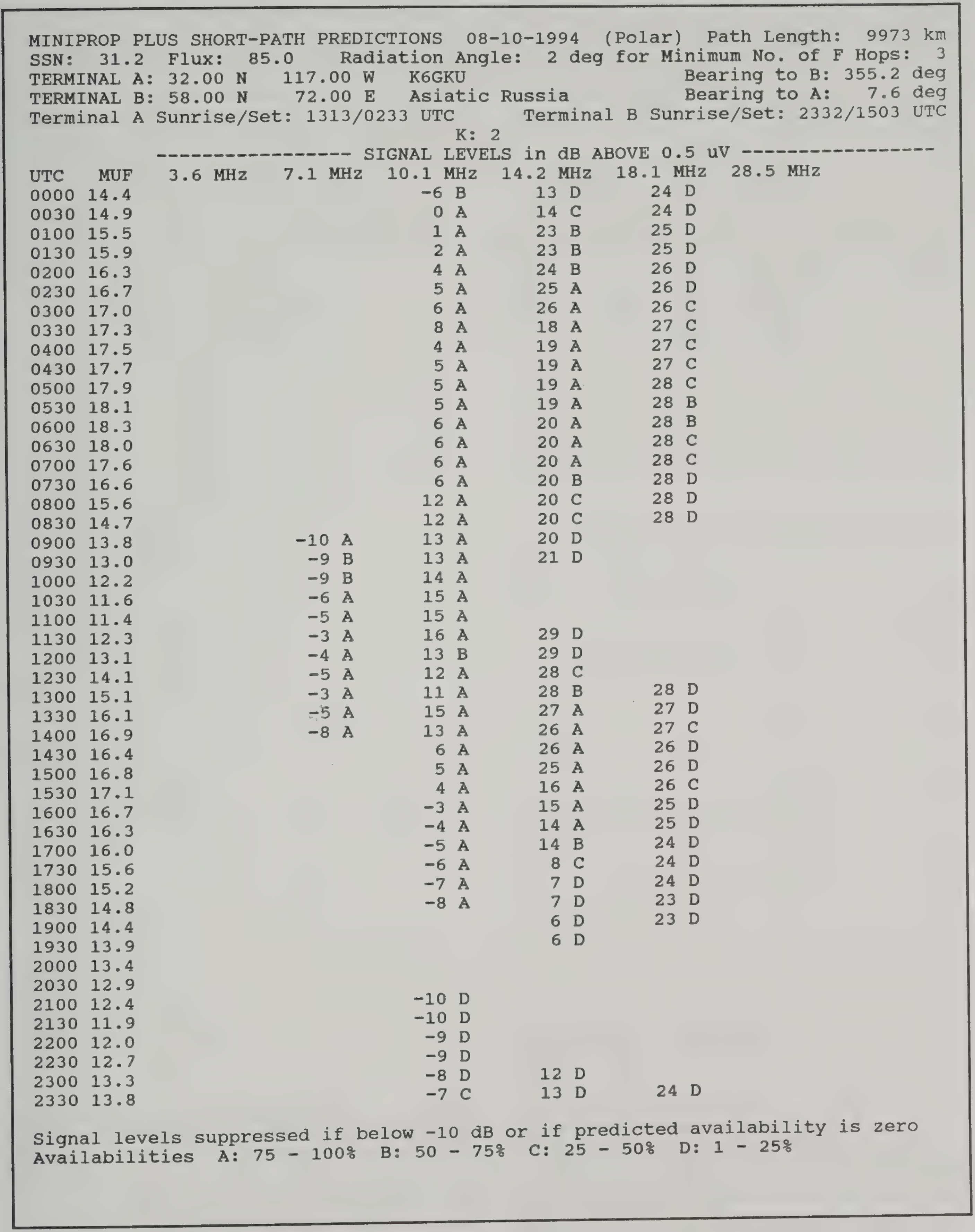

```
MINIPROP PLUS SHORT-PATH PREDICTIONS  08-10-1994  (Polar)  Path Length:  9973 km
SSN:  31.2  Flux:  85.0    Radiation Angle:  2 deg for Minimum No. of F Hops:  3
TERMINAL A: 32.00 N    117.00 W   K6GKU                   Bearing to B: 355.2 deg
TERMINAL B: 58.00 N     72.00 E   Asiatic Russia          Bearing to A:   7.6 deg
Terminal A Sunrise/Set: 1313/0233 UTC    Terminal B Sunrise/Set: 2332/1503 UTC
                                     K: 2
           ----------------- SIGNAL LEVELS in dB ABOVE 0.5 uV -----------------
UTC   MUF   3.6 MHz   7.1 MHz  10.1 MHz  14.2 MHz  18.1 MHz  28.5 MHz
0000 14.4                         -6 B      13 D      24 D
0030 14.9                          0 A      14 C      24 D
0100 15.5                          1 A      23 B      25 D
0130 15.9                          2 A      23 B      25 D
0200 16.3                          4 A      24 B      26 D
0230 16.7                          5 A      25 A      26 D
0300 17.0                          6 A      26 A      26 C
0330 17.3                          8 A      18 A      27 C
0400 17.5                          4 A      19 A      27 C
0430 17.7                          5 A      19 A      27 C
0500 17.9                          5 A      19 A      28 C
0530 18.1                          5 A      19 A      28 B
0600 18.3                          6 A      20 A      28 B
0630 18.0                          6 A      20 A      28 C
0700 17.6                          6 A      20 A      28 C
0730 16.6                          6 A      20 B      28 D
0800 15.6                         12 A      20 C      28 D
0830 14.7                         12 A      20 C      28 D
0900 13.8              -10 A      13 A      20 D
0930 13.0               -9 B      13 A      21 D
1000 12.2               -9 B      14 A
1030 11.6               -6 A      15 A
1100 11.4               -5 A      15 A
1130 12.3               -3 A      16 A      29 D
1200 13.1               -4 A      13 B      29 D
1230 14.1               -5 A      12 A      28 C
1300 15.1               -3 A      11 A      28 B      28 D
1330 16.1               -5 A      15 A      27 A      27 D
1400 16.9               -8 A      13 A      26 A      27 C
1430 16.4                          6 A      26 A      26 D
1500 16.8                          5 A      25 A      26 D
1530 17.1                          4 A      16 A      26 C
1600 16.7                         -3 A      15 A      25 D
1630 16.3                         -4 A      14 A      25 D
1700 16.0                         -5 A      14 B      24 D
1730 15.6                         -6 A       8 C      24 D
1800 15.2                         -7 A       7 D      24 D
1830 14.8                         -8 A       7 D      23 D
1900 14.4                                    6 D      23 D
1930 13.9                                    6 D
2000 13.4
2030 12.9
2100 12.4                        -10 D
2130 11.9                        -10 D
2200 12.0                         -9 D
2230 12.7                         -9 D
2300 13.3                         -8 D      12 D
2330 13.8                         -7 C      13 D      24 D

Signal levels suppressed if below -10 dB or if predicted availability is zero
Availabilities  A: 75 - 100%  B: 50 - 75%  C: 25 - 50%  D: 1 - 25%
```

Figure 6.9. *MINIPROP PLUS* mode search printout.

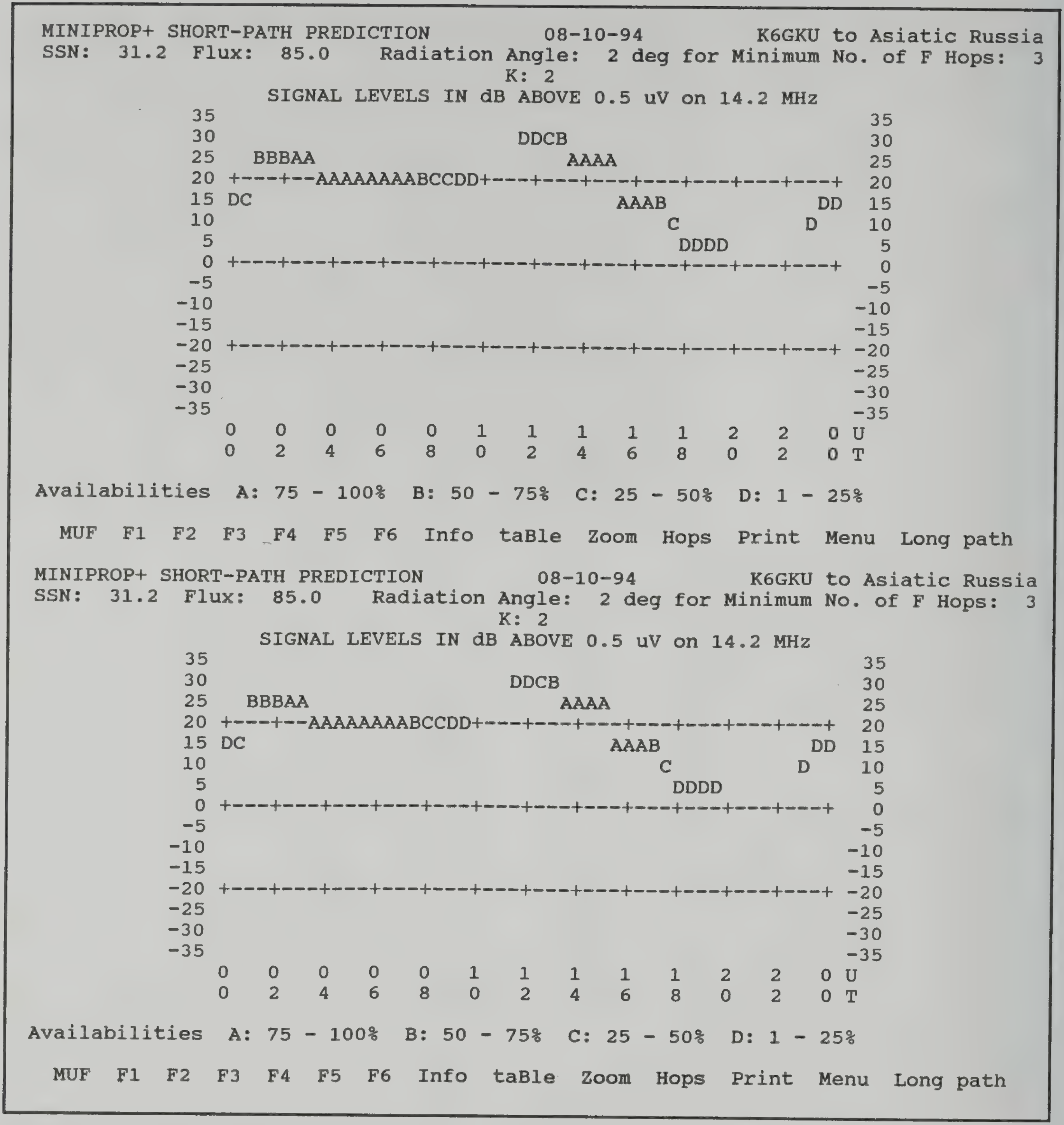

```
MINIPROP+ SHORT-PATH PREDICTION         08-10-94         K6GKU to Asiatic Russia
SSN:  31.2  Flux:  85.0    Radiation Angle:  2 deg for Minimum No. of F Hops:  3
                                     K: 2
                  SIGNAL LEVELS IN dB ABOVE 0.5 uV on 14.2 MHz
            35                                                    35
            30                        DDCB                        30
            25   BBBAA                    AAAA                    25
            20 +---+--AAAAAAAABCCDD+---+---+---+---+---+---+---+  20
            15 DC                             AAAB            DD  15
            10                                    C          D    10
             5                                     DDDD            5
             0 +---+---+---+---+---+---+---+---+---+---+---+---+   0
            -5                                                    -5
           -10                                                   -10
           -15                                                   -15
           -20 +---+---+---+---+---+---+---+---+---+---+---+---+ -20
           -25                                                   -25
           -30                                                   -30
           -35                                                   -35
               0   0   0   0   0   1   1   1   1   1   2   2   0 U
               0   2   4   6   8   0   2   4   6   8   0   2   0 T

Availabilities  A: 75 - 100%  B: 50 - 75%  C: 25 - 50%  D: 1 - 25%

  MUF  F1  F2  F3  F4  F5  F6  Info  taBle  Zoom  Hops  Print  Menu  Long path
```

```
MINIPROP+ SHORT-PATH PREDICTION         08-10-94         K6GKU to Asiatic Russia
SSN:  31.2  Flux:  85.0    Radiation Angle:  2 deg for Minimum No. of F Hops:  3
                                     K: 2
                  SIGNAL LEVELS IN dB ABOVE 0.5 uV on 14.2 MHz
            35                                                    35
            30                        DDCB                        30
            25   BBBAA                    AAAA                    25
            20 +---+--AAAAAAAABCCDD+---+---+---+---+---+---+---+  20
            15 DC                             AAAB            DD  15
            10                                    C          D    10
             5                                     DDDD            5
             0 +---+---+---+---+---+---+---+---+---+---+---+---+   0
            -5                                                    -5
           -10                                                   -10
           -15                                                   -15
           -20 +---+---+---+---+---+---+---+---+---+---+---+---+ -20
           -25                                                   -25
           -30                                                   -30
           -35                                                   -35
               0   0   0   0   0   1   1   1   1   1   2   2   0 U
               0   2   4   6   8   0   2   4   6   8   0   2   0 T

Availabilities  A: 75 - 100%  B: 50 - 75%  C: 25 - 50%  D: 1 - 25%

  MUF  F1  F2  F3  F4  F5  F6  Info  taBle  Zoom  Hops  Print  Menu  Long path
```

Figure 6.10. *MINIPROP PLUS* expected signal level for 14.2 MHz.

MINIPROP PLUS, the position of the Sun and the solar declination on any date are derived from Kepler's equations for an elliptical orbit (unlike many other programs, which assume the Earth's orbit is circular).

MINIPROP PLUS passed the first acid test: Could an average person use it without having to refer to the manual? In fact, it passed with flying colors! The program uses a protocol that is very user-friendly. The outputs are presented in such a manner that the program can serve a wide range of users having varied degrees of understanding with respect to HF propagation. Further, the manual is well written and complete.

In fact, it is recommended that the first thing *MINIPROP PLUS* users do is read the manual, because the author has an extensive knowledge of HF propagation, and he explains how the program works in a manner that is easily understood.

The program combines alphanumeric and graphical displays; the user can switch back and forth with relative ease. Using a "486" PC with a numeric coprocessor, *MINIPROP PLUS*'s calculation times range from several seconds to almost instantaneous following a carriage return. While slower, the program can be run without a numeric processor on most PCs.

MINIPROP PLUS calculates results on a path-by-path basis. It is quite easy to change paths with the extensive atlas of geographical locations provided with the software. Once the user has selected the desired path end-points, he or she is greeted with the bulletin shown in Figure 6.8. It confirms the geographical location of the end-points, sunrise and sunset times at both locations, gray-line times and beam headings, and great-circle beam headings.

One of the most impressive displays (remember our previous comments about man-machine interfaces) is the world map showing the terminator (gray-line coverage) and the long- and short-path routes (see Photo 6.A). This routine, which is easily brought up anytime within a session, quickly shows the user the parts of the world covered by the proposed HF circuit.

Figure 6.9 shows an example printout for the "mode-search" routine. Here, the program searches for the strongest mode of propagation (i.e., *E* layer, F_2 layer, F_2 layer with *E*-layer intervention, etc.) in 30-minute increments, in each frequency band of interest. This routine is very computer-intensive, and it will take some time to complete with smaller computers. The developer was quite careful to explain in the text exactly what is meant by "signal level."

Within the "mode-search" routine, the user is permitted to display the expected signal levels as a function of the time of day for each of the frequency bands previously specified. As seen in Figure 6.10, alphanotation denotes expected availability.

For users with smaller, slower computers, the "quick-look" product, shown in Figure 6.11, is more appropriate. Here, the predicted signal levels and mode availabilities are based on the assumption that propagation is via the lowest-order, pure *F*-layer mode (i.e., *E*-layer intervention is omitted).

MINIPROP PLUS also contains a DX Compass feature (see Figure 6.12) which shows the maximum one-hop MUF at 12 points around the compass. The user is again reminded that MUF calculations produce median values.

The "Hops" routine, shown in Figure 6.13, shows the dominant mode in each frequency band, the expected availability, the angle and the number of hops, and the *E/F*-layer combinations in mixed modes. This feature is for the serious student of propagation and is not for the casual user.

The last example of *MINIPROP PLUS* products is the world frequency map shown in Photo 6.B. Here, global coverage is displayed for each of the preselected frequency bands. This capability provides the user with a "quick look" at the parts of the world to which their favorite band is open.

In summary, *MINIPROP PLUS* is a quick, capable prediction program. Its development is well documented, and the program provides the user with a variety of useful information in a format that will appeal both to the casual operator or SWL as well as to the avid DXer.

Advanced Stand Alone Prediction System (ASAPS) V2.1

ASAPS[19] is an example of a top-end HF propagation prediction program that was designed by professionals to be used by those who make their living in HF-related industries. The program was developed by a team of scientists at the Ionospheric Prediction Service (IPS) in Australia. Because the HF spectrum still is widely used in Australia, both by the military as well as by commercial firms, there is a significant demand for an HF prediction program that can be used by operators having a wide variety of backgrounds and experience. While somewhat more "pricey" than the *DX* and *MINIPROP PLUS* programs, *ASAPS* is a more capable program and is fully supported by IPS (you can even talk to them on "e-mail" through INTERNET). Further, you can get a monthly newsletter from IPS with updated values for the *T*-index. What's the *T*-index? The monthly *T*-index is derived from the observed, monthly, median values of f_oF_2 for each hour at up to 40 ionospheric stations worldwide. These records become available from IPS stations in Australia very soon after the end of each month, but the majority of station data are received up to one year later. This means that the exact, observed value of the monthly *T*-index is not available until some months later. The *T*-index is used because it relates closely to measured variations in the ionosphere due to sunspot activity. Specifically, there is a close corre-

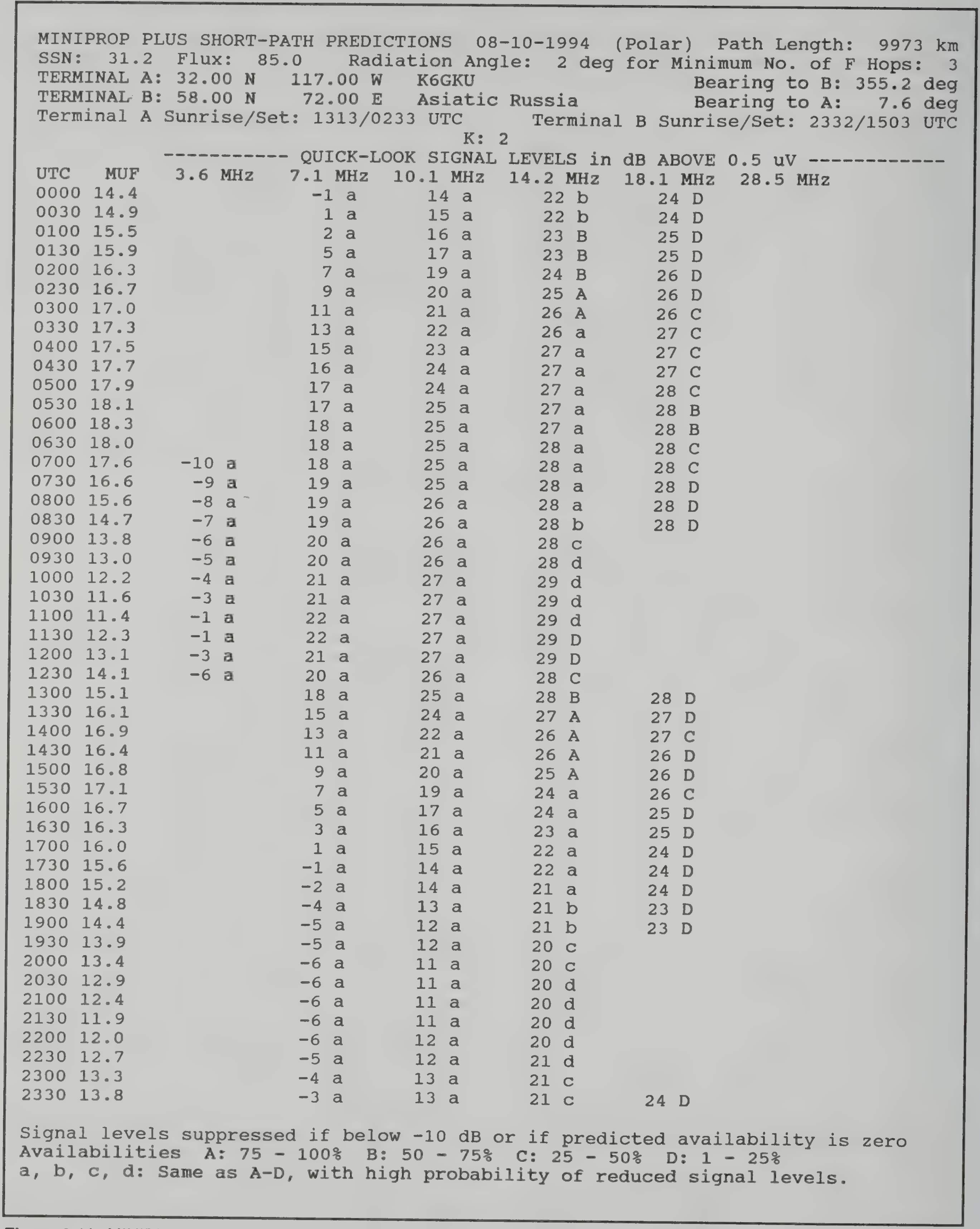

```
MINIPROP PLUS SHORT-PATH PREDICTIONS  08-10-1994  (Polar)  Path Length:  9973 km
SSN:  31.2  Flux:  85.0    Radiation Angle:  2 deg for Minimum No. of F Hops:  3
TERMINAL A: 32.00 N   117.00 W   K6GKU                     Bearing to B: 355.2 deg
TERMINAL B: 58.00 N    72.00 E   Asiatic Russia            Bearing to A:   7.6 deg
Terminal A Sunrise/Set: 1313/0233 UTC      Terminal B Sunrise/Set: 2332/1503 UTC
                                     K: 2
           ----------- QUICK-LOOK SIGNAL LEVELS in dB ABOVE 0.5 uV ------------
UTC  MUF    3.6 MHz   7.1 MHz  10.1 MHz  14.2 MHz  18.1 MHz  28.5 MHz
0000 14.4               -1 a      14 a      22 b      24 D
0030 14.9                1 a      15 a      22 b      24 D
0100 15.5                2 a      16 a      23 B      25 D
0130 15.9                5 a      17 a      23 B      25 D
0200 16.3                7 a      19 a      24 B      26 D
0230 16.7                9 a      20 a      25 A      26 D
0300 17.0               11 a      21 a      26 A      26 C
0330 17.3               13 a      22 a      26 a      27 C
0400 17.5               15 a      23 a      27 a      27 C
0430 17.7               16 a      24 a      27 a      27 C
0500 17.9               17 a      24 a      27 a      28 C
0530 18.1               17 a      25 a      27 a      28 B
0600 18.3               18 a      25 a      27 a      28 B
0630 18.0               18 a      25 a      28 a      28 C
0700 17.6   -10 a       18 a      25 a      28 a      28 C
0730 16.6    -9 a       19 a      25 a      28 a      28 D
0800 15.6    -8 a       19 a      26 a      28 a      28 D
0830 14.7    -7 a       19 a      26 a      28 b      28 D
0900 13.8    -6 a       20 a      26 a      28 c
0930 13.0    -5 a       20 a      26 a      28 d
1000 12.2    -4 a       21 a      27 a      29 d
1030 11.6    -3 a       21 a      27 a      29 d
1100 11.4    -1 a       22 a      27 a      29 d
1130 12.3    -1 a       22 a      27 a      29 D
1200 13.1    -3 a       21 a      27 a      29 D
1230 14.1    -6 a       20 a      26 a      28 C
1300 15.1               18 a      25 a      28 B      28 D
1330 16.1               15 a      24 a      27 A      27 D
1400 16.9               13 a      22 a      26 A      27 C
1430 16.4               11 a      21 a      26 A      26 D
1500 16.8                9 a      20 a      25 A      26 D
1530 17.1                7 a      19 a      24 a      26 C
1600 16.7                5 a      17 a      24 a      25 D
1630 16.3                3 a      16 a      23 a      25 D
1700 16.0                1 a      15 a      22 a      24 D
1730 15.6               -1 a      14 a      22 a      24 D
1800 15.2               -2 a      14 a      21 a      24 D
1830 14.8               -4 a      13 a      21 b      23 D
1900 14.4               -5 a      12 a      21 b      23 D
1930 13.9               -5 a      12 a      20 c
2000 13.4               -6 a      11 a      20 c
2030 12.9               -6 a      11 a      20 d
2100 12.4               -6 a      11 a      20 d
2130 11.9               -6 a      11 a      20 d
2200 12.0               -6 a      12 a      20 d
2230 12.7               -5 a      12 a      21 d
2300 13.3               -4 a      13 a      21 c
2330 13.8               -3 a      13 a      21 c      24 D

Signal levels suppressed if below -10 dB or if predicted availability is zero
Availabilities  A: 75 - 100%  B: 50 - 75%  C: 25 - 50%  D: 1 - 25%
a, b, c, d: Same as A-D, with high probability of reduced signal levels.
```

Figure 6.11. *MINIPROP PLUS* “quick-look” printout.

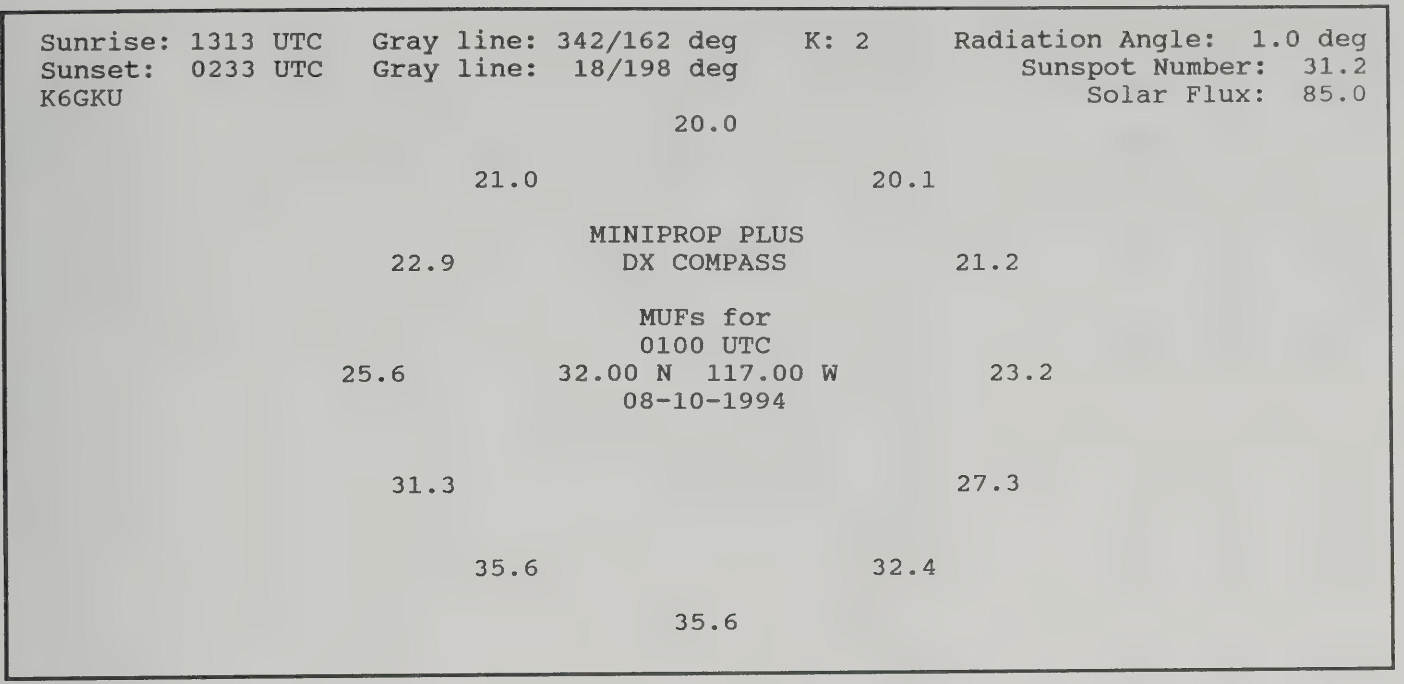

```
Sunrise: 1313 UTC   Gray line: 342/162 deg    K: 2     Radiation Angle:  1.0 deg
Sunset:  0233 UTC   Gray line:  18/198 deg                 Sunspot Number:  31.2
K6GKU                                                          Solar Flux:  85.0
                                         20.0

                           21.0                        20.1

                                     MINIPROP PLUS
                      22.9            DX COMPASS            21.2

                                       MUFs for
                                       0100 UTC
                   25.6             32.00 N  117.00 W           23.2
                                      08-10-1994


                      31.3                                  27.3


                           35.6                        32.4

                                         35.6
```

Figure 6.12. *MINIPROP PLUS* DX compass printout.

lation between the *T*-index and the smoothed sunspot number (SSN), and given the data from which it is derived, it would appear that the *T*-index should provide a better global representation of the ionosphere under a larger range of conditions. It is here, in the *T*-index, that *ASAPS* differs from *IONCAP*. In *IONCAP* the numerical maps for f_oF_2 were developed from data gathered in 1954 and 1957. In *ASAPS*, the numerical maps of the *T*-index (f_oF_2) reflect 40 years or more of data.

The predicted, smoothed monthly values of the *T*-index are computed by using a statistical analysis of the observed monthly *T*-indices for all solar cycles since 1938. In the absence of predicted *T*-index values, *ASAPS will take the predicted SSN and convert it to a T-index.*

ASAPS will run on most modern PCs with 512K RAM and a hard disk. *ASAPS* is not a program that a newcomer can sit down to and immediately start using. Its use does require a bit of initial preparation and some planning on: (1) antenna patterns; (2) transmitter/receiver names and locations (called terminals); and (3) how to pair terminals into what are called "circuits." The software should be accompanied by a recent copy of the IPS Solar-Geophysical Summary (published monthly). In each issue is a table (see Table 6.2) with 10 years of *T*-indices. The April 1994 Bulletin contains data from 1988 through 1997, the data for the latter four years being predicted values.

New users of *ASAPS* are greeted with the screen shown in Figure 6.14; nine function-key options are seen. Probably the first thing you should do is sit down and build the *T*-index database (F1). If you don't, the program will continue to remind you that the database is not there or has not yet been updated. Then, you should generate your "terminal" database, your "frequency set" database, and the "circuit" database. Finally, it would be worthwhile to spend the time necessary to generate an "antenna set" database that includes the antennas you use (or may be considering).

Once all of the databases have been generated and saved, the user should read pages 34 and 35 in the manual (the glossary of terms). The terminology used in *ASAPS* is somewhat different from other programs. On the screen you will see terms such as Absorption Limiting Frequency (ALF), Best Usable Frequency (BUF), *E*-layer Maximum Usable Frequency (EMUF), Optimum Working Frequency (OWF), and Upper Decile (UD).

Once the manual is read and understood, *ASAPS* is ready to use. The program has been designed to provide the user with a variety of information in a number of formats on many different circuits. Once properly set up, many plots can be generated very quickly. The program is particularly useful in revisiting predetermined scenarios such as those used in doing monthly coverage predictions for shortwave broadcast stations.

When *ASAPS* runs a calculation, the program con-

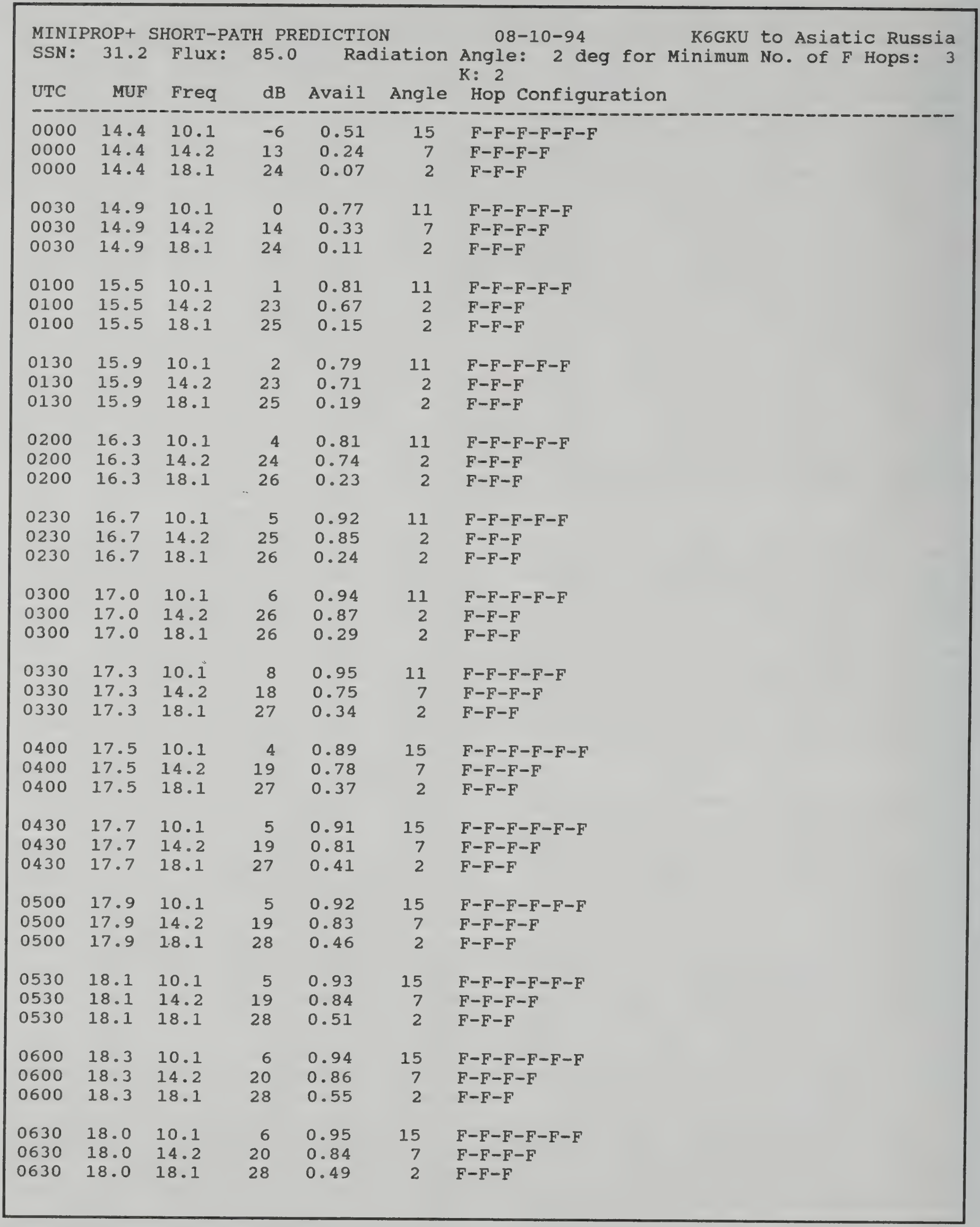

```
MINIPROP+ SHORT-PATH PREDICTION          08-10-94         K6GKU to Asiatic Russia
SSN:  31.2  Flux:  85.0    Radiation Angle:  2 deg for Minimum No. of F Hops:  3
                                       K: 2
UTC     MUF  Freq     dB  Avail  Angle  Hop Configuration
---------------------------------------------------------------------------------
0000   14.4  10.1     -6   0.51     15   F-F-F-F-F-F
0000   14.4  14.2     13   0.24      7   F-F-F-F
0000   14.4  18.1     24   0.07      2   F-F-F

0030   14.9  10.1      0   0.77     11   F-F-F-F-F
0030   14.9  14.2     14   0.33      7   F-F-F-F
0030   14.9  18.1     24   0.11      2   F-F-F

0100   15.5  10.1      1   0.81     11   F-F-F-F-F
0100   15.5  14.2     23   0.67      2   F-F-F
0100   15.5  18.1     25   0.15      2   F-F-F

0130   15.9  10.1      2   0.79     11   F-F-F-F-F
0130   15.9  14.2     23   0.71      2   F-F-F
0130   15.9  18.1     25   0.19      2   F-F-F

0200   16.3  10.1      4   0.81     11   F-F-F-F-F
0200   16.3  14.2     24   0.74      2   F-F-F
0200   16.3  18.1     26   0.23      2   F-F-F

0230   16.7  10.1      5   0.92     11   F-F-F-F-F
0230   16.7  14.2     25   0.85      2   F-F-F
0230   16.7  18.1     26   0.24      2   F-F-F

0300   17.0  10.1      6   0.94     11   F-F-F-F-F
0300   17.0  14.2     26   0.87      2   F-F-F
0300   17.0  18.1     26   0.29      2   F-F-F

0330   17.3  10.1      8   0.95     11   F-F-F-F-F
0330   17.3  14.2     18   0.75      7   F-F-F-F
0330   17.3  18.1     27   0.34      2   F-F-F

0400   17.5  10.1      4   0.89     15   F-F-F-F-F-F
0400   17.5  14.2     19   0.78      7   F-F-F-F
0400   17.5  18.1     27   0.37      2   F-F-F

0430   17.7  10.1      5   0.91     15   F-F-F-F-F-F
0430   17.7  14.2     19   0.81      7   F-F-F-F
0430   17.7  18.1     27   0.41      2   F-F-F

0500   17.9  10.1      5   0.92     15   F-F-F-F-F-F
0500   17.9  14.2     19   0.83      7   F-F-F-F
0500   17.9  18.1     28   0.46      2   F-F-F

0530   18.1  10.1      5   0.93     15   F-F-F-F-F-F
0530   18.1  14.2     19   0.84      7   F-F-F-F
0530   18.1  18.1     28   0.51      2   F-F-F

0600   18.3  10.1      6   0.94     15   F-F-F-F-F-F
0600   18.3  14.2     20   0.86      7   F-F-F-F
0600   18.3  18.1     28   0.55      2   F-F-F

0630   18.0  10.1      6   0.95     15   F-F-F-F-F-F
0630   18.0  14.2     20   0.84      7   F-F-F-F
0630   18.0  18.1     28   0.49      2   F-F-F
```

Figure 6.13. *MINIPROP PLUS* hops printout.

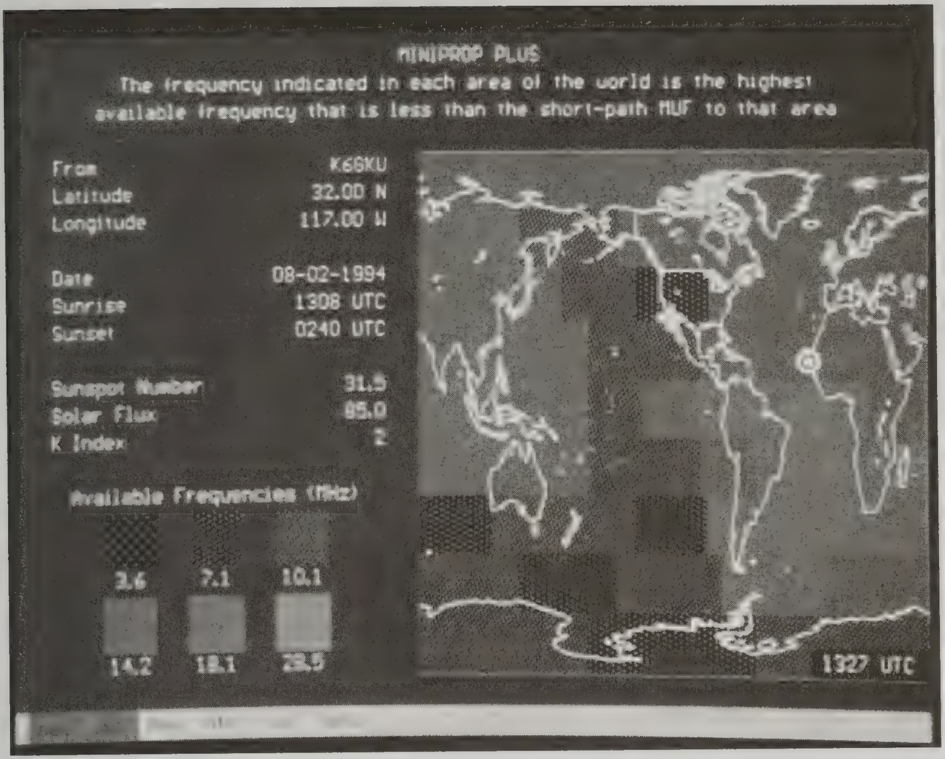

```
                         MINIPROP PLUS
      The frequency indicated in each area of the world is the highest
   available frequency that is less than the short-path MUF to that area

From                K6GKU
Latitude          32.00 N
Longitude        117.00 W

Date           08-02-1994
Sunrise          1308 UTC
Sunset           0240 UTC

Sunspot Number       31.5
Solar Flux           85.0
K Index                 2

 Available Frequencies (MHz)

    3.6     7.1    10.1

   14.2    18.1    28.5
                                                             1327 UTC
```

Photo 6.B. *MINIPROP PLUS* world coverage by frequency band.

structs two files: a field strength (FS) file and a GRAFEX file. If the field strength file is selected, the screen shown in Figure 6.15 will appear. While in this mode, the data can be reviewed in terms of the eight parameters shown at the bottom of the screen. In addition, the user can select between the modes of propagation; in this case, there were two: the 2*F* and the 3*F*. In this run, 16 different screens of data can be produced, printed, and/or stored. *ASAPS* can produce an immense amount of information in a very short period of time. Figure 6.16 illustrates the field strength printout expressed in dB above 1 microvolt/meter. Pressing the "S" key produces a signal-to-noise screen (see Figure 6.17). Pressing the "B" key produces the Best Usable Frequency (BUF) Prediction (see Figure 6.18). The BUF for each hour is defined as the frequency having the maximum signal-to-noise ratio from any mode that also satisfies the specified minimum angle and required signal-to-noise and probability levels.

Photo 6.C shows the graphical version of this output. If it seems that a user can be overwhelmed with the volume of data produced, that impression is valid. *ASAPS* solves each task in great detail, and gives the user many different ways to look at the solution.

Pressing the F5 key brings the user back to the "recompute" function. For every calculation run, there is an "F" file and a "G" file. The "F" file is the field strength file that we just have reviewed. Selection of the "G" file brings up the GRAFEX mode, in which alpha-numeric combinations, together with color combinations, convey a large amount of information on a single screen (see Figure 6.19).

Finally, *ASAPS* is useful for developing long-range statistics because up to 250 "F" files and "G" files are automatically retained. This means that you can revisit a given scenario when you have new or up-dated information on equipment or paths of interest.

IONCAP

One cannot discuss computerized propagation programs without mentioning *IONCAP*, the Ionospheric Communications Analysis and Prediction program.[20] It was developed in the late 1970s by the Institute of Telecommunication Sciences (ITS), U.S. Department of Commerce, Boulder, Colorado, as a mainframe program. Since then, it has become a standard by which other programs are judged, and it is used extensively by many government agencies and broadcasters around the world. Until the late 1980s, it was not available to the general public.

Some of the more important variables used in developing the *IONCAP* program are:

- Numerical maps of the median critical frequencies in the E, E_s, F_1, and F_2 layers.
- Numerical maps of atmospheric radio noise.

Latest *T*-Indices for IPS Advanced Stand-Alone Prediction System (*ASAPS*)
Last Update: April 1994 Solar-Geophysical Summary

Year	Jan.	Feb.	Mar.	Apr.	May	Jun.	Jul.	Aug.	Sep.	Oct.	Nov.	Dec.
1988	45	43	58	74	72	84	84	95	115	132	116	128
1989	147	164	135	140	141	157	162	149	143	159	164	152
1990	150	128	135	129	126	138	136	138	141	136	122	133
1991	142	176	172	164	136	118	141	128	136	131	121	130
1992	152	172	156	134	95	79	89	66	68	67	85	89
1993	75	78	80	65	63	63	55	47	34	31	37	58
1994	39*	37*	36*	35*	34*	31*	28*	26*	24*	22*	21*	19*
1995	18*	18*	17*	16*	15*	14*	14*	13*	12*	11*	11*	10*
1996	10*	9*	9*	8*	8*	8*	8*	9*	9*	10*	11*	12*
1997	13*	15*	17*	19*	21*	23*	26*	30*	33*	38*	43*	48*

**Asterisk indicates predicted value. For information concerning* ASAPS *for an IBM PC (or compatible), contact IPS.*

Table 6.2. IPS *T*-index 10-year table. It is interesting to note that these data suggest that the sunspot minimum will not occur until mid-1996.

- Numerical maps of layer thickness.
- F_2-layer heights from numerical maps of the M-3000 factor.
- Tables of values of the distribution of signal levels.
- Numerical maps of the distribution of radio noise.
- Tables of values for distribution of F_2-layer critical frequencies.
- Numerical coefficients for distribution of E_s-layer critical frequencies.
- Empirically derived equation for F_1-layer heights.
- Empirically derived constants for *E*- and F_1-layer thickness.
- Empirically derived constants for *E*-layer height.
- Empirically derived equations for over-the-MUF losses and their distribution.
- Numerical coefficients for the distribution of E_s-layer critical frequencies.
- Empirically derived equations for E_s reflection and losses.

In 1988, a PC version of *IONCAP* was developed, but it was very slow in operation, was not user friendly (poor MMI), and lacked adequate documentation.

Don Lucas, one of the leading developers of *IONCAP* at ITS, also is W0OMI. Upon his retirement, he decided to transform *IONCAP* into a PC-based pro-

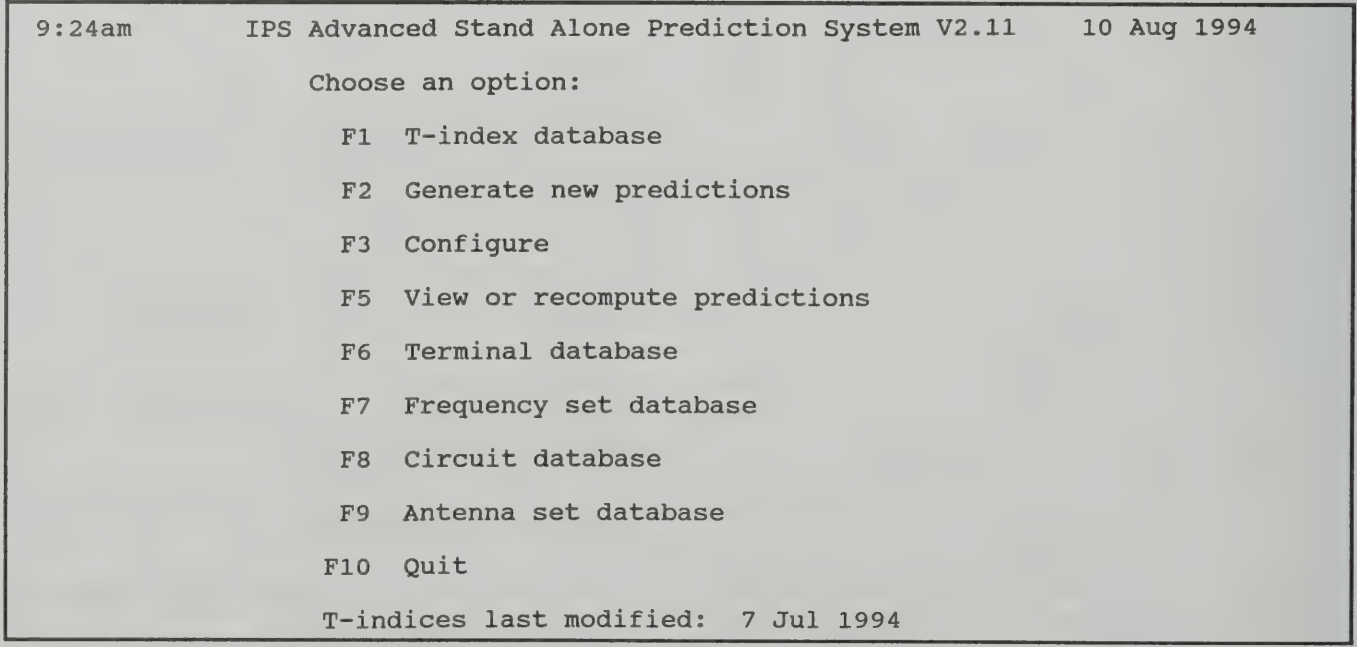

```
9:24am        IPS Advanced Stand Alone Prediction System V2.11    10 Aug 1994

                        Choose an option:

                          F1   T-index database

                          F2   Generate new predictions

                          F3   Configure

                          F5   View or recompute predictions

                          F6   Terminal database

                          F7   Frequency set database

                          F8   Circuit database

                          F9   Antenna set database

                         F10   Quit

                         T-indices last modified:  7 Jul 1994
```

Figure 6.14. *ASAPS* preamble menu.

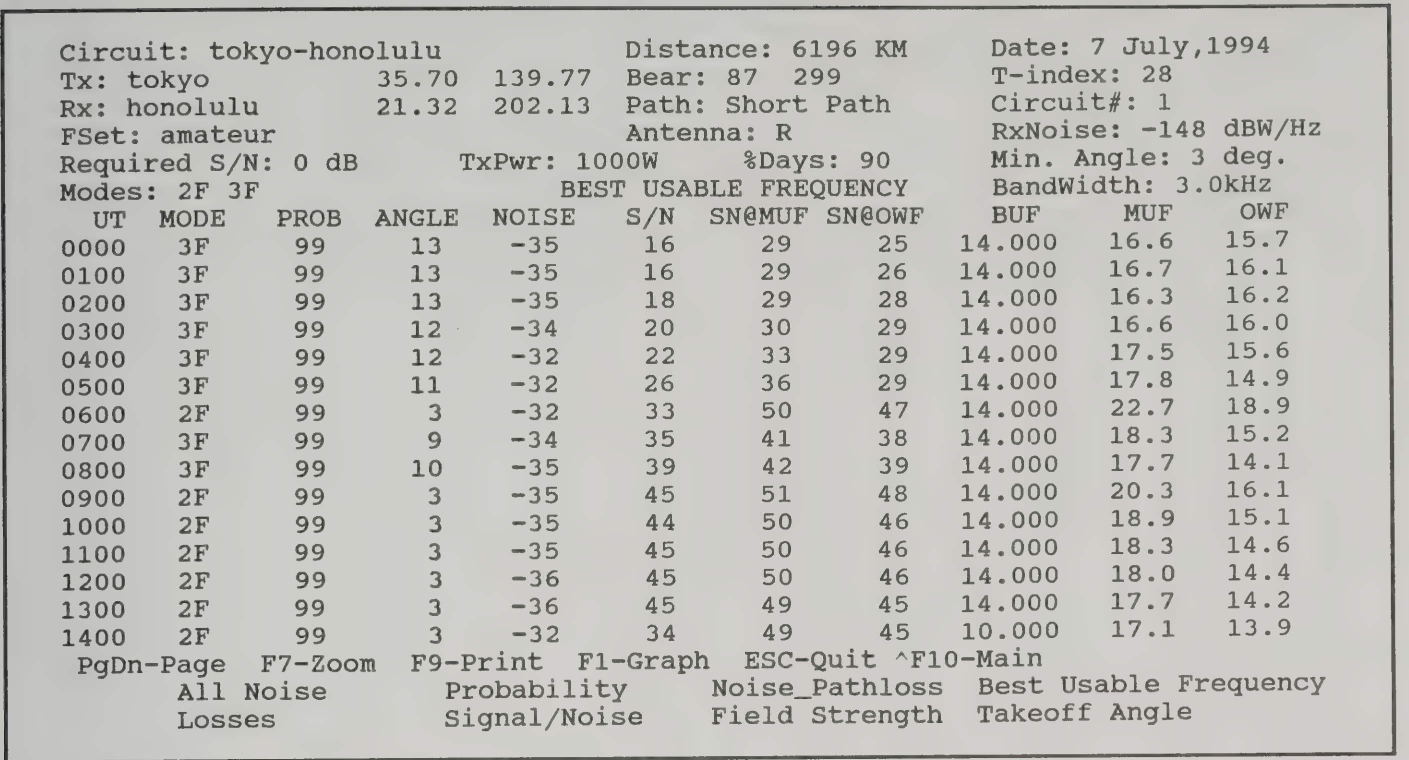

```
Circuit: tokyo-honolulu              Distance: 6196 KM     Date: 7 July,1994
Tx: tokyo            35.70  139.77  Bear: 87   299        T-index: 28
Rx: honolulu         21.32  202.13  Path: Short Path      Circuit#: 1
FSet: amateur                        Antenna: R            RxNoise: -148 dBW/Hz
Required S/N: 0 dB      TxPwr: 1000W      %Days: 90       Min. Angle: 3 deg.
Modes: 2F 3F                   BEST USABLE FREQUENCY       BandWidth: 3.0kHz
 UT   MODE    PROB  ANGLE   NOISE    S/N  SN@MUF SN@OWF     BUF      MUF     OWF
0000   3F      99     13     -35     16     29      25   14.000    16.6    15.7
0100   3F      99     13     -35     16     29      26   14.000    16.7    16.1
0200   3F      99     13     -35     18     29      28   14.000    16.3    16.2
0300   3F      99     12     -34     20     30      29   14.000    16.6    16.0
0400   3F      99     12     -32     22     33      29   14.000    17.5    15.6
0500   3F      99     11     -32     26     36      29   14.000    17.8    14.9
0600   2F      99      3     -32     33     50      47   14.000    22.7    18.9
0700   3F      99      9     -34     35     41      38   14.000    18.3    15.2
0800   3F      99     10     -35     39     42      39   14.000    17.7    14.1
0900   2F      99      3     -35     45     51      48   14.000    20.3    16.1
1000   2F      99      3     -35     44     50      46   14.000    18.9    15.1
1100   2F      99      3     -35     45     50      46   14.000    18.3    14.6
1200   2F      99      3     -36     45     50      46   14.000    18.0    14.4
1300   2F      99      3     -36     45     49      45   14.000    17.7    14.2
1400   2F      99      3     -32     34     49      45   10.000    17.1    13.9
 PgDn-Page  F7-Zoom  F9-Print  F1-Graph  ESC-Quit ^F10-Main
      All Noise       Probability     Noise_Pathloss  Best Usable Frequency
      Losses          Signal/Noise    Field Strength  Takeoff Angle
```

Figure 6.15. *ASAPS* FS working screen printout.

gram customized for radio amateur use. Working with Jim Tabor, KU5S, they developed the *CAPMAN* program, which stands for Computer Assisted Prediction Manager. *CAPMAN 2.0*[21] not only preserves the most recently updated version of the *IONCAP* kernel, but also, it adds many additional features for amateur radio use. Further, it overcomes the difficulties experienced previously with *IONCAP.*

CAPMAN is mouse/menu driven. Its output can contain all usable propagation parameters, including MUF, FOT, LUF, S/N, reliability, service probability, angles of take-off and arrival, field strength, modes of propagation (E, E_s, F_1, and F_2 layers), and more. The output can be set either for short-path or long-path calculations.

The data are presented in tabular or multi-colored graphical form. The program permits viewing and manipulating huge output files. Besides the usual, required circuit information, including date, path, power, etc., *CAPMAN* requires conveniently available data on the smoothed sunspot number or solar flux value. The effects of changing geomagnetic conditions can be assessed by inputs of *K*-index values.

A full-featured geographical database, indexed by both country name and amateur callsign prefix, provides access to over 490 prefixes. Each database entry establishes associated information such as prefix, continent, country, city, geographical coordinates, *CQ* zone, ITU zone, a 900-character note-pad for editing, short- and long-path bearings and distances, and current local sunrise and sunset times. Sunset and sunrise for any day are accessible through the use of a calendar that also displays the current Local Mean, Local Civil, and UTC times.

CAPMAN is the only program available that contains a wide choice of antenna routines, and it interfaces with the *ELNEC* and *MININEC* antenna evaluation programs. This permits propagation predictions to be made based on the actual antenna in use. The program contains an extensive on-line "help" system, and it includes a more than 40-page user's guide and tutorial. Help also is available by telephone and e-mail.

CAPMAN is a 32-bit program and requires an IBM or compatible "80386" or later processor running DOS 3.3 or higher, with at least 545K of available memory and a hard drive with at least 3MB of available free space. A graphics adaptor is required for display of output graphs. Mouse support is provided, but use of a mouse is optional. A numerical coprocessor, while not required, will speed up calculations to a few seconds or so.

CAPMAN is a professional-quality package customized for use by radio amateurs. It uses the most advanced propagation model available for PC-based

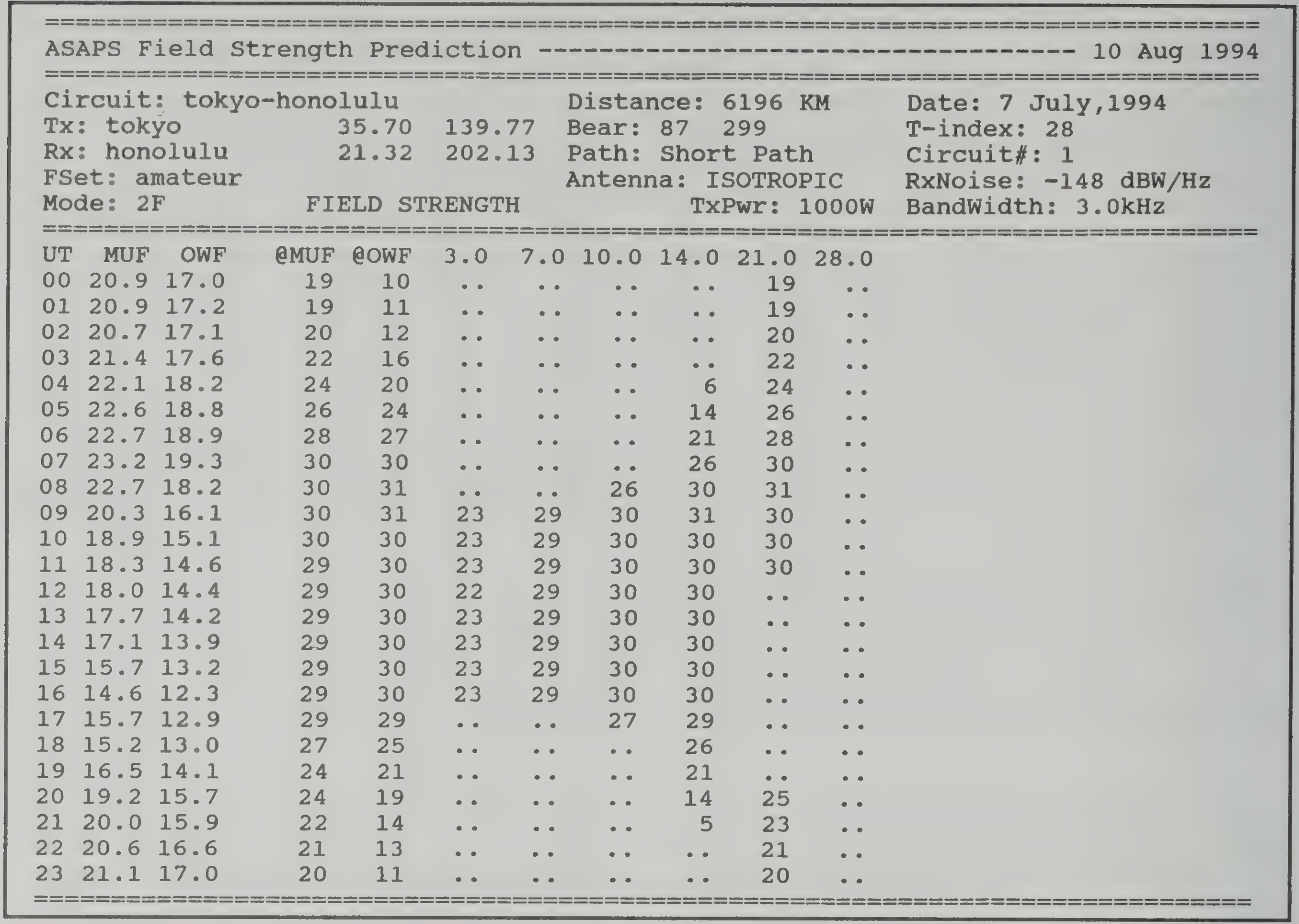

```
==============================================================================
ASAPS Field Strength Prediction ---------------------------------- 10 Aug 1994
==============================================================================
Circuit: tokyo-honolulu                Distance: 6196 KM     Date: 7 July,1994
Tx: tokyo             35.70  139.77  Bear: 87   299        T-index: 28
Rx: honolulu          21.32  202.13  Path: Short Path      Circuit#: 1
FSet: amateur                          Antenna: ISOTROPIC    RxNoise: -148 dBW/Hz
Mode: 2F           FIELD STRENGTH             TxPwr: 1000W  BandWidth: 3.0kHz
==============================================================================
UT  MUF  OWF    @MUF @OWF  3.0   7.0 10.0 14.0 21.0 28.0
00 20.9 17.0     19   10    ..    ..   ..   ..   19   ..
01 20.9 17.2     19   11    ..    ..   ..   ..   19   ..
02 20.7 17.1     20   12    ..    ..   ..   ..   20   ..
03 21.4 17.6     22   16    ..    ..   ..   ..   22   ..
04 22.1 18.2     24   20    ..    ..   ..    6   24   ..
05 22.6 18.8     26   24    ..    ..   ..   14   26   ..
06 22.7 18.9     28   27    ..    ..   ..   21   28   ..
07 23.2 19.3     30   30    ..    ..   ..   26   30   ..
08 22.7 18.2     30   31    ..    ..   26   30   31   ..
09 20.3 16.1     30   31    23    29   30   31   30   ..
10 18.9 15.1     30   30    23    29   30   30   30   ..
11 18.3 14.6     29   30    23    29   30   30   30   ..
12 18.0 14.4     29   30    22    29   30   30   ..   ..
13 17.7 14.2     29   30    23    29   30   30   ..   ..
14 17.1 13.9     29   30    23    29   30   30   ..   ..
15 15.7 13.2     29   30    23    29   30   30   ..   ..
16 14.6 12.3     29   30    23    29   30   30   ..   ..
17 15.7 12.9     29   29    ..    ..   27   29   ..   ..
18 15.2 13.0     27   25    ..    ..   ..   26   ..   ..
19 16.5 14.1     24   21    ..    ..   ..   21   ..   ..
20 19.2 15.7     24   19    ..    ..   ..   14   25   ..
21 20.0 15.9     22   14    ..    ..   ..    5   23   ..
22 20.6 16.6     21   13    ..    ..   ..   ..   21   ..
23 21.1 17.0     20   11    ..    ..   ..   ..   20   ..
==============================================================================
```

Figure 6.16. *ASAPS* FS field strength printout.

programs. Because of the many features that it incorporates and the vast amount of useful data it can produce, it may be of particular attraction to advanced radio amateurs and others with experience and a specialized interest in HF propagation. It is in the mid-level price range, and full particulars can be obtained from Reference 21. A detailed comparison between *CAPMAN* and *ASAPS* is contained in Reference 22.

Summary

In summary, we have reviewed four HF propagation prediction programs in detail. Did we compare their outputs with a common scenario? No, that would be meaningless, as has been noted earlier. We used these four as examples because we are comfortable with them. The best way to find the right program for you is to acquire an HF prediction program in your price range. Exercise it, and compare the results with your "on-the-air" observations. You will find cases where the predictions will be "right-on." Then again, there will be cases where the predictions are "dead-wrong." Compare notes with friends, especially those using other programs. The program that does the best job on your HF circuits probably will be the one you finally select. But only you can decide which is "best" for you. To assist you in this search, Table 6.3 lists additional HF prediction programs that are oriented towards the radio amateur and SWL communities. The reader is referred to Reference 23 for a review of many of the programs listed in Table 6.3.

6.7 The Future of HF Prediction Programs

In the near term, users of propagation prediction programs will continue to see evolutionary enhancements to the many products available today. For example, Figure 6.20 shows a broadcast coverage map for a 50 kW international broadcast station prepared using the *VOACAP* computerized propagation program. At the

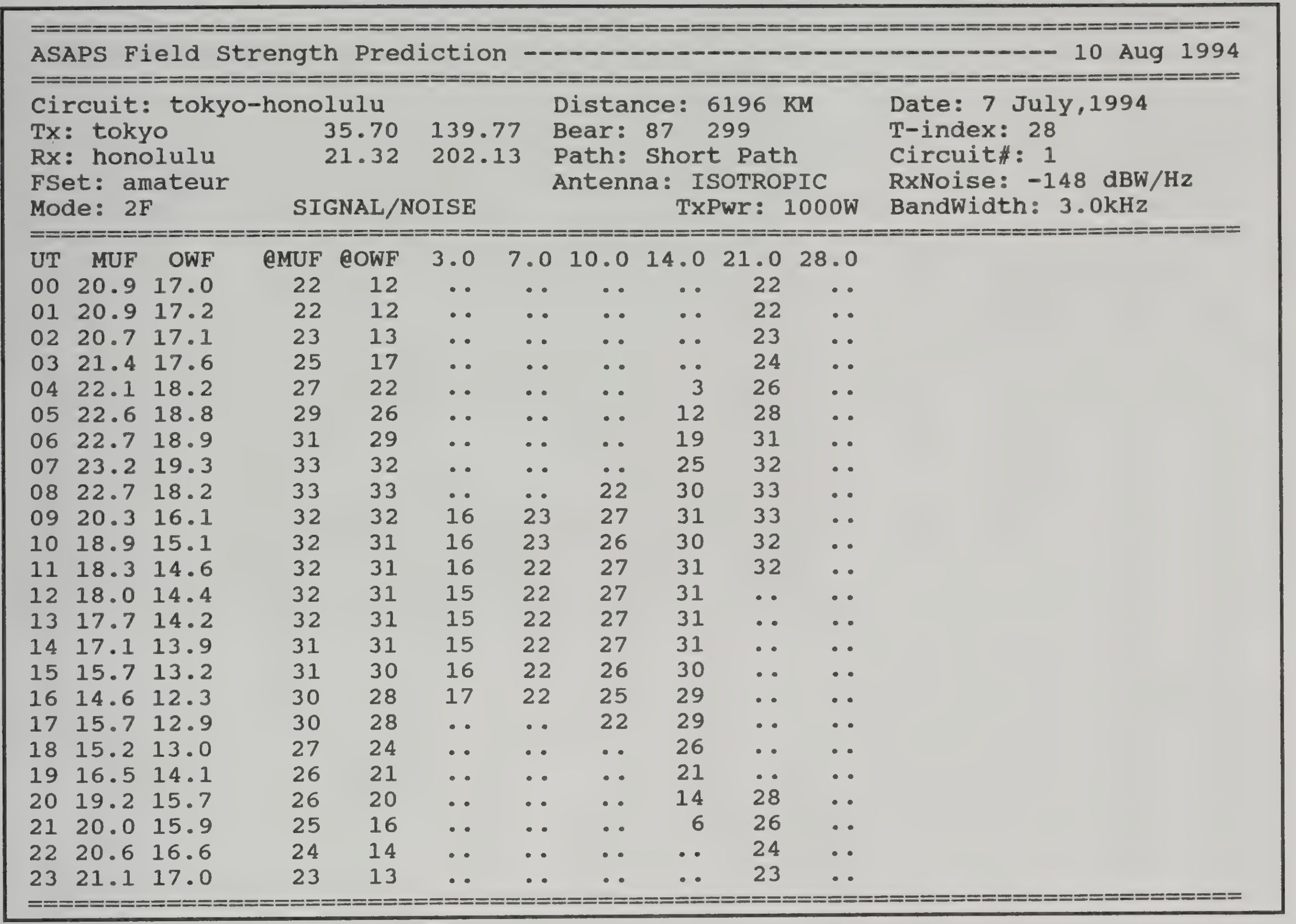

```
===============================================================================
ASAPS Field Strength Prediction ----------------------------------- 10 Aug 1994
===============================================================================
Circuit: tokyo-honolulu           Distance: 6196 KM     Date: 7 July,1994
Tx: tokyo          35.70  139.77  Bear: 87   299        T-index: 28
Rx: honolulu       21.32  202.13  Path: Short Path      Circuit#: 1
FSet: amateur                     Antenna: ISOTROPIC    RxNoise: -148 dBW/Hz
Mode: 2F         SIGNAL/NOISE             TxPwr: 1000W  BandWidth: 3.0kHz
===============================================================================
UT  MUF  OWF   @MUF @OWF  3.0  7.0 10.0 14.0 21.0 28.0
00 20.9 17.0     22   12   ..   ..   ..   ..   22   ..
01 20.9 17.2     22   12   ..   ..   ..   ..   22   ..
02 20.7 17.1     23   13   ..   ..   ..   ..   23   ..
03 21.4 17.6     25   17   ..   ..   ..   ..   24   ..
04 22.1 18.2     27   22   ..   ..   ..    3   26   ..
05 22.6 18.8     29   26   ..   ..   ..   12   28   ..
06 22.7 18.9     31   29   ..   ..   ..   19   31   ..
07 23.2 19.3     33   32   ..   ..   ..   25   32   ..
08 22.7 18.2     33   33   ..   ..   22   30   33   ..
09 20.3 16.1     32   32   16   23   27   31   33   ..
10 18.9 15.1     32   31   16   23   26   30   32   ..
11 18.3 14.6     32   31   16   22   27   31   32   ..
12 18.0 14.4     32   31   15   22   27   31   ..   ..
13 17.7 14.2     32   31   15   22   27   31   ..   ..
14 17.1 13.9     31   31   15   22   27   31   ..   ..
15 15.7 13.2     31   30   16   22   26   30   ..   ..
16 14.6 12.3     30   28   17   22   25   29   ..   ..
17 15.7 12.9     30   28   ..   ..   22   29   ..   ..
18 15.2 13.0     27   24   ..   ..   ..   26   ..   ..
19 16.5 14.1     26   21   ..   ..   ..   21   ..   ..
20 19.2 15.7     26   20   ..   ..   ..   14   28   ..
21 20.0 15.9     25   16   ..   ..   ..    6   26   ..
22 20.6 16.6     24   14   ..   ..   ..   ..   24   ..
23 21.1 17.0     23   13   ..   ..   ..   ..   23   ..
===============================================================================
```

Figure 6.17. *ASAPS* FS signal/noise printout.

time this book was written, this professional-level program was not yet available to the general public. However, it is very likely that in the not too distant future, it may be. Then, too, enhancements to other programs already available to the public may soon permit the calculation and plotting of such coverage contours for amateur radio stations.

Enhancements notwithstanding, the major problem encountered in the use of current HF prediction programs is that users have a wide range of experience and computer skills, and so, many find complicated, technically oriented software intimidating (so much so that they shy away from using it). A less-than-motivated user will do a poor job of setting up HF circuit scenarios, and accordingly, he or she will get poor results. Given this situation, next-generation HF propagation prediction programs will be designed to achieve a high level of performance and productivity, *regardless of the experience or motivation of the user.*

Some of the changes we will see in the years ahead will be revolutionary. For example, the man-machine interface of next-generation prediction programs will allow the user to converse with the system in the jargon of the science addressed by the programs. Further, because larger and larger amounts of propagation information are available every day, the programs will have the ability not only to *use* these data, but also to *peruse* it in order to determine whether or not they have application to the problem at hand. Complex scientific calculations involving propagation predictions and solar-terrestrial relationships will be performed in the "background," outside the user's view. In many cases, the operation of very complicated models, such as those found in *AMBCOM, ASAPS, IONCAP,* and the like, will be totally transparent to the user; they will be applied to the user's problem in a normal manner, and the result will reflect their use, but details relating to their actual operation will not appear in the foreground of the user's system.

Consider, too, that existing HF propagation predic-

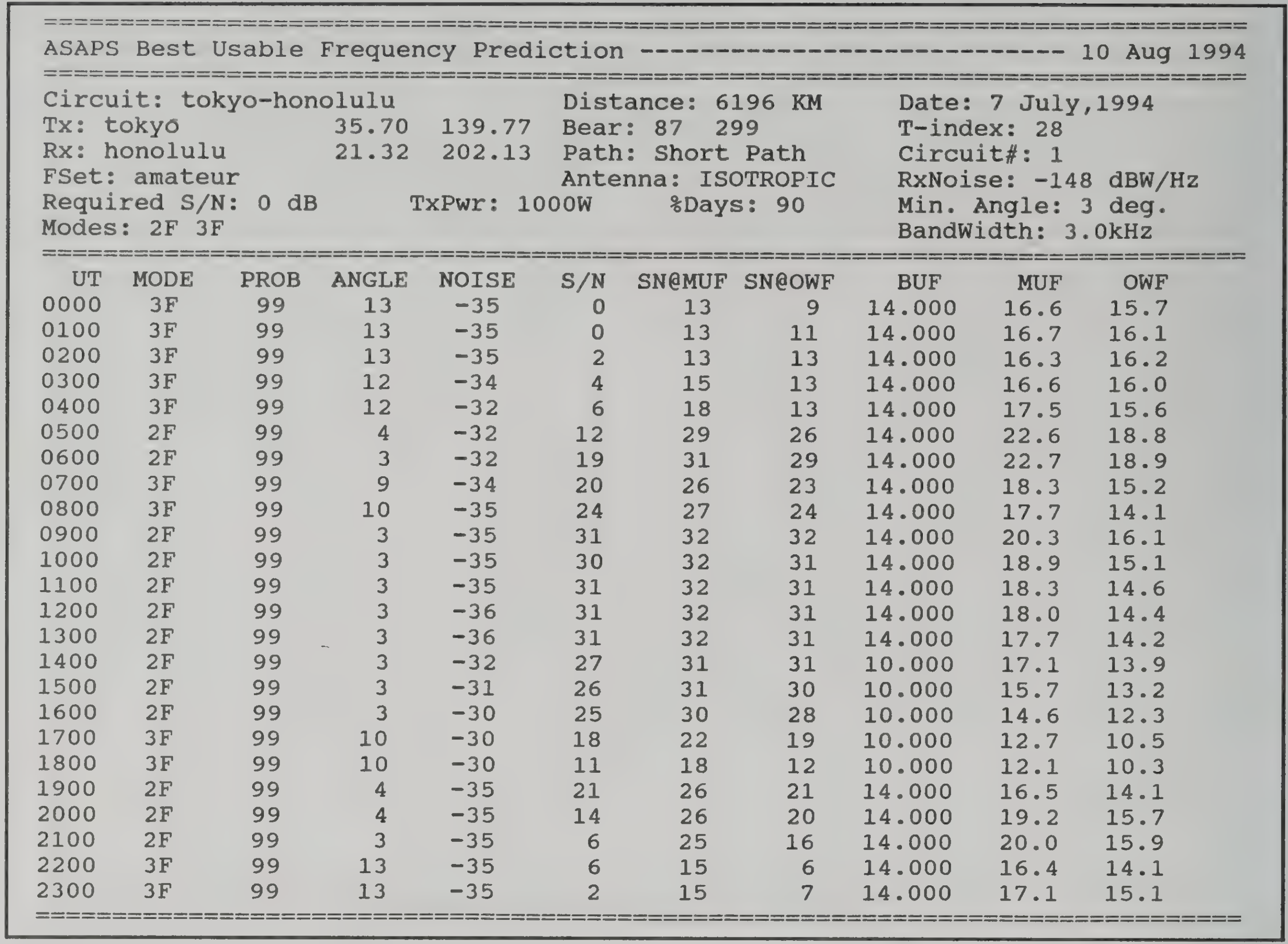

```
================================================================================
ASAPS Best Usable Frequency Prediction ---------------------------- 10 Aug 1994
================================================================================
Circuit: tokyo-honolulu                Distance: 6196 KM      Date: 7 July,1994
Tx: tokyo            35.70  139.77     Bear: 87   299          T-index: 28
Rx: honolulu         21.32  202.13     Path: Short Path        Circuit#: 1
FSet: amateur                          Antenna: ISOTROPIC      RxNoise: -148 dBW/Hz
Required S/N: 0 dB        TxPwr: 1000W       %Days: 90         Min. Angle: 3 deg.
Modes: 2F 3F                                                   BandWidth: 3.0kHz
================================================================================
  UT   MODE    PROB   ANGLE   NOISE    S/N  SN@MUF SN@OWF     BUF      MUF     OWF
0000   3F       99     13     -35       0     13      9     14.000    16.6    15.7
0100   3F       99     13     -35       0     13     11     14.000    16.7    16.1
0200   3F       99     13     -35       2     13     13     14.000    16.3    16.2
0300   3F       99     12     -34       4     15     13     14.000    16.6    16.0
0400   3F       99     12     -32       6     18     13     14.000    17.5    15.6
0500   2F       99      4     -32      12     29     26     14.000    22.6    18.8
0600   2F       99      3     -32      19     31     29     14.000    22.7    18.9
0700   3F       99      9     -34      20     26     23     14.000    18.3    15.2
0800   3F       99     10     -35      24     27     24     14.000    17.7    14.1
0900   2F       99      3     -35      31     32     32     14.000    20.3    16.1
1000   2F       99      3     -35      30     32     31     14.000    18.9    15.1
1100   2F       99      3     -35      31     32     31     14.000    18.3    14.6
1200   2F       99      3     -36      31     32     31     14.000    18.0    14.4
1300   2F       99      3     -36      31     32     31     14.000    17.7    14.2
1400   2F       99      3     -32      27     31     31     10.000    17.1    13.9
1500   2F       99      3     -31      26     31     30     10.000    15.7    13.2
1600   2F       99      3     -30      25     30     28     10.000    14.6    12.3
1700   3F       99     10     -30      18     22     19     10.000    12.7    10.5
1800   3F       99     10     -30      11     18     12     10.000    12.1    10.3
1900   2F       99      4     -35      21     26     21     14.000    16.5    14.1
2000   2F       99      4     -35      14     26     20     14.000    19.2    15.7
2100   2F       99      3     -35       6     25     16     14.000    20.0    15.9
2200   3F       99     13     -35       6     15      6     14.000    16.4    14.1
2300   3F       99     13     -35       2     15      7     14.000    17.1    15.1
================================================================================
```

Figure 6.18. *ASAPS* FS best usable frequency (BUF) printout.

tion programs calculate various parameters based on formulas that have been developed either from the physics involved in the propagation of electromagnetic waves through the atmosphere or from repeated observations of one phenomenon or another related to radio-wave propagation. However, many HF and VHF propagation problems cannot be solved by such analysis techniques. An example of the latter situation is the prediction of when and where sporadic-*E* will occur. Despite sporadic-*E*'s profound effect both on HF and VHF systems, it only can be described in qualitative terms (e.g., it generally occurs from May through August at local sunset, and drifts from the southeast to northwest). One of the most promising methods of dealing with these types of situations is to employ a subset of the science of artificial intelligence called "expert systems." An expert system is a computerized implementation of the thought processes that a human expert would employ in solving a problem. The major elements of an expert system include the "knowledge base" and the "inference engine." The "knowledge base" contains the body of information pertaining to the problem being addressed. Among other things, it may contain "subjective" rules of the sort used by human experts (that is, rules based on experience). From these rules, the system can construct "educated" solutions. The "inference engine" contains the strategies that are used to evaluate the knowledge base and to construct solutions.

In conclusion, the next generation of HF prediction programs will include hybrid systems that combine knowledge-based expert systems with traditional algorithmic functions such as those used in *ASAPS* and *IONCAP*. The expert system will specify, set up, and control complex HF connectivity and signal-assessment calculations produced by the prediction

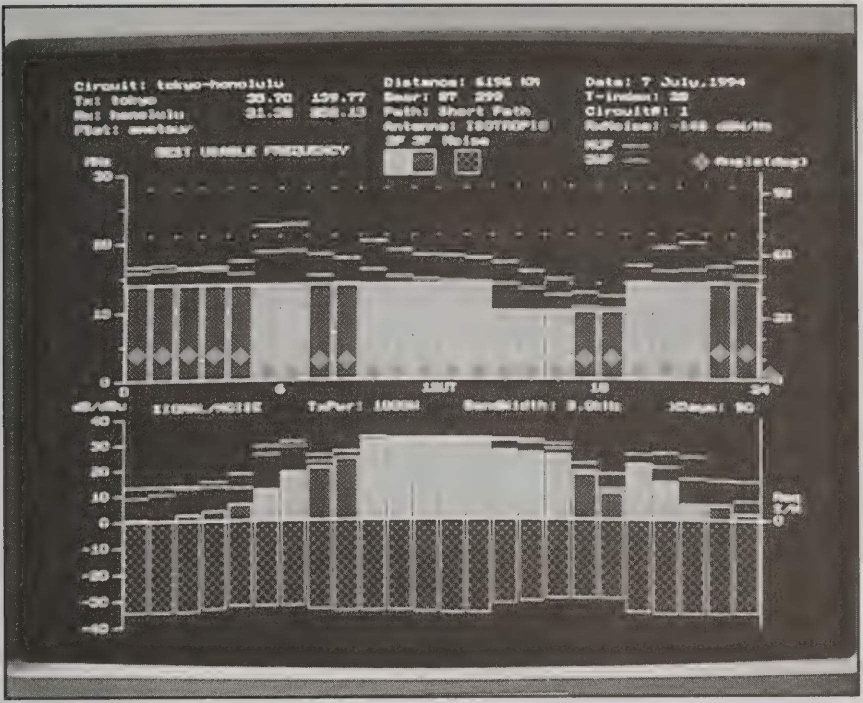

Photo 6.C. *ASAPS* graphical display of BUF.

program, and it will carry on a "user-friendly" query-response dialogue with the user. We're not quite there yet. But as they say, "The best is yet to come!"

6.8 References

1. Rose, R. B., J. N. Martin (NOSC), and P. H. Levine (Megatek Corp), "*MINIMUF-3*: A Simplified HF MUF Prediction," Naval Oceans Systems Center Technical Report TR186, San Diego, California, 1 February 1978.

2. Goodman, J. M., *HF Communications: Science and Technology,* Van Nostrand Reinhold, 1992, pp. 304–388.

3. Rose, R. B.,"*PROPHET* and Future Signal Warfare Decision Aids," AGARD Conference Proceedings on Operational Decision Aids for Exploiting or Mitigating Electromagnetic Effects, CP-453, 15–19 May 1989.

4. Rose, R. B., "*MINIMUF*: A Simplified MUF Prediction Program for Microcomputers," *QST,* Vol. LXVI No. 12, 1982, pp. 36–38.

5. Hatfield, V. E., "HF Communications Predictions 1978 (An Economical Up-to-Date Computer Code, AMBCOM)," Solar-Terrestrial Prediction Proceedings, Boulder, Colorado, 23–27 April 1979.

6. Barkhausen, A. F., J. W. Finney, L. L. Proctor, and L. D. Shultz, "Predicting Long-Term Operational Parameters of High Frequency Skywave Telecommunications Systems," ESSA Tech Rpt. ERL-110 - ITS-78, NTIS Doc. No. N70-24144, Boulder, Colorado, 1969.

7. Haydon, G. W., M. Leftin, and R. Rosich, "Predicting the Performance of High Frequency Skywave Telecommunication Systems (*HFMUFES 4*)," or Report 76-102, Dept. of Commerce, Boulder, Colorado, 1976.

8. Teeter, L. R., J. L. Lloyd, G. W. Haydon, and D. L. Lucas, "Estimating the Performance of Telecommunications Systems Using the Ionospheric Transmission Channel: Ionospheric Communications Analysis and Prediction Program (*IONCAP*) Users Manual," NTIA Report 83-127, NTIS Order No. N70-24144, Springfield, Virginia, 1983.

9. "*ASAPS*—Advanced Stand-Alone Prediction Program System," IPS Radio and Space Services, P.O. Box 5606, West Chatswood, N.S.W., Australia.

10. Sailors, D. B., Private Communication, 5 July 1994.

11. Danilov, A. D. "*SPARC*—System Prediction Analysis Radio Communications," Institute of Applied Geophysics, Rostokinskaya 9, 129226 Moscow, Russia, 1992.

12. Fricker, R., "A Microcomputer Program for the Critical Frequency and Height of the *F* Layer of the Ionosphere," 4th International Conference on Antennas and Propagation (ICAP 85), 16–19 April 1985, pp. 546–550.

13. Shallon, S. C., *MINIPROP PLUS*, W6EL Software, 11058 Queensland Street, Los Angeles,

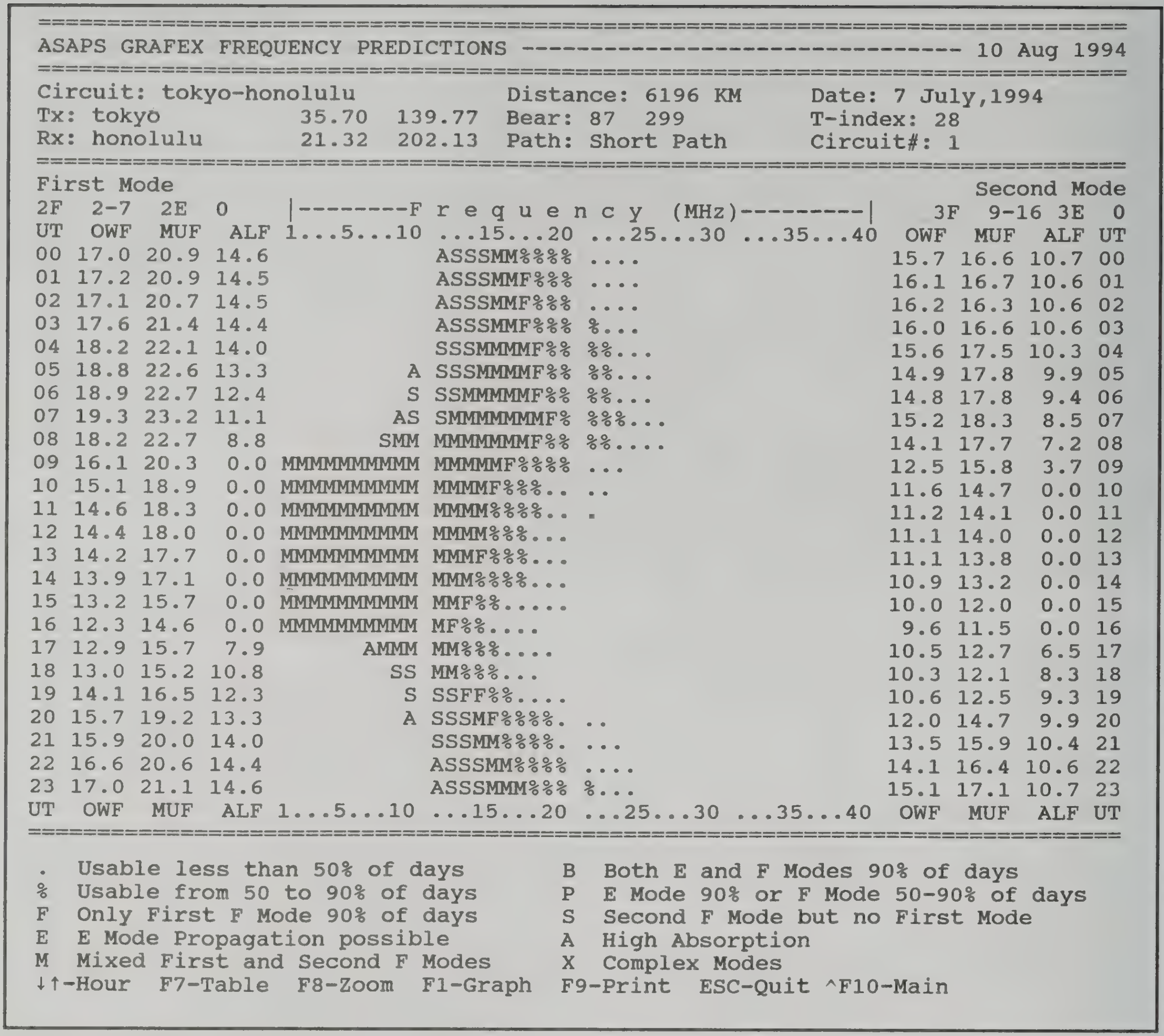

```
==============================================================================
ASAPS GRAFEX FREQUENCY PREDICTIONS ------------------------------- 10 Aug 1994
==============================================================================
Circuit: tokyo-honolulu           Distance: 6196 KM      Date: 7 July,1994
Tx: tokyo              35.70  139.77  Bear: 87   299      T-index: 28
Rx: honolulu           21.32  202.13  Path: Short Path    Circuit#: 1
==============================================================================
First Mode                                                          Second Mode
2F  2-7  2E  0    |--------F r e q u e n c y  (MHz)---------|  3F  9-16 3E  0
UT  OWF  MUF  ALF 1...5...10 ...15...20 ...25...30 ...35...40  OWF  MUF  ALF UT
00 17.0 20.9 14.6            ASSSMM%%%% ....                  15.7 16.6 10.7 00
01 17.2 20.9 14.5            ASSSMMF%%% ....                  16.1 16.7 10.6 01
02 17.1 20.7 14.5            ASSSMMF%%% ....                  16.2 16.3 10.6 02
03 17.6 21.4 14.4            ASSSMMF%%% %...                  16.0 16.6 10.6 03
04 18.2 22.1 14.0            SSSMMMMF%% %%...                 15.6 17.5 10.3 04
05 18.8 22.6 13.3          A SSSMMMMF%% %%...                 14.9 17.8  9.9 05
06 18.9 22.7 12.4          S SSMMMMMF%% %%...                 14.8 17.8  9.4 06
07 19.3 23.2 11.1         AS SMMMMMMMF% %%%...                15.2 18.3  8.5 07
08 18.2 22.7  8.8        SMM MMMMMMMF%% %%....                14.1 17.7  7.2 08
09 16.1 20.3  0.0 MMMMMMMMMM MMMMMF%%%% ...                   12.5 15.8  3.7 09
10 15.1 18.9  0.0 MMMMMMMMMM MMMMF%%%.. ..                    11.6 14.7  0.0 10
11 14.6 18.3  0.0 MMMMMMMMMM MMMM%%%%.. .                     11.2 14.1  0.0 11
12 14.4 18.0  0.0 MMMMMMMMMM MMMM%%%...                       11.1 14.0  0.0 12
13 14.2 17.7  0.0 MMMMMMMMMM MMMF%%%...                       11.1 13.8  0.0 13
14 13.9 17.1  0.0 MMMMMMMMMM MMM%%%%...                       10.9 13.2  0.0 14
15 13.2 15.7  0.0 MMMMMMMMMM MMF%%.....                       10.0 12.0  0.0 15
16 12.3 14.6  0.0 MMMMMMMMMM MF%%....                          9.6 11.5  0.0 16
17 12.9 15.7  7.9       AMMM MM%%....                         10.5 12.7  6.5 17
18 13.0 15.2 10.8         SS MM%%%...                         10.3 12.1  8.3 18
19 14.1 16.5 12.3          S SSFF%%....                       10.6 12.5  9.3 19
20 15.7 19.2 13.3          A SSSMF%%%%. ..                    12.0 14.7  9.9 20
21 15.9 20.0 14.0            SSSMM%%%%. ...                   13.5 15.9 10.4 21
22 16.6 20.6 14.4            ASSSMM%%%% ....                  14.1 16.4 10.6 22
23 17.0 21.1 14.6            ASSSMMM%%% %...                  15.1 17.1 10.7 23
UT  OWF  MUF  ALF 1...5...10 ...15...20 ...25...30 ...35...40  OWF  MUF  ALF UT
==============================================================================

 .  Usable less than 50% of days         B  Both E and F Modes 90% of days
 %  Usable from 50 to 90% of days        P  E Mode 90% or F Mode 50-90% of days
 F  Only First F Mode 90% of days        S  Second F Mode but no First Mode
 E  E Mode Propagation possible          A  High Absorption
 M  Mixed First and Second F Modes       X  Complex Modes
↓↑-Hour  F7-Table  F8-Zoom  F1-Graph    F9-Print  ESC-Quit ^F10-Main
```

Figure 6.19. *ASAPS* GRAFEX frequency predictions.

California 90034-3029. (As of this writing, price is $60 in the U.S. and Canada, and $65 elsewhere.)

14. Handwerker, J., *IONSOUND,* Version 3.0, Jacob Handwerkers User's Manual, Version 1.0, 1990.

15. Damboldt, The., and P. Suessman, "The FTZ HF propagation model for use on small computers and its accuracy," AGARD Conference Proceedings on Operational Decision Aids for Exploiting or Mitigating Electromagnetic Propagation Effects, CP-453, 15–19 May 1989.

16. Sailors, D. B., and W. K. Moision, "Quiet Time Lowest Observable Frequency Model," Naval Ocean Systems Center Technical Report 1189, August 1987.

17. Satterlee, B. (KD6SC), "*DX.BAS* Propagation Prediction Program," IBM-PC Version 4.3, 8210 Blossom Hill Court, Lemon Grove, California 91945-4232. (Shareware; as of this writing, price is $20.)

18. Damboldt, The., "Comparison of Deutsche Bunderpost Ionospheric HF Radio Propagation Predictions and Measured Field Strength," AGARD Conference Proceedings on Radio Systems and the Ionosphere, CP 173, 26–30 May 1976.

19. Ionospheric Prediction Service, Radio and Space Services, P.O. Box 5606, West Chatwwood, New South Wales, 2057, Australia. Distributed in North America by Jacques d'Avignon, VE3VIA, 965

Program Name	Type	Source	Comments*
BANDAID2/3	Empirical	24	Uses *MINIMUF 3.5* to develop simple HPF, MUF, FOT, LUF graphical screens. Developed by BASE(2) SYSTEMS
COMB6	Modified Statistical	25	Uses modification of Fricker's work. Computes mode, angle, number of days, and field strength. Outputs only to printer.
DXCAST	Modified Statistical	26	SWL-oriented program using Fricker's algorithm. The outputs are similar to those obtained from *COMB6*.
IONSOUND	Modified Statistical	27	Uses Fricker's algorithm. Produces alphanumeric and graphical outputs. Frequency database tailored for amateur operations.
MAPPER	Modified Stat. & Empirical	28	User selects use of *MINIMUF* or *MAXIMUF*. Graphical output with gray line.
MICROPREDIC	Empirical/ Statistical	29	Uses Canadian high-latitude database combined with an empirical mapping system. Very accurate above 35 degrees north latitude.
MINIFTZ4	Empirical	30	Developed in Germany from HF broadcast data. Accurate on longer range circuits. Outputs are alphanumeric to printer.
WHATSON	Empirical	31	Simple HPF/FOT/LUF BASIC programs that use the *MINIMUF* model. Usually found on Amateur/SWL bulletin boards.

**See also d'Avignon.[23]*

Table 6.3. Amateur/SWL-oriented HF prediction programs.

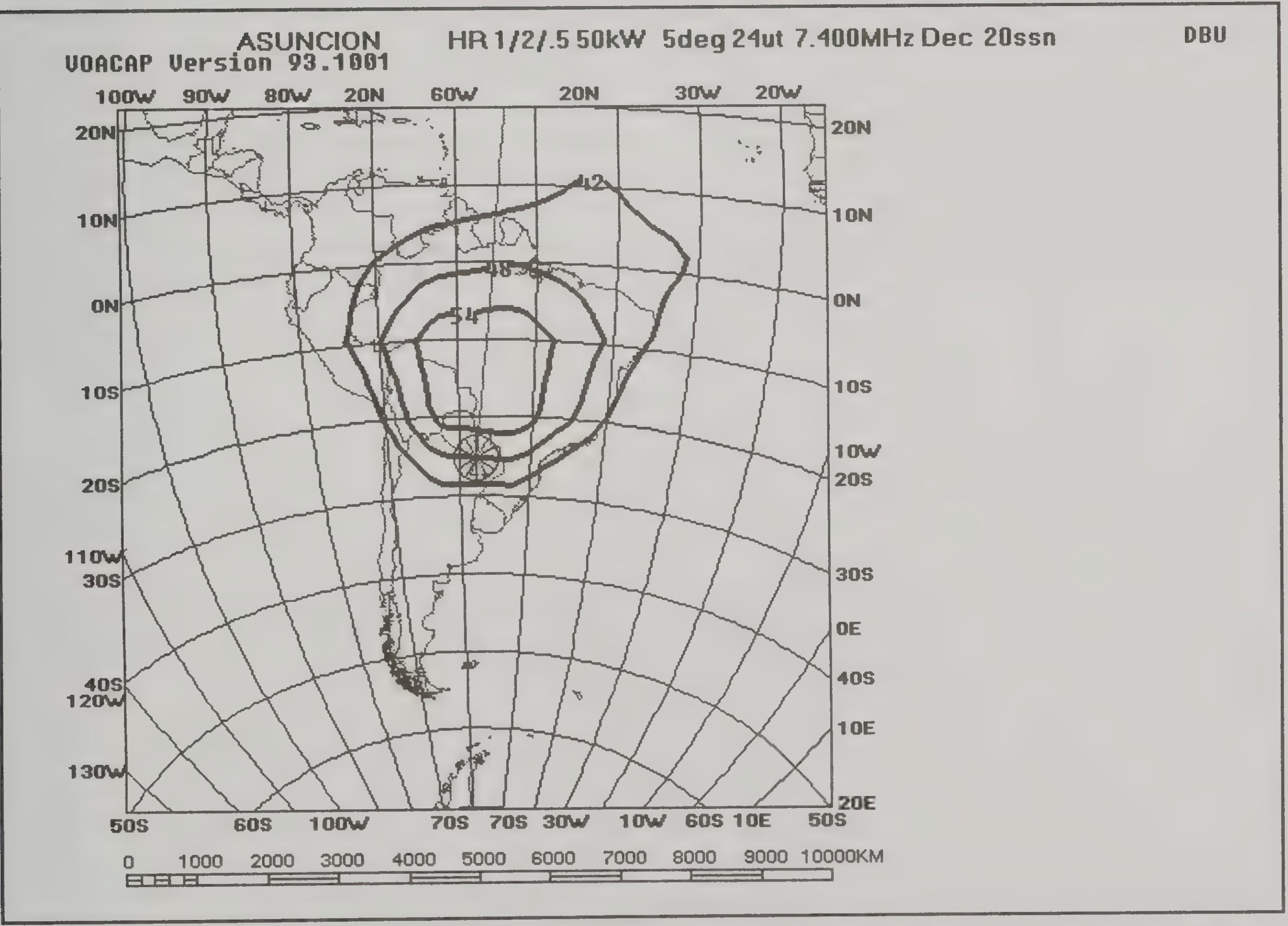

Figure 6.20. This contour map is based on a 50 kW shortwave broadcast transmitter using a 1×2 curtain antenna with reflector on a frequency of 7.4 MHz. In a few years, a similar program should be available for amateur radio use. (Courtesy of G. Jacobs & Associates.)

Lincoln Drive, Kingston, Ontario, Canada K7M 4Z3 (telephone: 613-634-1519; price, as of this writing, is $275 [U.S.]).

20. National Technical Information Service, U.S. Department of Commerce, 5285 Port Royal Road, Springfield, Virginia 22161. Order document: PB89 10 677 7 (price, as of this writing, is $150).

21. Lucas Radio/Kangaroo Tabor Software, 2900 Valmont Road, Suite "H," Boulder, Colorado 80301. (Price, as of this writing, $89.)

22. "*ASAPS* and *CAPMAN*: HF Propagation-Prediction Software for the IBM PC," *QST*, December 1994, pp. 77–89.

23. d'Avignon, Jacques, "Propagation Programs," published by Grove Enterprises, First Edition, August 1992.

24. Base(2) Systems, 2534 Nebraska Street, Saginaw, Michigan 48601. (Approximate price, as of this writing, is $50–$75.)

25. Michele D'Amico, Viale C. Colombo, 107, Foggia, 71100 Italy. e-mail: INTERNET\Damico @IPMEL1.POLIMI.IT (no cost).

26. Peter Oldfield, 250 Chemin Beaulne, Piedmont, Quebec, Canada, J0R 1K0 (no cost).

27. Jacob Handwerker/W1FM, 17 Pine Know Road, Lexington, Massachusetts 02173. (Price, as of this writing, is $35.)

28. Dennis F. Murray, 11165 McDonald Street, Culver City, California 90230. Available through Mannet Forum of Compuserve (no cost).

29. Petrie Telecommunications Ltd., 22 Barran Street, Nepean, Ontario, Canada K2J 1G4. (Cost varies; contact developer.)

30. Thom. Damboldt, Forschungsinstitut der DBP beim FTZ, Postfach 5000, D-6100 Darmstadt, Germany (price unknown).

31. Program found on ham-related bulletin boards and in shared ham-related utility programs (no cost).

Chapter 7

Unusual HF and VHF Ionospheric Propagation

Unusual ionospheric conditions can affect radio signals at frequencies well up into the VHF band (30 to 300 MHz), although at HF (3 to 30 MHz), many of the unusual effects are masked by conventional propagation modes. In the VHF band, however, unusual ionospheric effects appear more pronounced because signal propagation in this band usually involves line-of-sight paths over relatively short distances.

In this chapter we review some unusual conditions under which ionospheric propagation may be possible on the 50 and 144 MHz amateur bands, and the characteristics of such openings, which may result from regular F_2-layer reflection, sporadic-*E*, auroral and meteor ionization, and trans-equatorial and ionospheric scatter. We also will review some unusual propagation phenomena observed on the HF bands, including spread-*F*, gray-line (or twilight zone) propagation, propagation over paths that extend more than halfway around the world (long-path openings), one-way skip, and fading.

7.1 VHF Propagation By Regular F_2-layer Ionization

During most of any solar cycle, regular F_2-layer ionospheric openings generally occur at frequencies up to about 30 MHz. However, F_2-layer ionospheric

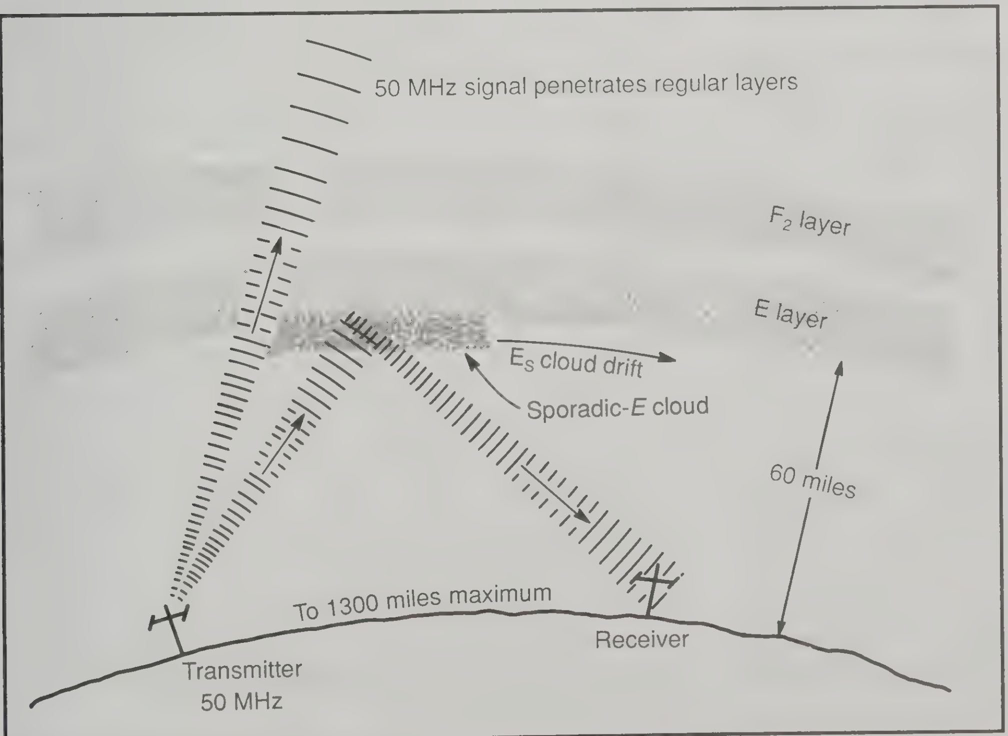

Figure 7.1. Fifty MHz short-skip propagation is possible by means of sporadic-*E* reflection.

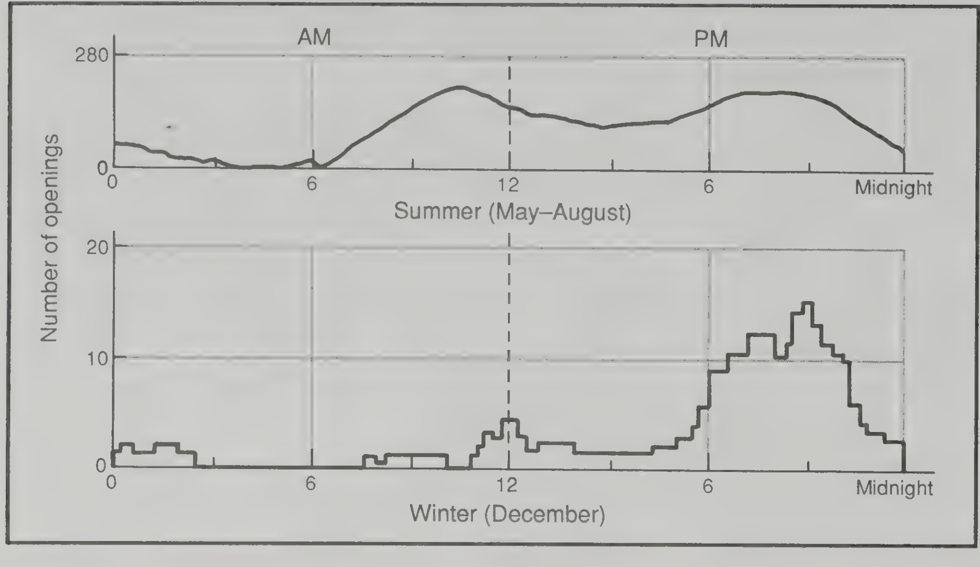

Figure 7.2. Hour-to-hour variation in E_s, summed for summer and winter, 1964–1970. (Note scale change in winter plot.)

openings may be possible on frequencies as high as, or higher than, 50 MHz during years of extremely high solar activity. In fact, trans-continental openings on the 50 MHz band took place for many hours at a time during the maximum periods of Cycles 18 through 22; 50 MHz openings also were observed between the United States and all other continents during these periods. Many trans-continental openings, and openings between North and South America, also were observed during the solar maxima of Cycles 18 through 22. The maximum of Cycle 22 (1988–1892: smoothed sunspot numbers in the range of 94–158) was characterized by a particularly sustained period of high solar activity that resulted in many 50 MHz DX openings.

For smoothed sunspot numbers over about 120, and for stations in the United States, F_2-layer openings on the 50 MHz band, if they do occur, peak during the winter months to Europe and the Far East, and during the spring and fall months to Africa, South America, Australasia, and other areas in the more-or-less southerly direction. Signal levels are often exceptionally strong during these openings, and communication over very great distances may be possible with relatively low power levels.

During periods of high solar activity, regular F_2-layer openings on 50 MHz are a daytime propagation phenomenon, with the band opening to Europe during the hours before noon, to Africa during the noontime period, to South America during the afternoon and sometimes extending into the early evening hours, and to the Far East and Australasia during the late afternoon and early evening hours, local standard time in the United States.

Propagation conditions in the 28 MHz band often provide indications of 50 MHz openings during the fall, winter, and spring months. When F_2-layer openings are observed on 28 MHz over distances of 1200 miles or less, the MUF is rising rapidly, and 50 MHz also may be open in the same general direction, but over a considerably greater distance.

There is little likelihood of any F_2-layer, 50 MHz openings taking place during periods of low solar activity.

The regular F_2 layer of the ionosphere is never sufficiently ionized to propagate signals on the 144 MHz band. This would require an F_2-layer critical frequency of greater than 48 MHz. However, during Cycle 22, especially in the winters of 1988–1989 and 1989–1990, f_oF_2 values in the southwest and on the west coast of the United States regularly approached 16 MHz, which is the lower limit where F_2-layer propagation will support 50 MHz communications.

7.2 Sporadic-*E* Ionization

Clouds or patches of abnormally intense ionization, which are capable of reflecting radio waves of frequencies much higher than those reflected by the regular *E* or *F* layers, frequently form immediately beneath the normal *E* layer of the ionosphere. These clouds usually cover a rather small geographical area, being approximately 50 to 100 miles in diameter. They occur more or less at random and are relatively short lived, usually dissipating within a few hours. Because this sporadic ionization generally occurs at about the same height as does the regular *E* layer, it is called sporadic-*E*, or E_s.

As a result of an intensely ionized sporadic-*E* cloud, it is possible, at times, to communicate over relatively long distances on the 50 MHz band, and on some occasions, on 144 MHz as well (see Figure 7.1). Further, the effects of sporadic-*E* are often observed on the HF bands.

The height at which sporadic-*E* usually occurs limits one-hop propagation to a maximum distance of approximately 1300 miles. For this reason, band openings due to E_s, whether on HF or VHF, are generally referred to as "short-skip" openings. During periods of geographically widespread sporadic-*E* ionization, which often happens during the summer months, multi-hop propagation is sometimes possible. Trans-Atlantic sporadic-*E* openings on 10 and 15 meters, consisting of at least 3 hops, have been reported, as have 50 MHz openings over 2-hop distances of up to 2600 miles.

Reflection from sporadic-*E* clouds takes place with very little signal loss, resulting in exceptionally strong signal levels during most openings, even when very low power levels are used. Quite often it is possible to maintain communications considerably off the great-circle path between two stations by means of back and side scatter from sporadic-*E* clouds. For example, a station in eastern New York state may be able work another station in the central part of the state if both stations point their antennas toward the same E_s cloud that is located, for example, over Georgia.

It also is possible for sporadic-*E* clouds to produce trans-Atlantic openings on the HF bands when no regular F_2-layer openings are possible.

The ionized clouds that produce sporadic-*E* are erratic in their behavior, and they are known to drift in a westerly or northwesterly direction at approximately 150 to 250 miles per hour. The drift appears to be due to winds that exist in the lower ionosphere. Because of this drift, skip zones change rapidly, and it is not uncommon for signal levels during sporadic-*E* openings to fade out completely from an S-9-plus level, often in a matter of minutes.

Sporadic-*E* ionization has long been the object of scientific investigation by amateur operators and research scientists. Studies have shown, for example, that in the mid-latitudes (United States, Europe, etc.), the diurnal variations in sporadic-*E* occurrence have a tendency to peak during the late morning hours and again around sunset, although E_s can occur at any time (see Figure 7.2). More specifically, during the summer months, peaks in sporadic-*E* activity are observed between 10 AM and noon, local time, and again from 6 to 8 PM. Thus, sporadic-*E* propagation is primarily a daytime phenomenon during the summer months, decreasing rapidly in occurrence after local sundown.

During the winter, while sporadic-*E* occurs at about the same local times as it does during the summer, the evening period of activity occurs well beyond sundown and extends into the night.

With respect to seasonal variations in the occurrence of mid-latitude E_s propagation, a summer maximum with a secondary winter peak is clearly observed (see Figure 7.3). In fact, nearly 80% of all E_s propagation observed in North America and Eur-

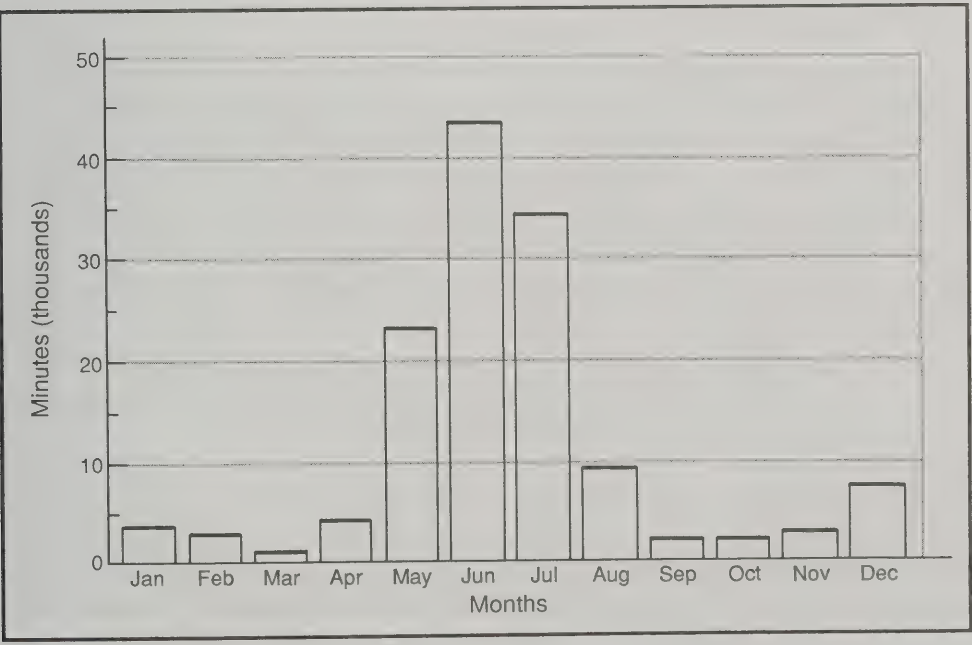

Figure 7.3. Fifty MHz E_s, monthly sums for 1964–1970.

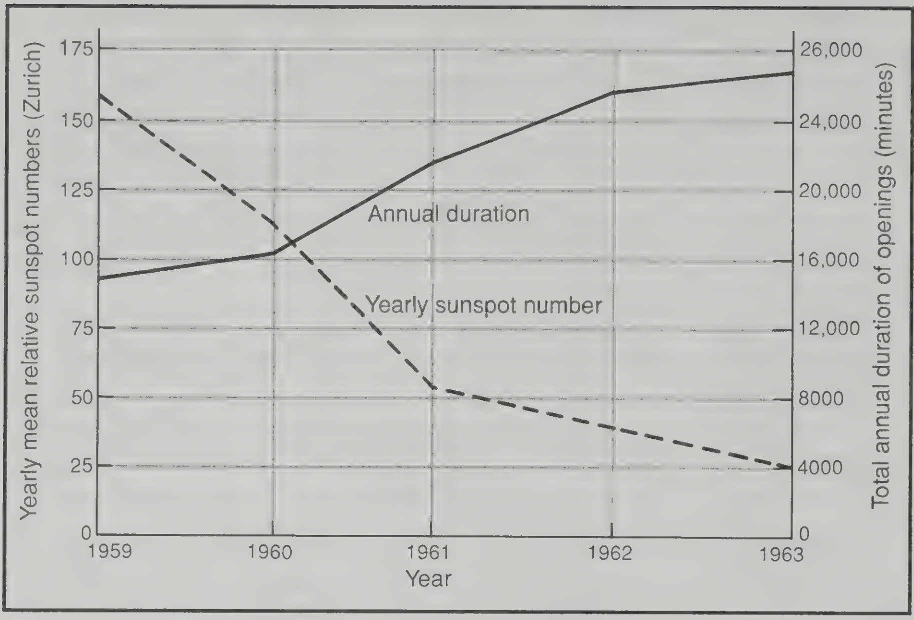

Figure 7.4. Relationship between annual duration of 50 MHz band openings, in minutes, and yearly mean relative sunspot numbers as determined by the Swiss Federal Observatory in Zurich. Solid line indicates annual duration of openings (read on scale at right); dotted line indicates yearly sunspot numbers (read scale on left).

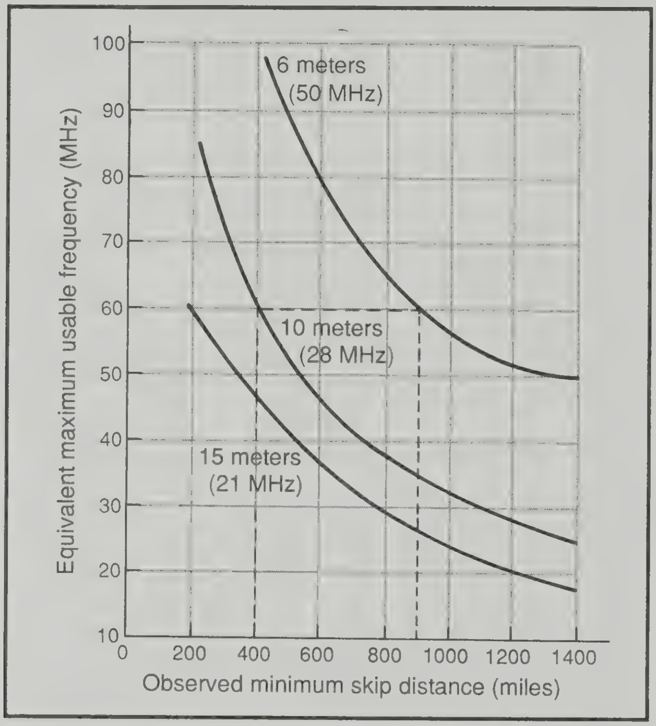

Figure 7.5. Chart describing correlation between sporadic-*E* openings on 10 and 15 meter amateur bands and possible 6 meter openings at the same time. The example shows a minimum skip distance of 400 miles observed on 10 meters; from the chart, 6 meters should be open with skip distance of greater than 900 miles.

ope takes place from May through August, with a maximum of openings occurring in June. (In the temperate zone of the southern hemisphere, similar patterns have been observed during the months of November to February, which corresponds to the summer season in that area.) A secondary maximum is evident in the month of December, with a definite minimum occurring in March.

Sporadic-*E* occurs most frequently, and with the greatest intensity, in equatorial and polar regions. In equatorial regions, E_s is essentially a daytime phenomenon, with little seasonal variation. In Southeast Asia, it appears almost daily. In the polar regions, sporadic-*E*, the mid-latitude type, occurs in the morning hours. In the evening hours, especially around local midnight, its high-latitude cousin, auroral-*E*, occurs year-around. The probability of auroral-*E* occurrence increases during the spring and fall, and during periods of high geomagnetic activity or radio storminess. Auroral-*E* will be discussed in more detail in Section 7.3.

Attempts have been made to determine the relationship between E_s occurrence and sunspot activity. Monroe and Monroe[1], for example, found that in the declining years of Cycle 19, F_2 propagation effects diminished as anticipated, but there persisted a marked *inverse* relationship between sunspot activity and available DX communication time in the 50–54 MHz range via E_s propagation. As sunspot numbers and F_2-supported DX declined steadily, with sunspot numbers dropping from 180 to 20 between 1959 and 1963, 50 MHz E_s-supported DX time increased steadily (see Figure 7.4).

Dyer[2] found a similar relationship from his studies. He observed that E_s occurrence was very high during 1965, a time when solar activity was very low (smoothed sunspot numbers on the order of 15). On the other hand, E_s occurrence was very low in 1969,

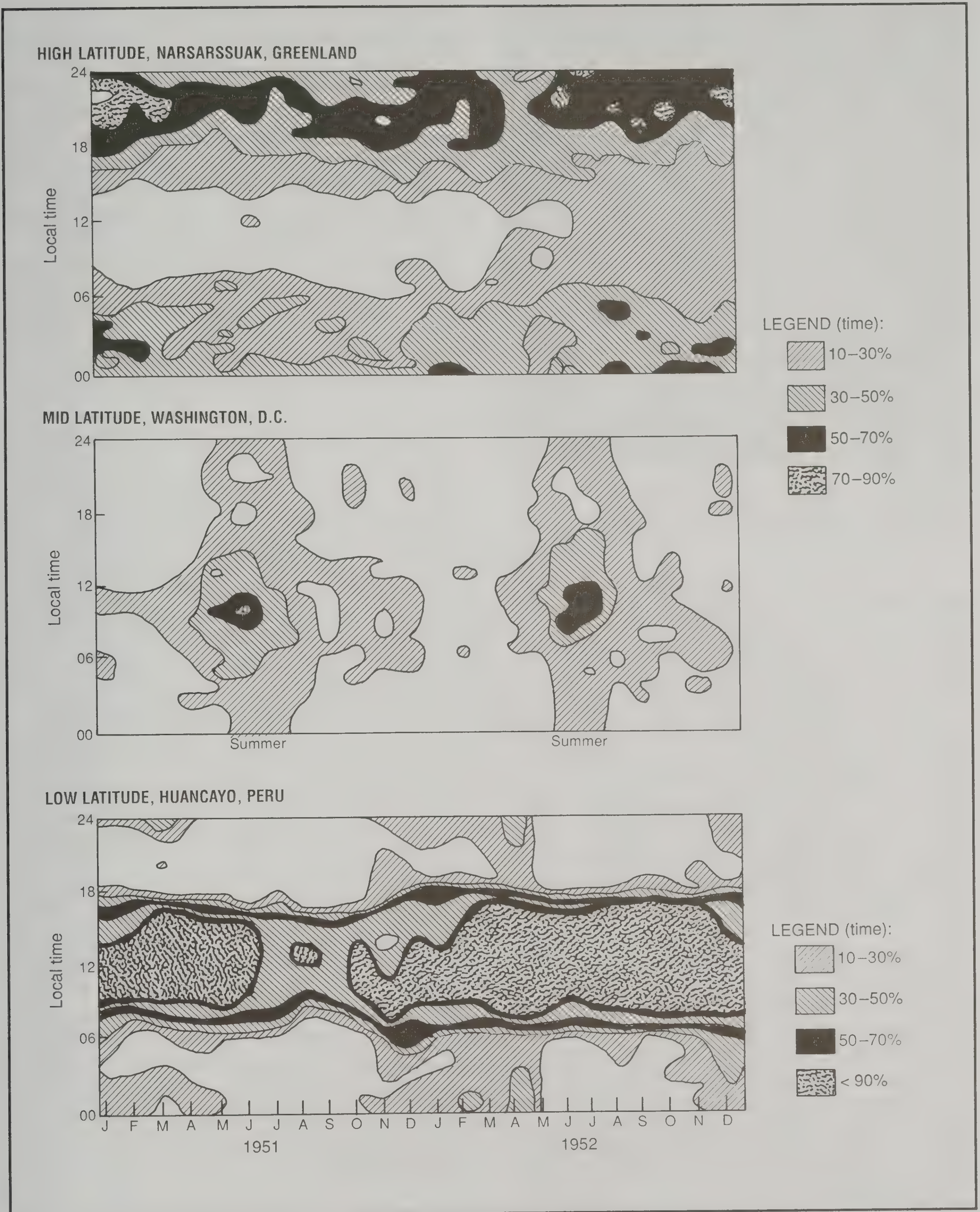

Figure 7.6. E_s Occurrence Contours vary considerably with latitude and time of day. (After E.K. Smith, "Worldwide Occurrence of Sporadic-E, NBS Circular 582, Washington, 1957.)

Photo 7.A. A brilliant aurora of the type associated with ionization intense enough to reflect 50 and 144 MHz signals between 300 and 1300 miles. The photo was taken in northern New York state.

when solar activity was at a peak (smoothed sunspot number on the order of 110). Dyer, however, also found a high level of E_s to have occurred during 1968, when solar activity was near maximum. Cycle 22 did nothing to resolve this controversy. For all of the volatility in solar activity that occurred in 1989, sporadic-*E* openings were somewhat above average in number but about the same as the number observed in the previous two years. Work by Pocock and Dyer[3] reported that E_s was observed on 85 days in 1989, with openings lasting a total of 7750 minutes. This number can be compared to 89 days in 1987, and 80 days in 1988, with the average for the period between 1980 and 1989 being 74.2 days. Roughly 81% of the openings in 1989 occurred in May, June, July, and August, while 13% occurred during November and December. We conclude at this time that there is no definitive relationship between E_s and the solar cycle.

Here is a useful tip for predicting 50 MHz short-skip E_s openings. The geometry of propagation is such that as the skip distance *decreases* on the 21 and 28 MHz bands, the highest frequency that will be reflected by a sporadic-*E* cloud *increases*. By observing the *minimum* skip distance heard on 21 and 28 MHz during an E_s opening, and by using the chart shown in Figure 7.5, it should be possible to tell whether or not 50 MHz is open, and if it is open, what the skip distance might be.

To demonstrate how this technique works, consider the following example. Suppose the minimum skip distance observed on 28 MHz in a southwesterly direction is 400 miles. (It is the distance to the nearest skip station heard that is important.) From Figure 7.5, the intersection between 400 miles and the 28 MHz curve corresponds to an equivalent Classical MUF of 60 MHz. This means that 50 MHz short-skip openings in a southwesterly direction are very likely to occur. The minimum skip distance expected on 50 MHz can now be found from Figure 7.5 by locating the intersection between 60 MHz on the vertical scale and the 50 MHz curve. The resulting distance on the horizontal scale is found to be 900 miles. A useful rule of thumb to remember is that when skip stations less than 500 miles away are heard on 28 MHz, or less than 250 miles away on 21 MHz, chances are very good that 50 MHz will open in the same direction.

From most locations in the continental United States, 1300-mile E_s openings should extend into both Canada and Mexico. From the southern third of the country, it also should be possible to work a rather large number of countries in Central America and in the West Indies during 15, 10, and 6 meter sporadic-*E* openings. Long-distance (DX) television reception also improves considerably during the summer months as a result of sporadic-*E* ionization. Signals from low-band VHF TV stations (Channels 2–5), which normally cannot be received at distances of more than 75 or 100 miles, suddenly are propagated up to 1300 miles, often with very strong signal levels.

The causes of sporadic-*E* ionization are not yet fully known. Since E_s occurs more often during the hours of daylight, it would appear that ultraviolet radiation might play some role in its formation. Since it also occurs at night, especially during the winter months, auroras are often suggested as possible sources of ionization. More recent theories indicate that the ionization might be caused by shearing forces associated with rapid wind movements in the ionosphere. Sporadic-*E* cannot be modeled theoretically, but it can be described statistically in terms of the likelihood of its occurrence as a function of the time of day, season, and geographical location (see Figure 7.6). Because sporadic-*E* supports signal propagation so well, statistical measures related to its occurrence should be enough to exploit it.

7.3 Auroral Ionization

Corpuscular radiation, consisting of charged particles that are emitted from time to time by the Sun (usually from solar flares), are channeled to the polar regions by the Earth's magnetic field. Here, they bombard the atoms and molecules of the gases present in the atmosphere, causing them to form an auroral display.

Of all natural phenomena, auroras are probably the most breathtaking and spectacular. They arc across the night sky as yellowish-green dancing ribbons and violently throbbing rays, or as great draperies folding and unfolding. Some of the rarer displays also may contain shades of red and purple. They occur at *E*-layer heights in the ionosphere, about 60 miles (110 km) above the Earth's surface, and can be seen obliquely from the ground for distances up to about 600 miles from the zenith point (see Photo 7.A). For those who have never seen an aurora, the Geophysical Institute at the University of Alaska in Fairbanks has produced a 27-minute color video of overhead aurora that captures the beauty of this natural phenomenon.[4]

Observations made over the past 100 years, and intensified during the past decade with investigations using high-flying airplanes and satellites, have defined areas of the world where auroras occur most frequently. The zones of maximum occurrence, where they are seen on approximately 250 nights a year, are belts about 23 degrees wide that are centered on the northern and southern magnetic poles. In the northern hemisphere, the zone arcs across northern Alaska, central Canada, the southern tip of Greenland and Iceland, the northern tip of Norway, and the northern coasts of Russia and Siberia (see Figure 7.7).

The shape of the oval is skewed, with the widest

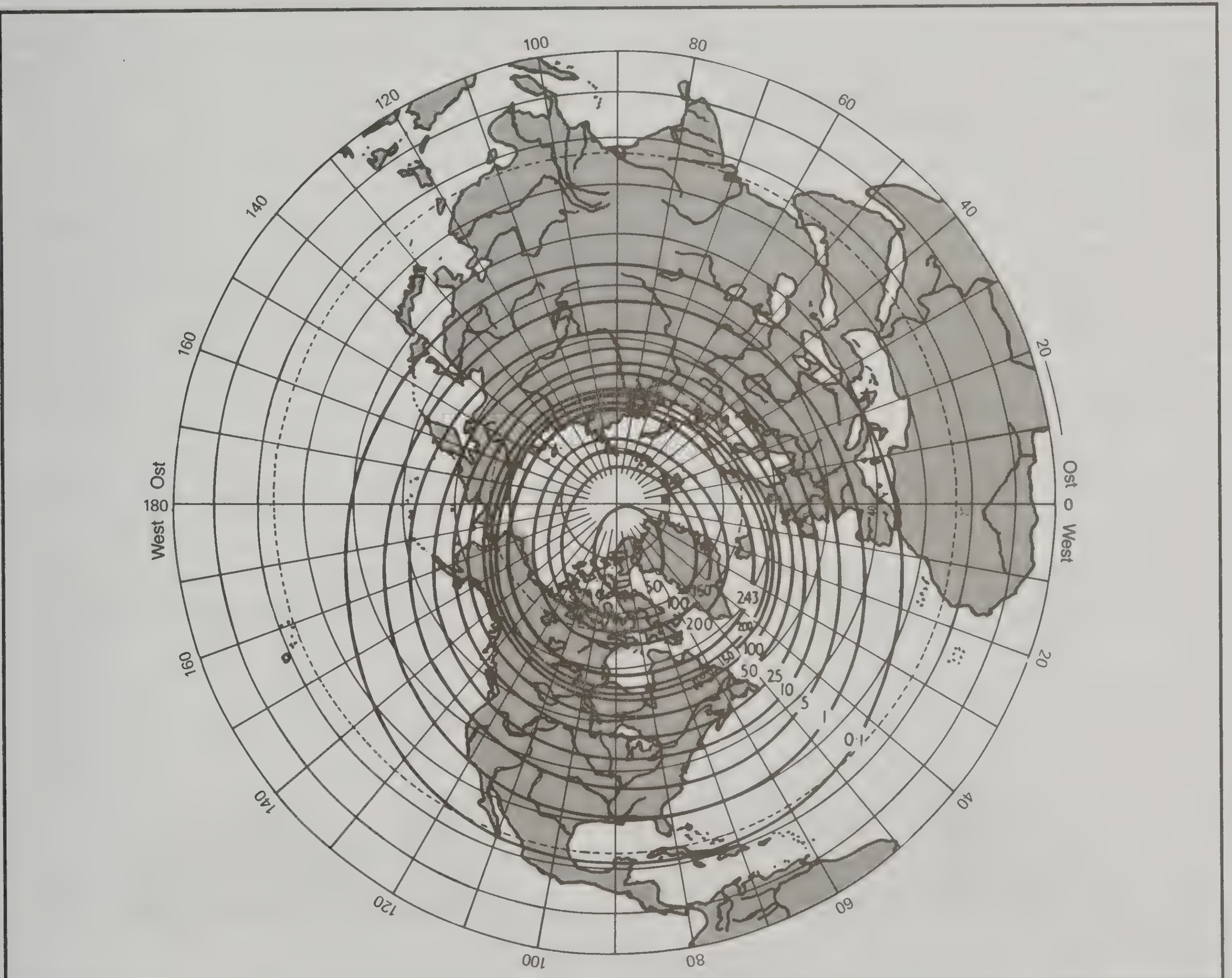

Figure 7.7. Geographical distribution of auroras over the northern hemisphere. The number of days during the year that auroras are likely to occur is indicated.

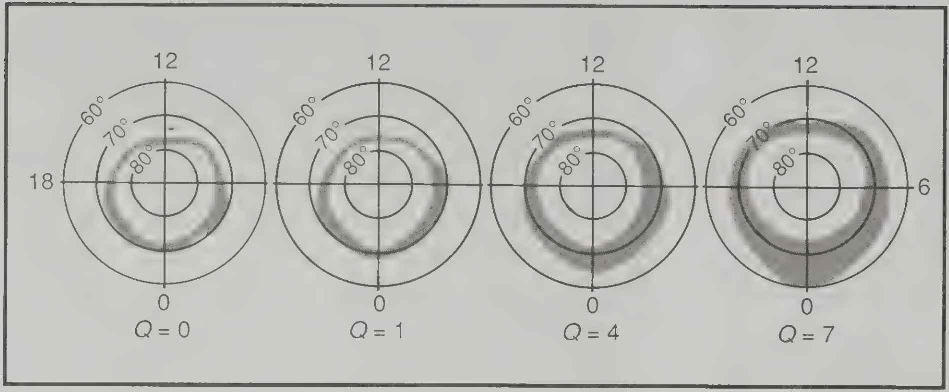

Figure 7.8. Changes in size of the auroral oval, in geomagnetic coordinates, for different values of geomagnetic *Q*-index. (*Q*-index is directly related to *K*-index.)

bulge occurring in the midnight sector and the narrowest portion facing towards the Sun in the noon sector. The Earth rotates under the auroral oval. As geomagnetic activity increases, the equatorward edge of the oval starts to migrate southward. The distance of this migration is proportional to the size of the disturbance. During quiet times, auroras may be seen 10 to 40 nights a year in the northern areas of the U.S. mainland. In the southern states, several years may pass before one is seen. In 1967, two Russian scientists, Starkov and Feldstein[5], modelled the expansion of the auroral oval as a function of geomagnetic activity (see Figure 7.8).

Auroras play havoc with shortwave communications. The excessive ionization that causes auroras also causes severe signal absorption. This absorption, called Auroral Zone Absorption (AZA), is strictly a high-latitude phenomenon, like the luminous aurora itself. Auroral Zone Absorption is caused by energetic electrons arriving in the ionosphere during geomagnetic disturbances. It can occur around-the-clock, with its major peak occurring in the mid-morning. The occurrence of AZA is most pronounced around the statistical center of the auroral zone band, with a latitudinal spread of about 8 degrees. It produces a sporadic interruption of usable signals caused by increased absorption in the *D* region. Its effects are quite short-lived (typically, tens of minutes) when compared to the effects of a PCA or an ionospheric storm.[6]

Absorption caused by an active (disturbed) auroral zone acts like a conducting screen, preventing shortwave transmissions from passing through the region. For this reason, transpolar communications to and from the Unites States are extremely difficult and often unreliable during periods of AZA. The presence of auroral effects on propagation frequently can be

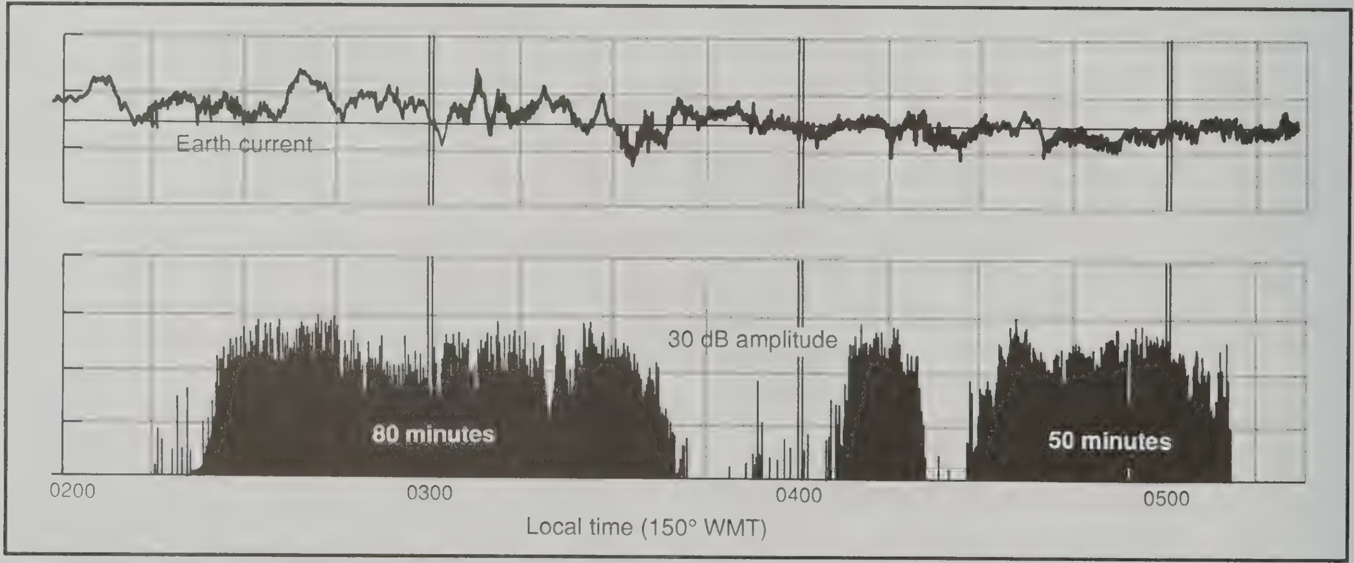

Figure 7.9. Long-duration auroral-*E* events, such as that above for 28 November 1991, can be used by radio amateurs for short skip propagated at 50 and 144 MHz.

Shower Name	Date of Peak Intensity	Shower Duration (Days)	Number of Meteors per Hour
Quadrantids	January 3	1	35–40
Lyrids	April 21	2	12–15
Eta Aquarids	May 5	7	12–20
Delta Aquarids	July 29	10	20-30
Perseids	August 12	5	50
Orionids	October 21	3	20–25
Taurids	November 5 & 12	20	12–15
Leonids	November 17	4	20–25
Geminids	December 13	5	40–50
Ursids	December 22	2	15

Table 7.1. A list of major meteor showers. The date of peak intensity may vary by a day, and the intensity of various showers may vary from year to year. About 20 other showers of less intensity also occur during the year—seven between January and June, and 13 between July and December.

detected by a unique fading component that consists of a low-frequency "flutter" (ranging from 100 to 1000 Hz) that the aurora superimposes on a signal. During periods of intense auroral activity, this fading component is often strong enough to render a voice signal unintelligible.

So-called "auroral flutter," or Doppler, is caused by the turbulence in the ionosphere, which in turn is caused by huge, electric ionospheric currents that exist at auroral and polar latitudes. The auroral and polar ionospheres, at *F*-layer altitudes, consist of a "patch-work quilt" of electron clouds, all being propelled along the high-latitude current system. When this system is bombarded with additional particle radiation, the current becomes turbulent, causing vast differences in the electron densities of the *F*-layer "patches." At times, the *F*-region may appear enhanced; oftentimes, it will disappear. Simply put, the ionosphere above 55 degrees north and south latitudes is not a simple, refracting layer, as it is usually modeled. Signals do not propagate through the polar regions as they do at mid-latitudes. Examples will be shown in Section 7.8.

There is a close relationship between ionospheric storms and the occurrence of auroras, because they are caused by the same phenomenon—the geomagnetic storm. The first effects of the geomagnetic storm are felt at high latitudes; then, these effects migrate southward as the storm intensifies. As the severity of the storm increases, the affected area spreads farther south. During the intense ionospheric storms of March 1989, auroras were observed overhead in Dallas, Texas.

While auroral displays can seriously disrupt communications on the amateur HF bands, propagation on 50 and 144 MHz often improves during these periods. Stated another way, the HF operator's famine often is the VHF operator's feast! This is good enough reason for the amateur interested in VHF propagation to check the WWV broadcast at 18 minutes after the hour, and to make use of Figures 5.8 through 5.12 (Chapter 5) in this book. When a combination of solar flux and current geomagnetic activity (the Boulder *K*-index) falls into the Below Normal or Disturbed regions of Figures 5.8 through 5.12, it is time to check 50 and 144 MHz for auroral-reflection and auroral-*E* (E_{au}) short-skip openings. Look, too, for sporadic-*E* openings. During high-latitude studies conducted in 1991, 1446 auroral-*E* observations (listed in Reference 7) show that auroral-*E* is predominately a nighttime phenomenon. Its occurrence centers around mid-path local midnight and several hours after local midnight. In the hours between 10 PM and 3 AM local time, when the *K*-index is sufficiently high so as to place the auroral oval over the propagation path, the likelihood of auroral-*E* is 50%. The average duration for such openings is 10–20 minutes, although a few will last in excess of an hour (see Figure 7.9). Auroral-*E* occurs on 75% of the days during the spring and fall, about 60% of the days during the summer, and only 36% of the time during the winter. The ionization is sufficient to elevate signals 20 to 30 dB above the noise.

Auroral-*E* propagation is restricted to paths where the reflection points lie in the auroral zone. During disturbed times, as the oval expands, the number of propagation opportunities increases. As implied above, to exploit auroral-*E*, users often must to stay up past midnight and into the early morning hours.

Ionization associated with auroras is often intense enough to reflect or scatter 50 and 144 MHz signals over distances of up to about 1200 miles when propagation over such paths by other modes may not be possible. Further, auroral ionization varies rapidly in intensity and height. This is what causes multi-path

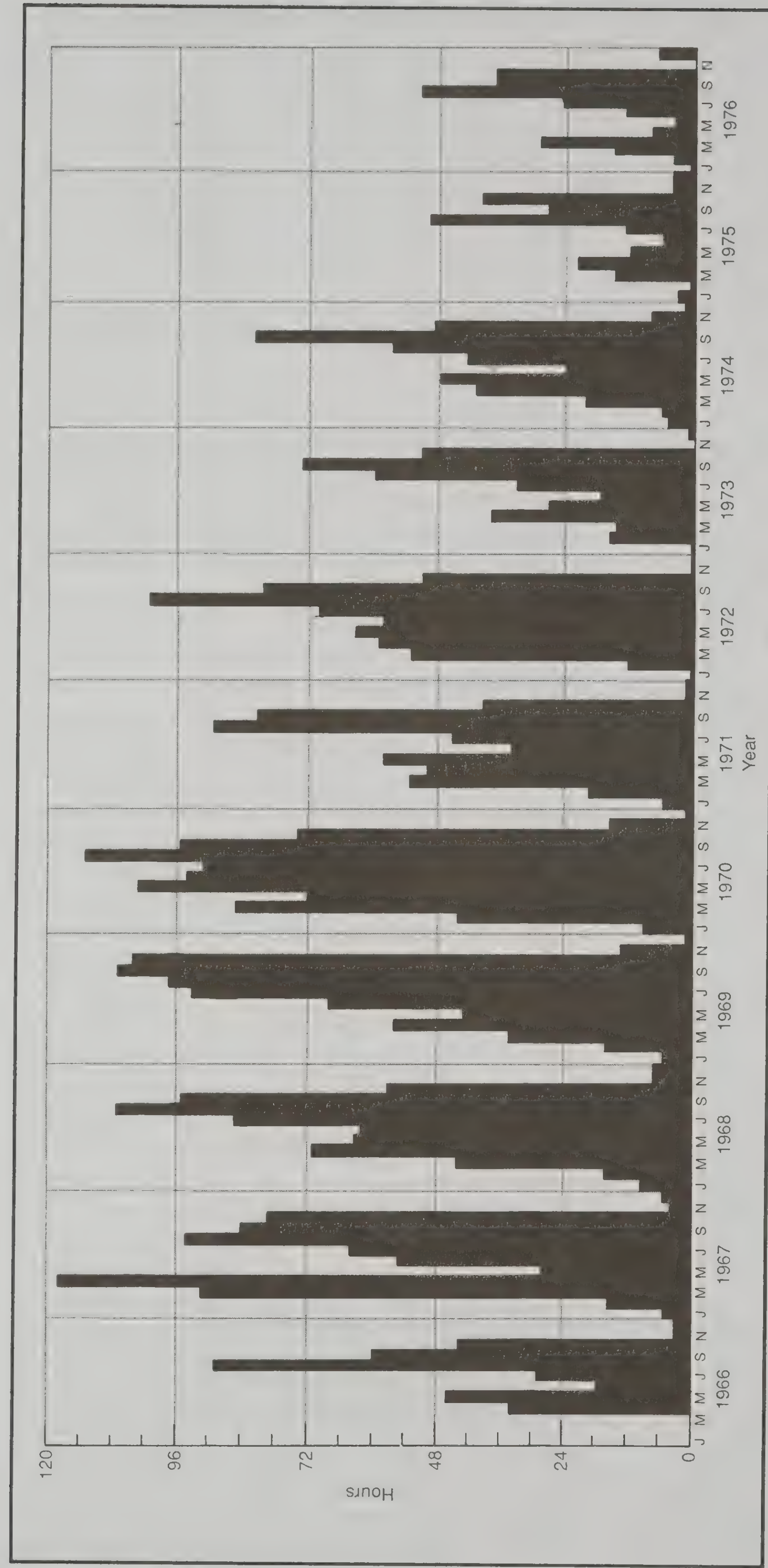

Figure 7.10. Hours-per-month of VHF trans-equatorial propagation (from Kingan, Reference 11). (Note: Horizontal axis designators are every other month—January, March, May, July, etc.)

distortion on VHF signals propagated by means of auroral-*E,* as well as on those signals reflected from an aurora. In both cases, voice modulation is often unintelligible on 50 MHz and is nearly always unusable on 144 MHz. Thus, while voice communications may be possible using SSB, experience has shown that CW is the most effective way to communicate.

Geographically, the more northerly the latitude, the greater the number of VHF auroral openings. In the U.S., the northern tier of states experience fairly good openings between 50 and 75 days a year. In the central states, openings may occur between 10 and 35 days a year, while considerably fewer openings occur in the southern tier of states. During prolonged geomagnetic storms, auroral openings may occur and re-occur several times throughout the day for several days in a row.

Because auroras occur in the northern areas of the northern hemisphere, north is the optimum antenna bearing to establish communications by auroral propagation modes. Once communications are established, antennas should be rotated slowly to maximize propagation.

Most auroras are produced by increased geomagnetic activity, which tends to stay at an elevated level for two to three years after the solar maximum. Auroral displays gradually decrease in number thereafter, occurring less frequently during periods of minimum solar activity.

A comprehensive auroral simulator computer program is available from the Solar Terrestrial Dispatch. The program simulates aurora in brilliant color, and is based on decades of auroral observations. The program permits a wide range of studies to be made of auroras, including their locations and effects on HF and VHF propagation, under controlled conditions. For more information and pricing, contact the Solar Terrestrial Dispatch directly.[8]

7.4 Meteor Ionization

Meteors, or "shooting stars" as they often are called, are particles of mineral and metallic matter that continually enter the Earth's atmosphere from outer space. It has been computed that hundreds of millions of meteors, most of them microscopic in size, enter the Earth's atmosphere every 24 hours. This figure increases significantly during certain times of the year when meteor showers occur.

As large meteors enter the Earth's atmosphere at velocities of up to 50 miles per second, the intense heat generated by friction due to the upper air causes the meteors to leave an ionized trail behind as they burn 30 to 100 miles (55 to 185 km) above the Earth. This ionization often is intense enough to reflect or scatter VHF signals over distances of several hundred miles. Signals reflected by meteor ionization can be identified by the very short, sudden burst in signal strength that takes place when the radio signal intersects the ionized trail. The signal level increase, on the order of 20 to 40 dB, is sharp and sudden; it may last from a few seconds to half a minute before fading into the background noise level. A Doppler shift also may be noticed on signals reflecting from a meteor trail. This is caused by the rapid motion of the reflecting point. In some cases, the shift may amount to as much as 2 kHz, and it can last for several seconds.

For the radio amateur, meteor-reflected signal bursts are of little communication value unless they occur frequently enough, or are of sufficient duration, to permit the transmission of information. A 50 MHz signal may appear as a few readable words, while on 144 MHz, the burst is shorter by almost a factor of 10, often being nothing more than a ping. At this rate, even during major meteor showers, it requires a great deal of time and patience to transmit information between stations. For this reason, high keying speeds are preferable to voice transmissions, although the exchange of voice information may at times be possible on 50 MHz, especially when using voice controlled (VOX) SSB.

Conventional communication techniques cannot be used for meteor-burst communications. Stations should arrange schedules and alternate their transmit-receive times. For example, a station could transmit for 15 seconds and then listen for 15 seconds. This is not to preclude random contacts by transmitting and listening in the "blind." Further, with modern multimode controllers, today's amateurs can generate very complex, high-data-rate signals. High-rate (50 wpm) machine-generated CW, as well as more sophisticated 1200-baud ARQ and AMTOR signals, now are being used for meteor-burst communications. While the frequency band between 30 and 60 MHz is about optimum for burst duration, the use of directive arrays can help to exploit this mode at 144 MHz. Meteor transmissions can be accomplished with modest transmitter power levels; however, the key element in the equation is "effective radiated power (ERP)"; that is, the combination of antenna gain and transmitter power. Because meteor showers tend to occur low in the morning sky, a directive antenna will help.

During a typical 24-hour period, between 300 and 500 meteor-reflected signal bursts lasting 5 seconds or longer can be counted on 50 MHz. Approximately 25% of these signal bursts will last from between 10 and 30 seconds, and occasionally, one may last considerably longer. A great number of bursts will be heard on 28 MHz and the lower frequency bands, while considerably fewer will be heard on 144 MHz and higher frequencies.

While meteors may appear at any time, most of them enter the Earth's atmosphere between midnight and dawn, peaking between 5 and 7 AM, local time. Because the optimum ionization altitude of meteor trails is between 45 and 65 miles (80 to 120 km), the optimum communication range is approximately 800 miles, with a maximum range of about 1200 miles. Seasonally, considerably more meteors enter the Earth's atmosphere during June and July than at any other time, with a minimum number observed during January and February.

From time to time, but on a regular basis, the Earth moves through areas in space in which there are very large swarms of meteors. During such periods, called meteor showers, meteors enter the Earth's atmosphere with more than average frequency. During many showers, meteors will appear at the rate of one or two a minute, and during certain very large showers, many thousands may be observed during a single night. The possibility of 50 and 144 MHz communications by means of ionized meteor trails increases considerably during meteor showers.

Table 7.1 lists the major showers, the approximate dates on which they occur, and the average number of

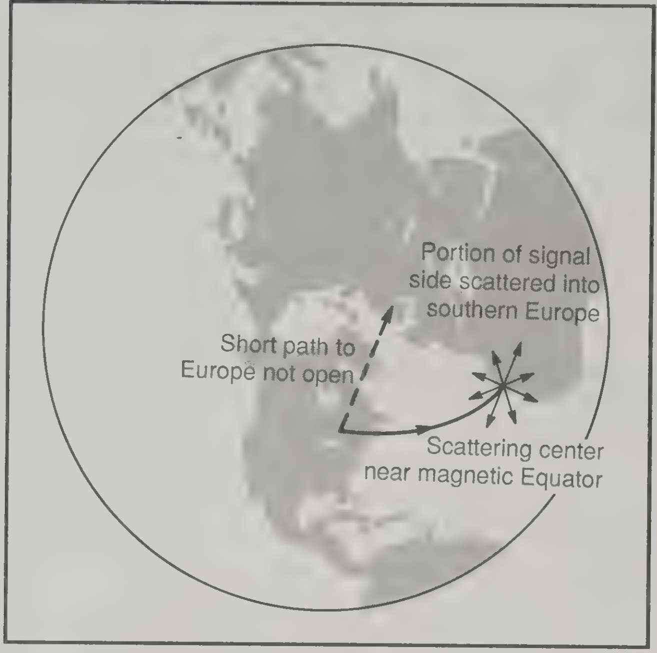
Portion of signal side scattered into southern Europe
Short path to Europe not open
Scattering center near magnetic Equator

Figure 7.11. It is possible to use side-scatter propagation for communications between the U.S. and Europe on 21, 24, and 28 MHz.

meteors that probably will enter the Earth's atmosphere each hour during these periods. While meteor-burst communication can be quite difficult, and can require a great deal of patience and time to move a small amount of information, it does provide a means of intermittent ionospheric communication on VHF bands over distances of between approximately 800 and 1200 miles.

7.5 Trans-Equatorial VHF Scatter

Strong 50 MHz band openings, and even moderately strong 144 MHz band openings, can occur, particularly during periods of moderate to high solar activity. These openings, which occur at times when the expected Classical MUF in the path is considerably lower than 50 MHz, are called trans-equatorial, or TE, openings.

Trans-equatorial propagation was first observed by radio amateurs during the solar maximum of Cycle 18, which took place during 1947. Amateurs also pioneered use of this mode of propagation during subsequent solar cycles.

In the early 1960s, Stanford Research Institute (SRI) scientists probed the ionospheric path that transited the magnetic equator between Hawaii and Rarotonga in the Cook Islands during the American High Altitude Nuclear tests. They found a mode of propagation that not only would support signals at frequencies greater than 64 MHz, but also, that occurred practically every night in the evening.[9,10] This mode of propagation was first observed in 1958, at the peak of Cycle 19, when a portable TV receiver taken to Rarotonga could routinely receive Hawaiian TV signals in the early evening. This phenomenon was first thought to be caused by exceptionally high critical frequencies due to the very intense solar maximum. However, the oblique sounder work of SRI in 1962 showed it to be a unique mode of propagation now known to be TE.

In 1966, a group of radio amateurs, led by Stuart Kingan (ZK1AA), started what turned out to be an eleven-year measurement project focusing on TE propagation over the path between Hawaii and Rarotonga. This path is unique because the magnetic and geographic equator almost coincide and because it is within one degree of being purely a north-south path. The project involved monitoring VHF signals from north of the equator (mostly TV signals) on a scanning receiver in Rarotonga. This project, which was conducted entirely by radio amateurs without any outside assistance, produced a very detailed look at TE propagation.

The nighttime mode of trans-equatorial propagation occurs across the magnetic equator. Propagation paths as short as 2500 km and as long as 5000 km can occur. This phenomenon never occurs before sunset, and it lasts until local midnight. Once conditions in the *F* region favor the onset of TE propagation on any particular longitude in the area affected, the strength and upper frequency limit all tend to increase up to 2200 local time, at which time TE propagation starts to wane. The conditions causing the phenomenon move from west to east at approximately 300 km per hour. Trans-equatorial propagation is very sensitive to solar activity. At solar maximum, TE openings occur between 24 and 30 days a month (or about 96–120 hours a month) with the peak months of occurrence being July through October. In early November, the mode abruptly disappears. At solar minimum, the occurrence rate drops off to 18–20 days a month (36–48 hours a month), with September being the single peak month. These characteristics can be seen in Figure 7.10, originally hand-drawn by Kingan.[11]

In the western hemisphere, the magnetic equator lies approximately 20 degrees south of the geographical equator, and it roughly follows an arc that extends from Lima, Peru, to Recife, Brazil, and that passes through La Paz, Bolivia. The optimum distances for

TE openings range between 1500 and 2500 miles above and below the equator. Thus, for example, typical TE paths exist between Puerto Rico and Argentina, and from southern Europe to southern Africa.

In the western hemisphere, and for smoothed sunspot numbers greater than 75, 50 MHz TE openings occur almost every night during the spring and summer, when the Sun is "over" the equator, over an area extending from Mexico City in the north to southern Chile and Argentina in the south. Within this area there is little variation in signal level from night to night, and circuit reliability is high. Less frequent openings extend into the southern and central area of the United States, with openings falling off rapidly at greater distances to the north.

Signal characteristics vary with path length, with serious flutter fading observed on short paths. Solid, voice-quality signals often are observed on the longer paths.

While we primarily have discussed 50 MHz TE skip and the spectacular openings that may result, TE openings also occur on the 10, 12, 15, 17, and 20 meter bands. Occurring during the evening hours (8 to 11 PM local time at the path mid-point), TE openings on these bands, particularly on 20 meters, can take place during periods of low solar activity. That is why openings between the western U.S., and Australia and New Zealand, are commonplace even at solar minimum.

Trans-equatorial propagation is believed to be due to a highly ionized, bell-shaped bulge in the ionosphere that is known to exist over the magnetic equator. Radio signals entering this region at a favorable angle are reflected considerable distances between the sides of the bulge in much the same manner that a ball rebounds off the sides of a billiard table. At times, this type of propagation may result in a long, single-hop opening, without intermediate ground reflection and with path lengths of up to 5000 miles.

Signals must cross the magnetic equator roughly in a north-south direction or trans-equatorial openings will not take place. A right-angle crossing is optimum, but TE contacts have been reported between stations as much as 20 degrees off a right-angle crossing.

The trans-equatorial Classical MUF is approximately 1.5 times greater than the daylight Classical MUF observed on the same path. Thus, 50 MHz TE openings may be expected during the evening hours when a

Table 7.2. Characteristics of unusual VHF ionospheric propagation modes.

Propagation Mode	VHF Bands Prop. Possible	Latitude Zone Peak	Time of Day Peak	Seasonal Peak	Optimum Sunspot Period	Approximate Communication Distance (miles)	Band Opening Period	Signal Characteristics
Regular *F*-Layer reflection	50 MHz	Temperate	Daytime	Winter	High	E-W paths 1800–5000 N-S paths 1800–6000	Several minutes to an hour or more	Exceptionally strong
	50 MHz	Low, Equatorial	Afternoon to late evening	Spring & Fall	High	E-W paths 1800–5000 N-S paths 1800–6000	Several minutes to an hour or more	Exceptionally strong
Sporadic-*E*	50 & 144 MHz	High, Polar	Night	Spring & Fall	High & Moderate	300–1300	Several minutes to an hour or more	Weak to strong with some flutter fading
	50 & 144 MHz	Temperate	Before noon & early evening	Late Spring & Summer	All	800–2400 on 50 MHz 1100–1300 on 144 MHz	Several minutes to an hour or more	Exceptionally strong
	50 & 144 MHz	Equatorial	All day	All seasons	All	800–2400 on 50 MHz 1100–1300 on 144 MHz	Several hours to complete day	Strong with flutter fading
Auroral ionization	50 & 144 MHz	High & Temperate	Late afternoon & early evening	Spring & Fall	High & Moderate	300–1200	Several minutes to an hour or more	Weak to moderately strong, with strong flutter fading. Voice badly distorted, CW recommended
Meteor ionization	50 & 144 MHz	All	Night & early morning	June & July and during specific shower periods	All	800–1200	Several seconds to a half minute or so per burst	Strong bursts High-speed CW recommended
Trans-equatorial	50 & 144 MHz	Low & Temperate	Evening through midnight	Spring & Fall	High & Moderate	2400–5400	From one to several hours	Weak to moderately strong, with some flutter fading at times
Ionospheric scatter	50 MHz	Low & High	Evening through midnight	Spring & Fall	High & Moderate	600–2400	A few minutes to several hours	Weak, fluttery signals

Classical MUF of 34 MHz is observed during the daytime. Note, too, that TE openings often may occur on 50 MHz when propagation is not possible on lower frequency bands, on the same path, and at the same time.

In sum, trans-equatorial openings occur most often during periods of moderate and high solar activity with the probability of occurrence dropping sharping during solar minimum. Although they may occur during any season, openings will occur most often in August and September; very seldom do they occur in November and December. Trans-equatorial propagation is a nighttime phenomenon, with most openings occurring between 8 and 11 PM, local time, at the path midpoint.

7.6 Ionospheric Scatter

When a signal is at a frequency equal to or below the Classical MUF, ionospheric propagation takes place by reflection from the ionized layers existing in the Earth's atmosphere. In this case, signals strike the ionosphere obliquely and are normally reflected in a forward direction, with a very small amount of energy scattered back towards the earth in more or less random directions. When the frequency is above the Classical MUF, the signal will penetrate the ionosphere, but a very small amount of energy also will be scattered in all directions. Scatter may take place from any of the ionosphere's layers, including the *D* layer.

Until the post-war introduction of super-sensitive receivers, advanced modulation techniques, and improved antenna designs, scatter signals were of little communication value. Today, with a good receiver, high-gain antennas, and high transmitter power, scatter openings often are observed, particularly on the 21, 24, 28, and 50 MHz bands, when these frequencies are considerably above the Classical MUF. However, only a small part of a signal's energy is returned to earth by scatter; such signals are generally, although not always, weak and fluttery.

Scatter appears to occur most often from ionospheric regions in the vicinity of the magnetic equator. In northern and temperate regions, ionospheric scattering increases considerably with increases in magnetic activity and during ionospheric storms. While 50 MHz scatter openings can occur at any time, they seem to peak during the evening hours of the spring and fall, and during periods of high and moderate solar activity.

To communicate by means of forward-scattered signals, it is usual for both stations to direct their antennas at each other along the great-circle path. To communicate by means of back- or side-scattered signals, it is often best to orient both antennas at the apparent point of scatter, which may be considerably off the great-circle path. This point often can be determined by slowly rotating antennas until signal strength is maximized.

Signals scattered in a forward direction from the *E* layer may permit 50 MHz openings over distances of between approximately 600 and 1200 miles while openings over considerably greater distances may be possible with signals scattered by the *F* layers. Back- or side-scattered signals often may permit ionospheric communications between stations separated by relatively small distances, although the signals themselves may have traversed considerable distances.

Side-scattered signals often can be used to establish communications on paths that deviate from a great circle. On the HF bands, and on the 10, 12, and 15 meter bands in particular, such off-path scatter reflections frequently produce unexpected band openings.

Figure 7.11 is an example of long-distance side-scatter propagation. Here, insufficient ionization in the atmosphere, or a high level of absorption (due, for example, to auroral activity), prevents communication on great-circle paths between the United States and Europe on the 10, 12, and 15 amateur bands. However, when amateurs in the U.S. point their antennas into central Africa, towards the magnetic equator, the higher level of ionization found there often causes signals to be scattered, with a portion of the energy being side-scattered into Europe. European operators, whose antennas should be pointed roughly south to southwest, should now be able to communicate with operators in the U.S., since a portion of their signals will be side-scattered to the west.

In using side scatter to communicate between the U.S. and western Europe, the path is optimized, roughly, between 1200 and 1500 UTC (or early afternoon in western Europe). During this period, the combination of east-west propagation between the U.S. and Africa, and of north-south propagation between Africa and western Europe, is favorable for the propagation of side-scattered signals on this path.

In passing, it should be noted that scattering centers for radio signals are not always located in the ionosphere. At times, signals that have been reflected from the ionosphere are scattered in all directions when they strike the ground. A portion of the ground scattered energy is then returned to the vicinity of the signal source via the same ionospheric path, and in this way,

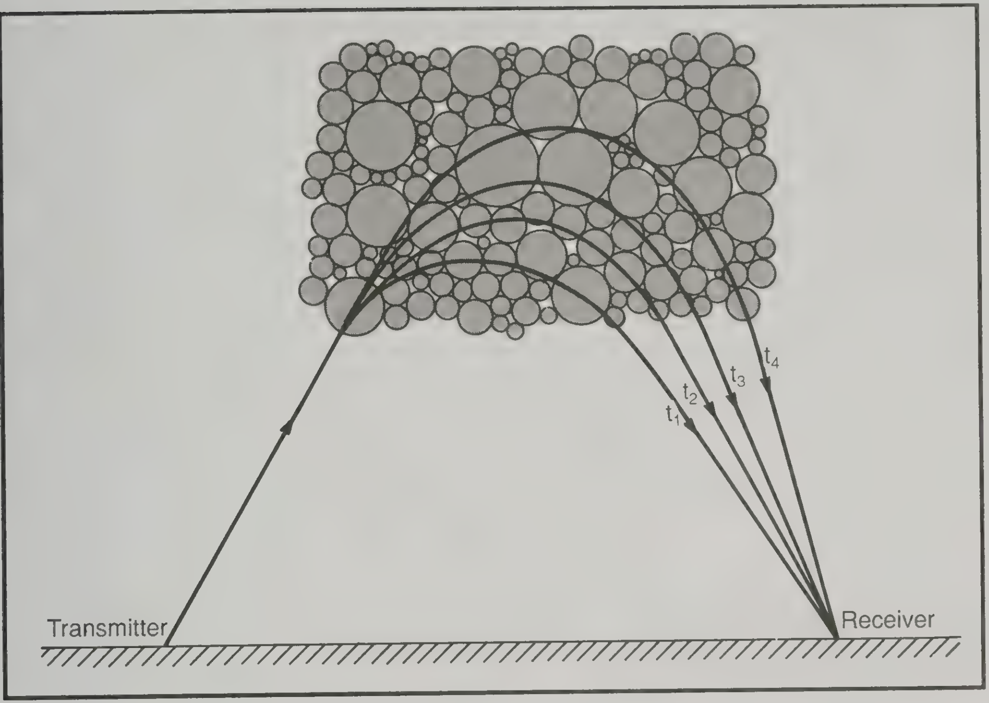

Figure 7.12. Conditions in the high-latitude ionosphere that produce spread-*F*. This type of patchy ionosphere is more common than most people think it is. Conditions like this are more likely to appear at night, but they do not occur all of the time.

communications can be established between stations whose separation prevents the use of surface waves or more conventional means of ionospheric propagation.

Finally, it is not possible to determine whether a signal has been scattered from the ionosphere or from the ground by listening to the quality of the scattered signal.

7.7 Summary of Unusual VHF Propagation Phenomena

The remainder of this chapter addresses unusual propagation phenomena that are observed only on the HF bands, and so, we pause here to summarize the various propagation anomalies and their signal characteristics that are more noticeable on the VHF bands (see Table 7.2). While propagation at any given time may be due to a single, particular mode, there are times when several modes may be involved. All in all, propagation due to phenomena in the ionosphere takes place often enough at the very high frequencies to add an extra dimension of interest to operators using the 50 and 144 MHz bands.

7.8 Spread-*F*

The existence of spread-*F* has been known for as long as there have been ionospheric measurements. Spread-*F* gets its name from the fact that vertical sounder measurements no longer show a nice, clear trace for the F_2 region, but rather, exhibit a fuzzy, diffuse trace that results from spreading of the return time delay. The question that immediately comes to mind is "What does spread-*F* do to an HF signal?" To answer this question, consider the following. During periods when spread-*F* occurs, the ionosphere's *F* layer is no longer a uniform, refracting layer; instead, it is better characterized as a turbulent medium made up of "blobs" (or patches) having different levels of electron densities. Figure 7.12 illustrates how an HF signal is split (or defocused) under these circumstances. As the signal ray enters the patchy ionosphere, it is split into many smaller, and weaker, signal rays. Each ray follows a more or less independent route, moving from one patch to another. Because each ray is in the ionosphere a different amount of time, the signal that finally emerges has been stretched in time. The effect on HF signals, then, is lower signal strength, signal stretching (distortion), and signal flutter. A second question is "How often is this a problem?" Studies conducted in 1992 and 1993 during Project PENEX[12] indicate that spread-*F* occurs more than is generally believed. When it occurs, spread-*F* produces a hollow, auroral warble with which most of us are familiar.

Historically, spread-*F* was thought to occur in the band that is bounded by plus or minus 20 degrees around the geomagnetic equator, and above 40 degrees geomagnetic latitude. It rarely occurs between 20 and 40 degrees geomagnetic latitudes.[13] The entire United States is above 40 degrees geomagnetic lati-

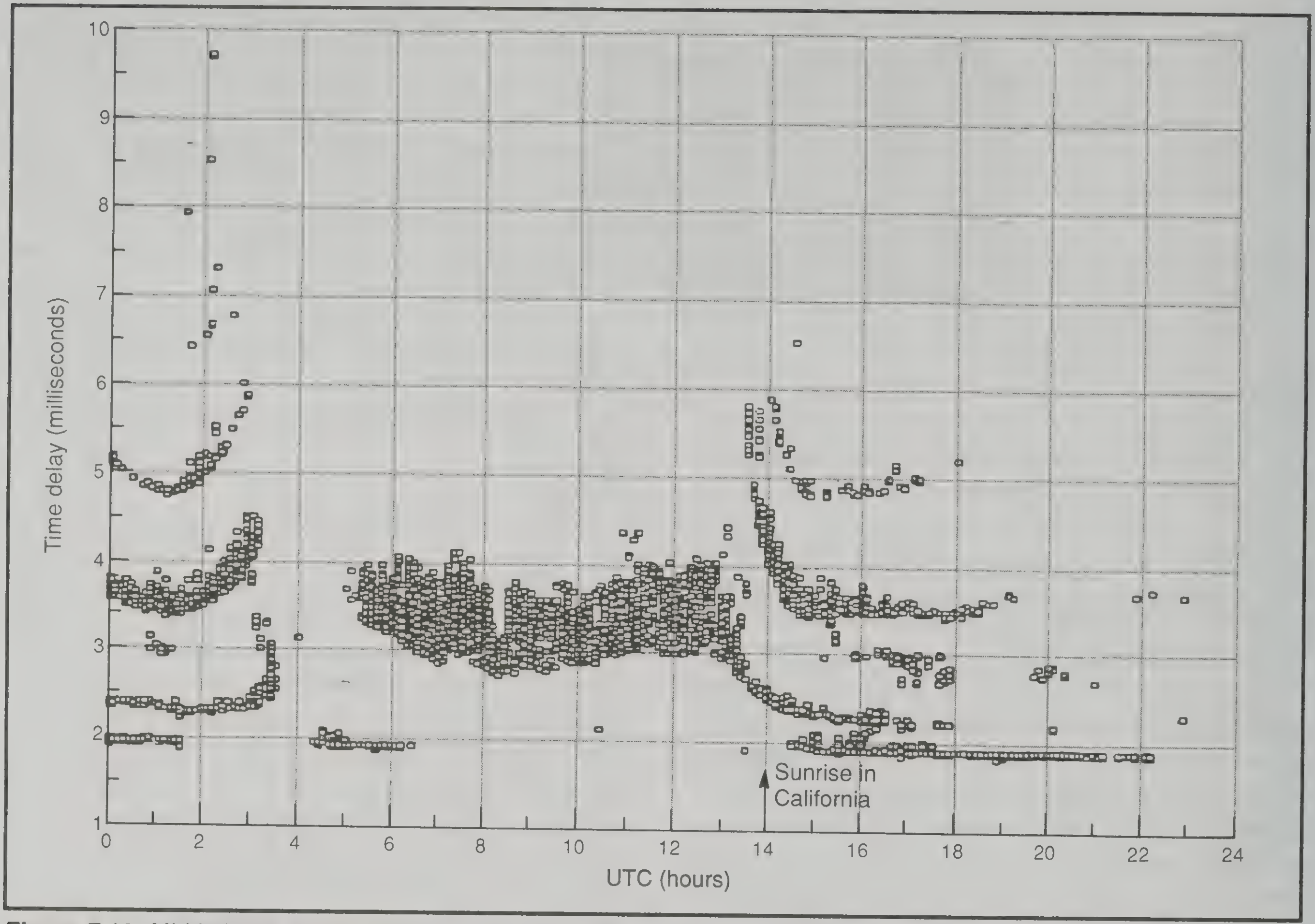

Figure 7.13. Mid-latitude (Monterey to San Diego, California, October 1992) spread-*F* is more prevalent than originally thought. (Courtesy of the U.S. Navy.)

tude, and so, it would be expected that spread-*F* should be relatively common.

In 1992, the U.S. Navy embarked on a project to make calibrated HF field strength measurements in order to calibrate the HF prediction programs that were commonly used at that time. This project was called **P**olar, **E**quatorial, **N**ear Vertical Incidence **EX**periment (PENEX). In this experiment, 40 kHz spread-spectrum signals were transmitted on 5.6, 11, and 16.8 MHz. This signal was generated by phase modulating a carrier with a pseudo-random noise (PN) digital sequence chosen to provide a very high correlation peak when matched with a reference sequence and to provide negligible correlation if the signal is not exactly aligned in time or is tested against interfering signals or noise. Pseudo-random noise sequences of 1K, 2K, 4K, and 8K bits were transmitted. Longer sequences provided more processing gain, but they are more susceptible to Doppler shift and other distortions. For the first time, scientists could operate anywhere in the HF band, undetected by standard 3 kHz bandwidth receivers and completely immune to standard broadcast or teletype signals. Because of the high processing gains involved (that is, the ability to receive signals buried deep in the noise), low transmitter powers were successfully used. The high level of time resolution provided by the system allowed scientists to view the ionosphere in great detail.

During the first transmitter tests in October 1992, between Monterey and San Diego, California, the first observations of mid-latitude spread-*F* were observed on 5.6 MHz (see Figure 7.13). Each little square is a single correlation peak, and it indicates that the receiver matched the transmitted signal at the time delay shown. Between 9 PM and 6 AM local time, propagation is purely via an *F* layer exhibiting significant spread-*F*. Spreading times ranged between 0.8 and 1.0 millisecond. At sunrise (6 AM), the formation of the daytime *F* layer is seen to start in the upper ionosphere, with the peak electron density moving downward as the Sun rises. The other interesting feature noted on all PENEX data is that the *E* layer (the straight trace at 2.0 milliseconds) provides a natural "sanity check" for the technique used. Spread-*F* observed over the path used in California was not as intense as that found when the measurement system was moved to higher latitudes (specifically Alaska).

The second example of spread-*F* (see Figure 7.14; this is the high-latitude version) was observed on a 900 km path between Fairbanks and Cape Wales, Alaska, in early June 1993. At this time, the path was illuminated by the Sun for almost 20 hours each day. Night, such as it was, was centered around 1000 hours UTC (local midnight). The *F* layer (time delays greater than 4 milliseconds) exhibits spread-*F* throughout the day. Subsequent data corroborated what is shown in Figure 7.14; that is, the auroral and polar regions' *F* layers are diffuse, turbulent medias, with spreading being more the norm than the exception. Modern HF prediction models have no capability to simulate the irregular, patchy *F* layer that PENEX signal probes observed. This is one reason why these models fail to accurately predict propagation conditions over high-latitude paths.

At geographical mid-latitudes, spread-*F* is a nighttime phenomena. At high latitudes, in the winter, it occurs almost 100% of the time, while in the summer, it occurs almost 100% of the time at night and 50–60% of the time during the day.

7.9 Gray-Line Propagation

The gray line, or the "twilight zone," as it is sometimes called, is that band around the Earth that separates the areas of daylight and darkness. In astronomical terms, the gray line is called the "terminator," and it is a somewhat fuzzy region because of the Earth's atmosphere (see Figure 7.15).

Propagation along the gray line is extremely efficient. A major reason for this is that for all intents and purposes, the *D* layer, which absorbs high-frequency signals, is absent in this zone. That is, the *D* region is rapidly disappearing on the sunset side of the gray line, while it has yet to build up in the areas experiencing sunrise. The F_2 layer exists throughout the nighttime hours, so it gets a "jump-start" on building its ionization levels to daytime levels at sunrise. At sunset, F_2-layer ionization drops slowly. So efficient is propagation along the gray line that at times, it is possible to send signals almost all the way around the world.

Because gray-line propagation is so efficient, it often can be one of the best modes to use for long-distance communications on the HF bands. In many cases, surprisingly good results can be obtained with antennas no fancier than dipoles and inverted Vs (the higher the better, of course), and best of all, you won't have to lose any sleep while chasing DX in this mode . . . well, at least not too much sleep. You see, at any given location, the gray line is in effect about two hours a day—one hour in the morning (plus or minus 30 minutes from sunrise) and one hour in the evening (plus or minus 30 minutes from sunset).

To understand how the orientation of the gray line varies with the season, let us take a few liberties with Copernican theory and bend some basic rules of astronomy.

Simply pretend that:

1. The Earth is the center of the universe;

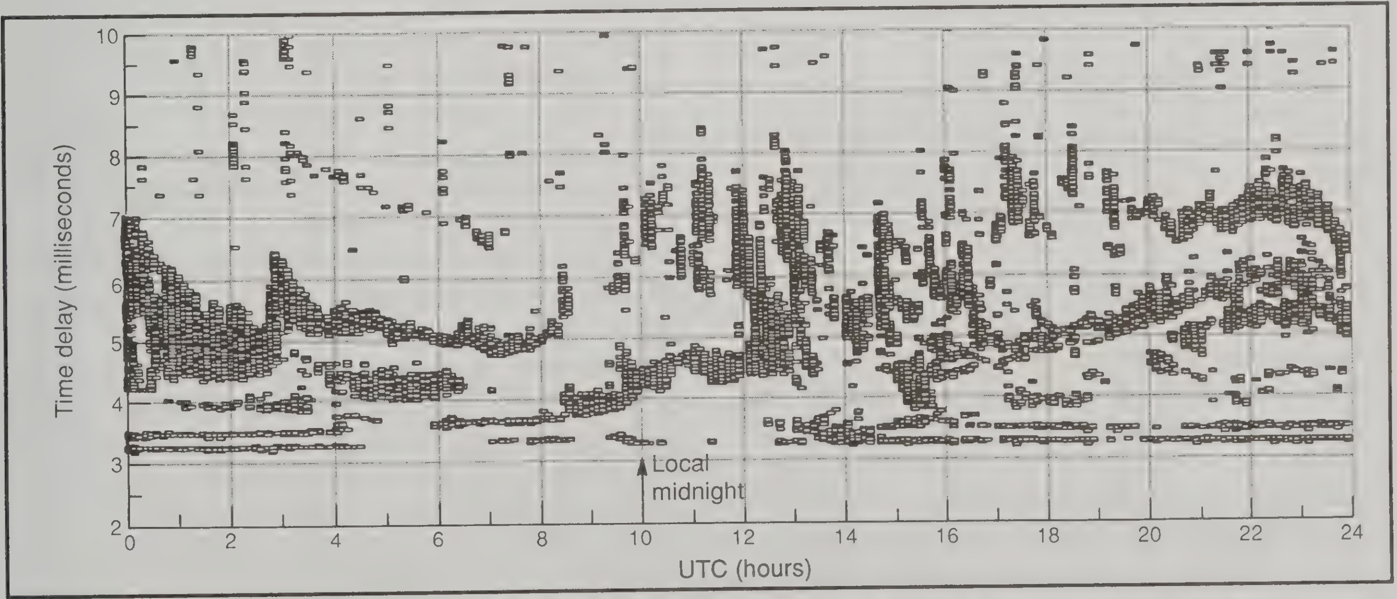

Figure 7.14. High-latitude spread-*F* observed in Alaska (June 1993) by Project PENEX. (Courtesy of the U.S. Navy.)

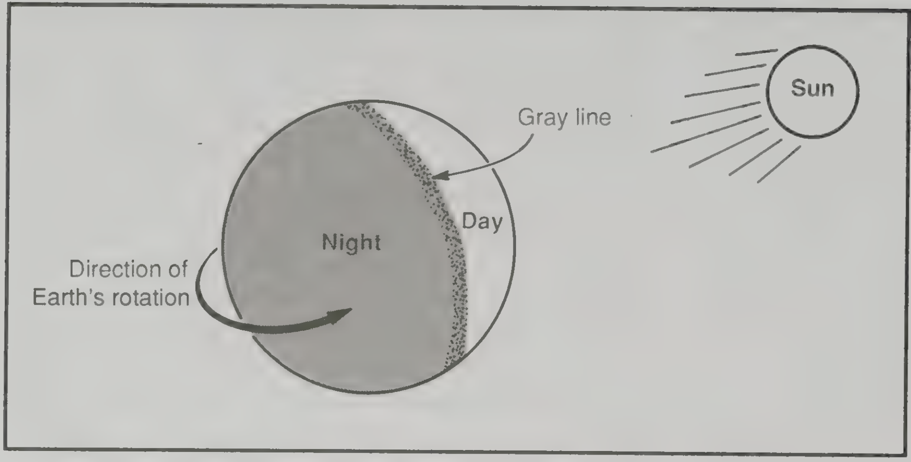

Figure 7.15. The gray line is the fuzzy band that separates the areas of daylight and darkness.

2. The Sun "travels" around our planet once a year;
3. The Earth's axis, which passes through the North and South Poles, is perfectly vertical (0°).

Now, looking at Figure 7.16[A], it can be seen that the Sun "travels" a maximum of 23 degrees north (Figure 7.16[B]) and 23 degrees south (Figure 7.16[C]) of the equator on its annual journey between the Tropic of Cancer and the Tropic of Capricorn. Because the Sun is going north on one trip and south on another, it crosses the equator twice a year (approximately March 21 and September 21), at times that are called the equinoxes.

Here's an idea on how to show where the gray line occurs, and one which the younger amateurs among us might even want to take to school as a science project. If you would like to see what DX you may be able to work using gray-line propagation on any given day, all that is needed are three items[14]:

1. The gray-line table (Table 7.3);
2. A globe (any one will do, even the kind used for children's coin banks); and
3. A piece of cardboard slightly larger than your globe.

Cut out a circle from the cardboard the diameter of your globe (Figure 7.17). Don't cut out too much—just enough to ensure that the cardboard fits snugly over the globe. Once the cardboard is mounted on the globe, it becomes your gray-line indicator (Figure 7.18).

Now, align the cardboard indicator on the globe using the gray-line estimator (Figure 7.19). This will bring you to within a few degrees of the correct orientation for the morning and evening periods.

To find the exact gray-line path, adjust the cardboard indicator to the angle given for today's date (or for the nearest date shown) in the gray-line table (Table 7.3). Let's assume you have chosen the morning period. Rotate the globe until the cardboard indicator slices through your location. You are now on the gray line.

Once you have your cardboard gray-line indicator properly oriented and over your location, run your finger along the cardboard to the other side of the world. All of the areas through which the indicator runs are in a position to be worked on that day—that is, the areas to be worked at your sunrise on that day.

A trick that can help you use your gray-line indicator is to think of the North Pole as zero degrees (rather than 90 degrees north latitude) and the Arctic Circle as 23 degrees to the south of north (rather than 67 degrees north); see Figure 7-20. The Arctic Circle usually is represented by a dotted ring on most globes. This will give you the two limit points between which your cardboard indicator will swing. Next, convert the other two high-latitude rings (80 and 70 degrees) to 10 and 20 degrees south or north, respectively. In this way, you will derive all of the reference points needed to use your gray-line indicator.

Let's say that it is December 21, and you live in San Francisco, California. What can you work this morning on the sunrise gray line?

Using the information from the gray-line table (Table 7.3), set your cardboard at 23 degrees to the south of the North Pole, and move the globe until the cardboard is over San Francisco. Now, run your finger down across the Pacific Ocean, and you will see that the gray line extends through the Malagasy Republic and Kenya, between Italy and Albania, and up to the Netherlands.

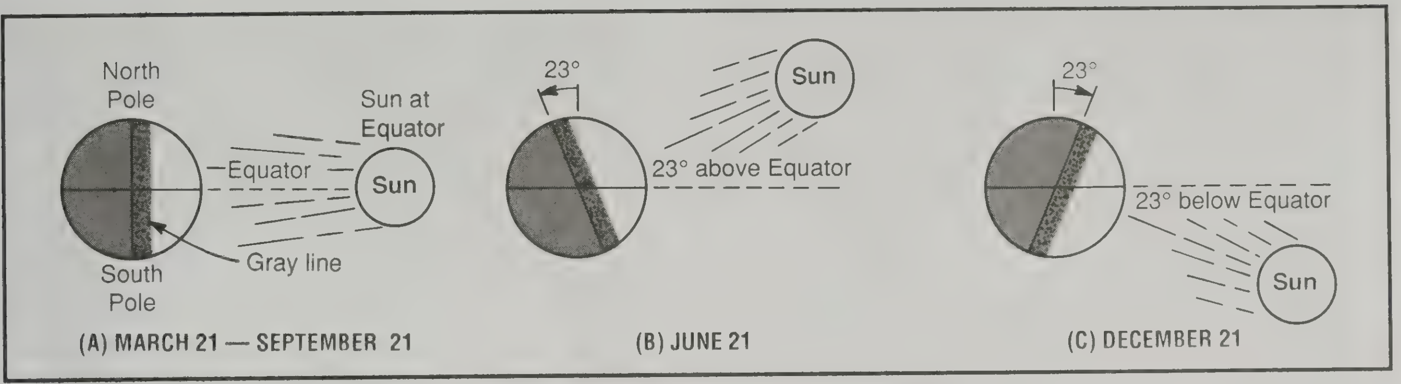

Figure 7.16. The Sun's relative angle to the Earth's equator varies throughout the year.

That's fine. But what happens in the evening, at sunset? Can you work into the same areas as you did in the morning? Absolutely not! You still obtain the gray-line orientations from Table 7.3, but now, you must do one very important thing—**reverse north and south.** That is, instead of setting your cardboard at 23 degrees south of the North Pole (as you did in the morning), set your cardboard at 23 degrees north of the South Pole. Running your finger down from San Francisco, you will see that the gray line crosses Mexico's Baja California Peninsula and the southern tip of South America, extends through Sri Lanka, and continues up through Bhutan and Mongolia. This certainly is a different gray line from the one you used this morning!

As another example of gray-line propagation, examine the sunrise gray line for the East Coast of the United States during the month of December. Using your cardboard indicator, you will find that the gray line passes through Central America, extends across

Month/Day	Angle from North Pole	Month/Day	Angle from South Pole	Month/Day	Angle from South Pole	Month/Day	Angle from North Pole
Jan. 1	23°S	Mar. 26	1°N	Jul. 3	22°N	Sept. 26	1°S
Jan. 2	23°S	Mar. 29	2°N	Jul. 12	21°N	Sept. 28	2°S
Jan. 10	22°S	Mar. 31	3°N	Jul. 19	20°N		
Jan. 16	21°S			Jul. 24	19°N	Oct. 1	3°S
Jan. 21	20°S			Jul. 28	18°N	Oct. 4	4°S
Jan. 25	19°S	Apr. 3	4°N			Oct. 6	5°S
Jan. 29	18°S	Apr. 5	5°N			Oct. 9	6°S
		Apr. 8	6°N	Aug. 2	17°N	Oct. 11	7°S
Feb. 2	17°S	Apr. 11	7°N	Aug. 5	16°N	Oct. 14	8°S
Feb. 5	16°S	Apr. 13	8°N	Aug. 9	15°N	Oct. 17	9°S
Feb. 8	15°S	Apr. 16	9°N	Aug. 12	14°N	Oct. 20	10°S
Feb. 12	14°S	Apr. 19	10°N	Aug. 16	13°N	Oct. 22	11°S
Feb. 15	13°S	Apr. 22	11°N	Aug. 19	12°N	Oct. 25	12°S
Feb. 18	12°S	Apr. 25	12°N	Aug. 22	11°N	Oct. 28	13°S
Feb. 20	11°S	Apr. 28	13°N	Aug. 25	10°N	Oct. 31	14°S
Feb. 23	10°S			Aug. 28	9°N		
Feb. 26	9°S	May 1	14°N	Aug. 31	8°N	Nov. 3	15°S
Feb. 28	8°S	May 5	15°N			Nov. 7	16°S
		May 8	16°N	Sept. 2	7°N	Nov. 10	17°S
Mar. 3	7°S	May 12	17°N	Sept. 5	6°N	Nov. 14	18°S
Mar. 6	6°S	May 16	18°N	Sept. 8	5°N	Nov. 18	19°S
Mar. 8	5°S	May 21	19°N	Sept. 10	4°N	Nov. 22	20°S
Mar. 11	4°S	May 26	20°N	Sept. 13	3°N	Nov. 27	21°S
Mar. 13	3°S			Sept. 16	2°N		
Mar. 16	2°S	Jun. 1	21°N	Sept. 18	1°N	Dec. 3	22°S
Mar. 18	1°S	Jun. 10	22°N	Sept. 21	0°	Dec. 12	23°S
Mar. 23	0°	Jun. 21	23°N	Sept. 23	0°	Dec. 23	23°S

Table 7.3. The gray-line table for sunrise. For sunset, read the same angle, but reverse north and south (i.e., for September 2 sunset, the figure is 7° south from the North Pole).

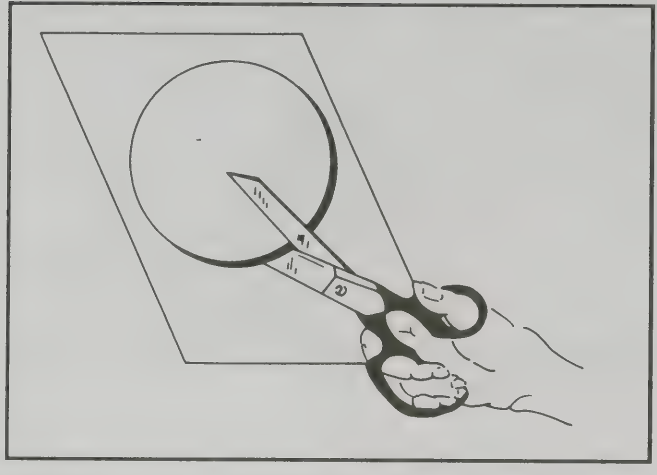

Figure 7.17. Cut a circle in the cardboard to match the size of the globe.

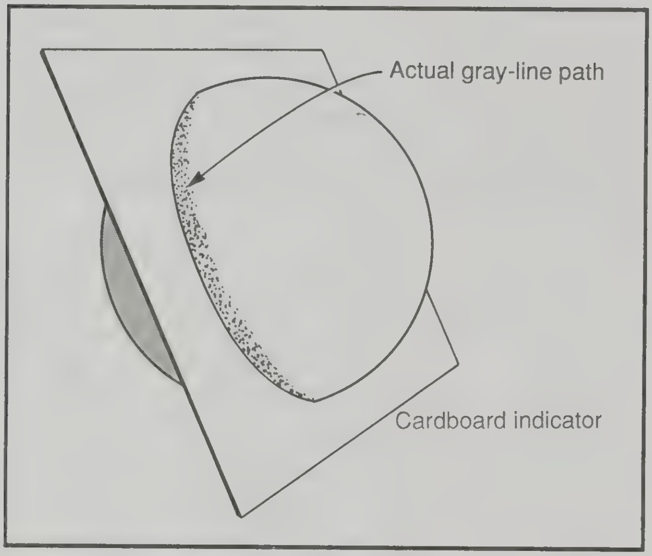

Figure 7.18. A cardboard gray-line indicator.

the South Pacific and south of New Zealand, runs along the west coast of Australia and through India, travels across Scandinavia, and extends south of Greenland. Thus, in addition to being able to work into Western Australia by using gray-line propagation, East Coast amateurs also should be able to communicate with stations in India, Pakistan, and even Russia **by beaming to the southwest**. By the way, that winter morning path into Western Australia, wherein East Coast amateurs beam south of New Zealand, makes it appear as if the signals undergo a dog-leg turn as they propagate into Australia (see Figure 7.21); hence, this path has been called the "crooked path." As we have seen, however, the crooked path is nothing more than a gray-line path.

Today, many "ham-utility" software programs and some of the newer HF prediction programs calculate, among other things, the gray line. Most use a world-map projection that shows, as a function of the time of day, which parts of the world are in daylight and which parts are in night, and thus, where the terminator lies. Most programs, using your computer's internal clock, also move the projection across the screen in real time. If a user wants to check what his or her gray-line paths are going to look like, however, he or she can remove the projection from its "real time" mode and enter the time for local sunrise or sunset. The screen will now display the gray-line path. Photos 7.B and 7.C show examples of screen displays produced by a computer program called *GEOCLOCK*.[15] Several other computer programs that display gray-line data were discussed in Chapter 6.

An excellent non-computerized, simple-to-use gray-line calculator is available from XANTEK Inc.[16], and is called The DX Edge. It consists of a durable plastic slide-rule map upon which is placed a transparent monthly solar zenith-angle plot. By setting the sunrise or sunset portion of the plot at the geographic longitude of your location, the gray line is immediately apparent. The DX Edge has been around since 1981, and it is a very convenient and easy way to identify all of the areas of the world that are in daylight or darkness at any time of day, and to show where the Sun is rising and setting. Figure 7.22 shows The DX Edge in use for September sunrise in Washington, D.C.

In sum, using the gray-line methods outlined here, you will be able to determine those days when the sunrise and sunset "windows" are open for you to work into certain areas. It is even possible to set up schedules months in advance, because the gray line will optimize your chances of communicating with (or hearing) stations in those elusive countries around the world.

7.10 Long-Path Propagation

Except for the antipodal point (a point exactly on the opposite side of the world), any two points on Earth are linked by both a short and a long great-circle path. The great-circle bearing along the short path is the reciprocal of the long-path bearing; that is, they differ by 180 degrees. The distance along the short path is always less than 12,000 miles, or about 20,000 kilometers, while the distance along the long path is equal to 24,000 miles (about 40,000 kilometers) minus the short-path distance. For example, the short-path great-circle bearing from a station in North Carolina to a

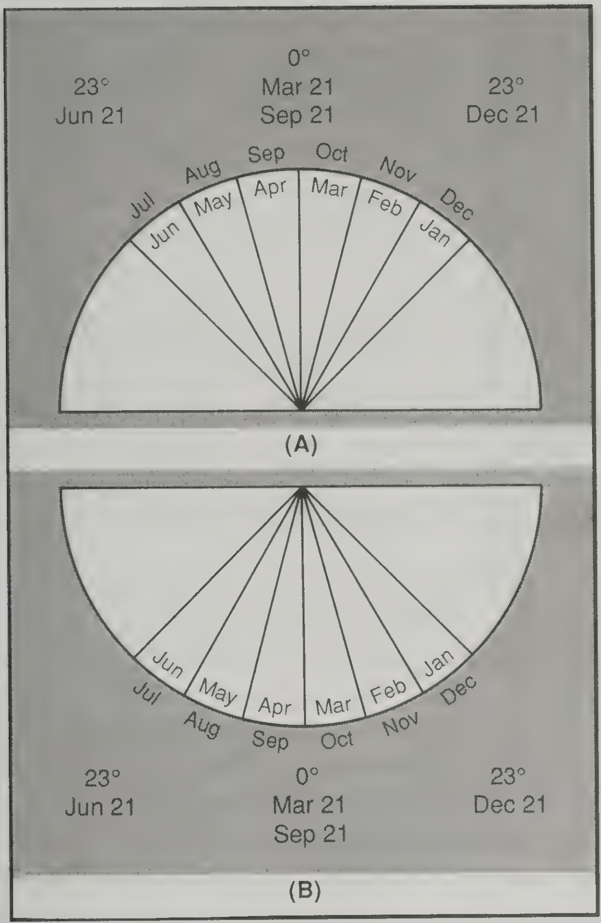

Figure 7.19. (A) Morning gray-line estimator (sunrise only). (B) Evening gray-line estimator (sunset only).

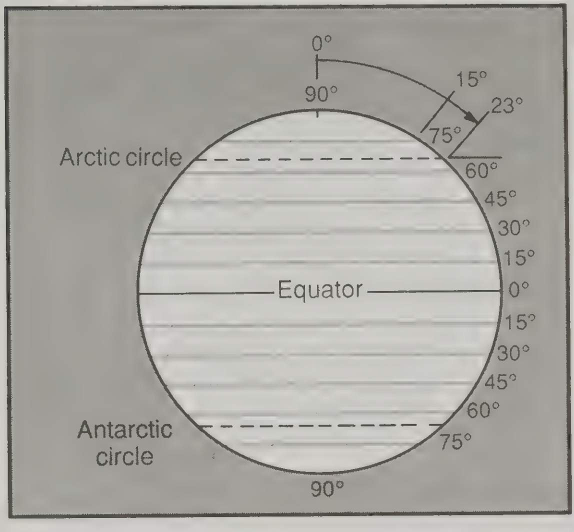

Figure 7.20. Thinking of the North Pole as 0 degrees and the Equator as 90 degrees to the south simplifies the location of reference points to plot the gray line.

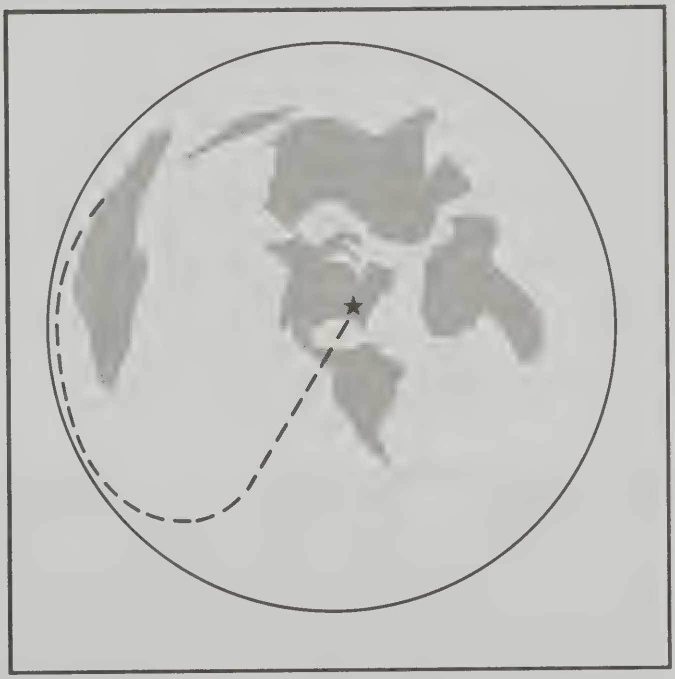

Figure 7.21. An azimuthal map centered on Washington, DC, showing the so-called "crooked path" into western Australia. By using your gray-line indicator, this path will be seen as the gray-line path that occurs at sunrise during the northern hemisphere's winter.

station in New Zealand is found to be 240 degrees, and the distance is approximately 8500 miles; the long-path bearing is 60 degrees, and the distance is approximately 15,500 miles.

Under normal conditions, a radio signal that is reflected from the ionosphere will propagate most effectively along the great-circle path that exhibits the least absorption. Further, everything else being equal, the amount by which a signal will be absorbed or weakened depends upon the amount of sunlight on the path (which, in turn, controls absorption in the *D* layer), the distance the signal must travel, and the proximity of the path to the zones of maximum overhead aurora. In most cases, total absorption will be less, and signals will be strongest, along the short path. On the other hand, there are often times when the long path exhibits the least absorption, even though the signal traveled more than half way around the world.

To explain why signals traversing the long path are at times the strongest, let us examine the special case of antipodal propagation. In this case, and only in this case, because both points are at opposite sides of the world, all paths between them are great-circle paths and all are 12,000 miles long!

Let us assume that the ionosphere is sufficiently strong so as to reflect a signal equally well on all possible paths. This is often the case on 20 and 40 meters.

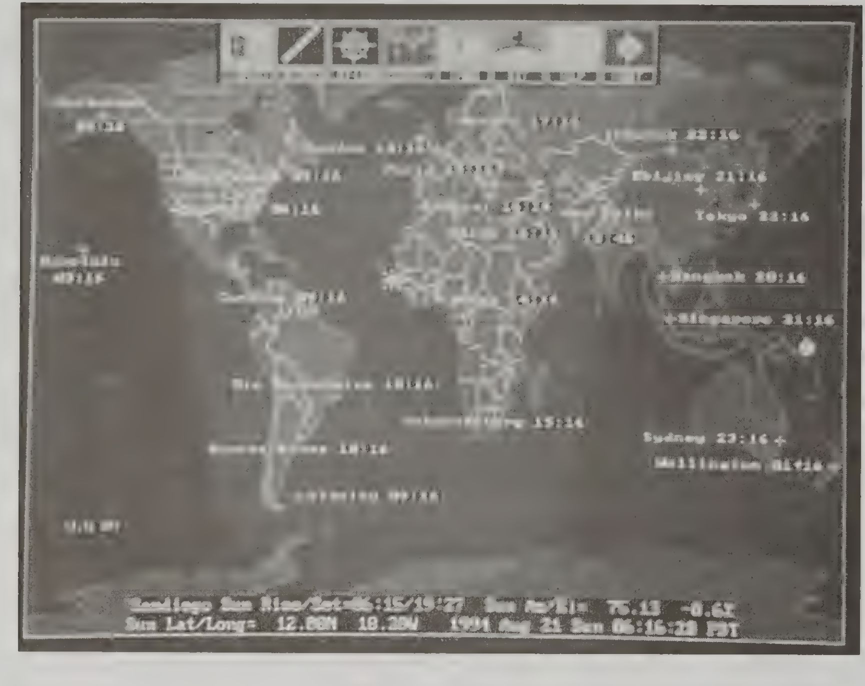

Photo 7.B. Day/Night terminator computer display produced by the *GEOCLOCK* program.[15]

Since for antipodal propagation all paths are of equal length, the main factor controlling signal intensity will be solar-induced absorption, or how much of the path is in sunlight. In fact, the path that has the shortest segment in daylight will be associated with the signal having the greatest strength. Put another way, for areas on the opposite side of the Earth from your location, the strongest signals should arrive over paths that extend through the nighttime side of the Earth. An example of antipodal propagation is the path between the East Coast of the United States and Western Australia. In the morning, East Coast time, the optimum path extends in a westerly direction over the Pacific, while in the afternoon, East Coast time, the optimum path extends in an easterly direction over Africa.

For paths less than 6000 miles (about 10,000 kilometers) in length—that is, paths for which the short-path length is about one third or less of the long path—the signal that travels along the short path almost always will arrive with greater signal strength. This occurs because signal losses caused by *D*-layer absorption and multi-hop ground reflection losses are

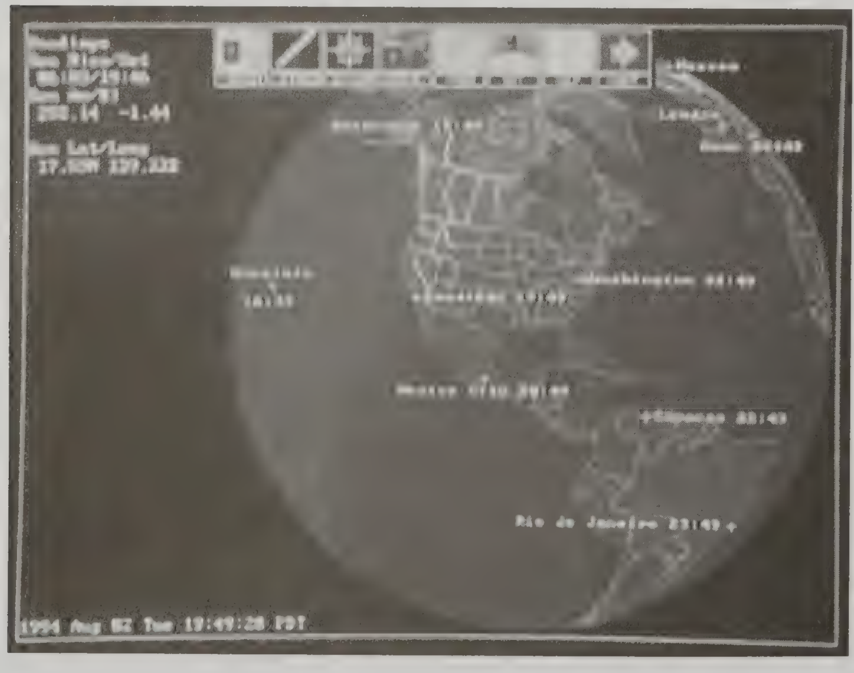

Photo 7.C. *GEOCLOCK* Space Display (shows the gray line as viewed from space).[15]

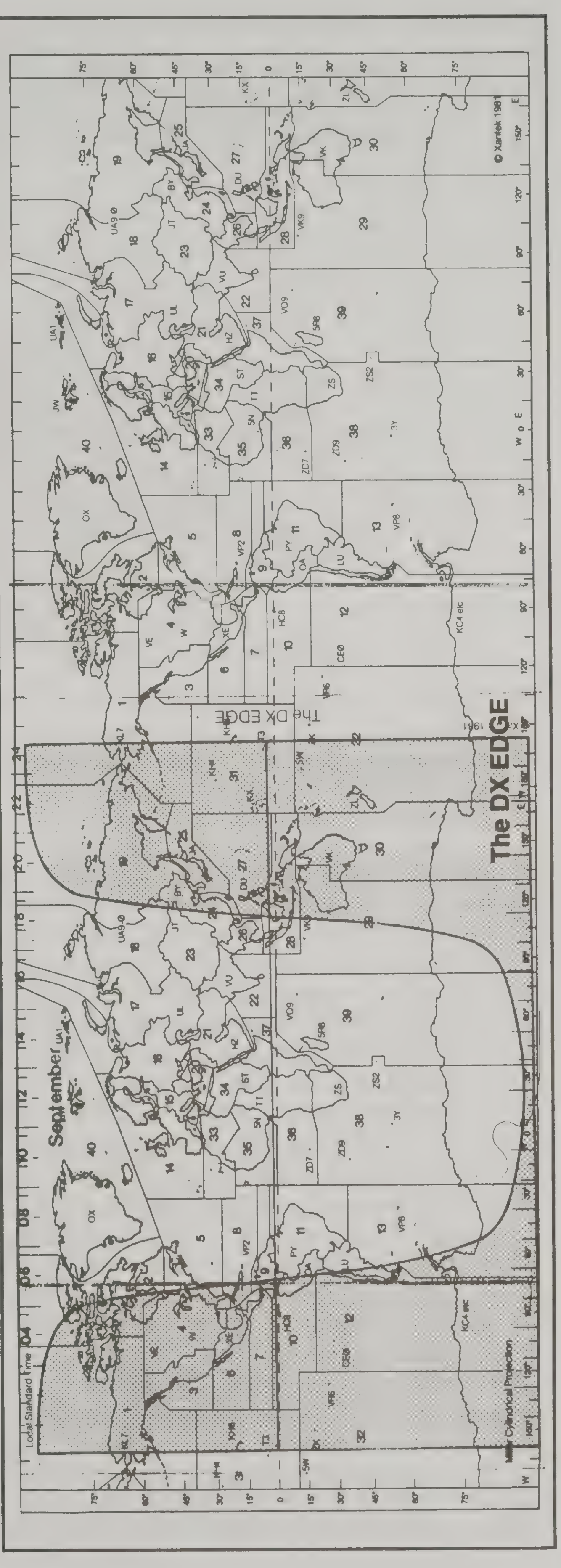

Figure 7.22. A sample of *The DX Edge* for sunrise at Washington, DC, during September. The shaded area of the world is in darkness; the unshaded area in daylight. The gray line is traced by the terminator contour that heads south through the west coast of South America, swinging north past Western Australia, and continuing north into eastern Asia.

considerably less than are the losses encountered on the long path. In general, roughly 6 dB are lost per hop due to absorption in the *D* layer (15 degree radiation angle, low solar activity, 14 MHz operating frequency) while another 6 dB are lost at each point of ground reflection (15 degree radiation angle, poorly conducting ground).

Newcomers are amazed when they hear their first long-path signal. An "opening" appears quickly, the footprint (or area with the other end) keeps changing, and then, it disappears abruptly. The major reason that these paths exist is that much of the distance is covered either in the night time sector of the Earth, where absorption is low, or where the signal is "ducted" (i.e., where the signal follows the curvature of the ionosphere without ground [and *D* layer] intervention), or both.

Russian scientists in the 1970s explored ducted propagation, and they uncovered many interesting facts. The optimum frequencies on which to establish regular ducted communications lie between 13 and 18 MHz. Ducted propagation has very critical signal entry and extraction requirements. There is a 2-to-5 degree angular window through which a signal must pass for it to enter or leave a ducted mode. Ionospheric anomalies set up these conditions. Features such as the equatorial bulge and other ionospheric irregularities provide changes in electron densities that bend the signal sufficiently to get it into a duct. Once in, it is refracted just enough to follow the curvature of the Earth until it encounters another region of changing electron densities that bends the signal down and out of the ionosphere. These modes are almost lossless, indicating very little *D*-layer passage. Ionospheric ray-tracing programs have been able to model ducted modes.

In the early 1980s, Navy scientists in San Diego were testing a new HF prediction system called *Advanced PROPHET.* One of its features was to divide the world into 5-degree-by-5-degree cells, and then, to determine whether or not the possibility exists that from a single, specified point, propagation can

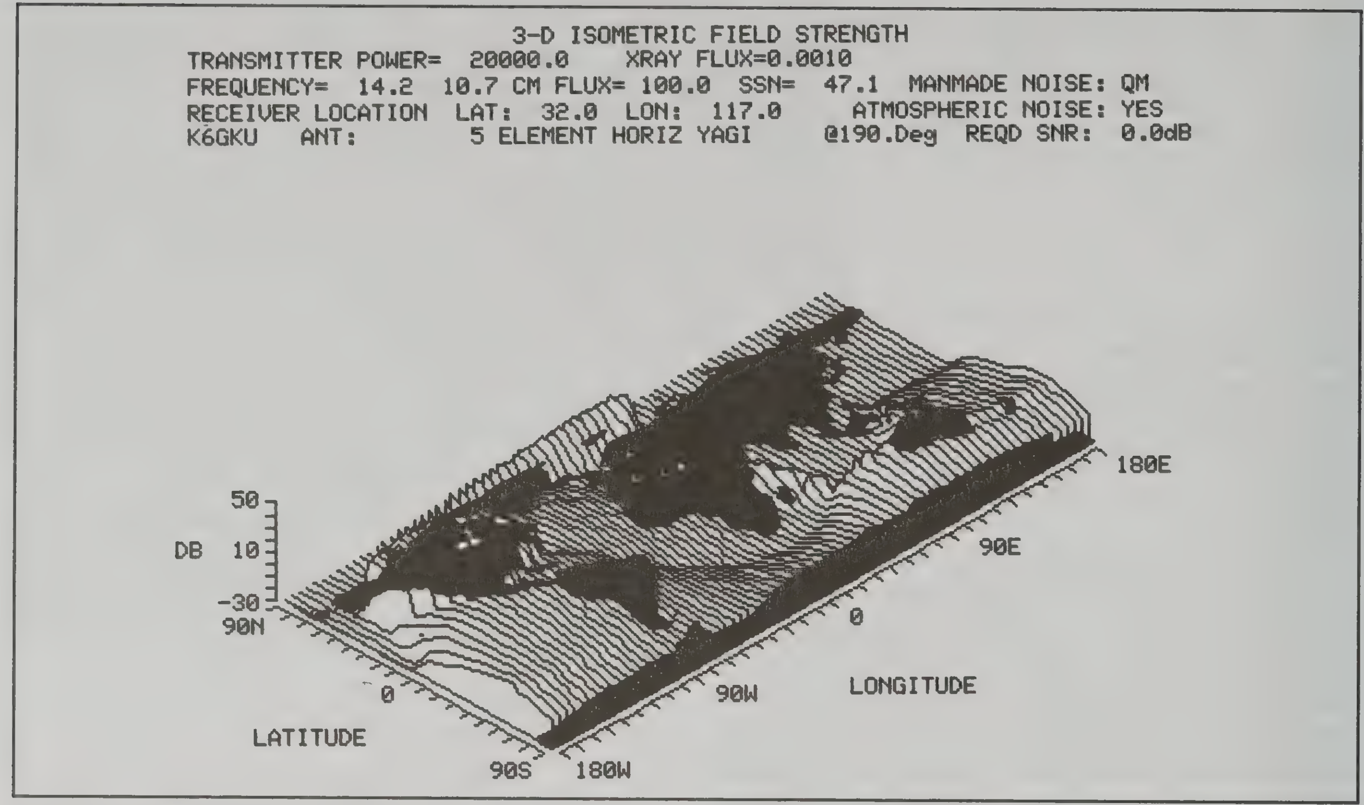

```
                    3-D ISOMETRIC FIELD STRENGTH
TRANSMITTER POWER=  20000.0    XRAY FLUX=0.0010
FREQUENCY=  14.2  10.7 CM FLUX= 100.0  SSN=  47.1  MANMADE NOISE: QM
RECEIVER LOCATION  LAT:  32.0  LON:  117.0     ATMOSPHERIC NOISE: YES
K6GKU   ANT:        5 ELEMENT HORIZ YAGI     @190.Deg  REQD SNR:  0.0dB
```

Figure 7.23. Sunrise (December 1983) 14 MHz long-path from San Diego, California. Moving west, the path moves under Australia and up the East Coast of Africa. The longitudinal contours show predicted signal strength (see scale at left in relative dB). (Courtesy of the U.S. Navy.)

occur to each cell. The expected signal level also was computed. The program was very useful for computing the global footprint of shortwave broadcast stations. However, it also was found to predict long-path propagation. Two examples, shown in Figures 7.23 and 7.24, illustrate 14.2 MHz long-path circuits that actually were confirmed with on-the-air observations. The first example (Figure 7.23) is an early morning (8 AM, local time) example (maybe late gray-line propagation) from the West Coast. This example was predicted in advance and confirmed with both two-way contacts and reception reports. From San Diego, California (and moving west), stations in Australia, the Southern Indian Ocean, eastern Africa, Israel, the Balkans, and central Europe were heard or worked. It took the footprint about 90 minutes to wander northward until it ceased to exist.

The second example (Figure 7.24) shows an evening long path from the East Coast of the United States. In this case, N4XX worked numerous stations over a 60-minute period, with the prediction showing the route of the observed long-path footprint.

If nothing else, long-path propagation provides one of the most mysterious dimensions of amateur radio. We don't exactly know how it works, but it does!

7.11 Non-Reciprocal Communications

The laws of reciprocity require that propagation of a radio signal from point A to point B should be via the same path that signals propagate from point B to point A. At times, however, this does not appear to be the case, and radio amateurs often refer to this condition as "one-way skip." In fact, non-reciprocal communications almost always can be shown to result from differences in the signal-to-noise ratios of the signals received at each end of an HF circuit. Put another way, even if two operators use identical stations, the signal-to-noise ratios of the received signals can differ, and they can do so by significant amounts! To see this, consider the fact that atmospheric noise levels throughout the world vary as a function of frequency, geographic location, time of day, and season of the year. Add to this the interference caused by other stations, together with manmade noise generated by

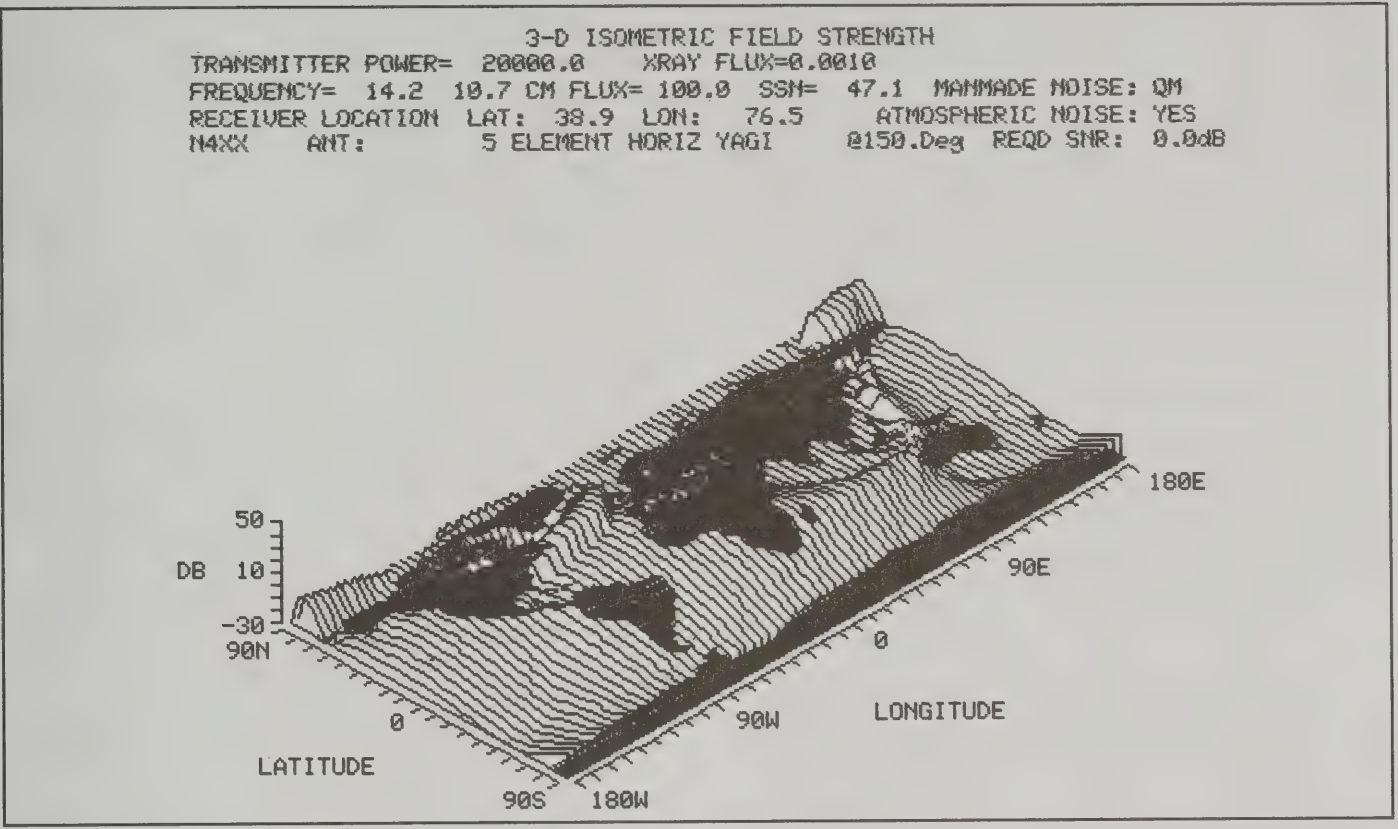

```
                    3-D ISOMETRIC FIELD STRENGTH
TRANSMITTER POWER=  20000.0    XRAY FLUX=0.0010
FREQUENCY=  14.2  10.7 CM FLUX= 100.0  SSN=  47.1  MANMADE NOISE: QM
RECEIVER LOCATION  LAT:  38.9  LON:   76.5    ATMOSPHERIC NOISE: YES
N4XX    ANT:        5 ELEMENT HORIZ YAGI     @150.Deg  REQD SNR:  0.0dB
```

Figure 7.24. Sunset (December 1983) 14 MHz long-path from the Washington, D.C., area. The path dips through Central Africa and extends into Western Australia before turning north and heading up the western rim of the Pacific Ocean. The longitudinal contours show predicted signal strength (see scale at left, in relative dB). (Courtesy of the U.S. Navy.)

appliances, power lines, and so forth, and it's not hard to imagine that the noise levels measured at any two stations could differ by 20 dB or more. Such situations often are encountered on the bands below 20 MHz, where atmospheric noise dominates.

For example, summertime noise levels in the northern hemisphere due to thunderstorm activity significantly degrade the signal-to-noise ratios of all signals received. However, everything else being equal, operators in the southern hemisphere, who are experiencing winter conditions, should receive signals with considerably higher signal-to-noise ratios than will their counterparts in the northern hemisphere. Under these conditions, and if you are in the northern hemisphere, operators in the southern hemisphere should be able to hear you (i.e., understand you) better that you are able to hear them. This may leave you both frustrated, as they continue to answer your CQs, while, at the same time, you are unable to hear their calls above the noise. Of course, for this example, the situation is reversed when it is winter in the northern hemisphere and summer in the southern hemisphere. Regardless of the situation, what appears to be "one-way skip" probably results from nothing more than a high noise level at one end of the circuit.

7.12 Fading

Some degree of fading, or fluctuation in signal level, occurs on all signals reflected by the ionosphere. Fading may be rapid or slow, deep or shallow. Slow fading causes signals to change in level over periods of a few minutes or more; rapid fading causes fluctuations over a period of a few seconds, or less. In practice, both slow and rapid fading can occur at the same time.

Slow fading is caused by variations in absorption in the *D* layer, and to a lesser extent in the *E* layer, and by slow, random movement or motion within the ionosphere itself, particularly in the vertical plane.

Rapid fading is caused by irregularities and instabilities that exist in the ionosphere, particularly in the equatorial region and in the auroral zones, and during periods of radio storminess. As we have seen, these irregularities cause a signal to separate along a number of similar but closely related paths, and to arrive at the receiver as a group of independent signals, with random phase relationships. These differences in phase, caused by multi-path propagation, produce a corresponding variation in signal strength. At one extreme, when the arriving signal components are all in phase, the signal level will be maximum. On the other hand, when they are completely out of phase, the signal will disappear entirely. At times, a fading cycle caused by multi-path propagation can be so rapid that it will render a signal unintelligible.

7.13 References

1. Monroe, M. (K7ALE), and D. Monroe (K7ALF), "50 MHz Propagation Effects," *CQ,* November 1964.

2. Dyer, Pat (WA5IYX), "A Seven Year Study of 50 MHz Sporadic-*E* Propagation," *CQ,* August 1972.

3. Pocock, E. (W3EP), and P. J. Dyer (WA5IYX)," The Sporadic-*E* Season of 1989 in Review," *QEX,* October 1990, pp. 17–19.

4. Brown, Hallinan & Osborne, "Aurora Color Television Project," Second Edition, Geophysical Institute, University of Alaska, Fairbanks, Alaska, 1985, 1986.

5. Fieldstein, Ya. I., and G.V. Starkov, "Dynamics of Auroral and Polar Geomagnetic Disturbances," *Planetary Space Sciences,* 15, 1967, p. 209.

6. Rose, R. B., "A High Latitude Ionospheric Disturbance Assessment System," *Radio Science,* 28 (1), January–February 1993, pp. 97–104.

7. Rose, R. B., and R. D. Hunsucker, "Auroral-*E* Observations: the First Year's Data," NRaD Technical Document 2449, Naval Command, Control and Ocean Surveillance Center, RDT&E Div., San Diego, California, February 1993.

8. Solar Terrestrial Dispatch, P.O. Box 357, Stirling, Alberta, Canada T0K 2E0.

9. Nielson, D. L., "Oblique Soundings of a Transequatorial Path," Stanford Research Institute, 1964.

10. Nielson, D. L., "Long-Range VHF Propagation Across the Geomagnetic Equator," Stanford Research Institute, 1969.

11. Kingan, S. G., "A Study of the Behavior and Geographical Distribution of Nighttime V.H.F. Transequatorial Propagation in the Central Pacific," *TEN-ERP,* Conf. Proceedings, June 22–24, 1993, Naval Postgraduate School, Monterey, California.

12. "Strays," *QST,* March 1994, p. 99.

13. Davis, K., *Ionospheric Radio,* Peter Peregrins Ltd., London, United Kingdom, 1990.

14. Hoppe, D. (K6UA), P. Dalton (W6NLZ), and F. Capossela (K6SSS), "The Gray Line Method of DXing," *CQ,* September 1975.

15. *GEOCLOCK* and other "ham utilities" are available from Joseph R. Ahlgren, 2218 North Tuckahoe Street, Arlington, Virginia 22205 (phone: [703] 241-2661; FAX: [703] 241-5809).

16. The DX Edge, XANTEK, Inc., P.O. Box 834, Madison Square Station, New York, New York 10159 (phone: [212] 673-7646).

Index

- Absorption, 1-1
  - Auroral, 5-5 to 5-6, 7-8 to 7-9, 7-14
  - *D* Layer, 1-8, 1-15 to 1-16, 1-19 to 1-20, 1-23, 5-3
- *a*-Index (see Magnetic, Indices)
- a_p-Index (see Magnetic, Indices)
- *A*-Index (see Magnetic, Indices)
- A_p-Index (see Magnetic, Indices)
- American Radio Relay League (ARRL), *The ARRL Antenna Book*, 1-19
- Angle of Arrival, 1-2
- Angle of Radiation, 1-13 to 1-14, 1-18 to 1-20, 7-23
- Anharmonic Frequency Analysis, 3-7, 3-9
- Antennas, 1-1, 1-18 to 1-20, 4-3, 7-10, 7-11, 7-14
- Appleton, Sir Edward, 1-2, 1-10
- Argon, 1-5
- Atmosphere
  - Composition, 1-5 to 1-7
  - Expansion, 1-11
  - Ionization, 1-1, 1-3 to 1-7
- Atmospheric Noise, 1-16, 1-21, 6-6 to 6-7, 7-24 to 7-25
- Attenuation (see Absorption)
- Aurora (Frequency of Occurrence), 5-5, 7-7 to 7-8
- Auroral
  - Displays, 1-26, 1-29, 7-6 to 7-11
  - E (E_{au}), 1-9, 7-1, 7-4, 7-9 to 7-10, 7-13
  - Flutter, 5-6, 7-9 to 7-10, 7-25
  - Zone Absorption (AZA), 7-8
  - Zones, 1-9, 5-5, 7-7 to 7-9, 7-17

- Backscatter (see Scatter)
- Beacons (HF), 5-16 to 5-18
- Belgium, Royal Observatory of, 2-1, 2-12
- Bending (of radio waves), 1-1, 1-4
- Blackouts, 1-17, 1-23, 1-25 to 1-26, 1-28
- Boykin and Richards, 3-4 to 3-5
- Bulletin Board Systems (BBS), 5-14 to 5-15, 5-17
- Briet and Tuve, 1-2

- CCIR (see ITU)
- Chapman and Milne, 1-7
- Chapman Layer, 1-9 to 1-10 (also see 1-9 [footnote])
- Charge, 1-15
- "Chirper" (see Ionosonde)
- Chromosphere, 3-2
- Circuit Analysis, 1-16 to 1-19
- Citizen's Band (CB), 1-15
- Classical MUF (see Maximum Usable Frequency)
- Computer Programs (for propagation prediction), 1-10, 1-15, 6-1 to 6-28
  - *AMBCOM*, 6-2
  - *ASAPS*, 6-3, 6-6, 6-15, 6-17 to 6-19, 6-20 to 6-27
  - *BANDAID, 2-3*, 6-27
  - *CAPMAN*, 6-6, 6-21 to 6-22
  - *CHIMPS*, 6-8
  - *COMB6*, 6-27
  - *DX Ver. 4.3*, 6-6 to 6-12
  - *DXCAST*, 6-27
  - *ESSA-ITSA-1*, 6-2
  - *GEOCLOCK* (for gray-line prediction only), 7-20, 7-22
  - *HFBC84*, 6-2
  - *HFMUFES4*, 6-2
  - *ICEPAC*, 6-8
  - *IONCAP*, 6-2 to 6-3, 6-6 to 6-9, 6-19 to 6-21, 6-24
  - *IONCAST*, 6-8
  - *IONSOUND*, 6-27
  - *ITS-78*, 6-2
  - *MAPPER*, 6-27
  - *MICROPREDIC*, 6-27
  - *MINIFTZ4*, 6-27
  - *MINIMUF 3/3.5*, 6-1, 6-5, 6-8 to 6-10, 6-12
  - *MINIPROP*, 6-4, 6-8
  - *MINIPROP PLUS*, 6-11 to 6-19
  - *MUF85*, 6-5
  - *PROPHET* (and *Advanced PROPHET*), 6-2 to 6-3
  - *PSYCHIC Ver. 1.2*, 6-8
  - *QLOF*, 6-4, 6-10
  - *RADARC*, 6-2
  - *SPARC*, 6-3
  - *VOACAP*, 6-6, 6-22 to 6-23, 6-27
  - *WHATSON*, 6-27

Control Point, 1-23
Coronal "Green Line," 3-7
Coronal Holes, 1-20, 1-24, 3-7
Coronal Mass Ejection (CME), 1-20, 1-24
Corpuscular Radiation (see Solar Radiation)
Cosmic Radiation (see Solar Radiation)
Critical Frequency, 1-3, 1-5, 1-9 (footnote), 1-11 to 1-15, 6-3 to 6-5
Crooked Path (see Path)
Cyclical Variations (in the Ionosphere; see Sunspots, Cycle)

Daily Sunspot Count (*R*) (see Sunspots, Daily Sunspot Number)
de Forest, Dr. Lee, 1-2
Dellenger, Dr. John H., 1-22
Dellenger Effect (see Sudden Ionospheric Disturbance [SID])
Disappearing (solar gas) Filaments, 1-20
D Layer, 1-7 to 1-8, 1-15 to 1-16, 1-19 to 1-20, 1-23, 5-3, 7-8, 7-17, 7-21 to 7-23
Doppler Shift (see Meteors, Doppler Shift)
Drift (of sporadic-*E* clouds), 1-9
Ducts (HF), 7-23

Echoes, 1-2, 1-24
Eclipse (solar), 1-1, 1-3
E Layer, 1-7 to 1-12, 1-18 to 1-19, 1-24 to 1-25
E_{au} (see Auroral, *E*)
E_s (see Sporadic-*E*)
Effective Radiated Power (ERP), 1-17, 4-3, 7-11
Electron
  As Part of an Atom, 1-5 to 1-6
  Density, 1-5 to 1-7, 1-15, 7-23
  Recombination, 1-6, 1-8, 1-10, 1-24
Ether, 1-2
Equinoxes (spring and fall; used in Master Propagation Charts), 4-1 to 4-31
Extreme Ultraviolet (EUV; see Solar Radiation)

Fading, 1-24, 7-1, 7-9 to 7-10, 7-13, 7-25 to 7-26
F Layer
  Above the *F* Layer, 1-10
  Definition, 1-7, 1-9 to 1-10
F_1 Layer, 1-9 to 1-11
F_2 Layer, 1-9 to 1-13, 1-18 to 1-19, 1-24 to 1-25, 5-3, 7-1 to 7-2, 7-13
F_2 Hang, 1-11
Forecasts (short-term ionospheric), 5-1, 5-6 to 5-9
Forward Scatter (see Scatter)
Frequency of Optimum Traffic (FOT), 1-17
Frequency vs. Wavelength, 1-1

Galileo, 2-3
Gases (atmosphere), 1-5 to 1-7
Geographical Variations (in the Ionosphere; see Ionospheric, Variations)
Geomagnetic (see Magnetic)
Gray Line (see Path)
Great Circle (see Path)
Ground
  Reflection, 5-3, 7-23
  Scatter, 7-14 to 7-15
Ground Level Event (GLE), 1-28 to 1-29

Hale, Dr. George E., 2-3
H-alpha (Hα) Filters, 3-2 to 3-3
Helium, 1-5
Hertz, Heinrich, 1-2
High Frequency (HF), 1-1
High-Speed Solar Wind System (HSSWS), 1-20, 1-24
Highest Possible Frequency (HPF), 1-17
Hydrogen, 1-20, 3-2

International Amateur Radio Union (IARU), 5-17 to 5-18
International Geophysical Year (IGY; 1957), 2-7
Ionization, 1-4 to 1-10, 1-19 to 1-20
Ionogram, 1-3 to 1-5
Ionosonde, 1-3 to 1-5
Ionosphere, 1-1, 2-5, 7-15
  Auroral, 7-9, 7-17
  Definition, 1-4 to 1-10
  Layers, 1-5 to 1-10
  Polar, 1-9, 1-25 to 1-29, 7-9, 7-17
Ionospheric
  Absorption, 1-1, 1-8, 1-15 to 1-16, 1-19 to 1-20, 1-23, 5-3, 5-5 to 5-6, 7-8, 7-17, 7-21 to 7-23
  Disturbances (including storms), 1-19 to 1-29, 5-5, 7-8 to 7-11
  Turbulence, 1-9, 7-9
  Variations
    Cyclical (see Sunspots, Cycle)
    Diurnal (day-night), 1-10 to 1-12
    Eclipse (during), 1-1, 1-3
    Geographical, 1-11 to 1-12
    Latitudinal, 1-11
    Longitudinal, 1-12
    Seasonal, 1-8 to 1-9, 1-11
Ions, 1-4 to 1-6
International Decade of Solar Cycle Studies (IDSCS), 3-2
INTERNET, 5-15, 5-17
ITU (International Telecommunication Union)
  CCIR (International Radio Consultative Committee; now, the Radio Communications Sector of the ITU), 1-5, 6-3 to 6-4, 6-12

Journal of Geophysical Research (JGR), 5-3
Jupiter Effect, 3-8

Kennelly-Heaviside Layer, 1-2, 1-4, 1-7
Koeckelenbergh, Dr. Andre, 2-14
K-Index (see Magnetic, Indices)

- K_p-Index (see Magnetic, Indices)

- Layer Formation, 1-3 to 1-6
- Layer Heights, 1-2 to 1-10, 1-14
- Latitude Variations (in the ionosphere; see Ionospheric, Variations)
- Longitude Variations (in the Ionosphere; see Ionospheric, Variations)
- Long-Term Propagation Predictions (see Predictions)
- Long Path (see Path)
- LORAN, 1-28
- Loss
  - Ionospheric Absorption (see Absorption)
  - Ground, 5-3, 7-23
- Lowest Usable Frequency (LUF), 1-16 to 1-18, 4-1, 6-5

- Magnetic (geomagnetic)
  - Activity, 1-23 to 1-24, 5-9, 7-10
  - Data (sources), 5-11 to 5-26
  - Disturbance, 1-9, 1-23 to 1-24, 1-26
  - Equator, 1-9, 7-12, 7-14, 7-15 to 7-16, 7-23, 7-25
  - Field of the Earth, 1-12, 1-23 to 1-24, 1-26, 1-28 to 1-29, 7-7
  - Indices
    - a-Index, 5-2 to 5-4
    - A-Index, 5-4
    - a_p-Index, 5-4
    - A_p-Index, 3-7, 5-4
    - K-Index, 1-9, 5-2 to 5-4, 7-9
    - K_p-Index, 6-4
  - Storms (geomagnetic), 1-23 to 1-24, 1-26, 1-28 to 1-29, 7-9
- Marconi, Guglielmo, 1-2, 1-4
- Master Propagation Charts, 3-12, 4-1 to 4-31, 5-1, 5-6, 6-9
  - Low Solar Phase (SSN 0-30)
    - DX, 4-7 to 4-11
    - Short-Skip, 4-11 to 4-12
  - Moderate Solar Phase (SSN 30-60)
    - DX, 4-12 to 4-17
    - Short-Skip, 4-17 to 4-18
  - High Solar Phase (SSN 60-90)
    - DX, 4-18 to 4-23
    - Short-Skip, 4-23 to 4-24
  - Very High Solar Phase (SSN 90-120)
    - DX, 4-24 to 4-30
    - Short-Skip, 4-30
  - Intense Solar Phase (SSN >120)
    - Use Very High Solar Phase (SSN 90-120) data above
- Maunder (sunspot) Minimum, 2-6
- Maunder, Walter, 2-6
- Maximum Entropy Spectral Analysis (MESA), 3-5, 3-7
- Maximum Observed Frequency (MOF), 1-11, 1-13
- Maximum Usable Frequency (MUF), 1-1
  - Calculation, 1-14 to 1-18, 4-1
  - Classical, 1-14 to 1-16, 7-6, 7-12, 7-13, 7-14
  - Median, 1-14, 5-2, 6-5
- Medieval (sunspot) Maximum, 2-6
- Meteors, 7-1
  - Doppler Shift, 7-9, 7-11
  - Ionization, 1-9, 7-11 to 7-13
  - Showers (including dates), 7-9, 7-11 to 7-12
- Monthly Mean Sunspot Number (R_m), 2-4
- Multi-Hop Propagation (See Path)
- Multi-Path (see Path)

- National Institutes of Standards and Technology (NIST; see WWV, WWVH)
- National Oceanic and Atmospheric Administration (NOAA), 5-11, 5-13 to 5-15
- Neutral Atoms, 1-5
- Nitrogen, 1-5
- Noise (see Atmospheric Noise)
- Non-Reciprocity (of propagated signals), 7-1, 7-24 to 7-25

- Ohl's Method, 3-5 to 3-6, 3-8
- One-Hop Propagation (see Path)
- One-Way Skip (see Non-Reciprocity)
- Optimum Radiation Angle, 1-18 to 1-20
- Optimum Working Frequency (OWF; see Frequency of Optimum Traffic [FOT])
- Oxygen, 1-5

- Path (ionospheric)
  - Crooked, 7-20, 7-21
  - Gray Line, 7-1, 7-17 to 7-23
  - Great Circle, 7-14
  - Long, 7-1, 7-20 to 7-25
  - Multi-Hop, 1-19, 7-3, 7-22 to 7-23
  - Multi-Path, 7-9, 7-26
  - One-Hop, 1-14, 1-18 to 1-19 7-3
  - Short, 7-20 to 7-21
- PENEX (Polar, Equatorial, Near Vertical Incidence Experiment), 7-15 to 7-17
- Pettit, Dr. Edison, 2-5
- Phase (of solar activity; see Solar, Phase)
- Photo-Ionizing Agents, 1-3, 2-5
- Plage, 2-2
- Planetary Indices (a_p, A_p, and K_p; see Magnetic, Indices)
- Plasma, 1-9 to 1-10, 1-20, 2-1
- Polar Blackouts, 1-25 to 1-27
- Polar Cap Absorption (PCA), 1-25 to 1-26, 7-8
- Polar Ionosphere (see Ionosphere)
- Predictions
  - Long-Term (band openings), 4-1 to 4-31, 5-1, 5-7 to 5-9
  - Solar (sunspots), 3-1 to 3-14
- Pre-Sunrise Depression (of f_oF_2), 1-11
- Propagation Indices, 4-1 to 4-4, 4-6, 5-7 to 5-9

- Quality of DX Propagation (see Signal Quality Rating)
- Quiet Geomagnetic Field, 5-5

- Radiation (see Solar Radiation)

Radiowaves, 1-1
Ray Path, 1-13 to 1-14, 1-18 to 1-19
Reciprocity, 7-24
Recombination, 1-6, 1-8, 1-10, 1-24
Reflection at Vertical Incidence, 1-2 to 1-4
Refraction (see Bending of Radio Waves)
Roman (sunspot) Maximum, 2-6
Royal Observatory of Belgium, 2-1, 2-5, 2-14
Satellites, 1-8, 1-26, 1-28 to 1-29, 2-11, 3-9
Scatter (ionospheric), 1-14, 7-1
  Forward, 7-6
  Side, 7-6
  Back, 7-6 to 7-7
Scheiner, Jesuit Friar Joseph, 2-1
Schwabe, Hendrick S., 2-4, 3-1
Seasonal Variations (in the ionosphere; see Ionospheric, Variations)
Secant Law (stated using the cosecant), 1-14
Short Path (see Path)
Short-Skip, 4-4, 4-6 to 4-7, 4-11 to 4-12, 4-17 to 4-18, 4-23 to 4-24, 4-30, 7-3, 7-6, 7-9
Shortwave, 1-1, 1-10
Shortwave Fadeout (SWF; see Sudden Ionospheric Disturbance)
Signal Quality Rating, 4-31, 5-3, 5-8 to 5-9, 5-11
Skip, 1-2
Skywave, 1-2, 1-8, 1-18
Solar
  Activity, 1-1
  Cycle (see Sunspot Cycle)
  Data (sources), 2-14, 5-11 to 5-26
  Flares, 1-20 to 1-29, 2-1
  Flux, 2-12 to 2-13, 5-2 to 5-4, 5-9, 7-9
  Phase, 3-11 to 3-12, 4-1 to 4-4
  Radiation
    Corpuscular (high and low energy solar particles), 1-20 to 1-29, 7-6
    Cosmic, 1-6, 2-12
    Extreme Ultraviolet, 1-3, 1-6, 1-9, 1-22, 3-2
    Rotation, 1-24
    Ultraviolet, 1-1, 1-4, 1-6 to 1-7, 1-10, 1-22, 2-1, 2-5, 2-12, 3-1, 7-6
    X-Ray, 1-6, 1-22 to 1-23, 2-1, 2-12
    Zenith Angle, 1-7, 1-10, 1-15, 1-23, 6-4 to 6-5
Sounder (see Ionosonde)
Sporadic-*E* (E_s), 1-9, 6-24, 7-1 to 7-6, 7-9, 7-13
Sporer (sunspot) Minimum, 2-6
Spread-*F*, 7-1, 7-15 to 7-17
Storms (see Ionospheric Disturbances, and Magnetic Storms)
Sudden Ionospheric Disturbance (SID), 1-22 to 1-23, 1-26, 1-29
Sun, 1-1 to 1-3, 1-6 to 1-7, 1-10 to 1-12, 1-20 to 1-22, 2-1, 3-1 to 3-2, 3-8, 5-2
Sunspots, 1-1 to 1-2, 1-12, 1-21, 1-24, 2-1 to 2-3, 3-1
  Average Cycle, 2-5 to 2-6
  Cycle, 1-1, 1-12, 2-1 to 2-4
  Cycle No. 19, 2-1, 2-6 to 2-7, 7-1, 7-12
  Cycle No. 20, 2-1, 2-6 to 2-9, 3-3, 7-1
  Cycle No. 21, 1-9, 1-22, 2-1, 2-6, 2-9 to 2-11, 3-3 to 3-4, 3-6, 3-8 to 3-9, 7-1
  Cycle No. 22, 1-1, 1-28 to 1-29, 2-1, 2-6 to 2-7, 2-10 to 2-13, 3-2, 3-4, 3-7, 3-9, 3-12, 4-3, 6-20, 7-1
  Cycle No. 23, 3-2, 3-10 to 3-12, 4-3
  Daily Sunspot Number (*R*), 2-4, 5-2
  Drift, 3-9 to 3-11
  Magnetic Fields, 2-2, 3-9 to 3-10
  Maximum, 1-24, 2-2, 2-4 to 2-7, 3-1 to 3-2
  Minimum, 2-1, 2-4 to 2-6, 3-1 to 3-2, 6-20
  Monthly Sunspot Number (R_m), 2-4
  Predictions, 3-1 to 3-14
  Proxy Data, 2-6
  Region No. 5395, 1-28 to 1-29, 2-2, 2-11
  Twelve-Month Running Smoothed Sunspot Numbers (R_s or SSN), 2-4, 2-14 to 2-18
Swiss Federal Observatory (Zurich Solar Observatory), 2-1, 2-3, 2-6, 2-14

Take-Off Angle (radiation angle), 1-13 to 1-14, 1-18 to 1-19
Television (DX), 2-7, 7-6, 7-12
Terminator (see Path, Gray Line)
Time Conversion, 4-5, 5-23
T-Index, 6-15, 6-17, 6-20
Trans-Equatorial (TE) Scatter, 7-1, 7-10, 7-12 to 7-14
Twenty-Seven-Day Recurrence, 1-24, 2-2 to 2-3, 3-7, 5-9 to 5-12, 6-4
Twilight Zone (see Path, Gray Line)

Ultraviolet Radiation (UV; see Solar Radiation)
Unreliability of HF Propagation, 2-11, 3-2
Unusual HF and VHF Propagation, 7-1 to 7-26

Van Allen, Dr. James, 1-28
Van Allen Belts, 1-28
Vertical Incidence Sounder (VIS) Stations, 1-5, 6-3
Very High Frequency (VHF) Propagation, 7-1 to 7-15

Waldmeier, Professor M., 2-14, 3-3
Watson-Watt, Sir Robert, 1-7
Wavelength vs. Frequency, 1-1
Wolf, Rudolf, 2-4
Wolf's Relative Sunspot Number (*R*; see Sunspots, Daily Sunspot Number)
WWV, WWVH, 2-13, 5-1 to 5-2, 5-6, 5-8 to 5-9, 5-11 to 5-14, 5-19 to 5-26, 6-11, 7-9

X-Rays (see Solar Radiation)

Zenith Angle of Sun (see Solar Zenith Angle)
Zurich Solar Observatory (see Swiss Federal Observatory)
Zurich Sunspot Numbers (*R*), 2-4, 2-14

The NEW Shortwave Propagation Handbook may well be the only book you'll need on the subject of ionospheric propagation for the next ten years or more! It is a "must read" for Radio Amateurs, Shortwave Listeners, and Radio Communicators of any type who need to make the most productive use of the radio spectrum, regardless of the time of day, the season of the year, or the state of the sunspot cycle. This is one book that is unlikely to sit on your bookshelf, unread, over the next few years. *The NEW Shortwave Propagation Handbook* will become your ever-present companion at the operating table as you master the art of shortwave radio propagation.

ISBN 0-943016-11-8
EAN
9

1 Brnsd Powell's Used $11.95
New Short Wave Propagation Han
Jacobs, George 9780943016115
COMP-ELEC RADIO 906 9/19/2023